

THE DEVELOPMENT OF REAGENTS AND
REACTIONS TO BE USED IN VISIBLE LIGHT
PHOTOCATALYSIS

By

MANJULA RATHNAYAKE

Bachelor of Science in Chemistry
University of Kelaniya
Sri Lanka
2013

Submitted to the Faculty of the
Graduate College of the
Oklahoma State University
in partial fulfillment of
the requirements for
the Degree of
DOCTOR OF PHILOSOPHY
July, 2020

THE DEVELOPMENT OF REAGENTS AND
REACTIONS TO BE USED IN VISIBLE LIGHT
PHOTOCATALYSIS

Dissertation Approved:

Dr Jimmie D. Weaver III

Dissertation Adviser

Dr Frank D. Blum

Dr Toby L. Nelson

Dr Laleh Tahsini

Dr Marimuthu Andiappan

ACKNOWLEDGEMENTS

I would like to express my sincere gratitude to my advisor Dr. Jimmie D. Weaver for his immense support during my Ph.D. study. His knowledge, skillful guidance, and continuous motivation were helped me to realize my potentials in the field of chemistry and I mostly enjoyed working in that type of research environment.

I would also like to acknowledge my committee members: Dr. Frank D. Blum, Dr. Toby Nelson, Dr. Laleh Tahsini, and Dr. Marimuthu Andiappan for their encouragements, valuable supports and helpful suggestions throughout these years.

I fully enjoyed working with all my lab mates Anuradha, Sameera, Amandeep, Jon, Kamaljeet, Kip, Mo, Sonal, Winston, Mukulesh, Ryne, Erik, Tim, Shivangi, and Sristy. I would like to thank them all. It was a great pleasure sharing ideas, helping, and learning from each other throughout these years.

It is my pleasure to thank my loving husband Asitha Karunathilaka for his continuous support throughout my graduate school period. Without his love and kind support, I would not have made through graduate school.

I would like to thank my father K.B. Rathnayake, my mother R. Thennakoon, and my brother Sanjeewa Rathnayake for their immense love and support throughout my life. Their guidance and motivation directed me to pursue this goal and I will forever be indebted for their sacrifices in supporting me.

Next, I would like to thank my professors of the University of Kelaniya where I completed my undergraduate studies. Their teaching and problem-solving skills showed me what the teaching should look like and it continuously amazed me. Their support and guidance helped a lot to enter graduate school.

Name: MANJULA RATHNAYAKE

Date of Degree: JULY, 2020

Title of Study: THE DEVELOPMENT OF REAGENTS AND REACTIONS TO BE
USED IN VISIBLE LIGHT PHOTOCATALYSIS

Major Field: CHEMISTRY

Abstract: Visible light photocatalysis has become a powerful synthetic tool that can be used to promote various functional group transformations through the use of visible light as a green and traceless reagent. Recently, we have attempted to develop a reagent capable of promoting visible-light prenylation. Prenylation is an essential reaction on which nature relies to modify properties of molecules and build terpenoids, but one which remains a challenging chemical reaction. Aiming to capitalize on recent advances in photocatalysis to cleanly generate a broad range of carbon based radicals, we have developed a prenyl transfer reagent that can capture transiently generated radicals. The reagent can be made in bulk, is bench stable, and broadly applicable such that it can be used with existing photocatalytic methods with very few changes to reaction conditions. In our next effort, we explored strategies to expand the scope of visible light mediated cross-couplings to alkyl halides. While aryl halides have proven to be competent precursors to aryl radicals, the extreme reduction potentials of unactivated alkyl halides limit their generality as radical precursors in organic synthesis via photocatalysis. To circumvent this limitation, we leveraged alkyl halides tendency towards substitution to install a functional group more inclined towards electron transfer and ultimately fragmentation to generate benzylic radicals from a variety of benzyl halides that would be sluggish, inert, or incompatible with current visible light photoredox catalysis. Applying this strategy, we demonstrate the use of collidinium salts as new reagents for formation of C–C bond which highlights the mild reaction conditions and high functional group tolerance. Finally, we demonstrated the visible light mediated photocatalyst free selective debromination of activated poly-bromides in the presence of amines. This visible light mediated alkyl bromide and chloride synthesis is a particularly convenient synthetic approach when coupled to perhalogenation reactions from the literature. This selective defunctionalization effectively separates the problems of bond formation and reaction selectivity and facilitates the synthesis of organo-bromides and –chlorides. We found that these photochemical reductions rely either on the formation of an electron donor-acceptor complex of the substrate and reductant, or alternatively on an auto-photocatalysis pathway.

TABLE OF CONTENTS

Chapter	Page
I. INTRODUCTION.....	1
1.1 Background	1
1.2 Discussion of photocatalysis	2
1.3 The development of reactions and reagents to be used in visible light photocatalysis.....	4
1.4 References.....	9
II. A GENERAL PHOTOCATALYTIC ROUTE TO PRENYLATION	18
2.1 Introduction.....	18
2.2 Development of photocatalytic prenylation reactions	22
2.3 Summary	36
2.4 Experimental section.....	37
2.5 References.....	137
III. ALKYL HALIDES VIA VISIBLE LIGHT MEDIATED DEHALOGENATION	148
3.1 Introduction.....	148
3.2 Development of methodology for the synthesis of alkyl halides.....	151
3.3 Summary	163
3.4 Experimental section.....	164
3.5 References.....	258

Chapter	Page
IV. COUPLING PHOTOCATALYSIS AND SUBSTITUTION CHEMISTRY; ENGAGING NON- REDOX ACTIVE HALIDES	268
4.1 Introduction.....	268
4.2 Generating radicals from non-redox active halides	271
4.3 Summary	289
4.4 Experimental section.....	290
4.5 References.....	411
 APPENDICES	 418

LIST OF SCHEMES

Schemes	Page
1.1 Oxidative and reductive quenching cycle of Ir(ppy) ₃	4
1.2 Reductive alkylation of 2-bromoazole	5
1.3 Visible light-mediated radical addition to alkene	5
1.4 Emerging strategies for radical formation	7
2.1 Approaches towards prenylated arenes	21
2.2 Challenges associated with transferring a prenyl group	22
2.3 Visible light-mediated radical addition to alkene	23
2.4 Reductive alkylation of 2-bromoazole	24
2.5 Allyl alcohol as a radical allylating agent	24
2.6 Allylation with α -substituted allyl sulfone	26
2.7 Synthesis of prenyl sulfones	27
2.8 Prenylation of azoles	27
2.9 Ary radicals from aryl diazonium salts	28
2.10 Prenylation of anilines	29
2.11 Reductive dehalogenation of aryl iodides	29
2.12 Prenylation of aryl iodides	30
2.13 Reductive dehalogenation alkyl halides	31
2.14 Prenylation of α -carbonyl bromides	31
2.15 General mechanism	32
2.16 Allylation with α -substituted allyl sulfone reagents	34
2.17 Photoredox thiol-yne reaction	34
2.18 Prenylation of thiophenol	34
2.19 Navigating photocatalysis	36
3.1 Visible light-mediated reductive dehalogenation	149
3.2 Alkyl halides by light irradiation of EDA complexes	150
3.3 Molecular sculpting approach to monohalogenation	156
3.4 Bach's visible light mediated intramolecular radical cyclization	160
3.5 General structure of streptocyanine dyes	160
3.6 Proposed mechanism and potential streptocyanine dye	161
3.7 Mechanistic experiments	163
4.1 Radical anion fragmentation	269
4.2 Emerging strategies for radical formation	270
4.3 Search for redox active salts	272

4.4 Redox activity of pyridinium salts	273
4.5 First reports on reduction of Katritzky salts with unactivated alkyl groups	274
4.6 Scope of pyridinium salts	285
4.7 Scope of acceptors	286
4.8 kinetic isotope experiments.....	288
4.9 Working mechanism.....	289

LIST OF TABLES

Tables	Page
2.1 Development of a prenyl transfer reagent.....	25
2.2 Isomerization of sulfone (1k).....	33
3.1 Optimization of dehalogenation.....	151
3.2 Optimization of amine	152
3.3 Optimization of solvent.....	153
3.4 Hydrodebromination with other potential reductants	154
3.5 Optimization of temperature	155
4.1 Optimization table.....	276
4.2 Photocatalyst screening.....	277
4.3 Photocatalyst loading	278
4.4 Acrylonitrile loading.....	279
4.5 Optimization of solvent.....	280
4.6 Optimization of temperature	280
4.7 Optimization of amine	281
4.8 Optimization of DIPEA equivalent.....	282
4.9 Effect of water.....	283
4.10 Deuterium incorporation.....	284

LIST OF FIGURES

Figure	Page
2.1 C5 isoprene units.....	19
2.2 Common examples of terpenes.....	19
2.3 Prenylated natural products.....	20
3.1 UV-Vis absorption of 7b,1b, and DIPEA	158
3.2 Rates of debromination reaction of 7b and 1b under different DIPEA concentrations	158
3.3 Time-dependent UV/Vis spectra of debromination reaction of 1b.....	159

CHAPTER I

INTRODUCTION

1.1 Background

The effect of the light on some chemical reactions has been known for many years. Photosynthesis, the quintessential example from nature, is the most fundamental example in which chlorophyll captures light energy and activates complex chemical reactions to convert CO₂ and H₂O into carbohydrate.¹ However, unlike chlorophyll which absorbs in the visible region, most simple organic molecules are colorless and can be photo-activated only by using relatively short wavelength, ultraviolet (UV) light. Irradiation of ultraviolet (UV) light to carry out organic reactions has a long history. In 1900, Giacomo Ciamician conducted experiments to study whether “light and light alone” would facilitate chemical reactions. Ciamician’s investigations are generally considered as the ground-breaking findings of modern synthetic photochemistry.² From the late 1950s onwards, organic transformations utilized ultraviolet (UV) light had increased steadily. Among them, Corey's synthesis of carophyllene alcohol,³ Eaton's cubane synthesis,⁴ and Wender's synthesis of cedrene⁵ are some remarkable findings. However, working with ultraviolet (UV) light frequently limits the functional group tolerance and leads to undesired side reactions. Furthermore, it requires specialized and expensive glassware, poses health and safety concerns, and can be challenging to run on large scales.⁶ As a result, ultraviolet (UV) light-mediated photochemistry has seen limited applications in organic synthesis. To overcome challenges associated with ultraviolet (UV) light, photocatalysis has emerged as powerful synthetic tool that allows

various functional group transformations using visible light as a green and traceless reagent.⁷ As a result, over the last two decades, the field of visible light photocatalysis has grown exponentially and is proving remarkably effective at catalytically generating a variety of radicals under near ambient conditions, often resulting in reactions that are tolerant of functional groups.⁷ In addition to their use in organic synthesis, photocatalysts have been utilized in organic light-emitting diodes,⁸ dye-sensitized solar cells,⁹ polymer synthesis,¹⁰ and photodynamic therapy.¹¹ However, in this discussion we focus on their use within organic synthesis.

1.2 Discussion of photocatalysis

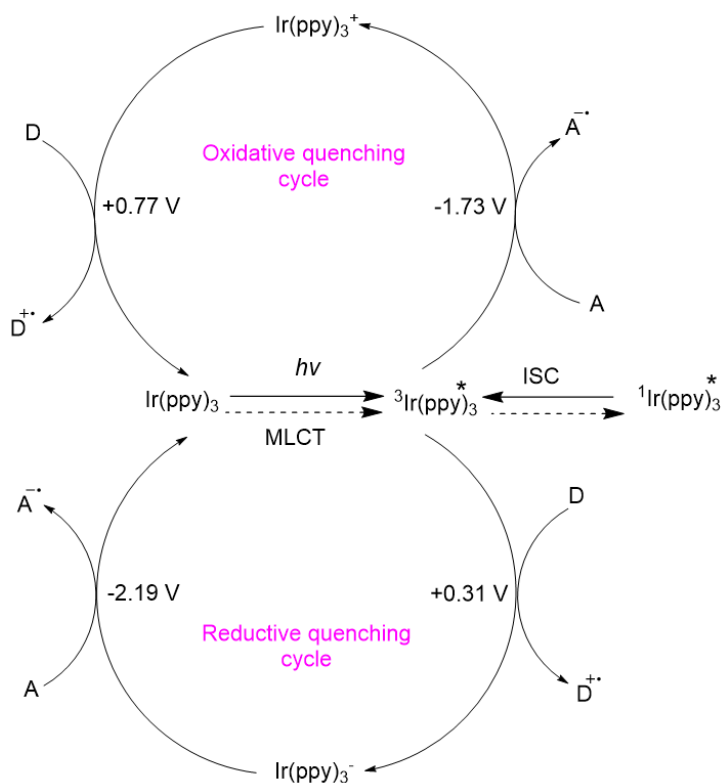
In photocatalysis, a photocatalyst absorbs light in the visible region to give long-lived photoexcited states¹² which can activate organic molecules by electron or energy transfer processes. While the excited states are very potent single-electron-transfer reagents, photocatalysts are generally poor single-electron reductants and oxidants in the ground state. Photocatalyst tris(2,2'-bipyridine) ruthenium(II), or Ru(bpy)₃²⁺ has been widely utilized in visible light-mediated organic transformations.^{7a} In 1981, Pac¹³ reported Ru(bpy)₃²⁺ mediated photoreduction of electron deficient alkenes in the presence of stoichiometric reductant 1-benzyl-1,4-dihydronicotinamide. This is the first report regarding ruthenium photocatalyst mediated small organic molecule activation. Furthermore, Fukuzumi and co-workers¹⁴ have described photocatalytic reduction of phenacyl halides utilizing the same catalyst. In 2008, MacMillan¹⁵ and Yoon¹⁶ have reported Ru(bpy)₃²⁺ employed α -alkylation of aldehydes and [2 + 2] cycloaddition, respectively. Shortly thereafter, Stephenson¹⁷ developed methodology to reductive dehalogenation of activated alkyl halides by the same catalyst. After these studies, organic transformations employed transition metal photocatalysts increased exponentially.

The well-investigated *fac*-tris(2-phenylpyridine) iridium(III), Ir(ppy)₃ is also a widely used photoredox catalyst in organic synthesis. It absorbs from 320 to 480 nm with a maximum absorption recorded at 375 nm.¹⁸ After absorption of a visible light photon, an electron present in the t_{2g} orbital of the metal is excited to a ligand-centered π* orbital which is the LUMO. This transition is called a metal to ligand charge transfer (MLCT). The MLCT singlet excited state rapidly undergoes intersystem crossing (ISC) to form the longer-lived lowest-energy triplet MLCT state which engages in single-electron transfer process. The longer lifetime of the triplet excited state of the photocatalyst is because its decay to the singlet ground state is spin forbidden process.^{12, 19} The photoexcited triplet species has the remarkable properties of being both oxidizing and reducing.

The excited photocatalyst can return to the ground state either by oxidative or by reductive quenching pathway.^{7a} In the oxidative quenching cycle, the *Ir(ppy)₃³⁺ serves as a reductant (E_{1/2}(IV)/(III)* = -1.73 V vs SCE)²⁰ and gives an electron to the electron acceptor (A) (scheme 1.1, upper half). The products formed after the single-electron-transfer event are the oxidized form of the photocatalyst Ir(ppy)₃⁴⁺ and the radical anion of A. This oxidized photocatalyst is a powerful oxidant (E_{1/2}(IV)/(III) = 0.77 V vs SCE) and may accept an electron from a donor (D). This electron transfer generates radical cation of D and returns the catalyst to the initial ground state completing the photocatalytic cycle.

The excited photocatalyst *Ir(ppy)₃³⁺ behaves as an oxidant (E_{1/2}(III)*/(II) = 0.31 V vs SCE)²¹ in the reductive quenching pathway (scheme 1.1, lower half). It accepts an electron from a donor (D) molecule to form the reduced species Ir(ppy)₃²⁺ and radical cation of D. The reduced Ir(II) intermediate is a strong reductant (E_{1/2}(III)/(II) = -2.19 V vs SCE) and may donate an electron to an acceptor molecule (A) to afford radical anion of A. Next, the catalyst returns to the ground state species to complete the photocatalytic cycle.

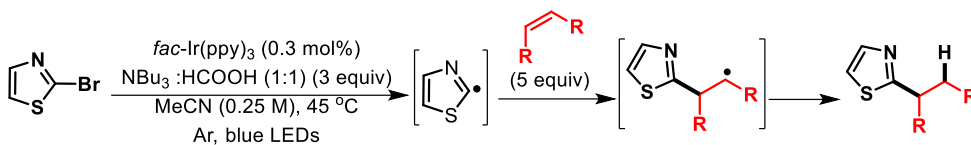
Scheme 1.1 Oxidative and reductive quenching cycle of Ir(ppy)₃



1.3 The development of reactions and reagents to be used in visible light photocatalysis

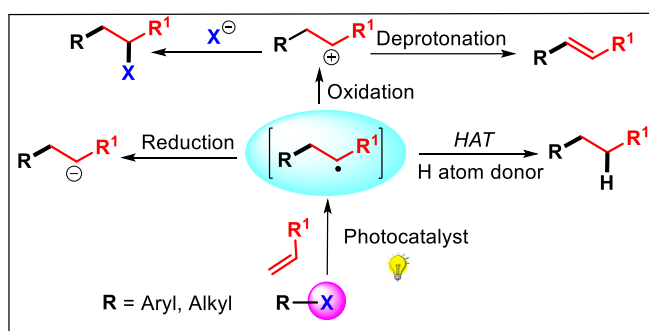
Among other things, our group has investigated strategies to utilize electron transfer to facilitate cross-couplings. More specifically, our group has looked at hard to functionalize C–F bonds²² as well as other important but problematic heterocycles²³ that can be mediated via visible light photocatalysis. This process leads to odd electron species capable of various types of coupling and our group has explored conditions that allow the coupling of alkenes, aryl groups, alkynes and amines. Among these works, former group members found that 2-bromoazoles can produce the azolyl radical in the presence of an amine, photocatalyst Ir(ppy)₃, and visible light. The generated azolyl radical undergoes smooth addition to unactivated π -bonds of alkenes to form alkylated azole product (scheme 1.2).^{23a} The azolyl radical showed a strong preference for the less substituted terminus, and, to a lesser degree, the more electron rich terminus of the double bond.

Scheme 1.2 Reductive alkylation of 2-bromoazole



Apart from this, in a number of cases photocatalytically generated radicals have proven capable of undergoing addition to alkenes.²⁴ Upon addition, a new alkyl radical intermediate is generated that has been oxidized,²⁵ reduced,¹⁶ or subjected to hydrogen atom transfer (HAT)²⁶ (scheme 1.3). Particularly, inherent selectivity is observed for the addition to the less substituted terminus of the double bond.

Scheme 1.3 Visible light-mediated radical addition to alkene



In this vein, a growing number of methods for the photocatalytic generation of different radicals have recently been disclosed.⁷ We became curious to know if we could use these methods to accomplish prenylation of various photocatalytically generated radicals. In order to accomplish this, we hoped to identify a reagent that tolerates the photocatalytic reaction conditions, rapidly intercepts these radicals, and delivers the prenylated product as a result. Based on the aforementioned literature, we believed that it should be possible to use an alkene to intercept the radical. Our hope was that we could use one of the subsequent intermediates to install the double bond of the prenyl group.

Prenylation is an important phenomena and nature prenylates proteins,²⁷ indole alkaloids,²⁸ flavonoids,²⁹ coumarins³⁰ and other aromatics³¹ to effect a number of biological purposes, and has

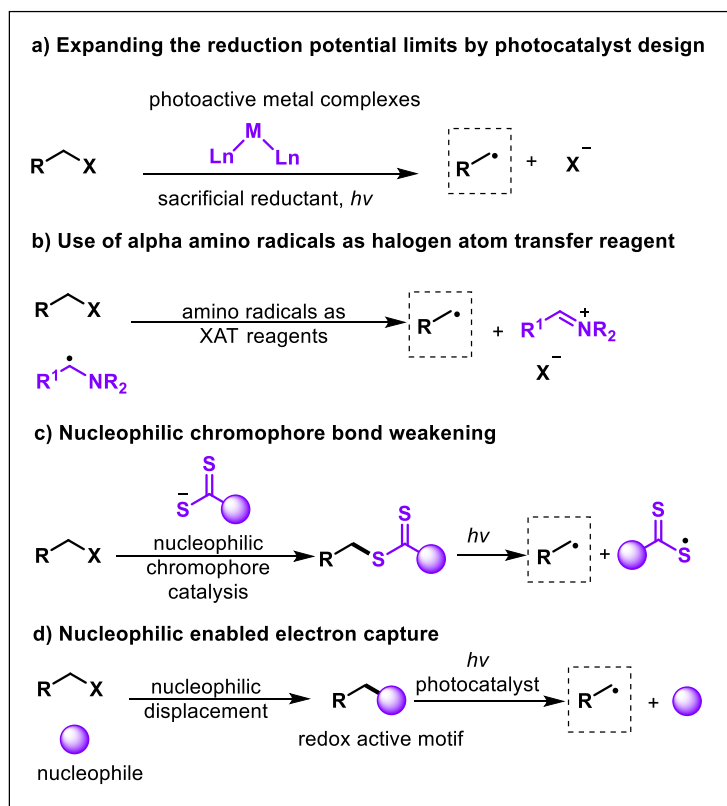
resulted in demand for prenylated molecules. We posited that we could capitalize on the high inherent regioselectivity of radical addition to alkenes to design a prenylating reagent that could be used broadly as a drop in solution to previously developed photocatalytic reaction which generate radicals. Furthermore, the ideal prenyl transfer reagent should be easily handled, shelf stable, non-toxic, inexpensive, and easily separated from the product. After screening multiple prenylating reagents, we identified iso-prenyl sulfone as a general photocatalytic prenylation reagent. We investigated its use in the visible light photocatalytic prenylation of 2-bromoazoles, iodoarenes, α -carbonyl alkyl bromides, thiols and anilines (via the insitu generated diazoniums). The reagent has demonstrated high functional group compatibility, proven bench stable, and is a crystalline solid that can be synthesized via allylation of benzene sulfinate followed by dimethylation in high yields. We anticipate that this reagent, along with rapid advancement of visible light photocatalysis will greatly expand prenylation efforts.

The prenylation work relies on the ability of photocatalysis to generate radicals. While aryl halides have often proven to be competent precursors to aryl radicals,³² the extreme reduction potentials of unactivated alkyl halides³³ has often pushed them beyond the scope of current photocatalytic methodologies. Generating radicals from aryl halides is possible due to the relatively low-lying unoccupied pi-star orbitals of the aromatic system into which an electron is transferred. En route to radical formation, an intramolecular electron transfer (ET) to the C–X sigma* orbital takes place, allowing the critical mesolytic fragmentation which yields the halide ion and carbon centered radical.³⁴ The rate of this intramolecular ET is dependent on a number of factors, including the energy of the pi*-orbitals, and electronic overlap with the fragmenting groups, among other factors.^{34b, 35} Practically speaking, useful rates of radical anion fragmentation are observed for ipso substituted halides, and alpha halo species, but drops with greater structural separation, and represents a real mechanistic limitation of radical anion fragmentation mechanism. This sensitivity to structure is particularly revealing in the case of alkyl halides in which the rate of fragmentation becomes highly dependent on the structure and

functional groups attached to the alkyl halide component.³⁶ Thus, methods for the generation of alkyl radicals are highly important process because they can enable the formation of new C–C bonds.

Recently, several diverse strategies have been explored to generate such alkyl radicals. Evolution of the photocatalyst structure aimed at pushing the reduction limits has been pursued by several groups (scheme 1.4a).³⁷ Among them, photocatalysts of low-valent group 6 (Cr, Mo, W) with isocyanide complexes have shown appealing photophysical and redox attributes,^{37a, 37b} and some success in photoredox transformations of difficult substrates.^{37b, 37c} Alternatively, Leonori has recently proposed the use of alpha amino radicals to facilitate halogen atom transfer (scheme 1.4b).³⁸ More relevant to this work, Melchiorre has identified a clever system that capitalizes on the electrophilicity of alkyl halides to be displaced by a nucleophilic chromophore (scheme 1.4c).³⁹

Scheme 1.4 Emerging strategies for radical formation



Encouraged by these findings, we have developed a conceptually related idea that capitalizes on the electrophilicity of alkyl halides but decouples the photon absorbing aspects of the catalyst from its nucleophilic aspects (scheme 1.4d). Our objective was to identify a nucleophile that upon addition to the alkyl halide would become easily reducible, and could thus serve as the electron capturing component where the halide failed, and ultimately, level substrate reduction potentials. We found that collidine as the optimal nucleophile. In chapter IV, we show that collidinium salts produced from the nucleophilic displacement of the halide by collidine can enable photoredox catalysis, not possible on the corresponding halide, to generate a range of alkyl radicals that can facilitate cross-couplings in a mild and efficient manner.

In the chapter III, we explore the concept of molecular sculpting and its application to the selective production of alkyl halides via visible light mediated (photocatalyst free) dehalogenation. Such alkyl bromides and chlorides are found in natural products⁴⁰ and play a central role in synthesis.⁴¹ Consequently, efforts have focused on the development of mono-⁴² and enantio-⁴³ selective halogenation. Often the increased reactivity of the products leads to inseparable mixtures un-, mono-, and di-halogenated material. Our group has approached the similar problem of organofluorine synthesis from an alternative direction,²² sculpting molecules by defluorinating poly- or per-fluorinated molecules to reveal the desired organofluorine left behind. In this chapter, we apply this concept to the production of alkyl halides which effectively separate the problems of bond formation and reaction selectivity- facilitating the synthesis of organo-bromides and -chlorides.

Recently, visible light-induced photocatalyst-free organic transformations have received considerable attention. As such, electron-donor-acceptor (EDA) complex-mediated reactions have played a critical role. An EDA complex is ground-state association between an electron-rich donor and an electron-poor acceptor.⁴⁴ EDA complexes have been postulated to undergo electron-transfer event when irradiated by visible light which in certain instances lead to bond fission or fusion.⁴⁵ Encouraged by the examples of successful reactions mediated by the photochemistry of EDA complexes, we studied the visible light

mediated selective debromination in the presence of amines. Further, we have shown that this visible light mediated alkyl bromide and chloride synthesis is a particularly convenient synthetic approach when coupled to perhalogenation reactions from the literature. The photochemical reductions require no photocatalyst, relying instead on the formation of an electron donor-acceptor complex of the substrate and reductant, or as will be discussed, alternatively auto-photocatalysis- which is used to explain how some reactions proceed despite any apparent photon absorption. Importantly, this work serves as a cautionary tale for other photochemical reactions involving amines-conditions common to photocatalysis.

1.4 References

1. Tanaka, A.; Makino, A., Photosynthetic Research in Plant Science. *Plant and Cell Physiology* **2009**, *50*, 681.
- 2.(a) Ciamician, G.; Silber, P., Chemische Lichtwirkungen. *Ber. Dtsch. Chem. Ges.* **1901**, *34*, 2040; (b) Ciamician, G., The Photochemistry of the Future. *Science* **1912**, *36*, 385.
- 3.(a) Corey, E. J.; Nozoe, S., Total Synthesis of α -Caryophyllene Alcohol. *J. Am. Chem. Soc.* **1964**, *86*, 1652; (b) Corey, E. J.; Nozoe, S., The Total Synthesis of α -Caryophyllene Alcohol. *J. Am. Chem. Soc.* **1965**, *87*, 5733.
4. Eaton, P. E.; Cole, T. W., Cubane. *J. Am. Chem. Soc.* **1964**, *86*, 3157.
5. Wender, P. A.; Howbert, J. J., Synthetic studies on arene-olefin cycloadditions: total synthesis of (+-)- α -cedrene. *J. Am. Chem. Soc.* **1981**, *103*, 688.
6. Albin, A.; Fagnoni, M., *Handbook of Synthetic Photochemistry*. Wiley: 2009.
- 7.(a) Prier, C. K.; Rankic, D. A.; MacMillan, D. W. C., Visible Light Photoredox Catalysis with Transition Metal Complexes: Applications in Organic Synthesis. *Chem. Rev.* **2013**, *113*, 5322; (b) Romero, N. A.; Nicewicz, D. A., Organic Photoredox Catalysis. *Chem. Rev.* **2016**, *116*, 10075; (c) Marzo, L.; Pagire, S. K.; Reiser, O.; König, B., Visible-Light Photocatalysis: Does It Make a Difference in Organic Synthesis? *Angew. Chem. Int. Ed.* **2018**, *57*, 10034; (d) Beatty, J. W.; Stephenson, C. R. J.,

Amine Functionalization via Oxidative Photoredox Catalysis: Methodology Development and Complex Molecule Synthesis. *Acc. Chem. Res.* **2015**, *48*, 1474.

8.Ulbricht, C.; Beyer, B.; Friebe, C.; Winter, A.; Schubert, U. S., Recent Developments in the Application of Phosphorescent Iridium(III) Complex Systems. *Adv. Mater.* **2009**, *21*, 4418.

9.Kalyanasundaram, K.; Grätzel, M., Applications of functionalized transition metal complexes in photonic and optoelectronic devices. *Coord. Chem. Rev.* **1998**, *177*, 347.

10.Fors, B. P.; Hawker, C. J., Control of a Living Radical Polymerization of Methacrylates by Light. *Angew. Chem. Int. Ed.* **2012**, *51*, 8850.

11.Howerton, B. S.; Heidary, D. K.; Glazer, E. C., Strained Ruthenium Complexes Are Potent Light-Activated Anticancer Agents. *J. Am. Chem. Soc.* **2012**, *134*, 8324.

12.Kalyanasundaram, K., Photophysics, photochemistry and solar energy conversion with tris(bipyridyl)ruthenium(II) and its analogues. *Coord. Chem. Rev.* **1982**, *46*, 159.

13.Pac, C.; Ihama, M.; Yasuda, M.; Miyauchi, Y.; Sakurai, H., Tris(2,2'-bipyridine)ruthenium(2+)-mediated photoreduction of olefins with 1-benzyl-1,4-dihydronicotinamide: a mechanistic probe for electron-transfer reactions of NAD(P)H-model compounds. *J. Am. Chem. Soc.* **1981**, *103*, 6495.

14.Fukuzumi, S.; Mochizuki, S.; Tanaka, T., Photocatalytic reduction of phenacyl halides by 9,10-dihydro-10-methylacridine: control between the reductive and oxidative quenching pathways of tris(bipyridine)ruthenium complex utilizing an acid catalysis. *J. Phys. Chem.* **1990**, *94*, 722.

15.Nicewicz, D. A.; MacMillan, D. W. C., Merging Photoredox Catalysis with Organocatalysis: The Direct Asymmetric Alkylation of Aldehydes. *Science* **2008**, *322*, 77.

16.Ischay, M. A.; Anzovino, M. E.; Du, J.; Yoon, T. P., Efficient Visible Light Photocatalysis of [2+2] Enone Cycloadditions. *J. Am. Chem. Soc.* **2008**, *130*, 12886.

17.Narayanam, J. M. R.; Tucker, J. W.; Stephenson, C. R. J., Electron-Transfer Photoredox Catalysis: Development of a Tin-Free Reductive Dehalogenation Reaction. *J. Am. Chem. Soc.* **2009**, *131*, 8756.

18. Singh, A.; Teegardin, K.; Kelly, M.; Prasad, K. S.; Krishnan, S.; Weaver, J. D., Facile synthesis and complete characterization of homoleptic and heteroleptic cyclometalated Iridium(III) complexes for photocatalysis. *J. Organomet. Chem.* **2015**, *776*, 51.
19. Hofbeck, T.; Yersin, H., The Triplet State of fac-Ir(ppy)₃. *Inorg. Chem.* **2010**, *49*, 9290.
20. Tucker, J. W.; Stephenson, C. R. J., Shining Light on Photoredox Catalysis: Theory and Synthetic Applications. *J. Org. Chem.* **2012**, *77*, 1617.
21. McNally, A.; Prier, C. K.; MacMillan, D. W. C., *Science* **2011**, *334*, 1114.
22. (a) Senaweera, S. M.; Singh, A.; Weaver, J. D., Photocatalytic Hydrodefluorination: Facile Access to Partially Fluorinated Aromatics. *J. Am. Chem. Soc.* **2014**, *136*, 3002; (b) Khaled, M. B.; El Mokadem, R. K.; Weaver, J. D., Hydrogen Bond Directed Photocatalytic Hydrodefluorination: Overcoming Electronic Control. *J. Am. Chem. Soc.* **2017**, *139*, 13092; (c) Singh, A.; Fennell, C. J.; Weaver, J. D., Photocatalyst size controls electron and energy transfer: selectable E/Z isomer synthesis via C–F alkenylation. *Chem. Sci.* **2016**, *7*, 6796; (d) Senaweera, S.; Weaver, J. D., Dual C–F, C–H Functionalization via Photocatalysis: Access to Multifluorinated Biaryls. *J. Am. Chem. Soc.* **2016**, *138*, 2520; (e) Singh, A.; Kubik, J. J.; Weaver, J. D., Photocatalytic C–F alkylation; facile access to multifluorinated arenes. *Chem. Sci.* **2015**, *6*, 7206; (f) Priya, S.; Weaver, J. D., Prenyl Praxis: A Method for Direct Photocatalytic Defluoroprenylation. *J. Am. Chem. Soc.* **2018**, *140*, 16020.
23. (a) Arora, A.; Teegardin, K. A.; Weaver, J. D., Reductive Alkylation of 2-Bromoazoles via Photoinduced Electron Transfer: A Versatile Strategy to Csp²–Csp³ Coupled Products. *Org. Lett.* **2015**, *17*, 3722; (b) Arora, A.; Weaver, J. D., Photocatalytic Generation of 2-Azoly Radical Intermediates for the Azoylation of Arenes and Heteroarenes via C–H Functionalization. *Org. Lett.* **2016**, *18*, 3996; (c) Singh, A.; Arora, A.; Weaver, J. D., Photoredox-Mediated C–H Functionalization and Coupling of Tertiary Aliphatic Amines with 2-Chloroazoles. *Org. Lett.* **2013**, *15*, 5390.
24. (a) Noble, A.; MacMillan, D. W. C., Photoredox α -Vinylolation of α -Amino Acids and N-Aryl Amines. *J. Am. Chem. Soc.* **2014**, *136*, 11602; (b) Heitz, D. R.; Rizwan, K.; Molander, G. A., Visible-Light-Mediated Alkenylation, Allylation, and Cyanation of Potassium Alkyltrifluoroborates with

Organic Photoredox Catalysts. *J. Org. Chem.* **2016**, *81*, 7308; (c) Hering, T.; Hari, D. P.; König, B., Visible-Light-Mediated α -Arylation of Enol Acetates Using Aryl Diazonium Salts. *J. Org. Chem.* **2012**, *77*, 10347; (d) Paul, S.; Guin, J., Radical C(sp³)-H alkenylation, alkynylation and allylation of ethers and amides enabled by photocatalysis. *Green Chem.* **2017**, *19*, 2530.

25.(a) Pirtsch, M.; Paria, S.; Matsuno, T.; Isobe, H.; Reiser, O., [Cu(dap)₂Cl] As an Efficient Visible-Light-Driven Photoredox Catalyst in Carbon-Carbon Bond-Forming Reactions. *Chem. Eur. J.* **2012**, *18*, 7336; (b) Paria, S.; Pirtsch, M.; Kais, V.; Reiser, O., Visible-Light-Induced Intermolecular Atom-Transfer Radical Addition of Benzyl Halides to Olefins: Facile Synthesis of Tetrahydroquinolines. *Synthesis* **2013**, *45*, 2689; (c) Qiang, L.; Hong, Y.; Jie, L.; Yuhong, Y.; Xu, Z.; Ziqi, Z.; Aiwen, L., Visible-Light Photocatalytic Radical Alkenylation of α -Carbonyl Alkyl Bromides and Benzyl Bromides. *Chem. Eur. J.* **2013**, *19*, 5120.

26.(a) Arora, A.; Teegardin, K. A.; Weaver, J. D., Reductive Alkylation of 2-Bromoazoles via Photoinduced Electron Transfer: A Versatile Strategy to Csp²-Csp³ Coupled Products. *Org. Lett.* **2015**, *17*, 3722; (b) Capaldo, L.; Ravelli, D., Hydrogen Atom Transfer (HAT): A Versatile Strategy for Substrate Activation in Photocatalyzed Organic Synthesis. *Eur. J. Org. Chem.* **2017**, *2017*, 2056.

27.(a) Sinensky, M.; Lutz, R. J., The prenylation of proteins. *Bioessays* **1992**, *14*, 25; (b) Deschenes, R. J.; Resh, M. D.; Broach, J. R., Acylation and prenylation of proteins. *Curr. Opin. Cell Biol.* **1990**, *2*, 1108.

28.Lindel, T.; Marsch, N.; Adla, S. K., Indole Prenylation in Alkaloid Synthesis. In *Alkaloid Synthesis*, Knölker, H.-J., Ed. Springer Berlin Heidelberg: Berlin, Heidelberg, 2012; pp 67.

29.Miranda, C. L.; Stevens, J. F.; Helmrich, A.; Henderson, M. C.; Rodriguez, R. J.; Yang, Y. H.; Deinzer, M. L.; Barnes, D. W.; Buhler, D. R., Antiproliferative and cytotoxic effects of prenylated flavonoids from hops (*Humulus lupulus*) in human cancer cell lines. *Food and Chemical Toxicology* **1999**, *37*, 271.

30. Li, X.-M.; Jiang, X.-J.; Yang, K.; Wang, L.-X.; Wen, S.-Z.; Wang, F., Prenylated Coumarins from *Heracleum stenopterum*, *Peucedanum praeruptorum*, *Clausena lansium*, and *Murraya paniculata*. *Nat Prod Bioprospect* **2016**, *6*, 233.
31. Wang, H.; Yan, Z.; Lei, Y.; Sheng, K.; Yao, Q.; Lu, K.; Yu, P., Concise synthesis of prenylated and geranylated chalcone natural products by regiospecific iodination and Suzuki coupling reactions. *Tetrahedron Lett.* **2014**, *55*, 897.
32. (a) Nguyen, J. D.; D'Amato, E. M.; Narayanam, J. M. R.; Stephenson, C. R. J., Engaging unactivated alkyl, alkenyl and aryl iodides in visible-light-mediated free radical reactions. *Nat Chem* **2012**, *4*, 854; (b) Hari, D. P.; Schroll, P.; König, B., Metal-Free, Visible-Light-Mediated Direct C–H Arylation of Heteroarenes with Aryl Diazonium Salts. *J. Am. Chem. Soc.* **2012**, *134*, 2958.
33. (a) Lambert, F. L.; Ingall, G. B., Voltammetry of organic halogen compounds. IV. The reduction of organic chlorides at the vitreous (glassy) carbon electrode. *Tetrahedron Lett.* **1974**, *15*, 3231; (b) Luo, Y. R., *Handbook of Bond Dissociation Energies in Organic Compounds*. CRC Press: 2002.
34. (a) Pause, L.; Robert, M.; Savéant, J.-M., Can Single-Electron Transfer Break an Aromatic Carbon–Heteroatom Bond in One Step? A Novel Example of Transition between Stepwise and Concerted Mechanisms in the Reduction of Aromatic Iodides. *J. Am. Chem. Soc.* **1999**, *121*, 7158; (b) Costentin, C.; Robert, M.; Savéant, J.-M., Fragmentation of Aryl Halide π Anion Radicals. Bending of the Cleaving Bond and Activation vs Driving Force Relationships. *J. Am. Chem. Soc.* **2004**, *126*, 16051; (c) Devery, J. J.; Nguyen, J. D.; Dai, C.; Stephenson, C. R. J., Light-Mediated Reductive Debromination of Unactivated Alkyl and Aryl Bromides. *ACS Catal.* **2016**, *6*, 5962.
35. (a) Arora, A.; Weaver, J. D., Visible Light Photocatalysis for the Generation and Use of Reactive Azolyl and Polyfluoroaryl Intermediates. *Acc. Chem. Res.* **2016**, *49*, 2273; (b) Konovalov, V. V.; Laev, S. S.; Beregovaya, I. V.; Shchegoleva, L. N.; Shteingarts, V. D.; Tsvetkov, Y. D.; Bilkis, I., Fragmentation of Radical Anions of Polyfluorinated Benzoates. *J. Phys. Chem. A* **2000**, *104*, 352; (c) Neta, P.; Behar, D., Intramolecular electron transfer in the anion radicals of nitrobenzyl halides. *J. Am. Chem. Soc.* **1980**, *102*, 4798; (d) Neta, P.; Behar, D., Intramolecular electron transfer and

dehalogenation of anion radicals. 3. Halobenzonitriles and cyanobenzyl halides. *J. Am. Chem. Soc.* **1981**, *103*, 103; (e) Behar, D.; Neta, P., Intramolecular electron transfer and dehalogenation of anion radicals. 4. Haloacetophenones and related compounds. *J. Am. Chem. Soc.* **1981**, *103*, 2280; (f) Andrieux, C. P.; Blocman, C.; Dumas-Bouchiat, J. M.; M'Halla, F.; Saveant, J. M., Determination of the lifetimes of unstable ion radicals by homogeneous redox catalysis of electrochemical reactions. Application to the reduction of aromatic halides. *J. Am. Chem. Soc.* **1980**, *102*, 3806; (g) Andrieux, C. P.; Saveant, J. M.; Zann, D., Relationship between reduction potentials and anion radical cleavage rates in aromatic molecules. *Nouv. J. Chim.* **1984**, *8*, 107.

36.(a) Isse, A. A.; Falciola, L.; Mussini, P. R.; Gennaro, A., Relevance of electron transfer mechanism in electrocatalysis: the reduction of organic halides at silver electrodes. *Chem. Commun.* **2006**, 344; (b) Koch, D. A., Carbanion and Radical Intermediacy in the Electrochemical Reduction of Benzyl Halides in Acetonitrile. *J. Electrochem. Soc.* **1987**, *134*, 3062; (c) Andrieux, C. P.; Le Gorande, A.; Saveant, J. M., Electron transfer and bond breaking. Examples of passage from a sequential to a concerted mechanism in the electrochemical reductive cleavage of arylmethyl halides. *J. Am. Chem. Soc.* **1992**, *114*, 6892; (d) Tanner, D. D.; Plambeck, J. A.; Reed, D. W.; Mojelsky, T. W., Polar radicals. 15. Interpretation of substituent effects on the mechanism of electrolytic reduction of the carbon-halogen bond in series of substituted benzyl halides. *J. Org. Chem.* **1980**, *45*, 5177.

37.(a) Sattler, W.; Ener, M. E.; Blakemore, J. D.; Rachford, A. A.; LaBeaume, P. J.; Thackeray, J. W.; Cameron, J. F.; Winkler, J. R.; Gray, H. B., Generation of Powerful Tungsten Reductants by Visible Light Excitation. *J. Am. Chem. Soc.* **2013**, *135*, 10614; (b) Büldt, L. A.; Guo, X.; Prescimone, A.; Wenger, O. S., A Molybdenum(0) Isocyanide Analogue of Ru(2,2'-Bipyridine)₃²⁺: A Strong Reductant for Photoredox Catalysis. *Angew. Chem. Int. Ed.* **2016**, *55*, 11247; (c) Herr, P.; Glaser, F.; Büldt, L. A.; Larsen, C. B.; Wenger, O. S., Long-Lived, Strongly Emissive, and Highly Reducing Excited States in Mo(0) Complexes with Chelating Isocyanides. *J. Am. Chem. Soc.* **2019**, *141*, 14394; (d) Shon, J.-H.; Teets, T. S., Potent Bis-Cyclometalated Iridium Photoreductants with β -Diketiminato Ancillary Ligands. *Inorg. Chem.* **2017**, *56*, 15295.

38. Constantin, T.; Zanini, M.; Regni, A.; Sheikh, N. S.; Juliá, F.; Leonori, D., Aminoalkyl radicals as halogen-atom transfer agents for activation of alkyl and aryl halides. *Science* **2020**, *367*, 1021.

39. Schweitzer-Chaput, B.; Horwitz, M. A.; de Pedro Beato, E.; Melchiorre, P., Photochemical generation of radicals from alkyl electrophiles using a nucleophilic organic catalyst. *Nature Chemistry* **2019**, *11*, 129.

40. (a) Gál, B.; Bucher, C.; Burns, N. Z., Chiral Alkyl Halides: Underexplored Motifs in Medicine. *Mar drugs* **2016**, *14*, 206; (b) Chung, W.-j.; Vanderwal, C. D., Stereoselective Halogenation in Natural Product Synthesis. *Angew. Chem. Int. Ed. Engl.* **2016**, *55*, 4396; (c) Gribble, G. W., *Naturally Occurring Organohalogen Compounds - A Comprehensive Update*. Springer Vienna: 2009; (d) Gribble, G. W., The diversity of naturally produced organohalogens. *Chemosphere* **2003**, *52*, 289.

41. (a) Kambe, N.; Iwasaki, T.; Terao, J., Pd-catalyzed cross-coupling reactions of alkyl halides. *Chem. Soc. Rev* **2011**, *40*, 4937; (b) Saito, B.; Fu, G. C., Alkyl-Alkyl Suzuki Cross-Couplings of Unactivated Secondary Alkyl Halides at Room Temperature. *J. Am. Chem. Soc.* **2007**, *129*, 9602; (c) Terao, J.; Kambe, N., Cross-Coupling Reaction of Alkyl Halides with Grignard Reagents Catalyzed by Ni, Pd, or Cu Complexes with π -Carbon Ligand(s). *Acc. Chem. Res.* **2008**, *41*, 1545; (d) McMurry, J., *Organic Chemistry*. Brooks/Cole Cengage Learning: 2011.

42. (a) Saikia, I.; Borah, A. J.; Phukan, P., Use of Bromine and Bromo-Organic Compounds in Organic Synthesis. *Chem. Rev.* **2016**, *116*, 6837; (b) Podgoršek, A.; Zupan, M.; Iskra, J., Oxidative Halogenation with “Green” Oxidants: Oxygen and Hydrogen Peroxide. *Angew. Chem. Int. Ed. Engl.* **2009**, *48*, 8424; (c) Kolvari, E.; Koukabi, N.; Khoramabadi-zad, A.; Shiri, A.; Ali Zolfigol, M., Alternative Methodologies for Halogenation of Organic Compounds. *Curr. Org. Synth.* **2013**, *10*, 837; (d) Sabuzi, F.; Pomarico, G.; Floris, B.; Valentini, F.; Galloni, P.; Conte, V., Sustainable bromination of organic compounds: A critical review. *Coord. Chem. Rev.* **2019**, *385*, 100; (e) Nishina, Y.; Ohtani, B.; Kikushima, K., Bromination of hydrocarbons with CBr₄, initiated by light-emitting diode irradiation. *Beilstein J. Org. Chem.* **2013**, *9*, 1663; (f) Cantillo, D.; Kappe, C. O., Halogenation of organic compounds using continuous flow and microreactor technology. *React. Chem. Eng.* **2017**, *2*, 7; (g)

Smith, A. M. R.; Hii, K. K., Transition Metal Catalyzed Enantioselective α -Heterofunctionalization of Carbonyl Compounds. *Chem. Rev.* **2011**, *111*, 1637; (h) Suryakiran, N.; Prabhakar, P.; Srikanth Reddy, T.; Chinni Mahesh, K.; Rajesh, K.; Venkateswarlu, Y., Chemoselective mono halogenation of β -keto-sulfones using potassium halide and hydrogen peroxide; synthesis of halomethyl sulfones and dihalomethyl sulfones. *Tetrahedron Lett.* **2007**, *48*, 877; (i) Poteat, C. M.; Lindsay, V. N. G., Controlled α -mono- and α,α -di-halogenation of alkyl sulfones using reagent–solvent halogen bonding. *Chem. Commun.* **2019**, *55*, 2912; (j) Erian, A. W.; Sherif, S. M.; Gaber, H. M., The Chemistry of α -Haloketones and Their Utility in Heterocyclic Synthesis. *Molecules* **2003**, *8*, 793; (k) Mohan, R. B.; Reddy, N. C. G., Regioselective α -Bromination of Alkyl Ketones Using N-Bromosuccinimide in the Presence of Montmorillonite K-10 Clay: A Simple and Efficient Method. *Synth. Commun.* **2013**, *43*, 2603; (l) Pravst, I.; Zupan, M.; Stavber, S., Halogenation of ketones with N-halosuccinimides under solvent-free reaction conditions. *Tetrahedron* **2008**, *64*, 5191; (m) Jagatheesan, R.; Joseph Santhana Raj, K.; Lawrence, S.; Christopher, C., Electroselective α -bromination of acetophenone using in situ bromonium ions from ammonium bromide. *RSC Adv* **2016**, *6*, 35602.

43.(a) Brochu, M. P.; Brown, S. P.; MacMillan, D. W. C., Direct and Enantioselective Organocatalytic α -Chlorination of Aldehydes. *J. Am. Chem. Soc.* **2004**, *126*, 4108; (b) Halland, N.; Braunton, A.; Bachmann, S.; Marigo, M.; Jørgensen, K. A., Direct Organocatalytic Asymmetric α -Chlorination of Aldehydes. *J. Am. Chem. Soc.* **2004**, *126*, 4790; (c) Bertelsen, S.; Halland, N.; Bachmann, S.; Marigo, M.; Braunton, A.; Jørgensen, K. A., Organocatalytic asymmetric α -bromination of aldehydes and ketones. *Chem. Commun.* **2005**, 4821; (d) Ueda, M.; Kano, T.; Maruoka, K., Organocatalyzed direct asymmetric α -halogenation of carbonyl compounds. *Org. Biomol. Chem.* **2009**, *7*, 2005.

44.Lima, C. G. S.; de M. Lima, T.; Duarte, M.; Jurberg, I. D.; Paixão, M. W., Organic Synthesis Enabled by Light-Irradiation of EDA Complexes: Theoretical Background and Synthetic Applications. *ACS Catal* **2016**, *6*, 1389.

45.(a) Postigo, A., Electron Donor-Acceptor Complexes in Perfluoroalkylation Reactions. *Eur. J. Org. Chem.* **2018**, *2018*, 6391; (b) Crisenza, G. E. M.; Mazzarella, D.; Melchiorre, P., Synthetic Methods

Driven by the Photoactivity of Electron Donor–Acceptor Complexes. *J. Am. Chem. Soc.* **2020**, *142*, 5461.

CHAPTER II

A GENERAL PHOTOCATALYTIC ROUTE TO PRENYLATION

2.1 Introduction

Prenylation is an essential biological transformation that involves the introduction of a C5 isoprene unit into a molecule via reaction with isopentenyl pyrophosphate or dimethylallyl pyrophosphate (figure 2.1).¹ The isoprene unit is an important moiety in natural product terpenes which represent one of the largest and most diverse classes of natural products.² The tremendous structural diversity of terpenes shows a wide range of biological properties^{2a,3} including pharmacological properties,⁴ primary constituents of essential oils of medicinal plants and flowers,⁵ and natural flavoring compounds in the food industry.⁶ The most common terpenes (figure 2.2) includes limonene (anti-inflammatory, antioxidant, and anticancer),⁷ alpha-pinene (antibiotic resistance modulation, antitumor, anticoagulant, and antimicrobial),⁸ myrcene (sedative as well as motor relaxant effects),⁹ beta-caryophyllene (cardioprotective, hepatoprotective, immunomodulatory agent, and gastroprotective),¹⁰ terpinolene (antioxidant, and anticancer),¹¹ and humulene (anti-inflammatory and analgesic properties).¹² Terpenoids have contributed to six major drug classes namely steroids, taxanes, tocopherols, artemisinins, ingenanes and cannabinoids.¹³

In addition to terpenes, nature prenylates indole alkaloids,¹⁴ flavonoids,¹⁵ coumarins¹⁶ and other aromatics¹⁷(figure 2.3) which have attracted attention in synthesis because of their unique anti-

microbial, anti-oxidant, anti-inflammatory, anti-viral and anti-cancer properties.¹⁸ The structure of these prenylated arenes varies widely with respect to (1) the mode of addition of the prenyl group (linear or branched), (2) the position of the prenyl group (C-, N-, O-prenylation) and (3) the number of prenyl groups (mono-, di-, or triprenyl).¹⁹ Furthermore, once introduced, the prenyl unit can undergo chemical modification by cyclization, hydroxylation, oxidation and reduction to diversify the prenylation pattern.^{19a}

Figure 2.1 C5 isoprene units

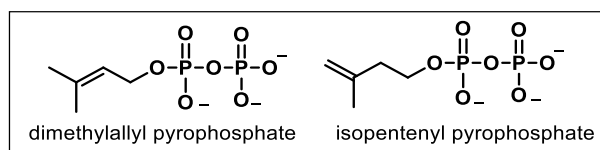


Figure 2.2 Common examples of terpenes

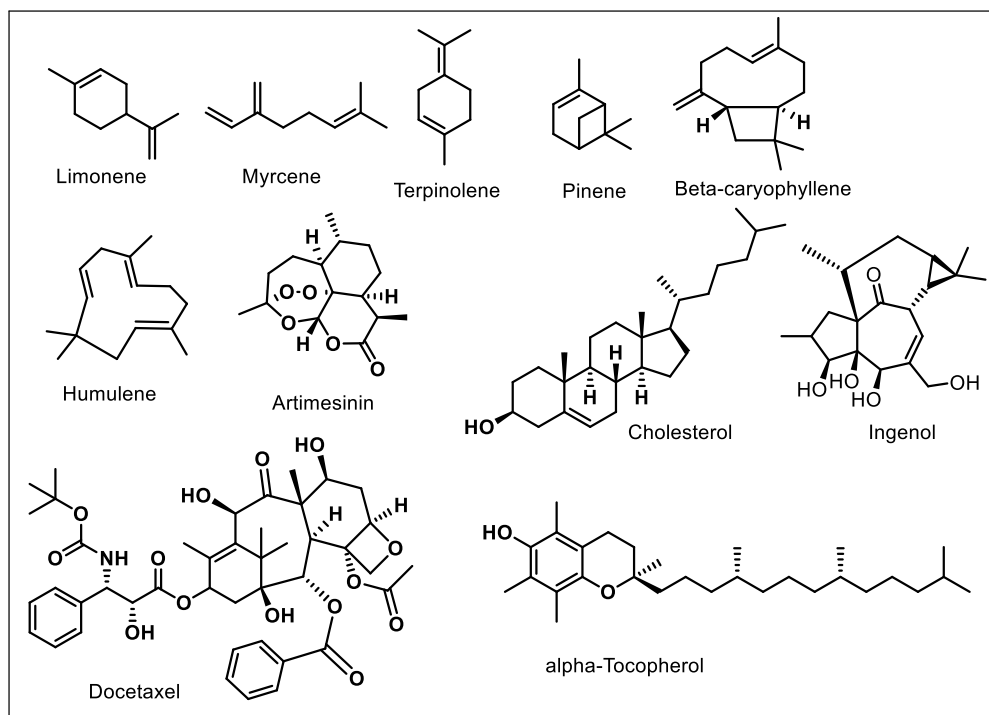
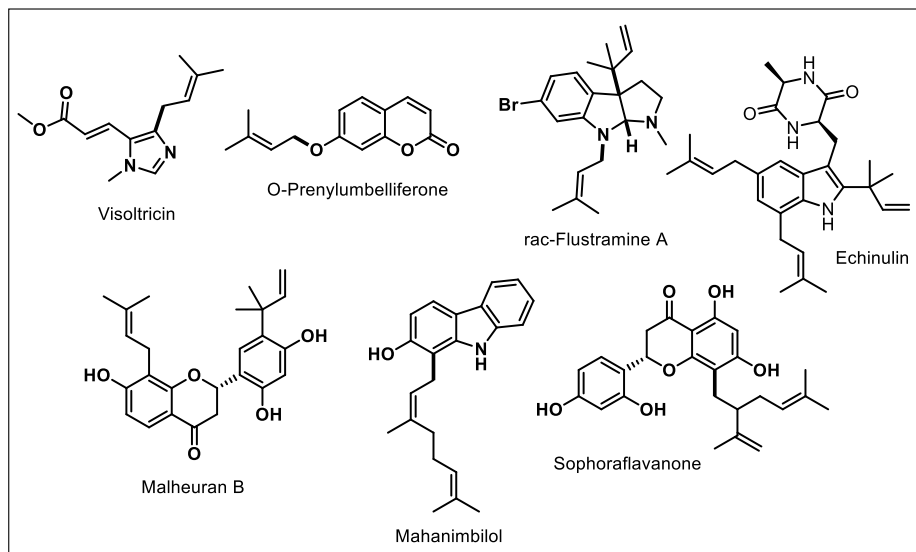


Figure 2.3 Prenylated natural products



Given the number of prominent examples of prenylated molecules and similarity to allylation, it is tempting to assume prenylation is as well developed as allylation chemistry, which differs subtly by the replacement of the terminal methylene for a geminal dimethyl group. However, the impact of this substitution should not be underestimated. While remarkable progress (scheme 2.1) has been made, these methods²⁰ are designed to be used with specific classes of substrates.

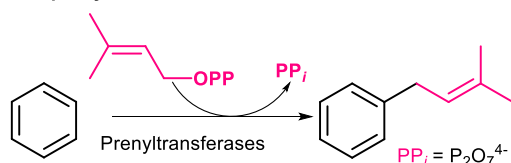
Nature uses an enzyme called prenyl transferase to introduce prenyl groups into molecules (scheme 2.1a). This is a heavily studied and versatile biosynthetic pathway.^{20a} While substantial effort has been made to exploit this pathway, indole prenyltransferases that prenylate at all possible positions of the indole ring²¹ and several other aromatic prenyltransferases²² have been discovered. So far, synthetic applications have been relatively limited to specific substrates. Among those, synthetic introduction of prenyl units to arenes has received considerable attention.

Synthesis can take place via direct addition of prenyl unit to an arene or through a series of functional group transformations to achieve prenylation. Recently, transition-metal-catalyzed prenylation of aryl C–H bond with the support of *directing group* has been developed^{20b, 20c} (scheme 2.1b). However, the

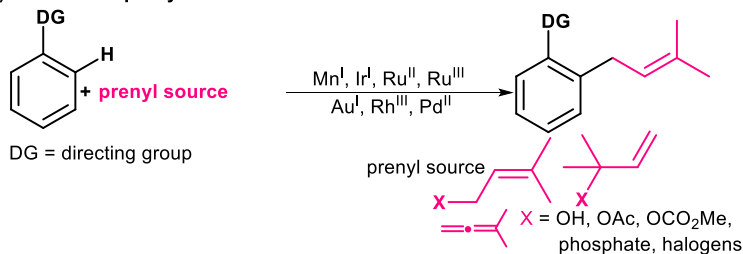
necessity of a directing group limits the scope of the C–H prenylation. Alternatively, transition-metal-catalyzed cross-coupling of aryl halides and organoboron or organozinc as prenylating reagents^{20e, 20f} (scheme 2.1c) is one of the most general ways to introduce a prenyl group to prefunctionalized arenes (i.e. bromides and chlorides). However, controlling the regioisomerism of the prenylation has proven challenging in this transformation. Both the ligand of the transition-metal catalyst as well as the structure of the organometallic prenylating reagent employed impact the selectivity.²³

Scheme 2.1 Approaches towards prenylated arenes

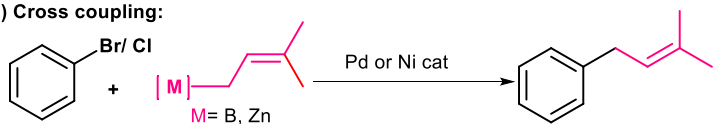
a) Biosynthetic prenylation:



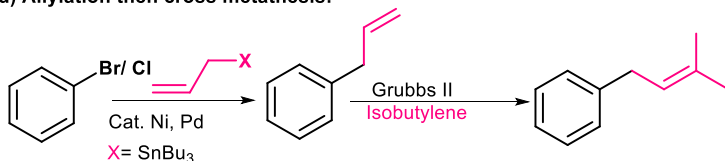
b) Direct C–H prenylation:



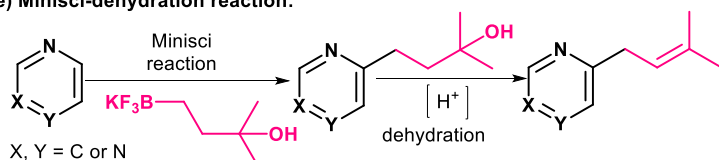
c) Cross coupling:



d) Allylation then cross metathesis:



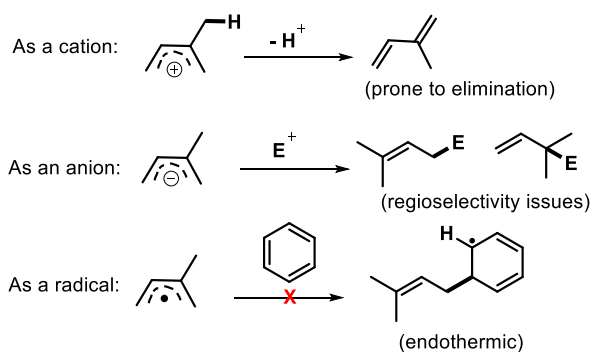
e) Minisci-dehydration reaction:



Owing to the complexity of direct prenylation, a more common practice is indirect prenylation (scheme 2.1d) in which the substrate is first allylated and then subjected to cross-metathesis using isobutylene and Grubbs II catalyst to install the missing methyl groups.^{20g 24} N-heteroarenes are important motifs in pharmaceutical chemistry and their prenylation²⁰ⁱ has been achieved through a Minisci cascade reaction using a new coupling reagent, potassium (3-hydroxy-3-methylbut-1-yl)trifluoroborate and subsequent acid-promoted dehydration sequence (scheme 2.1e). This circumvents the issue of radical addition to the alkene by masking the alkene during the radical addition and later revealing it through acid catalyzed dehydration.

While useful, the application of the aforementioned methods to accomplish prenylation still have substantial limitations that leave much room for improvement in terms of scope expansion and general use. As such, prenyl units as electrophiles are prone to elimination, and as anions, prenylation can cause regioselectivity issues. Further, the prenyl radical might add selectively, however the addition to an arene is expected to be a highly endergonic process (scheme 2.2).²⁵

Scheme 2.2 Challenges associated with transferring a prenyl group

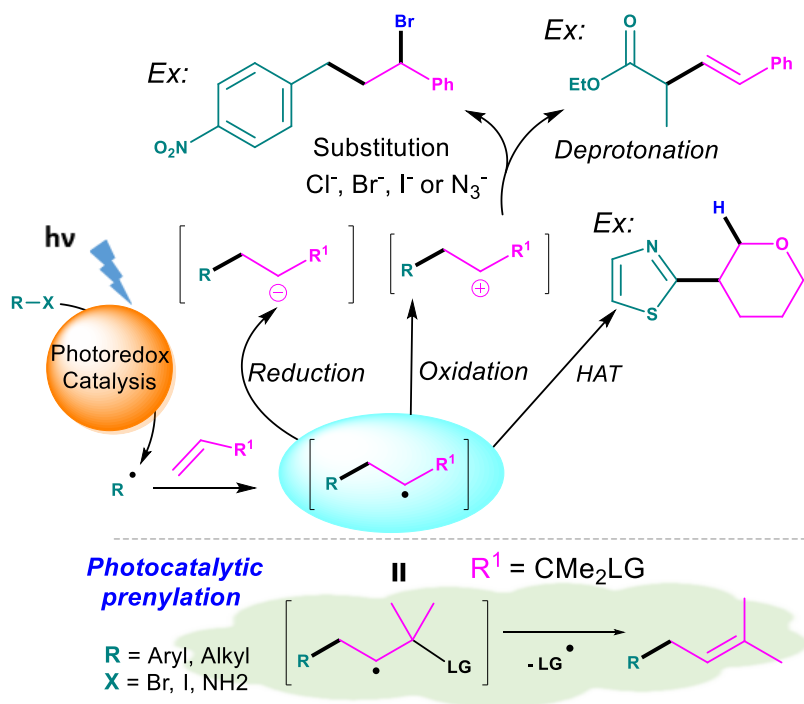


2.2 Development of photocatalytic prenylation reactions

Recently, visible light photocatalysis has proven effective at catalytically generating a variety of radicals under near ambient conditions, often resulting in useful reactions that are remarkably tolerant of functional groups.²⁶ In a number of cases these photocatalytically generated radicals have proven

capable of undergoing addition to alkenes.²⁷ Upon addition, a new alkyl radical is generated that can be oxidized,²⁸ reduced,²⁹ or subjected to hydrogen atom transfer (HAT)³⁰ (scheme 2.3).

Scheme 2.3 Visible light-mediated radical addition to alkene

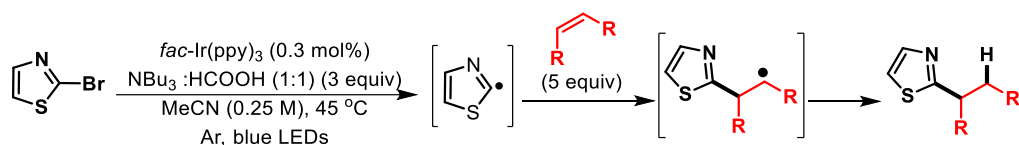


The literature shows that a number of unactivated alkenes can easily intercept photocatalytically generated radicals.³¹ Thus, we anticipated that a terminal methylene group of an isoprenyl molecule would undergo addition to the unsubstituted terminus with high selectivity. Then, if the alkene were appropriately substituted with a leaving group capable of homolytic fragmentation it could out compete other competing processes, such as oxidation, reduction, and HAT and instead yield the key double bond. Thus, we set about trying to develop a reagent amenable to photocatalytic reactions, and capable of intercepting a diverse set of photocatalytically generated radicals.

Substituted azoles are an important class of compounds found natural products and drugs.³² As such, the Weaver group has developed methodologies for the functionalization of azoles.^{30a, 33} Previous members of the group^{30a, 33} demonstrated that 2-bromoazoles can lead to azolyl radicals in the presence of amine, photocatalyst, and visible light irradiation. Furthermore, that the generated azolyl radical

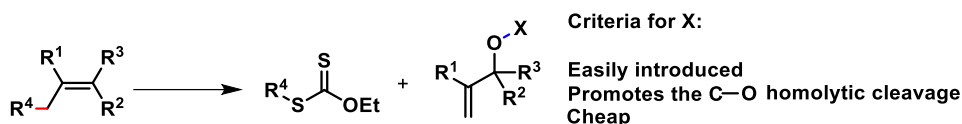
could be intercepted with an unactivated alkene to form a new C–C bond, and after HAT, an alkylated azole product (scheme 2.4).^{30a}

Scheme 2.4 Reductive alkylation of 2-bromoazole



To accomplish general prenylation (scheme 2.3, below), we needed to identify a prenylating reagent that can facilitate prenylation in high yield and also be prepared from low cost and readily available starting materials. In this sense, alcohols are cheap and readily accessible molecules that are ideal for the synthesis of reagents. We were attracted to the seminal work by Zard³⁴ which provided key insight into how to accelerate the desired fragmentation. Specifically, using thermally generated radicals from the homolysis of alkyl xanthate esters, he demonstrated their efficient addition to alkenes as well as their ability to undergo homolytic cleavage of the normally strong C–O bond. In order to transform allylic alcohols into radical trapping allylating reagents, we would need to identify an X appendage (scheme 2.5), that would weaken the strong C–O bond. We hypothesized that weakening this bond would accelerate beta fragmentation, allowing it to be used as a radical allylating (prenylating) reagent.^{34e}

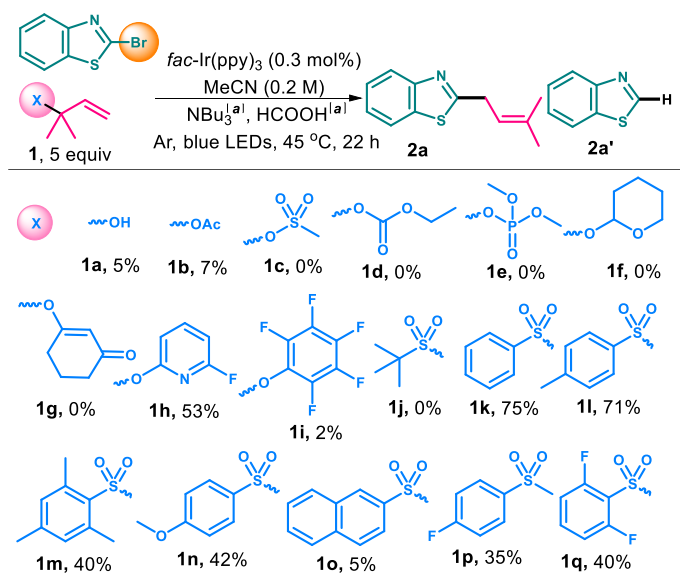
Scheme 2.5 Allyl alcohol as a radical allylating agent



We initiated screening of each prenylating reagent with 2-bromobenzothiazole in the presence of three equivalents of NBu₃ (tributylamine), three equivalents of formic acid and five equivalents of the potential prenylating reagent and a catalytic amount of *fac*-Ir(ppy)₃ (table 2.1). Following the Zard's

work, we started with isoprenyl alcohol derivatives (1a-1i, table 2.1). Not surprisingly, groups 1a-1e are expected to have a relatively strong C–O bond, and provided very little of the prenylated product, 2a. Next, we moved to derivatives expected to have weaker C–O bonds. However, 1f and 1g did not provide product. The use of a pyridyl activating group (1h) which had been previously studied by Zard^{34a} in lauroyl peroxide mediated transfer of xanthates to olefins gave full conversion and 53% yield. The mass balance was primarily accounted for by reduced azole. Further efforts to optimize the reaction using 1h did not increase the yield and we observed some [3,3] sigmatropic rearrangement of 1h. Next, we looked at prenylating reagent 1i which was also recently developed by the Weaver group to allow the prenylation of fluorinated arenes under mild conditions.^{25d} However, in the case of 2-bromoazole, 1i did not produce 2a in appreciable quantities. Attempts to use 1i failed to give any more than 2% prenylation with any of the substrate classes studied in this work. Therefore, 1i could not serve as a general prenylation source.

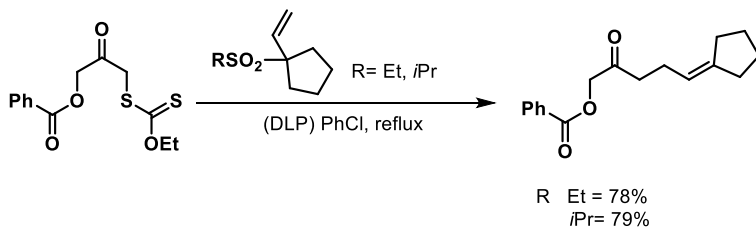
Table 2.1 Development of a prenyl transfer reagent



^{a1}(3 equiv). Assay yield determined by GCMS. No further conversion to product over extended time

In addition to allylic alcohol derivatives, radical allylation reactions have been carried out using allyl-halides, -sulfones, -stannanes, -Co, and -Ga reagents.^{34c, 34e, 35} Again, the key feature among all these reagents is a relatively weak allyl-X bond which facilitates the homolytic fragmentation, or beta scission. We expanded our search to include sulfones (1j-1q), since the C-S bond of sulfones is relatively weak (for MeOH, C-O BDE = 91 kcal/mol while MeSH, C-S BDE = 73 kcal/mol).³⁶ Sulfones are also attractive because they are easily handled, generally shelf-stable, and can be easily elaborated via alkylation chemistry. Zard^{34c} has explored lauroyl peroxide mediated allylation of xanthate esters with α -substituted allylic alkyl sulfones, which suggests it should be possible to use sulfones (scheme 2.6) in concert with photocatalytic generation of radicals to accomplish prenylation. Furthermore, more recently Ollivier,³⁷ Kamijo,³⁸ Zhu,³⁹ Chen⁴⁰ and Flechsig⁴¹ have shown that photocatalytically generated radicals can react with a range of sulfonyl reagents which are capable of trapping radicals, suggesting that it might be possible to identify a prenyl transfer reagent capable of working under photocatalytic conditions.

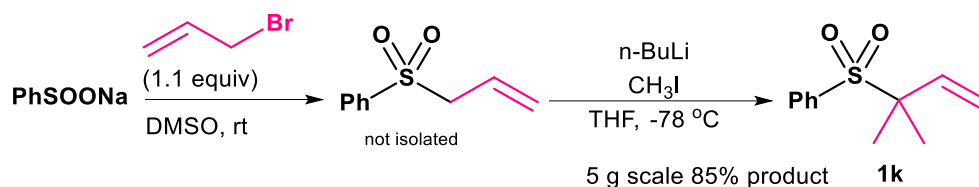
Scheme 2.6 Allylation with α -substituted allyl sulfone



Thus, we synthesized and tested a library of isoprenyl sulfones (1j-1q). Use of alkyl sulfone 1j resulted in trace conversion to the reduced azole 2a'. In sharp contrast, aryl sulfones generally worked well. Aryl sulfones bearing electron donating methyl (1m) and methoxy (1n) substituents were found to give lower yields compared to phenyl sulfone (1k). Moreover, phenyl sulfones having electron withdrawing fluorine substituents (1p) and (1q) or extended conjugation (1o) also exhibited comparatively lower yields. Thus, we selected phenyl sulfone (1k) which gave the best yield, 75% of 2a, for further studies.

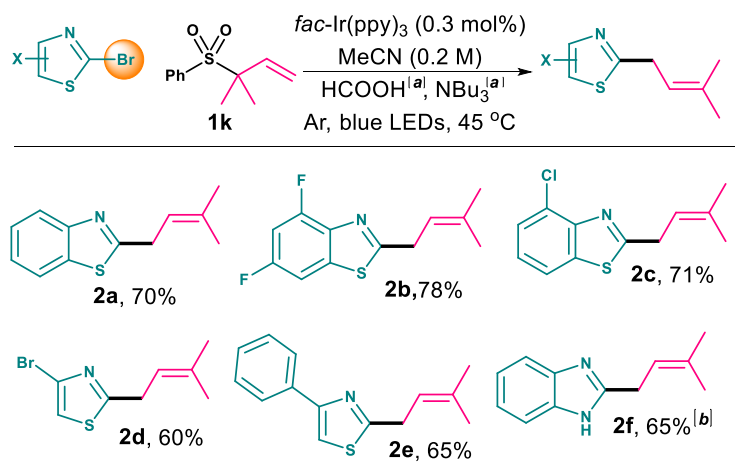
Reagent **1k** is a bench stable, crystalline solid that can be made via allylation of benzene sulfinate, then in a chromatography free, telescoped fashion, dimethylated yielding the isolation of **1k** in pure form in 75-85% yield (scheme 2.7).⁴²

Scheme 2.7 Synthesis of prenyl sulfones



With prenylating reagent **1k** in hand, we began exploring recently developed photocatalytic reactions. Using the same conditions developed for the hydroazoylation of alkenes⁴³ and the C–H azoylation of arenes,⁴⁴ along with the addition of reagent **1k** in lieu of the original coupling alkene or arene partners, we attempted the prenylation of several bromoazoles (scheme 2.8).

Scheme 2.8 Prenylation of azoles



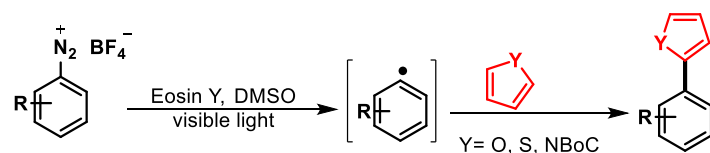
1k (5 equiv),^[a](3 equiv). Yields are of isolated product. ^[b]Reaction did not go to completion even after increasing the amount of NBU₃, sulfone or catalyst.

The prenyl transfer reagent **1k** proved to be general, as the prenylated azoles (**2a-2f**) were obtained in 60-78% yield. The reduced azole, the result of HAT to the azoyl radical, accounted for the mass balance. Importantly, the reaction displayed both perfect regioselectivity giving no branched product,

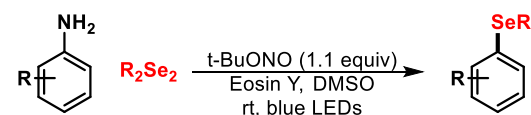
and displaying perfect chemoselectivity for the 2-Br, allowing other bromine and chlorine substituents (2c, 2d) to remain untouched. The photocatalytic prenylation of 2-bromobenzimidazole was sluggish as was seen previously in the related alkylation reaction,^{33b} and the reaction did not go to completion. Aryl diazonium salts have attracted attention as an excellent precursor of aryl radicals, in part, because of their facile reduction.⁴⁵ Recently, König has demonstrated the visible light mediated, eosin Y catalyzed direct C–H arylation of heteroarenes with aryl diazonium salts via photocatalysis (scheme 2.9a).^{28d} However, the use of diazonium salts can undermine the utility of the method because the shelf-stability of diazonium salts can vary widely from substrate to substrate. Furthermore, their use often raises significant safety concerns⁴⁶ that might limit their applications on scale. For this reason, Ranu has developed a method for the *in situ* generation of the diazonium salt from anilines and demonstrated their use within photocatalysis in the synthesis of organoselenides (scheme 2.9b). In this reaction, *tert*-butylnitrite converts the aryl amine into the diazonium salt which is consumed as it is made, and to some extent, helps circumvent some of the aforementioned issues with diazoniums.⁴⁷

Scheme 2.9 Ary radicals from aryl diazonium salts

a) Direct C-H arylation



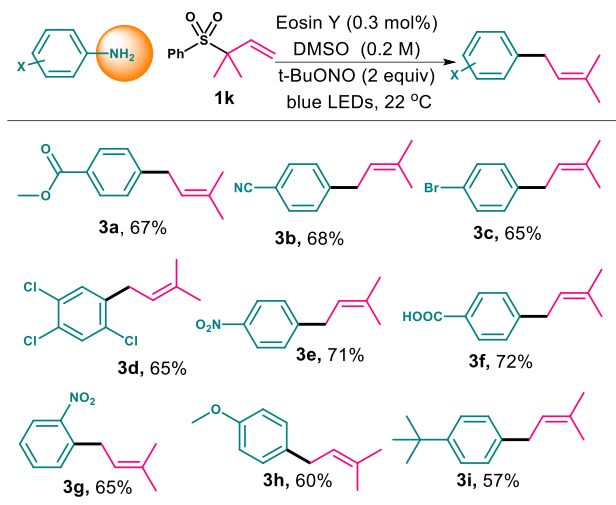
b) Synthesis of diaryl selenides



Thus, we inspected whether this method could be adapted to allow prenylation of aryl amines (scheme 2.10). Indeed, the desired prenylated arene was formed as the major product in reasonable yield along with a minor amount of the reduced arene. Further optimizations were carried out to improve the yields. The reaction worked well for arenes with electron withdrawing- (3a, 3b, 3e, 3f and 3g), and neutral-groups (3c). However, more electron rich aryl amines were somewhat sluggish and gave slightly

lowered yields (3h and 3j). The mild reaction conditions are compatible with a wide range of functional groups such as a nitro, ester, cyano, bromide, chloride and carboxylic acid. The broad functional group tolerance should facilitate further synthetic elaboration.

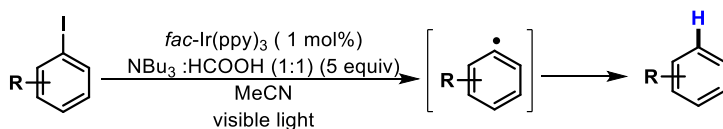
Scheme 2.10 Prenylation of anilines



1k (5 equiv). Yields are of isolated product.

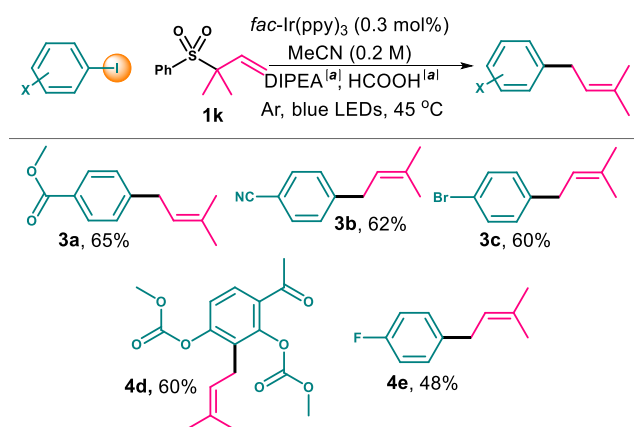
Next, we looked at prenylation of aryl iodides. Unactivated carbon-iodide bonds have decidedly negative reduction potentials. For example, the reduction potential of iodobenzene has been measured to be -1.59 V versus SCE.⁴⁸ Stephenson⁴⁹ and coworkers have introduced a protocol to generate radicals from unactivated alkyl, alkenyl and aryl iodide in the presence of *fac*-Ir(ppy)₃ upon irradiation (scheme 2.11). In these cases, the radicals underwent hydrogen atom abstraction (HAT) or intramolecular cyclization.

Scheme 2.11 Reductive dehalogenation of aryl iodides



Based on their protocol, we looked at prenylation of aryl iodides using prenyl transfer reagent **1k** (scheme 2.12). The standard conditions i.e. photocatalyst, *N,N*-diisopropylethylamine, formic acid, and aryl iodide were used along with **1k** to give prenylated product in moderate to good yields. Electron rich aryl iodides were more sluggish towards prenylation than electron deficient aryl iodide, potentially because of challenges associated with the initial electron transfer from the photocatalyst due to their extremely negative potentials. As expected halogens⁴⁹ lighter than iodide were tolerated in the reaction, (4c, and 4e) and should allow advanced synthetic manipulation.

Scheme 2.12 Prenylation of aryl iodides

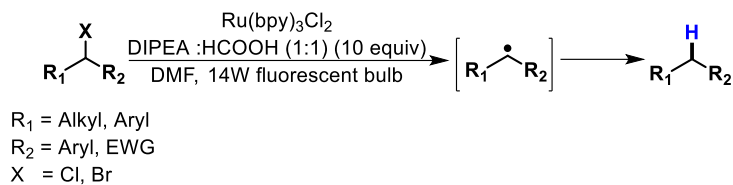


^[a](3 equiv), **1k** (5 equiv). Yields are of isolated product.

Even a sterically hindered aryl iodide gave moderate amount of prenylated product (**4d**), highlighting the ability of the radical and the reagent to form sterically demanding bonds. In fact, yields may have been higher, but the carbonates of **4d** were somewhat unstable under the reaction conditions, as we observed some deprotection of carbonates during the reaction and made no attempt to optimize the reaction.

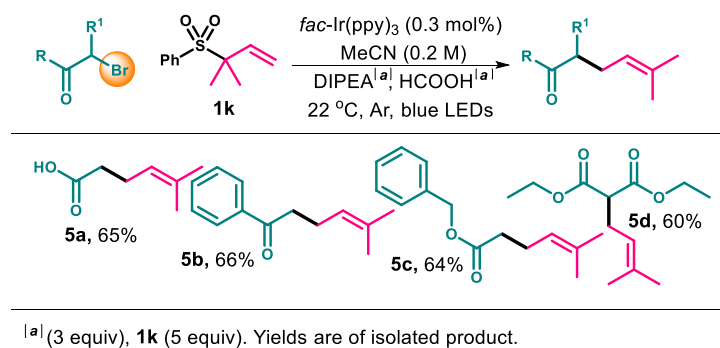
Visible light promoted reductive dehalogenation⁵⁰ and alkenylation^{28c} reactions of α -carbonyl alkyl bromides/ chlorides and benzyl bromides have been reported presence of Ru(bpy)_3^{2+} (scheme 2.13).

Scheme 2.13 Reductive dehalogenation alkyl halides



Using conditions also developed by Stephenson,⁵⁰ we attempted the prenylation of α -bromo carbonyls using reagent **1k** (scheme 2.14). Changing the photocatalyst from $\text{Ru}(\text{bpy})_3^{2+}$ to *fac*- $\text{Ir}(\text{ppy})_3$ and some minor tweaking of reaction conditions, made it possible to obtain prenylated carbonyl products as the major product. The acid **5a** serves as a valuable precursor for many synthetic sequences,⁵¹ and this procedure should expedite access to this compound. Additionally, the reaction works well for ketones (**5b**), esters (**5c**), and diesters (**5d**).

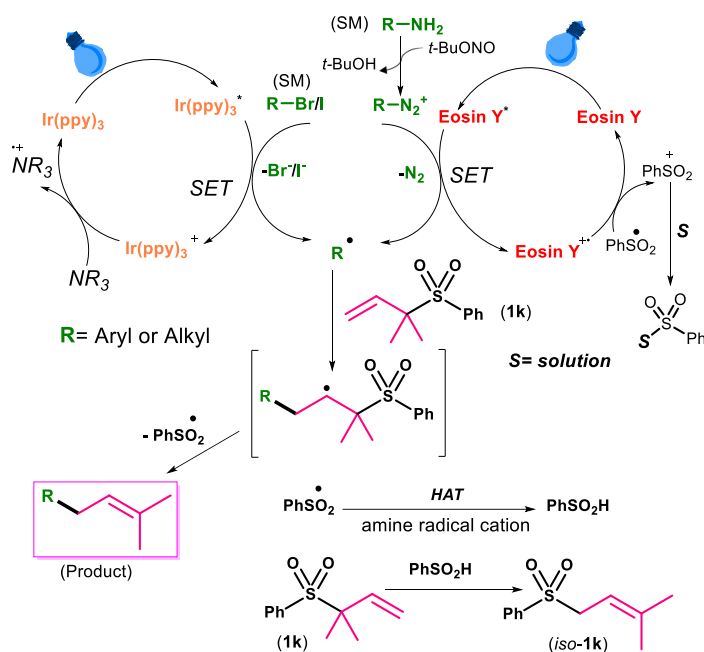
Scheme 2.14 Prenylation of α -carbonyl bromides



Among the different classes of substrates we have studied, there are assuredly mechanistic variations. However, a generic mechanism is outlined below (scheme 2.15). All reactions begin with the irradiation of the photocatalyst to give an excited state catalyst (PC^*). From PC^* single electron transfer (SET) to the halogenated (or pseudo-halogenated) substrate occurs, converting the photocatalyst to its more oxidized state which is then reduced by the sacrificial reductant. Meanwhile, mesolytic fragmentation of the halide (or pseudo-halide) takes place and generates a carbon based radical. We recognize that in some cases reductive quenching of the photocatalyst may be operative,

but still results in an electron transfer to the halide which proceeds as described. Addition of the photocatalytically generated radical to isoprenyl sulfone (1k) generates the β -sulfonyl radical. Finally, beta fragmentation of a sulfinyl radical generates the key double bond, providing the prenylated aryl or alkyl product.

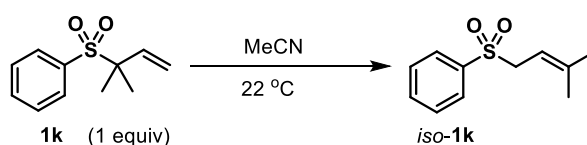
Scheme 2.15 General mechanism



The α -C-H bond of the amine radical cation is significantly weakened to an estimated bond dissociation energy ~ 42 kcal/mol.⁵² Phenylsulfonic acid PhS(O)O-H has a bond dissociation energy ~ 77.2 kcal/mol.⁵³ Therefore, it is feasible that the sulfinyl radical abstracts a hydrogen atom from amine radical cation to generate sulfonic acid that can then be subsequently deprotonated by excess amine. During the prenylation reaction, we observed that some of 1k underwent a formal 1,3-rearrangement to form the thermodynamically more stable, linear, and non-productive prenylated sulfone. Uguen⁵⁴ and coworkers have shown that allylic sulfones undergo allylic isomerization when treated with arenesulfonic acid. To study the isomerization of sulfones several experiments were performed (table 2.2). A reaction was set up adding PhSO₂Na to a solution of 1k in acetonitrile (entry 1) and we did not

observe any sulfone isomerization (*iso*-1k). PhSO₂Na was less soluble in acetonitrile. A similar experiment was run in DMSO (rather than acetonitrile) which completely solubilized the PhSO₂Na, however, no sulfone isomerization was observed (entry 2). Carrying out the reaction with PhSO₂Na and HCOOH resulted complete isomerization of sulfone (entry 3). A Similar observation was noted when the reaction was carried out with NBu₃ & HCOOH (1:1). The experimental outcomes reveal that *in situ* generated sulfinic acid is responsible for the isomerization of sulfone. Importantly, the rate of isomerization 1k increases with temperature (entry 7 & 8).

Table 2.2 Isomerization of sulfone (1k)

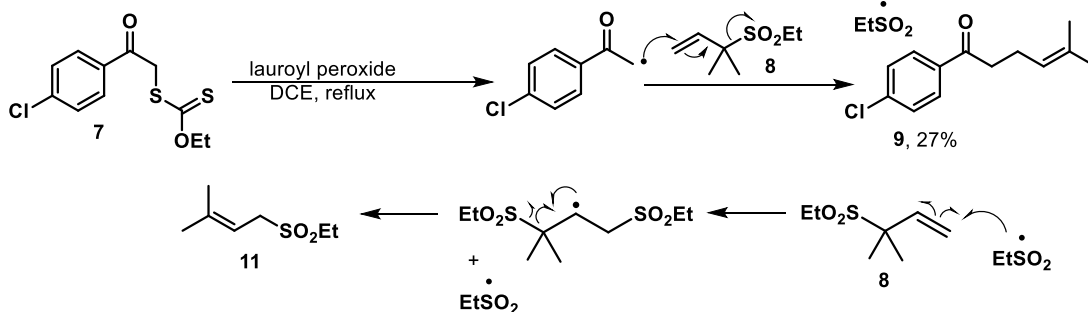


entry	modification	time	conv ^a
1	PhSO ₂ Na (1 equiv)	21 h	0% ^b
2	PhSO ₂ Na (1 equiv), DMSO instead of MeCN	30 h	0% ^b
3	PhSO ₂ Na (1 equiv), HCOOH (2 equiv)	21 h	100%
4	PhSO ₂ H (1 equiv)	17 h	100%
5	PhSO ₂ Na (1 equiv), NBu ₃ :HCOOH (1:1) (3 equiv)	21 h	100%
6	PhSO ₂ Na (1 equiv), <i>fac</i> -Ir(ppy) ₃ (0.3 mol%)	30 h	0% ^b
7	entry 3 45 °C	17 h	100%
8	entry 3 0 °C	21 h	50% ^b

^aConversion determined by ¹H NMR. ^bReaction did not proceed with extended time

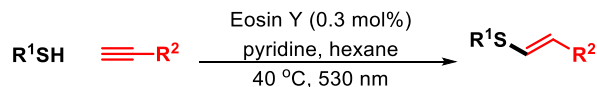
Zard and coworkers have observed sulfone isomerization in radical allylation with α -branched allyl sulfones (scheme 2.16).^{34c} For instance, the reaction of xanthate 7 with α, α -dimethyl-allyl ethyl sulfone 8 in presence of lauroyl-peroxide under reflux condition was sluggish and resulted only 27% of the desired product 9 (Scheme 2.16). They observed the formation of a considerable amount of rearranged sulfone 11 and proposed that this occurred by addition–fragmentation of ethylsulfonyl radicals with α, α -dimethylallyl ethyl sulfone 8. The persistence of the ethyl-sulfonyl radicals in the reaction turns out to be a problem. Based on all evidences, we believe that both sulfinic acid and sulfinyl radical are causative agents for sulfone isomerization in our prenylation reactions. However, this issue can simply overcome by the addition of 1k to compensate for loss of the reactant due to isomerization.

Scheme 2.16 Allylation with α -substituted allyl sulfone reagents

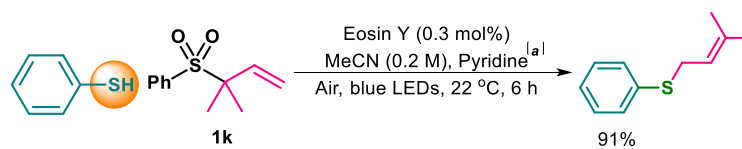


All the prenylation examples discussed thus far work by the generation of radicals via reductive fragmentation of the C–X bond. However, we believe the prenylation method should also be amenable to oxidatively generated radicals. Thus, we looked at the one-electron photocatalytic oxidation of thiols described by Yoon⁵⁵ and Ananikov⁵⁶ to generate a thiol radical cation which mesolytically fragments into a proton and an electrophilic thiyl radical, which we believed would react with **1k** to accomplish the prenylation of thiols. In this case, we used the similar conditions of photoredox thiol-yne click reaction developed by Ananikov (scheme 2.17).⁵⁶ Indeed, the desired prenylated thiol was formed as the major product in high yield (scheme 2.18). In the control experiment, irradiation of the reaction mixture absent of Eosin Y, produced only 6% of the product within the same time frame. This suggests that **1k** can also be expected to work with reactions that proceed through oxidative fragmentations.

Scheme 2.17 Photoredox thiol–yne reaction



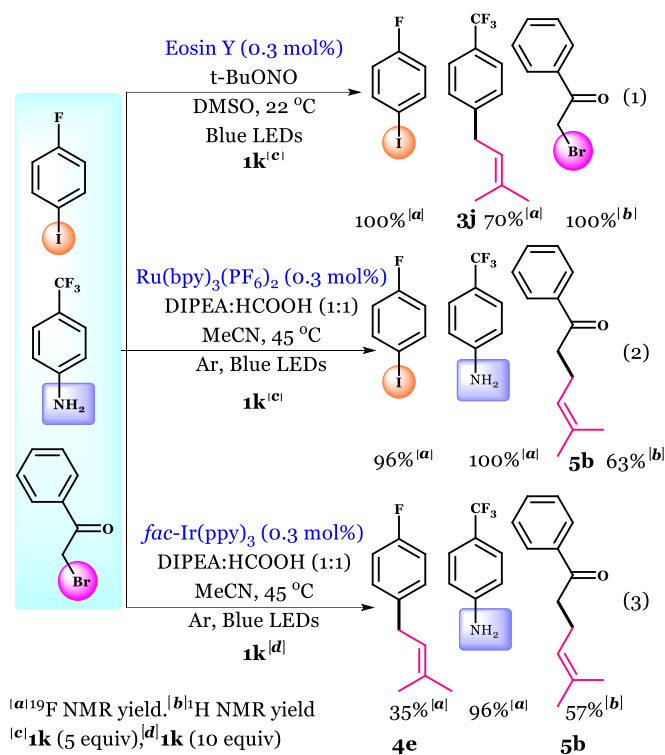
Scheme 2.18 Prenylation of thiophenol



^a (1 equiv), **1k** (3 equiv). Yields are of isolated product.

Visible light photocatalysis conditions are often tolerant of various functional groups and the synthetic community continues to find new uses. However, selectivity within photocatalytic pathways is less explored despite that many conditions are orthogonal, or rely on different phenomena.⁵⁷ To demonstrate selective photocatalysis, we performed the prenylation of different photocatalytically active substrates by judicious choice of reaction conditions. We observed selective prenylation of CF₃-aniline via selective reduction of the *in situ* generated diazonium by eosin Y (scheme 2.19, eqn 1). Electron transfer from eosin Y to the bromo-ketone or the aryl iodide, would be endothermic, and consequently happens infrequently. Similarly, use of a more reducing Ru(bpy)₃²⁺ (eqn 2) allows the reduction of the bromo-ketone but only very sluggishly reduces the aryl iodide, and does not affect the aniline. We had hoped to accomplish prenylation of the aryl iodide (-1.59 V)⁴⁸ selectively over the bromo-ketone (-0.78 V)⁵⁸ via Marcus-selectivity.⁵⁹ Electron transfer reactions are expected to slow when they become excessively thermodynamically favorable, a counterintuitive interplay of kinetics and thermodynamics termed the inverted region in Marcus theory. As such, we believed that SET to more easily reduced substrate (bromo-ketone) should become sluggish allowing SET to the less easily reduced substrate (aryl iodide) (eqn 3). Indeed, we did observe a relative increase in the rate of consumption of the aryl iodide compared to the bromo-ketone, however, it was not synthetically useful. One potential explanation for why we fail to see complete selectivity could simply be due to unselective electron transfer from the photocatalyst any electron acceptor, i.e. the iodide or the bromide. Another explanation could be that we did in fact selectively transfer the electron to the aryl iodide, but that radical anion of the aryl iodide undergoes exothermic SET to the bromo-ketone faster than mesolytic fragmentation of the iodide-masking Marcus selectivity. However, literature has reported that addition of an electron to an aryl iodide can result concerted bond cleavage rather formation of a radical anion, in which case the latter argument seems less likely.⁶⁰ Nonetheless, it is still remarkable to see that the relative preference for the more easily reduced bromide is significantly lessened, and suggests that Marcus selectivity may still find applications in other systems.

Scheme 2.19 Navigating photocatalysis



2.3 Summary

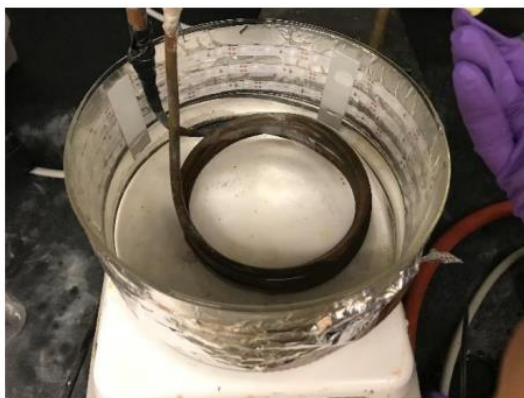
Prenylation is an essential reaction on which nature relies to modify properties of molecules and build terpenoids, but remains a challenging chemical reaction. We have developed a visible light photoredox-mediated, efficient and general method for prenylation of 2-bromo-azoles, aryl iodides, α -bromo-carbonyls, anilines via *in situ* generated diazoniums using bench stable, and easy to handle iso-prenyl sulfone, **1k**. We anticipate that this reagent, along with rapid advancement of visible light photocatalysis will greatly facilitate prenylation efforts.

2.4 Experimental section

All reagents were obtained from commercial suppliers (Aldrich, VWR, TCI Chemicals, and Oakwood Chemicals) and used without further purification unless otherwise noted. Acetonitrile (CH_3CN) was dried over molecular sieves. Diisopropylethylamine was distilled and stored over KOH pellets. Photocatalysts *fac*-tris(2-phenylpyridine) iridium(III), $\text{Ir}(\text{ppy})_3$ and all other iridium photocatalysts were synthesized according to the literature procedure.⁶¹ Eosin Y was purchased from VWR.

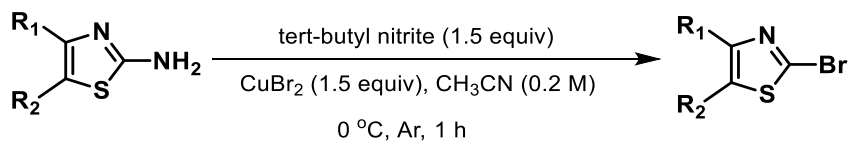
Reactions were monitored by thin layer chromatography (TLC), (obtained from sorbent technology Silica XHL TLC Plates, w/UV254, glass backed, 250 μm , 20 x 20 cm) and were visualized with ultraviolet light, potassium permanganate stain, GC-MS (QP 2010S, Shimadzu equipped with auto sampler) and ^1H NMR. Isolations were carried out using Teledyne Isco Combiflash Rf 200i flash chromatograph with Redisep Rf normal phase silica (4 g, 12 g, 24 g, 40 g) with product detection at 254 and 288 nm and by ELSD (evaporative light scattering detection). Some isolations were performed using Sorbent Technology Silica Prep TLC Plates, w/UV254, glass backed, 1000 μm , 20 x 20 cm, and were visualized with ultraviolet light. NMR spectra were obtained on a 400 MHz Bruker Avance III spectrometer and 400 MHz Unity Inova spectrometer. ^1H and ^{13}C NMR chemical shifts are reported in ppm relative to the residual protio solvent peak (^1H , ^{13}C).

Photocatalytic reactions were set up in a light bath as described below. Blue LEDs (in the form of strips i.e., 18 LEDs/ft from Solid Apollo) were wrapped around the walls of glass crystallization dish and secured with masking tape and then wrapped with aluminum foil. A lid which rest on the top was fashioned from cardboard and holes were made such that reaction tubes were held firmly in the cardboard lid which was placed on the top of bath. Water was added to the bath such that the tubes were submerged in the water which was maintained at 45 °C with the aid of a sand bath connected to a thermostat. In some cases, the same light bath set up was used with water in it which was maintained at 22 °C with the aid of circulating water through a coil of copper tubing placed in the bath.



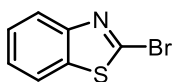
Synthesis of Substrates

General procedure A for synthesis of 2-bromothiazoles and 2-bromobenzothiazoles^{30a}

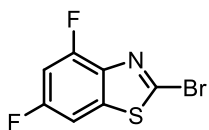


The aminoazole (9.5 mmol, 1.0 equiv) and CuBr₂ (14.5 mmol, 1.5 equiv) in MeCN (48 mL) was added to a round bottom flask and cooled to 0 °C under argon. Next, tert-butyl nitrite (14.5 mmol, 1.5 equiv.) was added drop wise to the reaction flask. The reaction mixture was stirred at 0 °C for 1 h and then at room temperature until full consumption of the starting material. The reaction was monitored by TLC. After consumption of the starting material, the mixture was diluted with H₂O (15 mL) and acidified

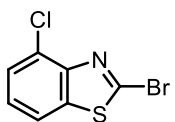
with 12 N HCl (until pH<1 by indicator paper) then extracted with CH₂Cl₂ (3×20 mL). The organic layers were combined and dried with MgSO₄. The crude product was concentrated in vacuo and purified via normal phase chromatography.



The general procedure **A** was followed using benzothiazol-2-amine (3.00 g, 20.0 mmol), tert-butyl nitrite (3.09 g, 3.57 mL, 30.0 mmol), CuBr₂ (6.70 g, 30.0 mmol) and 100 mL of MeCN to afford 2-bromobenzo[d]thiazole in 65% yield after isolation (2.78 g, 13.0 mmol) as a light orange solid. The substrate was purified via automated flash chromatography using EtOAc in hexanes (0% to 100%) with product eluting at 8% on a 120 g silica column.

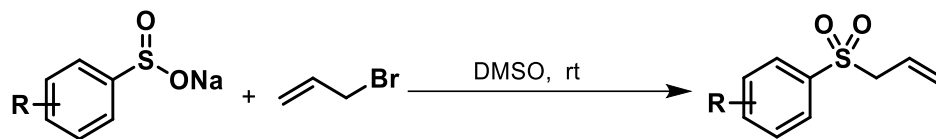


The general procedure **A** was followed using 4,6-difluorobenzothiazol-2-amine (500 mg, 2.29 mmol), tert-butyl nitrite (416.09 mg, 0.48 mL, 4.04 mmol), CuBr₂ (901.3 mg, 4.04 mmol) and 12 mL of MeCN to afford 2-bromo-4,6-difluorobenzo[d]thiazole in 68% yield after isolation (390.1 mg, 1.56 mmol) as a white solid. The substrate was purified via automated flash chromatography using EtOAc in hexanes (0% to 100%) with product eluting at 10% on 24 g silica column.

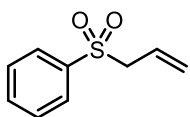


The general procedure **A** was followed using 4-chlorobenzothiazol-2-amine (500 mg, 2.71 mmol), tert-butyl nitrite (419.7 mg, 0.48 mL, 4.07 mmol), CuBr₂ (909.1 mg, 4.07 mmol) and 14 mL of MeCN to afford 2-bromo-4-chlorobenzo[d]thiazole in 52% yield after isolation (350 mg, 1.41 mmol) as a white solid. The substrate was purified via automated flash chromatography using EtOAc in hexanes (0% to 100%) with product eluting at 12% on a 24 g silica column.

General procedure B for synthesis of allyl sulfones

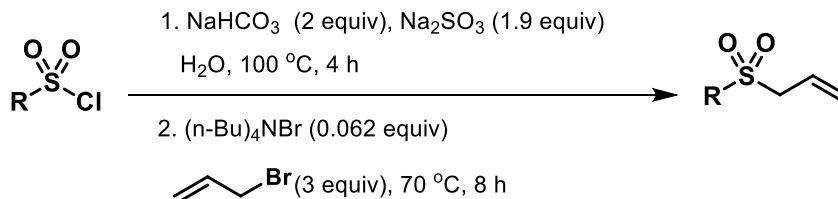


To a solution of sodium benzenesulphinate (61 mmol, 1 equiv) in DMSO (100 mL) stirring at room temperature, was added allyl bromide (67.1 mmol, 1.1 equiv). The reaction mixture was stirred at room temperature. The reaction was monitored by TLC. When TLC indicated the reaction was complete, the reaction mixture was poured into a separating funnel containing ethyl acetate (100 mL) which caused the precipitation of sodium bromide as white crystals. Water (200 mL) was added and the layers separated. The aqueous layer was extracted with ethyl acetate (3 x 100 mL) and combined organic layers were washed with water (2 x 100 mL), brine (100 mL), and then dried (MgSO_4). The solvent was removed under reduced pressure to give the product.

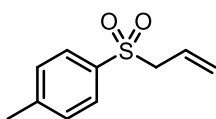


Allyl phenyl sulfone was prepared by general procedure **B**. To a solution of sodium benzenesulphinate (20 g, 122 mmol) in DMSO (200 mL) stirring at room temperature, was added allyl bromide (16.2 g, 11.6 mL, 134 mmol). The reaction mixture was stirred at room temperature for 6 h. After workup, the product (crude yield = 98%) was isolated as a pale yellow oil.

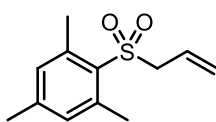
General procedure C for synthesis of allyl sulfones⁶²



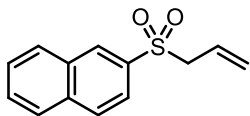
A stirred mixture of sulfonyl chloride (10 mmol, 1 equiv), sodium bicarbonate (20 mmol, 2 equiv), and sodium sulfite (19 mmol, 1.9 equiv) was heated in water (12 mL) at 100 °C for 3 h. The reaction was cooled to ~ 50 °C, treated with (n-Bu)₄NBr (0.62 mmol, 0.062 equiv) and allyl bromide (30 mmol, 3 equiv) and heated at 70 °C for 8 h. The reaction was cooled, treated with water (10 mL) and extracted with dichloromethane (3 × 15 mL). The extracts were combined and dried with MgSO₄, concentrated in vacuo and chromatographed on silica gel using ethyl acetate/hexanes to afford allyl sulfone.



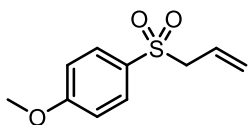
1-(allylsulfonyl)-4-methylbenzene was prepared by general procedure C. To a solution of 4-methylbenzenesulfonyl chloride (3.6 g, 18.9 mmol) in H₂O (23 mL) was added sodium bicarbonate (3.18 g, 37.8 mmol) and sodium sulfite (4.52 g, 35.9 mmol). The reaction mixture was heated at 100 °C for 3 h. Then treated with (n-Bu)₄NBr (377.8 mg, 1.17 mmol) and allyl bromide (6.9 g, 5 mL, 56.7 mmol) and heated at 70 °C for 8 h. The crude was purified via automated flash chromatography using EtOAc in hexanes (0% to 100%) with product eluting at 19% on 40 g silica column to afford the product in 80% yield (2.97 g, 15.12 mmol) as a white solid.



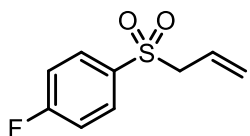
2-(allylsulfonyl)-1,3,5-trimethylbenzene was prepared by general procedure C. To a solution of 2,4,6-trimethylbenzenesulfonyl chloride (6.78 g, 31.1 mmol) in H₂O (38 mL) was added sodium bicarbonate (5.2 g, 62.2 mmol) and sodium sulfite (7.43 g, 59 mmol). The reaction mixture was heated at 100 °C for 3 h. Then treated with (n-Bu)₄NBr (621.6 mg, 1.92 mmol) and allyl bromide (11.3 g, 8 mL, 93.3 mmol) and heated at 70 °C for 8 h. The crude material was purified by flash chromatography using EtOAc in hexane (0% to 100%) with product eluting at 8% on a 40 g silica column to the product in 65% yield (4.5 g, 20.06 mmol) as a white solid.



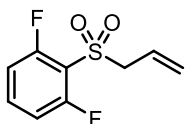
2-(allylsulfonyl)naphthalene was prepared by general procedure C. To a solution of naphthalene-2-sulfonyl chloride (3.6 g, 15.9 mmol) in H₂O (19 mL) was added sodium bicarbonate (2.67 g, 31.8 mmol) and sodium sulfite (3.8 g, 30.2 mmol). The reaction mixture was heated at 100 °C for 3 h. Then treated with (n-Bu)₄NBr (317.8 mg, 0.99 mmol) and allyl bromide (5.8 g, 2.3 mL, 26.5 mmol) and heated at 70 °C for 8 h. The crude material was purified by flash chromatography using EtOAc in hexane (0% to 100%) with product eluting at 10% on a 40 g silica column to afford the product in 73% yield (2.7 g, 11.62 mmol) as a white solid.



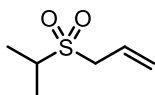
1-(allylsulfonyl)-4-methoxybenzene was prepared by general procedure C. To a solution of 4-methoxybenzenesulfonyl chloride (3.0 g, 14.52 mmol) in H₂O (18 mL) was added sodium bicarbonate (2.44 g, 29.04 mmol) and sodium sulfite (3.48 g, 27.6 mmol). The reaction mixture was heated at 100 °C for 3 h. Then treated with (n-Bu)₄NBr (290.2 mg, 0.9 mmol) and allyl bromide (5.3 g, 3.8 mL, 43.6 mmol) and heated at 70 °C for 8 h. The crude material was purified by flash chromatography using EtOAc in hexane (0% to 100%) with product eluting at 20% on a 40 g silica column to afford the product in 71% yield (2.19 g, 10.31 mmol) as a white solid.



1-(allylsulfonyl)-4-fluorobenzene was prepared by general procedure C. To a solution of 4-fluorobenzenesulfonyl chloride (3.5 g, 18 mmol) in H₂O (22 mL) was added sodium bicarbonate (3.02 g, 36 mmol) and sodium sulfite (4.3 g, 34.2 mmol). The reaction mixture was heated at 100 °C for 3 h. Then treated with (n-Bu)₄NBr (356.8 mg, 1.12 mmol) and allyl bromide (6.5 g, 4.7 mL, 54 mmol) and heated at 70 °C for 8 h. The crude material was purified by flash chromatography using EtOAc in hexane (0% to 100%) with product eluting at 20% on a 40 g silica column to afford the product in 69% yield (2.49 g, 12.4 mmol) as a colorless liquid.

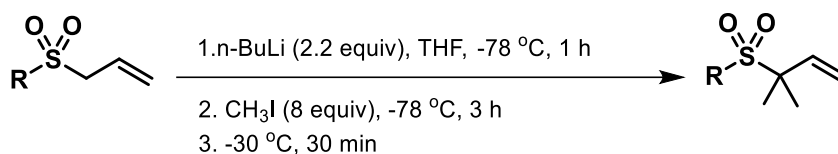


2-(allylsulfonyl)-1,3-difluorobenzene was prepared by general procedure C. To a solution of 2,6-difluorobenzenesulfonyl chloride (3.0 g, 14.1 mmol) in H₂O (17 mL) was added sodium bicarbonate (2.37 g, 28.2 mmol) and sodium sulfite (3.38 g, 26.8 mmol). The reaction mixture was heated at 100 °C for 3 h. Then treated with (n-Bu)₄NBr (281.8 mg, 0.87 mmol) and allyl bromide (5.1 g, 3.7 mL, 42.3 mmol) and heated at 70 °C for 8 h. The crude material was purified by flash chromatography using EtOAc in hexane (0% to 100%) with product eluting at 8% on a 40 g silica column to afford the product in 67% yield (2.06 g, 9.45 mmol) as a white solid.



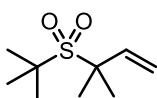
3-(isopropylsulfonyl)prop-1-ene was prepared by general procedure C. To a solution of propane-2-sulfonyl chloride (4.4 g, 3.48 mL, 30.9 mmol) in H₂O (37 mL) was added sodium bicarbonate (5.19 g, 61.8 mmol) and sodium sulfite (7.4 g, 58.7 mmol). The reaction mixture was heated at 100 °C for 3 h. Then treated with (n-Bu)₄NBr (617.6 mg, 1.92 mmol) and allyl bromide (11.2 g, 8 mL, 92.7 mmol) and heated at 70 °C for 8 h. After workup, the product was isolated as a colorless oil in 85% crude yield (3.9 g, 26.27 mmol).

General procedure D for synthesis of *iso*-prenylated sulfones⁶³

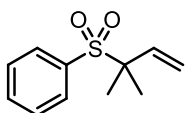


A solution of allylic sulfone (10 mmol, 1 equiv) in dry THF (50 mL) was cooled to -78 °C. 1.6 M n-butyllithium solution in hexane (22 mmol, 2.2 equiv.) was added dropwise via syringe under argon, and the colorless solution became yellow-orange. The reaction mixture was maintained at -78 °C and stirred for a further 1 h. Then, methyl iodide (80 mmol, 8 equiv.) was added dropwise via syringe and the resulting mixture was stirred at -78 °C for further 3 h. Then the temperature was raised to -30 °C and stirred for a further 30 min. Aqueous sodium bicarbonate solution was added to quench the reaction

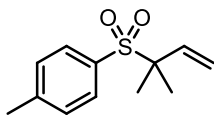
and extracted with diethyl ether and washed with water and brine. The organic extracts were combined and dried with MgSO₄. The solvent was removed under reduced pressure to give methylated sulfone and purified via normal phase chromatography.



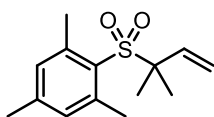
3-(tert-butylsulfonyl)-3-methylbut-1-ene (**1j**) was prepared by general procedure **D**. To a solution of 3-(isopropylsulfonyl)prop-1-ene (1.0 g, 6.7 mmol) in dry THF (33 mL) at -78 °C was added 1.6 M n-butyllithium solution in hexane (9.2 mL, 14.7 mmol). After 1 h stirring, methyl iodide (7.6 g, 3.3 mL, 53.6 mmol) was added and the resulting mixture was stirred at -78 °C for a further 3 h. Then the temperature was raised to -30 °C and stirred for a further 30 min. The crude material was purified by flash chromatography using EtOAc in hexane (0% to 100%) with product eluting at 14% on a 24 g silica column to afford the product in 55% yield (0.7 g, 3.7 mmol) as a colorless liquid.



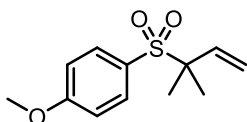
((2-methylbut-3-en-2-yl)sulfonyl)benzene (**1k**) was prepared by general procedure **D**. To a solution of (allylsulfonyl)benzene (5.0 g, 27.5 mmol) in dry THF (130 mL) at -78 °C was added 1.6 M n-butyllithium solution in hexane (38 mL, 60.4 mmol). After 1 h stirring, methyl iodide (31.2 g, 14 mL, 219.6 mmol) was added and the resulting mixture was stirred at -78 °C for a further 3 h. Then the temperature was raised to -30 °C and stirred for a further 30 min. The crude material was purified by flash chromatography using EtOAc in hexane (0% to 100%) with product eluting at 5% on an 80 g silica column to afford the product in 85% yield (4.9 g, 23.4 mmol) as a white solid.



1-methyl-4-((2-methylbut-3-en-2-yl)sulfonyl)benzene (**11**) was prepared by general procedure **D**. To a solution of 1-(allylsulfonyl)-4-methylbenzene (1.0 g, 5.1 mmol) in dry THF (25.5 mL) at -78 °C was added 1.6 M n-butyllithium solution in hexane (7 mL, 11.22 mmol). After 1 h stirring, methyl iodide (5.79 g, 2.5 mL, 40.8 mmol) was added and the resulting mixture was stirred at -78 °C for a further 3 h. Then the temperature was raised to -30 °C and stirred for a further 30 min. The crude material was purified by flash chromatography using EtOAc in hexane (0% to 100%) with product eluting at 4% on a 24 g silica column to afford the product in 85% yield (0.97 g, 4.34 mmol) as a white solid.

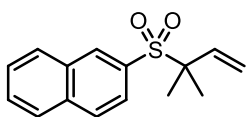


1,3,5-trimethyl-2-((2-methylbut-3-en-2-yl)sulfonyl)benzene (**1m**) was prepared by general procedure **D**. To a solution of 2-(allylsulfonyl)-1,3,5-trimethylbenzene (1.0 g, 4.5 mmol) in dry THF (22.5 mL) at -78 °C was added 1.6 M n-butyllithium solution in hexane (6.2 mL, 9.9 mmol). After 1 h stirring, methyl iodide (5.11 g, 2.2 mL, 36 mmol) was added and the resulting mixture was stirred at -78 °C for a further 3 h. Then the temperature was raised to -30 °C and stirred for a further 30 min. The crude material was purified by flash chromatography using EtOAc in hexane (0% to 100%) with product eluting at 5% on 24 g silica column to afford the product in 75% yield (0.85 g, 3.38 mmol) as a white solid.

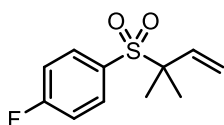


1-methoxy-4-((2-methylbut-3-en-2-yl)sulfonyl)benzene (**1n**) was prepared by general procedure **D**. To a solution of 1-(allylsulfonyl)-4-methoxybenzene (1.0 g, 4.7 mmol) in dry THF (23.5 mL) at -78 °C was added 1.6 M n-butyllithium solution in hexane (6.5 mL, 10.3 mmol). After 1 h stirring, methyl iodide (5.3 g, 2.3 mL, 37.6 mmol) was added and the resulting mixture was stirred at -78 °C for a further 3 h. Then the temperature was raised to -30 °C and stirred for a further 30 min. The crude material was purified by flash chromatography using EtOAc in

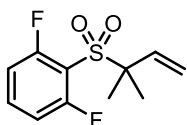
hexane (0% to 100%) with product eluting at 7% on a 24 g silica column to afford the product in 70% yield (0.79 g, 3.3 mmol) as a white solid.



2-((2-methylbut-3-en-2-yl)sulfonyl)naphthalene (**1o**) was prepared by general procedure **D**. To a solution of 2-(allylsulfonyl)naphthalene (1 g, 4.3 mmol) in dry THF (21.5 mL) at -78 °C was added 1.6 M n-butyllithium solution in hexane (5.9 mL, 9.46 mmol). After 1 h stirring, methyl iodide (4.88 g, 2.1 mL, 34.4 mmol) was added and the resulting mixture was stirred at -78 °C for a further 3 h. Then the temperature was raised to -30 °C and stirred for a further 30 min. The crude material was purified by flash chromatography using EtOAc in hexane (0% to 100%) with product eluting at 3% on a 24 g silica column to afford the product in 60% yield (0.67 g, 2.58 mmol) as a white solid.



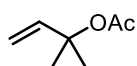
1-fluoro-4-((2-methylbut-3-en-2-yl)sulfonyl)benzene (**1p**) was prepared by general procedure **D**. To a solution of 1-(allylsulfonyl)-4-fluorobenzene (1.2 g, 6 mmol) in dry THF (30 mL) at -78 °C was added 1.6 M n-butyllithium solution in hexane (8.3 mL, 13.2 mmol). After 1 h stirring, methyl iodide (6.8 g, 3 mL, 48 mmol) was added and the resulting mixture was stirred at -78 °C for a further 3 h. Then the temperature was raised to -30 °C and stirred for a further 30 min. The crude material was purified by flash chromatography using EtOAc in hexane (0% to 100%) with product eluting at 1% on a 24 g silica column to afford the product in 65% yield (0.89 g, 3.9 mmol) as a white solid.



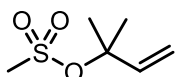
1,3-difluoro-2-((2-methylbut-3-en-2-yl)sulfonyl)benzene (**1q**) was prepared by general procedure **D**. To a solution of 2-(allylsulfonyl)-1,3-difluorobenzene (1.0 g,

4.6 mmol) in dry THF (23 mL) at -78 °C was added 1.6 M n-butyllithium solution in hexane (6.3 mL, 10.1 mmol). After 1 h stirring, methyl iodide (5.2 g, 2.3 mL, 36.8 mmol) was added and the resulting mixture was stirred at -78 °C for a further 3 h. Then the temperature was raised to -30 °C and stirred for a further 30 min. The crude material was purified by flash chromatography using EtOAc in hexane (0% to 100%) with product eluting at 0.3% on a 24 g silica column to afford the product in 60% yield (0.68 g, 2.76 mmol) as a white solid.

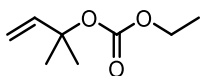
Synthesis of prenylating reagents from 2-methylbut-3-en-2-ol



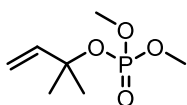
2-methylbut-3-en-2-yl acetate (**1b**) was prepared according to the following method. 2-methylbut-3-en-2-ol (2.5 mL, 25.1 mmol), triethylamine (13.3 mL, 95.7 mmol), DMAP (25 mg, 0.20 mmol) and dry DCM (13 mL) were added in to a flame dried 100 mL flask. The flask was cooled in an ice bath and acetic anhydride (9 mL, 95.7 mmol) was added dropwise. The resulting solution was stirred under argon at room temperature until TLC analysis showed no remaining starting material. The reaction was quenched with water and washed with NaHCO₃ (2 x 100 mL), 10% NaOH (2 x 100 mL), brine (100 mL), and dried with MgSO₄. Solvent was removed in vacuo and crude product was obtained as a slightly yellow oil which was distilled (130-150 °C at 760 mmHg) to yield 68%.



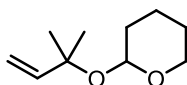
2-methylbut-3-en-2-yl methanesulfonate (**1c**) was prepared according to the following method. To a solution of 2-methylbut-3-en-2-ol (4.3 mL, 41.6 mmol) and triethylamine (8 mL, 57.4 mmol) at -30 °C in DCM (75 mL) was added methanesulfonyl chloride (5.7 g, 50 mmol) dropwise. After 45 min at -30 °C the slurry was warmed to room temperature and was transferred to a separatory funnel with ice/water (20 mL) and the organic layer was separated. The aqueous layer was extracted with DCM (3 x 10 mL) and the combined organic layers dried over MgSO₄ and concentrated in vacuo to afford crude product to yield 4.6 g, 67 %.



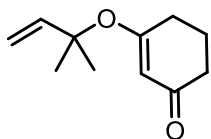
ethyl (2-methylbut-3-en-2-yl) carbonate (**1d**) was prepared according to the following method. To a solution of 2-methylbut-3-en-2-ol (1.7 mL, 16.64 mmol) and pyridine (2 mL, 25 mmol) in benzene (50 mL), ethyl chloroformate (2.1 mL, 21.63 mmol) was added slowly over 10 min at 0 °C. The reaction mixture was stirred for 3 h at room temperature and quenched with aq. NH₄Cl (30 mL). The mixture was diluted with ethyl acetate (40 mL) and the combined organic phase was washed with water and brine, dried over MgSO₄, and concentrated in vacuo. The crude material was purified by flash chromatography using EtOAc/ hexane 1:3 as a yellowish oil, yield 2.2 g, 84%.



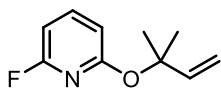
Dimethyl (2-methylbut-3-en-2-yl) phosphate (**1e**) was prepared according to the following method. Dimethyl phosphorochloridate (7.225 g, 50 mmol) was added to a solution of 2-methyl-3-buten-2-ol (3.876 g, 45 mmol) and pyridine (4 mL) in dichloromethane (50 mL) at 0 °C for 5 min. The resulting white slurry was stirred for 6 h at room temperature. The reaction mixture was diluted with diethyl ether and washed successively with 10 % HCl, saturated aqueous NaHCO₃ and brine. The organic layer was dried over anhydrous MgSO₄. After removal of the solvent in vacuo, the crude product was purified by column chromatography hexane/EtOAc 95:5 to yield 5.6 g, 65 %.



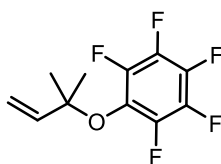
2-((2-methylbut-3-en-2-yl)oxy)tetrahydro-2H-pyran (**1f**) was prepared according to the following method. To a solution of 2-methylbut-3-en-2-ol (0.9 mL, 9 mmol) in DCM (35 mL) 2,3-dihydro-4H-pyran (0.8 mL, 9 mmol) and trifluoroacetic acid (0.1 mL, 1.8 mmol) were added. The reaction was stirred at room temperature and monitored by TLC. After completion of the reaction, it was quenched with NaHCO₃ and extracted with DCM. The organic phase was washed with water and brine, dried over MgSO₄, and concentrated in vacuo. The crude material was purified by flash chromatography using hexane/ EtOAc 99:1 as a colorless oil, yield 1.07 g, 70%.



3-((2-methylbut-3-en-2-yl)oxy)cyclohex-2-en-1-one (**1g**) was prepared according to the following method. To a solution of 2-methylbut-3-en-2-ol (3.1 mL, 29.7 mmol) in DCM (75 mL) 1, 3-cyclohexanedione (4 g, 35.7 mmol) and nitric acid (0.92 mL, 14.9 mmol) were added. The reaction was stirred at room temperature and monitored by TLC. After completion of the reaction, it was quenched with NaHCO₃ and extracted with DCM. Organic phase was washed with water and brine, dried over MgSO₄, and concentrated in vacuo. The crude material was purified by flash chromatography using hexane/ EtOAc 90:10 as a colorless oil, yield 3.2 g, 60%.



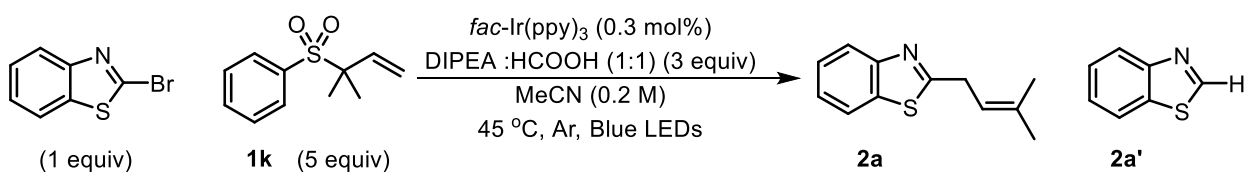
2-fluoro-6-((2-methylbut-3-en-2-yl)oxy)pyridine (**1h**) was prepared according to the following method.^{34a} 2,6-difluoropyridine (3.1 mL, 34.4 mmol) was added to a solution of 2-methyl-3-buten-2-ol (3 mL, 28.7 mmol), and NaH (0.89 g, 37.3 mmol) in THF (25 mL) at room temperature. The resulting solution was stirred for 8 h. The reaction mixture was quenched with water, diluted with diethyl ether and washed with brine. The organic layer was dried over anhydrous MgSO₄. After removal of the solvent in vacuo, the crude product was purified by column chromatography hexane/EtOAc 95:5 to yield 3.8 g, 75 %.



Benzene, [(1,1-dimethyl-2-propenyl)oxy]pentafluoro (**1i**) was prepared according to the following method.⁵ Hexafluorobenzene (0.37 mL, 3.1 mmol) was added to a solution of 2-methyl-3-buten-2-ol (0.4 mL, 3.83 mmol), and NaH (0.12 g, 4.37 mmol) in THF (10 mL) at room temperature. The resulting solution was stirred for 8 h. The reaction mixture was quenched with water, diluted with diethyl ether and was washed with brine. The organic layer was dried over anhydrous MgSO₄. After removal of the solvent in vacuo, the crude product was purified by column chromatography hexane/EtOAc 99:1 to yield 0.68 g, 87 %.

Optimization of Photocatalytic Prenylation:

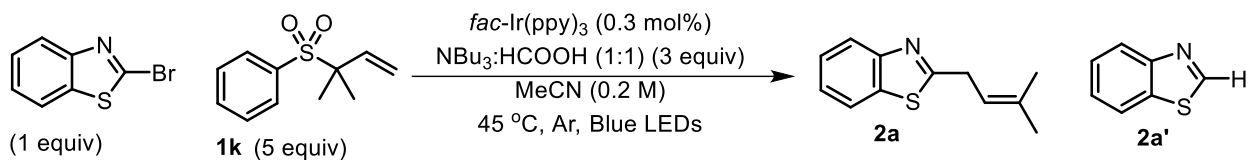
Optimization of photocatalytic prenylation of 2-bromoazoles with prenyl sulfones:



entry	modification	2a:2a' ^a	time	conv ^a
1	none	71:29	23 h	100%
2	used NBu ₃ instead of DIPEA	78:22	23 h	100%
3	used DIPEA with out HCOOH	62:38	30 h	100%
4	NBu ₃ :HCOOH (1:1) (4 equiv)	70:30	18 h	100%
5	NBu ₃ :HCOOH (1:1) (2 equiv)	81:19	35 h	65% ^b
6	DMF instead of MeCN	25:75	23 h	100%
7	DMSO instead of MeCN	30:70	23 h	100%
8	DCM instead of MeCN	16:84	43 h	36% ^b
9	entry 2, 4 equiv of alkene	65:35	29 h	100%
10	entry 2, 6 equiv of alkene	80:20	22 h	100%
11	entry 2, 60 °C	63:37	18 h	100%
12	entry 2, 22 °C	75:25	48 h	100%
13	in air	60:40	21 h	65% ^b
14	no amine or no Ir(ppy) ₃	na	24 h	0%
15	TEMPO (1.5 equiv)	60:40	24 h	15% ^b

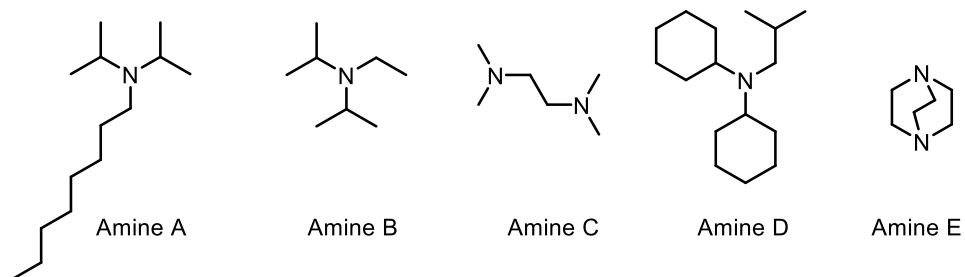
^aConversion and product ratio **2a:2a'** determined by GCMS. ^bReaction did not proceed with extended time.

Optimization of amine in prenylation of 2-bromoazoles:

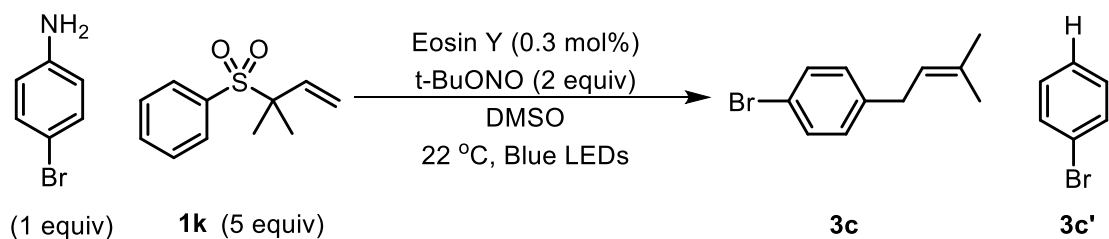


entry	modification	2a:2a' ^a	time	conv ^a
1	none	78:22	23 h	100%
2	Amine A instead of NBu_3	86:14	30 h	28% ^b
3	Amine B instead of NBu_3	71:29	23 h	100%
4	Amine C instead of NBu_3	90:10	35 h	33% ^b
5	Amine D instead of NBu_3	13:87	35 h	69% ^b
6	Amine E instead of NBu_3	na	24 h	0% ^b

^aConversion and product ratio **2a:2a'** determined by GCMS. ^bReaction did not proceed with extended time



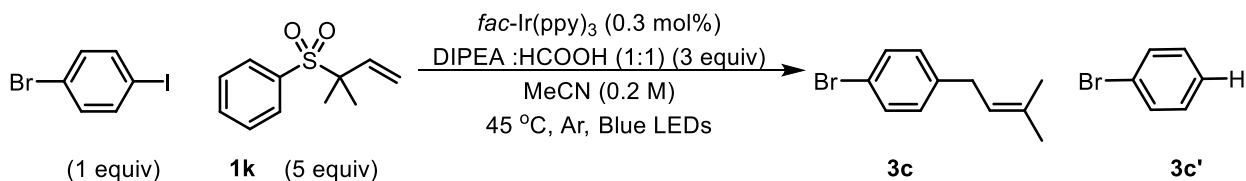
Optimization of photocatalytic prenylation of aniline with prenyl sulfones:



entry	modification	3c:3c' ^a	time	conv ^a
1	none	72:28	15 h	100%
2	t-BuONO (1.3 equiv)	37:63	24 h	24% ^b
3	t-BuONO (1.6 equiv)	64:36	24 h	48% ^b
4	t-BuONO (2.3 equiv)	72:28	15 h	100%
5	No t-BuONO	na	20 h	0% ^b
6	No light	41:58	20 h	6% ^b
7	No Eosin Y	50:50	20 h	5% ^b
8	Green LEDs instead of Blue LEDs	67:33	21 h	100%
9	DMF instead of DMSO	10:90	16 h	100%
10	MeCN instead of DMSO	19:81	18 h	45% ^b
11	MeOH instead of DMSO	51:49	18 h	100%
12	Isoamyl Nitrite instead of t-BuONO	27:73	24 h	44% ^b
13	NaNO ₂ (2 equiv), HCl instead of t-BuONO	45:55	18 h	20% ^b
14	30 °C	35:65	12 h	100%

^aConversion and product ratio **3c:3c'** determined by GCMS. ^bReaction did not proceed with extended time

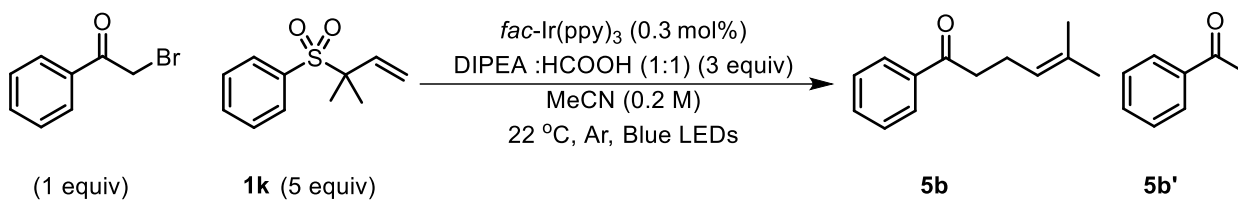
Optimization of photocatalytic prenylation of iodoarenes with prenyl sulfone:



entry	modification	3c:3c' ^a	time	conv ^a
1	none	65:35	33 h	100%
2	used DIPEA with out HCOOH	21:79	35 h	100%
3	used 4-methoxytriphenyl amine instead of DIPEA	0:100	48 h	95% ^b
4	1,4-Diazabicyclo[2.2.2]octane (DABCO) instead of DIPEA	na	22 h	0% ^b
5	1-Azabicyclo[2.2.2]octane (Quinuclidine) instead of DIPEA	na	22 h	0% ^b
6	<i>N</i> -cyclohexyl- <i>N</i> -isobutylcyclohexanamine (low soluble amine)	26:74	35 h	60% ^b
7	used CH ₃ COOH instead of HCOOH	38:62	28 h	100%
8	used CH ₃ CH ₂ COOH instead of HCOOH	32:68	28 h	100%
9	DIPEA:HCOOH (1:1) (4 equiv)	51:49	30 h	100%
10	DIPEA:HCOOH (1:1) (2 equiv)	68:32	58 h	90% ^b
11	DMF instead of MeCN	13:87	40 h	85% ^b
12	DMSO instead of MeCN	45:55	40 h	89% ^b
13	DCM instead of MeCN	20:80	40 h	64% ^b
14	60 °C instead of 45 °C	55:45	28 h	100%
15	22 °C instead of 45 °C	68:32	40 h	60% ^b
16	Ru(bpy) ₃ PF ₆ instead of <i>fac</i> -Ir(ppy) ₃	10:90	22 h	10% ^b
17	<i>fac</i> -Ir(4'-F-ppy) ₃ instead of <i>fac</i> -Ir(ppy) ₃	25:75	32 h	64% ^b
18	<i>fac</i> -Ir(4'-CF ₃ -ppy) ₃ instead of <i>fac</i> -Ir(ppy) ₃	29:71	32 h	73% ^b
19	<i>fac</i> -Ir(<i>t</i> Bu-ppy) ₃ instead of <i>fac</i> -Ir(ppy) ₃	44:56	30 h	32% ^b
20	no amine or no Ir(ppy) ₃	na	24 h	0% ^b

^aConversion and product ratio **3c:3c'** determined by GCMS. ^bReaction did not proceed with extended time

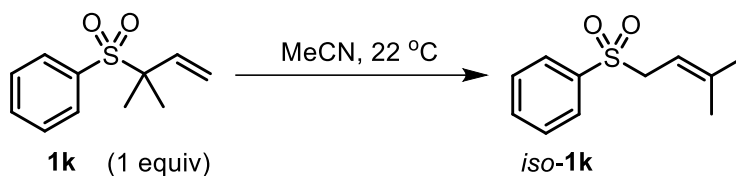
Optimization of photocatalytic prenylation of α -carbonyl bromides with prenyl sulfone:



entry	modification	5b:5b' ^a	time	conv ^a
1	none	68:32	23 h	100%
2	used NBU ₃ instead of DIPEA	62:38	23 h	100%
3	used DIPEA with out HCOOH	48:52	23 h	100%
4	NBU ₃ :HCOOH (1:1) (4 equiv)	54:46	19 h	100%
5	NBU ₃ :HCOOH (1:1) (2 equiv)	48:52	30 h	70% ^b
6	DMF instead of MeCN	28:72	25 h	100%
7	DMSO instead of MeCN	40:60	25 h	100%
8	Ru(bpy) ₃ Cl ₂ instead of <i>fac</i> -Ir(ppy) ₃	55:45	25 h	80% ^b
9	Ru(bpy) ₃ PF ₆ instead of <i>fac</i> -Ir(ppy) ₃	58:42	25 h	90%
10	45 °C	53:47	19 h	100%
11	no amine or no Ir(ppy) ₃	na	24 h	0% ^b

^aConversion and product ratio **5b:5b'** determined by GCMS. ^bReaction did not proceed with extended time

Experiments to confirm isomerization of sulfones:

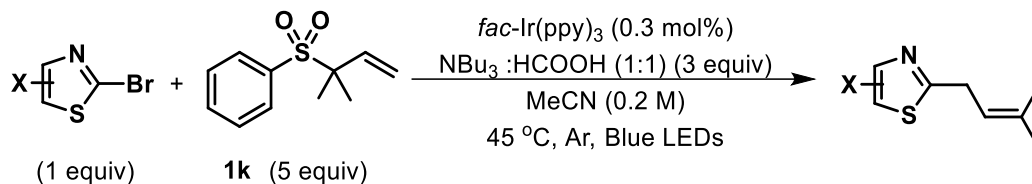


entry	modification	time	conv ^a
1	PhSO ₂ Na (1 equiv)	21 h	0% ^b
2	PhSO ₂ Na (1 equiv), DMSO instead of MeCN	30 h	0% ^b
3	PhSO ₂ Na (1 equiv), HCOOH (2 equiv)	21 h	100%
4	PhSO ₂ Na (1 equiv), H ₂ O (4 equiv), (n-Bu) ₄ NBr (0.003 equiv)	30 h	0% ^b
5	PhSO ₂ H (1 equiv)	17 h	100%
6	PhSO ₂ Na (1 equiv), NBu ₃ :HCOOH (1:1) (3 equiv)	21 h	100%
7	PhSO ₂ Na (1 equiv), <i>fac</i> -Ir(ppy) ₃ (0.3 mol%)	30 h	0% ^b
8	entry 3 45 °C	17 h	100%
9	entry 3 0 °C	21 h	50% ^b
10	HCOOH (1.5 equiv)	21 h	0% ^b
11	NBu ₃ (1.5 equiv)	21 h	0% ^b
12	HCOOH (1.5 equiv), <i>fac</i> -Ir(ppy) ₃ (0.3 mol%)	21 h	0% ^b
13	NBu ₃ (1.5 equiv), <i>fac</i> -Ir(ppy) ₃ (0.3 mol%)	21 h	0% ^b
14	NBu ₃ :HCOOH (1:1) (1.5 equiv), <i>fac</i> -Ir(ppy) ₃ (0.3 mol%)	21 h	0% ^b

^aConversion determined by ¹H NMR. ^bReaction did not proceed with extended time

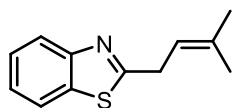
Photocatalytic Prenylation

General procedure E for the photocatalytic prenylation of 2-bromoazoles with prenyl sulfone (limiting azole)



A 12×75 mm borosilicate tube fitted with a rubber septum was charged with *fac*-tris(2-phenylpyridinato-C2, N) Iridium(III) (Ir(ppy)₃) (0.6 mM, 0.6 mL in MeCN), 2-bromoazoles (0.12 mmol, 1 equiv), tributylamine (0.36 mmol, 85.6 μL, 3 equiv), formic acid (0.36 mmol, 13.6 μL, 3 equiv) and ((2-methylbut-3-en-2-yl)sulfonyl)benzene (**1k**) (0.6 mmol, 126.2 mg, 5 equiv). Then the reaction mixture was degassed via Ar bubbling for 10 min and then left under positive Ar pressure by removing the exit needle. The tube was placed in a light bath (description above) and the lower portion of the tube was submerged under the water bath which was maintained at 45 °C. The reaction was monitored by TLC and GC-MS. After the complete consumption of 2-bromoazoles, MeCN was removed via rotovap and the residue was treated with sat. NaHCO₃ solution (2 mL) and extracted with DCM (3 x 2 mL). The organic portions were combined and dried over anhydrous MgSO₄. The crude product was concentrated in vacuo and purified via normal phase chromatography.

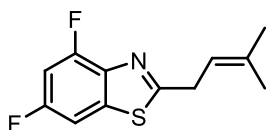
2a 2-(3-methylbut-2-en-1-yl)benzo[d]thiazole



The general procedure **E** was followed using 2-bromobenzo[d]thiazole (25.7 mg, 0.12 mmol), tributylamine (85.6 μL, 0.36 mmol), formic acid (13.6 μL, 0.36 mmol), ((2-methylbut-3-en-2-yl)sulfonyl)benzene (126.2 mg, 0.6 mmol) and 0.6 mL of stock solution of Ir(ppy)₃ in MeCN. After the completion of the reaction 23 h, the crude was purified via automated

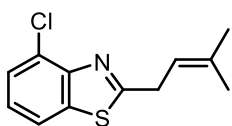
flash chromatography using EtOAc in hexanes (0% to 100%) with product eluting at 3% on a 4 g silica column to afford **2a** in 70% yield (17 mg, 0.084 mmol) as an oil. ^1H NMR (400 MHz, CDCl_3) δ 7.96 (d, $J = 8.2$ Hz, 1H), 7.82 (d, 1H), 7.44 (td, $J = 8.3, 7.3, 1.2$ Hz, 1H), 7.33 (td, 1H), 5.56 – 5.47 (m, 1H), 3.83 (d, $J = 7.4$ Hz, 2H), 1.81 (s, 3H), 1.76 (s, 3H). ^{13}C NMR (101 MHz, CDCl_3) δ 172.9, 153.7, 137.1, 135.7, 126.3, 125.1, 122.9, 121.9, 119.5, 33.6, 26.2, 18.5. GC/MS (m/z, relative intensity) 203 (M^+ , 70), 188 (90), 162 (50).

2b 4,6-difluoro-2-(3-methylbut-2-en-1-yl)benzo[d]thiazole



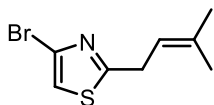
The general procedure **E** was followed using 2-bromo-4,6-difluorobenzo[d]thiazole (30 mg, 0.12 mmol), tributylamine (85.6 μl , 0.36 mmol), formic acid (13.6 μl , 0.36 mmol), ((2-methylbut-3-en-2-yl)sulfonyl)benzene (126.2 mg, 0.6 mmol) and 0.6 mL of stock solution of $\text{Ir}(\text{ppy})_3$ in MeCN. After the completion of the reaction 21 h, the crude was purified via silica prep TLC plate using EtOAc/hexanes 1:99 to afford **2b** in 78% yield (22 mg, 0.094 mmol) as an oil. ^1H NMR (400 MHz, CDCl_3) δ 7.31 (dd, 1H), 6.95 (td, $J = 10.2, 10.2, 2.3$ Hz, 1H), 5.55 – 5.44 (m, 1H), 3.82 (d, $J = 7.4$ Hz, 2H), 1.81 (s, 3H), 1.75 (s, 3H). ^{19}F NMR (376 MHz, CDCl_3) δ -113.6 – -113.7 (m), -118.4 (dd, $J = 10.2, 5.3$ Hz). ^{13}C NMR (101 MHz, CDCl_3) δ 173.3, 160.2 (dd, $J = 246.7, 10.4$ Hz), 155.2 (dd, $J = 258.5, 13.4$ Hz), 139.4 (dd, $J = 13.2, 2.4$ Hz), 138.6 (dd, $J = 12.6, 5.0$ Hz), 137.8, 119.1, 104.0 (dd, $J = 26.3, 4.6$ Hz), 102.2 (dd, $J = 28.3, 21.9$ Hz), 33.6, 26.1, 18.5. GC/MS (m/z, relative intensity) 239 (M^+ , 90), 224 (100), 198 (50).

2c 4-chloro-2-(3-methylbut-2-en-1-yl)benzo[d]thiazole



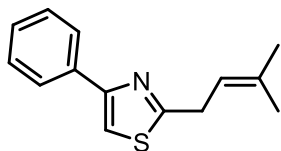
The general procedure **E** was followed using 2-bromo-4-chlorobenzo[d]thiazole (29.8 mg, 0.12 mmol), tributylamine (85.6 μ l, 0.36 mmol), formic acid (13.6 μ l, 0.36 mmol), ((2-methylbut-3-en-2-yl) sulfonyl)benzene (126.2 mg, 0.6 mmol) and 0.6 mL of stock solution of Ir(ppy)₃ in MeCN. After the completion of the reaction 22 h, the crude was purified via automated flash chromatography using EtOAc in hexanes (0% to 100%) with product eluting at 0.2% on a 4 g silica column to afford **2c** in 71% yield (20 mg, 0.085 mmol) as an oil. ¹H NMR (400 MHz, CDCl₃) δ 7.72 (d, *J* = 8.0 Hz, 1H), 7.46 (d, *J* = 7.8 Hz, 1H), 7.27 (t, 1H), 5.57 – 5.45 (m, 1H), 3.88 (d, *J* = 7.4 Hz, 2H), 1.82 (s, 3H), 1.76 (s, 3H). ¹³C NMR (101 MHz, CDCl₃) δ 174.3, 150.6, 137.4, 136.9, 127.3, 126.2, 125.2, 120.2, 119.1, 33.4, 25.9, 18.2. GC/MS (*m/z*, relative intensity) 237 (M⁺, 100), 222 (95), 196 (55).

2d 4-bromo-2-(3-methylbut-2-en-1-yl)thiazole



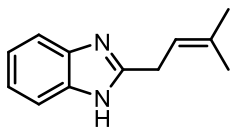
The general procedure **E** was followed using 2,4-dibromothiazole (29 mg, 0.12 mmol), tributylamine (85.6 μ l, 0.36 mmol), formic acid (13.6 μ l, 0.36 mmol), ((2-methylbut-3-en-2-yl)sulfonyl)benzene (126.2 mg, 0.6 mmol) and 0.6 mL of stock solution of Ir(ppy)₃ in MeCN. After the completion of the reaction 26 h, the crude was purified via automated flash chromatography using EtOAc in hexanes (0% to 100%) with product eluting at 0.2% on a 4 g silica column to afford **2d** in 60% yield (17 mg, 0.072 mmol) as an oil. ¹H NMR (400 MHz, CDCl₃) δ 7.08 (s, 1H), 5.51 – 5.35 (m, 1H), 3.70 (d, *J* = 7.4 Hz, 2H), 1.79 (s, 3H), 1.71 (s, 3H). ¹³C NMR (101 MHz, CDCl₃) δ 173.0, 137.3, 124.4, 118.8, 116.3, 32.4, 25.8, 18.1. GC/MS (*m/z*, relative intensity) 231 (M⁺, 40), 216 (45), 152 (80).

2e 2-(3-methylbut-2-en-1-yl)-4-phenylthiazole



The general procedure **E** was followed using 2-bromo-4-phenylthiazole (28.8 mg, 0.12 mmol), tributylamine (85.6 μ l, 0.36 mmol), formic acid (13.6 μ l, 0.36 mmol), ((2-methylbut-3-en-2-yl)sulfonyl)benzene (126.2 mg, 0.6 mmol) and 0.6 mL of stock solution of Ir(ppy)₃ in MeCN. After the completion of the reaction 23 h, the crude was purified via automated flash chromatography using EtOAc in hexanes (0% to 100%) with product eluting at 0.2% on a 4 g silica column to afford **2e** in 65% yield (18 mg, 0.078 mmol) as an oil. ¹H NMR (400 MHz, CDCl₃) δ 7.89 (d, 2H), 7.41 (t, *J* = 7.5, 7.5 Hz, 2H), 7.33 (s, 1H), 7.31 (t, *J* = 7.3 Hz, 1H), 5.58 – 5.42 (m, 1H), 3.79 (d, *J* = 7.3 Hz, 2H), 1.81 (s, 3H), 1.75 (s, 3H). ¹³C NMR (101 MHz, CDCl₃) δ 171.9, 155.2, 136.4, 134.6, 128.9, 128.1, 126.5, 119.8, 112.4, 32.5, 25.9, 18.2. GC/MS (*m/z*, relative intensity) 229 (M⁺, 100), 214 (60), 188 (45).

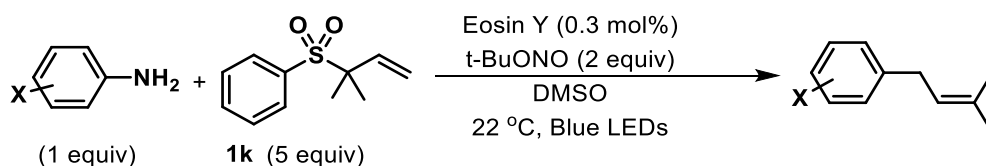
2f 2-(3-methylbut-2-en-1-yl)-1H-benzo[d]imidazole



The general procedure **E** was followed using 2-bromo-1H-benzo[d]imidazole (24 mg, 0.12 mmol), tributylamine (85.6 μ l, 0.36 mmol), formic acid (13.6 μ l, 0.36 mmol), ((2-methylbut-3-en-2-yl)sulfonyl)benzene (126.2 mg, 0.6 mmol) and 0.6 mL of stock solution of Ir(ppy)₃ in MeCN. The photocatalytic reaction did not go to further conversion after 4 days. After adding tributylamine (28.5 μ l, 0.12 mmol), formic acid (4.5 μ l, 0.12 mmol), ((2-methylbut-3-en-2-yl)sulfonyl)benzene (50.5 mg, 0.24 mmol) and 0.1 mL of Ir(ppy)₃ to the reaction, slight further conversion was observed and it afforded **2f** in 70% ¹H NMR yield after 6 days. The crude was purified via automated flash chromatography using EtOAc/hexanes under 1% Et₃N with product eluting at 23% EtOAc on a 4 g silica column to afford **2f** in 65% yield as an oil which includes 19% starting material. ¹H NMR (400 MHz, CDCl₃) δ 7.60 – 7.53 (m, 2H), 7.28 – 7.21 (m, 2H), 5.59 – 5.36 (m, 1H), 3.73 (d, *J* = 7.3 Hz, 2H), 1.75 (s, 3H), 1.71 (s, 3H). ¹³C NMR (101 MHz, CDCl₃) δ 153.9, 137.5, 126.4, 123.2,

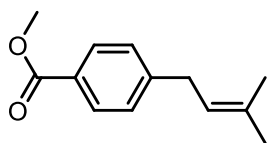
122.9, 117.3, 114.7, 28.2, 25.9, 18.2. GC/MS (m/z, relative intensity) 186 (M⁺, 100), 171 (100), 145 (75).

General procedure F for the photocatalytic prenylation of aniline with prenyl sulfone (limiting aniline)



A 12×75 mm borosilicate tube fitted with a rubber septum was charged with Eosin Y (0.6 mM, 0.6 mL in DMSO), aniline (0.12 mmol, 1 equiv), t-BuONO (0.24 mmol, 2 equiv) and ((2-methylbut-3-en-2-yl)sulfonyl)benzene (0.6 mmol, 126.2 mg, 5 equiv). Then the tube was placed in a light bath (description above) and the lower portion of the tube was submerged under the water bath which was maintained at 22 °C. The reaction was monitored by TLC and GC-MS. After completion of the reaction, water (5 mL) was added and extracted with ethyl acetate (3 mL). The organic fraction was washed with water (10 mL) and brine (10 mL). Then the organic phase was dried over MgSO₄ and evaporated to leave the crude product, which was purified by column chromatography.

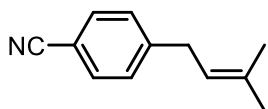
3a methyl 4-(3-methylbut-2-en-1-yl)benzoate



The general procedure **F** was followed using methyl 4-aminobenzoate (18 mg, 0.12 mmol), t-BuONO (24.7 mg, 28.5 μl, 0.24 mmol), ((2-methylbut-3-en-2-yl)sulfonyl)benzene (126.2 mg, 0.6 mmol) and 0.6 mL of stock solution of Eosin Y in DMSO. After the completion of the reaction 15 h, the crude was purified via automated flash chromatography using EtOAc in hexanes (0% to 100%) with product eluting at 0.1% on a 4 g silica column to afford **3a** in 67% yield (16 mg, 0.08 mmol) as an oil. ¹H NMR (400 MHz, CDCl₃) δ 7.94 (d, *J* = 8.2 Hz, 2H), 7.24 (d, *J* = 8.2 Hz, 2H), 5.37 – 5.25 (m, 1H), 3.90 (s, 3H), 3.39 (d, *J* = 7.3

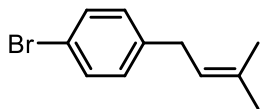
Hz, 2H), 1.76 (s, 3H), 1.72 (s, 3H). ^{13}C NMR (101 MHz, CDCl_3) δ 167.3, 147.5, 133.6, 129.9, 128.5, 127.8, 122.2, 52.1, 34.6, 25.9, 18.0. GC/MS (m/z, relative intensity) 204 (M^+ , 35), 189 (20), 145 (100).

3b 4-(3-methylbut-2-en-1-yl)benzonitrile



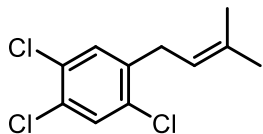
The general procedure **F** was followed using 4-aminobenzonitrile (14.2 mg, 0.12 mmol), t-BuONO (24.7 mg, 28.5 μl , 0.24 mmol), ((2-methylbut-3-en-2-yl)sulfonyl)benzene (126.2 mg, 0.6 mmol) and 0.6 mL of stock solution of Eosin Y in DMSO. After the completion of the reaction 15 h, the crude was purified via automated flash chromatography using EtOAc in hexanes (0% to 100%) with product eluting at 0.2% on a 4 g silica column to afford **3b** in 68% yield (14 mg, 0.082 mmol) as an oil. ^1H NMR (400 MHz, CDCl_3) δ 7.56 (apd, $J = 8.2$ Hz, 2H), 7.27 (d, $J = 7.5$ Hz, 2H), 5.34 – 5.19 (m, 1H), 3.39 (d, $J = 7.4$ Hz, 2H), 1.76 (s, 3H), 1.71 (s, 3H). ^{13}C NMR (101 MHz, CDCl_3) δ 147.6, 134.4, 132.3, 129.2, 121.5, 119.3, 109.7, 34.6, 25.9, 18.0. GC/MS (m/z, relative intensity) 171 (M^+ , 50), 156 (100), 142 (40).

3c 1-bromo-4-(3-methylbut-2-en-1-yl)benzene



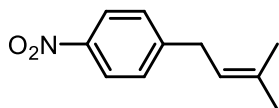
The general procedure **F** was followed using 4-bromoaniline (20.6 mg, 0.12 mmol), t-BuONO (24.7 mg, 28.5 μl , 0.24 mmol), ((2-methylbut-3-en-2-yl)sulfonyl)benzene (126.2 mg, 0.6 mmol) and 0.6 mL of stock solution of Eosin Y in DMSO. After the completion of the reaction 15 h, the crude was purified via automated flash chromatography using EtOAc in hexanes (0% to 100%) with product eluting at 100% hexane on a 4 g silica column to afford **3c** in 65% yield (18 mg, 0.078 mmol) as an oil. ^1H NMR (400 MHz, CDCl_3) δ 7.41 – 7.33 (apd, 2H), 7.05 (d, $J = 8.3$ Hz, 2H), 5.31 – 5.25 (m, 1H), 3.29 (d, $J = 7.3$ Hz, 2H), 1.75 (s, 3H), 1.71 (s, 3H). ^{13}C NMR (101 MHz, CDCl_3) δ 141.2, 133.6, 131.8, 130.5, 122.9, 119.9, 34.2, 26.2, 18.3. GC/MS (m/z, relative intensity) 224 (M^+ , 20), 145 (40), 130 (100).

3d 1,2,4-trichloro-5-(3-methylbut-2-en-1-yl)benzene



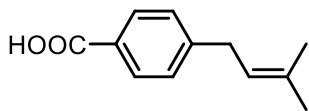
The general procedure **F** was followed using 2,4,5-trichloroaniline (23.6 mg, 0.12 mmol), t-BuONO (24.7 mg, 28.5 μ l, 0.24 mmol), ((2-methylbut-3-en-2-yl)sulfonyl)benzene (126.2 mg, 0.6 mmol) and 0.6 mL of stock solution of Eosin Y in DMSO. After completion of the reaction, 13 h, the crude was purified via automated flash chromatography using EtOAc in hexanes (0% to 100%) with product eluting at 0.1% on a 4 g silica column to afford **3d** in 65% yield (19.5 mg, 0.078 mmol) as an oil. ^1H NMR (400 MHz, CDCl_3) δ 7.44 (s, 1H), 7.27 (s, 1H), 5.28 – 5.03 (m, 1H), 3.36 (d, $J = 7.3$ Hz, 2H), 1.77 (s, 3H), 1.70 (s, 3H). ^{13}C NMR (101 MHz, CDCl_3) δ 139.9, 135.5, 133.1, 131.5, 131.3, 130.9, 130.8, 120.3, 31.9, 26.2, 18.4. GC/MS (m/z, relative intensity) 247 (M^+ , 15), 195 (30), 176 (35).

3e 1-(3-methylbut-2-en-1-yl)-4-nitrobenzene



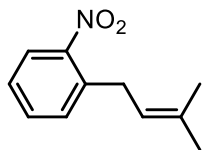
The general procedure **F** was followed using 4-nitroaniline (17 mg, 0.12 mmol), t-BuONO (24.7 mg, 28.5 μ l, 0.24 mmol), ((2-methylbut-3-en-2-yl)sulfonyl)benzene (126.2 mg, 0.6 mmol) and 0.6 mL of stock solution of Eosin Y in DMSO. After the completion of the reaction 14 h, the crude was purified via automated flash chromatography using EtOAc in hexanes (0% to 100%) with product eluting at 0.1% on a 4 g silica column to afford **3e** in 71% yield (16.2 mg, 0.085 mmol) as an oil. ^1H NMR (400 MHz, CDCl_3) δ 8.17 – 8.11 (apd, 2H), 7.32 (d, $J = 8.7$ Hz, 2H), 5.35 – 5.17 (m, 1H), 3.44 (d, $J = 7.3$ Hz, 2H), 1.77 (s, 3H), 1.72 (s, 3H). ^{13}C NMR (101 MHz, CDCl_3) δ 149.5, 146.1, 134.3, 128.9, 123.5, 121.0, 34.1, 25.6, 17.7. GC/MS (m/z, relative intensity) 191 (M^+ , 20), 174 (30), 130 (100).

3f 4-(3-methylbut-2-en-1-yl)benzoic acid



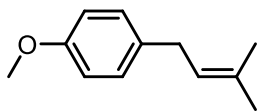
The general procedure **F** was followed using 4-aminobenzoic acid (16.5 mg, 0.12 mmol), t-BuONO (24.7 mg, 28.5 μ l, 0.24 mmol), ((2-methylbut-3-en-2-yl)sulfonyl)benzene (126.2 mg, 0.6 mmol) and 0.6 mL of stock solution of Eosin Y in DMSO. After completion of the reaction 15 h, the crude was purified via automated flash chromatography using EtOAc in hexanes 1% acetic acid (0% to 100%) with product eluting at 70% on a 4 g silica column to afford **3f** in 72% yield (16.4 mg, 0.086 mmol) as a white solid. ^1H NMR (400 MHz, CDCl_3) δ 7.95 (d, $J = 6.9$ Hz, 2H), 7.20 (d, $J = 7.5$ Hz, 2H), 5.28 – 5.18 (m, 1H), 3.34 (d, $J = 7.2$ Hz, 2H), 1.69 (s, 3H), 1.65 (s, 3H). ^{13}C NMR (101 MHz, CDCl_3) δ 171.8, 148.4, 133.7, 130.4, 128.5, 126.8, 121.9, 34.5, 25.7, 17.9. GC/MS (m/z , relative intensity) 190 (M^+ , 30), 145 (100), 131 (100).

3g 1-(3-methylbut-2-en-1-yl)-2-nitrobenzene



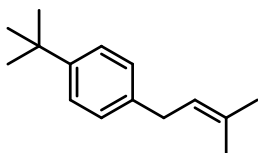
The general procedure **F** was followed using 2-nitroaniline (17 mg, 0.12 mmol), t-BuONO (24.7 mg, 28.5 μ l, 0.24 mmol), ((2-methylbut-3-en-2-yl)sulfonyl)benzene (126.2 mg, 0.6 mmol) and 0.6 mL of stock solution of Eosin Y in DMSO was used. After the completion of the reaction 14 h, the crude was purified via automated flash chromatography using EtOAc in hexanes (0% to 100%) with product eluting at 0.1% on a 4 g silica column to afford **3g** in 65% yield (15 mg, 0.078 mmol) as an oil. ^1H NMR (400 MHz, CDCl_3) δ 7.87 (d, $J = 8.1$ Hz, 1H), 7.51 (t, $J = 7.4, 7.4$ Hz, 1H), 7.38 – 7.30 (m, 2H), 5.29 – 5.20 (m, 1H), 3.63 (d, $J = 7.1$ Hz, 2H), 1.75 (s, 3H), 1.71 (s, 3H). ^{13}C NMR (101 MHz, CDCl_3) δ 149.6, 136.7, 134.8, 132.9, 131.5, 127.0, 124.6, 120.8, 31.4, 25.9, 18.1. GC/MS (m/z , relative intensity) 174 (20), 144 (95), 128 (100).

3h 1-methoxy-4-(3-methylbut-2-en-1-yl)benzene



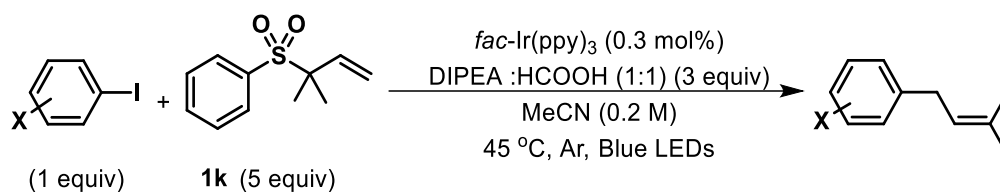
The general procedure **F** was followed using 4-methoxyaniline (15 mg, 0.12 mmol), t-BuONO (24.7 mg, 28.5 μ l, 0.24 mmol), ((2-methylbut-3-en-2-yl)sulfonyl)benzene (126.2 mg, 0.6 mmol) and 0.6 mL of stock solution of Eosin Y in DMSO. After completion of the reaction 19 h, the crude was purified via automated flash chromatography using EtOAc in hexanes (0% to 100%) with product eluting at 0.2% on a 4 g silica column to afford **3h** in 60% yield (12.6 mg, 0.072 mmol) as an oil. ^1H NMR (400 MHz, CDCl_3) δ 7.11 (dd, J = 8.4, 2.2 Hz, 2H), 6.85 (dd, J = 8.8, 2.5 Hz, 2H), 5.45 – 5.24 (m, 1H), 3.80 (d, J = 1.9 Hz, 3H), 3.30 (d, J = 7.3 Hz, 2H), 1.76 (s, 3H), 1.73 (s, 3H). ^{13}C NMR (101 MHz, Chloroform- d) δ 158.2, 134.4, 132.6, 129.6, 124.1, 114.2, 55.7, 33.9, 26.2, 18.2. GC/MS (m/z , relative intensity) 176 (M^+ , 60), 161 (100), 146 (30).

3i 1-(tert-butyl)-4-(3-methylbut-2-en-1-yl)benzene



The general procedure **F** was followed using 4-(tert-butyl)aniline (17.9 mg, 0.12 mmol), tBuONO (24.7 mg, 28.5 μ l, 0.24 mmol), ((2-methylbut-3-en-2-yl)sulfonyl)benzene (126.2 mg, 0.6 mmol) and 0.6 mL of stock solution of Eosin Y in DMSO. After completion of the reaction 19 h, the crude was purified via automated flash chromatography using EtOAc in hexanes (0% to 100%) with product eluting at 0.1% on a 4 g silica column to afford **3i** in 57% yield (13.8 mg, 0.068 mmol) as an oil. ^1H NMR (400 MHz, CDCl_3) δ 7.33 – 7.29 (apd, 2H), 7.13 (d, J = 8.4 Hz, 2H), 5.40 – 5.28 (m, 1H), 3.32 (d, J = 7.4 Hz, 2H), 1.75 (s, 3H), 1.73 (s, 3H), 1.31 (s, 9H). ^{13}C NMR (101 MHz, CDCl_3) δ 148.6, 138.9, 132.4, 128.1, 125.4, 123.5, 34.5, 34.0, 31.6, 25.9, 18.0. GC/MS (m/z , relative intensity) 202 (M^+ , 45), 187 (100), 145 (60). The compound produced a thermally generated rearranged product under GC conditions that was otherwise not observed in ^1H or ^{13}C NMR.

General procedure G for the photocatalytic prenylation of iodoarenes with prenyl sulfone (limiting iodoarene)

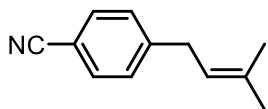


This procedure is identical to general procedure **E** except with following changes, where, Iodoarene (0.12 mmol, 1 equiv) and N,N-diisopropylethylamine (0.36 mmol, 62.7 μ l, 3 equiv) were used in MeCN (0.2 M with respect to iodoarene).

3a methyl 4-(3-methylbut-2-en-1-yl)benzoate

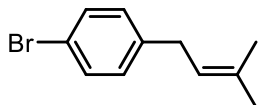
The general procedure **G** was followed using methyl 4-iodobenzoate (31.4 mg, 0.12 mmol), N,N-diisopropylethylamine (62.7 μ l, 0.36 mmol), formic acid (13.6 μ l, 0.36 mmol), ((2-methylbut-3-en-2-yl)sulfonyl)benzene (126.2 mg, 0.6 mmol) and 0.6 mL of stock solution of Ir(ppy)₃ in MeCN. After completion of the reaction, 32 h, the crude was purified via automated flash chromatography using EtOAc in hexanes (0% to 100%) with product eluting at 0.1% on a 4 g silica column to afford **3a** in 65% yield (16 mg, 0.078 mmol) as an oil. ¹H NMR (400 MHz, CDCl₃) δ 7.94 (d, *J* = 8.2 Hz, 2H), 7.24 (d, *J* = 8.2 Hz, 2H), 5.37 – 5.25 (m, 1H), 3.90 (s, 3H), 3.39 (d, *J* = 7.3 Hz, 2H), 1.76 (s, 3H), 1.72 (s, 3H). ¹³C NMR (101 MHz, CDCl₃) δ 167.3, 147.5, 133.6, 129.9, 128.5, 127.8, 122.2, 52.1, 34.6, 25.9, 18.0. GC/MS (*m/z*, relative intensity) 204 (M⁺, 35), 189 (20), 145 (100).

3b 4-(3-methylbut-2-en-1-yl)benzonitrile



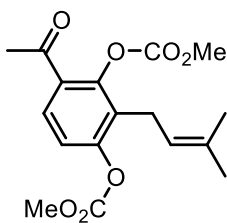
The general procedure **G** was followed using 4-iodobenzonitrile (27.5 mg, 0.12 mmol), N,N-diisopropylethylamine (62.7 μ l, 0.36 mmol), formic acid (13.6 μ l, 0.36 mmol), ((2-methylbut-3-en-2-yl)sulfonyl)benzene (126.2 mg, 0.6 mmol) and 0.6 mL of stock solution of Ir(ppy)₃ in MeCN. After the completion of the reaction, 30 h, the crude was purified via automated flash chromatography using EtOAc in hexanes (0% to 100%) with product eluting at 0.2% on a 4 g silica column to afford **3b** in 62% yield (12.7 mg, 0.074 mmol) as an oil. ¹H NMR (400 MHz, CDCl₃) δ 7.56 (apd, *J* = 8.2 Hz, 2H), 7.27 (d, *J* = 7.5 Hz, 2H), 5.34 – 5.19 (m, 1H), 3.39 (d, *J* = 7.4 Hz, 2H), 1.76 (s, 3H), 1.71 (s, 3H). ¹³C NMR (101 MHz, CDCl₃) δ 147.6, 134.4, 132.3, 129.2, 121.5, 119.3, 109.7, 34.6, 25.9, 18.0. GC/MS (*m/z*, relative intensity) 171 (M⁺, 50), 156 (100), 142 (40).

3c 1-bromo-4-(3-methylbut-2-en-1-yl)benzene



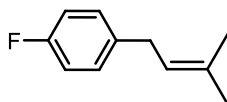
The general procedure **G** was followed using 1-bromo-4-iodobenzene (34 mg, 0.12 mmol), N,N-diisopropylethylamine (62.7 μ l, 0.36 mmol), formic acid (13.6 μ l, 0.36 mmol), ((2-methylbut-3-en-2-yl)sulfonyl)benzene (126.2 mg, 0.6 mmol) and 0.6 mL of stock solution of Ir(ppy)₃ in MeCN. After the completion of the reaction 33 h, the crude was purified via automated flash chromatography using EtOAc in hexanes (0% to 100%) with product eluting at 100% hexane on a 4 g silica column to afford **3c** in 60% yield (16.2 mg, 0.072 mmol) as an oil. ¹H NMR (400 MHz, CDCl₃) δ 7.41 – 7.33 (apd, 2H), 7.05 (d, *J* = 8.3 Hz, 2H), 5.31 – 5.25 (m, 1H), 3.29 (d, *J* = 7.3 Hz, 2H), 1.75 (s, 3H), 1.71 (s, 3H). ¹³C NMR (101 MHz, CDCl₃) δ 141.2, 133.6, 131.8, 130.5, 122.9, 119.9, 34.2, 26.2, 18.3. GC/MS (*m/z*, relative intensity) 224 (M⁺, 20), 145 (40), 130 (100).

4d 4-acetyl-2-(3-methylbut-2-en-1-yl)-1,3-phenylene dimethyl bis(carbonate)



The general procedure **G** was followed using 4-acetyl-2-iodo-1,3-phenylene dimethyl bis(carbonate) (47.3 mg, 0.12 mmol), *N,N*-diisopropylethylamine (62.7 μ l, 0.36 mmol), formic acid (13.6 μ l, 0.36 mmol), ((2-methylbut-3-en-2-yl)sulfonyl)benzene (126.2 mg, 0.6 mmol) and 0.6 mL of stock solution of Ir(ppy)₃ in MeCN. After completion of the reaction 33 h, the crude was purified via automated flash chromatography using EtOAc in hexanes (0% to 100%) with product eluting at 20% on a 4 g silica column to afford **4d** in 60% yield as an oil which includes 24% reduced product. ¹H NMR (400 MHz, CDCl₃) δ 7.72 (d, *J* = 8.6 Hz, 2H), 7.20 (d, *J* = 8.5 Hz, 2H), 5.05 – 4.99 (m, 1H), 3.92 (s, 3H), 3.91 (s, 3H), 3.32 (d, *J* = 7.0 Hz, 2H), 2.55 (s, 3H), 1.72 (s, 3H), 1.66 (s, 3H). ¹³C NMR (101 MHz, CDCl₃) δ 196.9, 154.4, 153.5, 153.2, 152.9, 133.5, 128.9, 128.7, 128.2, 120.1, 119.9, 118.9, 55.9, 29.2, 25.8, 23.8, 17.8. GC/MS (*m/z*, relative intensity) 336 (*M*⁺, 5), 304 (15), 277 (40).

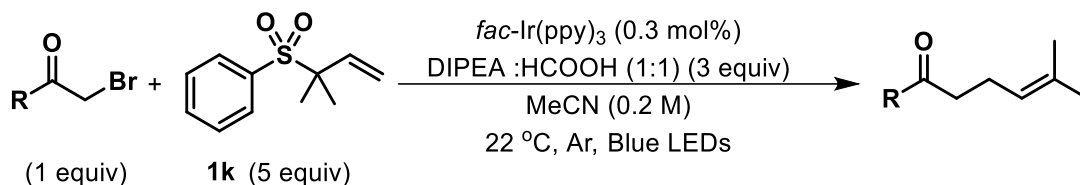
4e 1-fluoro-4-(3-methylbut-2-en-1-yl)benzene



The general procedure **G** was followed using 1-fluoro-4-iodobenzene (14 μ l, 0.12 mmol), *N,N*-diisopropylethylamine (62.7 μ l, 0.36 mmol), formic acid (13.6 μ l, 0.36 mmol), ((2-methylbut-3-en-2-yl)sulfonyl)benzene (126.2 mg, 0.6 mmol) and 0.6 mL of stock solution of Ir(ppy)₃ in MeCN. After the completion of the reaction 33 h, it afforded **8a** in 55% ¹⁹F NMR yield. The crude material was purified by using Prep TLC with 100% hexanes and afforded **4e** in 48% yield. Minimal effort was given to evaporate the solvent due to volatile nature of the product. ¹H NMR (400 MHz, CDCl₃) δ 7.15 – 7.07 (m, 2H), 7.01 – 6.89 (m, 2H), 5.39 – 5.19 (m, 1H), 3.31 (d, *J* = 7.1 Hz, 2H), 1.75 (s, 3H), 1.71 (s, 3H). ¹⁹F NMR (376 MHz, CDCl₃) δ -118.12 (ddd, *J* = 14.2, 8.8, 5.5 Hz). ¹³C NMR (101 MHz, CDCl₃) δ 161.3 (d, *J* = 243.1 Hz), 137.5 (d, *J* = 3.2 Hz), 132.9, 129.7 (d, *J* = 7.7

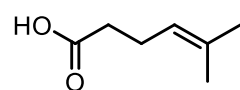
Hz), 123.2, 115.2 (d, $J = 21.1$ Hz), 33.6, 25.9, 17.9. GC/MS (m/z, relative intensity) 164 (M^+ , 50), 149 (100), 109 (90).

General procedure H for the photocatalytic prenylation of α carbonyl bromides with prenyl sulfone (limiting α -carbonyl bromides)

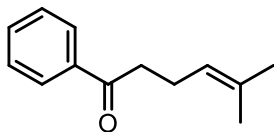


This procedure is identical to general procedure **G** except the reactions were carried out in a light bath where the temperature was maintained at 22 °C.

5a 5-methylhex-4-enoic acid

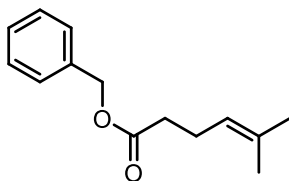
 The general procedure **H** was followed using 2-bromoacetic acid (16.7 mg, 0.12 mmol), N,N-diisopropylethylamine (62.7 μ l, 0.36 mmol), formic acid (13.6 μ l, 0.36 mmol), ((2-methylbut-3-en-2-yl)sulfonyl)benzene (126.2 mg, 0.6 mmol) and 0.6 mL of stock solution of Ir(ppy)₃ in MeCN. After completion of the reaction 24 h, the crude was purified via automated flash chromatography using EtOAc in hexanes (0% to 100%) under 1% acetic acid with product eluting at 60% on a 4 g silica column to afford **5a** in 65% yield (10 mg, 0.078 mmol) as an oil. ¹H NMR (400 MHz, CDCl₃) δ 5.25 – 4.92 (m, 1H), 2.40 – 2.35 (m, 2H), 2.35 – 2.28 (m, 2H), 1.69 (s, 3H), 1.63 (s, 3H). ¹³C NMR (101 MHz, CDCl₃) δ 179.2, 133.6, 122.2, 34.3, 25.8, 23.5, 17.8. GC/MS (m/z, relative intensity) 128 (M^+ , 40), 110 (5), 69 (100). The compound produced some thermally generated impurities under GC conditions.

5b 5-methyl-1-phenylhex-4-en-1-one



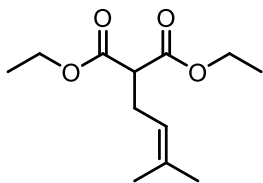
The general procedure **H** was followed using 2-bromo-1-phenylethan-1-one (23.9 mg, 0.12 mmol), N,N-diisopropylethylamine (62.7 μ l, 0.36 mmol), formic acid (13.6 μ l, 0.36 mmol), ((2-methylbut-3-en-2-yl)sulfonyl)benzene (126.2 mg, 0.6 mmol) and 0.6 mL of stock solution of Ir(ppy)₃ in MeCN. After completion of the reaction 23 h, the crude was purified via automated flash chromatography using EtOAc in hexanes (0% to 100%) with product eluting at 0.2% on a 4 g silica column to afford **5b** in 66% yield (15 mg, 0.08 mmol) as an oil. ¹H NMR (400 MHz, CDCl₃) δ 7.99 – 7.93 (m, 2H), 7.59 – 7.52 (m, 1H), 7.46 (t, *J* = 7.5, 7.5 Hz, 2H), 5.22 – 5.12 (m, 1H), 3.02 (t, 2H), 2.42 (q, *J* = 7.4, 7.4, 7.3 Hz, 2H), 1.69 (s, 3H), 1.64 (s, 3H). ¹³C NMR (101 MHz, CDCl₃) δ 200.1, 137.0, 132.9, 132.8, 128.5, 128.1, 122.9, 38.8, 25.7, 22.9, 17.7. GC/MS (*m/z*, relative intensity) 188 (M⁺, 5), 170 (10), 105 (100).

5c benzyl 5-methylhex-4-enoate



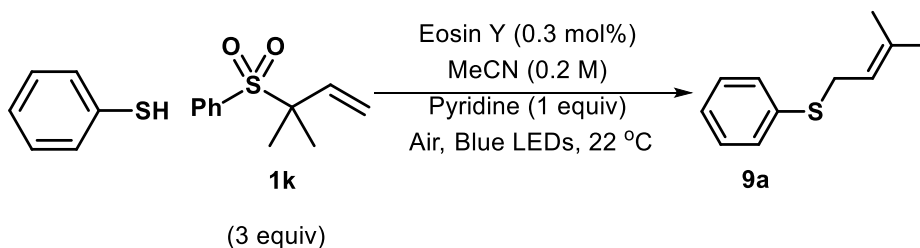
The general procedure **H** was followed using benzyl 2-bromoacetate (27.5 mg, 0.12 mmol), N,N-diisopropylethylamine (62.7 μ l, 0.36 mmol), formic acid (13.6 μ l, 0.36 mmol), ((2-methylbut-3-en-2-yl)sulfonyl)benzene (126.2 mg, 0.6 mmol) and 0.6 mL of stock solution of Ir(ppy)₃ in MeCN. After the completion of the reaction 21 h, the crude was purified via automated flash chromatography using EtOAc in hexanes (0% to 100%) with product eluting at 0.1% on a 4 g silica column to afford **5c** in 64% yield (16.7 mg, 0.077 mmol) as an oil. ¹H NMR (400 MHz, Chloroform-*d*) δ 7.38 – 7.32 (m, 5H), 5.12 (s, 1H), 5.11 – 5.06 (m, 1H), 2.38 (dd, *J* = 8.1, 5.1 Hz, 2H), 2.36 – 2.29 (m, 2H), 1.67 (s, 3H), 1.60 (s, 3H). ¹³C NMR (101 MHz, Chloroform-*d*) δ 173.4, 136.3, 133.3, 128.7, 128.3, 128.3, 122.5, 66.3, 34.7, 25.8, 23.8, 17.8. GC/MS (*m/z*, relative intensity) 182 (15), 127 (50), 91 (100). The compound produced some thermally generated impurities under GC conditions.

5d diethyl 2-(3-methylbut-2-en-1-yl)malonate



The general procedure **H** was followed using diethyl 2-bromomalonate (28.7 mg, 0.12 mmol), *N,N*-diisopropylethylamine (62.7 μ l, 0.36 mmol), formic acid (13.6 μ l, 0.36 mmol), ((2-methylbut-3-en-2-yl)sulfonyl)benzene (126.2 mg, 0.6 mmol) and 0.6 mL of stock solution of Ir(ppy)₃ in MeCN. After the completion of the reaction 25 h, the crude was purified via automated flash chromatography using EtOAc in hexanes (0% to 100%) with product eluting at 8% on a 4 g silica column to afford **5d** in 60% yield (11 mg, 0.08 mmol) as an oil. ¹H NMR (400 MHz, CDCl₃) δ 5.12 – 5.00 (m, 1H), 4.19 (q, *J* = 7.1, 7.1, 7.1 Hz, 4H), 3.32 (t, *J* = 7.7, 7.7 Hz, 1H), 2.58 (t, *J* = 7.5, 7.5 Hz, 2H), 1.68 (s, 3H), 1.63 (s, 3H), 1.26 (t, *J* = 7.1, 7.1 Hz, 6H). ¹³C NMR (101 MHz, CDCl₃) δ 169.4, 135.0, 119.8, 61.4, 52.4, 27.7, 25.9, 17.9, 14.2. GC/MS (*m/z*, relative intensity) 228 (M⁺, 10), 160 (30), 139 (40). The compound produced a thermally generated impurity under GC conditions that was otherwise not observed in ¹H or ¹³C NMR.

Photocatalytic prenylation via photooxidative process

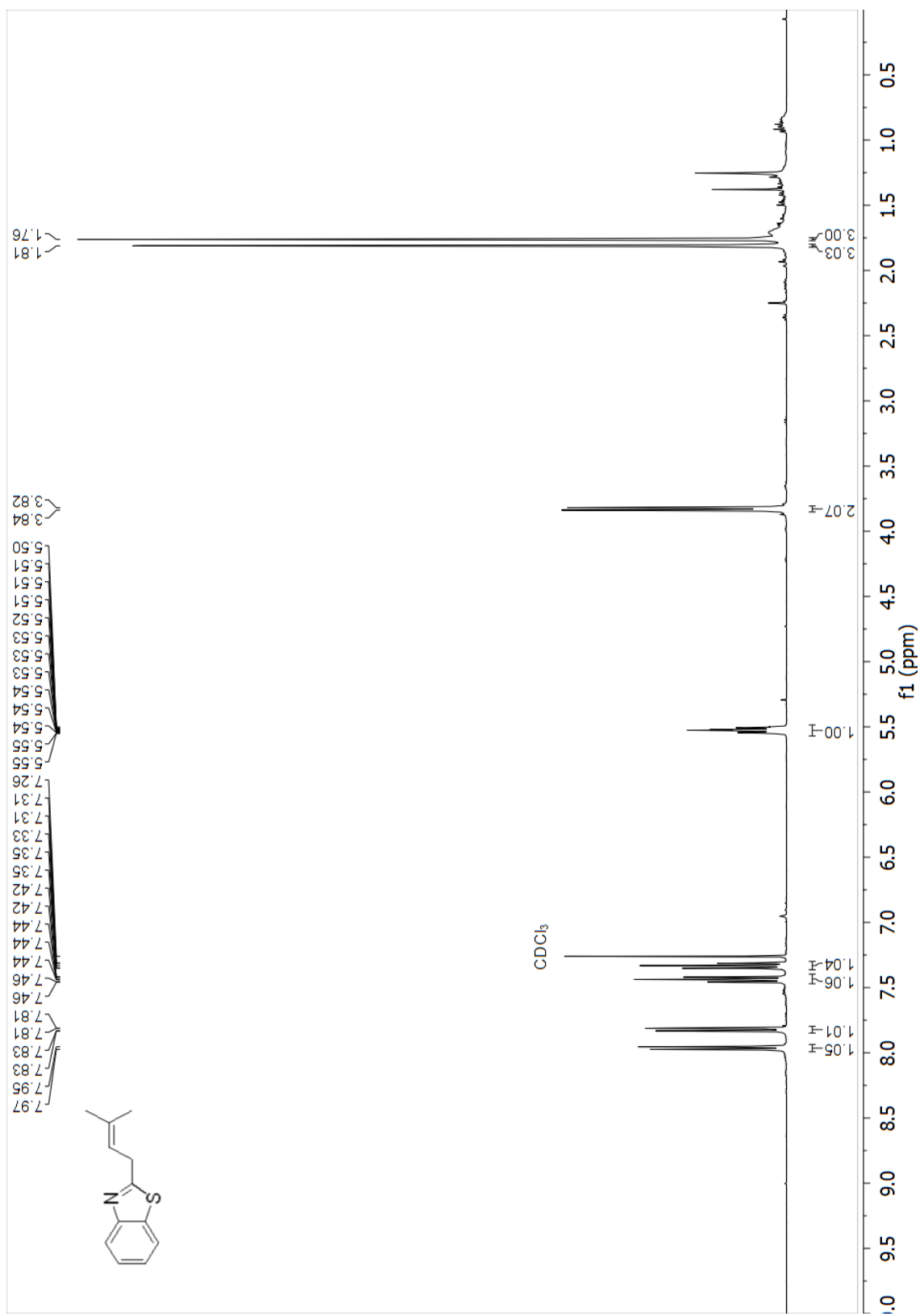


Thiophenol (13.2 mg, 0.12 mmol), ((2-methylbut-3-en-2-yl)sulfonyl)benzene (82 mg, 0.39 mmol), pyridine (0.12 mmol) and 0.6 mL of stock solution of Eosin Y (0.003 mmol) in MeCN. Then the tube was placed in a light bath. After completion of the reaction 6 h, the crude was purified via automated flash chromatography using EtOAc in hexanes (0% to 100%) with product eluting at 0.1% on a 4 g

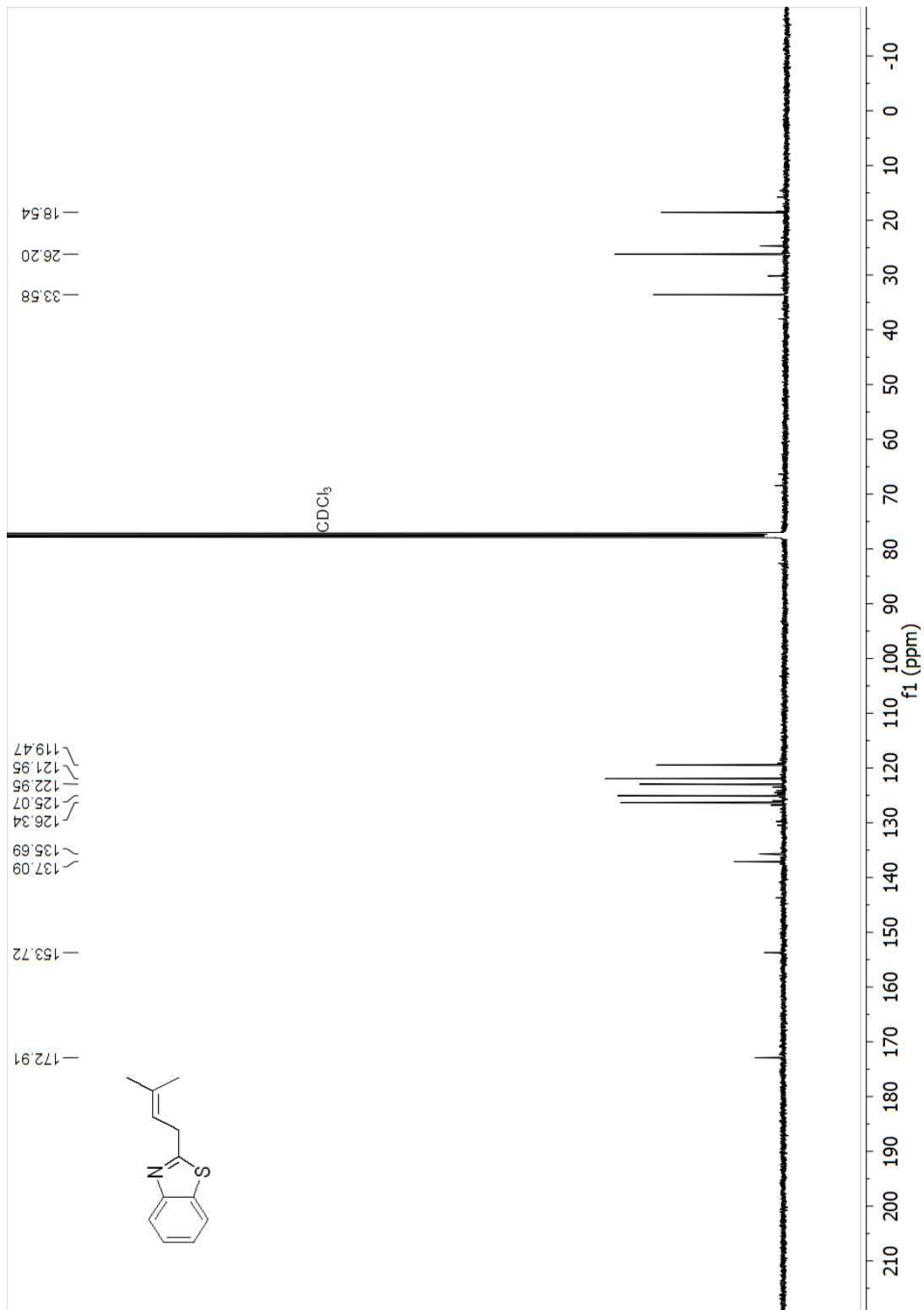
silica column to afford the product in 91% yield. ^1H NMR shifts match with literature values. GC/MS showed the mass of the product 178 (M^+).

Irradiation of the reaction mixture absence of Eosin Y, produced only 6% of product after 6 h.

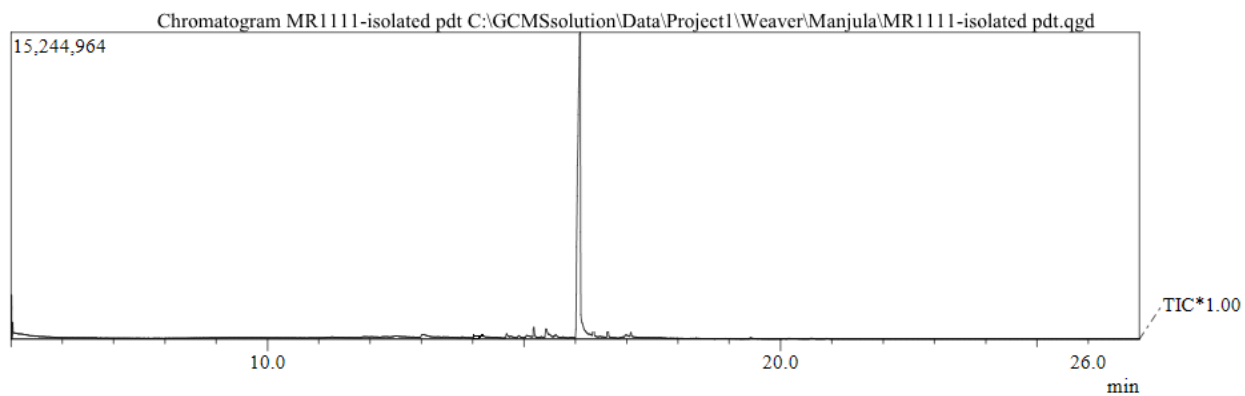
^1H NMR (400 MHz, Chloroform-d) spectrum of 2a (2-(3-methylbut-2-en-1-yl)benzo[d]thiazole)



^{13}C NMR (101 MHz, Chloroform-d) spectrum of 2a (2-(3-methylbut-2-en-1-yl)benzo[d]thiazole)

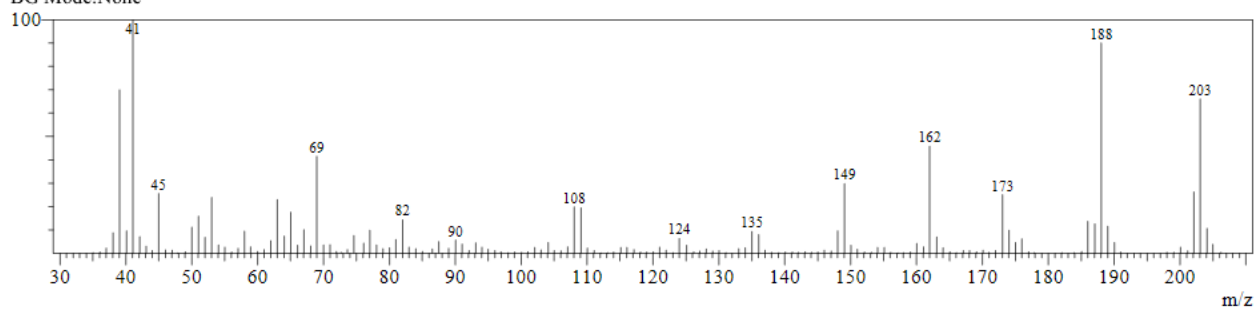


GC and MS of 2a (2-(3-methylbut-2-en-1-yl)benzo[d]thiazole)

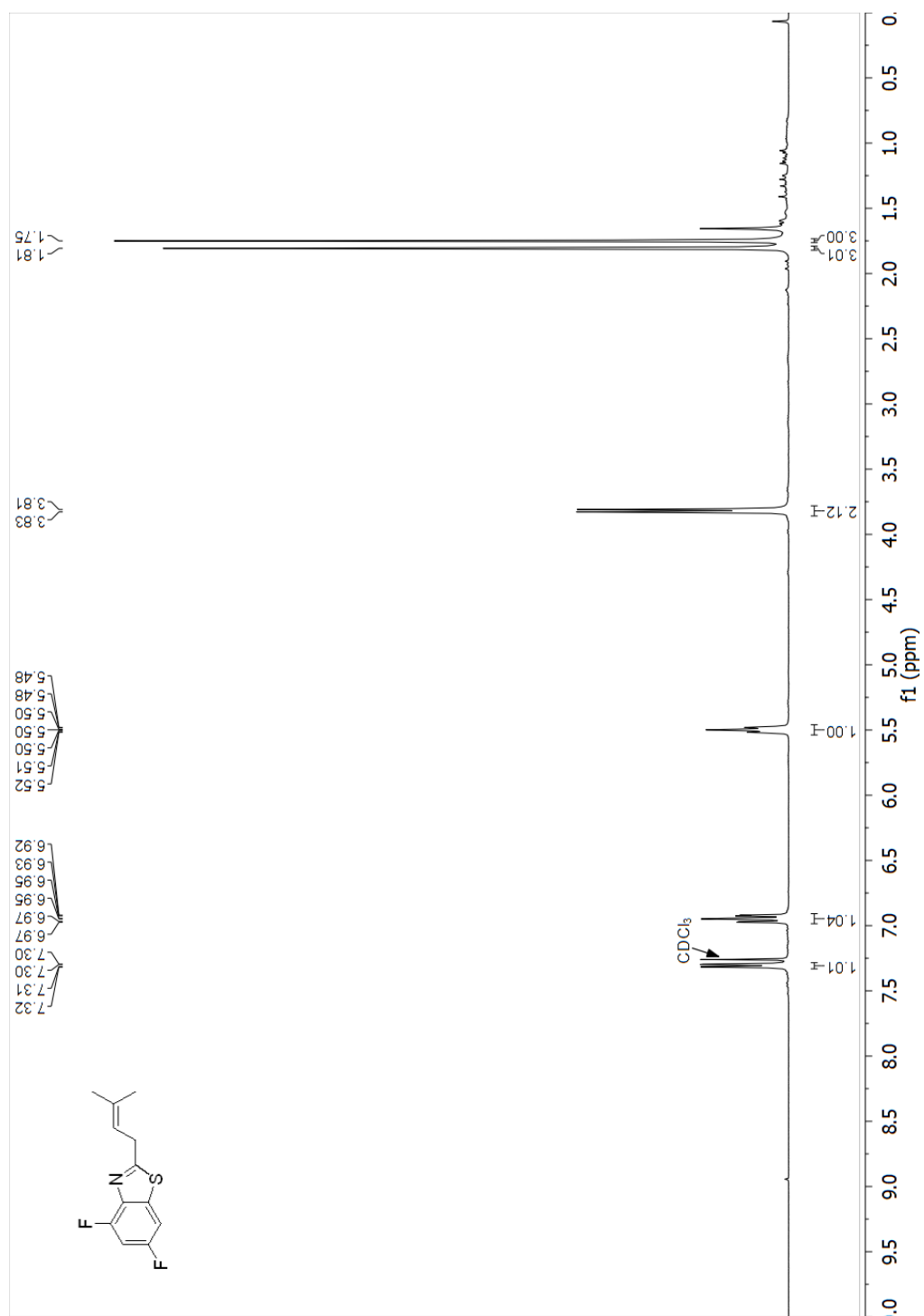


Spectrum

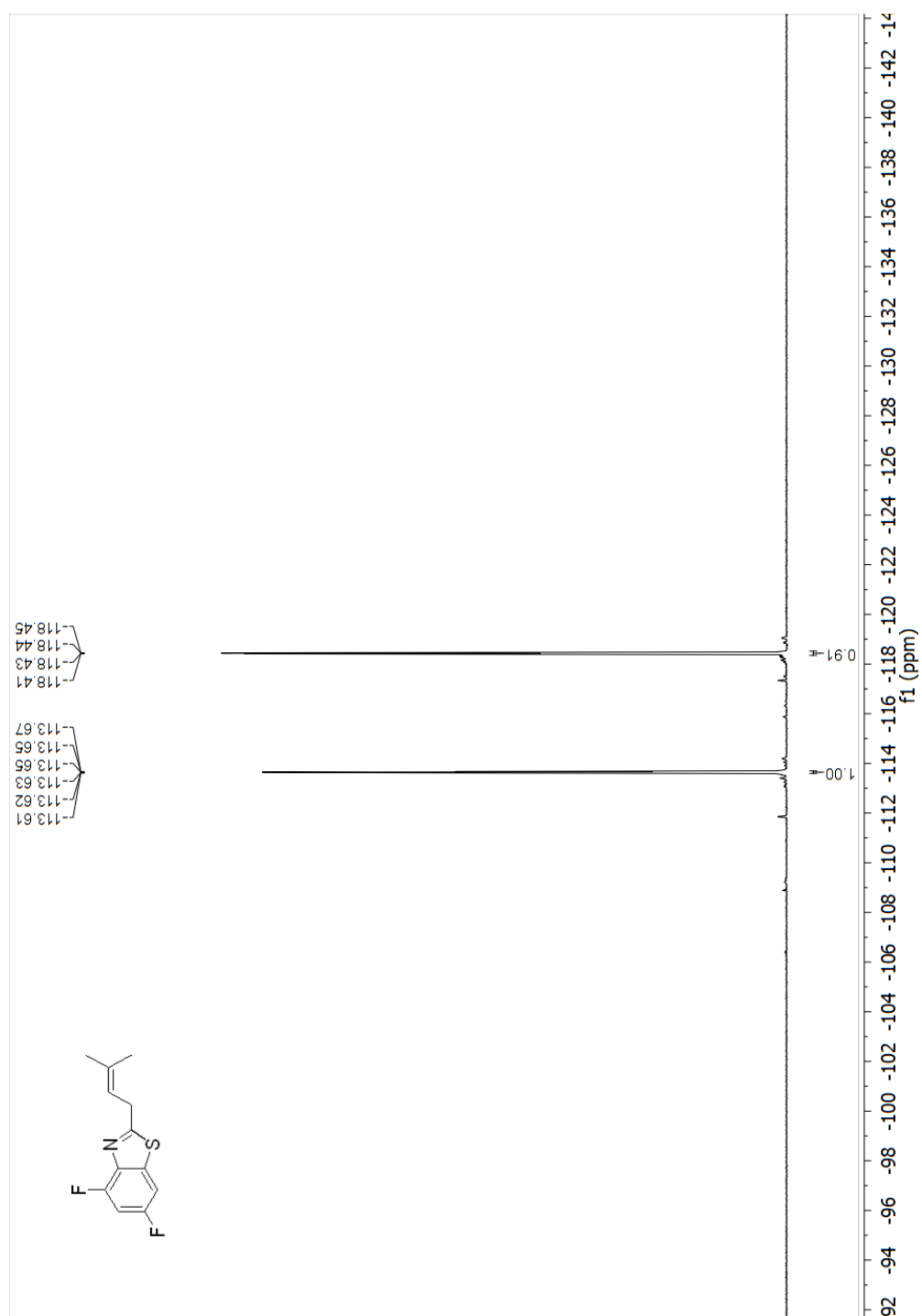
Line#:1 R.Time:16.0(Scan#:1326)
MassPeaks:160
RawMode:Single 16.0(1326) BasePeak:41(825548)
BG Mode:None



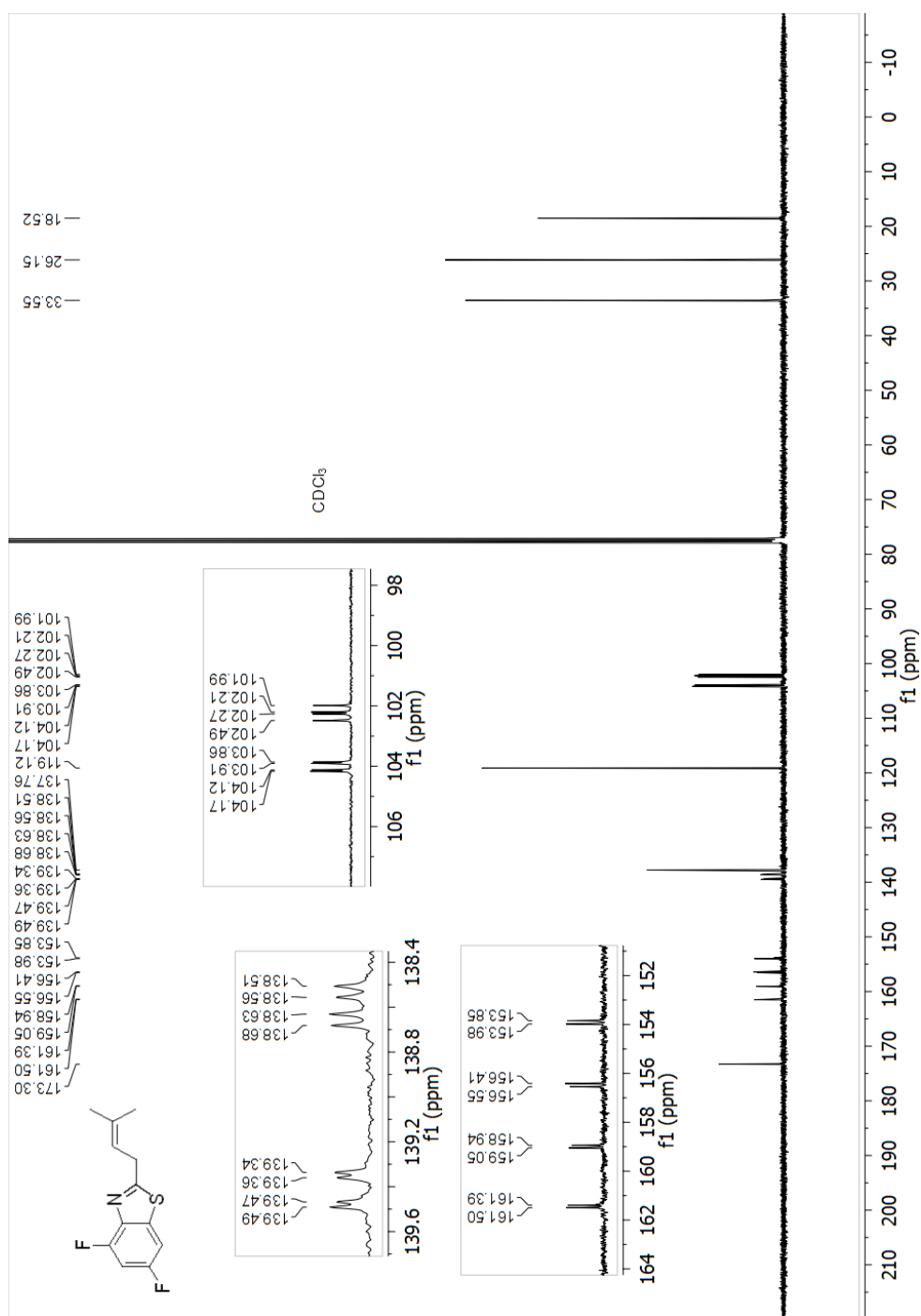
¹H NMR (400 MHz, Chloroform-d) spectrum of 2b (4,6-difluoro-2-(3-methylbut-2-en-1-yl)benzo[d]thiazole)



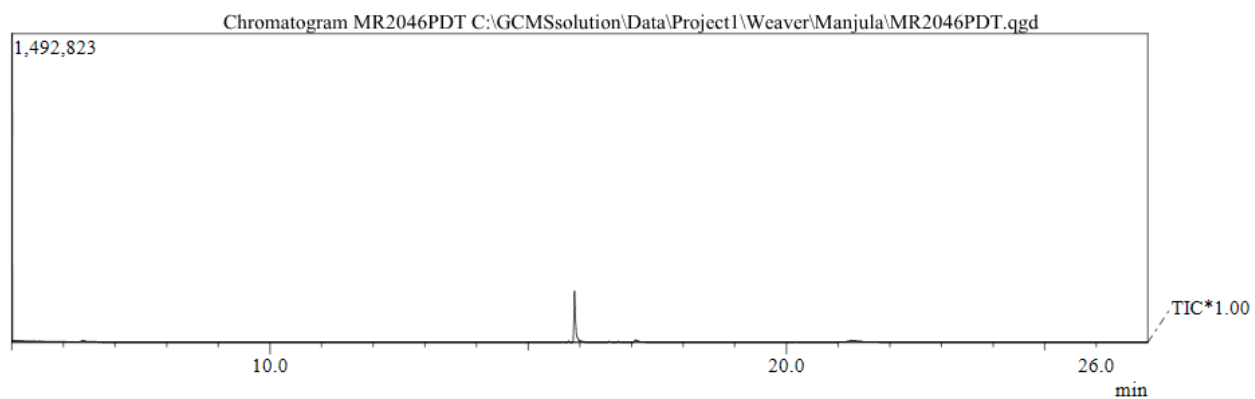
^{19}F NMR (376 MHz, Chloroform-d) spectrum of 2b (4,6-difluoro-2-(3-methylbut-2-en-1-yl)benzo[d]thiazole)



¹³C NMR (101 MHz, Chloroform-d) spectrum of 2b (4,6-difluoro-2-(3-methylbut-2-en-1-yl)benzo[d]thiazole)

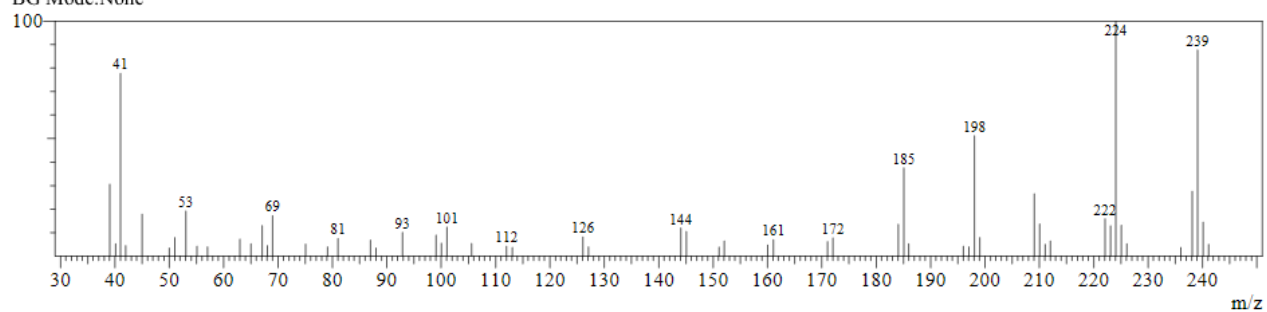


GC and MS of 2b (4,6-difluoro-2-(3-methylbut-2-en-1-yl)benzo[d]thiazol

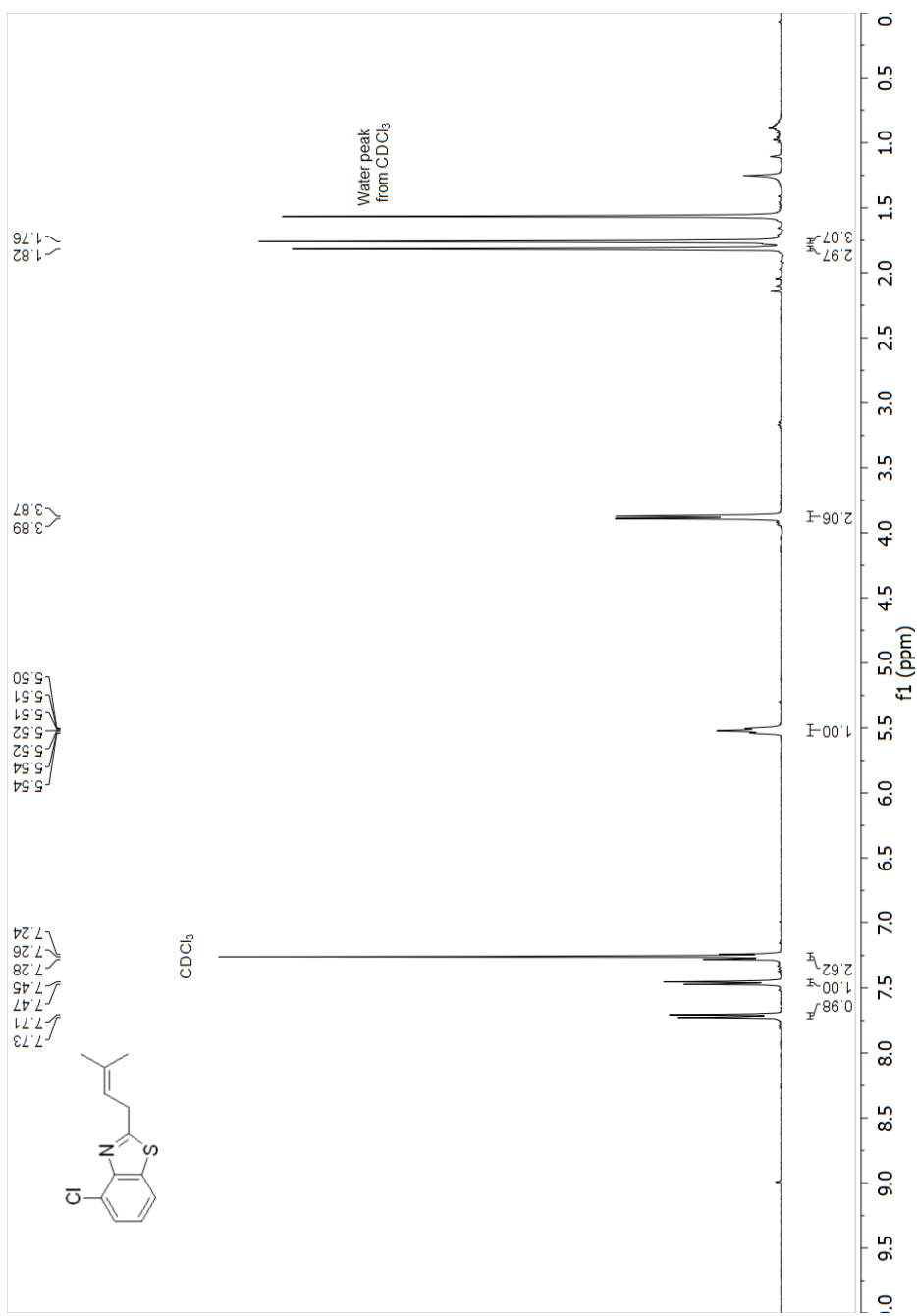


Spectrum

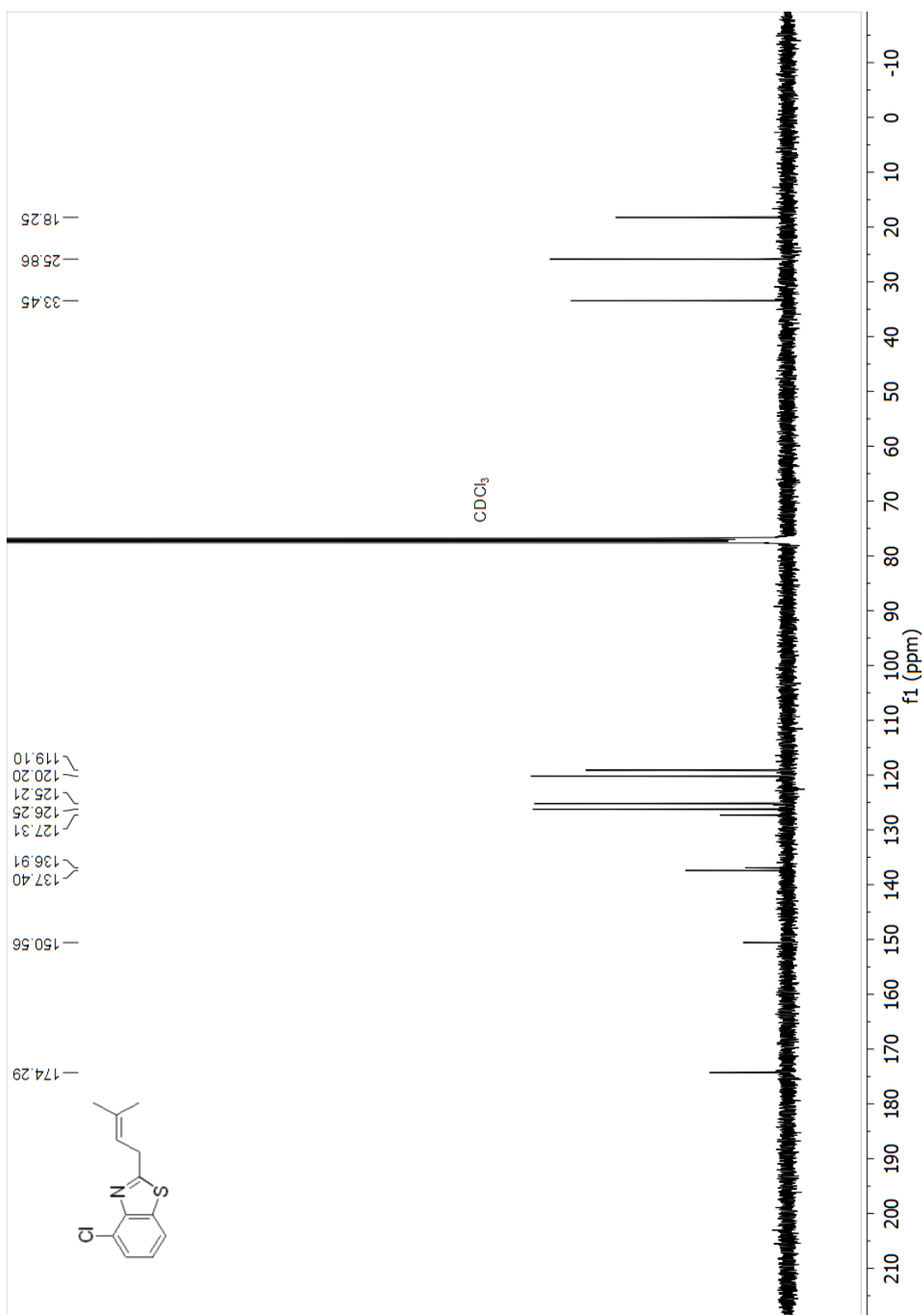
Line#:1 R.Time:15.9(Scan#:1309)
MassPeaks:58
RawMode:Single 15.9(1309) BasePeak:224(29994)
BG Mode:None



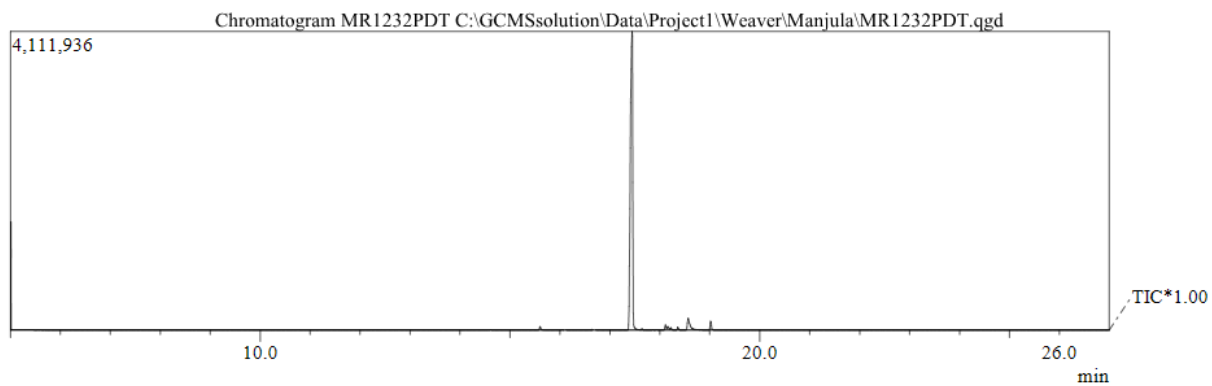
¹H NMR (400 MHz, Chloroform-d) spectrum of 2c (4-chloro-2-(3-methylbut-2-en-1-yl)benzo[d]thiazole)



^{13}C NMR (101 MHz, Chloroform-d) spectrum of 2c (4-chloro-2-(3-methylbut-2-en-1-yl)benzo[d]thiazole)

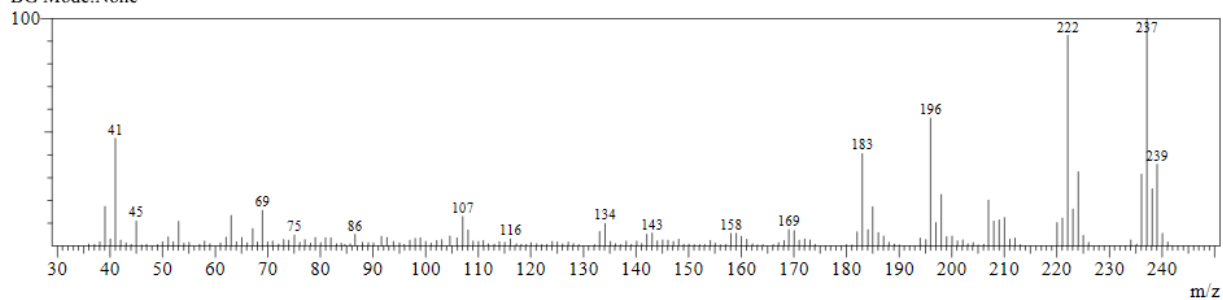


GC and MS of 2c (4-chloro-2-(3-methylbut-2-en-1-yl)benzo[d]thiazole)

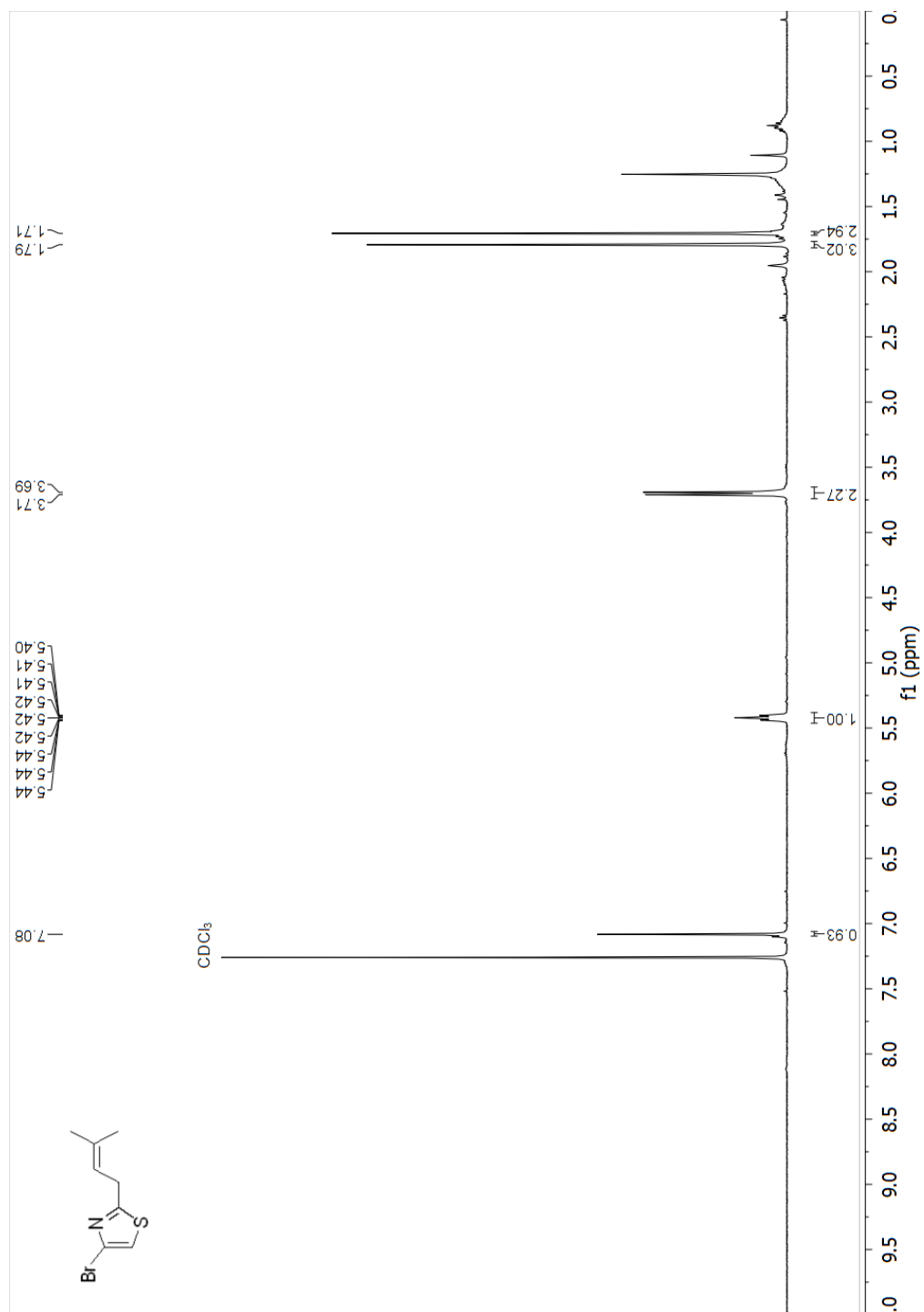


Spectrum

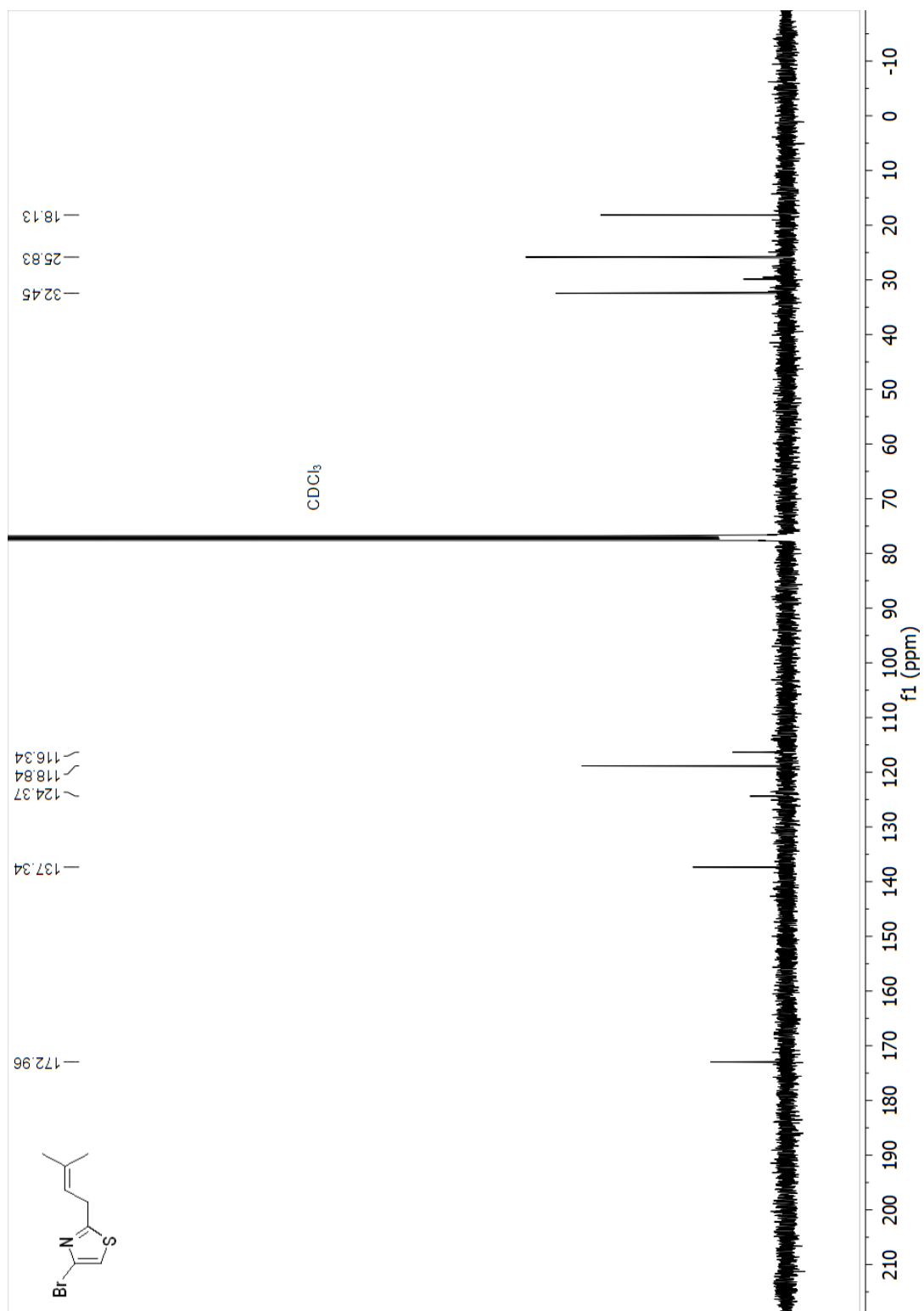
Line#:1 R.Time:17.4(Scan#:1491)
MassPeaks:177
RawMode:Single 17.4(1491) BasePeak:237(304010)
BG Mode:None



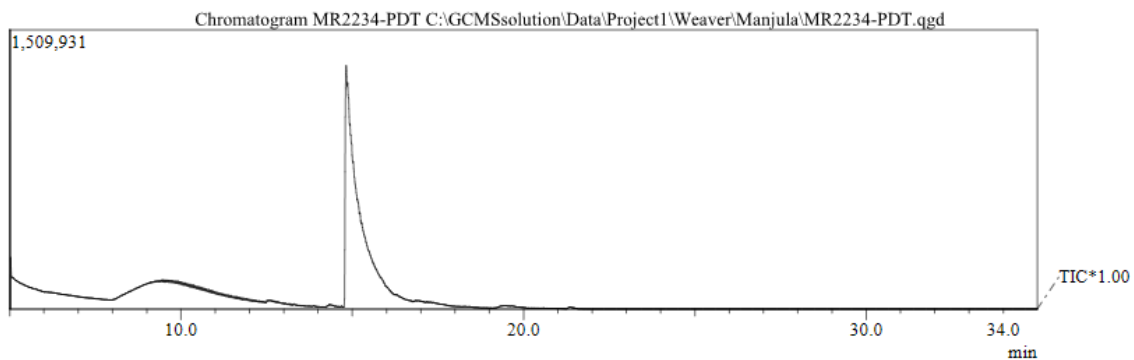
^1H NMR (400 MHz, Chloroform-d) spectrum of 2d (4-bromo-2-(3-methylbut-2-en-1-yl)thiazole)



^{13}C NMR (101 MHz, Chloroform-d) spectrum of 2d (4-bromo-2-(3-methylbut-2-en-1-yl)thiazole)

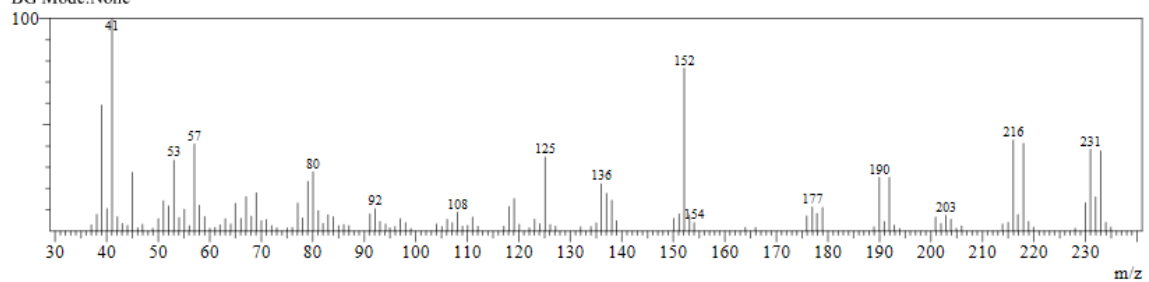


GC and MS of 2d (4-bromo-2-(3-methylbut-2-en-1-yl)thiazole)

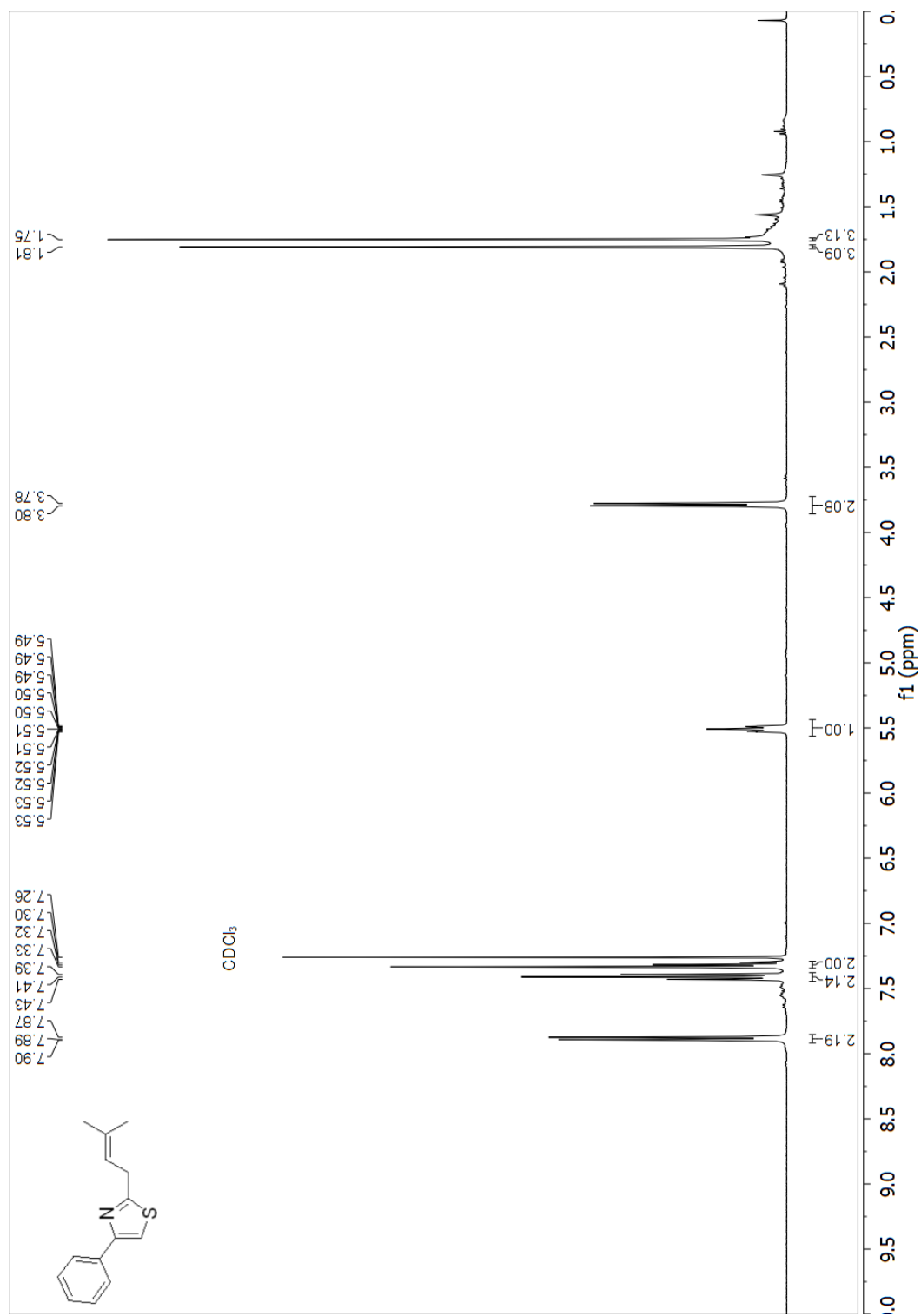


Spectrum

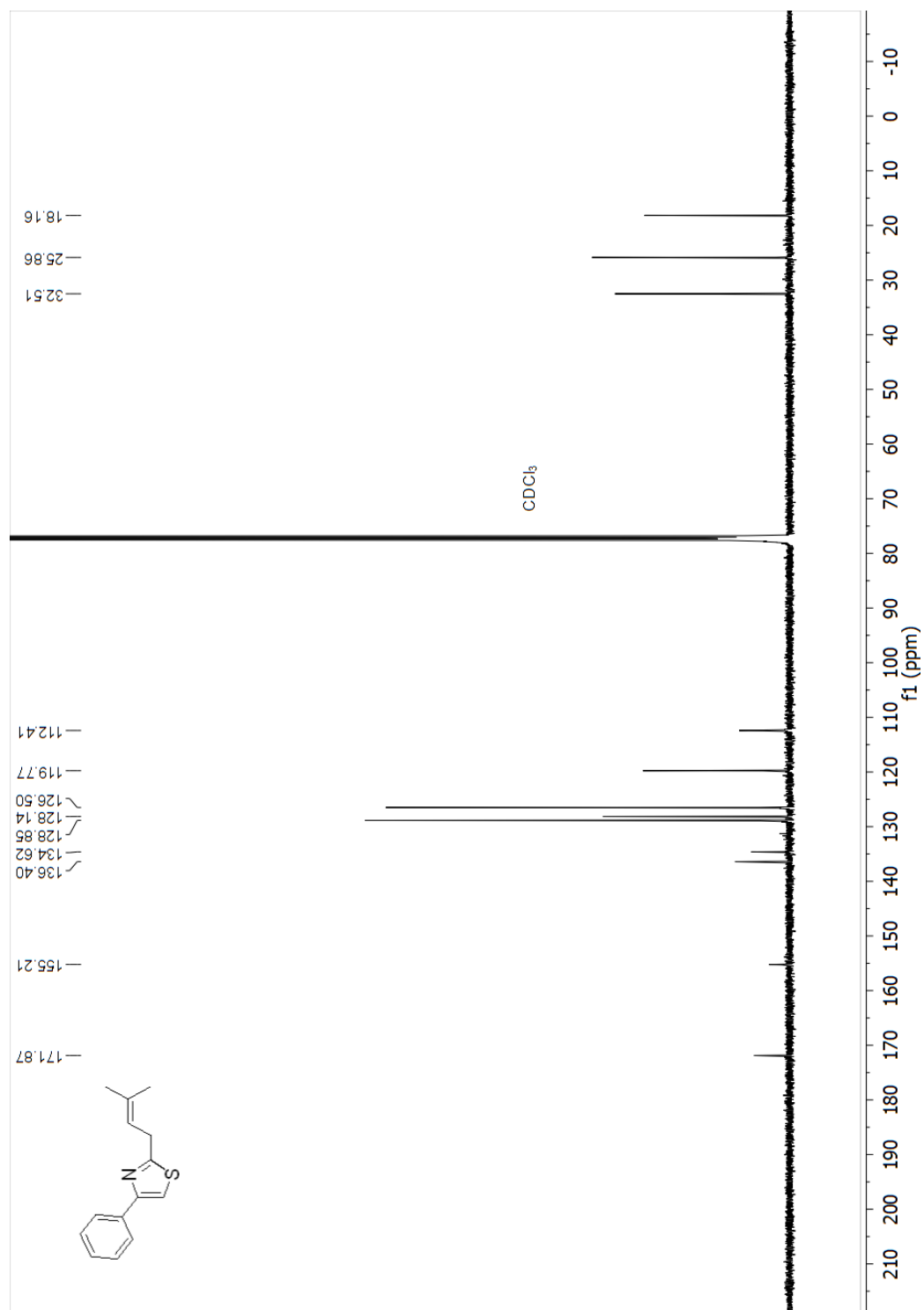
Line#:1 R.Time:14.9(Scan#:1190)
MassPeaks:121
RawMode:Single 14.9(1190) BasePeak:41(83462)
BG Mode:None



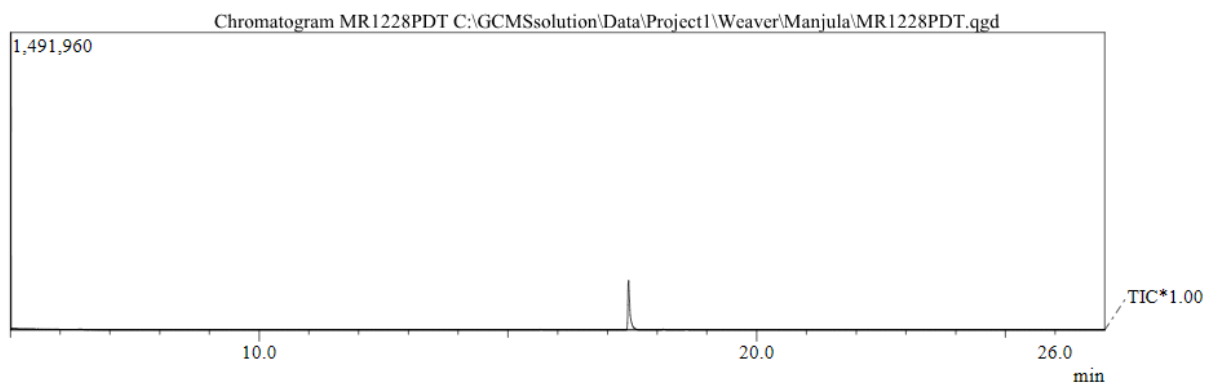
¹H NMR (400 MHz, Chloroform-d) spectrum of 2e (2-(3-methylbut-2-en-1-yl)-4-phenylthiazole)



¹³C NMR (101 MHz, Chloroform-d) spectrum of 2e (2-(3-methylbut-2-en-1-yl)-4-phenylthiazole)

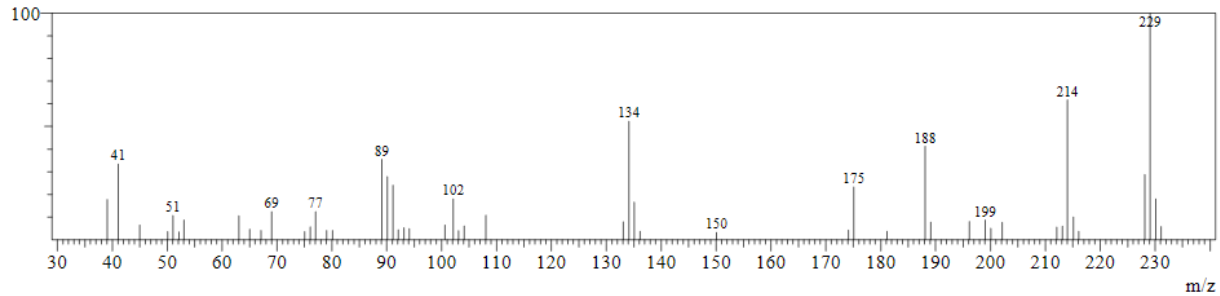


GC and MS of 2e (2-(3-methylbut-2-en-1-yl)-4-phenylthiazole)

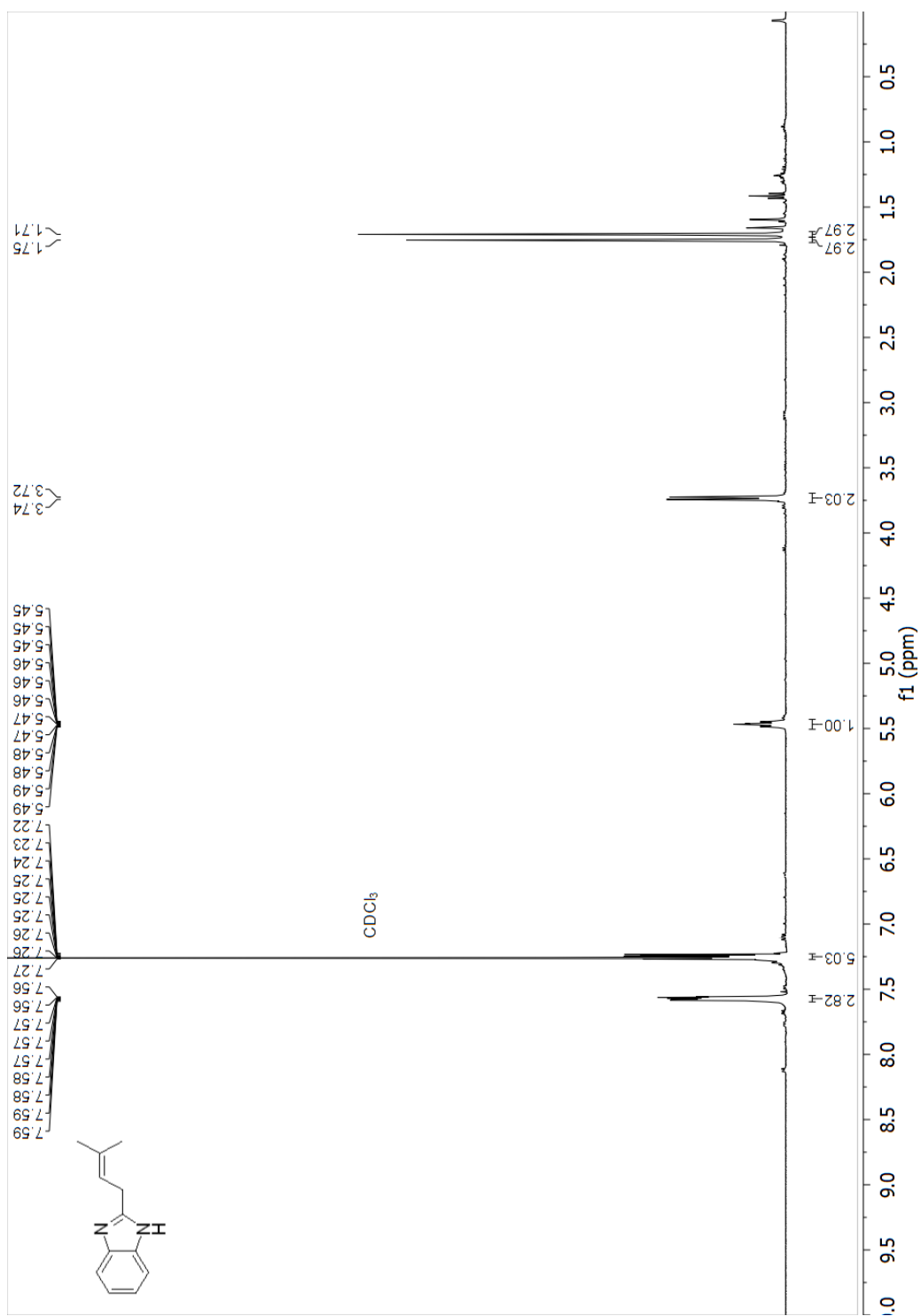


Spectrum

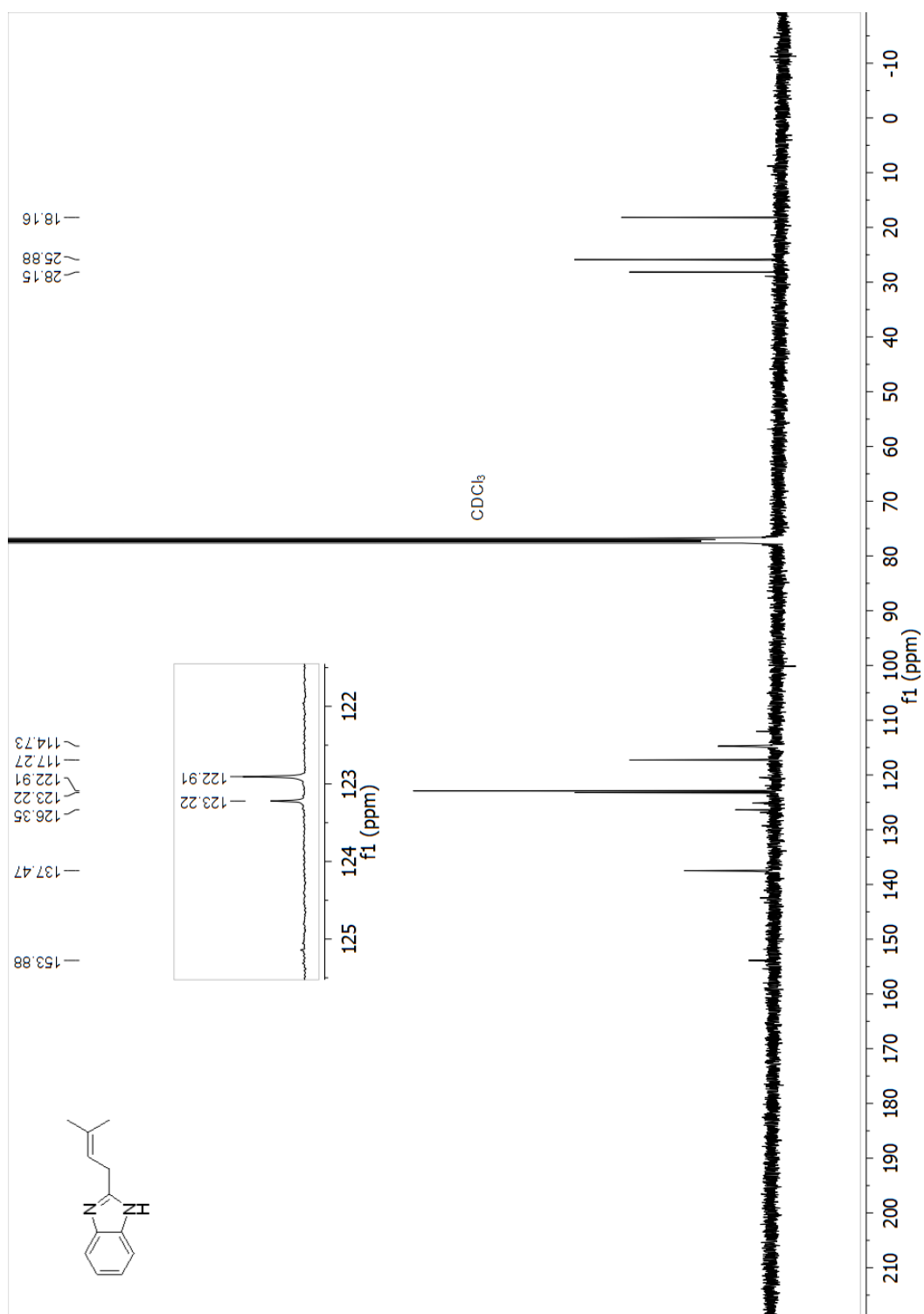
Line#:1 R.Time:17.4(Scan#:1491)
MassPeaks:50
RawMode:Single 17.4(1491) BasePeak:229(31460)
BG Mode:None



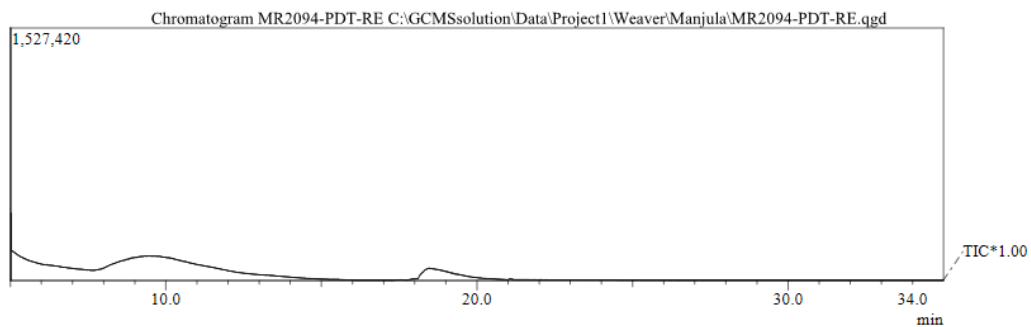
^1H NMR (400 MHz, Chloroform-d) spectrum of 2f (2-(3-methylbut-2-en-1-yl)-1H-benzo[d]imidazole)



^{13}C NMR (101 MHz, Chloroform-d) spectrum of 2f (2-(3-methylbut-2-en-1-yl)-1H-benzo[d]imidazole)



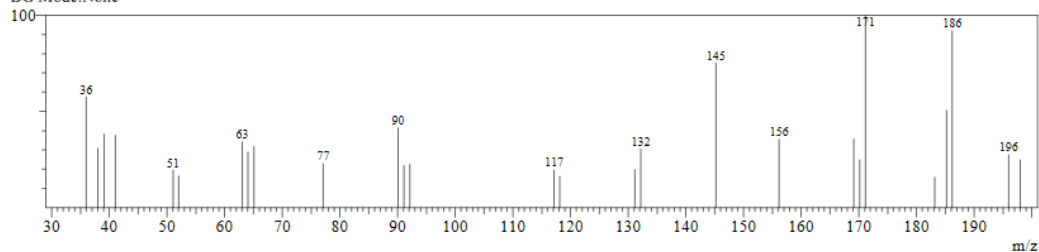
GC and MS of 2f (2-(3-methylbut-2-en-1-yl)-1H-benzo[d]imidazole)



Spectrum

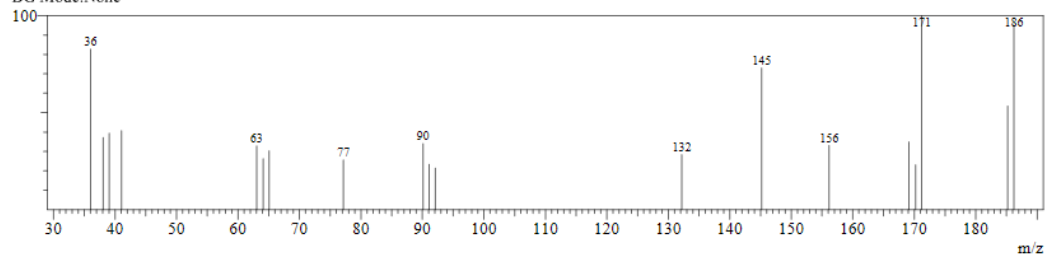
Starting material

Line#:1 R.Time:18.6(Scan#:1631)
MassPeaks:27
RawMode:Single 18.6(1631) BasePeak:171(7220)
BG Mode:None

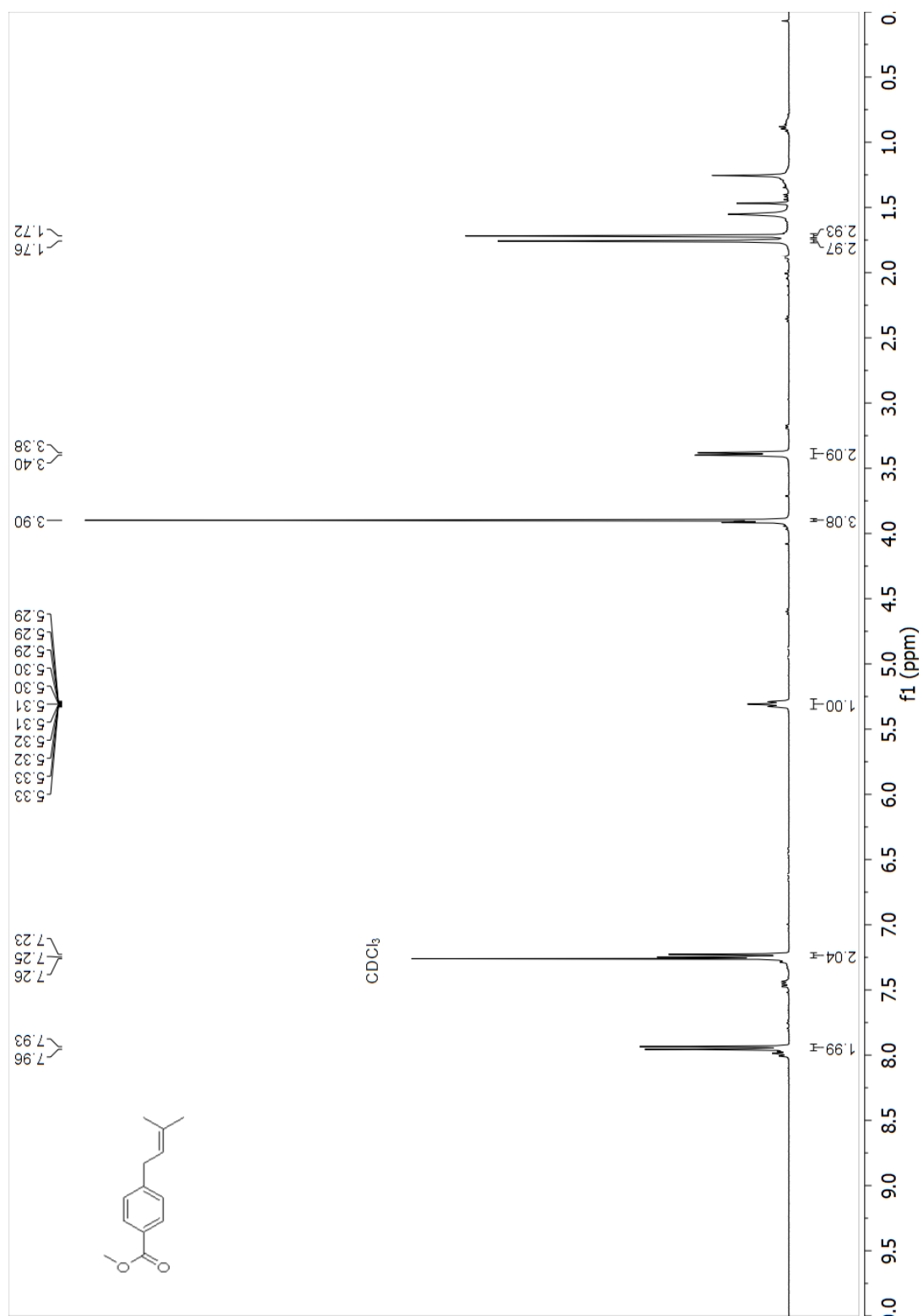


Product

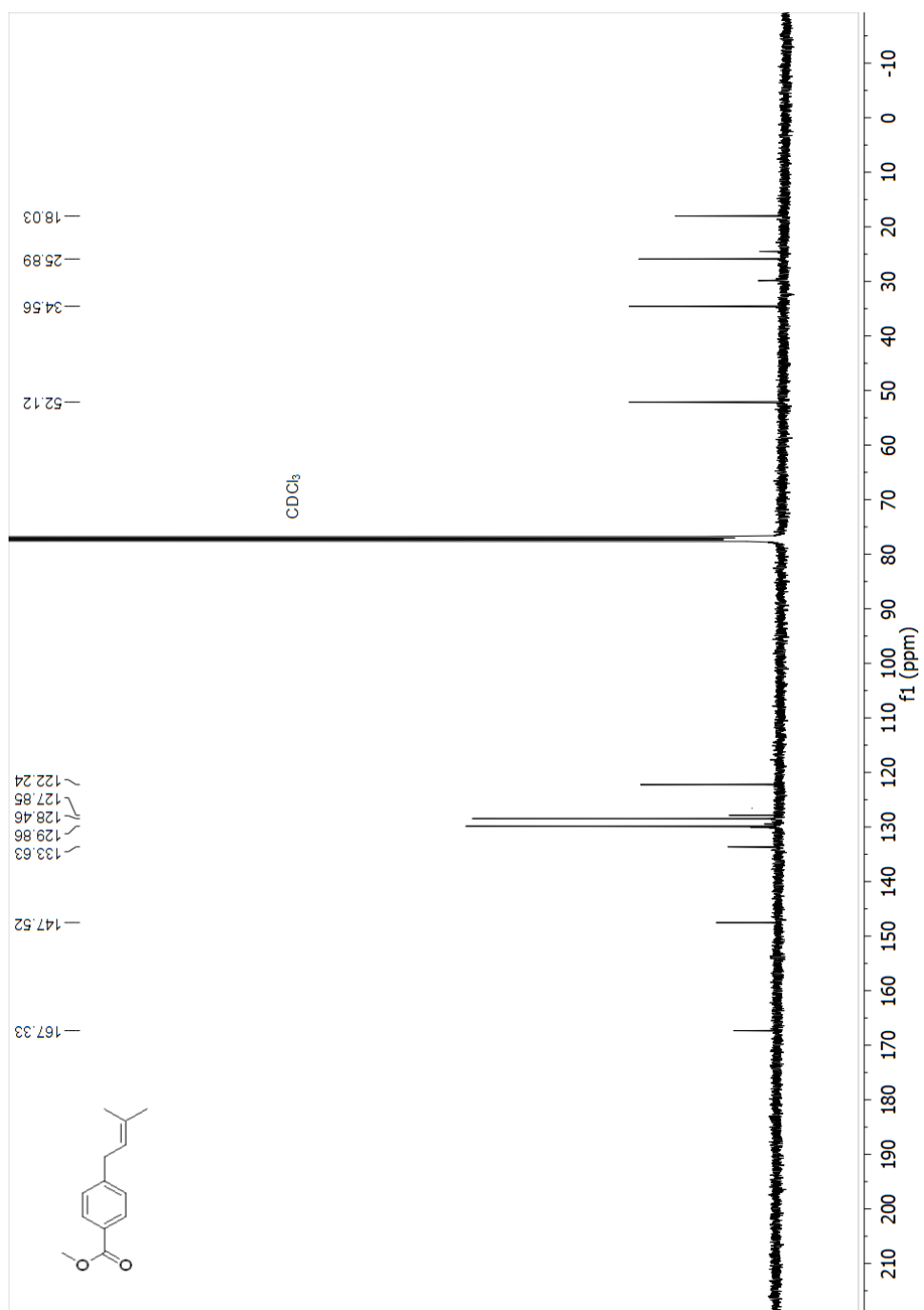
Line#:1 R.Time:19.2(Scan#:1710)
MassPeaks:19
RawMode:Single 19.2(1710) BasePeak:171(4924)
BG Mode:None



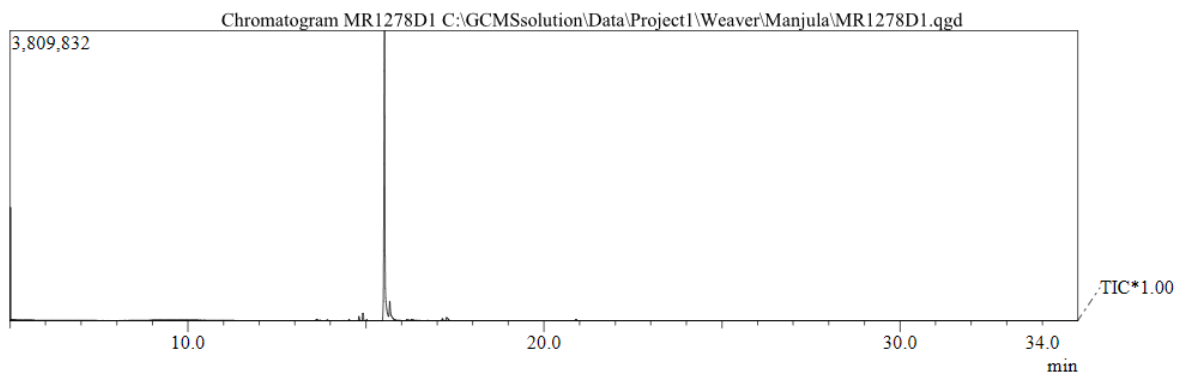
¹H NMR (400 MHz, Chloroform-d) spectrum of 3a (methyl 4-(3-methylbut-2-en-1-yl)benzoate)



^{13}C NMR (101 MHz, Chloroform-d) spectrum of 3a (methyl 4-(3-methylbut-2-en-1-yl)benzoate)

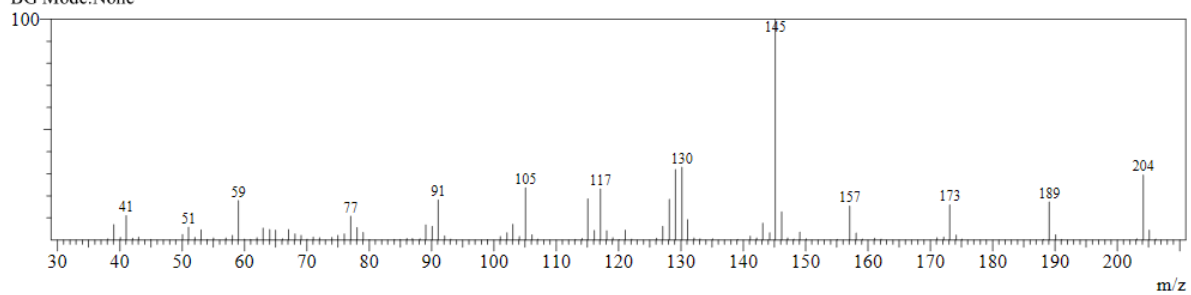


GC and MS of 3a (methyl 4-(3-methylbut-2-en-1-yl)benzoate)

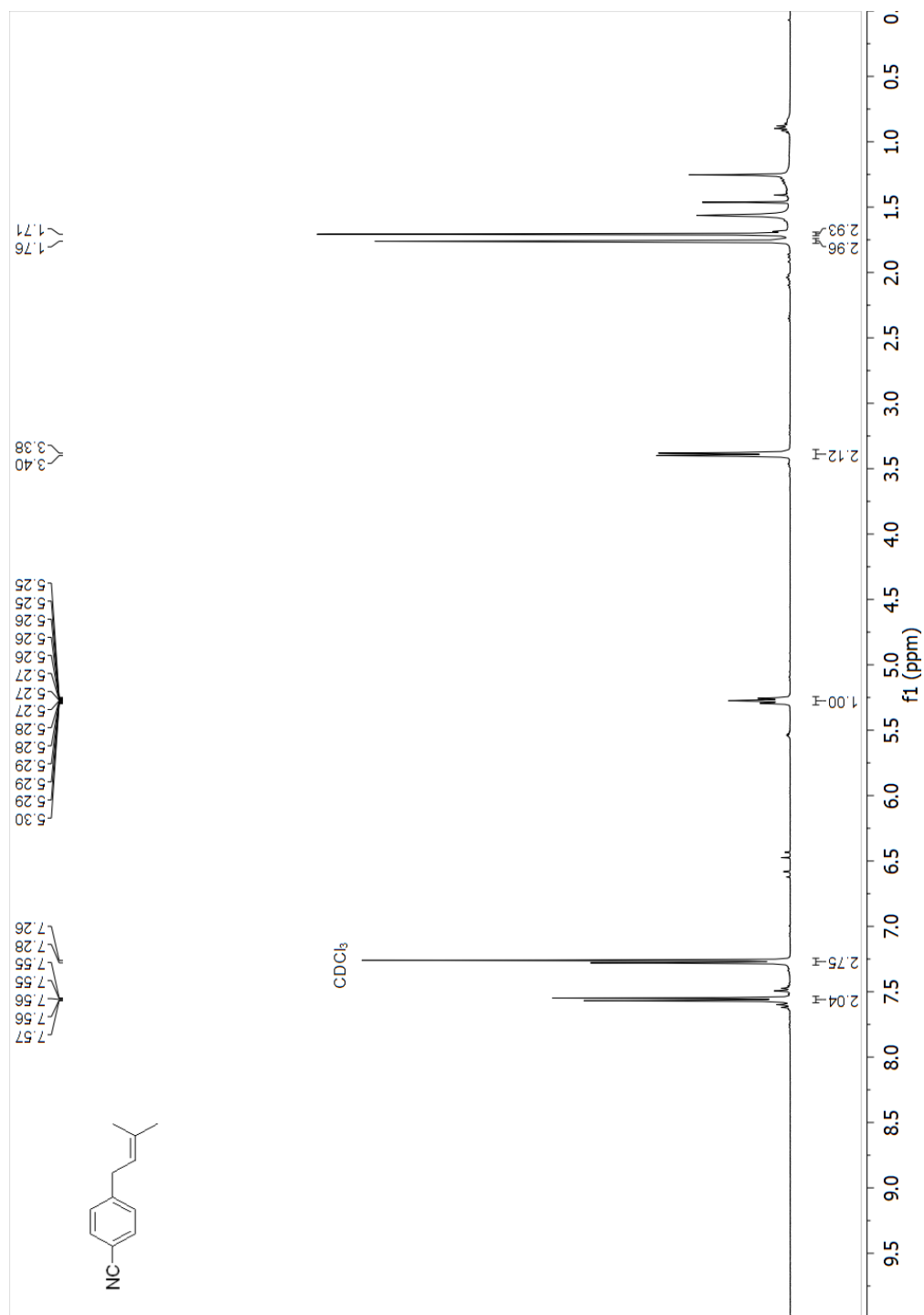


Spectrum

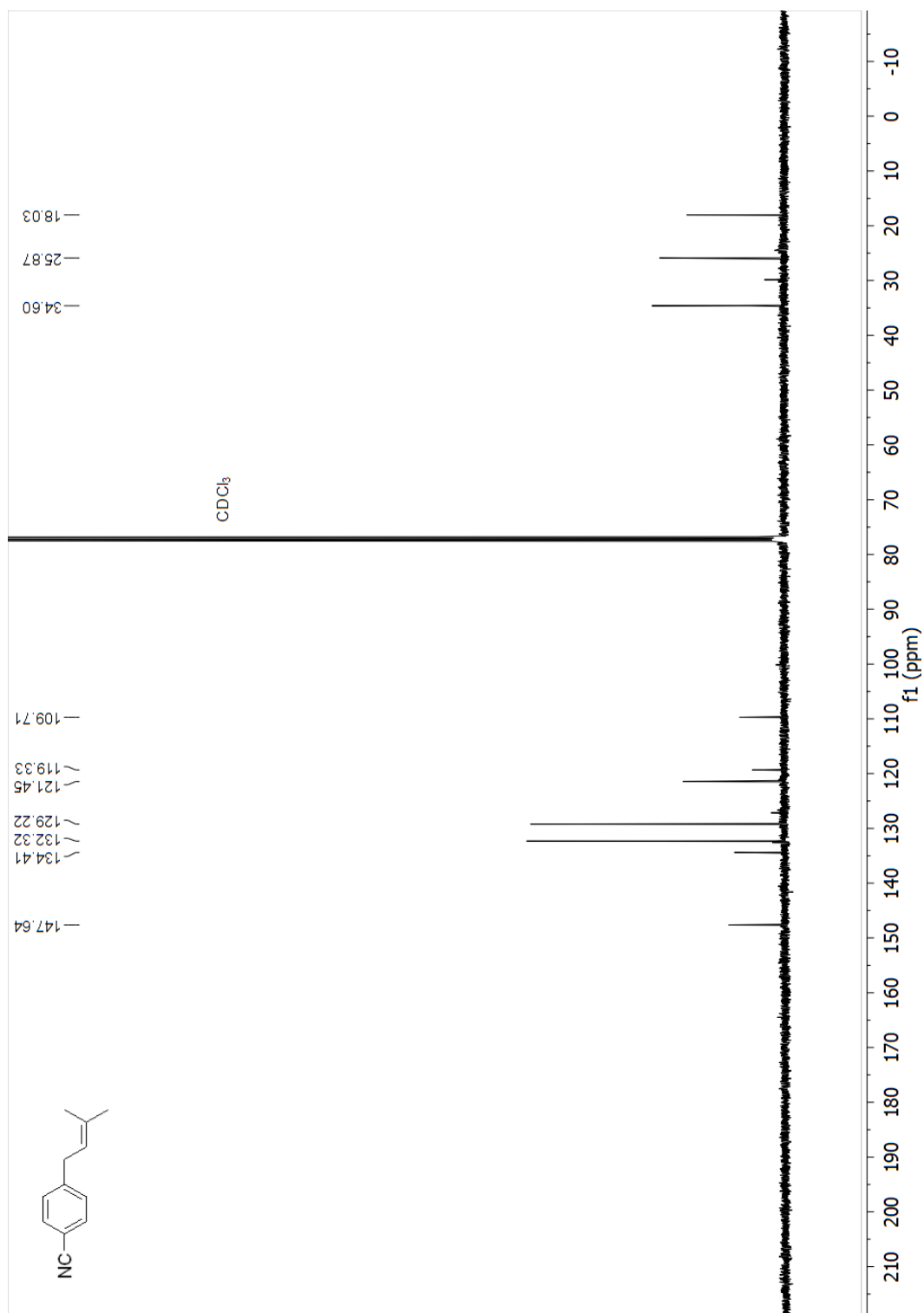
Line#:1 R.Time:15.5(Scan#:1262)
MassPeaks:103
RawMode:Single 15.5(1262) BasePeak:145(569762)
BG Mode:None



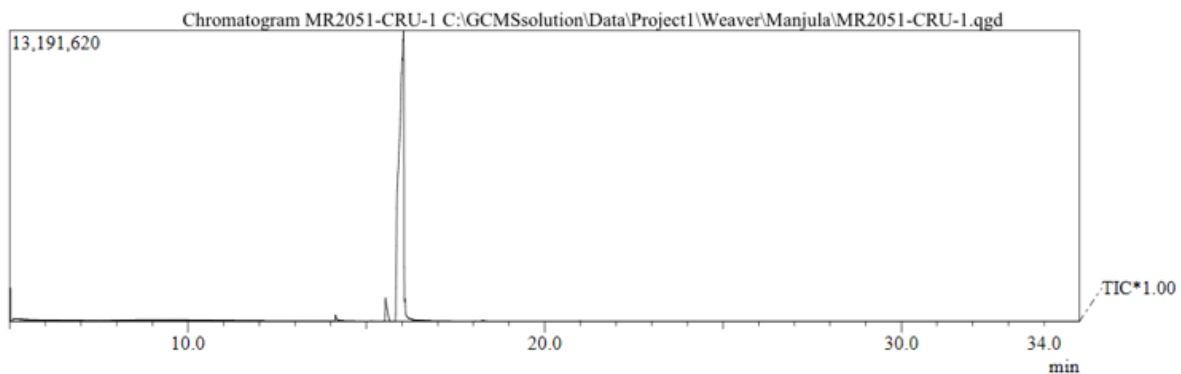
¹H NMR (400 MHz, Chloroform-d) spectrum of 3b (4-(3-methylbut-2-en-1-yl)benzotrile)



^{13}C NMR (101 MHz, Chloroform-d) spectrum of 3b (4-(3-methylbut-2-en-1-yl)benzonitrile)

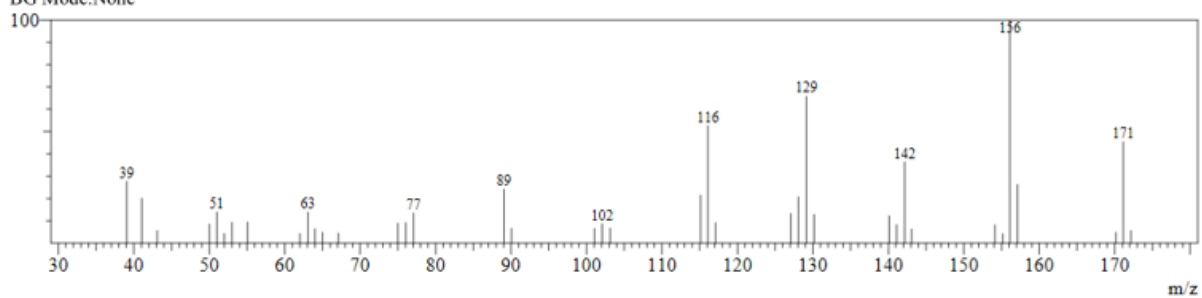


GC and MS of 3b (4-(3-methylbut-2-en-1-yl)benzocnitrile)

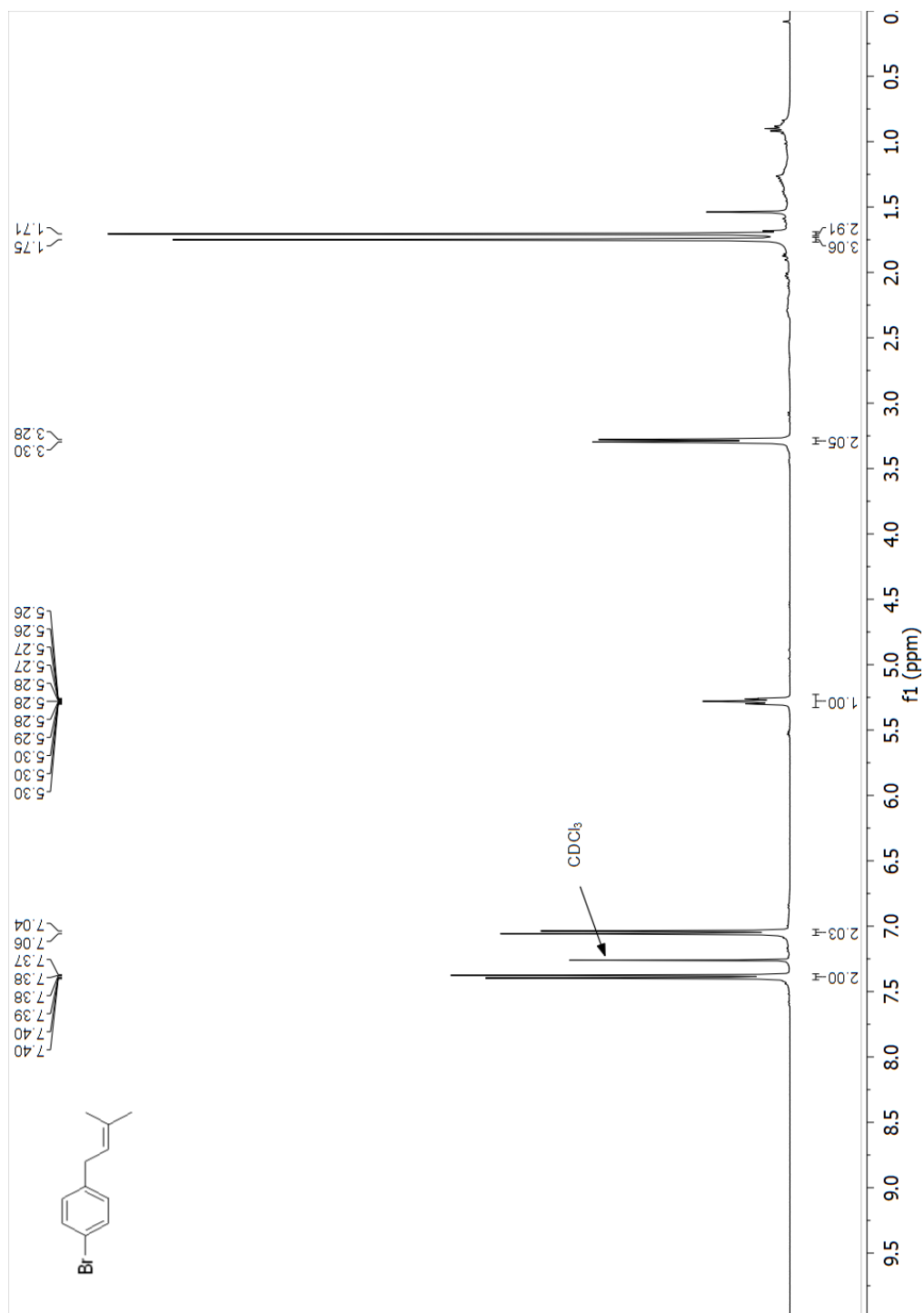


Spectrum

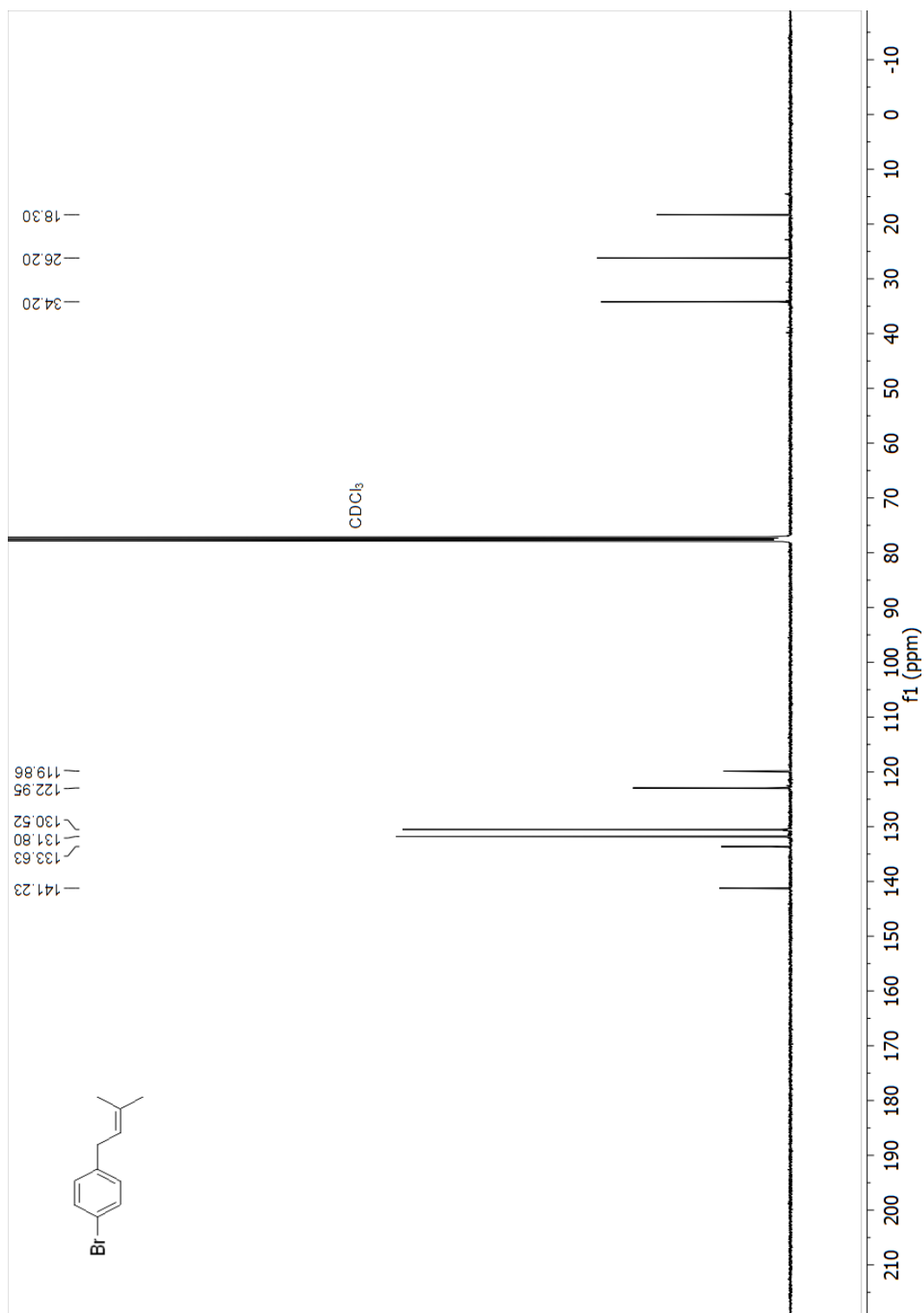
Line#:1 R.Time:16.0(Scan#:1316)
MassPeaks:39
RawMode:Single 16.0(1316) BasePeak:156(24318)
BG Mode:None



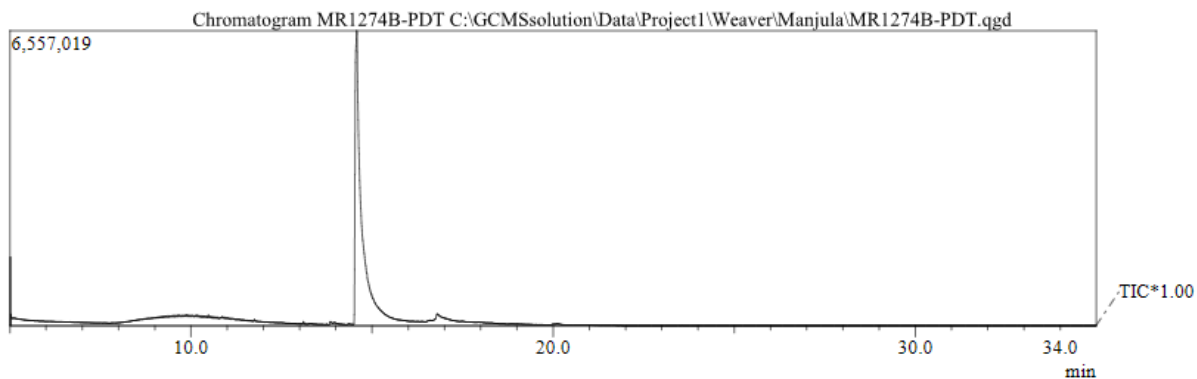
^1H NMR (400 MHz, Chloroform-d) spectrum of 3c (1-bromo-4-(3-methylbut-2-en-1-yl)benzene)



^{13}C NMR (101 MHz, Chloroform-d) spectrum of 3c (1-bromo-4-(3-methylbut-2-en-1-yl)benzene)

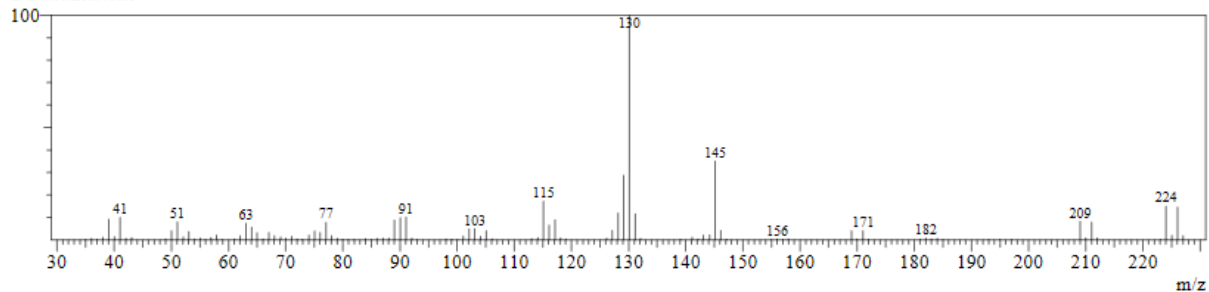


GC and MS of 3c (1-bromo-4-(3-methylbut-2-en-1-yl)benzene)

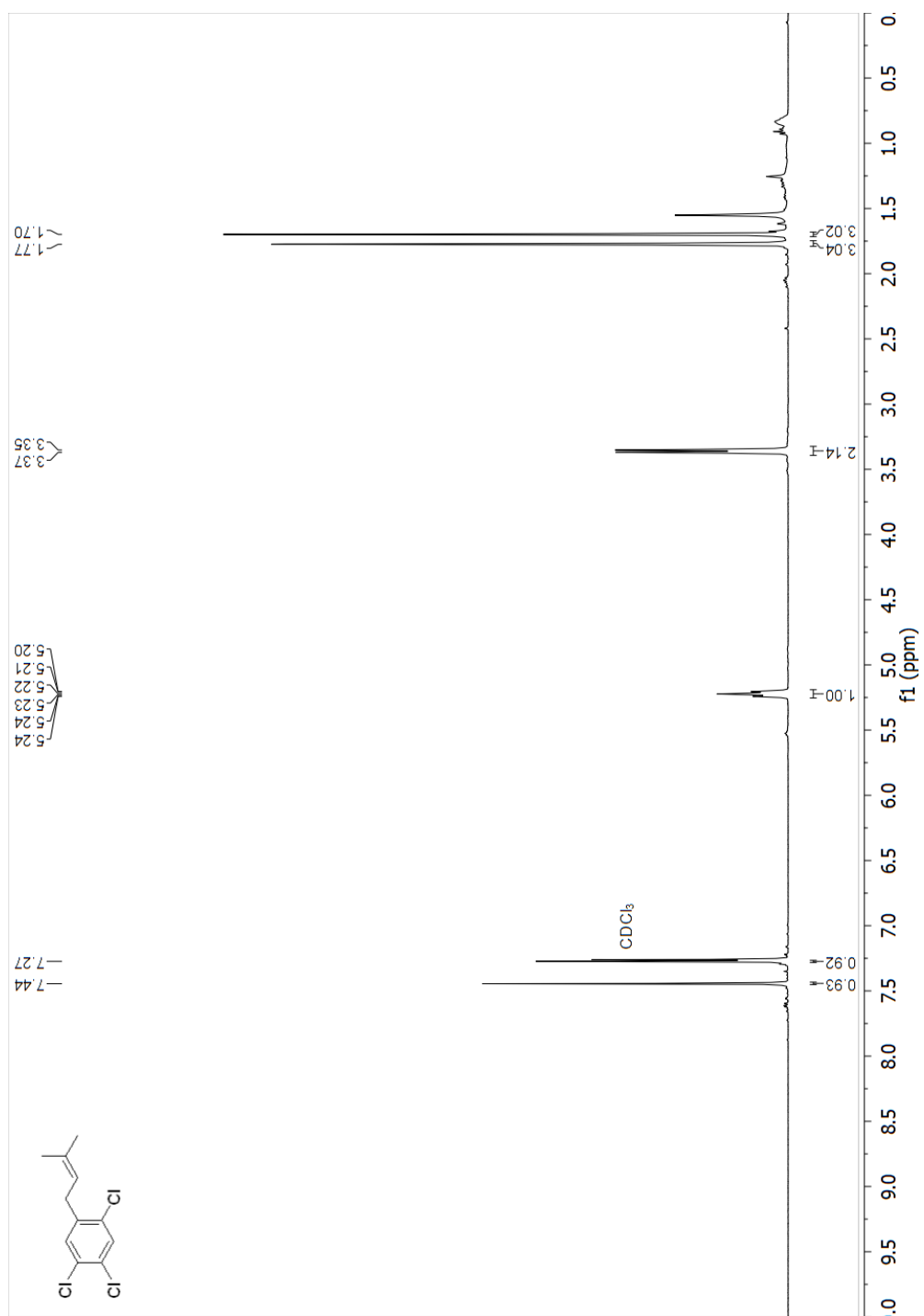


Spectrum

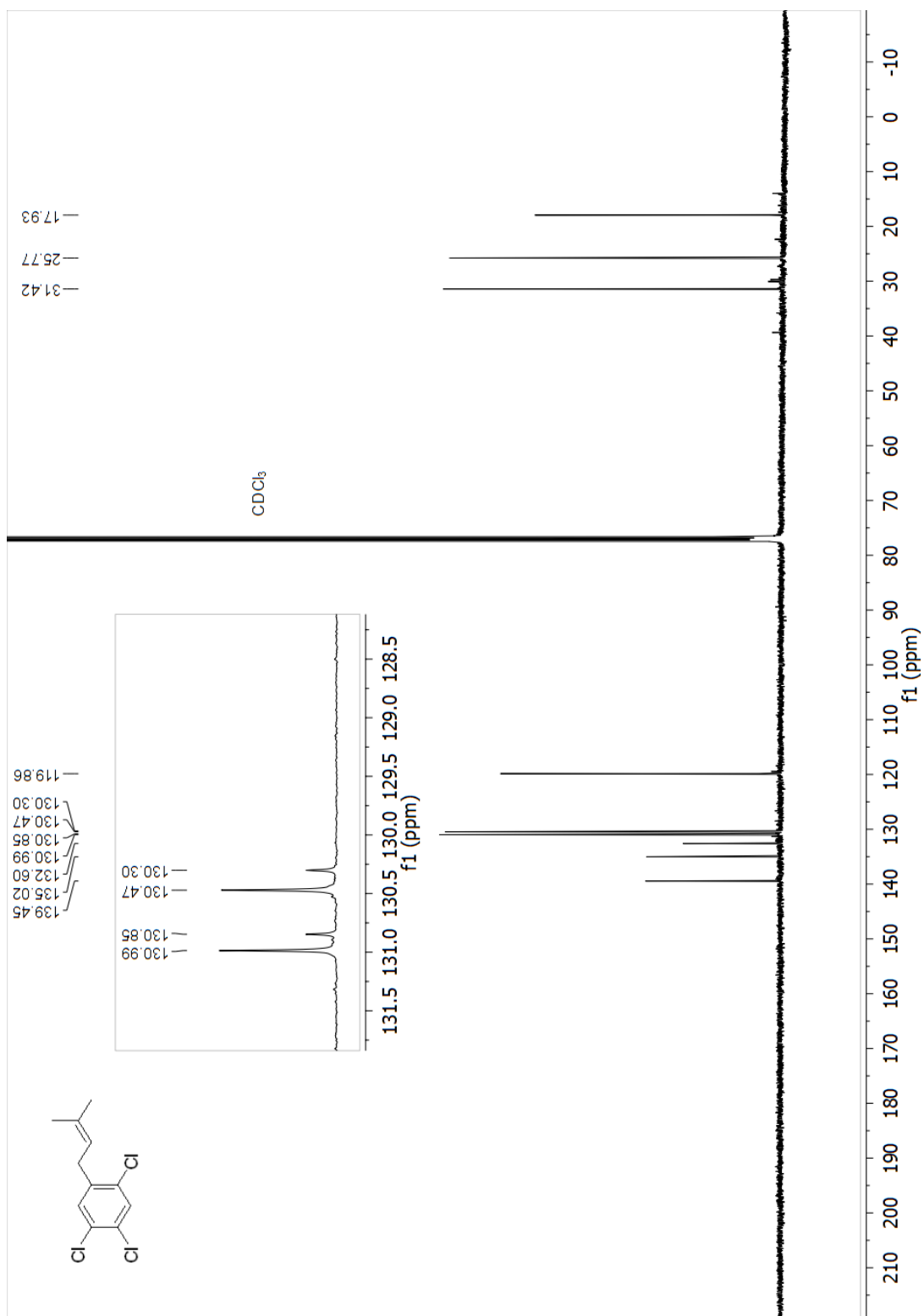
Line#:1 R.Time:14.6(Scan#:1156)
MassPeaks:108
RawMode:Single 14.6(1156) BasePeak:130(941128)
BG Mode:None



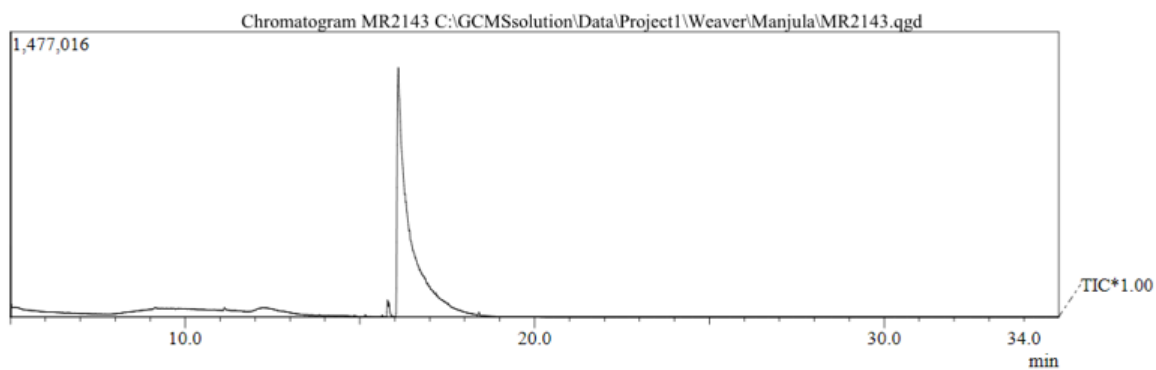
^1H NMR (400 MHz, Chloroform-d) spectrum of 3d (1,2,4-trichloro-5-(3-methylbut-2-en-1-yl)benzene)



^{13}C NMR (101 MHz, Chloroform-d) spectrum of 3d (1,2,4-trichloro-5-(3-methylbut-2-en-1-yl)benzene)



GC and MS of 3d (1,2,4-trichloro-5-(3-methylbut-2-en-1-yl)benzene)



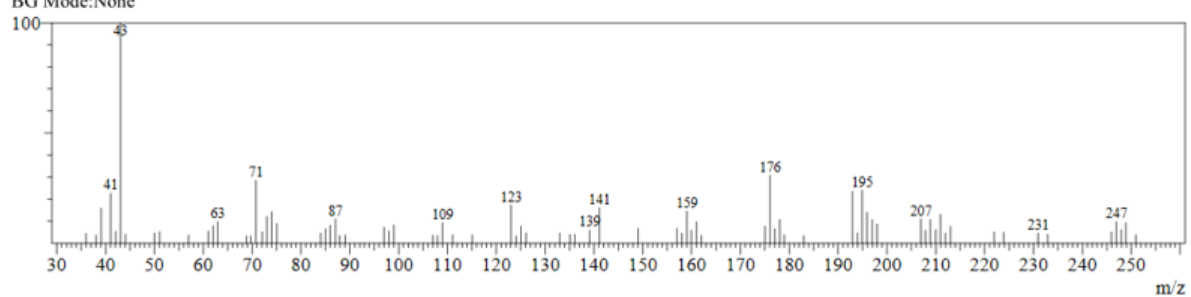
Spectrum

Line#:1 R.Time:16.8(Scan#:1422)

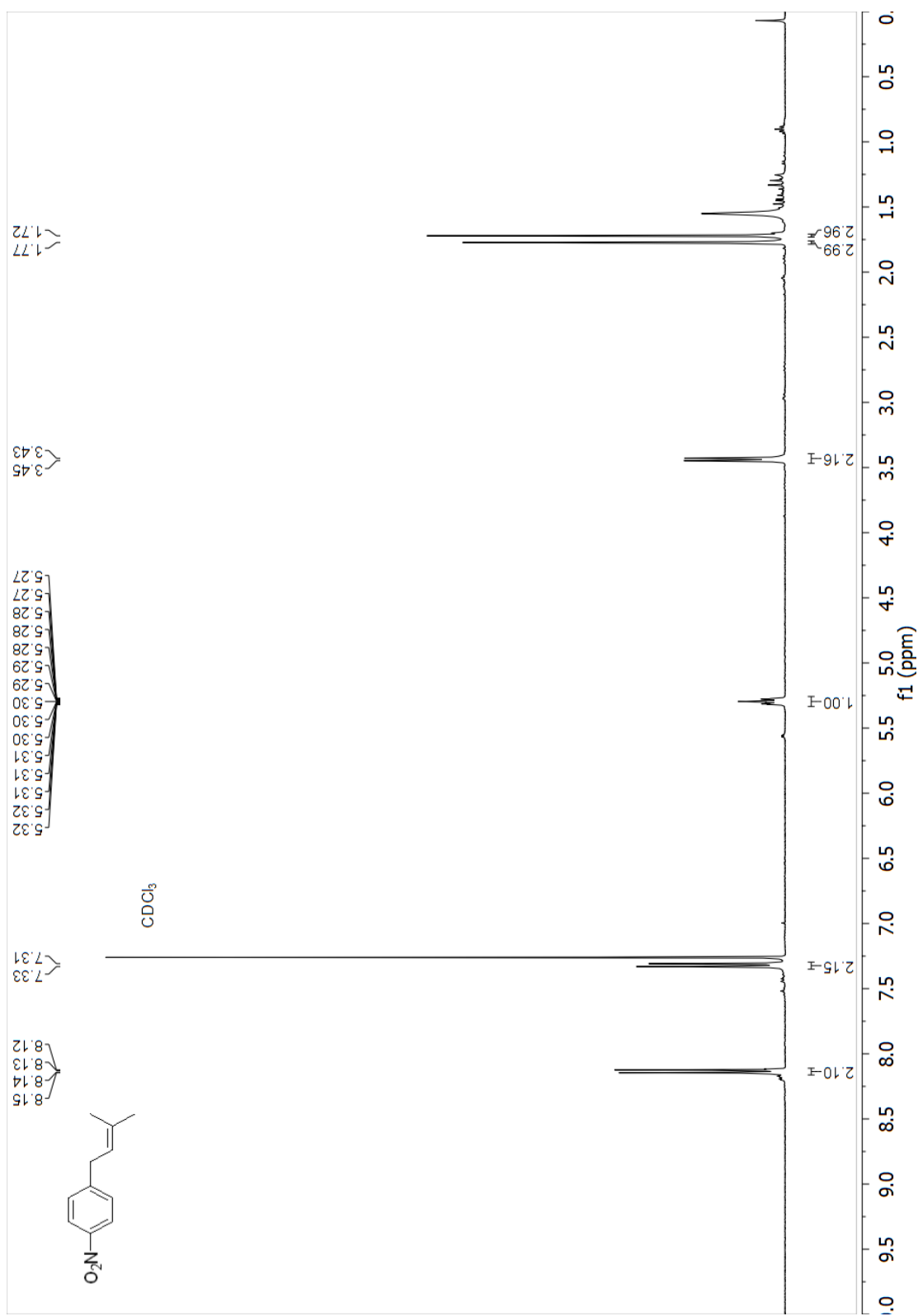
MassPeaks:78

RawMode:Single 16.8(1422) BasePeak:43(30759)

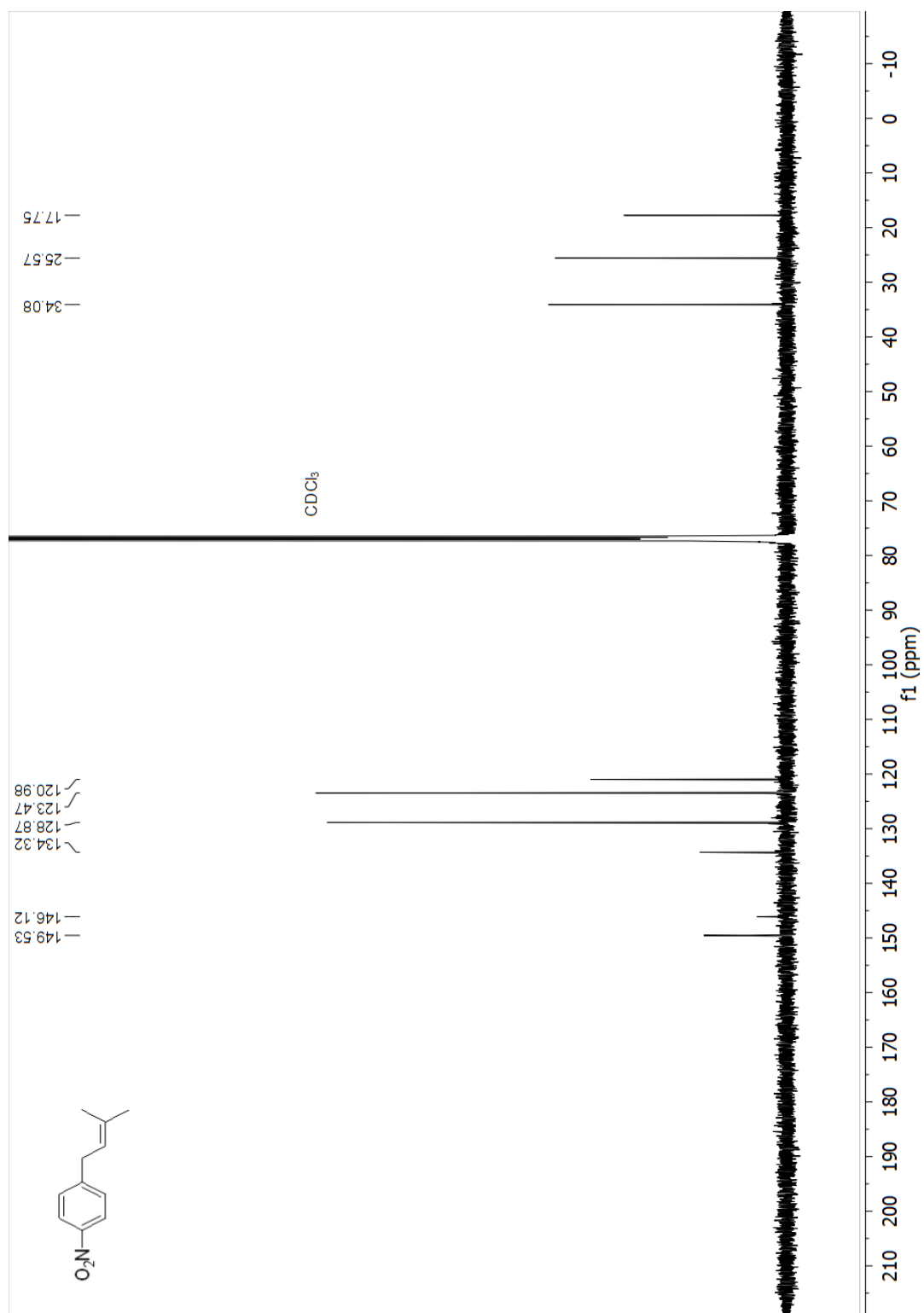
BG Mode:None



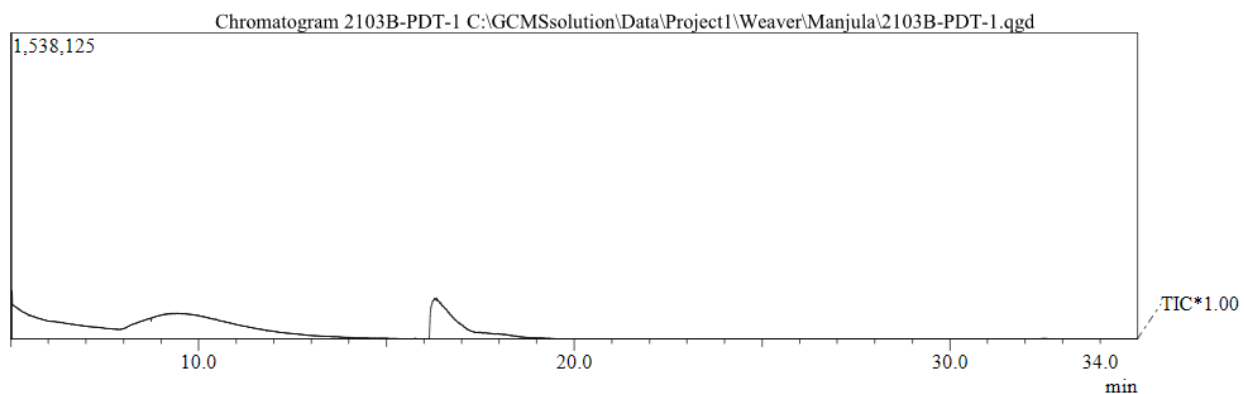
¹H NMR (400 MHz, Chloroform-d) spectrum of 3e (1-(3-methylbut-2-en-1-yl)-4-nitrobenzene)



^{13}C NMR (101 MHz, Chloroform-d) spectrum of 3e (1-(3-methylbut-2-en-1-yl)-4-nitrobenzene)

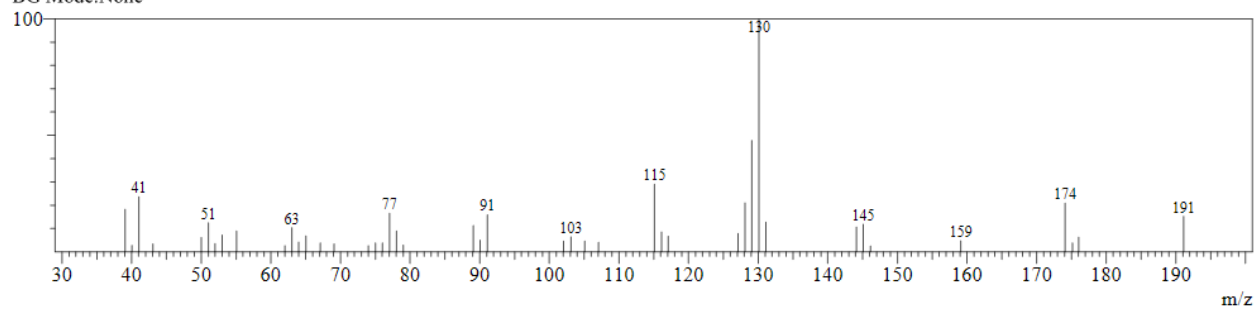


GC and MS of 3e (1-(3-methylbut-2-en-1-yl)-4-nitrobenzene)

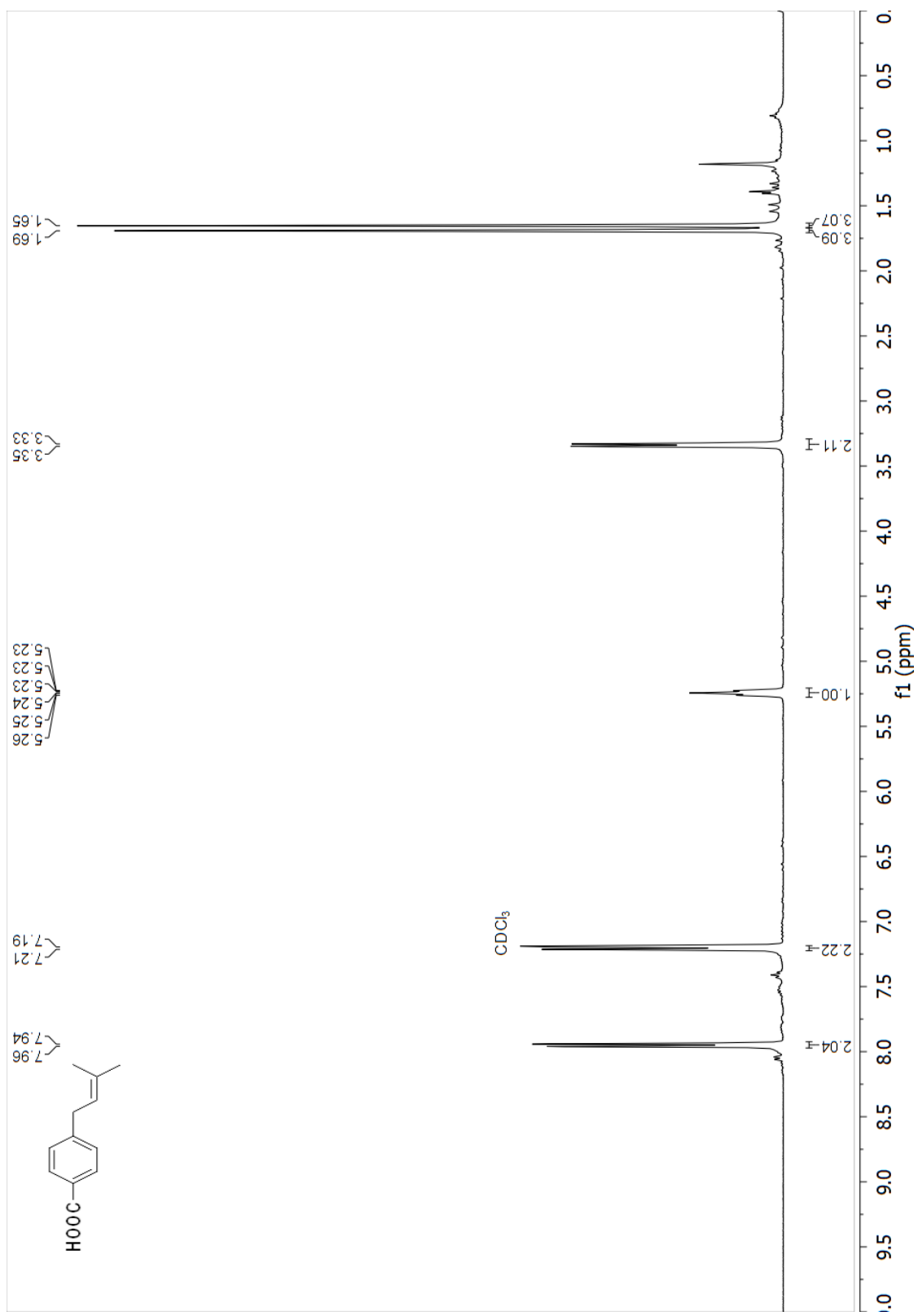


Spectrum

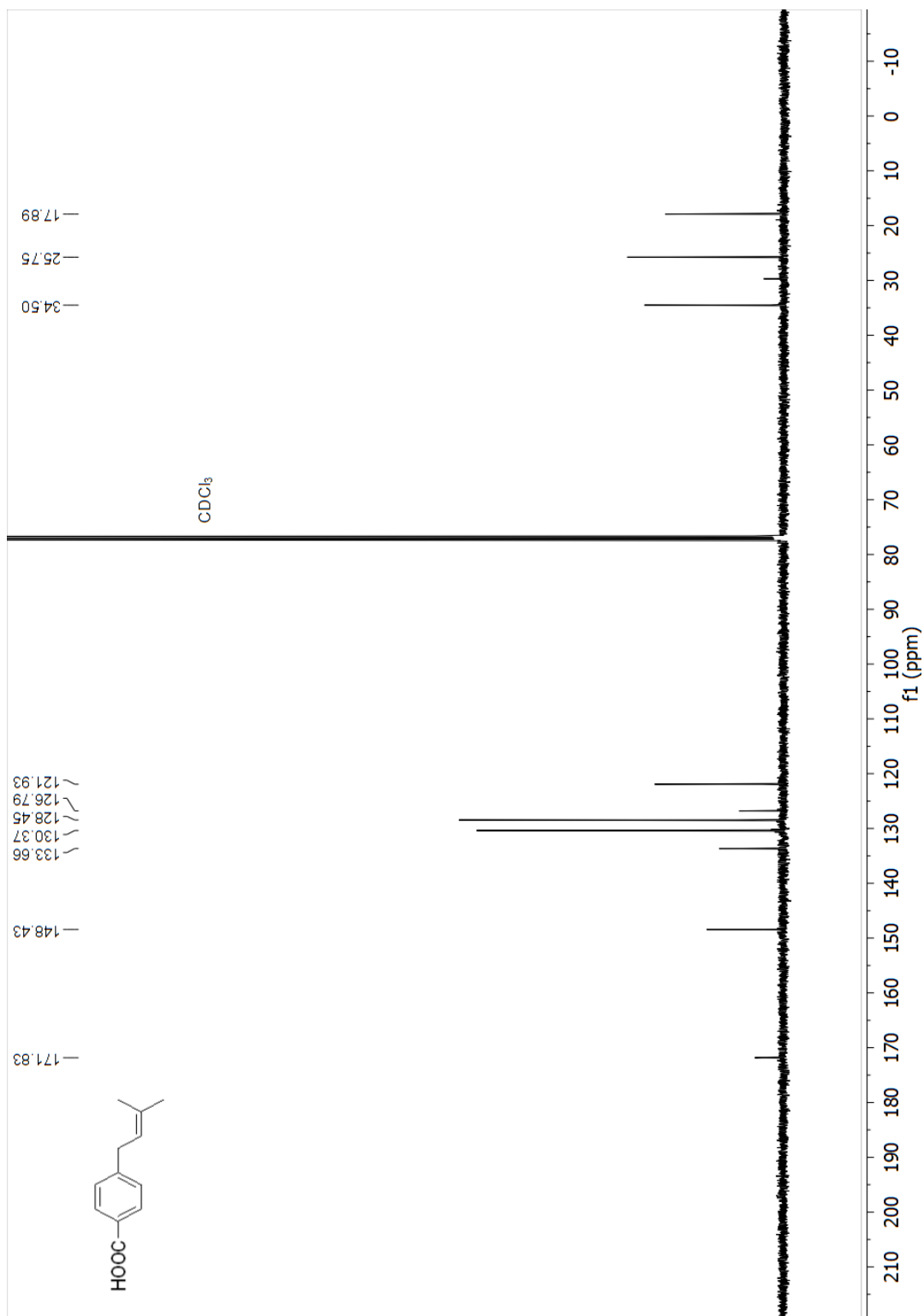
Line#:1 R.Time:16.3(Scan#:1361)
MassPeaks:44
RawMode:Single 16.3(1361) BasePeak:130(39820)
BG Mode:None



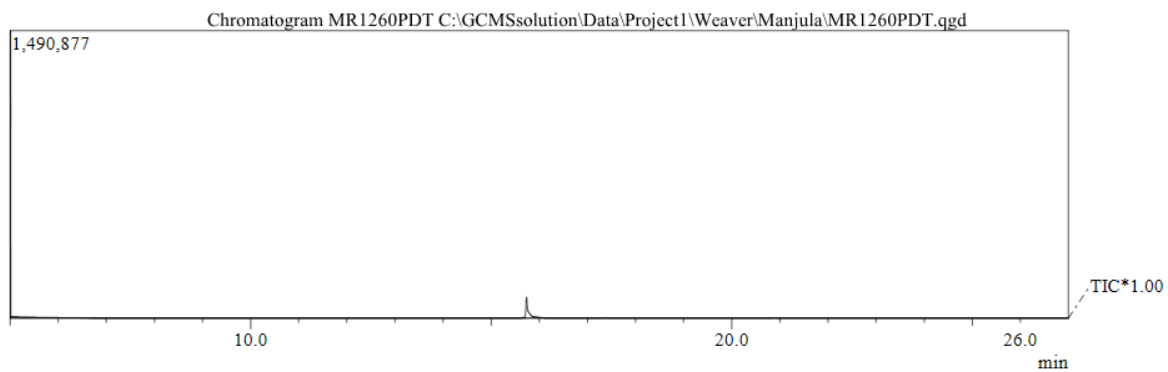
¹H NMR (400 MHz, Chloroform-d) spectrum of 3f (4-(3-methylbut-2-en-1-yl)benzoic acid)



^{13}C NMR (101 MHz, Chloroform-d) spectrum of 3f (4-(3-methylbut-2-en-1-yl)benzoic acid)

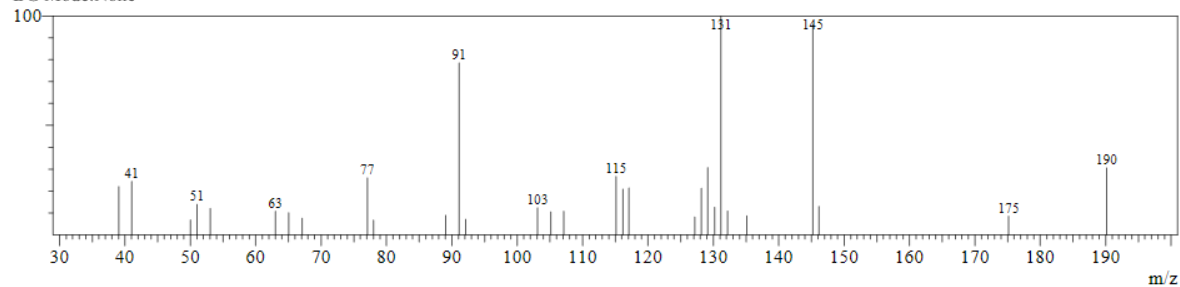


GC and MS of 3f (4-(3-methylbut-2-en-1-yl)benzoic acid)

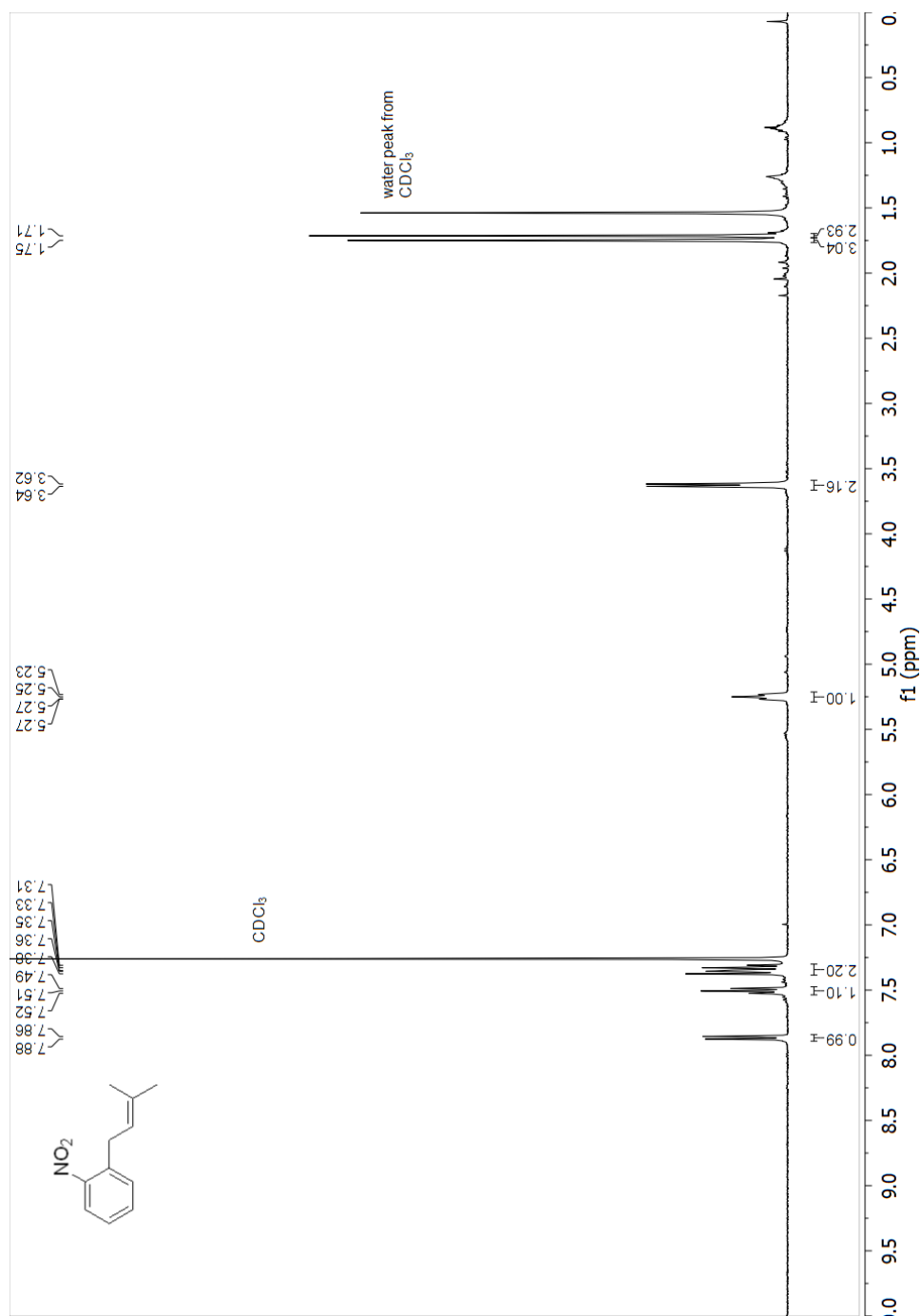


Spectrum

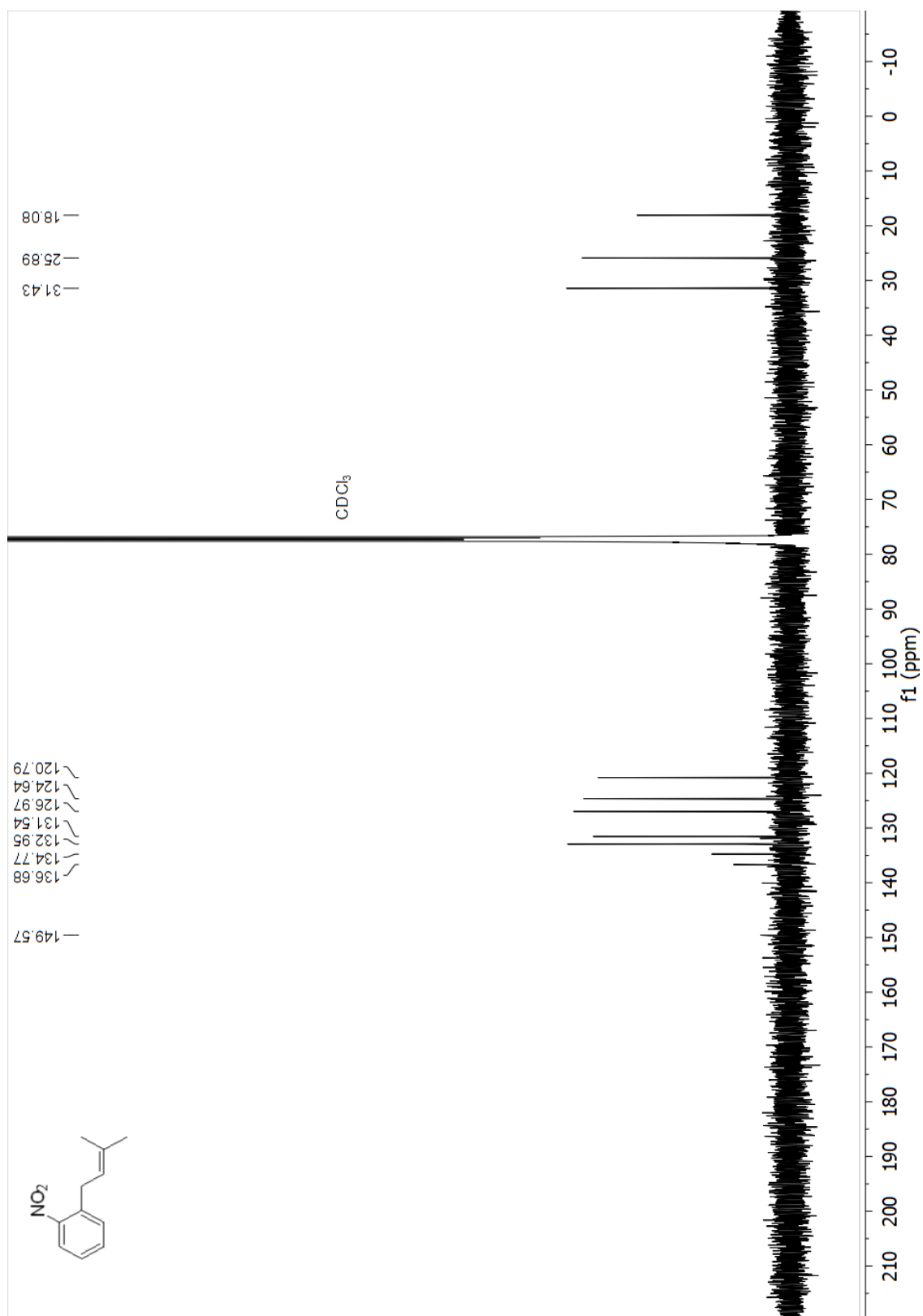
Line#:1 R.Time:15.7(Scan#:1289)
MassPeaks:30
RawMode:Single 15.7(1289) BasePeak:131(16148)
BG Mode:None



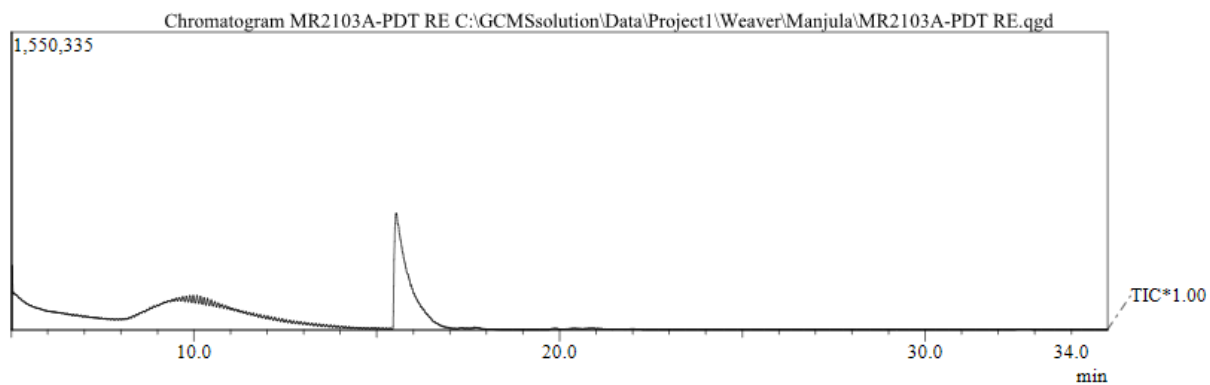
¹H NMR (400 MHz, Chloroform-d) spectrum of 3g (1-(3-methylbut-2-en-1-yl)-2-nitrobenzene)



¹³C NMR (101 MHz, Chloroform-d) spectrum of 3g (1-(3-methylbut-2-en-1-yl)-2-nitrobenzene)

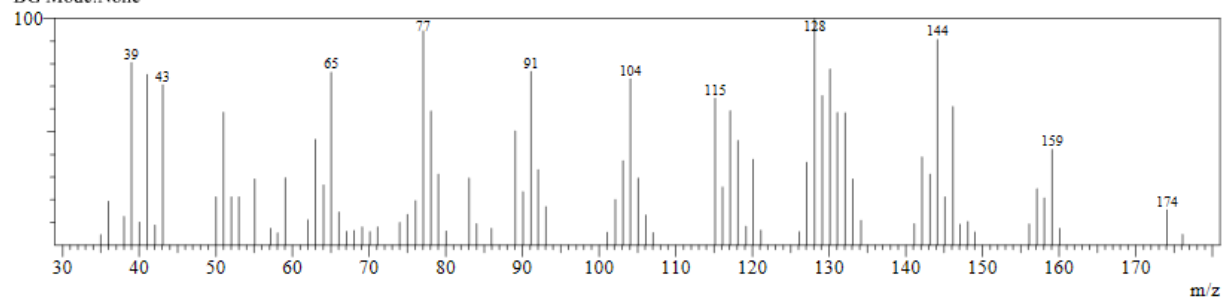


GC and MS of 3g (1-(3-methylbut-2-en-1-yl)-2-nitrobenzene)

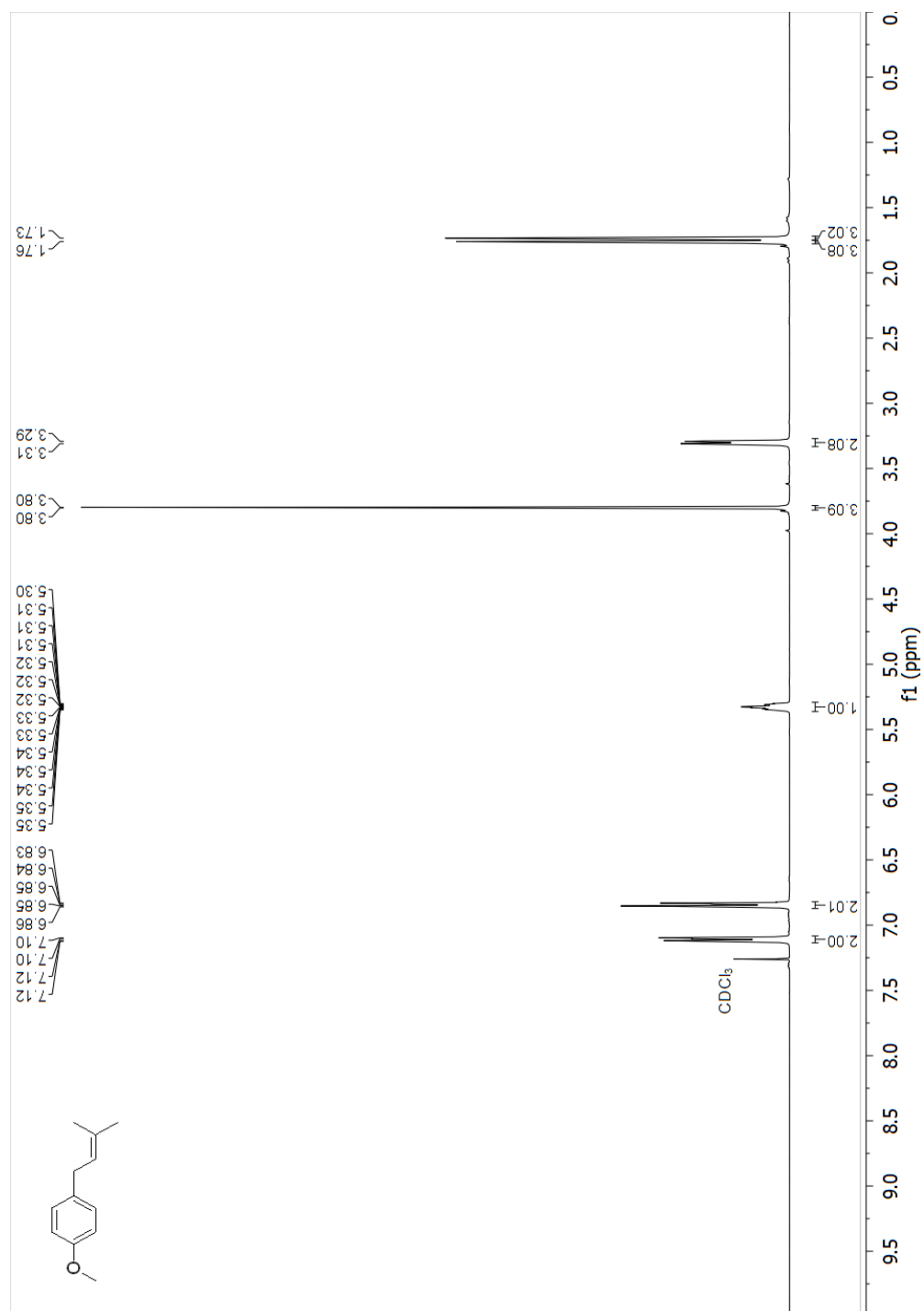


Spectrum

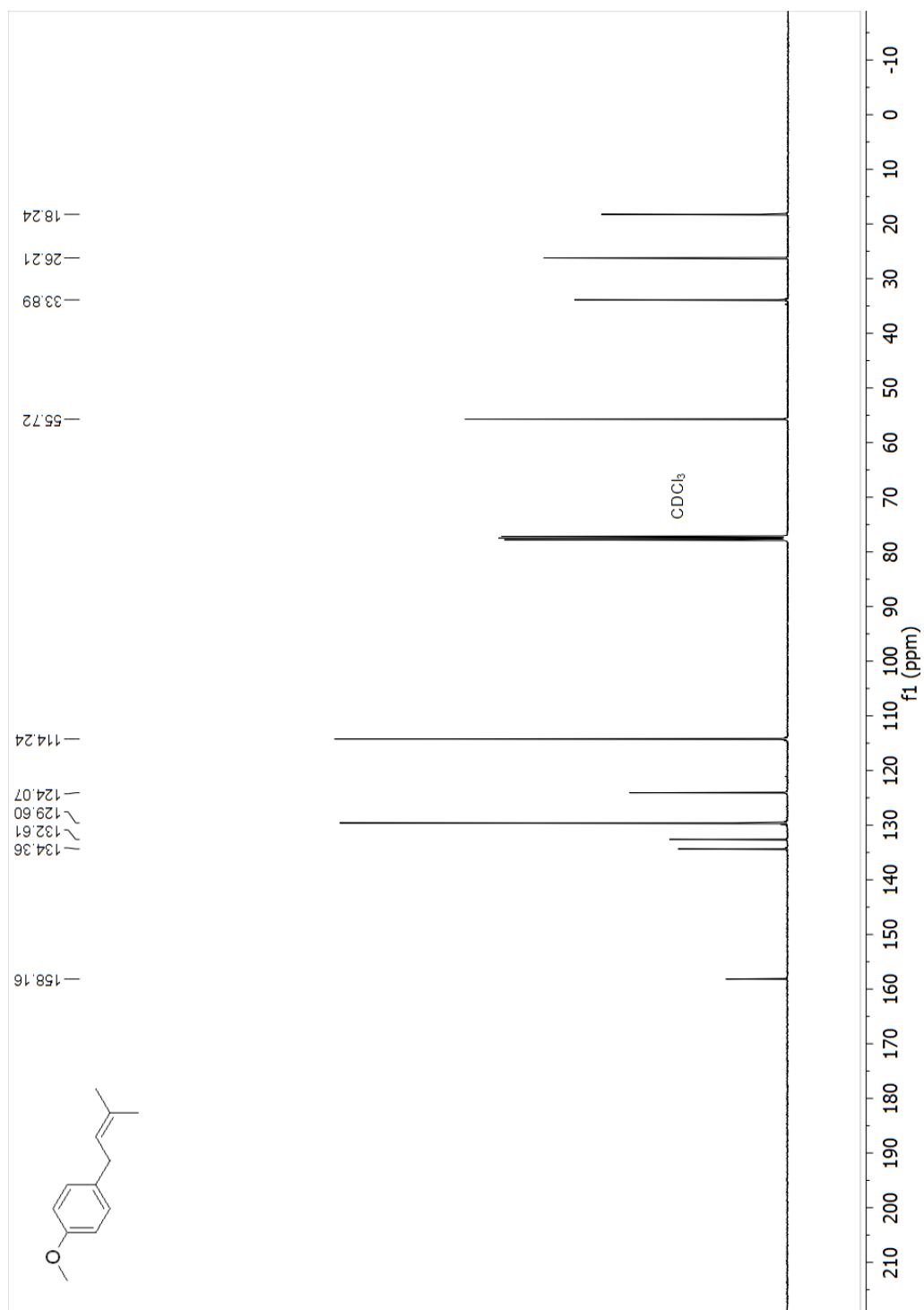
Line#:1 R.Time:15.6(Scan#:1271)
MassPeaks:80
RawMode:Single 15.6(1271) BasePeak:128(22370)
BG Mode:None



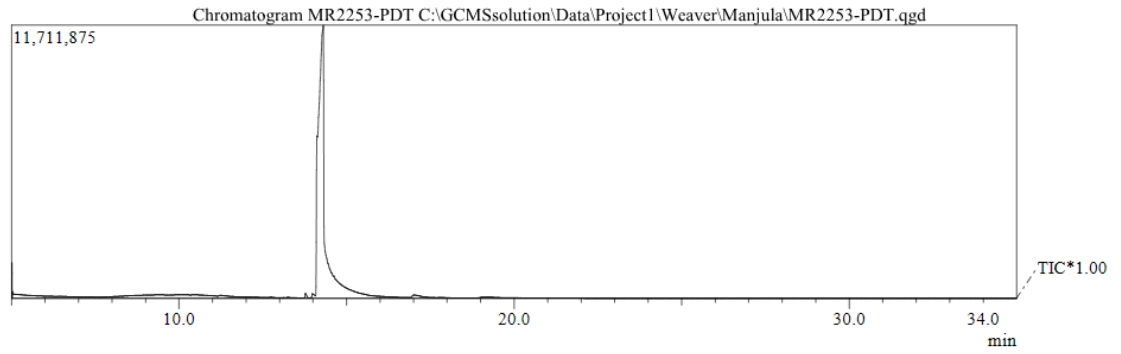
¹H NMR (400 MHz, Chloroform-d) spectrum of 3h (1-methoxy-4-(3-methylbut-2-en-1-yl)benzene)



^{13}C NMR (101 MHz, Chloroform-d) spectrum of 3h (1-methoxy-4-(3-methylbut-2-en-1-yl)benzene)

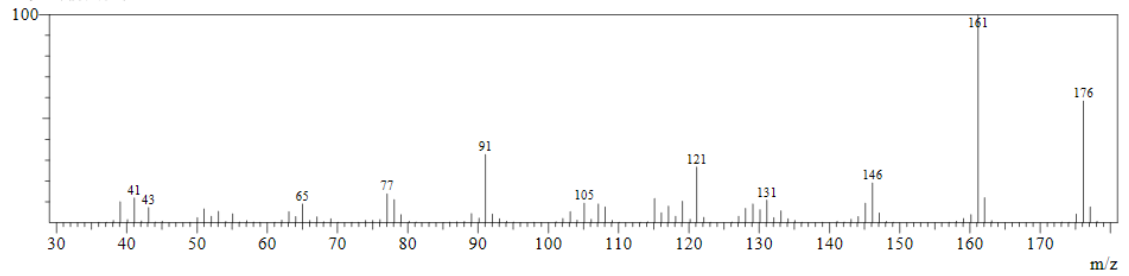


GC and MS of 3h (1-methoxy-4-(3-methylbut-2-en-1-yl)benzene)

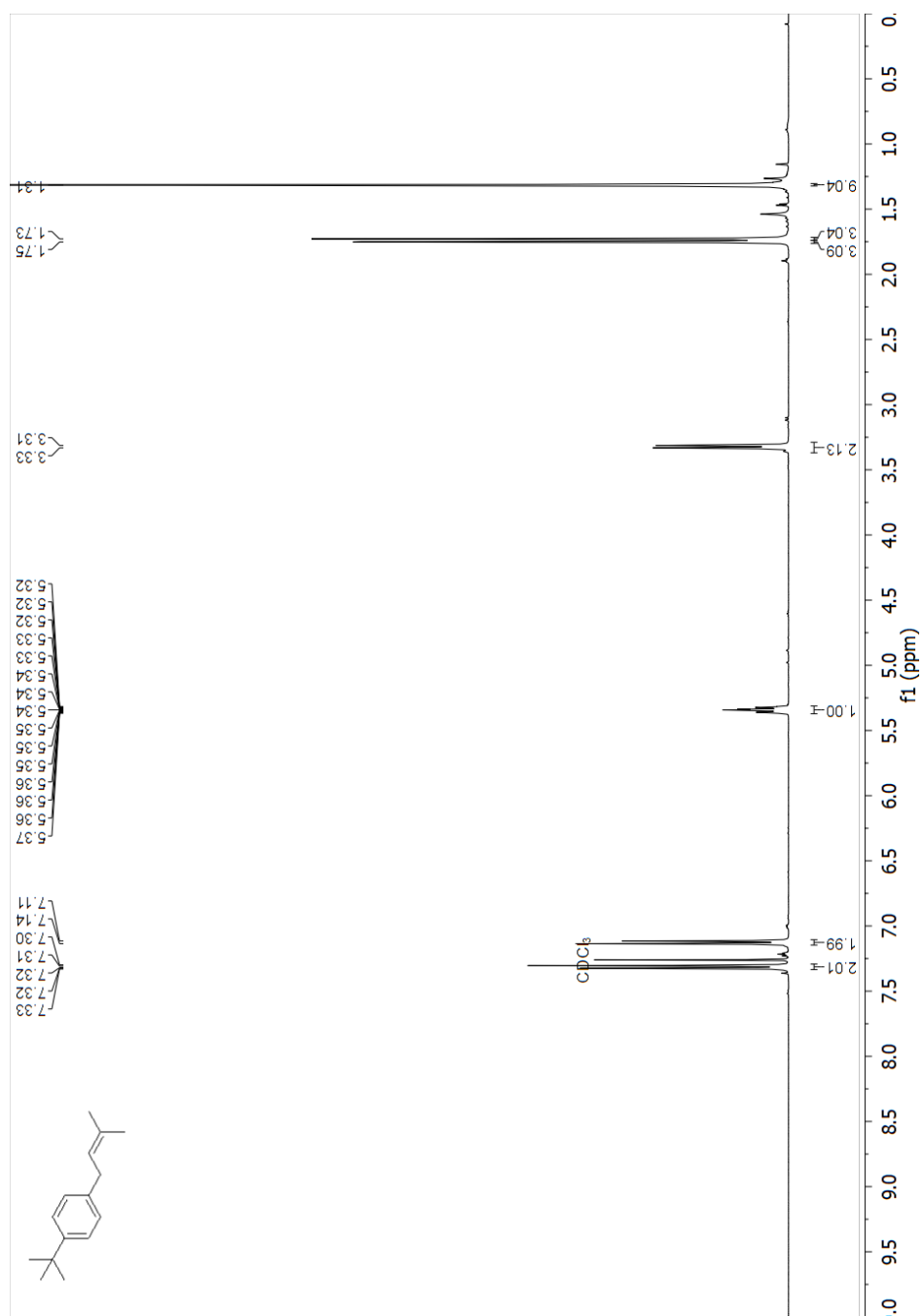


Spectrum

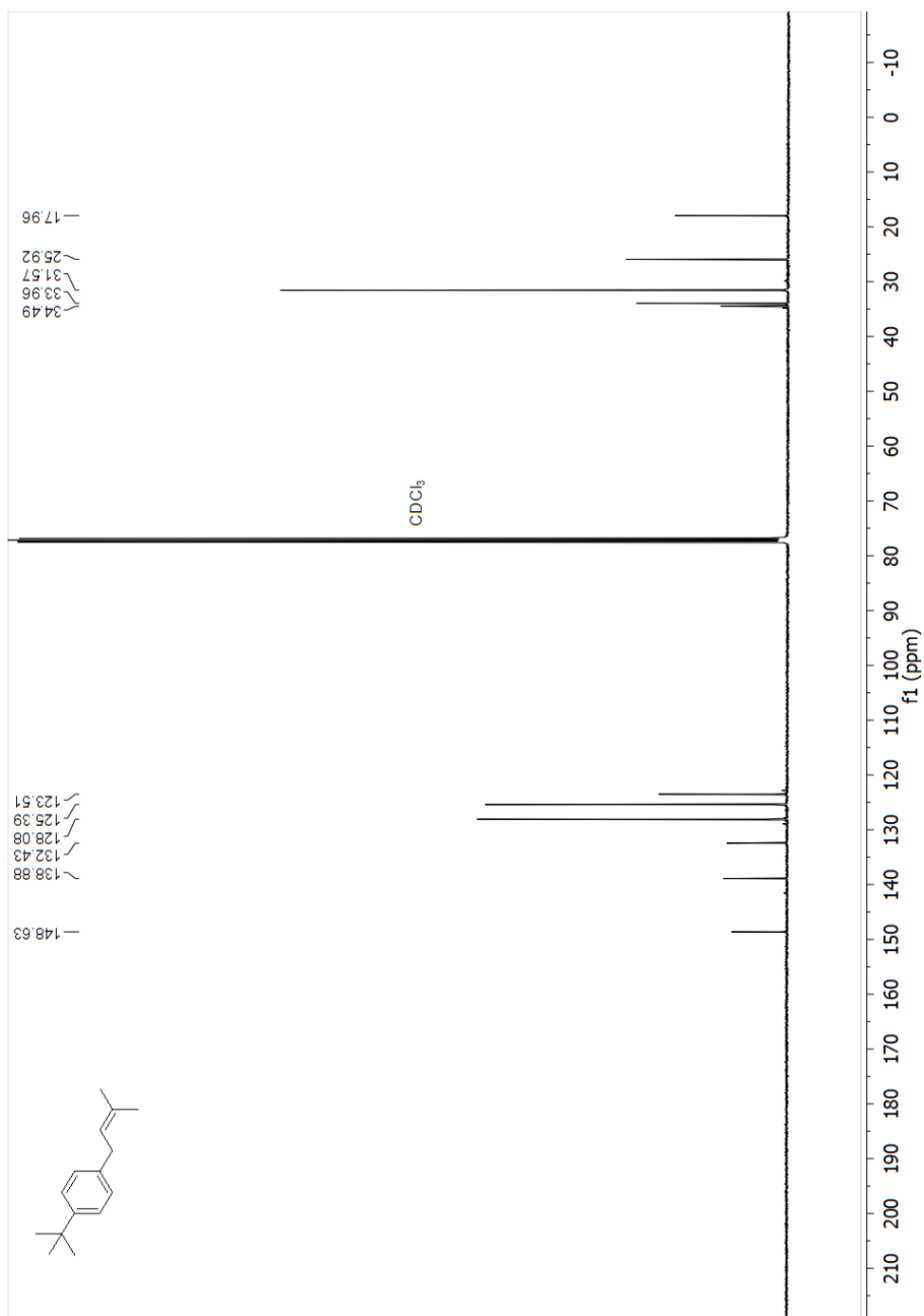
Line#:1 R.Time:14.2(Scan#:1109)
MassPeaks:111
RawMode:Single 14.2(1109) BasePeak:161(1866892)
BG Mode:None



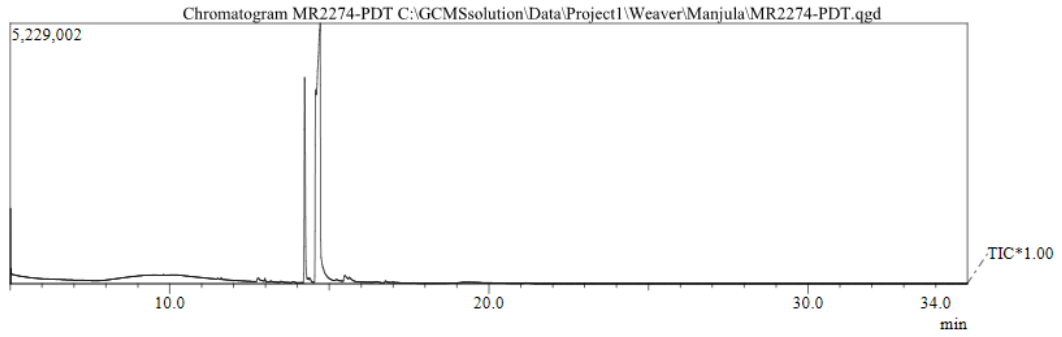
^1H NMR (400 MHz, Chloroform-d) spectrum of 3i (1-(tert-butyl)-4-(3-methylbut-2-en-1-yl)benzene)



^{13}C NMR (101 MHz, Chloroform-d) spectrum of 3i (1-(tert-butyl)-4-(3-methylbut-2-en-1-yl)benzene)

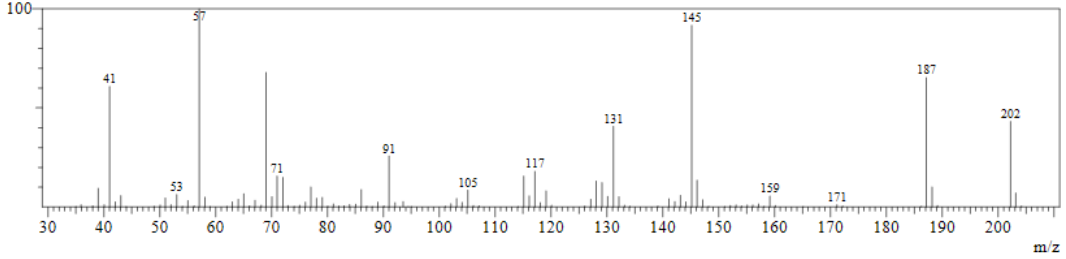


GC and MS of 3i (1-(tert-butyl)-4-(3-methylbut-2-en-1-yl)benzene)

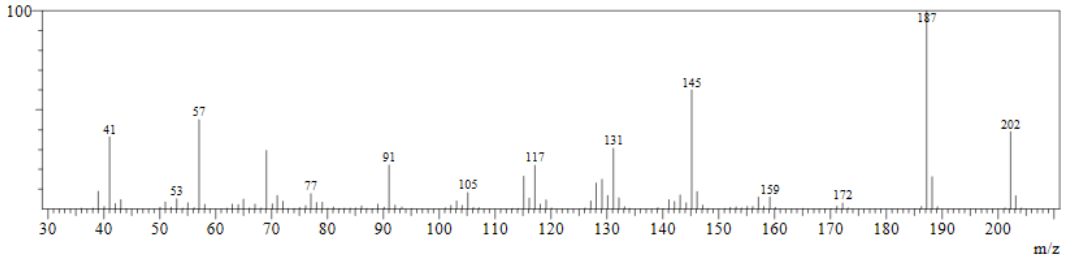


Spectrum

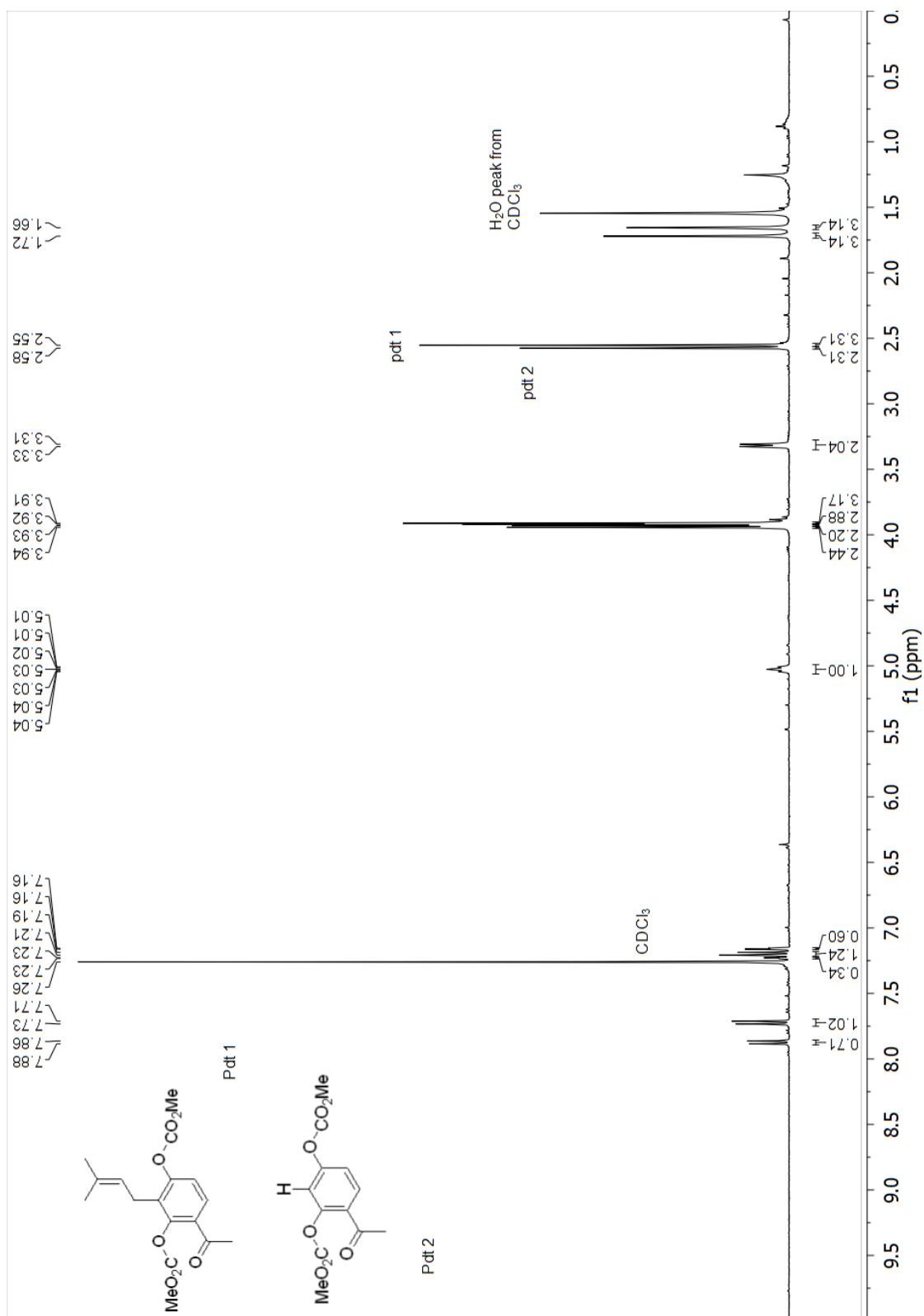
Line#:1 R.Time:14.2(Scan#:1109)
MassPeaks:106
RawMode:Single 14.2(1109) BasePeak:57(497473)
BG Mode:None



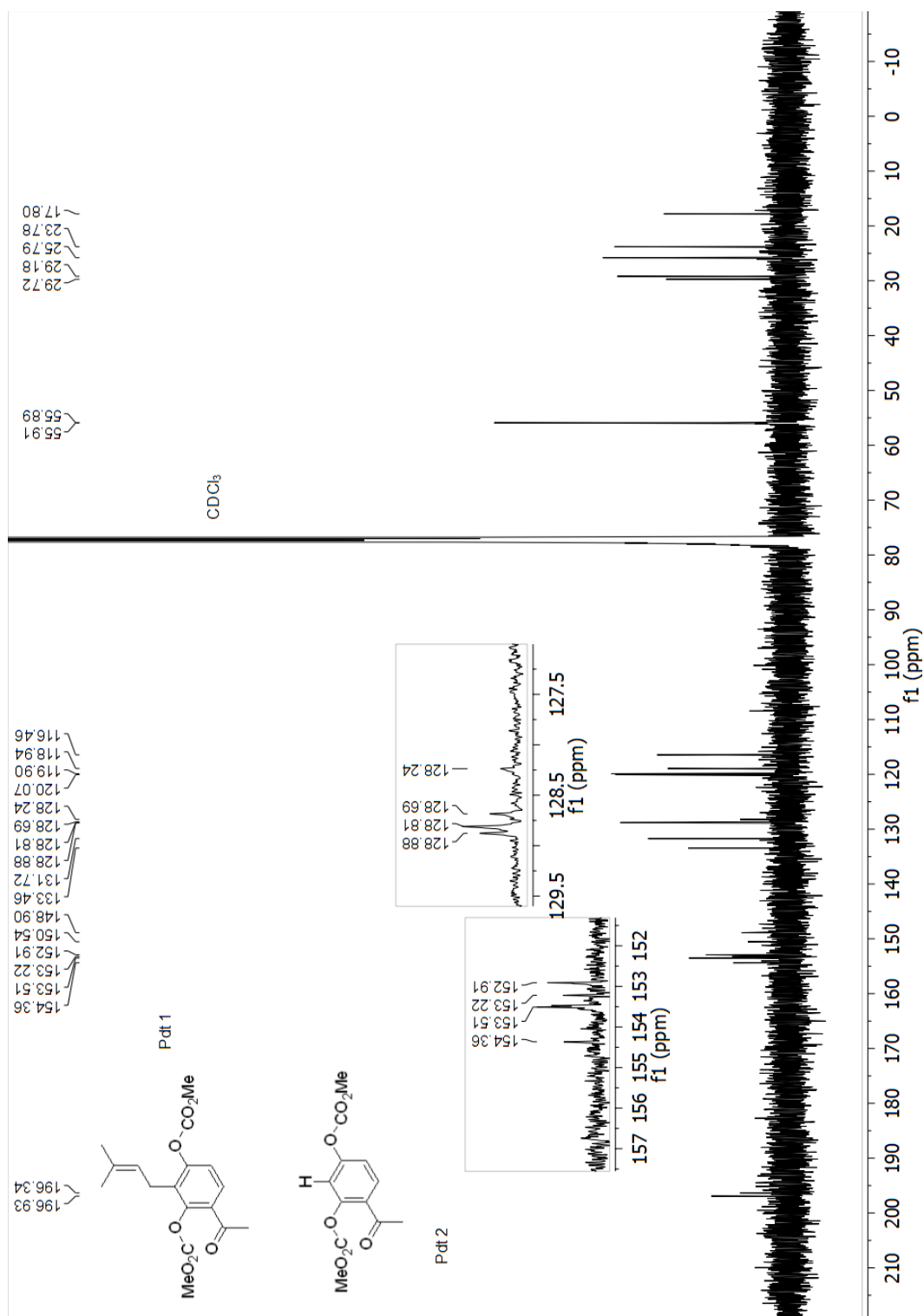
Line#:2 R.Time:14.6(Scan#:1156)
MassPeaks:109
RawMode:Single 14.6(1156) BasePeak:187(633089)
BG Mode:None



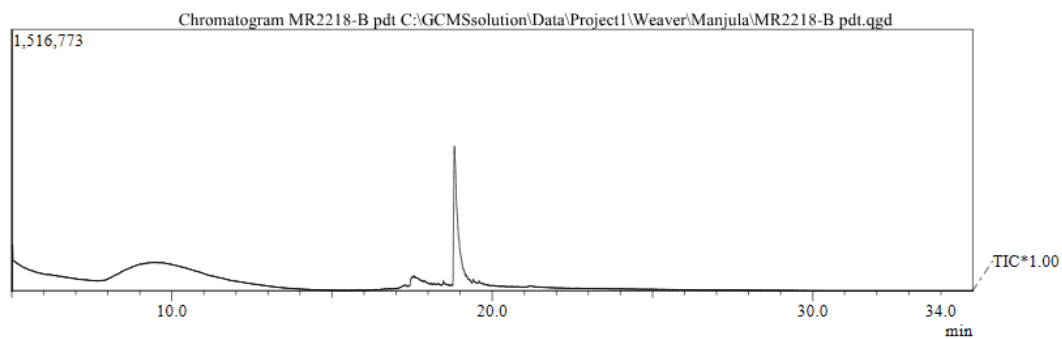
¹H NMR (400 MHz, Chloroform-d) spectrum of 4d (4-acetyl-2-(3-methylbut-2-en-1-yl)-1,3-phenylene dimethyl bis(carbonate))



¹³C NMR (101 MHz, Chloroform-d) spectrum of 4d (4-acetyl-2-(3-methylbut-2-en-1-yl)-1,3-phenylene dimethyl bis(carbonate))



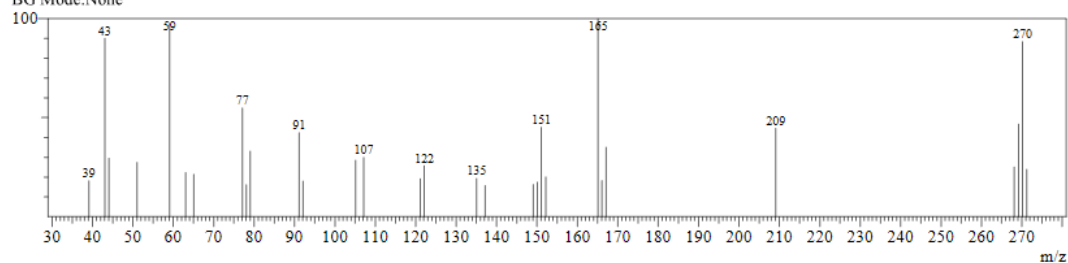
GC and MS of 4d (4-acetyl-2-(3-methylbut-2-en-1-yl)-1,3-phenylene dimethyl bis(carbonate))



Spectrum

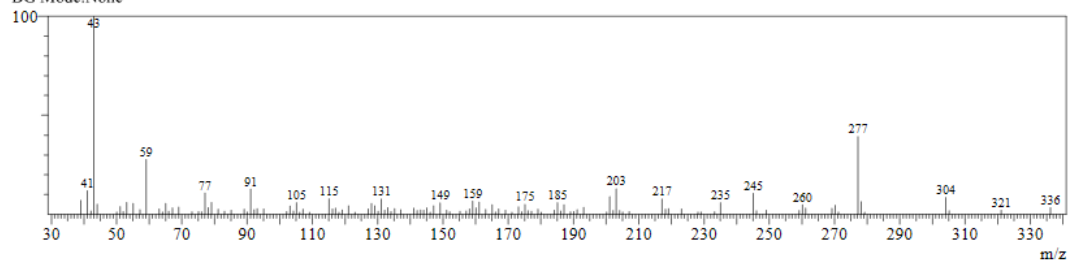
Line#:1 R.Time:17.7(Scan#:1519)
MassPeaks:30
RawMode:Single 17.7(1519) BasePeak:165(6673)
BG Mode:None

Reduced product

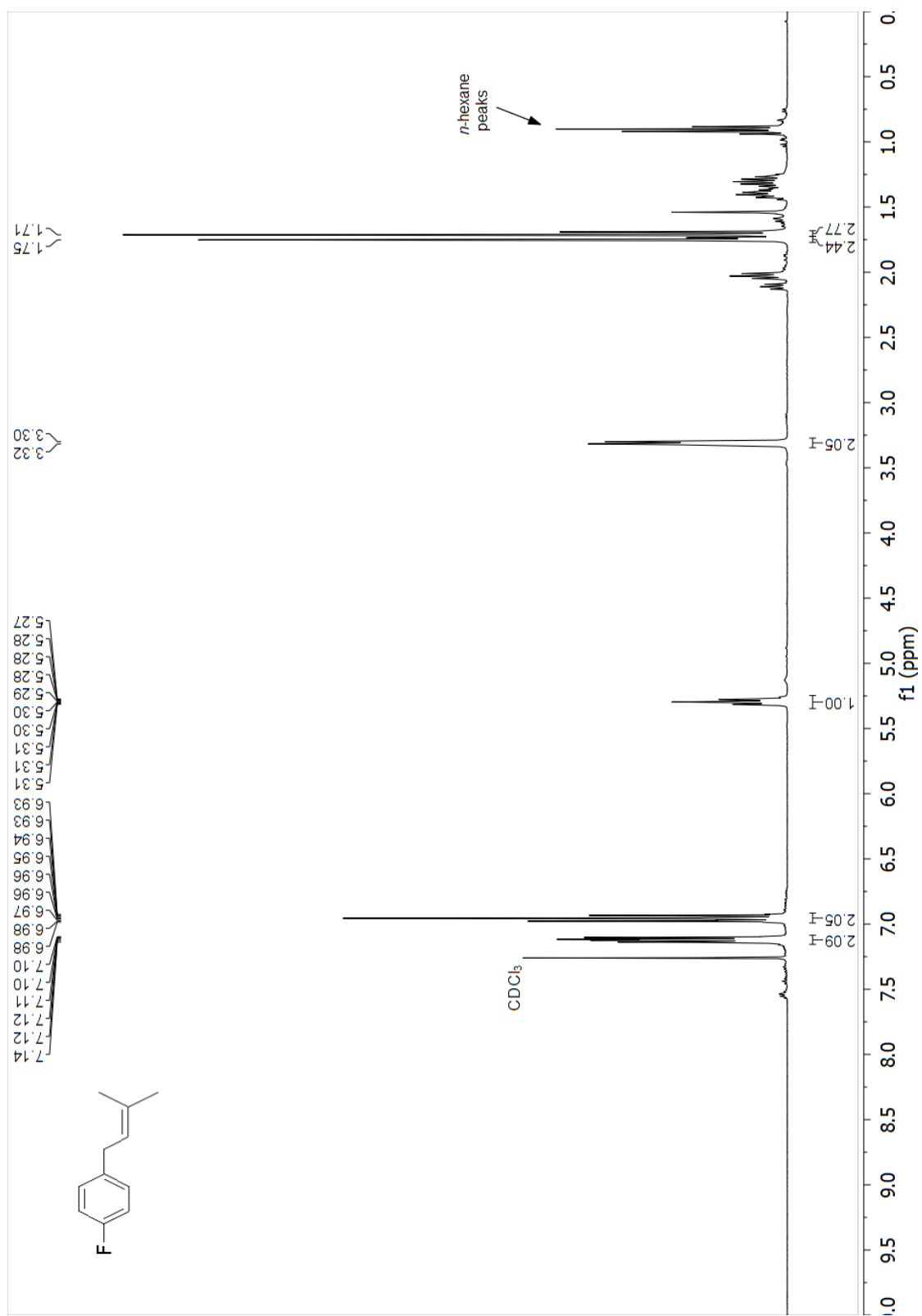


Line#:2 R.Time:18.9(Scan#:1666)
MassPeaks:125
RawMode:Single 18.9(1666) BasePeak:43(94351)
BG Mode:None

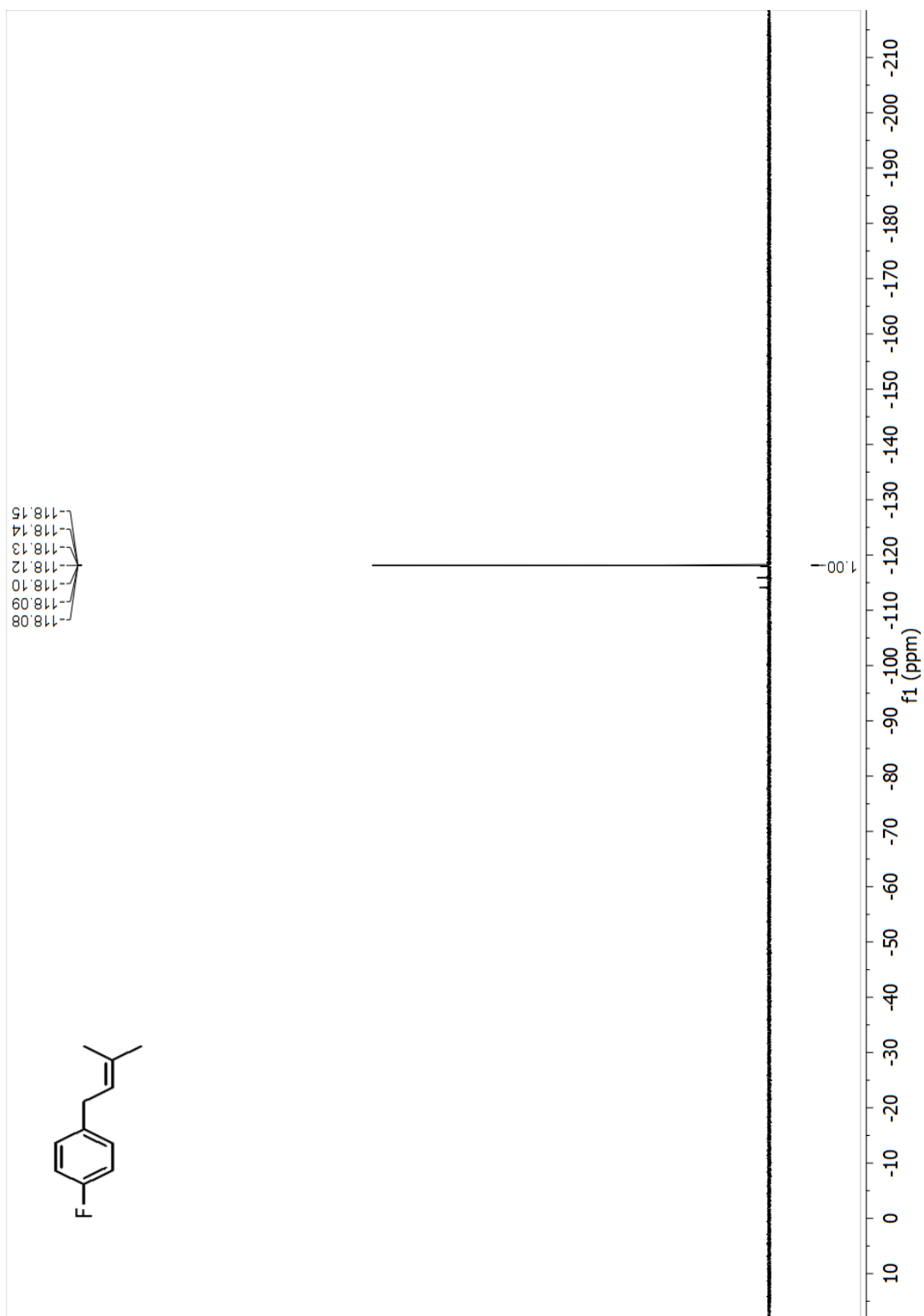
product



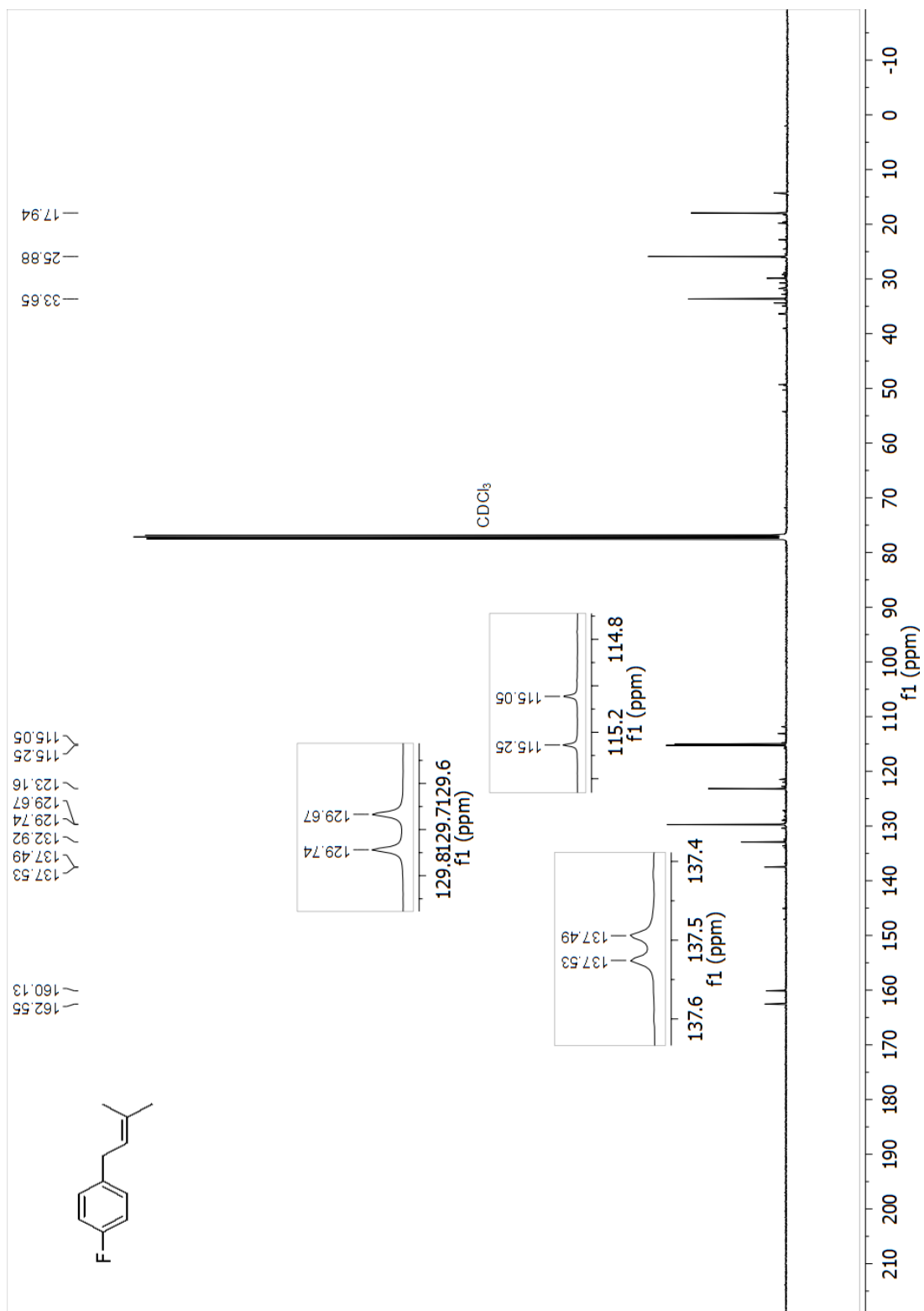
¹H NMR (400 MHz, Chloroform-d) spectrum of 4e (1-fluoro-4-(3-methylbut-2-en-1-yl)benzene)



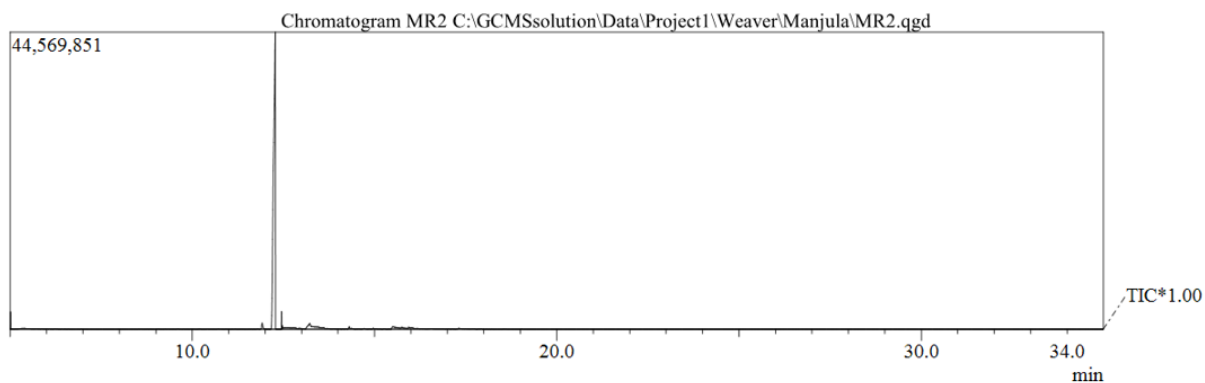
^{19}F NMR (376 MHz, Chloroform-d) spectrum of 4e (1-fluoro-4-(3-methylbut-2-en-1-yl)benzene)



¹³C NMR (101 MHz, Chloroform-d) spectrum of 4e (1-fluoro-4-(3-methylbut-2-en-1-yl)benzene)

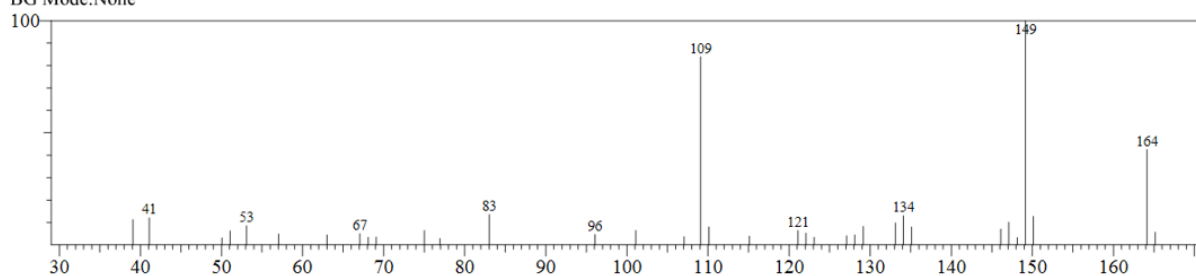


GC and MS of 4e (1-fluoro-4-(3-methylbut-2-en-1-yl)benzene)

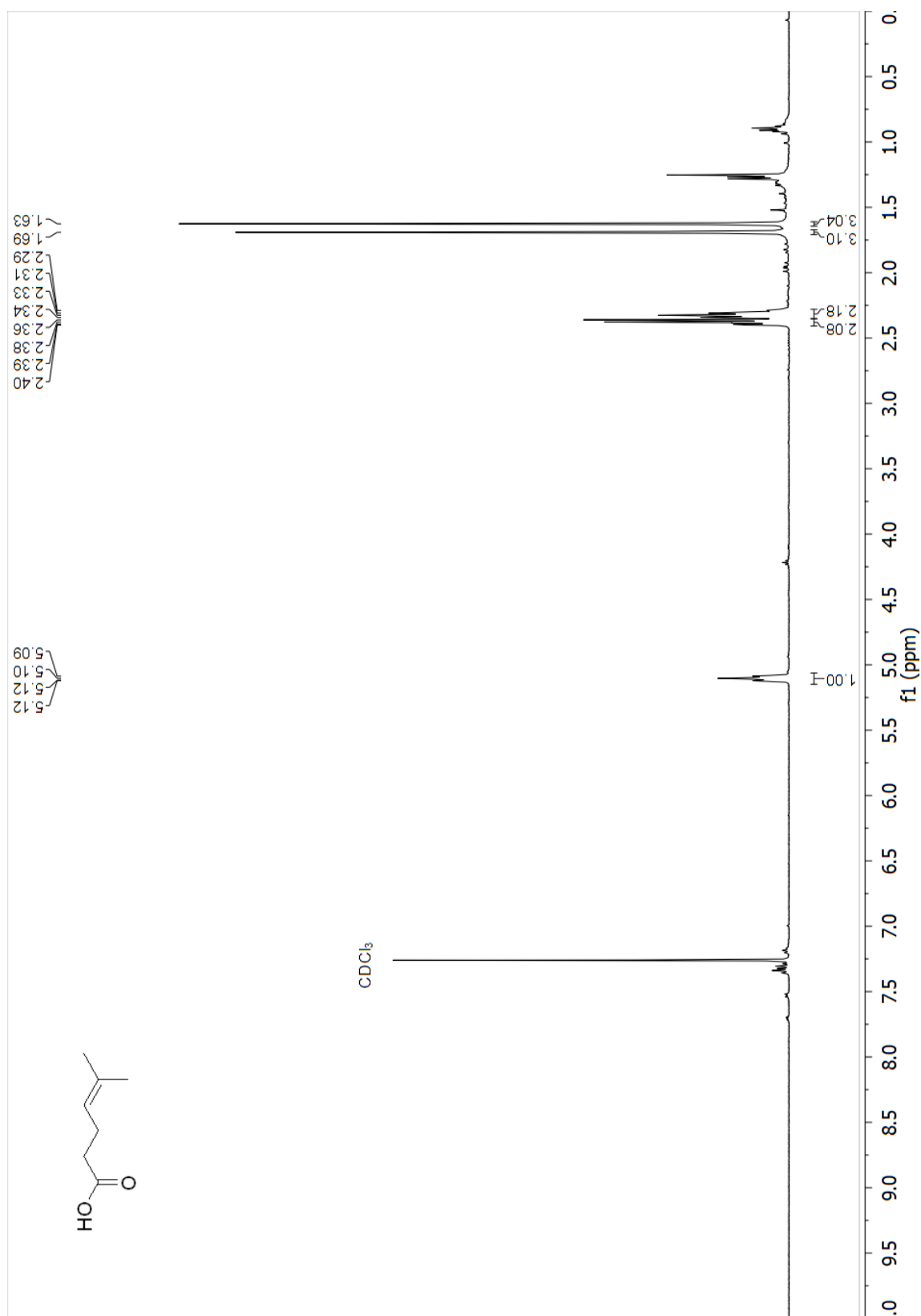


Spectrum

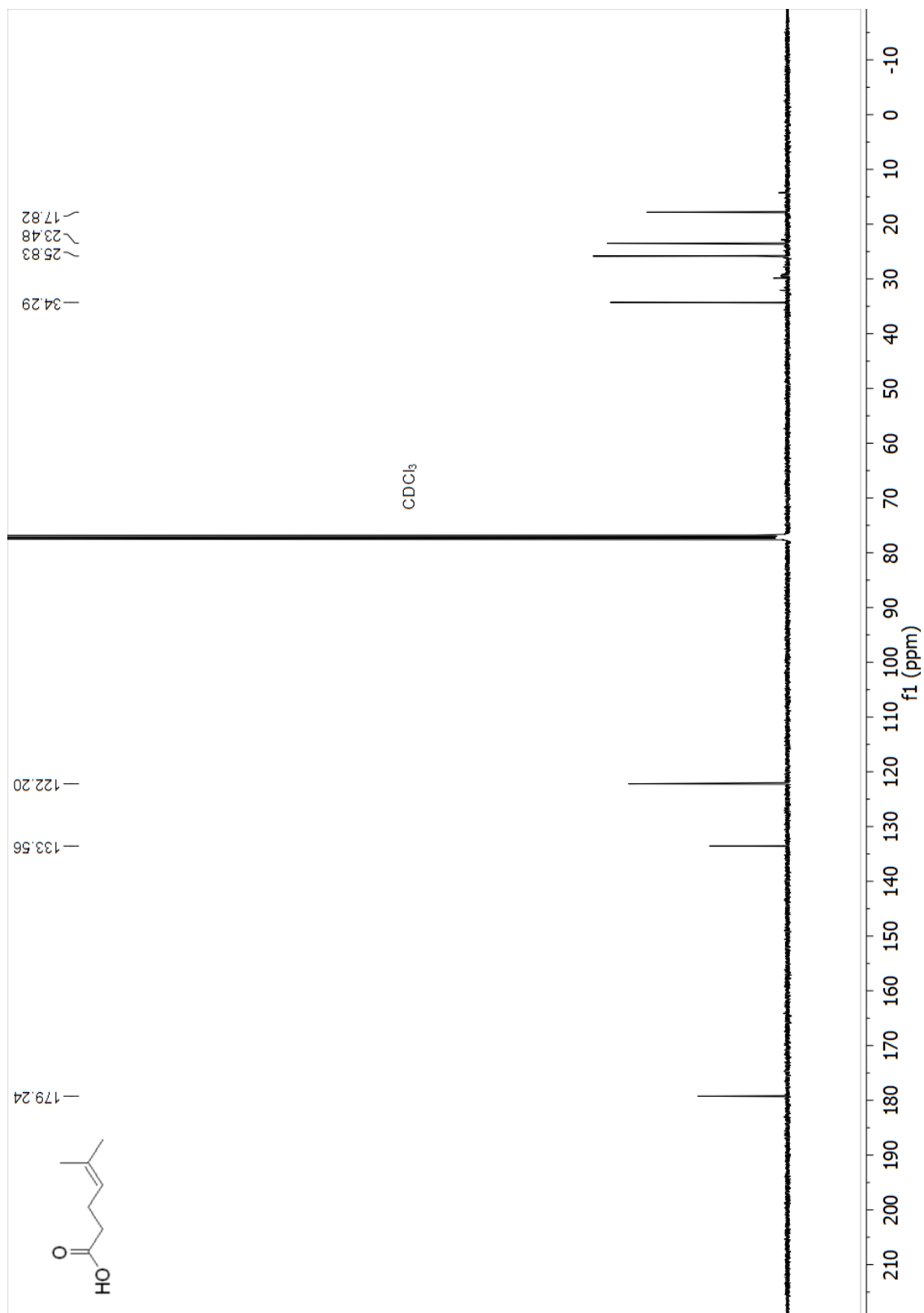
Line#:1 R.Time:12.3(Scan#:876)
MassPeaks:35
RawMode:Single 12.3(876) BasePeak:149(37037)
BG Mode:None



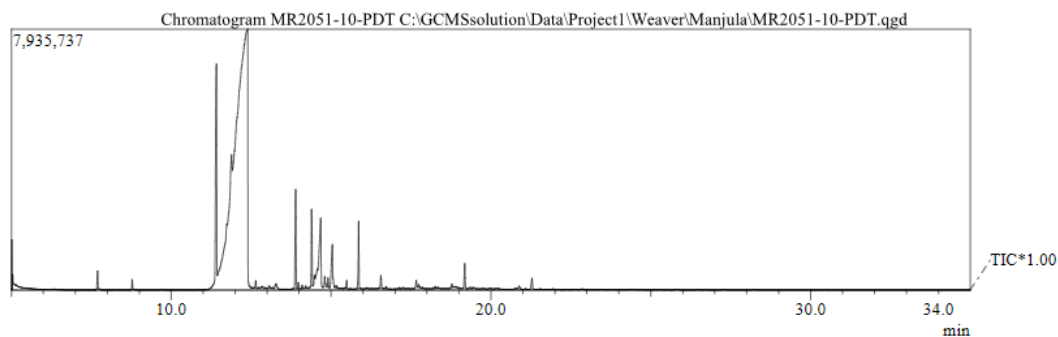
¹H NMR (400 MHz, Chloroform-d) spectrum of 5a (5-methylhex-4-enoic acid)



^{13}C NMR (101 MHz, Chloroform-d) spectrum of 5a (5-methylhex-4-enoic acid)

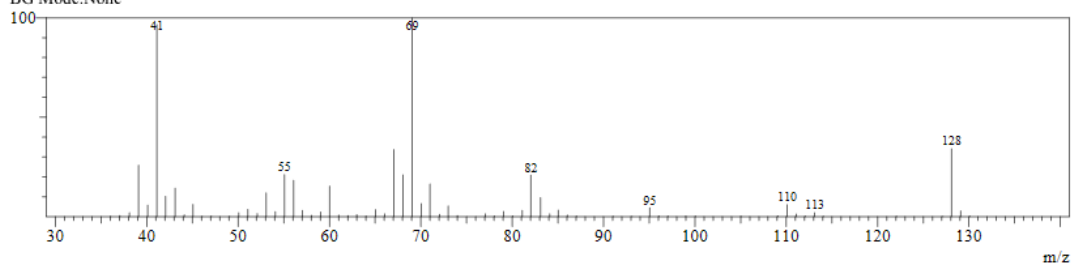


GC and MS of 5a (5-methylhex-4-enoic acid)

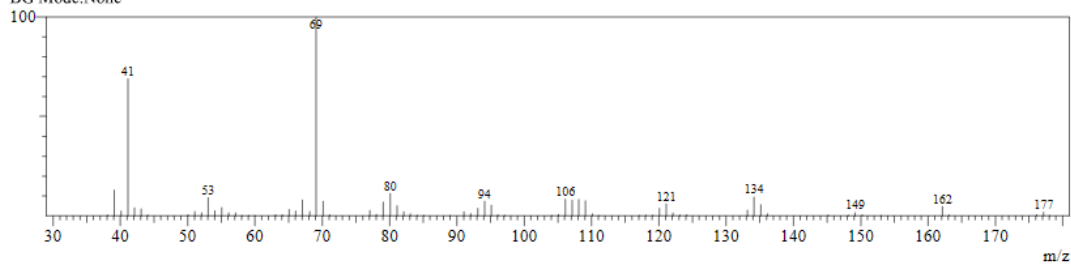


Spectrum

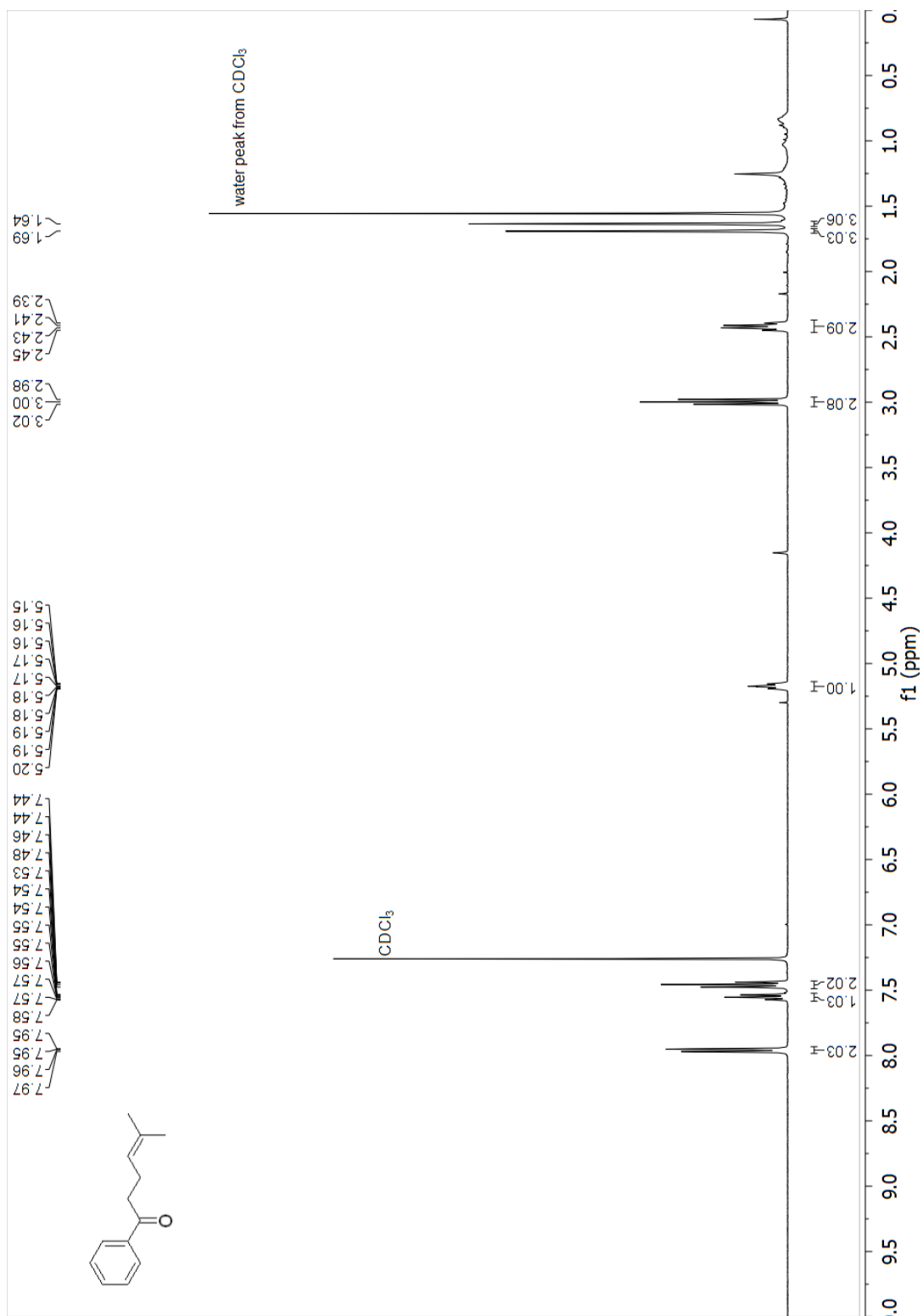
Line#:1 R.Time:11.9(Scan#:834)
MassPeaks:68
RawMode:Single 11.9(834) BasePeak:69(724308)
BG Mode:None



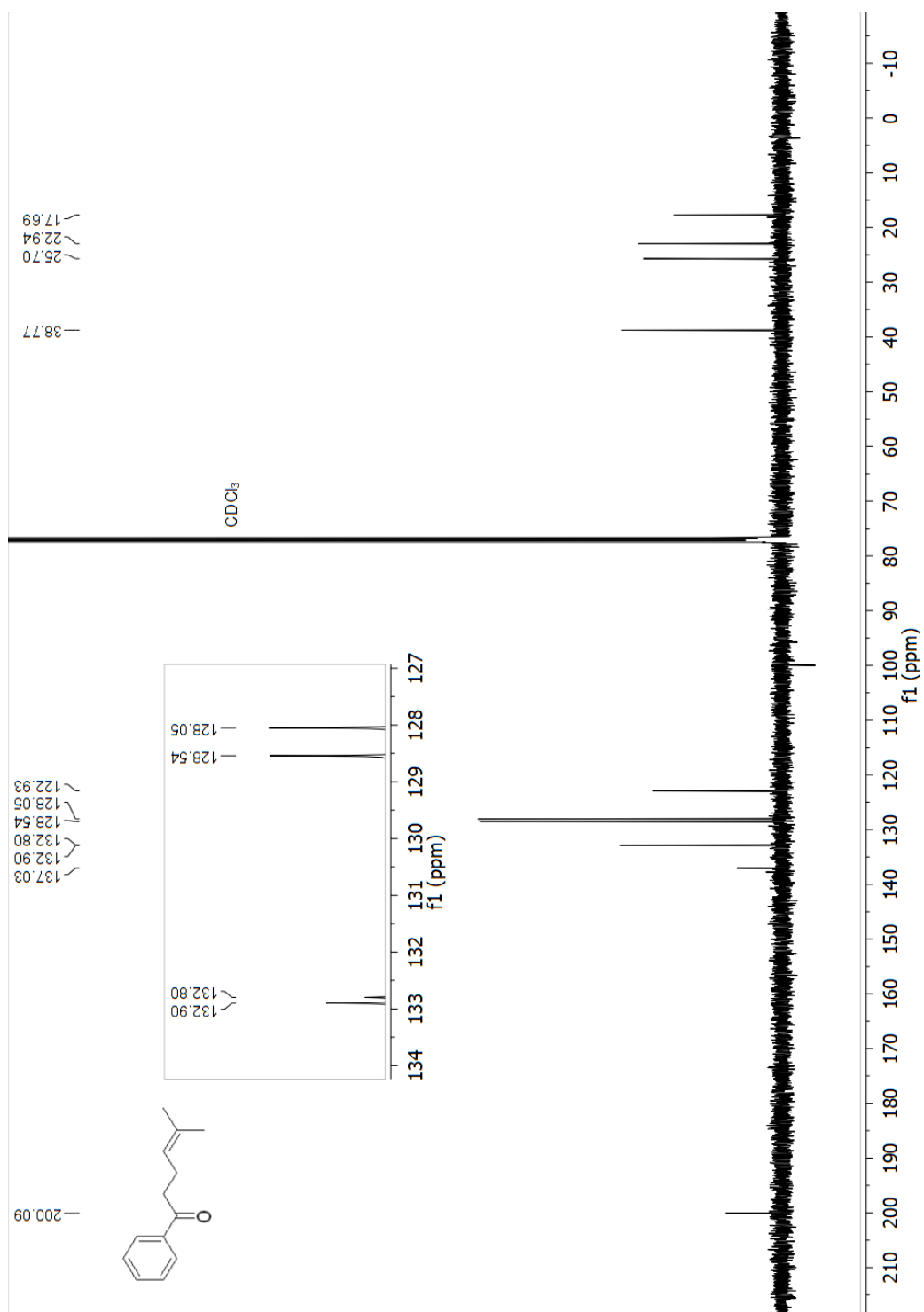
Line#:2 R.Time:13.9(Scan#:1066)
MassPeaks:74
RawMode:Single 13.9(1066) BasePeak:69(434355)
BG Mode:None



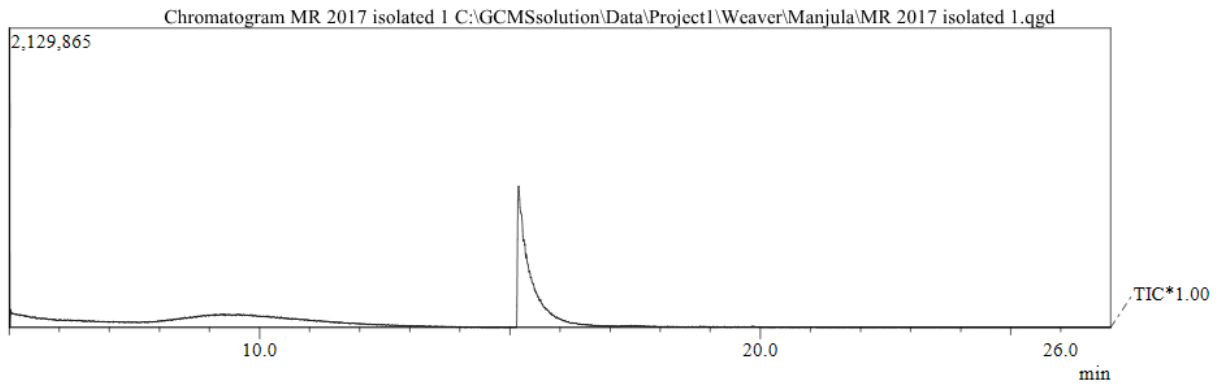
¹H NMR (400 MHz, Chloroform-d) spectrum of 5b (5-methyl-1-phenylhex-4-en-1-one)



^{13}C NMR (101 MHz, Chloroform-d) spectrum of 5b (5-methyl-1-phenylhex-4-en-1-one)

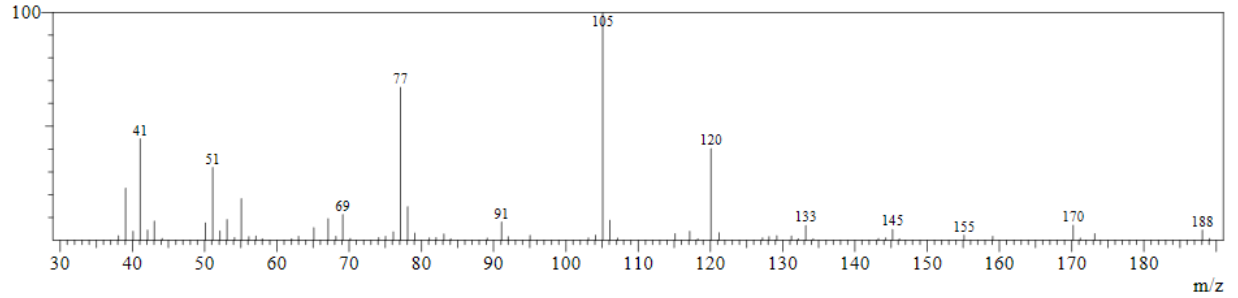


GC and MS of 5b (5-methyl-1-phenylhex-4-en-1-one)

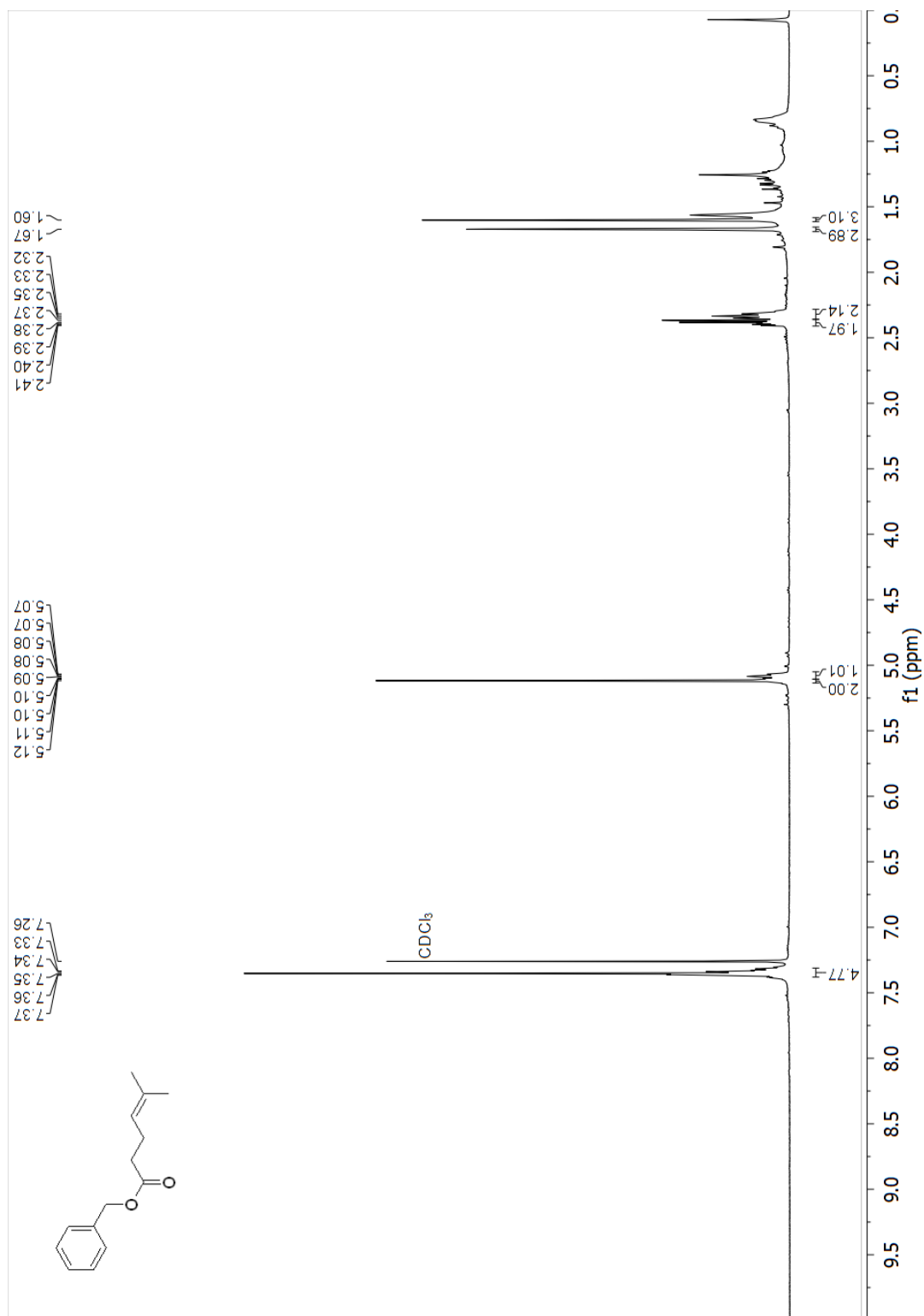


Spectrum

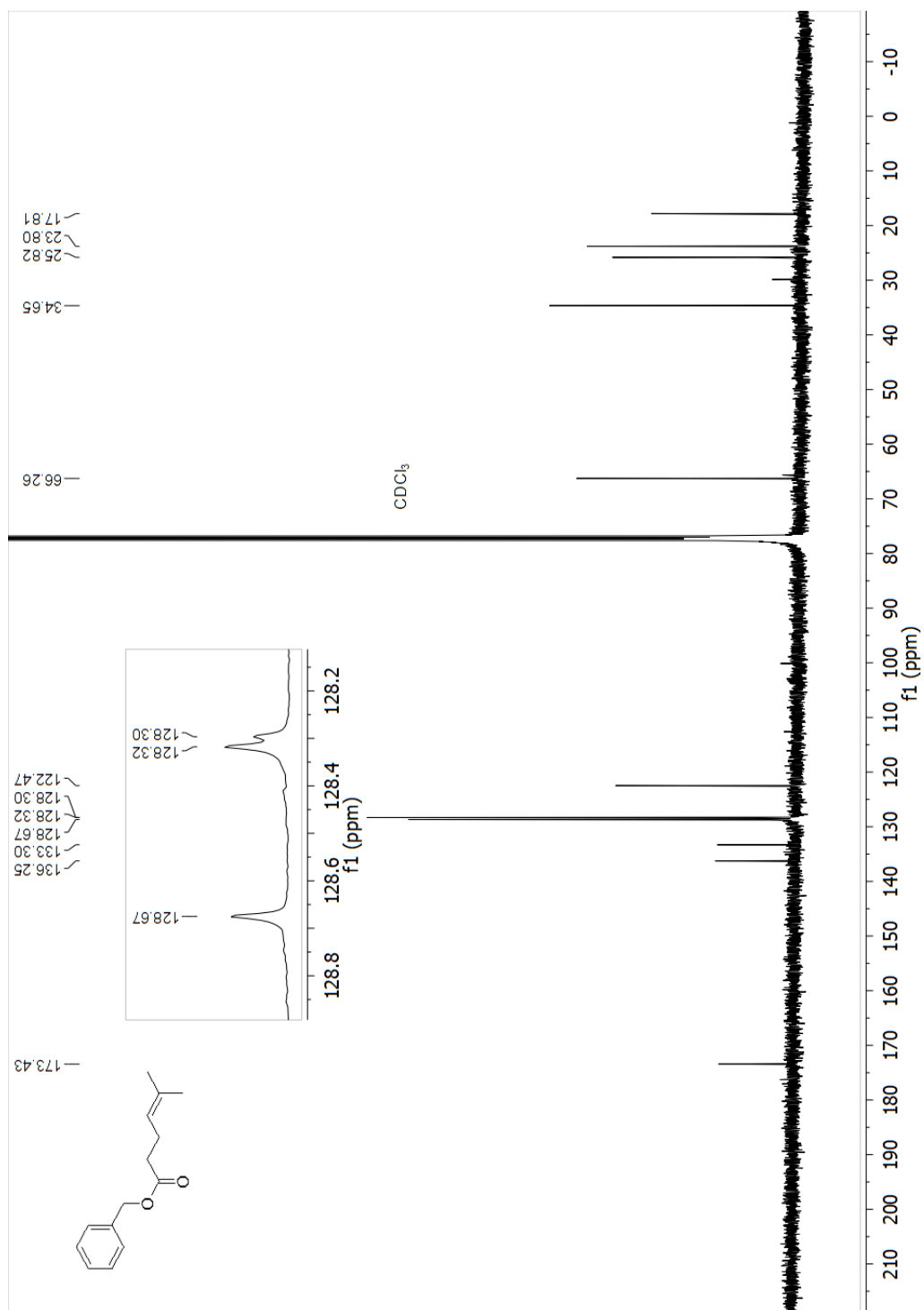
Line#:1 R.Time:15.2(Scan#:1227)
MassPeaks:65
RawMode:Single 15.2(1227) BasePeak:105(160118)
BG Mode:None



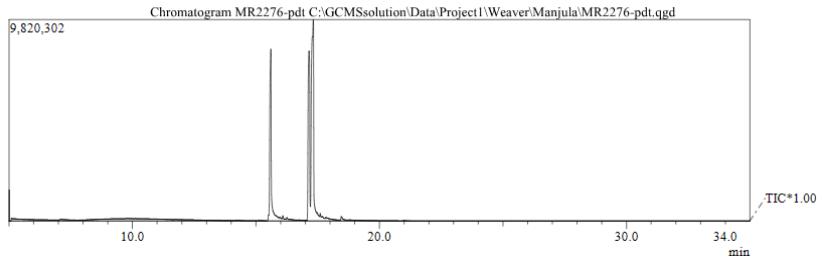
¹H NMR (400 MHz, Chloroform-d) spectrum of 5c (benzyl 5-methylhex-4-enoate)



¹³C NMR (101 MHz, Chloroform-d) spectrum of 5c (benzyl 5-methylhex-4-enoate)

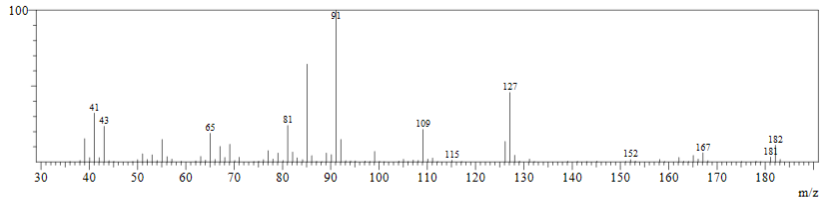


GC and MS of 5c (benzyl 5-methylhex-4-enoate)

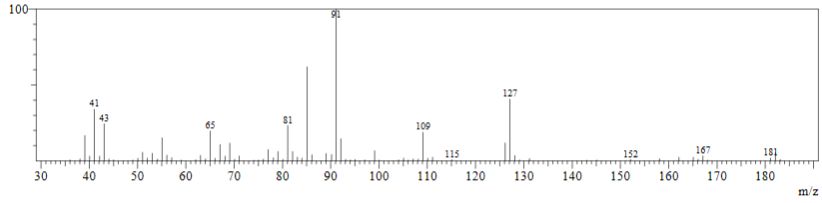


Spectrum

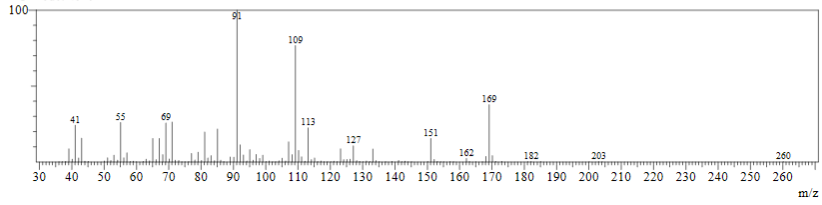
Line#:1 R.Time:15.5(Scan#:1266)
MassPeaks:95
RawMode:Single 15.5(1266) BasePeak:91(362081)
BG Mode:None



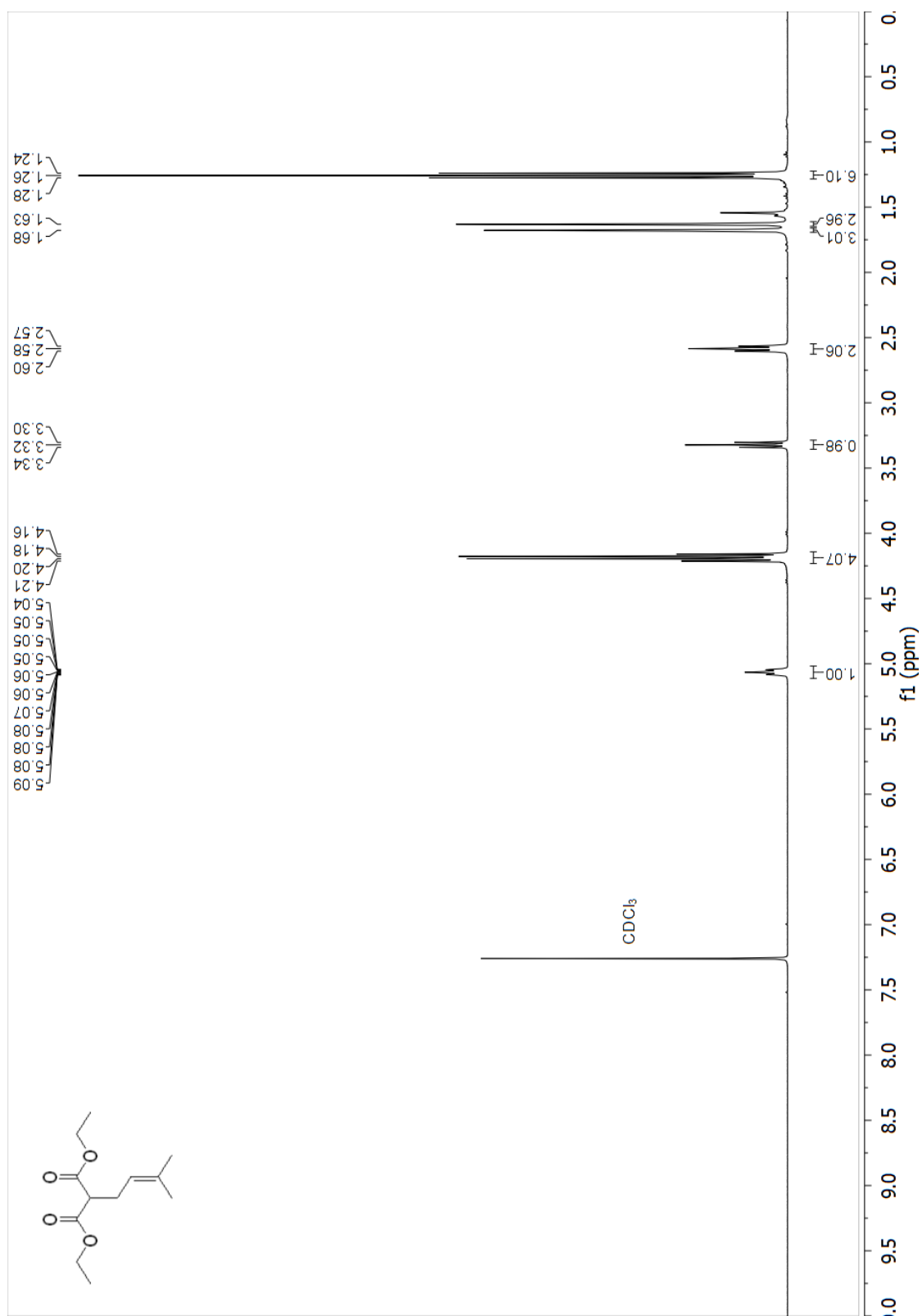
Line#:2 R.Time:15.6(Scan#:1276)
MassPeaks:78
RawMode:Single 15.6(1276) BasePeak:91(233852)
BG Mode:None



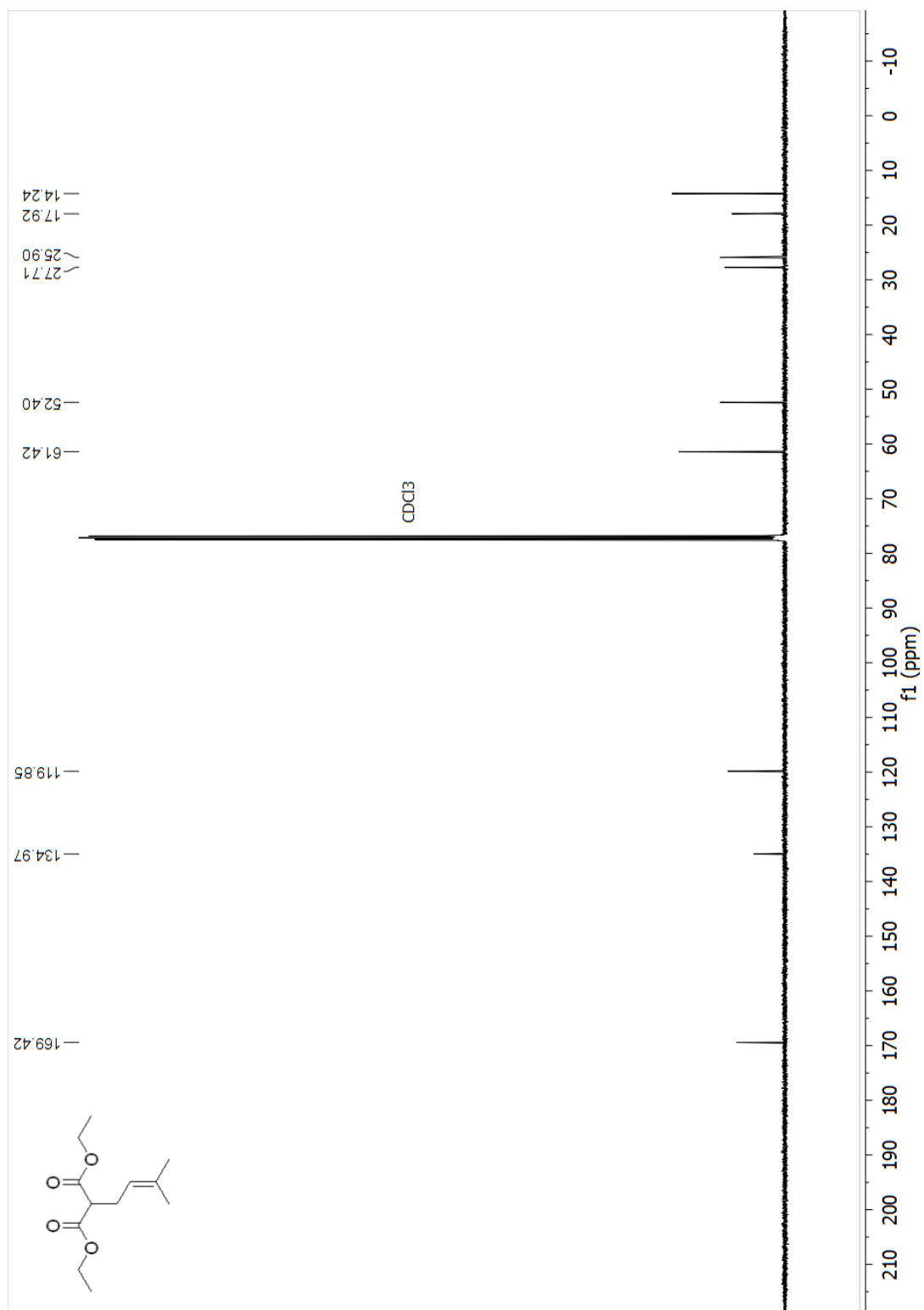
Line#:3 R.Time:17.2(Scan#:1460)
MassPeaks:125
RawMode:Single 17.2(1460) BasePeak:91(1249239)
BG Mode:None



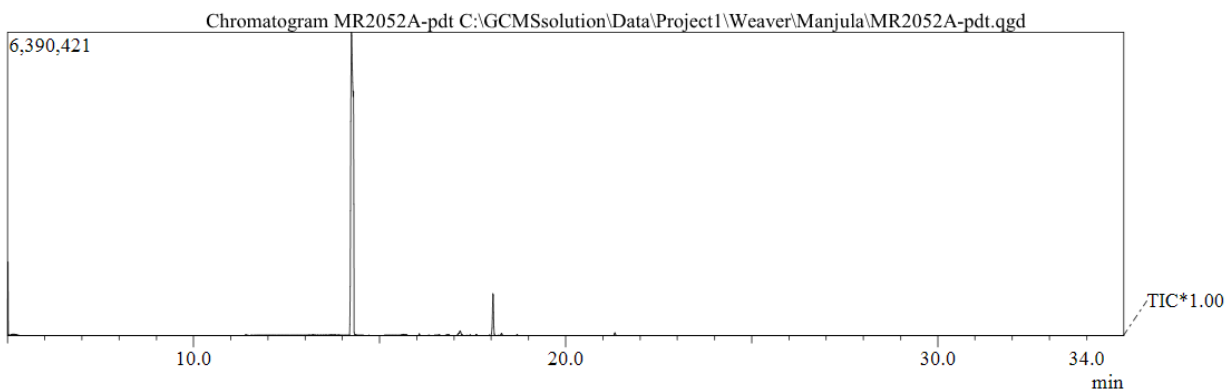
¹H NMR (400 MHz, Chloroform-d) spectrum of 5d (diethyl 2-(3-methylbut-2-en-1-yl)malonate)



¹³C NMR (101 MHz, Chloroform-d) spectrum of 5d (diethyl 2-(3-methylbut-2-en-1-yl)malonate)

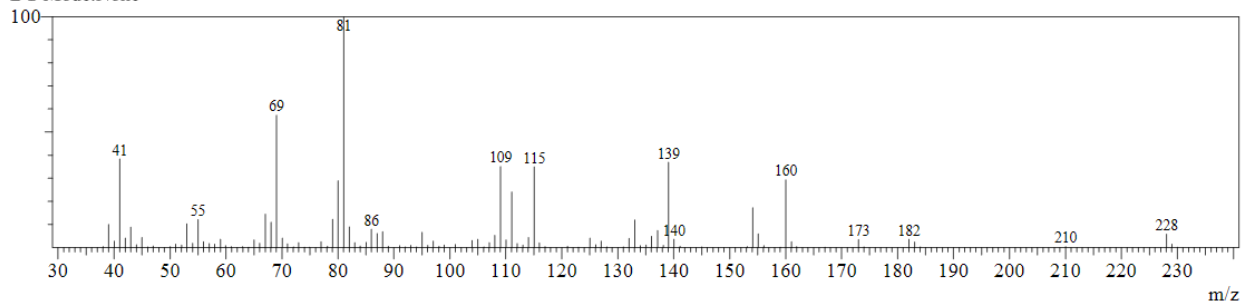


GC and MS of 5d (diethyl 2-(3-methylbut-2-en-1-yl)malonate)



Spectrum

Line#:1 R.Time:14.3(Scan#:1113)
MassPeaks:108
RawMode:Single 14.3(1113) BasePeak:81(827412)
BG Mode:None



2.5 References

- 1.(a) Kuzuyama, T., Biosynthetic studies on terpenoids produced by Streptomyces. *The Journal Of Antibiotics* **2017**, *70*, 811; (b) Sacchettini, J. C.; Poulter, C. D., Creating Isoprenoid Diversity. *Science* **1997**, *277*, 1788.
- 2.(a) Maimone, T. J.; Baran, P. S., Modern synthetic efforts toward biologically active terpenes. *Nat. Chem. Biol.* **2007**, *3*, 396; (b) Gershenzon, J.; Dudareva, N., The function of terpene natural products in the natural world. *Nat. Chem. Biol.* **2007**, *3*, 408.
- 3.Tholl, D., Terpene synthases and the regulation, diversity and biological roles of terpene metabolism. *Current Opinion in Plant Biology* **2006**, *9*, 297.
- 4.(a) Paduch, R.; Kandefer-Szerszeń, M.; Trytek, M.; Fiedurek, J., Terpenes: substances useful in human healthcare. *Arch. Immunol. Ther. Exp.* **2007**, *55*, 315; (b) Fernández, M. A.; de las Heras, B.; García, M. D.; Sáenz, M. T.; Villar, A., New insights into the mechanism of action of the anti-inflammatory triterpene lupeol. *J. Pharm. Pharmacol.* **2001**, *53*, 1533.
- 5.(a) Isman, M. B., Plant essential oils for pest and disease management. *Crop Protection* **2000**, *19*, 603; (b) Batish, D. R.; Singh, H. P.; Kohli, R. K.; Kaur, S., Eucalyptus essential oil as a natural pesticide. *For. Ecol. Manag.* **2008**, *256*, 2166.
- 6.Caputi, L.; Aprea, E., Use of terpenoids as natural flavouring compounds in food industry. *Recent patents on food, nutrition & agriculture* **2011**, *3*, 9.
- 7.(a) Gurgel do Vale, T.; Couto Furtado, E.; Santos, J. G.; Viana, G. S. B., Central effects of citral, myrcene and limonene, constituents of essential oil chemotypes from *Lippia alba* (Mill.) N.E. Brown. *Phytomedicine : international journal of phytotherapy and phytopharmacology* **2002**, *9*, 709; (b) Mizrahi, B.; Shapira, L.; Domb, A. J.; Hourii-Haddad, Y., Citrus oil and MgCl₂ as antibacterial and anti-inflammatory agents. *J Periodontol.* **2006**, *77*, 963; (c) Hirota, R.; Roger, N. N.; Nakamura, H.; Song, H. S.; Sawamura, M.; Suganuma, N., Anti-inflammatory effects of limonene from yuzu (*Citrus junos* Tanaka) essential oil on eosinophils. *J. Food Sci.* **2010**, *75*, H87.

- 8.(a) Kim, D.-S.; Lee, H.-J.; Jeon, Y.-D.; Han, Y.-H.; Kee, J.-Y.; Kim, H.-J.; Shin, H.-J.; Kang, J.-W.; Lee, B. S.; Kim, S.-H.; Kim, S.-J.; Park, S.-H.; Choi, B.-M.; Park, S.-J.; Um, J.-Y.; Hong, S.-H., Alpha-Pinene Exhibits Anti-Inflammatory Activity Through the Suppression of MAPKs and the NF- κ B Pathway in Mouse Peritoneal Macrophages. *Am. J. Chin. Med.* **2015**, *43*, 731; (b) Salehi, B.; Upadhyay, S.; Erdogan Orhan, I.; Kumar Jugran, A.; S, L. D. J.; D, A. D.; Sharopov, F.; Taheri, Y.; Martins, N.; Baghalpour, N.; Cho, W. C.; Sharifi-Rad, J., Therapeutic Potential of α - and β -Pinene: A Miracle Gift of Nature. *Biomolecules* **2019**, *9*.
- 9.(a) do Vale, T. G.; Furtado, E. C.; Santos, J. G., Jr.; Viana, G. S., Central effects of citral, myrcene and limonene, constituents of essential oil chemotypes from *Lippia alba* (Mill.) n.e. Brown. *Phytomedicine : international journal of phytotherapy and phytopharmacology* **2002**, *9*, 709; (b) Costa, L. G.; Garrick, J.; Roque, P. J.; Pellacani, C., Chapter 1 - Nutraceuticals in CNS Diseases: Potential Mechanisms of Neuroprotection. In *Nutraceuticals*, Gupta, R. C., Ed. Academic Press: Boston, 2016; pp 3.
- 10.(a) Diniz, L. R. L.; Vieira, C. F. X.; Chaves dos Santos, E.; Lima, G. C.; Aragao, K. K. V.; Vasconcelos, R. P.; Araujo, P. C. d. C.; Vasconcelos, Y. d. A. G.; Cunha de Oliveira, A.; David de Oliveira, H.; Portella, V. G.; Coelho-de-Souza, A. N., Gastroprotective effects of the essential oil of *Hyptis crenata* Pohl ex Benth. on gastric ulcer models. *J. Ethnopharmacol.* **2013**, *149*, 694; (b) Younis, N. S.; Mohamed, M. E., β -Caryophyllene as a Potential Protective Agent Against Myocardial Injury: The Role of Toll-Like Receptors. *Molecules* **2019**, *24*; (c) Varga, Z. V.; Matyas, C.; Erdelyi, K.; Cinar, R.; Nieri, D.; Chicca, A.; Nemeth, B. T.; Palocz, J.; Lajtos, T.; Corey, L.; Hasko, G.; Gao, B.; Kunos, G.; Gertsch, J.; Pacher, P., β -Caryophyllene protects against alcoholic steatohepatitis by attenuating inflammation and metabolic dysregulation in mice. *Br. J. Pharmacol.* **2018**, *175*, 320.
11. Bhalla, Y.; Gupta, V. K.; Jaitak, V., Anticancer activity of essential oils: a review. *J. Sci. Food Agric.* **2013**, *93*, 3643.

12. Fernandes, E. S.; Passos, G. F.; Medeiros, R.; da Cunha, F. M.; Ferreira, J.; Campos, M. M.; Pianowski, L. F.; Calixto, J. B., Anti-inflammatory effects of compounds alpha-humulene and (-)-trans-caryophyllene isolated from the essential oil of *Cordia verbenacea*. *Eur. J. Pharmacol.* **2007**, *569*, 228.
13. Dewick, P. M., *Medicinal Natural Products: A Biosynthetic Approach*. Wiley: 2002.
- 14.(a) Lindel, T.; Marsch, N.; Adla, S. K., Indole Prenylation in Alkaloid Synthesis. In *Alkaloid Synthesis*, Knölker, H.-J., Ed. Springer Berlin Heidelberg: Berlin, Heidelberg, 2012; pp 67; (b) Tanner, M. E., Mechanistic studies on the indole prenyltransferases. *Nat. Prod. Rep.* **2015**, *32*, 88.
- 15.(a) Yang, X.; Jiang, Y.; Yang, J.; He, J.; Sun, J.; Chen, F.; Zhang, M.; Yang, B., Prenylated flavonoids, promising nutraceuticals with impressive biological activities. *Trends Food Sci Technol* **2015**, *44*, 93; (b) Chen, X.; Mukwaya, E.; Wong, M.-S.; Zhang, Y., A systematic review on biological activities of prenylated flavonoids. *Pharm. Biol.* **2014**, *52*, 655.
- 16.(a) Li, X.-M.; Jiang, X.-J.; Yang, K.; Wang, L.-X.; Wen, S.-Z.; Wang, F., Prenylated Coumarins from *Heracleum stenopterum*, *Peucedanum praeruptorum*, *Clausena lansium*, and *Murraya paniculata*. *Nat Prod Bioprospect* **2016**, *6*, 233; (b) Lin, T.-T.; Huang, Y.-Y.; Tang, G.-H.; Cheng, Z.-B.; Liu, X.; Luo, H.-B.; Yin, S., Prenylated Coumarins: Natural Phosphodiesterase-4 Inhibitors from *Toddalia asiatica*. *Nat. Prod. Rep.* **2014**, *77*, 955.
- 17.(a) Vogel, S.; Heilmann, J., Synthesis, Cytotoxicity, and Antioxidative Activity of Minor Prenylated Chalcones from *Humulus lupulus*. *J. Nat. Prod.* **2008**, *71*, 1237; (b) García, P.; Hernández, Á.; San Feliciano, A.; Castro, M., Bioactive Prenyl- and Terpenyl-Quinones/Hydroquinones of Marine Origin †. *Mar Drugs* **2018**, *16*, 292.
- 18.(a) Pisco, L.; Kordian, M.; Peseke, K.; Feist, H.; Michalik, D.; Estrada, E.; Carvalho, J.; Hamilton, G.; Rando, D.; Quincoces, J., Synthesis of compounds with antiproliferative activity as analogues of prenylated natural products existing in Brazilian propolis. *Eur. J. Med. Chem.* **2006**, *41*, 401; (b) Vogel, S.; Ohmayer, S.; Brunner, G.; Heilmann, J., Natural and non-natural prenylated chalcones: Synthesis, cytotoxicity and anti-oxidative activity. *Bioorg. Med. Chem.* **2008**, *16*, 4286; (c) Chen, X.; Mukwaya, E.; Wong, M.-S.; Zhang, Y., A systematic review on biological activities of prenylated

flavonoids. *Pharm. Biol.* **2014**, *52*, 655; (d) Zhang, H.; Zhang, D.-D.; Lao, Y.-Z.; Fu, W.-W.; Liang, S.; Yuan, Q.-H.; Yang, L.; Xu, H.-X., Cytotoxic and Anti-Inflammatory Prenylated Benzoylphloroglucinols and Xanthenes from the Twigs of *Garcinia esculenta*. *J. Nat. Prod.* **2014**, *77*, 1700.

19.(a) Oleg, L.; Catherine, B.-P.; Svitlana, S., The Synthetic and Biological Aspects of Prenylation as the Versatile Tool for Estrogenic Activity Modulation. *ChemistrySelect* **2017**, *2*, 6577; (b) Saleh, O.; Haagen, Y.; Seeger, K.; Heide, L., Prenyl transfer to aromatic substrates in the biosynthesis of aminocoumarins, meroterpenoids and phenazines: The ABBA prenyltransferase family. *Phytochemistry* **2009**, *70*, 1728.

20.(a) Liang, P. H.; Ko, T. P.; Wang, A. H. J., Structure, mechanism and function of prenyltransferases. *Eur. J. Biochem.* **2002**, *269*, 3339; (b) Zhang, Y. J.; Skucas, E.; Krische, M. J., Direct Prenylation of Aromatic and α,β -Unsaturated Carboxamides via Iridium-Catalyzed C–H Oxidative Addition–Allene Insertion. *Org. Lett.* **2009**, *11*, 4248; (c) Chen, S.-Y.; Li, Q.; Wang, H., Manganese(I)-Catalyzed Direct C–H Allylation of Arenes with Allenes. *J. Org. Chem.*

2017, *82*, 11173; (d) Tarselli, M. A.; Liu, A.; Gagné, M. R., Gold(I)-catalyzed intermolecular hydroarylation of allenes with nucleophilic arenes: scope and limitations. *Tetrahedron* **2009**, *65*, 1785; (e) Farmer, J. L.; Hunter, H. N.; Organ, M. G., Regioselective Cross-Coupling of Allylboronic Acid Pinacol Ester Derivatives with Aryl Halides via Pd-PEPPSI-IPent. *J. Am. Chem. Soc.* **2012**, *134*, 17470; (f) Yang, Y.; Mustard, T. J. L.; Cheong, P. H. Y.; Buchwald, S. L., Palladium-Catalyzed Completely Linear-Selective Negishi Cross-Coupling of Allylzinc Halides with Aryl and Vinyl Electrophiles. *Angew. Chem. Int. Ed.* **2013**, *52*, 14098; (g) Grenning, A. J.; Boyce, J. H.; Porco, J. A., Rapid Synthesis of Polyprenylated Acylphloroglucinol Analogs via Dearomative Conjunctive Allylic Annulation. *J. Am. Chem. Soc.* **2014**, *136*, 11799; (h) Tan, D.-H.; Zeng, Y.-F.; Liu, Y.; Lv, W.-X.; Li, Q.; Wang, H., Direct Assembly of Prenylated Heteroarenes through a Cascade Minisci Reaction/Dehydration Sequence. *ChemistryOpen* **2016**, *5*, 535; (i) Dong-Hang, T.; Yao-Fu, Z.; Yao, L.; Wen-Xin, L.;

Qingjiang, L.; Honggen, W., Direct Assembly of Prenylated Heteroarenes through a Cascade Minisci Reaction/Dehydration Sequence. *ChemistryOpen* **2016**, *5*, 535.

21. Tanner, M. E., Mechanistic studies on the indole prenyltransferases. *Nat Prod Rep* **2015**, *32*, 88.

22.(a) Kuzuyama, T.; Noel, J. P.; Richard, S. B., Structural basis for the promiscuous biosynthetic prenylation of aromatic natural products. *Nature* **2005**, *435*, 983; (b) Pojer, F.; Wemakor, E.; Kammerer, B.; Chen, H.; Walsh, C. T.; Li, S.-M.; Heide, L., CloQ, a prenyltransferase involved in clorobiocin biosynthesis. *Proceedings of the National Academy of Sciences* **2003**, *100*, 2316; (c) Edwards, D. J.; Gerwick, W. H., Lyngbyatoxin Biosynthesis: Sequence of Biosynthetic Gene Cluster and Identification of a Novel Aromatic Prenyltransferase. *J. Am. Chem. Soc.* **2004**, *126*, 11432.

23.(a) Hatanaka, Y.; Goda, K.-i.; Hiyama, T., α -Selective cross-coupling reaction of allyltrifluorosilanes: Remarkable ligand effect on the regiochemistry. *Tetrahedron Lett.* **1994**, *35*, 6511; (b) Echavarren, A. M.; Stille, J. K., Palladium-catalyzed coupling of aryl triflates with organostannanes. *J. Am. Chem. Soc.* **1987**, *109*, 5478; (c) Takaoka, S.; Nakade, K.; Fukuyama, Y., The first total synthesis and neurotrophic activity of clusiparalicoline A, a prenylated and geranylated biaryl from *Clusia paralicola*. *Tetrahedron Lett.* **2002**, *43*, 6919; (d) Yamamoto, Y.; Takada, S.; Miyaura, N., γ -Selective cross-coupling of potassium allyltrifluoroborates with aryl and 1-alkenyl bromides catalyzed by a Pd(OAc)₂/D-t-BPF complex. *Chem. Lett.* **2006**, *35*, 704; (e) Sebelius, S.; Olsson, V. J.; Szabó, K. J., Palladium Pincer Complex Catalyzed Substitution of Vinyl Cyclopropanes, Vinyl Aziridines, and Allyl Acetates with Tetrahydroxydiboron. An Efficient Route to Functionalized Allylboronic Acids and Potassium Trifluoro(allyl)borates. *J. Am. Chem. Soc.* **2005**, *127*, 10478; (f) Gerbino, D. C.; Mandolesi, S. D.; Schmalz, H.-G.; Podesta, J. C., Introduction of Allyl and Prenyl Side-Chains into Aromatic Systems by Suzuki Cross-Coupling Reactions. *Eur. J. Org. Chem.* **2009**, 3964.

24.(a) Kawamura, T.; Hayashi, M.; Mukai, R.; Terao, J.; Nemoto, H., An Efficient Method for C8-Prenylation of Flavonols and Flavanones. *Synthesis* **2012**, *44*, 1308; (b) Takamatsu, N.; Inoue, S.; Kishi, Y., Synthetic study on echinulin and related compounds. Part I. acid-catalyzed amino claisen rearrangement of allyl- and 3,3-dimethylallyl-aniline derivatives. *Tetrahedron Lett.* **1971**, *12*, 4661; (c)

Gester, S.; Metz, P.; Zierau, O.; Vollmer, G., An efficient synthesis of the potent phytoestrogens 8-prenylnaringenin and 6-(1,1-dimethylallyl)naringenin by europium(III)-catalyzed Claisen rearrangement. *Tetrahedron* **2001**, *57*, 1015.

25.(a) Marsden, S. P.; Depew, K. M.; Danishefsky, S. J., Stereoselective Total Syntheses of Amauromine and 5-N-Acetylardeemin. A Concise Route to the Family of "Reverse-Prenylated" Hexahydropyrroloindole Alkaloids. *J. Am. Chem. Soc.* **1994**, *116*, 11143; (b) Trost, B. M.; Malhotra, S.; Chan, W. H., Exercising Regiocontrol in Palladium-Catalyzed Asymmetric Prenylations and Geranylation: Unifying Strategy toward Flustramines A and B. *J. Am. Chem. Soc.* **2011**, *133*, 7328; (c) Iwasaki, T.; Okamoto, K.; Kuniyasu, H.; Kambe, N., Cu-catalyzed reductive coupling of perfluoroarenes with 1,3-dienes. *Chem. Lett.* **2017**, *46*, 1504; (d) Priya, S.; Weaver, J. D., 3rd, Prenyl Praxis: A Method for Direct Photocatalytic Defluoroprenylation. *J. Am. Chem. Soc.* **2018**, *140*, 16020.

26.(a) Narayanam, J. M. R.; Stephenson, C. R. J., Visible light photoredox catalysis: applications in organic synthesis. *Chem. Soc. Rev.* **2011**, *40*, 102; (b) Tucker, J. W.; Stephenson, C. R. J., Shining Light on Photoredox Catalysis: Theory and Synthetic Applications. *J. Org. Chem.* **2012**, *77*, 1617; (c) Prier, C. K.; Rankic, D. A.; MacMillan, D. W. C., Visible Light Photoredox Catalysis with Transition Metal Complexes: Applications in Organic Synthesis. *Chem. Rev.* **2013**, *113*, 5322; (d) Shaw, M. H.; Twilton, J.; MacMillan, D. W. C., Photoredox Catalysis in Organic Chemistry. *J. Org. Chem.* **2016**, *81*, 6898; (e) König, B., Photocatalysis in Organic Synthesis – Past, Present, and Future. *Eur. J. Org. Chem.* **2017**, *2017*, 1979; (f) Goddard, J.-P.; Ollivier, C.; Fensterbank, L., Photoredox Catalysis for the Generation of Carbon Centered Radicals. *Acc. Chem. Res.* **2016**, *49*, 1924; (g) Marzo, L.; Pagire, S. K.; Reiser, O.; König, B., Visible-Light Photocatalysis: Does It Make a Difference in Organic Synthesis? *Angew. Chem. Int. Ed.* **2018**, *57*, 10034.

27.(a) Noble, A.; MacMillan, D. W. C., Photoredox α -Vinylolation of α -Amino Acids and N-Aryl Amines. *J. Am. Chem. Soc.* **2014**, *136*, 11602; (b) Heitz, D. R.; Rizwan, K.; Molander, G. A., Visible-Light-Mediated Alkenylation, Allylation, and Cyanation of Potassium Alkyltrifluoroborates with Organic Photoredox Catalysts. *J. Org. Chem.* **2016**, *81*, 7308; (c) Hering, T.; Hari, D. P.; König, B.,

Visible-Light-Mediated α -Arylation of Enol Acetates Using Aryl Diazonium Salts. *J. Org. Chem.* **2012**, *77*, 10347; (d) Paul, S.; Guin, J., Radical C(sp³)-H alkenylation, alkynylation and allylation of ethers and amides enabled by photocatalysis. *Green Chem.* **2017**, *19*, 2530.

28.(a) Pirtsch, M.; Paria, S.; Matsuno, T.; Isobe, H.; Reiser, O., [Cu(dap)₂Cl] As an Efficient Visible-Light-Driven Photoredox Catalyst in Carbon-Carbon Bond-Forming Reactions. *Chem. Eur. J.* **2012**, *18*, 7336; (b) Paria, S.; Pirtsch, M.; Kais, V.; Reiser, O., Visible-Light-Induced Intermolecular Atom-Transfer Radical Addition of Benzyl Halides to Olefins: Facile Synthesis of Tetrahydroquinolines. *Synthesis* **2013**, *45*, 2689; (c) Qiang, L.; Hong, Y.; Jie, L.; Yuhong, Y.; Xu, Z.; Ziqi, Z.; Aiwen, L., Visible-Light Photocatalytic Radical Alkenylation of α -Carbonyl Alkyl Bromides and Benzyl Bromides. *Chem. Eur. J.* **2013**, *19*, 5120; (d) Hari, D. P.; Schroll, P.; König, B., Metal-Free, Visible-Light-Mediated Direct C-H Arylation of Heteroarenes with Aryl Diazonium Salts. *J. Am. Chem. Soc.* **2012**, *134*, 2958.

29. Broggi, J.; Terme, T.; Vanelle, P., Organic Electron Donors as Powerful Single-Electron Reducing Agents in Organic Synthesis. *Angew. Chem. Int. Ed.* **2014**, *53*, 384.

30.(a) Arora, A.; Teegardin, K. A.; Weaver, J. D., Reductive Alkylation of 2-Bromoazoles via Photoinduced Electron Transfer: A Versatile Strategy to Csp²-Csp³ Coupled Products. *Org. Lett.* **2015**, *17*, 3722; (b) Capaldo, L.; Ravelli, D., Hydrogen Atom Transfer (HAT): A Versatile Strategy for Substrate Activation in Photocatalyzed Organic Synthesis. *Eur. J. Org. Chem.* **2017**, *2017*, 2056.

31.(a) Mizuta, S.; Verhoog, S.; Engle, K. M.; Khotavivattana, T.; O'Duill, M.; Wheelhouse, K.; Rassias, G.; Médebielle, M.; Gouverneur, V., Catalytic Hydrotrifluoromethylation of Unactivated Alkenes. *J. Am. Chem. Soc.* **2013**, *135*, 2505; (b) Chen, Y.; Shu, C.; Luo, F.; Xiao, X.; Zhu, G., Photocatalytic acylarylation of unactivated alkenes with diaryliodonium salts toward indanones and related compounds. *Chem. Commun.* **2018**, *54*, 5373; (c) Liu, Q.; Yi, H.; Liu, J.; Yang, Y.; Zhang, X.; Zeng, Z.; Lei, A., Visible-Light Photocatalytic Radical Alkenylation of α -Carbonyl Alkyl Bromides and Benzyl Bromides. *Chem. Eur. J.* **2013**, *19*, 5120; (d) Nakajima, M.; Lefebvre, Q.; Rueping, M., Visible light photoredox-catalysed intermolecular radical addition of α -halo amides to olefins. *Chem.*

Commun. **2014**, *50*, 3619; (e) Prasad Hari, D.; Hering, T.; König, B., The Photoredox-Catalyzed Meerwein Addition Reaction: Intermolecular Amino-Arylation of Alkenes. *Angew. Chem. Int. Ed.* **2014**, *53*, 725.

32. Badenock, J. C.; Gribble, G. W., Chapter Four - Metal-Catalyzed Coupling with Heterocycles. In *Advances in Heterocyclic Chemistry*, Scriven, E. F. V.; Ramsden, C. A., Eds. Academic Press: 2016; Vol. 120, pp 99.

33.(a) Arora, A.; Weaver, J. D., Photocatalytic Generation of 2-Azoly Radical Intermediates for the Azoylation of Arenes and Heteroarenes via C–H Functionalization. *Org. Lett.* **2016**, *18*, 3996; (b) Singh, A.; Arora, A.; Weaver, J. D., Photoredox-Mediated C–H Functionalization and Coupling of Tertiary Aliphatic Amines with 2-Chloroazoles. *Org. Lett.* **2013**, *15*, 5390.

34.(a) Charrier, N.; Quiclet-Sire, B.; Zard, S. Z., Allylic Alcohols as Radical Allylating Agents. An Overall Olefination of Aldehydes and Ketones. *J. Am. Chem. Soc.* **2008**, *130*, 8898; (b) Quiclet-Sire, B.; Zard, S. Z., New Radical Allylation Reaction. *J. Am. Chem. Soc.* **1996**, *118*, 1209; (c) Charrier, N.; Zard, S. Z., Radical Allylation with α -Branched Allyl Sulfones. *Angew. Chem. Int. Ed.* **2008**, *47*, 9443; (d) Quiclet-Sire, B.; Zard, S., Z., Fun with radicals: Some new perspectives for organic synthesis. *Pure Appl. Chem.* **2011**, *83*, 519; (e) Debien, L.; Quiclet-Sire, B.; Zard, S. Z., Allylic Alcohols: Ideal Radical Allylating Agents? *Acc. Chem. Res.* **2015**, *48*, 1237.

35. Sumino, S.; Uno, M.; Huang, H.-J.; Wu, Y.-K.; Ryu, I., Palladium/Light Induced Radical Alkenylation and Allylation of Alkyl Iodides Using Alkenyl and Allylic Sulfones. *Org. Lett.* **2018**, *20*, 1078.

36.(a) Kerr, J. A., Bond Dissociation Energies by Kinetic Methods. *Chem. Rev.* **1966**, *66*, 465; (b) Mackle, H.; McClean, R. T. B., Studies in the thermochemistry of organic sulphides. Part 4.—Heat of formation of the mercaptyl radical. *J. Chem. Soc. Faraday Trans.* **1962**, *58*, 895.

37. Baralle, A.; Fensterbank, L.; Goddard, J.-P.; Ollivier, C., Aryl Radical Formation by Copper(I) Photocatalyzed Reduction of Diaryliodonium Salts: NMR Evidence for a CuII/CuI Mechanism. *Chem. Eur. J.* **2013**, *19*, 10809.

- 38.(a) Kamijo, S.; Kamijo, K.; Maruoka, K.; Murafuji, T., Aryl Ketone Catalyzed Radical Allylation of C(sp³)–H Bonds under Photoirradiation. *Org. Lett.* **2016**, *18*, 6516; (b) Kamijo, S.; Takao, G.; Kamijo, K.; Hirota, M.; Tao, K.; Murafuji, T., Photo-induced Substitutive Introduction of the Aldoxime Functional Group to Carbon Chains: A Formal Formylation of Non-Acidic C(sp³)–H Bonds. *Angew. Chem.* **2016**, *128*, 9847.
- 39.Duan, Y.; Zhang, M.; Ruzi, R.; Wu, Z.; Zhu, C., The direct decarboxylative allylation of N-arylglycine derivatives by photoredox catalysis. *Org Chem Front* **2017**, *4*, 525.
- 40.Zhang, J.; Li, Y.; Zhang, F.; Hu, C.; Chen, Y., Generation of Alkoxy Radicals by Photoredox Catalysis Enables Selective C(sp³)–H Functionalization under Mild Reaction Conditions. *Angew. Chem. Int. Ed.* **2016**, *55*, 1872.
- 41.Wu, K.; Wang, L.; Colón-Rodríguez, S.; Flechsig, G.-U.; Wang, T., Amidyl Radical Directed Remote Allylation of Unactivated sp³ C–H Bonds by Organic Photoredox Catalysis. *Angew. Chem. Int. Ed.* **2019**, *58*, 1774.
- 42.Sun, X.; Wang, L.; Zhang, Y., A Convenient Synthesis of Sulfones Using Zinc Mediated Coupling Reaction of Sulfonyl Chlorides with Alkyl Halides in Aqueous Media. *Synth. Commun.* **1998**, *28*, 1785.
- 43.Arora, A.; Teegardin, K. A.; Weaver, J. D., Reductive Alkylation of 2-Bromoazoles via Photoinduced Electron Transfer: A Versatile Strategy to Csp²–Csp³ Coupled Products. *Org. Lett.* **2015**, *17*, 3722.
- 44.Arora, A.; Weaver, J. D., Photocatalytic Generation of 2-Azoly Radicals: Intermediates for the Azolylation of Arenes and Heteroarenes via C–H Functionalization. *Org. Lett.* **2016**, *18*, 3996.
- 45.(a) Allongue, P.; Delamar, M.; Desbat, B.; Fagebaume, O.; Hitmi, R.; Pinson, J.; Savéant, J.-M., Covalent Modification of Carbon Surfaces by Aryl Radicals Generated from the Electrochemical Reduction of Diazonium Salts. *J. Am. Chem. Soc.* **1997**, *119*, 201; (b) Galli, C., Radical reactions of arenediazonium ions: An easy entry into the chemistry of the aryl radical. *Chem. Rev.* **1988**, *88*, 765; (c) Milanesi, S.; Fagnoni, M.; Albini, A., (Sensitized) Photolysis of Diazonium Salts as a Mild General

Method for the Generation of Aryl Cations. Chemoselectivity of the Singlet and Triplet 4-Substituted Phenyl Cations. *J. Org. Chem.* **2005**, *70*, 603.

46.(a) Sheng, M.; Frurip, D.; Gorman, D., Reactive chemical hazards of diazonium salts. *J. Loss. Prev. Process Ind.* **2015**, *38*, 114; (b) Ullrich, R.; Grewer, T., Decomposition of aromatic diazonium compounds. *Thermochim Acta* **1993**, *225*, 201.

47.Kundu, D.; Ahammed, S.; Ranu, B. C., Visible Light Photocatalyzed Direct Conversion of Aryl-/Heteroarylamines to Selenides at Room Temperature. *Org. Lett.* **2014**, *16*, 1814.

48.Fry, A. J.; Krieger, R. L., Electrolyte effects upon the polarographic reduction of alkyl halides in dimethyl sulfoxide. *J. Org. Chem.* **1976**, *41*, 54.

49.Nguyen, J. D.; D'Amato, E. M.; Narayanam, J. M. R.; Stephenson, C. R. J., Engaging unactivated alkyl, alkenyl and aryl iodides in visible-light-mediated free radical reactions. *Nat Chem* **2012**, *4*, 854.

50.Narayanam, J. M. R.; Tucker, J. W.; Stephenson, C. R. J., Electron-Transfer Photoredox Catalysis: Development of a Tin-Free Reductive Dehalogenation Reaction. *J. Am. Chem. Soc.* **2009**, *131*, 8756.

51.(a) Johnson, W. S.; Werthemann, L.; Bartlett, W. R.; Brocksom, T. J.; Li, T.-T.; Faulkner, D. J.; Petersen, M. R., Simple stereoselective version of the Claisen rearrangement leading to trans-trisubstituted olefinic bonds. Synthesis of squalene. *J. Am. Chem. Soc.* **1970**, *92*, 741; (b) Eng, H. M.; Myles, D. C., 1. Synthesis of the common C.1–C.13 hydrophobic domain of the B-type amphidinolides. *Tetrahedron Lett.* **1999**, *40*, 2275; (c) Mura, S.; Zouhiri, F.; Lerondel, S.; Maksimenko, A.; Mouglin, J.; Gueutin, C.; Brambilla, D.; Caron, J.; Sliwinski, E.; LePape, A.; Desmaele, D.; Couvreur, P., Novel Isoprenoyl Nanoassembled Prodrug for Paclitaxel Delivery. *Bioconjugate Chem.* **2013**, *24*, 1840.

52.Beatty, J. W.; Stephenson, C. R. J., Amine Functionalization via Oxidative Photoredox Catalysis: Methodology Development and Complex Molecule Synthesis. *Acc. Chem. Res.* **2015**, *48*, 1474.

53.Griesser, M.; Chauvin, J.-P. R.; Pratt, D. A., The hydrogen atom transfer reactivity of sulfinic acids. *Chem. Sci.* **2018**, *9*, 7218.

54.Julia, M. N., M.; Uguen, D., , Organic synthesis with sulfones. XLI. Nucleophilic substitutions of allylic sulfones. *Bulletin de la Societe Chimique de France* **1987**, *3*, 487.

55. Tyson, E. L.; Ament, M. S.; Yoon, T. P., Transition Metal Photoredox Catalysis of Radical Thiol-Ene Reactions. *J. Org. Chem.* **2013**, *78*, 2046.
56. Zaleskiy, S. S.; Shlapakov, N. S.; Ananikov, V. P., Visible light mediated metal-free thiol-yne click reaction. *Chem. Sci.* **2016**, *7*, 6740.
- 57.(a) Ishiguro, K.; Nakano, T.; Shibata, H.; Sawaki, Y., Redox Reaction of Benzyl Radicals with Aromatic Radical Ions Photogenerated. The Marcus Inverted Region and the Selective Formation of Carbocations or Carbanions. *J. Am. Chem. Soc.* **1996**, *118*, 7255; (b) Mayer, J. M., Understanding Hydrogen Atom Transfer: From Bond Strengths to Marcus Theory. *Acc. Chem. Res.* **2011**, *44*, 36.
58. Tanner, D. D.; Singh, H. K., Reduction of α -halo ketones by organotin hydrides. An electron-transfer-hydrogen atom abstraction mechanism. *J. Org. Chem.* **1986**, *51*, 5182.
- 59.(a) Marcus, R. A., On the Theory of Oxidation-Reduction Reactions Involving Electron Transfer. I. *J. Chem. Phys.* **1956**, *24*, 966; (b) Marcus, R. A., Chemical and Electrochemical Electron-Transfer Theory. *Annu. Rev. Phys. Chem.* **1964**, *15*, 155.
60. Pause, L.; Robert, M.; Savéant, J.-M., Can Single-Electron Transfer Break an Aromatic Carbon-Heteroatom Bond in One Step? A Novel Example of Transition between Stepwise and Concerted Mechanisms in the Reduction of Aromatic Iodides. *J. Am. Chem. Soc.* **1999**, *121*, 7158.
61. Singh, A.; Teegardin, K.; Kelly, M.; Prasad, K. S.; Krishnan, S.; Weaver, J. D., Facile synthesis and complete characterization of homoleptic and heteroleptic cyclometalated Iridium(III) complexes for photocatalysis. *J. Organomet. Chem.* **2015**, *776*, 51.
62. Bernotas, R. C.; Dooley, R. J., Efficient syntheses of 1,2,3,4,4a,5-hexahydro-pyrazino[2,1-c][1,4]benzothiazine-6,6-dioxide. *Tetrahedron* **2010**, *66*, 2273.
63. Smith, T. A. K.; Whitham, G. H., Radical induced 1,3-rearrangement-cyclisations of some unsaturated allylic sulphones. *J. Chem. Soc., Perkin Trans. 1* **1989**, 319.

CHAPTER III

ALKYL HALIDES VIA VISIBLE LIGHT MEDIATED DEHALOGENATION

3.1 Introduction

Alkyl halides found in natural products are potential source of new medicinal drugs.¹ Consequently, a significant amount of the bioactive halogenated compounds have been discovered from marine-derived sources, terrestrial plants, lichen, fungi, bacteria, and insects over the past decades.^{1d} In addition, alkyl halides are important as they play a central role in synthesis as starting materials and synthetic intermediates.² As a result, numerous efforts have focused on the development of and enantioselective -³ mono⁴alogenation. Often this is a challenging feat, owing to the increased reactivity of the products which leads to inseparable mixtures un-, mono-, and di-halogenated material.

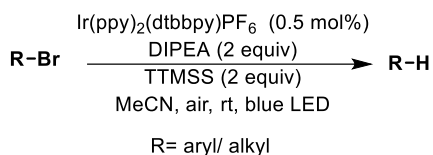
Meanwhile, the Weaver group has approached a parallel problem of organofluorines from an alternative approach. Namely, rather than attempting to control the selectivity of the halogenation (fluorination in this case) step, they have found that a molecular sculpting approach to organofluorines is a versatile and arguably underutilized strategy. In this approach, starting with the synthetically more accessible per- or fully-fluorinated molecule and subjecting it to selective defluorination reveals the desired partially fluorinated organofluorine.⁵ This approach effectively separates the problems of bond formation and selectivity. The objective of this project is to explore this concept in the context of accessing organo-bromides and -chlorides.

The replacement of a halogen by hydrogen is known as hydrodehalogenation, and a number of strategies exist in the literature. Traditional methods of hydrodehalogenation include metal halogen exchange,⁶ nucleophilic hydride substitution,⁷ atom transfer,⁸ or single electron transfer fragmentation.⁹ However, these methods suffer from drawbacks including undesired side reactions, extreme basicity, functional group intolerance, explosive,¹⁰ toxic,¹¹ and stoichiometric loadings of metals.

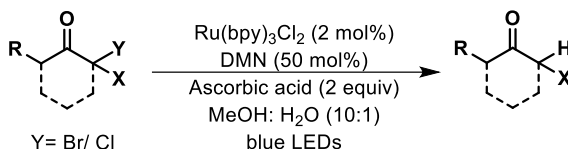
Recently, Stephenson has shown that hydrodehalogenation is possible using a silane via an iridium mediated photocatalysis (scheme 3.1a).¹² While a mild and efficient protocol with broad functional group tolerance, it requires superstoichiometric amounts of relatively expensive tris(trimethylsilane) in addition to an iridium catalyst which could complicate scaling of the reaction.

Scheme 3.1 Visible light-mediated reductive dehalogenation

a) Reductive debromination of unactivated alkyl compounds



b) Reductive dehalogenation of alpha-haloketones



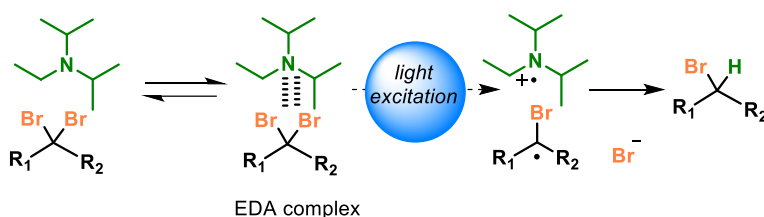
Reiser and coworkers have reported visible light-mediated reductive dehalogenation of α -haloketones using 1,5-dimethoxynaphthalene (DMN) and ascorbate in the presence of catalytic $\text{Ru}(\text{bpy})_3\text{Cl}_2$ (scheme 3.1b).¹³ This method is amenable to both α -bromocarbonyl compounds and α -chlorocarbonyl compounds. While a mild and efficient protocol with broad functional group tolerance, the substrate scope was limited to α -haloketones.

Recently, visible light-induced photocatalyst-free organic transformations have received considerable attention.¹⁴ Among these, electron-donor–acceptor (EDA) complex-mediated electron-transfer reactions are particularly intriguing. The diffusion controlled, ground-state association between a donor

D- which is usually an electron-rich compound, and an acceptor A- which is usually an electron-poor molecule, produces an electron donor–acceptor (EDA) complex often characterized by the appearance of a weak absorption band due to charge-transfer from donor to acceptor. In many cases, the energy of this transition lies within the visible range, thus producing a characteristic strong coloration.¹⁵ Often, when compared to hydrogen bonding, EDA complexes display weak, less directional, and reversible ground-state interactions.¹⁶ Furthermore, these interactions are sensitive to variations of solvent, concentration, and temperature.¹⁷

EDA complexes have been postulated to involve in organic transformations when irradiated by visible light.¹⁸ Recently, the photophysical properties of EDA complexes have been studied extensively,^{17a, 19} however, their use in synthetic chemistry has been more limited, though notable examples of their utility exists. They include radical-nucleophilic aromatic substitutions,²⁰ nitration of substituted benzene compounds,²¹ arylation of pyrroles at the 2-position with diaryliodonium salts,²² intramolecular cyclization of α,β -unsaturated lactams, lactones, and cycloalkenones with pendant alkyl iodides,²³ asymmetric α -alkylation of aldehydes with alkyl halides²⁴ and α -C–H functionalization of tertiary amines.²⁵ It is relatively well-known that tertiary amines can be involved in electron-donor–acceptor (EDA) complexes and in subsequent photoinduced electron transfer reactions.^{15, 26} Encouraged by the examples of successful reactions mediated by the photochemistry of EDA complexes, we began studying the visible light mediated debromination of polybrominated alkanes by *N,N*-diisopropylethylamine (DIPEA) (scheme 3.2).

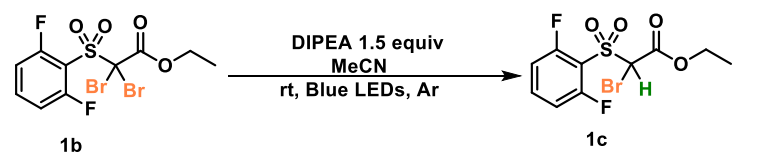
Scheme 3.2 Alkyl halides by light irradiation of EDA complexes



3.2 Development of methodology for the synthesis of alkyl halides

We chose α, α -dibromo sulfonyl acetate (**1b**) for optimization of the debromination reaction (table 3.1). The debromination of **1b** was carried out with 1.5 equiv of DIPEA with blue LED irradiation at room temperature. Initial solvent screening (entry 2) revealed that dichloromethane, toluene and tetrahydrofuran gave low conversion, while polar solvents (entry 3) facilitated the complete conversion of the reaction with high yield. However, MeCN was found to be the optimal solvent (entry 1) for the debromination.

Table 3.1 Optimization of dehalogenation



entry	modification	time	conv% ^a	1c% ^a
1	none	45 min	100	96
2	DCM, Tol or THF instead of MeCN	90 min	<39	38-20
3	DMF or DMSO instead of MeCN	60 min	100	85-87 ^b
4	1 equiv of DIPEA	73 min	100	90
5	2 equiv of DIPEA	30 min	100	84 ^b
6	1.5 equiv of Et ₃ N instead of DIPEA	90 min	78	75
7	1.5 equiv of DBU instead of DIPEA	90 min	94	75
8	1.5 equiv of K ₂ CO ₃ instead of DIPEA	45 min	0	0
9	1.5 equiv of Hantzsch Ester instead of DIPEA	75 min	63	51
10	3 equiv of water	35 min	100	87 ^b
11	Green LEDs instead of Blue LEDs	45 min	5	5
12	Purple LEDs instead of Blue LEDs	30 min	100	89 ^b
13	In dark or no DIPEA	45 min	0	0
14	1.5 equiv of TEMPO	45 min	3	3

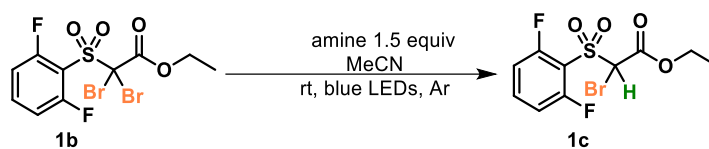
^adetermined by ¹⁹F NMR. ^bformed dibrominated product is 10% or more (see SI).

The rate of the reaction did appear to depend on the equivalents of amine (entries 1, 4 and 5) and an increase in the amount of amine led to dibrominated product. Use of 1.5 equiv of amine gave the highest yield for mono-debromination. Exploration of other amines showed diminished reactivity or low yield with triethylamine (entry 6) and DBU (entry 7). The use of inorganic base, potassium

carbonate, did not form any product (entry 8). The reaction did proceed when Hantzsch ester was used instead of amine, but showed relatively slow conversion (entry 9). Adding water accelerated the reaction (entry 10), but led to undesired didebrominated product. Thus, dry conditions provided higher yields. When the reaction was irradiated with lower energy green light (entry 11) the reaction gave only trace conversion, while higher energy violet light (entry 12) more rapidly gave complete conversion, but also led to didebrominated product, thus we opted to use blue light so as to maintain better control of the product distribution. Control studies demonstrated the necessity of both amine and light (entry 13). The addition of 1.5 equiv TEMPO led to only trace conversion, suggesting the presence of a radical intermediate (entry 14).

These optimization data were summarized after a more extensive study that included variations in several parameters and careful optimizations.

Table 3.2 Optimization of amine.



entry	amine	time	conv% ^a	1c% ^a
1	Et ₃ N	90 min	78 ^b	75
2	Bu ₃ N	90 min	98 ^b	65
3	DIPEA	45 min	100	96
4	DABCO	90 min	47	2
5	DBU	90 min	94 ^b	75
6	4-Methoxy- <i>N,N</i> -diphenylbenzenamine	90 min	3	3
7	2,2,6,6-tetramethylpiperidine	90 min	2	2

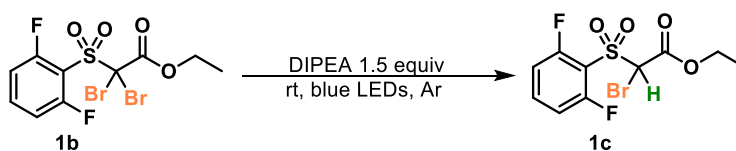
^adetermined by ¹⁹F NMR. ^bdidebrominated product is 10-15%.

Exploration of amines showed diminished reactivity with trimethylamine (Et₃N) (table 3.2 entry 1) and low yield with tributylamine (Bu₃N) (entry 2). DBU (entry 5) was also able to form the desired

debrominated product but in a relatively lower yield. Switching the amine to DABCO (entry 4) formed undesired didebrominated product. 4-Methoxy-*N,N*-diphenylbenzenamine and 2,2,6,6-tetramethylpiperidine (entry 6 & 7) did result trace amount of product formation. DIPEA was found to be the optimal amine (entry 3) for the debromination.

Next, we studied the mechanism of the reaction associated with DIPEA, and we were able to draw several conclusions. However, given the differences in the nature of the reductants, it is likely that multiple mechanisms are operative, and we make no claim concerning the others. We postulate that a streptocyanine dye of some kind is formed under the reaction conditions, and that it is responsible for debromination. According to the literature, streptocyanine dye formation from Et₃N and NBu₃ can undergo a similar transformation to DIPEA.²⁷ However, it is not known with respect to DBU and DABCO.

Table 3.3 Optimization of solvent

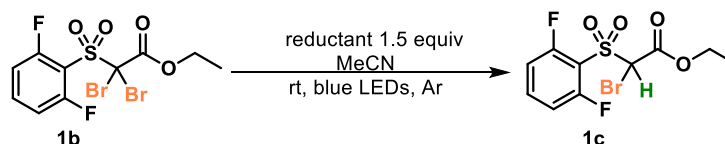


entry	solvent	time	conv% ^a	1c% ^a
1	Toluene	90 min	37	37
2	THF	90 min	39	38
3	DCM	90 min	20	20
4	NMP	60 min	40	23
5	MeCN	45 min	100	96
6	DMF	60 min	100 ^b	87
7	DMSO	60 min	100 ^b	85
8	MeOH	60 min	100 ^b	60

^adetermined by ¹⁹F NMR. ^bdidebrominated product is 10-15%

The debromination reaction gave low conversion in toluene, tetrahydrofuran (THF), and dichloromethane (DCM) (table 3.3 entry 1-3). While polar solvents DMF, DMSO, and MeOH (entry 6-8) showed the complete conversion of the reaction with good yield. However, they formed more didebrominated product. MeCN was found to be the optimal solvent (entry 5) for the debromination.

Table 3.4 Hydrodebromination with other potential reductants

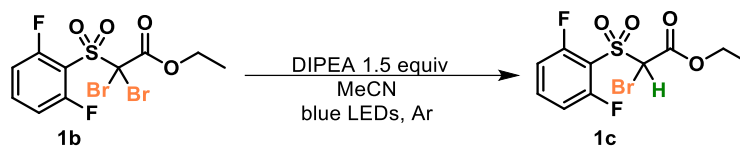


entry	reductant	time	conv% ^a	1c% ^a
1	Hantzsch ester	75 min	63 ^b	51
2	4-fluorothiophenol	75 min	7	7
3	Sodium ascorbate	75 min	1	1
4	Sodium oxalate	75 min	0	0

^adetermined by ¹⁹F NMR. ^bdidebrominated product is 12%.

Instead of amine other potential reductants for hydrodebromination were screened. The reaction did proceed with Hantzsch ester but gave relatively slow conversion (table 3.4 entry 1). Other reductants 4-fluorothiophenol, sodium ascorbate, and sodium oxalate (entries 2-4) formed only a trace amount of hydrodebrominated product. However, this could be due to the low solubility of sodium ascorbate and sodium oxalate in MeCN.

Table 3.5 Optimization of temperature



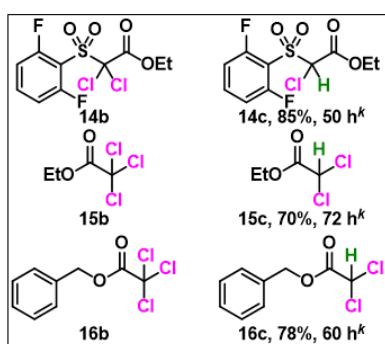
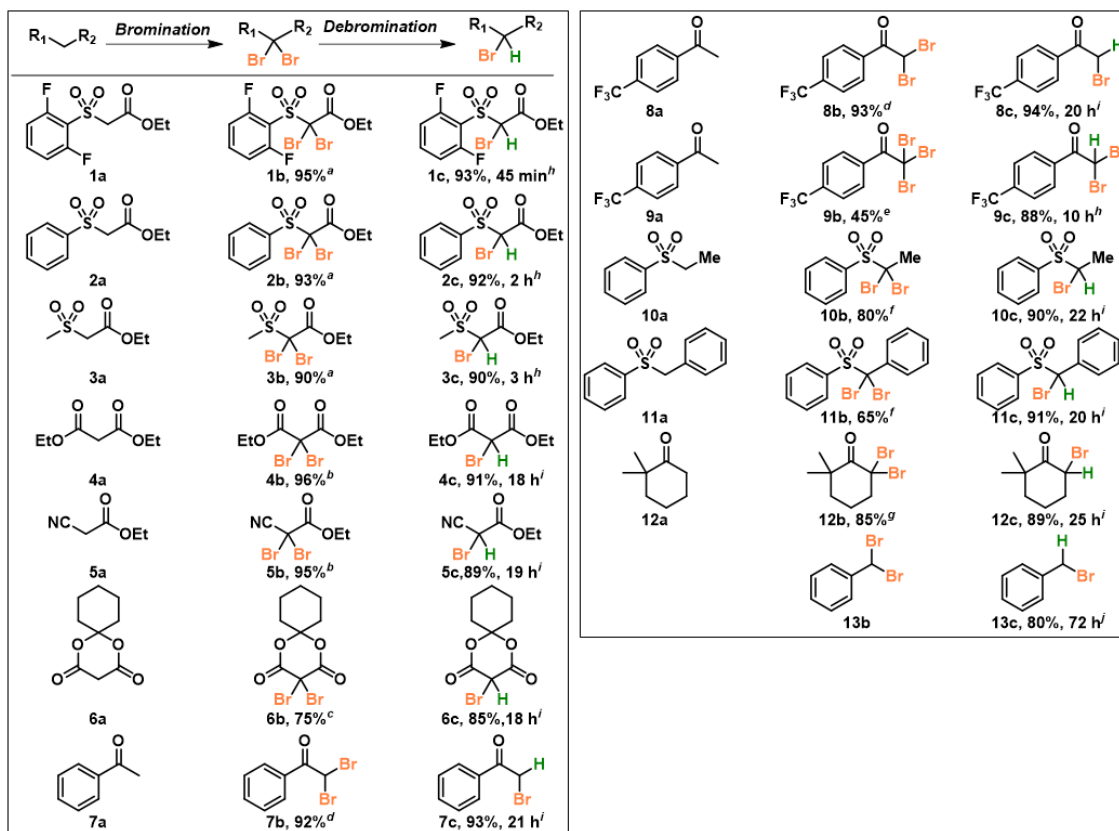
entry	temperature	time	conv% ^a	1c% ^a
1	0 °C	90 min	87	83
2	28 °C (rt)	45 min	100	96
3	45 °C	30 min	100	90

^adetermined by ¹⁹F NMR.

Temperature screening is another important parameter which affected both the rate of reactions and product distribution (debrominated pdt: didebrominated pdt) (table 3.5). Hydrodebromination reaction at 0 °C was relatively slow and resulted 83% of desired product. Carrying out the reaction at 45 °C accelerated hydrodebromination (entry 3), but led to undesired didebrominated product. Reaction at 28 °C was found to be the optimal temperature (entry 2) and resulted 96% desired product.

Having optimized the reaction conditions, we next sought to explore the substrate scope (scheme 3.3). However, as a first step, we synthesized a series of fully-brominated ketones, esters and sulfones substrates (1b-12b). The synthetic utility of our approach hinges on facile perhalogenation, and we show that by using established literature procedures the di- or tri-brominated starting materials can generally be synthesized in high yields.^{4h, 28} Next, the hydrodebromination was performed. Sulfonyl esters (1b-3b) showed complete conversion within a short time period (0.75-2 h) and formed the intended debrominated product (1c-3c) in excellent yield. Whereas α -bromo ketones, esters and mono-activated sulfones (4b-12b) required longer reaction times and increased DIPEA loading (2 vs. 1.5 equiv) compared to sulfonyl esters, but gave mono-debrominated products in high yield.

Scheme 3.3 Molecular sculpting approach to monohalogenation



^aEt₃N 3 equiv, Br₂ 4 equiv, DCM, rt

^bBr₂ 4 equiv, DCM, rt

^c2M NaOH, Br₂ 2.2 equiv, 0 °C

^dBr₂ 2.2 equiv, 1,4 dioxane, rt,

^eAcOH:H₂O (1:2) Br₂ 6 equiv, reflux

^fn-BuLi, -78 °C, Br₂ 2.2 equiv, THF, rt

^gNBS 2.2 equiv, p-toluenesulfonic acid 0.2 equiv, DCM, reflux

^hDIPEA 1.5 equiv, blue LEDs, rt

ⁱDIPEA 2 equiv, blue LEDs, rt

^jDIPEA 4 equiv, blue LED, rt

^kDIPEA 4 equiv, purple LEDs, rt

Yields are of isolated product

Furthermore, it is conceivable that enolizable substrate including 7b & 8b may undergo debromination via a different mechanism under the reaction condition.²⁹ Dibromotoluene, 13b, required longer reaction time and higher amine loading, but good conversion was achieved.

Upon further investigation, we found that this protocol was also amenable to the dechlorination of α -chloroketones (15b, 16b) and sulfonyl esters (14b). Longer reaction times were found to be necessary to achieve good yields, however. Moreover, the dechlorination reaction took place faster upon switching to higher energy violet LEDs.

During the course of our studies we noticed that a marked yellow color appeared immediately upon mixing ketone 7b with the DIPEA. We suspected the formation of an EDA complex³⁰ and that this complex was responsible for the apparent photochemistry. To gain insight, we performed several UV-Vis spectroscopic experiments. As shown in figure 3.1, while the UV-Vis spectra of both 7b and DIPEA in MeCN absorb below 380 nm, the spectrum of a mixture of both components shows a bathochromic shift above 400 nm. The observation of this charge transfer band strongly supports the existence of the EDA complex. The formation of a yellow solution upon mixing of the substrates and DIPEA was generally a good indicator that the reaction would take place via an EDA complex (7b, 8b and 9b), though for some substrates an EDA complex formed it was not visible (10b, 11b, 13b). Moreover, following the debromination of 7b via ¹H NMR (figure 3.2, left) demonstrated the benefit of the additional amine, which gave overall greater formation of the product at a faster rate. In stark contrast to ketone 7b, sulfone 1b did not form any visually detectable EDA complex which was supported by UV-Vis experiments (figure 3.1, right). Control studies reassured us that this was indeed a photochemical reaction, but by appearances the reaction, in apparent violation of Grotthuss-Draper law, did not absorb a visible photon. As shown in Figure 3.1 (right) the absorption of 1b in MeCN approaches zero near 310 nm but a 1:1.5 mixture of 1b and DIPEA showed a slight bathochromic displacement but its absorbance too drops off before it reaches the visible region. Interestingly, following the debromination of 1b by ¹⁹F NMR (figure 3.2, right) revealed a *sigmoidal* profile. The reaction had a conspicuous lag time in first few minutes. Such a kinetic profile is consistent with autocatalysis.³¹

Figure 3.1 UV-Vis absorption of 7b, 1b, and DIPEA

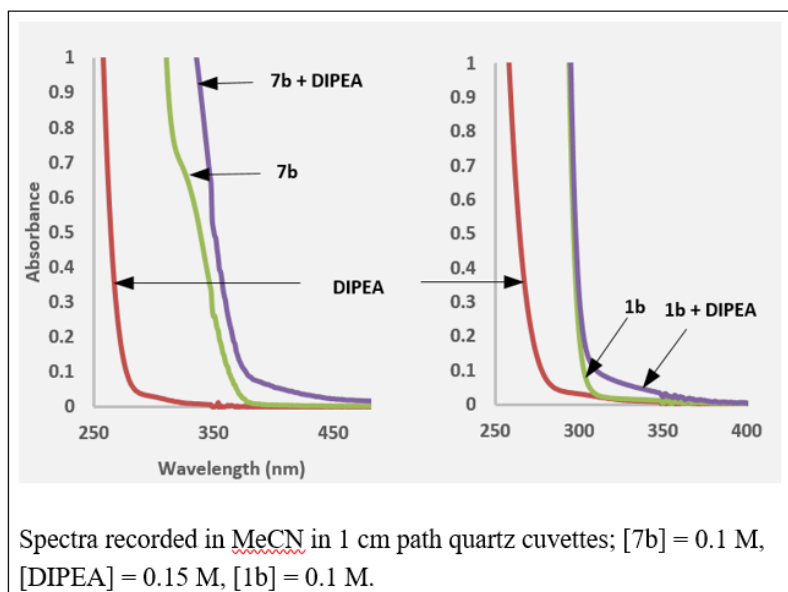
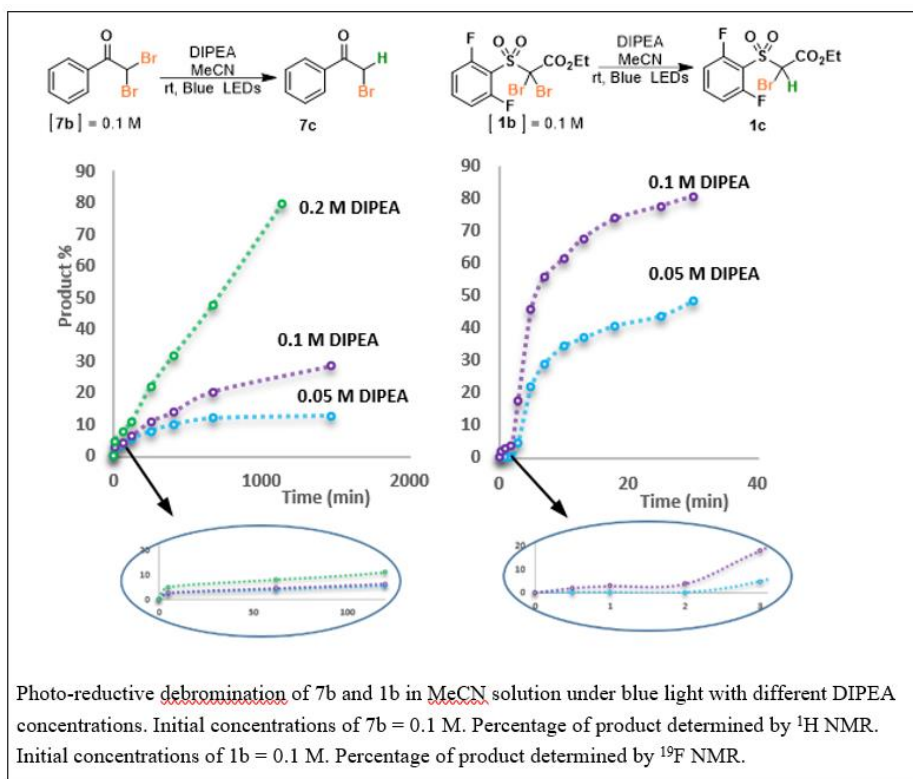
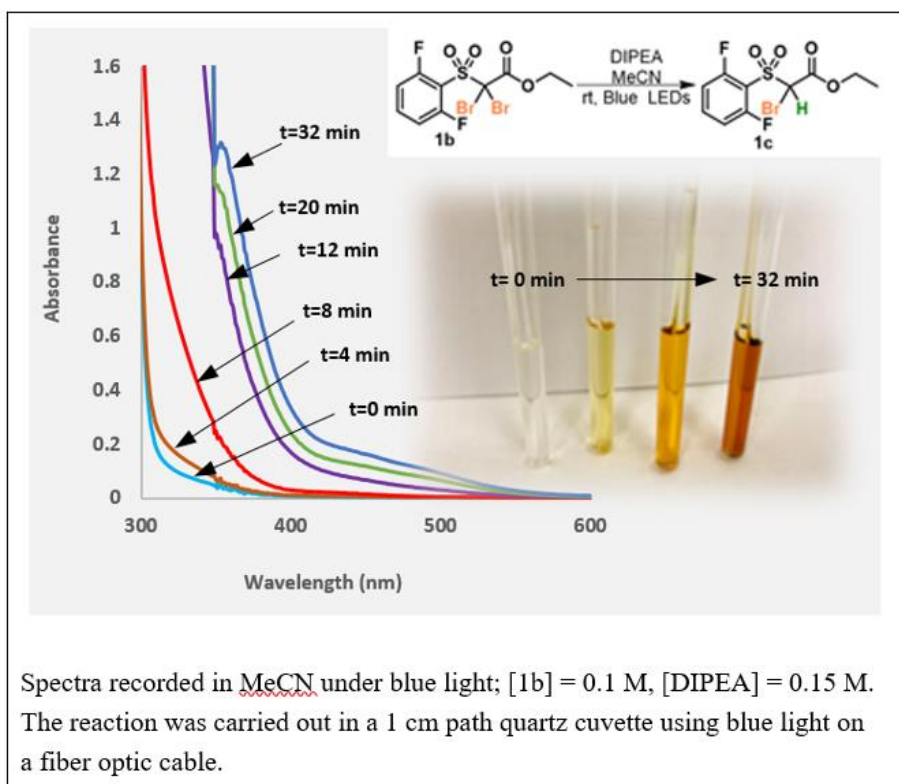


Figure 3.2 Rates of debromination reaction of 7b and 1b under different DIPEA concentrations



Furthermore, during the debromination reactions of 1b, upon irradiation of the reaction mixture with blue light, it was noted that the appearance of the reaction mixture changed from colorless to deep yellow and later to yellowish brown (See inset figure 3.3). We studied the origin of the prominent color change via UV-Vis spectroscopy. Monitoring the UV-Vis absorption spectra of a reaction mixture taken every 2 min for 32 min during the debromination (figure 3.3). Initially, only a strong band below 350 nm was noted. But after just 4 minutes had elapsed, new bands started to emerge and became quite prominent after 8 minutes, the solution becoming a deep yellow.

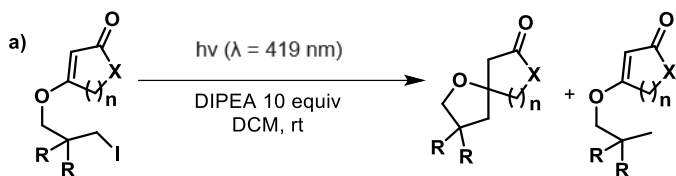
Figure 3.3 Time-dependent UV/Vis spectra of debromination reaction of 1b



Recently, Bach and coworkers³² noted a similar observation during the intramolecular cyclization of α,β -unsaturated lactams, lactones, and cycloalkenones with pendant alkyl iodides upon irradiation with visible light ($\lambda=419$ nm) in the presence of DIPEA (scheme 3.4a). The intensely colored by-products

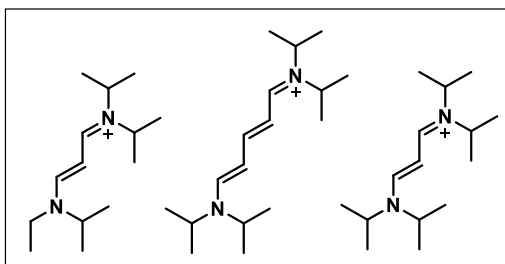
were proposed to be streptocyanine dyes, based on mass spectrometric evidence and comparison with known compounds (scheme 3.4b). Importantly, they were shown to be key to successful reaction.

Scheme 3.4 Bach's visible light mediated intramolecular radical cyclization



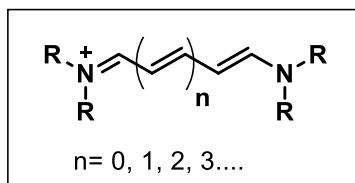
X = CH₂, O

b) Streptocyanine dyes formed in the reaction



Streptocyanine dyes³³ are part of the family of polymethine dyes.³⁴ These organic compounds are cationic, contain an odd numbered carbon chain, which terminates in two acyclic nitrogen atoms (scheme 3.5). When the nitrogen atoms are heterocyclic they are simply called cyanine dyes.^{33a, 35} These dyes are potentially formed from the dimerization of amines, conjugating an enamine and an iminium. Depending on the number of conjugated vinyl units, they are known to absorb photons that can run the energy gamut from the UV to IR region.^{32, 36}

Scheme 3.5 General structure of streptocyanine dyes

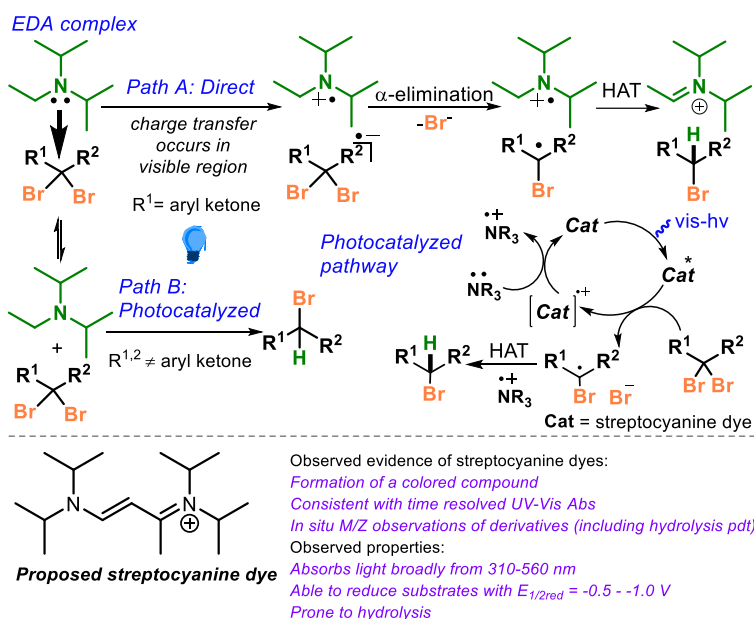


The cationic nature of the amine makes it ideal for staining cell surfaces for which it is currently used extensively.³⁷ Furthermore, they have been used as photocatalysts to excite electrons into the conduction band of titanate complexes.³⁸ However, to our knowledge they have not been used as

catalysts in visible light photocatalysis—at least from the outset of the reaction. The absence of their use in photocatalysis may stem from their tendency to decompose via any number of pathways, including photo-,³⁹ thermal-,^{39f} and hydrolytic-pathways. However, we posit that if they can be reliably generated *in situ*, and their reactivity anticipated, they can become another useful tool for the synthetic chemist.

Based on mass spectrometric and UV-Vis spectroscopy evidences we have proposed the structure of *in situ* generated streptocyanine dye (scheme 3.6, bottom). This streptocyanine dye absorbs light broadly from 310-560 nm. It is able to reduce substrates with $E_{1/2red} = -0.5 - -1.0$ V. We postulate that the streptocyanine dye of some kind (scheme 3.6, bottom) formed under the reaction conditions, that it is responsible for photoinduced electron transfer to the substrate, generation of a radical anion, subsequent alpha-elimination of the halide and formation of the alkyl radical. The alkyl radical can then undergo hydrogen atom transfer with an amine radical cation. DIPEA reduces the oxidized dye and completes the cycle (scheme 3.6)

Scheme 3.6 Proposed mechanism and potential streptocyanine dye



Although our attempts to directly characterize the dye failed, we were able to perform several experiments that probed the nature of the active photocatalyst (scheme 3.7). When the debromination of sulfone 2b was run to *ca.* 50% conversion, a small aliquot was transferred to a fresh solution involving a different dibromo-substrate (scheme 3.7, eqn 1). When compared to a control reaction, in which no aliquot from the partially converted reaction had been added, the reaction did not display the aforementioned lag time.

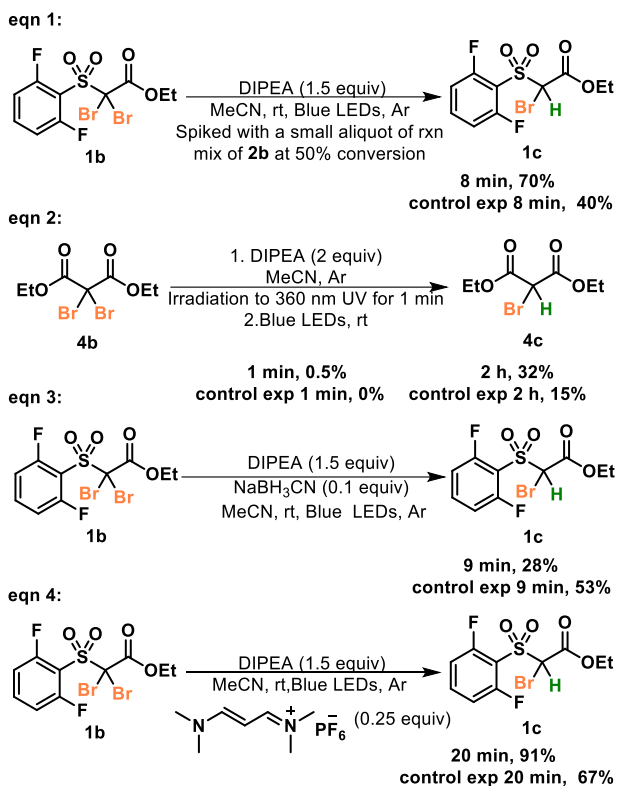
Given that streptocyanine dyes were not present at the beginning of the reaction and therefore could not be the causative agent at the beginning of the reaction, we expected that trace amounts of adventitious UV light might lead to a photoinduced single electron transfer (SET) from the amine to the dibromide substrate and initiate a process that ultimately leads to the formation of a visible light absorbing dye *in situ* that was itself capable of the photoinduced SET and primarily responsible for subsequent visible light mediated hydrodebromination. Consistent with this idea, figure 3.1 (right) displayed an EDA complex, though weak and in the UVA region, between sulfone 1b and DIPEA. We probed this idea by intentionally subjecting dibromomalonate 4b, which normally took 18 h to reach completion, to UV-light with a hand-held UV lamp-designed for TLC analysis for just 1 minute and then returned the reaction to the blue LED light bath, we observed that the lag-time could also be avoided (scheme 3.7, eqn 2).

In another attempt to probe the nature of the active catalyst which we suspected were streptocyanine dyes, we added 10 mol% sodium cyanoborohydride which we anticipated, and verified, would reduce the iminium but not the sulfone. Indeed, we observed that sodium cyanoborohydride slowed the conversion to the mono-bromide, though it did not stop it completely. (scheme 3.7, eqn 3). The solution with the sodium cyanoborohydride remained colorless for longer than the control reaction, before eventually coloring. The delayed coloring is consistent with reduction of the conjugated dye.

Using a related commercially available streptocyanine dye, we were able to probe its catalytic ability (scheme 3.7, eqn 4). Sulfone 2b was subjected to debromination in the presence of a catalytic amount

of the commercial streptocyanine dye, which resulted in a rate enhancement compared with the standard.

Scheme 3.7 Mechanistic experiments



Conversion determined by ^{19}F NMR of **1c**. Conversion determined by ^1H NMR of **4c**.

3.3 Summary

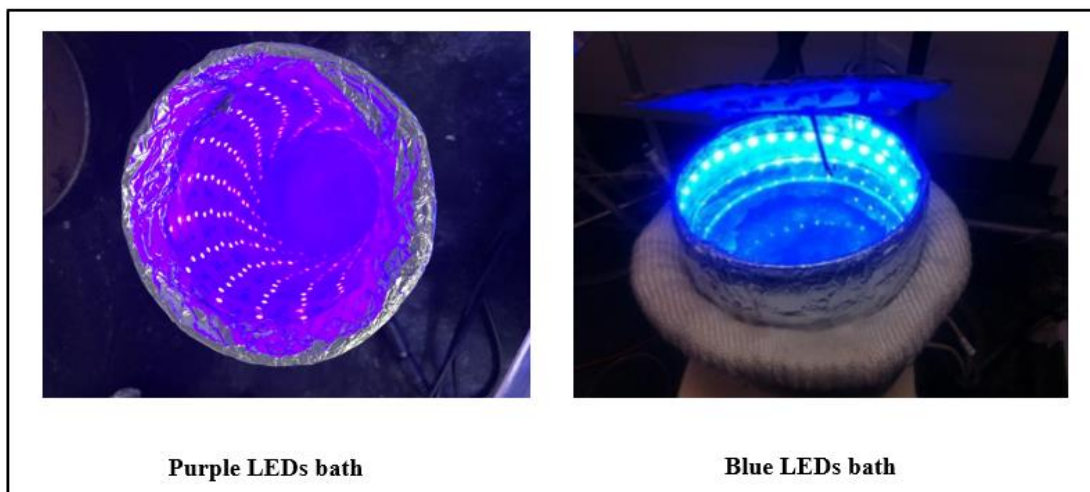
We have shown that two-step bromination/debromination is a viable approach to bromination, affording valuable building blocks in high yields. We have also shown that the potential for a photochemical reaction should not be assumed based on the presences/absence of an EDA complex, and have provided useable insight into some of the causative agents at work. Given the frequency of the use of tertiary amines in photocatalysis work, care should be taken to ensure that any added photocatalyst is truly the causative agent in respective applications-as formation of streptocyanine dyes may be occurring during the course of the reaction.

3.4 Experimental section

All reagents were obtained from commercial suppliers (Aldrich, VWR, TCI Chemicals, and Oakwood Chemicals) and used without further purification unless otherwise noted. Acetonitrile (CH₃CN) was dried for 48 h over activated 3 Å molecular sieves. Distilled diisopropylethylamine was stored over KOH pellets with air tight light resistant container.

Reactions were monitored by a combination of thin layer chromatography (TLC), (obtained from sorbent technologies Silica XHL TLC Plates, w/UV254, glass backed, 250 µm, 20 x 20 cm) and were visualized with ultraviolet light, potassium permanganate stain, GC-MS (QP 2010S, Shimadzu equipped with auto sampler) 19F NMR and 1H NMR (*vide infra*). Isolations were carried out using Teledyne Isco Combiflash Rf 200i flash chromatograph with Redisep Rf normal phase silica (4 g, 12 g, 24 g, 40 g) with product detection at 254 and 288 nm and by ELSD (evaporative light scattering detection). NMR spectra were obtained on a 400 MHz Bruker Avance III spectrometer and Neo 600 MHz. 1H and 13C NMR chemical shifts are reported in ppm relative to the residual protio solvent peak (1H, 13C). Photophysical properties were studied on Varian Cary Eclipse spectrophotometer. Mass spectra (HRMS) analysis was performed on LTQ-OrbitrapXL by Thermo Scientific ltd using a Heatedelectrospray ionization (H-ESI) source.

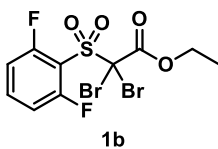
Reactions were set up in a light bath which consists of Blue LEDs (λ_{max} emission ~ 450 nm) or purple LEDs (λ_{max} emission ~ 410 nm) as described below. Blue LEDs (200 LEDs)/ purple LEDs (240 LEDs) were wrapped around the walls of glass crystallization dish and secured with masking tape and then wrapped with aluminum foil. A lid which rest on the top was fashioned from cardboard and holes were made such that reaction tubes were held firmly in the cardboard lid which was placed on the top of bath. Water was added to the bath such that the tubes were submerged in the water which was at 28 °C. (Temperature of the bath was maintained at 28 °C using a fan).



Synthesis of alkyl bromide/chloride substrates:

Alkyl bromides and alkyl chlorides were synthesized according to the literature procedures and some procedures were modified slightly to increase the yield of alkyl bromides and chlorides.^{4h, 28, 40}

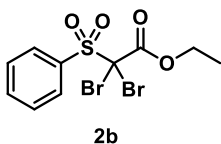
Ethyl 2,2-dibromo-2-((2,6-difluorophenyl)sulfonyl)acetate



Ethyl 2-((2,6-difluorophenyl)sulfonyl)acetate (1.0 g, 3.9 mmol, 1 equiv) and triethylamine (1.2 g, 11.7 mmol, 3 equiv) in 25 mL of DCM was stirred for 20 min. Bromine (2.5 g, 15.6 mmol, 4 equiv) was added in to the reaction. The progress of the reaction was monitored by TLC. The reaction was stirred at room temperature for 15 h. After consumption of the starting material, the mixture was diluted with H₂O (15 mL) and then extracted with EtOAc (3×15 mL). The organic layers were combined and washed with brine then dried with MgSO₄. The crude product was concentrated *in vacuo* and purified via automated flash chromatography using EtOAc in hexanes (0% to 100%) with product eluting at 19% on a 40 g silica column to afford **1b** in 95% yield (3.7 mmol, 1.6 g).^{4h} ¹H NMR (400 MHz, CDCl₃) δ 7.72 (tt, *J* = 8.4, 5.7 Hz, 1H), 7.11 (ap t, *J* = 8.4 Hz, 2H), 4.39 (q, *J* = 7.2 Hz, 2H), 1.36 (t, *J* = 7.2 Hz, 3H). ¹⁹F NMR (376 MHz, CDCl₃) δ -98.4 – -98.5 (m). ¹³C NMR (101 MHz, CDCl₃) δ 163.4, 161.4 – 160.5 (dd), 138.8

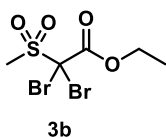
(qd, $J = 9.7, 8.2, 4.6$ Hz), 114.1 (d, $J = 4.6$ Hz), 113.9 (d, $J = 5.8$ Hz), 71.0, 66.6, 14.1. HRMS (ESI) calcd. for $[\text{C}_{10}\text{H}_8\text{Br}_2\text{F}_2\text{O}_4\text{SNa}]^+ [\text{M}+\text{Na}]^+$: m/z , 444.8355 found 444.8355.

Ethyl 2,2-dibromo-2-(phenylsulfonyl)acetate



Ethyl 2-(phenylsulfonyl)acetate (0.9 g, 3.9 mmol, 1 equiv) and triethylamine (1.2 g, 11.7 mmol, 3 equiv) in 25 mL of DCM was stirred for 20 min. Bromine (2.5 g, 15.6 mmol, 4 equiv) was added in to the reaction. The progress of the reaction was monitored by TLC. The reaction was stirred at room temperature for 17 h. After consumption of the starting material, the mixture was diluted with H_2O (15 mL) and then extracted with EtOAc (3×15 mL). The organic layers were combined and washed with brine then dried with MgSO_4 . The crude product was concentrated *in vacuo* and purified via automated flash chromatography using EtOAc in hexanes (0% to 100%) with product eluting at 21% on a 40 g silica column to afford **2b** in 93% yield (3.6 mmol, 1.4 g).^{4h} ^1H NMR (400 MHz, CDCl_3) δ 8.12 (dd, 2H), 7.75 (t, 1H), 7.60 (t, $J = 7.9$ Hz, 2H), 4.35 (q, $J = 7.1$ Hz, 2H), 1.33 (t, $J = 7.1$ Hz, 3H). ^{13}C NMR (101 MHz, CDCl_3) δ 161.8, 135.9, 133.1, 132.9, 129.1, 69.2, 66.0, 14.1. HRMS (ESI) calcd. for $[\text{C}_{10}\text{H}_{10}\text{Br}_2\text{O}_4\text{SNa}]^+ [\text{M}+\text{Na}]^+$: m/z , 408.8544 found 408.8541.

Ethyl 2,2-dibromo-2-(methylsulfonyl)acetate



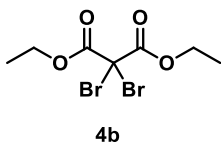
Ethyl 2-(methylsulfonyl)acetate (0.7 g, 3.9 mmol, 1 equiv) and triethylamine (1.2 g, 11.7 mmol, 3 equiv) in 25 mL of DCM was stirred for 20 min. Bromine (2.5 g, 15.6 mmol, 4 equiv) was added in to the reaction. The progress of the reaction was monitored by TLC. The reaction was stirred at room temperature for 20 h. After consumption of the starting material, the mixture was diluted with H_2O (15 mL) and then extracted with EtOAc (3×15 mL). The organic layers were combined and washed with brine then dried with MgSO_4 . The crude product was concentrated *in vacuo* and purified via automated flash chromatography using EtOAc in hexanes (0% to 100%) with product eluting at 27% on a 40 g silica column to afford **3b** in 90% yield (3.5 mmol,

1.1 g).^{4h} ¹H NMR (400 MHz, CDCl₃) δ 4.42 (q, *J* = 7.1 Hz, 2H), 3.50 (s, 3H), 1.39 (t, *J* = 7.1 Hz, 3H).

¹³C NMR (101 MHz, CDCl₃) δ 162.4, 67.1, 66.2, 37.3, 14.1. HRMS (ESI) calcd. for [C₅H₈Br₂O₄SNa]

⁺ [M+Na]⁺: *m/z*, 346.8387 found 346.8385.

Diethyl 2,2-dibromomalonate

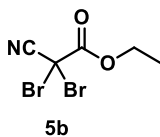


Bromine (2 g, 12.5 mmol, 4 equiv) was added into a solution of diethyl malonate (0.5 g, 3.12 mmol, 1 equiv) in 30 mL DCM. Then, the reaction was stirred at room temperature for 20 h. The progress of the reaction was monitored by TLC. After

consumption of the starting material, the mixture was diluted with H₂O (20 mL) and then extracted with EtOAc (3×15 mL). The organic layers were combined and washed with brine then dried with MgSO₄.

The crude product was concentrated *in vacuo* and purified via automated flash chromatography using EtOAc in hexanes (0% to 100%) with product eluting at 7% on a 24 g silica column to afford **4b** in 96% yield (3 mmol, 0.95 g).^{40b, 41}

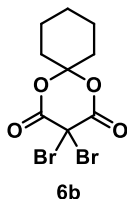
Ethyl 2,2-dibromo-2-cyanoacetate



Bromine (2 g, 12.5 mmol, 4 equiv) was added into a solution of ethyl 2-cyanoacetate (0.4 g, 3.1 mmol, 1 equiv) in 30 mL DCM. The progress of the reaction was monitored by TLC. The reaction was stirred at room temperature for 20 h. After consumption of

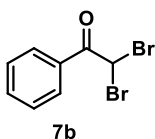
the starting material, the mixture was diluted with H₂O (20 mL) and then extracted with EtOAc (3×15 mL). The organic layers were combined and washed with brine then dried with MgSO₄. The crude product was concentrated *in vacuo* and purified via automated flash chromatography using EtOAc in hexanes (0% to 100%) with product eluting at 9% on a 24 g silica column to afford **5b** in 95% yield (3 mmol, 0.80 g).^{40b, 42}

3,3-Dibromo-1,5-dioxaspiro[5.5]undecane-2,4-dione



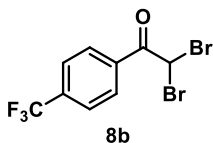
To a chilled (0 °C) 2 M solution of NaOH (5 mL), 1,5-dioxaspiro[5.5]undecane-2,4-dione (0.9 g, 5 mmol, 1 equiv) was added and stirred for 15 min to get homogeneous reaction mixture. Then, bromine (1.6 g, 10 mmol, 2 equiv) was added dropwise at 0 °C. After addition, the reaction was stirred for 45 minutes at 0 °C and solid crude was observed at the end of the reaction. Then, it was filtered and washed with distilled water and extracted with toluene (3 x 3 mL). The organic layers were dried over MgSO₄ and concentrated *in vacuo* to afford **6b** in 75% yield (3.8 mmol, 1.3 g).^{28d} ¹H NMR (400 MHz, CDCl₃) δ 2.05 (t, 4H), 1.77 (p, *J* = 6.3 Hz, 4H), 1.52 (p, *J* = 6.0 Hz, 2H). ¹³C NMR (101 MHz, CDCl₃) δ 161.0, 108.6, 39.2, 36.8, 23.9, 22.3. HRMS (ESI) calcd. for [C₉H₁₀Br₂O₄Na]⁺ [M+Na]⁺: *m/z*, 364.8823 found 364.8822.

2,2-dibromo-1-phenylethan-1-one



Bromine (1.4 g, 9 mmol, 2 equiv) was added dropwise over a period of 20 minutes into 3 mL of anhydrous 1,4-dioxane at room temperature under a flow of Ar. Then, the reaction mixture was stirred for another 30 minutes. A solution of acetophenone (0.5 g, 4.2 mmol, 1 equiv) in 2 mL of dioxane was added into the reaction mixture at once and stirred for another 5 h. At the end of the reaction, ice cold water (50 mL, 10 volumes with respect to the dioxane) was added to the reaction flask causing the product to precipitate which was filtered from solution. The filtrate was washed with hexane to afford **7b** in 92% yield (3.9 mmol, 1.1 g).^{28a, 43}

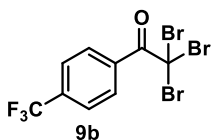
2,2-Dibromo-1-(4-(trifluoromethyl)phenyl)ethan-1-one



Bromine (1.4 g, 9 mmol, 2 equiv) was added dropwise over a period of 20 minutes into 3 mL of anhydrous 1,4-dioxane at room temperature under a flow of Ar. Then, the reaction mixture was stirred for another 30 minutes. 1-(4-(trifluoromethyl)phenyl)ethan-1-one (0.8 g, 4.2 mmol, 1 equiv) in 2 mL of dioxane was added into the reaction mixture at once and stirred for another 5 h. At the end of the reaction, ice cold water (50 mL,

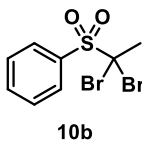
10 volumes with respect to the dioxane) was added to the reaction flask causing the product to precipitate which was filtered from solution. The filtrate was washed with hexane to afford **8b** in 93% yield (3.9 mmol, 1.4 g).^{28a, 44}

2,2,2-tribromo-1-(4-(trifluoromethyl)phenyl)ethan-1-one



To a solution of 1-(4-(trifluoromethyl)phenyl)ethan-1-one (0.5 g, 2.7 mmol, 1 equiv) in AcOH (10 mL) and 3 mL of water, Br₂ (2.1 g, 13.5 mmol, 5 equiv) was added at 0 °C. Then, the reaction mixture was brought to reflux for 60 h. The reaction mixture was diluted with water and extracted with ethylacetate (3×10 mL). The organic layers were combined and washed with water, saturated aqueous NaHCO₃ and brine. The organic layer was dried over MgSO₄ and concentrated *in vacuo*. The crude product was purified via automated flash chromatography using DCM in hexanes (0% to 100%) with product eluting at 0.2% on a 40 g silica column to afford **9b** in 45% yield (1.2 mmol, 0.5 g).⁴⁵

((1,1-Dibromoethyl)sulfonyl)benzene



To (ethylsulfonyl)benzene (0.4 g, 2.2 mmol, 1 equiv) in anhydrous THF (11 mL) at -78 °C was added n-BuLi (3 mL, 4.8 mmol, 1.6 M in hexane). Before addition of n-BuLi, it should be titrated to find the exact concentration of n-BuLi (as given below). After addition, the yellow mixture was allowed to warm to room temperature and then again cooled to -78 °C. Bromine (1.1 g, 6.6 mmol, 3 equiv) was added slowly, and the mixture was then warmed to room temperature. The reaction was stirred at room temperature for 13 h. The reaction was diluted with 1 M NaHSO₃, the mixture was extracted with diethyl ether (3 x 10 mL) and the combined extracts were dried over MgSO₄ and concentrated. The collected crude was purified via automated flash chromatography using EtOAc in hexanes (0% to 100%) with product eluting at 10% on a 24 g silica column to afford **10b** in 80% yield (1.8 mmol, 0.6 g).^{4i, 28b}

General procedure for n-BuLi titration:

An oven dried 25 ml three neck flask equipped with an argon inlet adapter, a stirring bar and two rubber septa. The flask was charged with menthol (0.64 mmol, 100 mg), 2,2'-dipyridyl (2.5 mg) and 10 mL of dry THF. To the resulting solution is added n-BuLi via 1.0 mL syringe (graduated in 0.01 mL increments) in a dropwise fashion. During addition, it was observed that periodic quantities of a red colored complex appeared in the solution. It could be noted that in the early stage of the titration this red color dispersed rapidly. As one nears the endpoint, the red coloration required longer periods of time to disperse. At this point, it is necessary to slow the rate of addition. Eventually, the addition of a single drop of n-BuLi caused a persistent red coloration of the solution. Then, find the difference between initial and final volumes of n-BuLi to get the used volume of n-BuLi in the titration. Finally, calculate the molarity of n-BuLi.

Calculation:

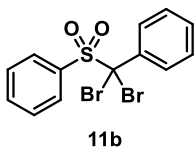
100 mg menthol = 0.64 mmol which reacts with 0.64 mmol n-BuLi.

This amount of n-BuLi is present in V ml (used volume in the titration) of the analyte.

Since molarity equals mol/L, it also equals mmol/mL. Thus:

$$0.64 \text{ mmol} / V \text{ mL} = \text{Concentration of n-BuLi solution}$$

((Dibromo(phenyl)methyl)sulfonyl)benzene

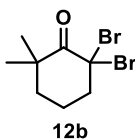


To (benzylsulfonyl)benzene (0.5 g, 2.2 mmol, 1 equiv) in anhydrous THF (11 mL) at -78 °C was added n-BuLi (3 mL, 4.8 mmol, 1.6 M in hexane). The yellow mixture was warmed to room temperature and then again cooled to -78 °C. Bromine (1.1 g,

6.6 mmol, 3 equiv) was added in a single portion, and the mixture was then warmed to room

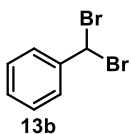
temperature. The reaction was stirred at room temperature for 10 h. The reaction was diluted with 1 M NaHSO₃, the mixture was extracted with diethyl ether (3 x 10 mL) and the combined extracts were dried over MgSO₄ and concentrated. The crude was purified via automated flash chromatography using EtOAc in hexanes (0% to 100%) with product eluting at 4% on a 24 g silica column to afford **11b** in 65% yield (1.43 mmol, 0.55 g).^{4i, 28b}

2,2-Dibromo-6,6-dimethylcyclohexan-1-one



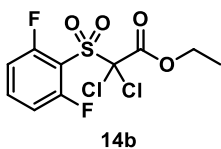
A solution of 2,2-dimethylcyclohexan-1-one (0.5 g, 4 mmol, 1 equiv) in DCM (2 mL) was added dropwise to a solution of *n*-bromosuccinimide (1.6 g, 8.8 mmol, 2.2 equiv) and *p*-TsOH (0.13 g, 0.8 mmol, 0.2 equiv) in DCM (15 mL) at 0 °C. The reaction mixture was then brought to reflux for 15 h. After addition of H₂O (10 mL), the organic layer was separated, and the aqueous layer was extracted with CH₂Cl₂ (3 x 10 mL). The combined organic layer was washed with saturated aqueous NaHCO₃ and brine, dried over anhydrous MgSO₄, and concentrated under reduced pressure. The residue was purified via automated flash chromatography using EtOAc in hexanes (0% to 100%) with product eluting at 0.1% on a 24 g silica column to afford **12b** in 85% yield (3.4 mmol, 1.0 g).^{28c, 46}

(Dibromomethyl)benzene



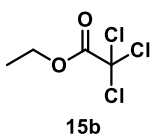
13b was synthesized according to a modified literature procedure. Benzyl bromide (0.4 g, 2.3 mmol, 1 equiv), *N*-bromosuccinimide (0.5 g, 2.6 mmol, 1.1 equiv) and azobis(isobutyronitrile) (3 mg, 0.01 mmol, 0.006 equiv) in 10 mL of CCl₄ was heated for 10 h under reflux. The mixture was cooled and the precipitate (succinimide) was filtered off and washed with 5 mL of CCl₄, and the filtrate was washed in succession with a 5% solution of Na₂SO₃, a 10% solution of Na₂CO₃, and water and dried over MgSO₄. The solvent was removed, and the residue was purified via automated flash chromatography using EtOAc in hexanes (0% to 100%) with product eluting at 0.1% on a 24 g silica column to afford **13b** in 70% yield (1.6 mmol, 0.4 g).⁴⁷

Ethyl 2,2-dichloro-2-((2,6-difluorophenyl)sulfonyl)acetate



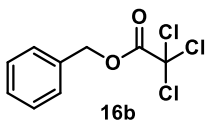
Ethyl 2-((2,6-difluorophenyl)sulfonyl)acetate (1 g, 3.9 mmol, 1 equiv) and triethylamine (1.18 g, 11.7 mmol, 3 equiv) in 25 mL of DCM was stirred for 20 min. N-chlorosuccinimide (1.6 g, 11.7 mmol, 3 equiv) was added in to the reaction. The progress of the reaction was monitored by TLC. The reaction was stirred at room temperature for 21 h. After consumption of the starting material, the mixture was diluted with H₂O (15 mL) and then extracted with EtOAc (3×10 mL). The organic layers were combined and washed with brine then dried with MgSO₄. The crude product was concentrated *in vacuo* and purified via automated flash chromatography using EtOAc in hexanes (0% to 100%) with product eluting at 30% on a 40 g silica column to afford **14b** in 80% yield (3.1 mmol, 1.01 g). ¹H NMR (400 MHz, CDCl₃) δ 7.74 (tt, *J* = 8.5, 5.7 Hz, 1H), 7.11 (ap t, *J* = 16.8 Hz, 2H), 4.42 (q, *J* = 7.2 Hz, 2H), 1.38 (t, *J* = 7.2 Hz, 3H). ¹⁹F NMR (376 MHz, CDCl₃) δ -99.3 (ddd, *J* = 8.9, 5.8, 2.9 Hz). ¹³C NMR (151 MHz, CDCl₃) δ 161.6 (dd, *J* = 266.5, 2.6 Hz), 160.4, 138.4 (t, *J* = 11.5 Hz), 113.6, 113.4 (d, *J* = 4.6 Hz), 93.6, 66.0, 13.6. HRMS (ESI) calcd. for [C₁₀H₈Cl₂F₂O₄SNa]⁺ [M+Na]⁺: *m/z*, 354.9386 found 354.9383.

Ethyl 2,2,2-trichloroacetate



A mixture of trichloroacetic acid (0.7 g, 4.3 mmol, 1 equiv), concentrated sulfuric acid (0.1 mL), and ethanol (5 mL) was refluxed for 7 h. Then the flask was cooled to room temperature, water (10 mL) was added to the content of the flask, and the crude was extracted with diethyl ether (3×10 mL). The organic layers were combined and washed with a 10% sodium carbonate solution and dried with anhydrous MgSO₄. The solvent was removed, and the residue was purified via automated flash chromatography using EtOAc in hexanes (0% to 100%) with product eluting at 8% on a 24 g silica column to afford **15b** in 85% yield (3.7 mmol, 0.70 g).^{40a, 48}

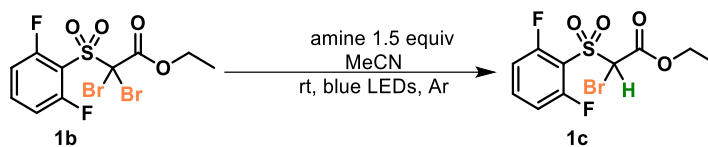
Benzyl 2,2,2-trichloroacetate



A mixture of trichloroacetic acid (0.7 g, 4.3 mmol, 1 equiv), concentrated sulfuric acid (0.1 mL), and benzyl alcohol (1.4 g, 12.9 mmol, 3 equiv) in 10 mL of MeCN was refluxed for 5 h. Then the flask was cooled to room temperature, water (10 mL) was added to the content of the flask, and the crude was extracted with diethyl ether (3×10 mL). The combined organic extracts were washed with a 10% sodium carbonate solution and dried with anhydrous MgSO₄. The solvent was removed, and the residue was purified via automated flash chromatography using EtOAc in hexanes (0% to 100%) with product eluting at 0.5% on a 24 g silica column to afford **16b** in 70% yield (3 mmol, 0.76 g).^{40a, 49}

Optimization of hydrodebromination:

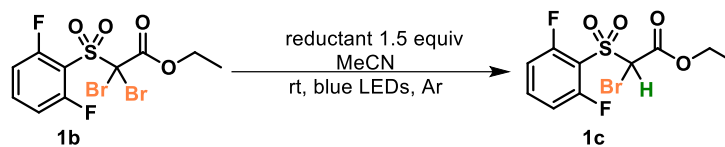
Optimization of amine structure:



entry	amine	time	conv% ^a	1c % ^a
1	Et ₃ N	90 min	78 ^b	75
2	Bu ₃ N	90 min	98 ^b	65
3	DIPEA	45 min	100	96
4	DABCO	90 min	47	2
5	DBU	90 min	94 ^b	75
6	4-methoxytriphenylamine	90 min	3	3
7	2,2,6,6-tetramethylpiperidine	90 min	2	2

^adetermined by ¹⁹F NMR. ^bdibrominated product is 10-15%.

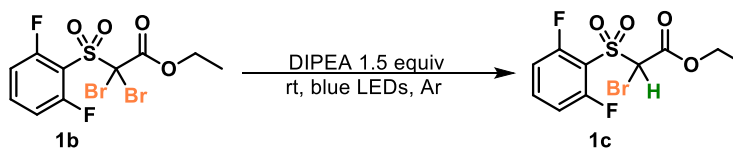
Attempted hydrodebromination with other potential reductants:



entry	reductant	time	conv% ^a	1c % ^a
1	Hantzsch ester	75 min	63 ^b	51
2	4-fluorothiophenol	75 min	7	7
3	Sodium ascorbate	75 min	1	1
4	Sodium oxalate	75 min	0	0

^adetermined by ¹⁹F NMR. ^bdidebrominated product is 12%.

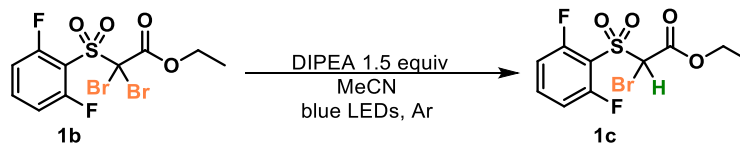
Solvent optimization:



entry	solvent	time	conv% ^a	1c % ^a
1	Toluene	90 min	37	37
2	THF	90 min	39	38
3	DCM	90 min	20	20
4	NMP	60 min	40	23
5	MeCN	45 min	100	96
6	DMF	60 min	100 ^b	87
7	DMSO	60 min	100 ^b	85
8	MeOH	60 min	100 ^b	60

^adetermined by ¹⁹F NMR. ^bdidebrominated product is 10-15%

Temperature optimization:



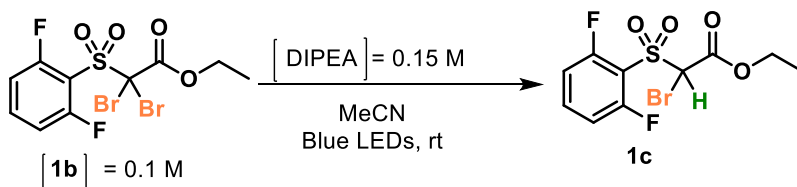
entry	temperature	time	conv% ^a	1c % ^a
1	0 °C	90 min	87	83
2	28 °C (rt)	45 min	100	96
3	45 °C	30 min	100	90

^adetermined by ¹⁹F NMR.

Mechanistic experiments

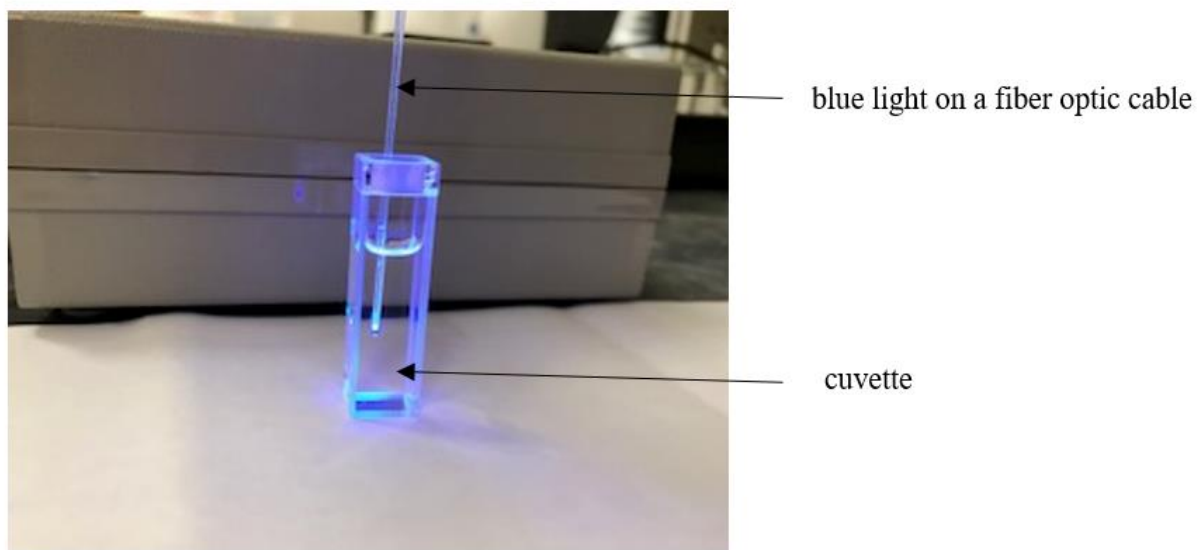
UV-Vis experiments:

Time-dependent UV/Vis spectra of hydrodebromination reaction of **1b**:

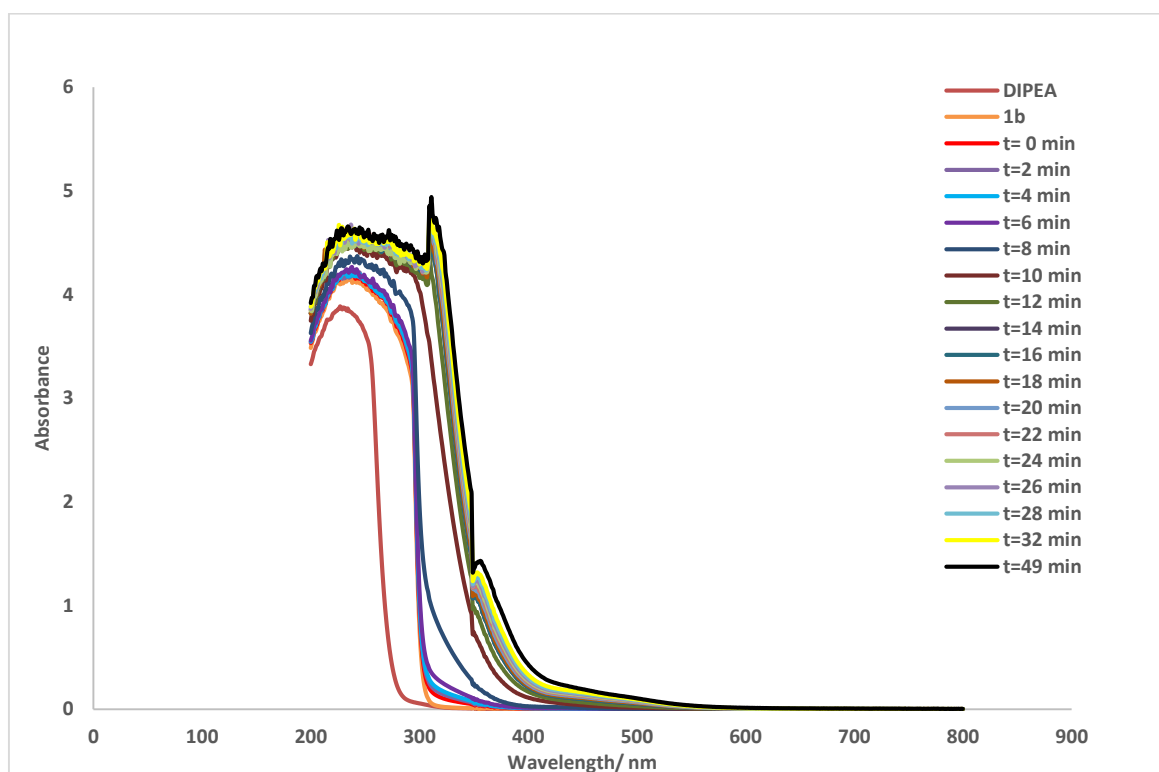


Brominated compound **1b** (101.3 mg, 0.24 mmol, 1 equiv) and *N,N*-diisopropylethylamine (62.8 μ L, 0.36 mmol, 1.5 equiv) was added into 1 cm path quartz cuvette and total volume was adjusted to 2.4 mL by adding MeCN to the cuvette. Then, the blue light on a fiber optic cable was dipped in the cuvette and reaction was irradiated. UV-Vis spectra were recorded for the reaction at different reaction times using Varian Cary Eclipse spectrophotometer. The appearance of an absorption band in the visible

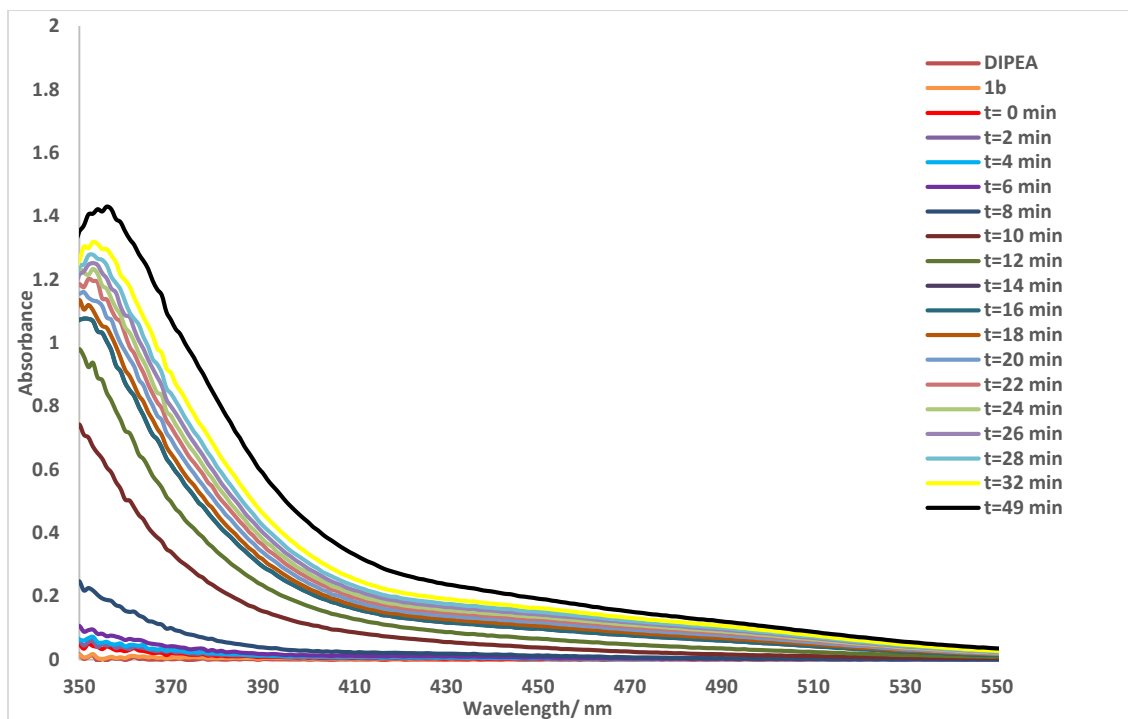
region as a function of time is consistent with the formation of a streptocyanine dye as the reaction progresses.



Time-dependent UV/Vis spectra of debromination reaction of **1b**

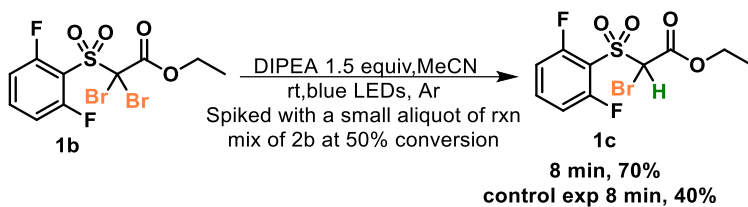


Expansion of the above spectrum:



Exp 1:

Spiking experiment:

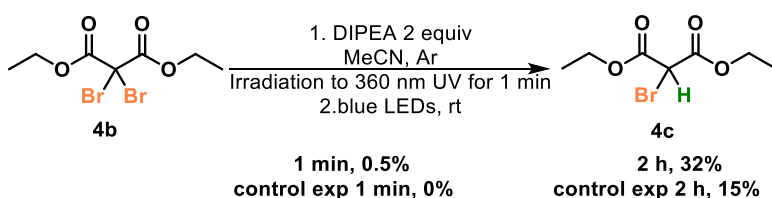


Reaction of **2b** used for above spiking:



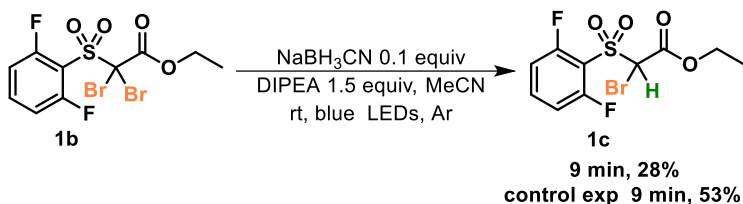
An NMR tube fitted with a rubber septum was charged with brominated sulfone **1b** (50.6 mg, 0.12 mmol, 1 equiv), *N, N*-diisopropylethylamine (31.4 μ L, 0.18 mmol, 1.5 equiv) and MeCN (1.2 mL). Then the reaction mixture was spiked with a 20 μ L aliquot of reaction mixture of **2b** at 50% conversion. The reaction tube was covered with piece of aluminum foil to avoid ambient light and degassed via Ar bubbling for 10 min. Then the piece of aluminum foil was removed and the tube was placed in a blue LED bath. Meanwhile, a control experiment was set up without any reaction mixture of **2b**. The reactions were monitored by ^{19}F NMR. After 8 min, the spiked reaction showed 70% conversion while the control experiment showed only 40% conversion, indicating that a species formed during the reaction of a different substrate was capable of accelerating the formation of a different product. This is suggestive that the postulated streptocyanine dye is capable of catalyzing this hydrodebromination reaction.

Exp 2:



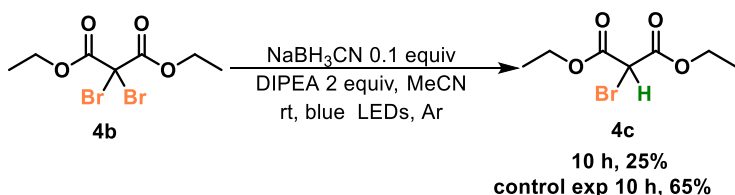
An NMR tube fitted with a rubber septum was charged with brominated compound **4b** (38.15 mg, 0.12 mmol, 1 equiv), *N, N*-diisopropylethylamine (41.8 μ L, 0.24 mmol, 2 equiv) and MeCN (01.2 mL). The reaction tube was covered with piece of aluminum foil to avoid ambient light and degassed via Ar bubbling for 10 min. The piece of aluminum foil was removed and the colorless reaction mixture was irradiated with the long wavelength UV light (360 nm) produced by a hand held TLC lamp, for 1 min. Then, the tube was returned to a blue LED bath. Meanwhile, the control experiment was immediately placed in the same blue LED bath. The reactions were monitored by ^1H NMR. After 2 h, the UV-exposed reaction mixture showed 32% conversion while the control experiment showed only 15% conversion. This experiment suggests that UV light can initiate reaction faster than blue light.

Exp 3:



An NMR tube fitted with a rubber septum was charged with brominated compound **1b** (50.6 mg, 0.12 mmol, 1 equiv), *N,N*-diisopropylethylamine (31.4 μ L, 0.18 mmol, 1.5 equiv), NaBH₃CN (0.8 mg, 0.012 mmol, 0.1 equiv) and MeCN (1.2 mL). The reaction tube was covered with piece of aluminum foil to avoid ambient light and degassed via Ar bubbling for 10 min. Then, the piece of aluminum foil was removed and the tube was placed in a blue LED bath. Meanwhile, a control experiment was set up containing no NaBH₃CN. The reactions were monitored by ¹⁹F NMR. After 9 min, the reaction mixture containing NaBH₃CN showed only 28% conversion, while the positive control experiment showed 53% conversion. Indicating the presence of the hydride source retarded the rate of the reaction. Importantly, a dark version of this reaction showed that the NaBH₃CN did not reduce the substrate.

Exp 4:

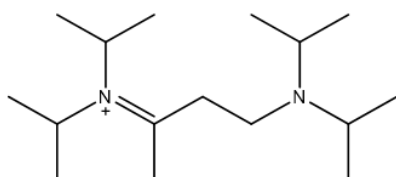


An NMR tube fitted with a rubber septum was charged with brominated compound **4b** (38.15 mg, 0.12 mmol, 1 equiv), *N,N*-diisopropylethylamine (41.8 μ L, 0.24 mmol, 2 equiv), NaBH₃CN (0.8 mg, 0.012 mmol, 0.1 equiv) and MeCN (1.2 mL). The reaction tube was covered with piece of aluminum foil to avoid ambient light and degassed via Ar bubbling for 10 min. Then, the piece of aluminum foil was removed and the tube was placed in a blue LED bath. The control experiment was set up without adding

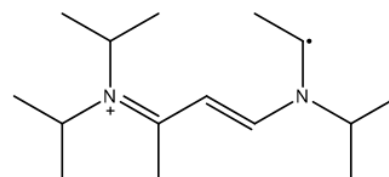
NaBH₃CN. The reactions were monitored by ¹H NMR. After 10 h, the reaction containing the NaBH₃CN showed only 25% conversion while the positive control experiment gave 65% conversion. Again, this experiment shows that the presence of the hydride source retarded the rate of the reaction. Importantly, a dark version of this reaction showed that the NaBH₃CN did not reduce the substrate. A further observation concerning experiments 3 and 4 was the slowing of the formation of colored reaction mixture. These observations are consistent with a streptocyanine based dye in which the iminium functional group would be expected to be reduced by the NaBH₃CN.

Evidence for streptocyanine dye:

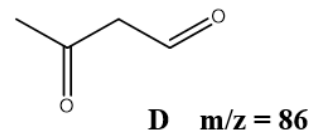
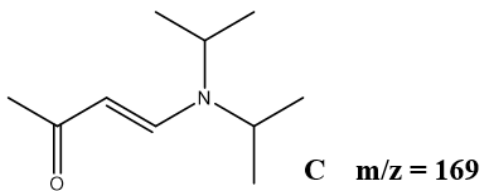
A 12×75 mm borosilicate tube fitted with a rubber septum was charged with brominated compound **1b** (50.6 mg, 0.12 mmol, 1 equiv), *N, N*-diisopropylethylamine (31.4 μL, 0.18 mmol, 1.5 equiv) and MeCN (1.2 mL). The reaction tube was covered with piece of aluminum foil to avoid ambient light and degassed via Ar bubbling for 10 min. The tube was placed in a blue LED bath which was at 28 °C. The reaction was monitored by the Expression Compact Mass Spectrometer (CMS)- Advion in the positive detection mode to detect the cyanine dyes. Mass spectrum of crude reaction when t=7 min has given below. It revealed masses of 255, 238 and 169 which could explain the following streptocyanine dye and its hydrolyzed products. Furthermore, after complete conversion of **1b**, crude reaction was subjected to GCMS. It also showed hydrolyzed product of streptocyanine dye. Attempts to isolate the colored material failed as its quantity seemed to be very low.



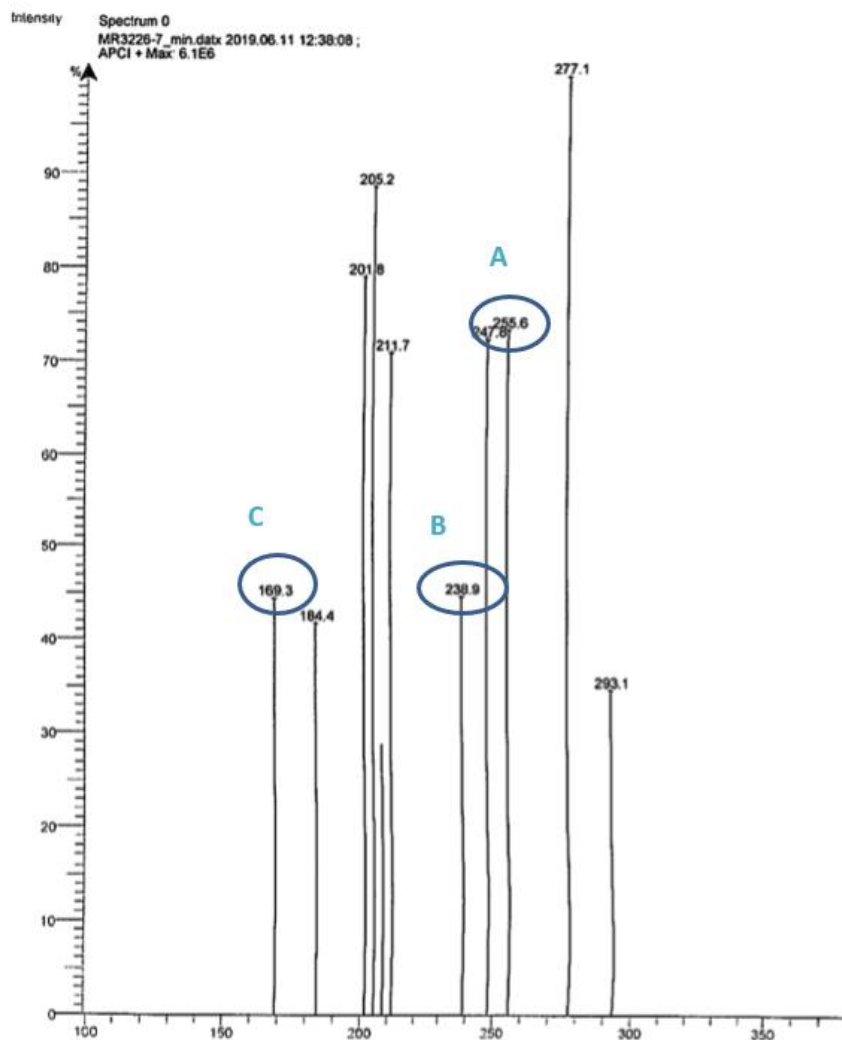
A m/z = 255



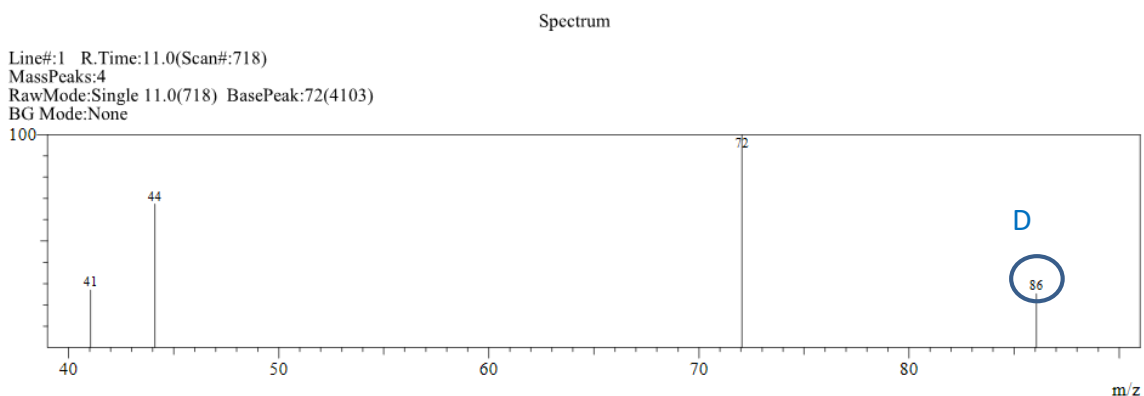
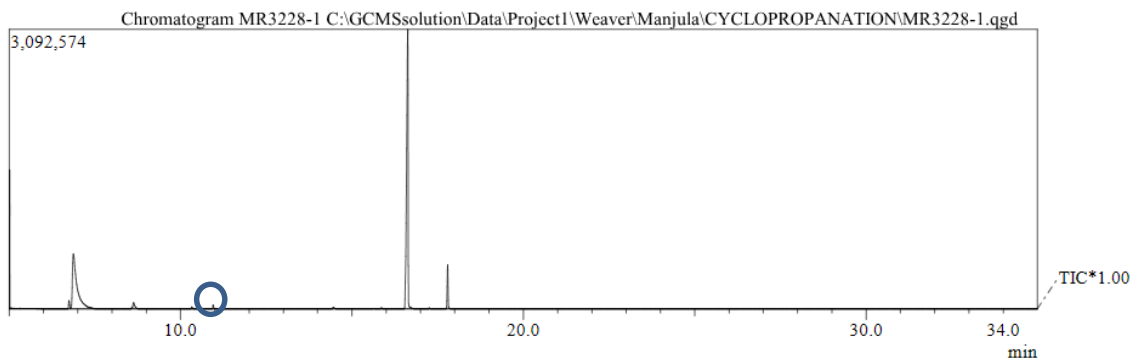
B m/z = 238



CMS- Mass spectrum of crude reaction of 1b when $t = 7$ min



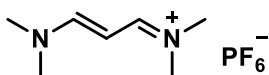
GC- MS of crude reaction when t= 45 min



Supportive experiments:

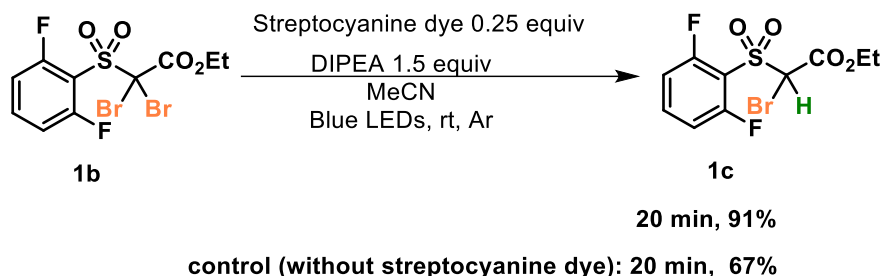
1) Experiments related to streptocyanine dye

We postulate that a streptocyanine dye formed under the reaction conditions, and that it is responsible for photoinduced electron transfer process. We have performed several experiments that are consistent with our hypothesis. While the exact dye we believe to be involved was not commercially available, we were able to purchase the following related streptocyanine dye.



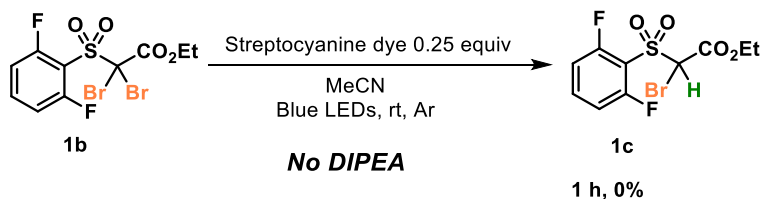
Methanaminium, N-[3-(dimethylamino)-2-propen-1-ylidene]-N-methyl-, hexafluorophosphate

Following reaction was performed using a catalytic amount of this streptocyanine dye. This allowed to see if the reaction was accelerated by the presence of this dye.



An NMR tube fitted with a rubber septum was charged with brominated sulfone **1b** (50.6 mg, 0.12 mmol, 1 equiv), *N,N*-diisopropylethylamine (31.4 μ L, 0.18 mmol, 1.5 equiv), streptocyanine dye (8.2 mg, 0.03 mmol, 0.25 equiv) and MeCN (1.2 mL). The reaction tube was covered with piece of aluminum foil to avoid ambient light and degassed via Ar bubbling for 10 min. Then, the piece of aluminum foil was removed and the tube was placed in a blue LED bath. Meanwhile, a control experiment was set up without any streptocyanine dye in the reaction. The reactions were monitored by ^{19}F NMR. After 20 min, streptocyanine dye contained reaction showed 91% conversion while the control experiment (without streptocyanine dye) showed only 67% conversion, indicating that having streptocyanine dye accelerates the rate of the reaction.

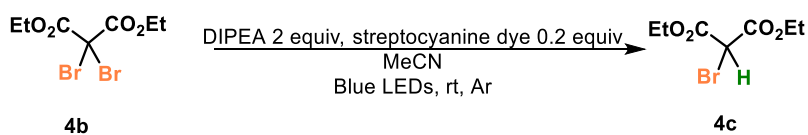
A control experiment showing that the streptocyanine dye itself does not serve as a stoichiometric reagent in the debromination was performed.



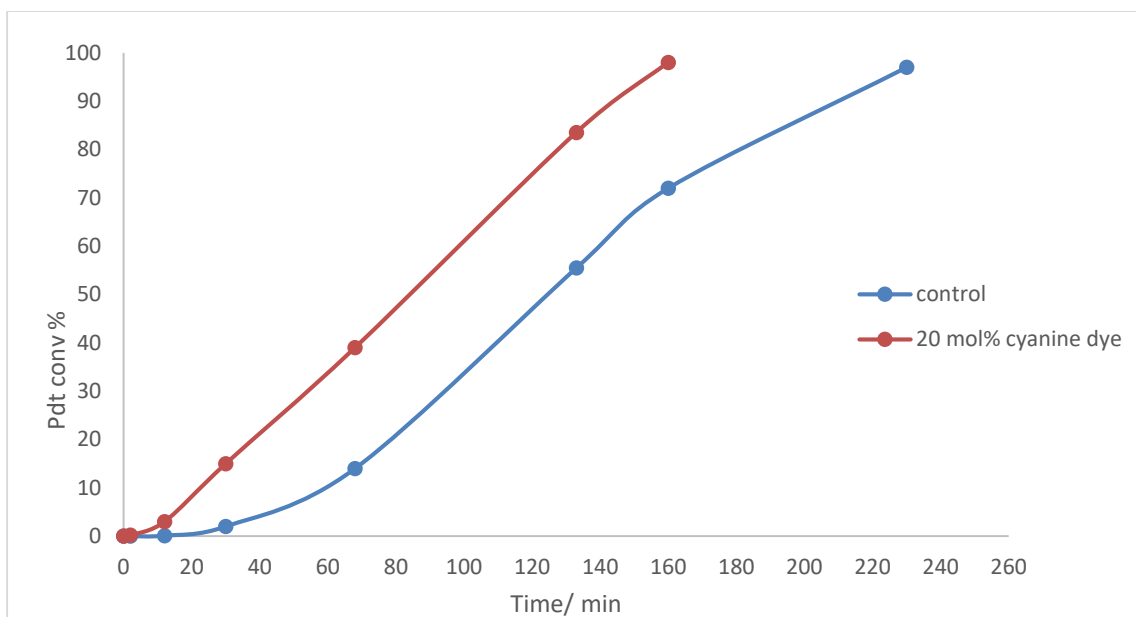
An NMR tube fitted with a rubber septum was charged with brominated sulfone **1b** (50.6 mg, 0.12 mmol, 1 equiv), streptocyanine dye (8.2 mg, 0.03 mmol, 0.25 equiv) and MeCN (1.2 mL). The reaction

tube was covered with piece of aluminum foil to avoid ambient light and degassed via Ar bubbling for 10 min. Then, the piece of aluminum foil was removed and the tube was placed in a blue LED bath. The reaction was monitored by ^{19}F NMR. After 1 h, reaction showed 0% conversion indicating that having DIPEA is necessary for the reaction.

A similar experiment was performed on a second substrate. Again, a similar acceleration was seen. It should be noted that the inflection in the rate profile is still observed. We believe that this explained by the formation of the dye during the course of the reaction, which may be even more active than the commercially available dye.



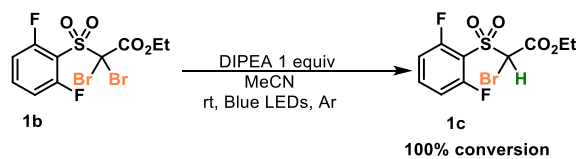
An NMR tube fitted with a rubber septum was charged with diethyl 2,2-dibromomalonate **4b** (19.1 mg, 0.06 mmol, 1 equiv), *N,N*-diisopropylethylamine (21 μL , 0.12 mmol, 2 equiv) streptocyanine dye (3.3 mg, 0.012 mmol, 0.2 equiv) and MeCN (0.6 mL). The reaction tube was covered with piece of aluminum foil to avoid ambient light and degassed via Ar bubbling for 10 min. Then the piece of aluminum foil was removed and the tube was placed in a blue LED bath. Meanwhile, a control experiment was set up without any streptocyanine dye in the reaction. The reactions were monitored by ^1H NMR. Different time points were collected to plot a graph time vs product conversion as below. It indicates that having streptocyanine dye accelerates the rate of the reaction.



UV-Vis experiments of streptocyanine dye:

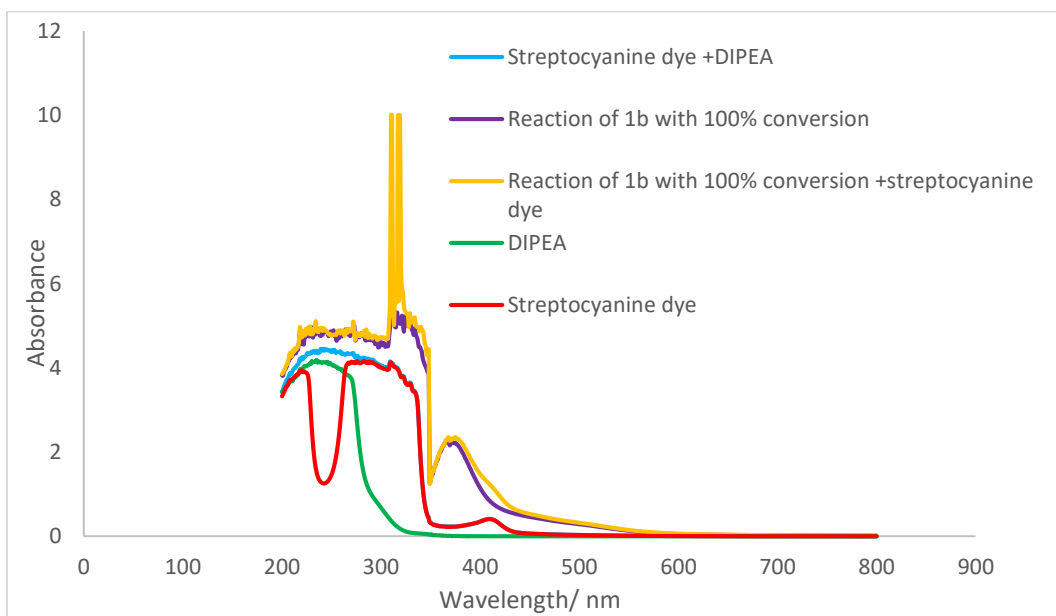
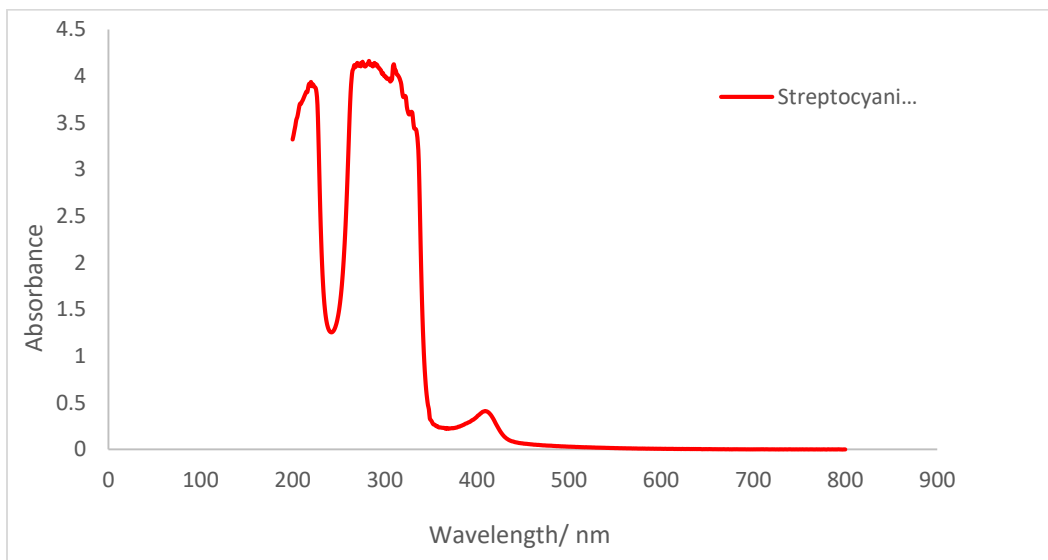
UV/Vis spectra were recorded using 1 cm path quartz cuvette and Varian Cary Eclipse spectrophotometer. MeCN was used as the solvent. UV/Vis spectra were recorded for following mixtures.

1. Streptocyanine dye (0.012 mmol of streptocyanine dye in 2.1 ml total volume of MeCN)
2. DIPEA (0.06 mmol of DIPEA in 2.1 ml total volume of MeCN)
3. Streptocyanine dye and DIPEA (0.012 mmol of streptocyanine dye and 0.06 mmol of DIPEA in 2.1 ml total volume of MeCN)
4. Reaction of **1b** with 100% conversion



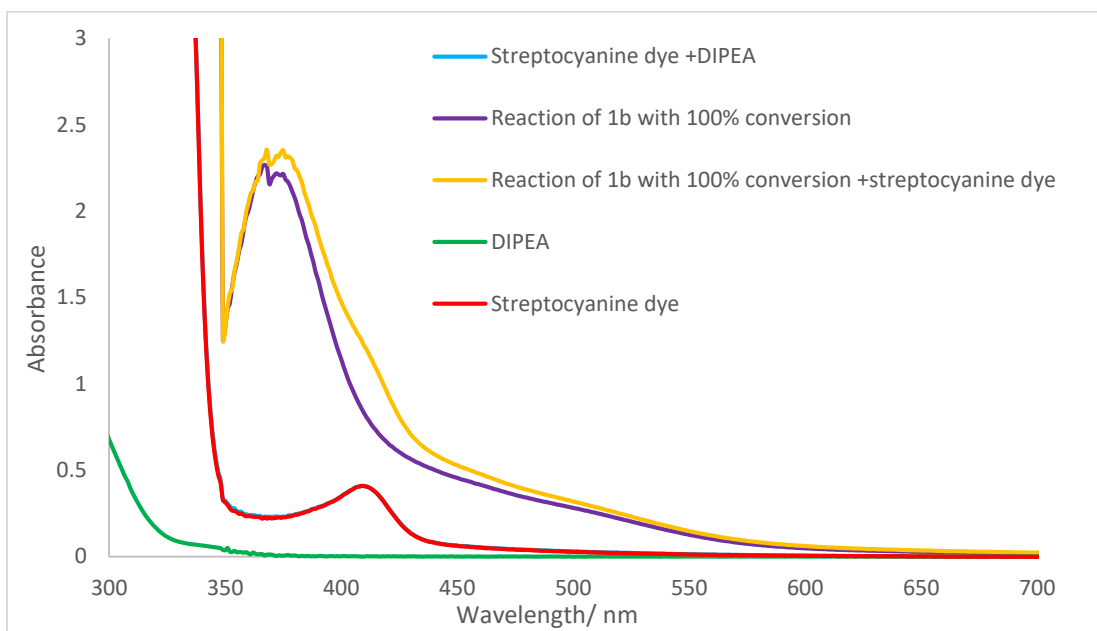
(**1b** 0.12 mmol, DIPEA 0.06 mmol in total volume of 2.1 mL of MeCN)

5. Reaction of **1b** with 100% conversion and streptocyanine dye (0.012 mmol)



Commercial streptocyanine dye absorbs in the visible region with $\lambda = 413$ nm. Reaction of **1b** with 100% conversion also absorbs in the same visible region.

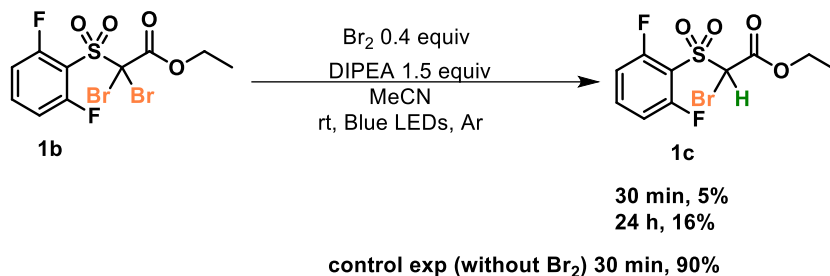
Expansion of the above spectrum:



2) Br₂ related experiments

During the debromination reactions, upon irradiation of the reaction mixture with blue LEDs, it was noted that the appearance of the reaction mixture changed from colorless to deep yellow and later to yellowish brown. It was suggested that the brownish color may result from the formation of Br₂. The following experiments probed the formation of Br₂.

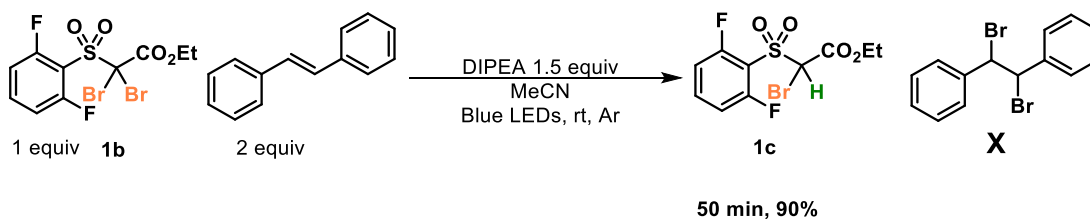
Experiment 1: Addition of Br₂ to the reaction



An NMR tube fitted with a rubber septum was charged with brominated sulfone **1b** (50.6 mg, 0.12 mmol, 1 equiv), *N,N*-diisopropylethylamine (31.4 μ L, 0.18 mmol, 1.5 equiv), bromine (2.5 μ L, 0.048 mmol, 0.4 equiv) and MeCN (1.2 mL). The reaction tube was covered with piece of aluminum foil to avoid ambient light and degassed via Ar bubbling for 10 min. Then the piece of aluminum foil was removed and the tube was placed in a blue LED bath. Meanwhile, a control experiment was set up without any bromine in the reaction. The reactions were monitored by ¹⁹F NMR. After 30 min, the bromine contained reaction showed only 5% conversion while the control experiment (normal conditions-no Br₂) gave 90% conversion, indicating that bromine significantly retarded the rate of the reaction.

Experiment 2: Addition of bromine scavenger to the reaction

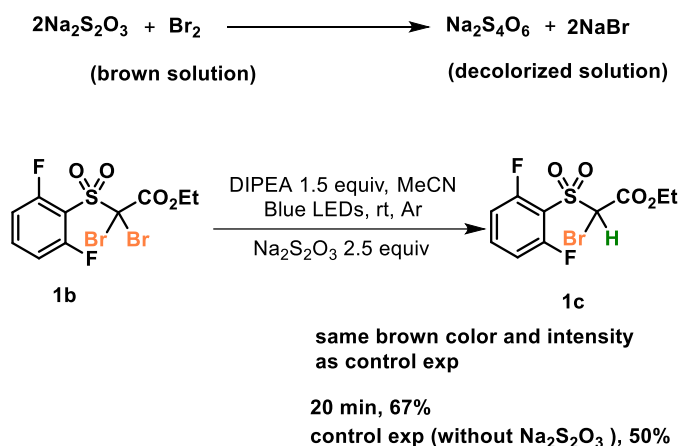
Bromination of (*E*)-1,2-diphenylethene is well known reaction in literature.^{13, 50} If the reaction forms bromine in the reaction, (*E*)-1,2-diphenylethene would react with bromine and form the di-brominated product. Therefore, following reaction was set up.



An NMR tube fitted with a rubber septum was charged with brominated sulfone **1b** (50.6 mg, 0.12 mmol, 1 equiv), *N,N*-diisopropylethylamine (31.4 μ L, 0.18 mmol, 1.5 equiv), (*E*)-1,2-diphenylethene (43.3 mg, 0.24 mmol, 2 equiv) and MeCN (1.2 mL). The reaction tube was covered with piece of aluminum foil to avoid ambient light and degassed via Ar bubbling for 10 min. Then the piece of aluminum foil was removed and the tube was placed in a blue LED bath. After 50 min, the reaction was monitored by ^{19}F NMR and it showed complete conversion with 90% product. Then, the reaction was subjected to GCMS. It did not show the mass of the dibrominated stilbene product.

Experiment 3: Addition of bromine scavenger $\text{Na}_2\text{S}_2\text{O}_3$ to the reaction

$\text{Na}_2\text{S}_2\text{O}_3$ can react with bromine and which would be expect to decolorize the brownish colored solution.



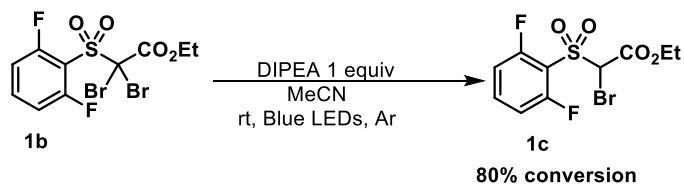
An NMR tube fitted with a rubber septum was charged with brominated sulfone **1b** (50.6 mg, 0.12 mmol, 1 equiv), *N,N*-diisopropylethylamine (31.4 μ L, 0.18 mmol, 1.5 equiv), $\text{Na}_2\text{S}_2\text{O}_3$ (47.4 mg, 0.3 mmol, 2.5 equiv) and MeCN (1.2 mL). The reaction tube was covered with piece of aluminum foil to avoid ambient light and degassed via Ar bubbling for 10 min. Then the piece of aluminum foil was removed and the tube was placed in a blue LED bath. After 20 min, the reaction was monitored by ^{19}F NMR. $\text{Na}_2\text{S}_2\text{O}_3$ contained reaction showed 67% conversion while the control experiment showed 50%

conversion. By visual inspection, the same brown color and intensity was observed for both the reactions.

Experiment 4: UV-Vis experiment

UV/Vis spectra were recorded using 1 cm path quartz cuvette and Varian Cary Eclipse spectrophotometer. MeCN was used as the solvent. UV/Vis spectra were recorded for following mixtures.

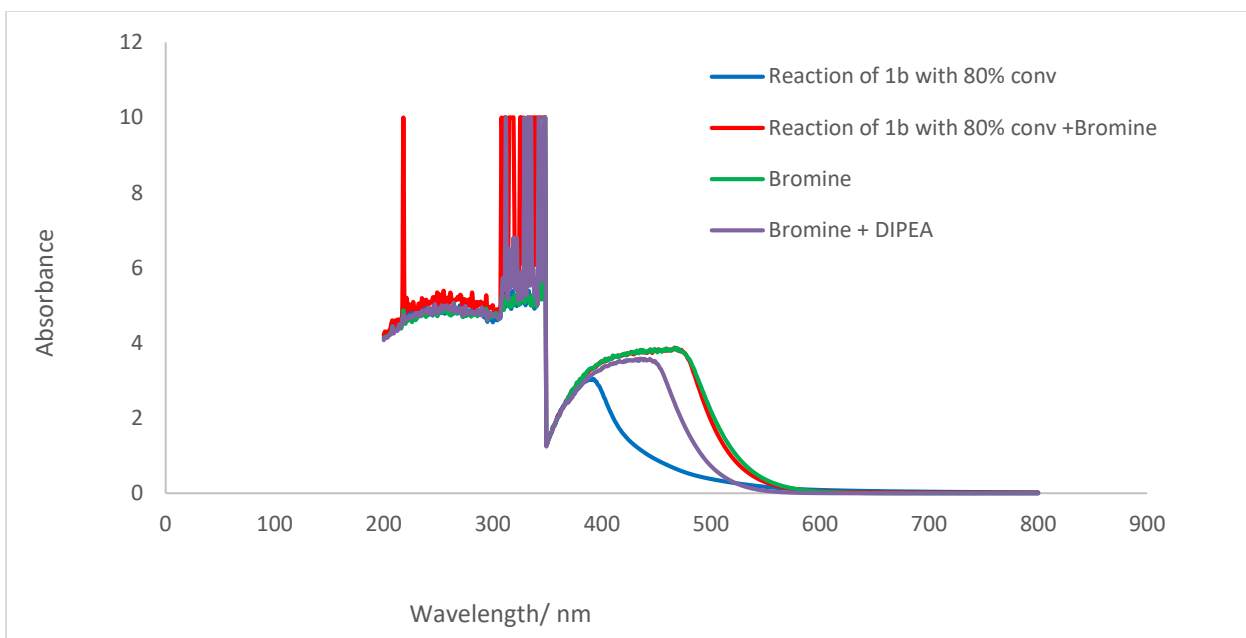
1. Bromine (0.06 mmol of Br₂ in 2.1 ml total volume of MeCN)
2. Bromine and DIPEA (0.06 mmol of Br₂ and 0.06 mmol of DIPEA in 2.1 ml total volume of MeCN)
3. Reaction of **1b** at 80% conversion



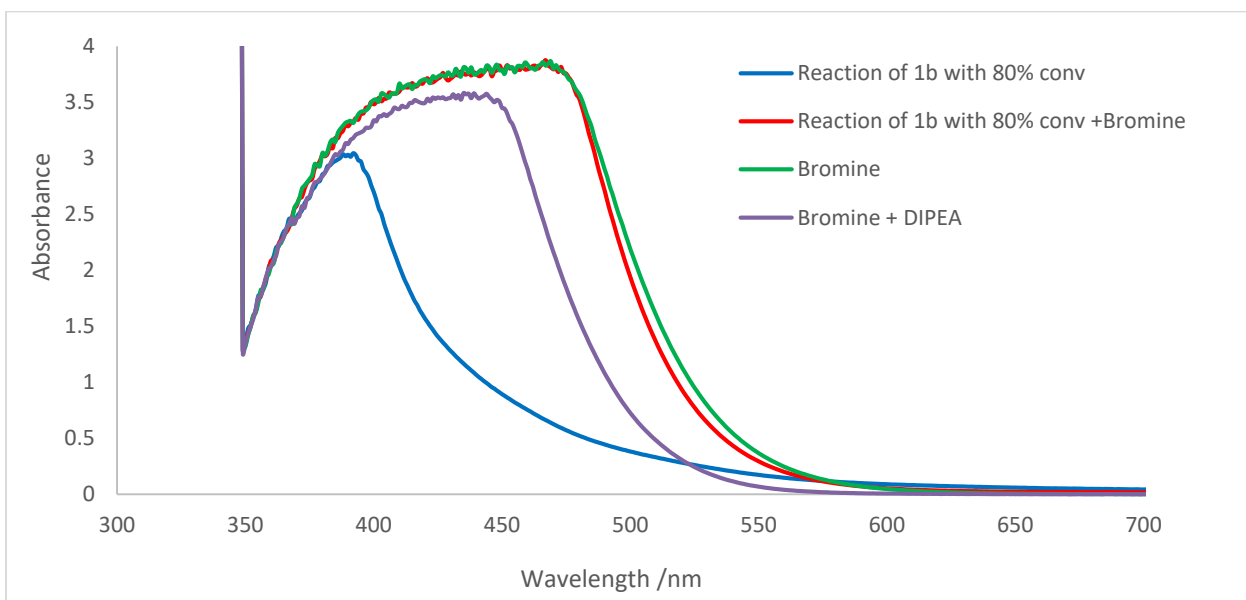
(**1b** 0.12 mmol, DIPEA 0.06 mmol in total volume of 2.1 ml of MeCN)

4. Reaction of **1b** at 80% conversion (as above) and bromine (0.06 mmol)

While bromine does absorb in the visible region with $\lambda_{\text{max}} = 468$ nm, the reaction mixture of **1b** (at 80% conversion) absorbs the visible region with $\lambda_{\text{max}} = 393$ nm. This suggests that bromine is neither present or involved in the reaction.



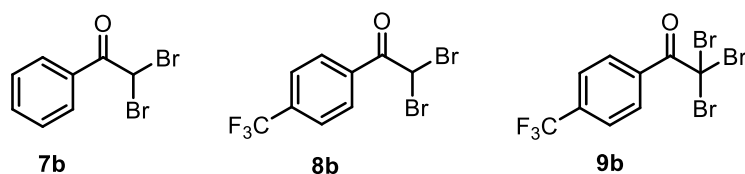
Expansion of the above spectrum:



3) For the direct EDA pathway, it is proposed that a halogen-nitrogen EDA complex results in a bathochromic shift which enables excitation and subsequent loss of a bromide anion. This is based on a UV shift observed with substrate **7b** when mixed with DIPEA. The UV shift could be as a direct result of deprotonation forming a charged species leading to a UV shift and not due to the EDA complex.

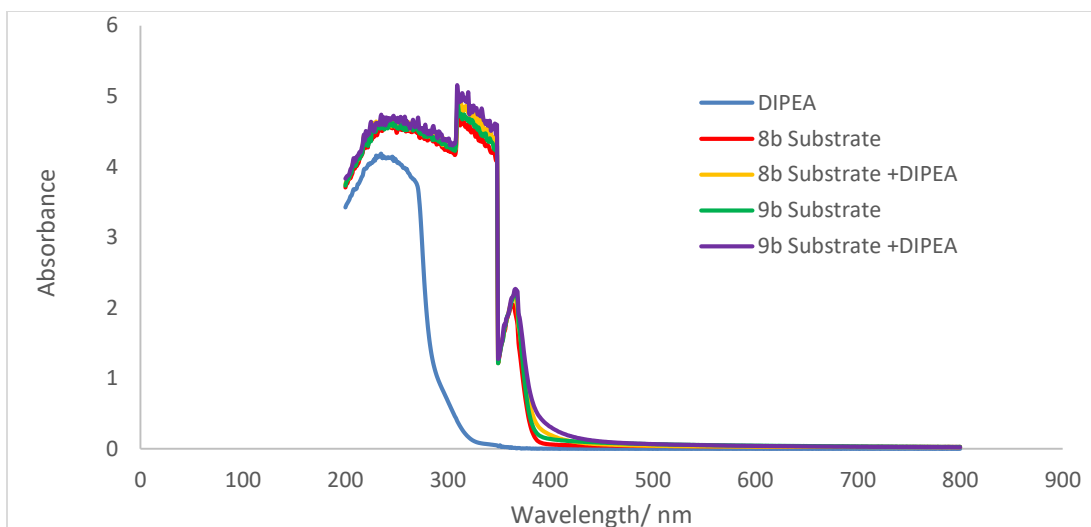
To be clear, this is only possible for two substrates **7b** and **8b** which have acidic protons. Arguably, if we formed the enolate, the absorption spectrum would likely look substantially different than the EDA complex. Thus, we performed UV-Vis experiments on **8b** and **9b**, which are nearly identical except that the last acidic proton is replaced with a bromine. We observed similar spectra, and think it is likely that these two classes of substrates still proceed through an EDA complex, though we cannot completely rule out the suggested possibility.

A UV-Vis experiment was performed on **9b** which could not undergo such a mechanism as that suggested by the reviewer. Like **8b**, it also displays a bathochromic shift **7b**, suggesting that these two may be undergoing the same mechanism. The following spectra were recorded.

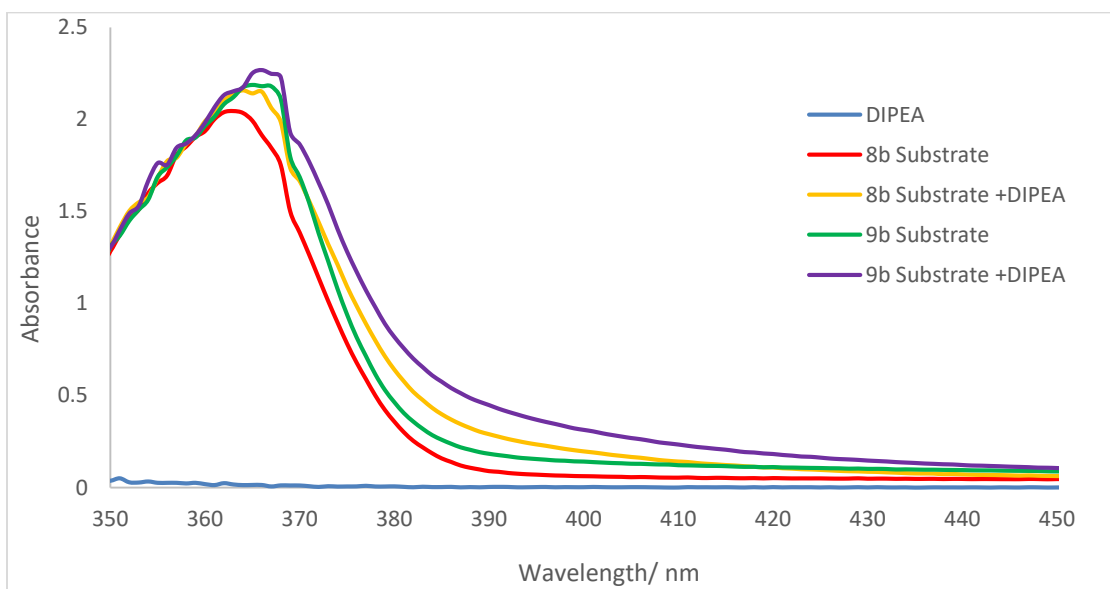


1. **8b** or **9b** (0.21 mmol of **8b** or **9b** in 2.1 mL total volume of MeCN)

2. **8b** or **9b** with DIPEA (0.21 mmol of **8b** or **9b** with 0.315 mmol of DIPEA in 2.1 mL total volume of MeCN)



Expansion of the above spectrum:



- 4) Purple LEDs and a vast excess of DIPEA are used in particular for dehalogenation of chlorides. This supports a hypothesis that an initial homolytic cleavage is necessary which ultimately leads to propagation in the system.

These conditions also are expected to facilitate the reaction under our proposed mechanism, unlike the proposed homolysis radical chain mechanism.

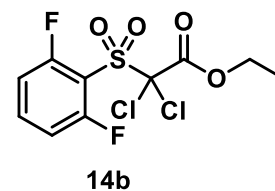
Sulfone **14b** formed an EDA complex that absorbed in the UV region (given in the below), but not in the visible (hence not visually detectable). As shown below the absorption of in MeCN approaches zero near 319 nm but a 1:4 mixture of **14b** and DIPEA showed a slight bathochromic displacement but its absorbance drops off before it reaches the visible region. This study, included in the SI, indicates that the EDA complex is likely the only species that can absorb a photon, suggesting that a radical chain mechanism that involves continual homolysis is unlikely.

UV/Vis spectra were recorded using 1 cm path quartz cuvette and Varian Cary Eclipse spectrophotometer. MeCN was used as the solvent. UV/Vis spectra were recorded for following mixtures.

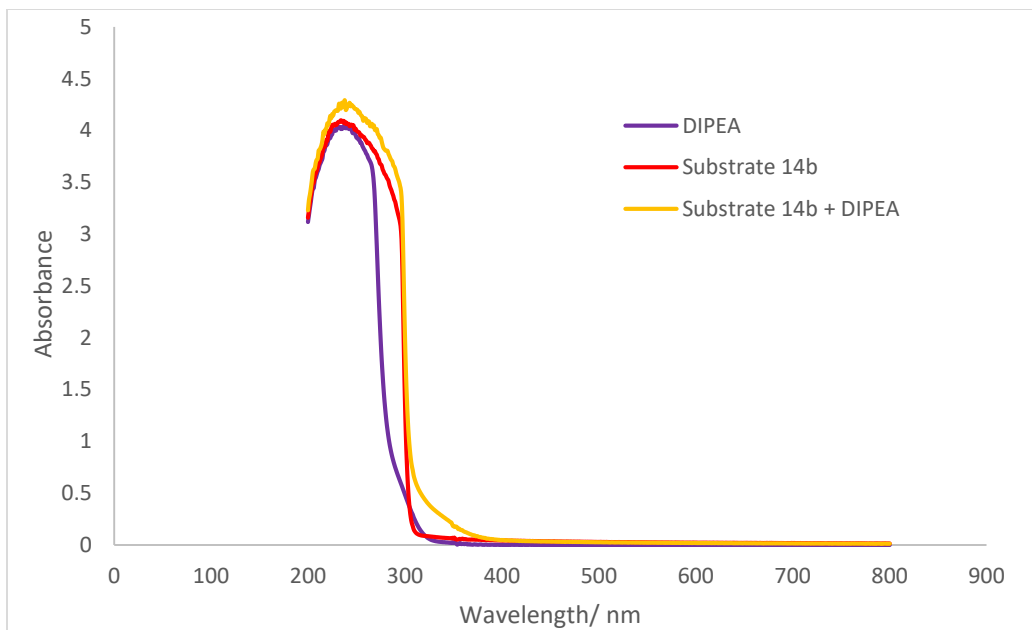
1. **14b** (0.06 mmol of **14b** in 2.1 mL total volume of MeCN)

2. DIPEA (0.24 mmol of DIPEA in 2.1 mL total volume of MeCN)

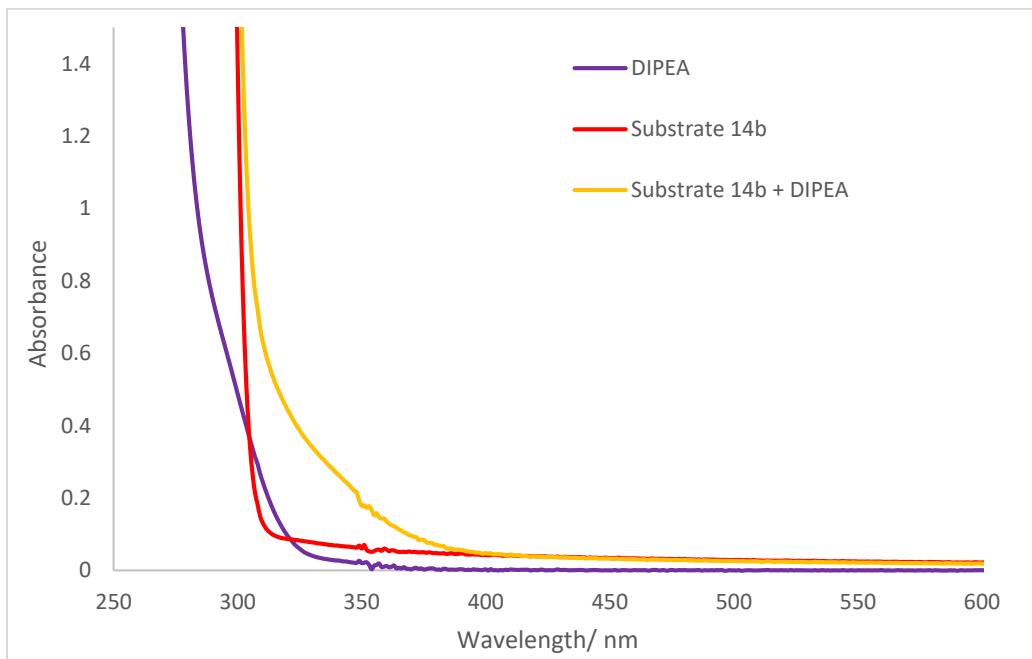
3. **14b** & DIPEA (0.06 mmol of **14b** and 0.24 mmol of DIPEA in 2.1 mL total volume of MeCN)



sulfone **14b** did not form any visually detectable EDA complex which was supported by UV-Vis experiments. As shown below the absorption of in MeCN approaches zero near 319 nm but a 1:4 mixture of **14b** and DIPEA showed a slight bathochromic displacement but its absorbance too drops off before it reaches the visible region.

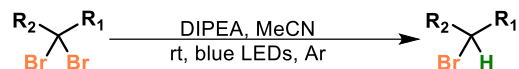


Expansion of the above spectrum:



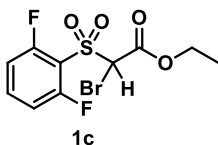
Light mediated dehalogenation

General procedure a for hydrodebromination:



A 12×75 mm borosilicate tube fitted with a rubber septum was charged with brominated compound (0.12 mmol, 1 equiv), *N, N*-diisopropylethylamine (X equivalent of amine) and MeCN (1.2 mL). The reaction tube was covered with piece of aluminum foil to avoid ambient light and degassed via Ar bubbling for 10 min and then left under positive Ar pressure by removing the exit needle. Then, the piece of aluminum foil was removed and the tube was placed in a blue LED bath (description above) and the lower portion of the tube was submerged under the water bath which was at 28 °C. The reaction was monitored by TLC, ¹H NMR or GC-MS. After the completion of selective debromination, MeCN was removed via rotovap and the residue was treated with sat. NaHCO₃ solution (2 mL) and extracted with DCM (3 x 2 mL). The organic portions were combined and dried over anhydrous MgSO₄. The crude product was concentrated *in vacuo* and purified via normal phase chromatography.

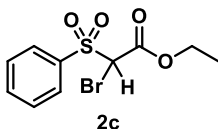
Ethyl 2-bromo-2-((2,6-difluorophenyl)sulfonyl)acetate



The general procedure **A** was followed using ethyl 2,2-dibromo-2-((2,6-difluorophenyl)sulfonyl)acetate (50.6 mg, 0.12 mmol, 1 equiv) and *N, N*-diisopropylethylamine (31.4 μL, 0.18 mmol, 1.5 equiv) in 1.2 mL MeCN. After the completion of the reaction in 45 min, the crude was purified via automated flash chromatography using ether in hexanes (0% to 100%) with product eluting at 30% on a 4 g silica column to afford **1c** in 93% yield (38 mg, 0.112 mmol) as an oil. ¹H NMR (400 MHz, CDCl₃) δ 7.69 (tt, *J* = 8.5, 5.9 Hz, 1H),

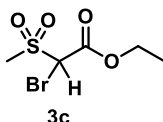
7.10 (t, $J = 8.4$ Hz, 2H), 5.48 (s, 1H), 4.36 – 4.24 (m, 2H), 1.29 (t, $J = 7.1$ Hz, 3H). ^{19}F NMR (376 MHz, CDCl_3) δ -103.4 (dd, $J = 8.4, 5.8$ Hz). ^{13}C NMR (101 MHz, CDCl_3) δ 161.1 (dd, $J = 263.5, 3.0$ Hz), 161.3, 137.7 (t, $J = 11.4$ Hz), 113.8 – 113.6 (m), 113.6 – 113.4 (m), 64.5, 60.4, 13.9. GC/MS (m/z, relative intensity) 263 (30), 224 (1), 154 (100). The compound produced thermally generated impurities under GC conditions. HRMS (ESI) calcd. for $[\text{C}_{10}\text{H}_8\text{BrF}_2\text{O}_4\text{S}]^-$ $[\text{M}-\text{H}]^-$ m/z, 340.9295 found 340.9301.

Ethyl 2-bromo-2-(phenylsulfonyl)acetate



The general procedure **A** was followed using ethyl 2,2-dibromo-2-(phenylsulfonyl)acetate (46.3 mg, 0.12 mmol) and *N,N*-diisopropylethylamine (31.4 μL , 0.18 mmol, 1.5 equiv) in 1.2 mL MeCN. After the completion of the reaction in 2 h, the crude was purified via automated flash chromatography using EtOAc in hexanes (0% to 100%) with product eluting at 23% on a 4 g silica column to afford **2c** in 92% yield (33.8 mg, 0.11 mmol) as an oil. ^1H NMR (400 MHz, CDCl_3) δ 7.98 (d, $J = 7.3$ Hz, 2H), 7.73 (t, $J = 7.5$ Hz, 1H), 7.60 (t, $J = 7.8$ Hz, 2H), 5.24 (s, 1H), 4.25 (q, $J = 7.1$ Hz, 2H), 1.26 (t, $J = 7.1$ Hz, 3H). ^{13}C NMR (101 MHz, CDCl_3) δ 162.1, 134.9, 134.5, 130.4, 128.8, 63.7, 58.4, 13.6. GC/MS (m/z, relative intensity) 306 (M^+ , 1), 280 (1), 141 (60). The compound produced thermally generated impurities under GC conditions. HRMS (ESI) calcd. for $[\text{C}_{10}\text{H}_{10}\text{BrO}_4\text{S}]^-$ $[\text{M}-\text{H}]^-$ m/z, 304.9483 found 304.9492.

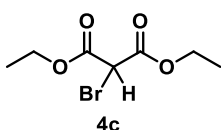
Ethyl 2-bromo-2-(methylsulfonyl)acetate



The general procedure **A** was followed using ethyl 2,2-dibromo-2-(methylsulfonyl)acetate (38.9 mg, 0.12 mmol) and *N,N*-diisopropylethylamine (31.4 μL , 0.18 mmol, 1.5 equiv) in 1.2 mL MeCN. After the completion of the reaction in 3 h, the crude was purified via automated flash chromatography using ether in hexanes (0% to 100%) with product eluting at 28% on a 4 g silica column to afford **3c** in 90% yield (26.5 mg, 0.108 mmol) as an oil. ^1H

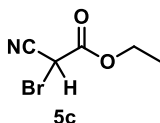
NMR (400 MHz, CDCl₃) δ 5.04 (s, 1H), 4.35 (q, $J = 7.1$ Hz, 2H), 3.28 (s, 3H), 1.36 (t, $J = 7.1$ Hz, 3H). ¹³C NMR (101 MHz, CDCl₃) δ 163.2, 64.3, 55.8, 37.2, 13.9. GC/MS (m/z, relative intensity) 216 (10), 166 (10), 120 (100). The compound produced thermally generated impurities under GC conditions. HRMS (ESI) calcd. for [C₅H₈BrO₄S]⁻[M-H]⁻ m/z, 242.9327 found 242.9335.

Diethyl 2-bromomalonate



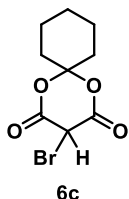
The general procedure **A** was followed using diethyl 2,2-dibromomalonate (38.15 mg, 0.12 mmol) and *N,N*-diisopropylethylamine (41.8 μ L, 0.24 mmol, 2 equiv) in 1.2 mL MeCN. After the completion of the reaction in 18 h, the crude was purified via automated flash chromatography using EtOAc in hexanes (0% to 100%) with product eluting at 7% on a 4 g silica column to afford **4c** in 91% yield (26.2 mg, 0.109 mmol) as an oil. NMR chemical shifts and mass spectrum details have reported in literature⁵¹ and NMR chemical shifts match with the literature values. ¹H NMR (400 MHz, CDCl₃) δ 4.81 (s, 1H), 4.28 (q, $J = 7.1$ Hz, 4H), 1.30 (t, $J = 7.1$ Hz, 6H). ¹³C NMR (101 MHz, CDCl₃) δ 165.0, 63.7, 42.8, 14.3.

Ethyl 2-bromo-2-cyanoacetate



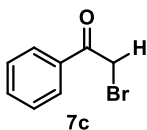
The general procedure **A** was followed using ethyl 2,2-dibromo-2-cyanoacetate (32.5 mg, 0.12 mmol) and *N,N*-diisopropylethylamine (41.8 μ L, 0.24 mmol, 2 equiv) in 1.2 mL MeCN. After the completion of the reaction in 19 h, the crude was purified via automated flash chromatography using EtOAc in hexanes (0% to 100%) with product eluting at 12% on a 4 g silica column to afford **5c** in 89% yield (20.5 mg, 0.107 mmol) as an oil. NMR chemical shifts and mass spectrum details have reported in literature⁵² and NMR chemical shifts match with the literature values. ¹H NMR (400 MHz, CDCl₃) δ 5.78 (s, 1H), 4.38 (q, $J = 7.1$ Hz, 2H), 1.36 (t, $J = 7.1$ Hz, 3H).

3-Bromo-1,5-dioxaspiro[5.5]undecane-2,4-dione



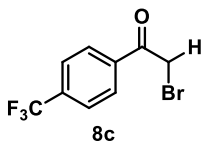
The general procedure **A** was followed using 3,3-dibromo-1,5-dioxaspiro[5.5]undecane-2,4-dione (41 mg, 0.12 mmol) and *N,N*-diisopropylethylamine (41.8 μ L, 0.24 mmol, 2 equiv) in 1.2 mL MeCN. After the completion of the reaction in 18 h, the crude was purified via silica plug to afford **6c** in 85% yield as a mixture of 89:11 monodebrominated to didebrominated product based on ^1H NMR. ^1H NMR (400 MHz, CDCl_3) δ 5.13 (s, 1H), 2.17 – 2.09 (m, 2H), 2.04 – 1.94 (m, 4H), 1.81 – 1.72 (m, 4H), 1.57 – 1.44 (m, 2H). ^{13}C NMR (101 MHz, CDCl_3) δ 161.4, 108.6, 37.2, 37.0, 35.1, 24.3, 22.7, 22.6. This compound decomposed under GC conditions. HRMS (ESI) calcd. for $[\text{C}_9\text{H}_{10}\text{BrO}_4]^-$ $[\text{M}-\text{H}]^-$ m/z , 260.9762 found 260.9782.

2-Bromo-1-phenylethan-1-one



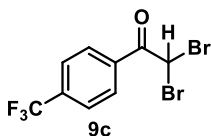
The general procedure **A** was followed using 2,2-dibromo-1-phenylethan-1-one (33.4 mg, 0.12 mmol) and *N,N*-diisopropylethylamine (41.8 μ L, 0.24 mmol, 2 equiv) in 1.2 mL MeCN. After the completion of the reaction in 21 h, the crude was purified via automated flash chromatography using EtOAc in hexanes (0% to 100%) with product eluting at 3% on a 4 g silica column to afford **7c** in 93% yield (22.2 mg, 0.112 mmol) as an oil. NMR chemical shifts and mass spectrum details have reported in literature⁵³ and NMR chemical shifts match with the literature values. ^1H NMR (400 MHz, CDCl_3) δ 7.98 (dd, 2H), 7.61 (tt, $J = 6.9, 1.3$ Hz, 1H), 7.55 – 7.45 (m, 2H), 4.46 (s, 2H). ^{13}C NMR (101 MHz, CDCl_3) δ 191.4, 134.1, 129.1, 129.0, 31.1.

2-Bromo-1-(4-(trifluoromethyl)phenyl)ethan-1-one



The general procedure **A** was followed using 2,2-dibromo-1-(4-(trifluoromethyl)phenyl)ethan-1-one (41.5 mg, 0.12 mmol) and *N,N*-diisopropylethylamine (41.8 μ L, 0.24 mmol, 2 equiv) in 1.2 mL MeCN. After the completion of the reaction in 20 h, the crude was purified via automated flash chromatography using EtOAc in hexanes (0% to 100%) with product eluting at 1% on a 4 g silica column to afford **8c** in 94% yield (30.1 mg, 0.113 mmol) as an oil. ^1H NMR (400 MHz, CDCl_3) δ 8.11 (d, $J = 8.2$ Hz, 2H), 7.77 (d, $J = 8.3$ Hz, 2H), 4.45 (s, 2H). ^{19}F NMR (376 MHz, CDCl_3) δ -63.3. ^{13}C NMR (101 MHz, CDCl_3) δ 190.5, 137.5 – 136.0 (m), 135.3 (q, $J = 32.8$ Hz), 129.5, 126.1 (q, $J = 3.7$ Hz), 123.5 (q, $J = 272.9$ Hz), 30.4. GC/MS (m/z , relative intensity) 266 (M^+ , 1), 173 (100), 145 (50). The compound produced thermally generated impurities under GC conditions. HRMS (ESI) calcd. for $[\text{C}_9\text{H}_5\text{BrF}_3\text{O}]^-$ $[\text{M}-\text{H}]^-$ m/z , 264.9476 found 264.9484.

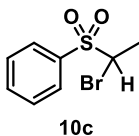
2,2-Dibromo-1-(4-(trifluoromethyl)phenyl)ethan-1-one



The general procedure **A** was followed using 2,2,2-tribromo-1-(4-(trifluoromethyl)phenyl)ethan-1-one (51 mg, 0.12 mmol) and *N,N*-diisopropylethylamine (31.4 μ L, 0.18 mmol, 1.5 equiv) in 1.2 mL MeCN. After the completion of the reaction in 10 h, the crude was purified via automated flash chromatography using EtOAc in hexanes (0% to 100%) with product eluting at 0.1% on a 4 g silica column to afford **9c** in 88% yield (36.7 mg, 0.106 mmol) as an oil. ^1H NMR (400 MHz, CDCl_3) δ 8.23 (d, $J = 8.2$ Hz, 2H), 7.78 (d, $J = 8.3$ Hz, 2H), 6.62 (s, 1H). ^{19}F NMR (376 MHz, CDCl_3) δ -63.4. ^{13}C NMR (101 MHz, CDCl_3) δ 185.5, 136.0 (q, $J = 33.0$ Hz), 134.4 – 133.9 (m), 130.7, 127.81 (q, $J = 272.9$ Hz), 126.4 (q, $J = 3.7$ Hz), 39.5. GC/MS (m/z , relative intensity) 327(1), 266 (1), 173 (100). The compound produced

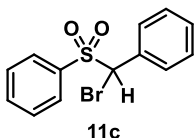
thermally generated impurities under GC conditions. HRMS (ESI) calcd. for $[\text{C}_9\text{H}_4\text{Br}_2\text{F}_3\text{O}]^- [\text{M-H}]^-$ m/z , 344.8561 found 344.8568.

((1-Bromoethyl)sulfonyl)benzene



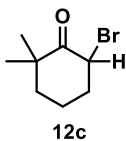
The general procedure **A** was followed using ((1,1-dibromoethyl)sulfonyl)benzene (39.4 mg, 0.12 mmol) and *N,N*-diisopropylethylamine (41.8 μL , 0.24 mmol, 2 equiv) in 1.2 mL MeCN. After the completion of the reaction in 22 h, the crude was purified via automated flash chromatography using EtOAc in hexanes (0% to 100%) with product eluting at 10% on a 4 g silica column to afford **10c** in 90% yield (27 mg, 0.108 mmol) as an oil. NMR chemical shifts and mass spectrum details have reported in literature⁴ⁱ and mass spectrum details match with the literature values. GC/MS (m/z , relative intensity) 248 (M^+ , 2), 250 ($\text{M}^+ + 2$, 2), 125 (90), 77 (100).

((Bromo(phenyl)methyl)sulfonyl)benzene



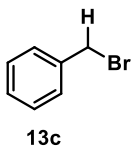
The general procedure **A** was followed using ((dibromo(phenyl)methyl)sulfonyl)benzene (46.8 mg, 0.12 mmol) and *N,N*-diisopropylethylamine (41.8 μL , 0.24 mmol, 2 equiv) in 1.2 mL MeCN. After the completion of the reaction in 20 h, the crude was purified via automated flash chromatography using EtOAc in hexanes (0% to 100%) with product eluting at 6% on a 4 g silica column to afford **11c** in 91% yield (34 mg, 0.109 mmol) as an oil. NMR chemical shifts and mass spectrum details have reported in literature⁴ⁱ and NMR chemical shifts match with the literature values. ¹H NMR (400 MHz, CDCl_3) δ 7.70 (dd, $J = 8.4, 1.2$ Hz, 2H), 7.66 – 7.61 (m, 1H), 7.50 – 7.43 (m, 2H), 7.40 – 7.33 (m, 3H), 7.33 – 7.27 (m, 2H), 5.70 (s, 1H). ¹³C NMR (101 MHz, CDCl_3) δ 135.0, 134.6, 131.2, 130.5, 130.4, 130.2, 129.0, 128.7, 65.8.

6-Bromo-2,2-dimethylcyclohexan-1-one



The general procedure **A** was followed using 2,2-dibromo-6,6-dimethylcyclohexan-1-one (34.1 mg, 0.12 mmol) and *N,N*-diisopropylethylamine (41.8 μ L, 0.24 mmol, 2 equiv) in 1.2 mL MeCN. After the completion of the reaction in 25 h, the crude was purified via automated flash chromatography using diethyl ether in hexanes (0% to 100%) with product eluting at 1% on a 4 g silica column to afford **12c** in 89% yield (21.9 mg, 0.107 mmol) as an oil. NMR chemical shifts and mass spectrum details have reported in literature⁵⁴ and mass spectrum details match with the literature values. GC/MS (*m/z*, relative intensity) 204 (M^+ , 10), 206 ($M^+ + 2$, 10), 97 (70), 69 (100).

(Bromomethyl)benzene



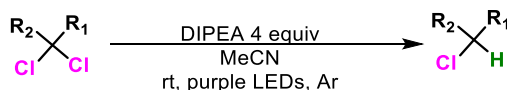
The general procedure **A** was followed using (dibromomethyl)benzene (30 mg, 0.12 mmol) and *N,N*-diisopropylethylamine (83.6 μ L, 0.48 mmol, 4 equiv) in 1.2 mL MeCN. After the completion of the reaction in 72 h, the crude was purified via automated flash chromatography using EtOAc in hexanes (0% to 100%) with product eluting at 0.1% on a 4 g silica column to afford **13c** in 80% yield (16.4 mg, 0.096 mmol) as an oil. NMR chemical shifts match with the literature values.⁵⁵ ¹H NMR (400 MHz, CDCl₃) δ 7.40 (dd, *J* = 8.2, 1.5 Hz, 2H), 7.35 (ddd, *J* = 7.4, 5.9, 1.5 Hz, 2H), 7.32 – 7.27 (m, 1H), 4.51 (s, 2H). ¹³C NMR (101 MHz, CDCl₃) δ 138.2, 129.5, 129.3, 128.9, 34.0.

Hydrodebromination in large scale



A 18×150 mm borosilicate tube fitted with a rubber septum was charged with **1b** (422 mg, 1 mmol, 1 equiv), *N,N*-diisopropylethylamine (349 μ L, 2 mmol, 2 equiv) and MeCN (10 mL). The reaction tube was covered with piece of aluminum foil to avoid ambient light and degassed via Ar bubbling for 30 min and then left under positive Ar pressure by removing the exit needle. Then, the piece of aluminum foil was removed and the tube was placed in a blue LED bath (description above) and the lower portion of the tube was submerged under the water bath which was at 28 °C and the reaction was stirred. The reaction was monitored by ^{19}F NMR. After the complete consumption of **1b** (6 h), crude reaction showed 80% of **1c** product according to ^{19}F NMR. MeCN was removed via rotovap and the residue was treated with sat. NaHCO_3 solution (20 mL) and extracted with DCM (3 x 10 mL). The organic portions were combined and dried over anhydrous MgSO_4 . The crude product was concentrated *in vacuo* and purified via normal phase chromatography using EtOAc in hexanes (0% to 100%) with product eluting at 26% on a 40 g silica column to afford **1c** in 76% as a solid.

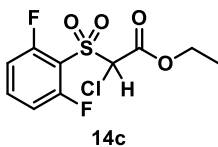
General procedure B for hydrodechlorination



This procedure is identical to general procedure **A** except that the blue LEDs were exchanged with violet LEDs and increased loading of amine was used. This procedure was used for all the hydrodechlorination reactions. Substrate (0.12 mmol, 1 equiv) and *N,N*-diisopropylethylamine (83.6

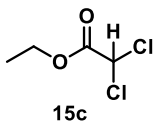
μL , 0.48 mmol, 4 equiv) in 1.2 mL MeCN. The tube was placed in a purple LEDs bath. The reaction was monitored by TLC, ^1H NMR or GC-MS. After the completion of selective dechlorination, MeCN was removed via rotovap and the residue was treated with sat. NaHCO_3 solution (2 mL) and extracted with DCM (3 x 2 mL). The organic portions were combined and dried over anhydrous MgSO_4 . The crude product was concentrated *in vacuo* and purified via normal phase chromatography.

Ethyl 2-chloro-2-((2,6-difluorophenyl)sulfonyl)acetate



The general procedure **B** was followed using ethyl 2,2-dichloro-2-((2,6-difluorophenyl)sulfonyl)acetate (40 mg, 0.12 mmol) and *N,N*-diisopropylethylamine (83.6 μL , 0.48 mmol, 4 equiv) in 1.2 mL MeCN. After the completion of the reaction in 50 h, the crude was purified via automated flash chromatography using EtOAc in hexanes (0% to 100%) with product eluting at 20% on a 4 g silica column to afford **14c** in 85% yield (30.5 mg, 0.102 mmol) as an oil. ^1H NMR (400 MHz, CDCl_3) δ 7.70 (tt, $J = 8.5, 5.9$ Hz, 1H), 7.10 (t, $J = 8.5$ Hz, 2H), 5.44 (s, 1H), 4.35 (qq, $J = 6.8, 3.6$ Hz, 2H), 1.32 (t, $J = 7.1$ Hz, 3H). ^{19}F NMR (376 MHz, CDCl_3) δ -103.5 (dd, $J = 8.5, 5.8$ Hz). ^{13}C NMR (101 MHz, CDCl_3) δ 161.2 (dd, $J = 263.8, 3.1$ Hz), 161.1, 137.8 (t, $J = 11.3$ Hz), 113.8 – 113.7 (m), 113.6 – 113.4 (m), 72.6, 64.5, 13.9. GC/MS (m/z, relative intensity) 270 (5), 177 (100), 161 (60). The compound produced thermally generated impurities under GC conditions. HRMS (ESI) calcd. for $[\text{C}_{10}\text{H}_8\text{ClF}_2\text{O}_4\text{S}]^-$ $[\text{M}-\text{H}]^-$ m/z, 296.9800 found 296.9808.

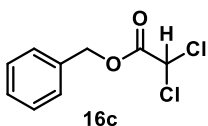
ethyl 2,2-dichloroacetate



The general procedure **B** was followed using ethyl 2,2,2-trichloroacetate (23 mg, 0.12 mmol) and *N,N*-diisopropylethylamine (83.6 μL , 0.48 mmol, 4 equiv) in 1.2 mL MeCN.

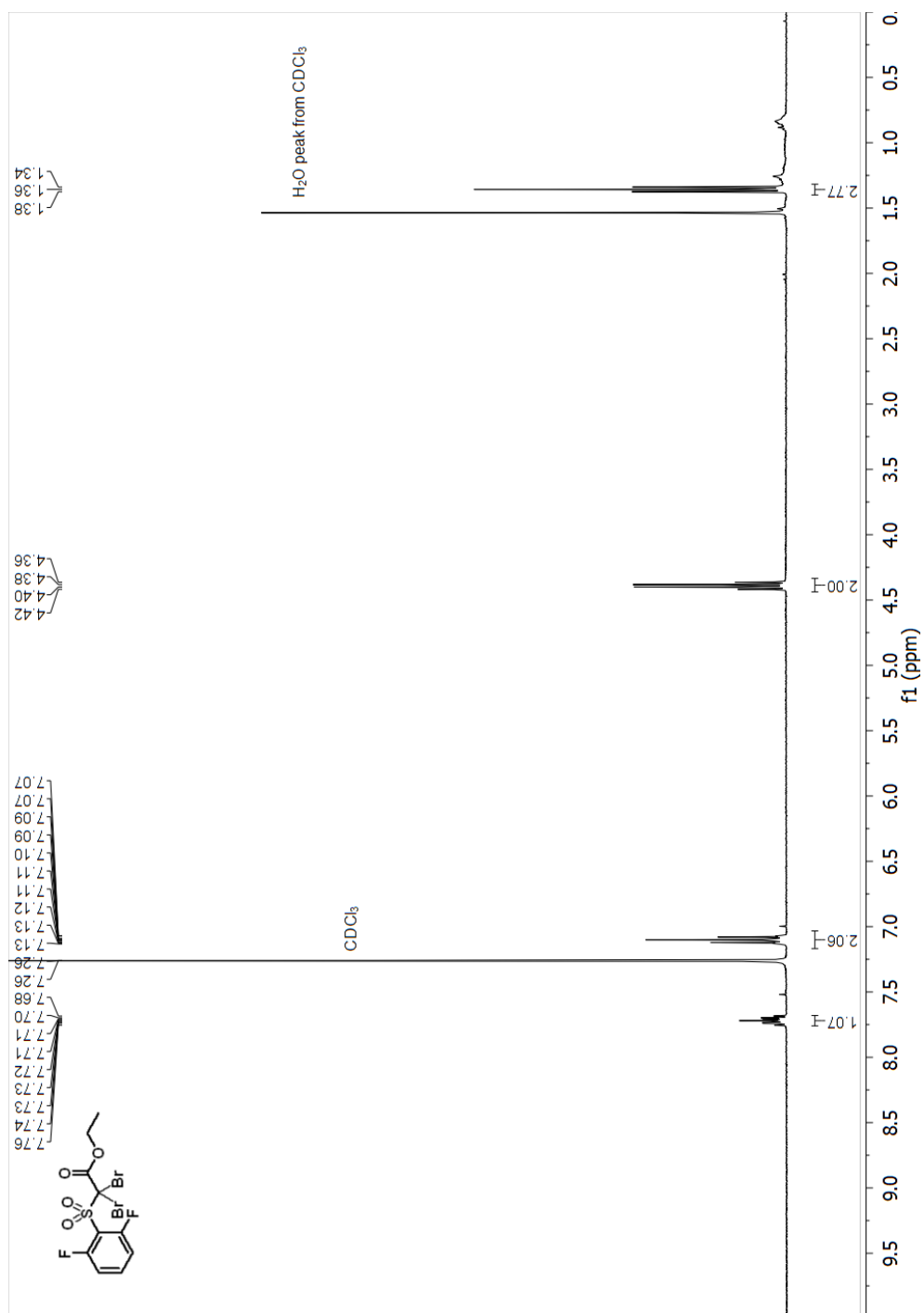
After the completion of the reaction in 72 h, the crude was purified via automated flash chromatography using EtOAc in hexanes (0% to 100%) with product eluting at 10% on a 4 g silica column to afford **15c** in 70% yield (13.2 mg, 0.084 mmol) as an oil. NMR chemical shifts and mass spectrum details have reported in literature⁵⁶ and NMR chemical shifts match with the literature values. ¹H NMR (400 MHz, CDCl₃) δ 5.93 (s, 1H), 4.33 (qd, *J* = 7.1, 1.5 Hz, 2H), 1.35 (td, *J* = 8.7, 6.7, 1.6 Hz, 3H). ¹³C NMR (101 MHz, CDCl₃) δ 165.0, 64.8, 64.2, 14.3.

Benzyl 2,2-dichloroacetate

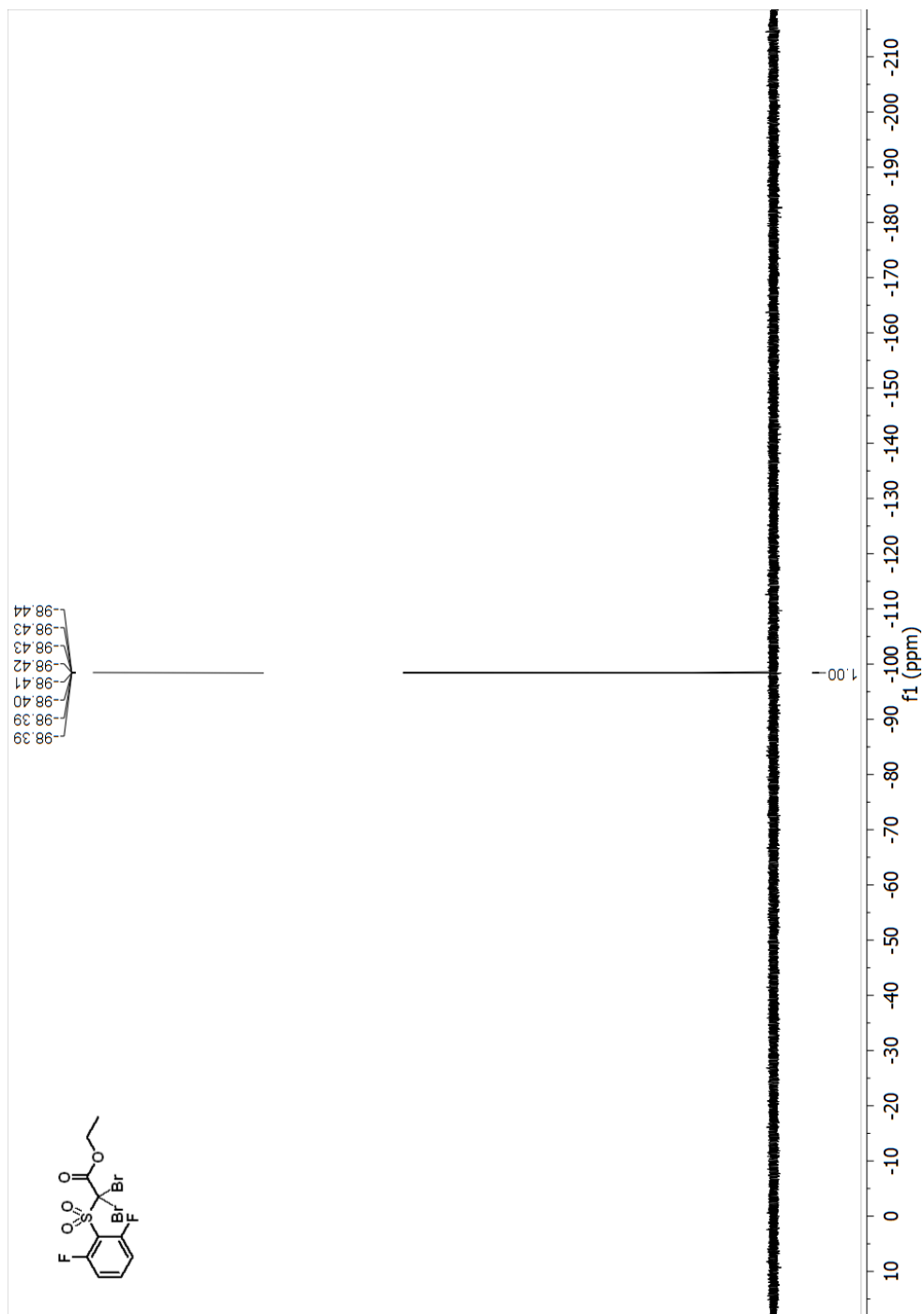


The general procedure **B** was followed using benzyl 2,2,2-trichloroacetate (30.4 mg, 0.12 mmol) and *N,N*-diisopropylethylamine (83.6 μL, 0.48 mmol, 4 equiv) in 1.2 mL MeCN. After the completion of the reaction in 60 h, the crude was purified via automated flash chromatography using EtOAc in hexanes (0% to 100%) with product eluting at 20% on a 4 g silica column to afford **16c** in 78% yield (20.5 mg, 0.094 mmol) as an oil. ¹H NMR (400 MHz, CDCl₃) δ 7.39 (s, 5H), 5.98 (s, 1H), 5.29 (s, 2H). ¹³C NMR (101 MHz, CDCl₃) δ 164.8, 134.6, 129.4, 129.2, 128.9, 69.5, 64.7. GC/MS (*m/z*, relative intensity) 218 (*M*⁺, 10), 107 (18), 91 (100). The compound produced thermally generated impurities under GC conditions. HRMS (ESI) calcd. for [C₉H₇Cl₂O₂]⁻ [*M*-H]⁻ *m/z*, 216.9823 found 216.9785.

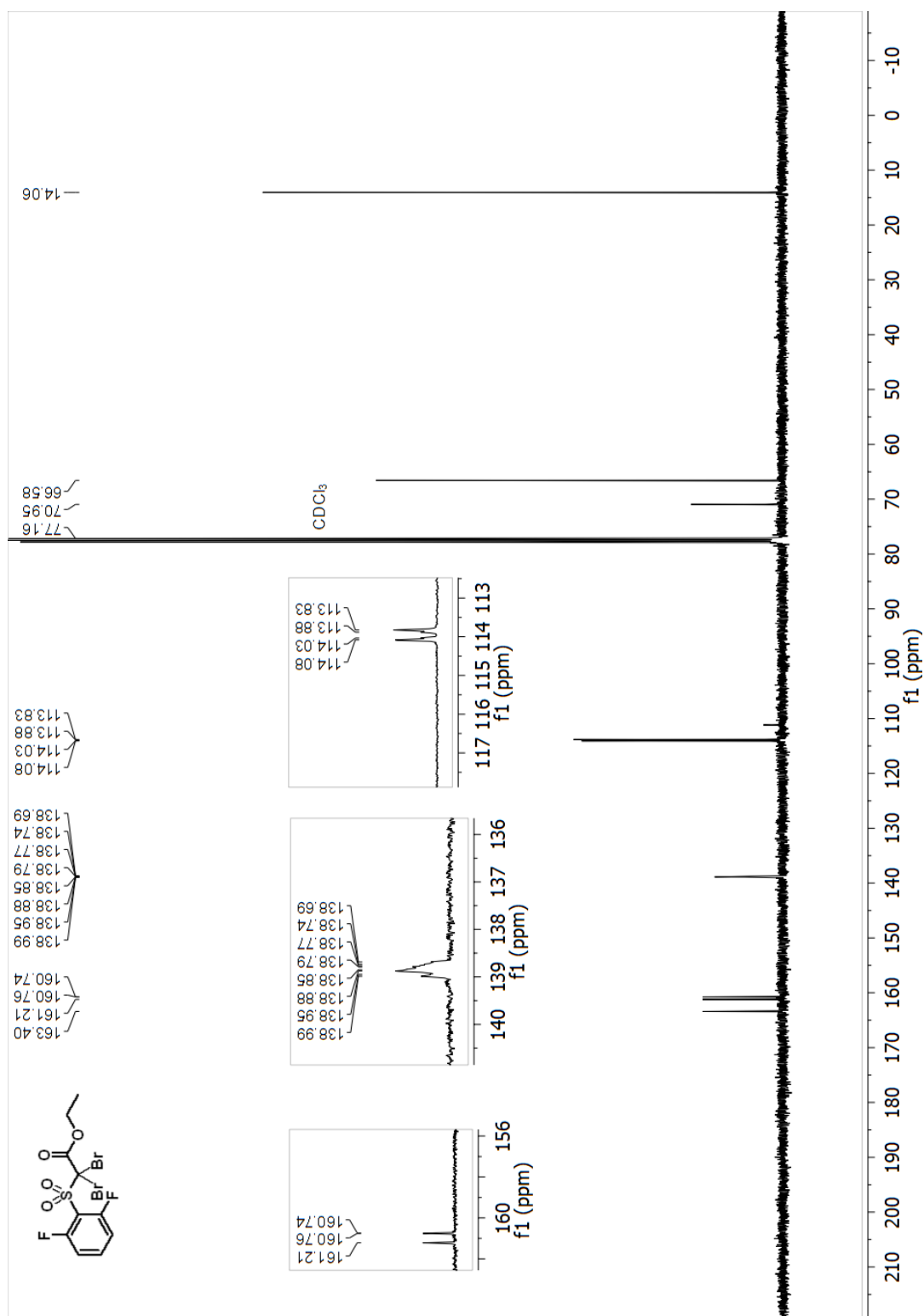
^1H NMR (400 MHz, CDCl_3) spectrum of 1b Ethyl 2,2-dibromo-2-((2,6-difluorophenyl)sulfonyl)acetate



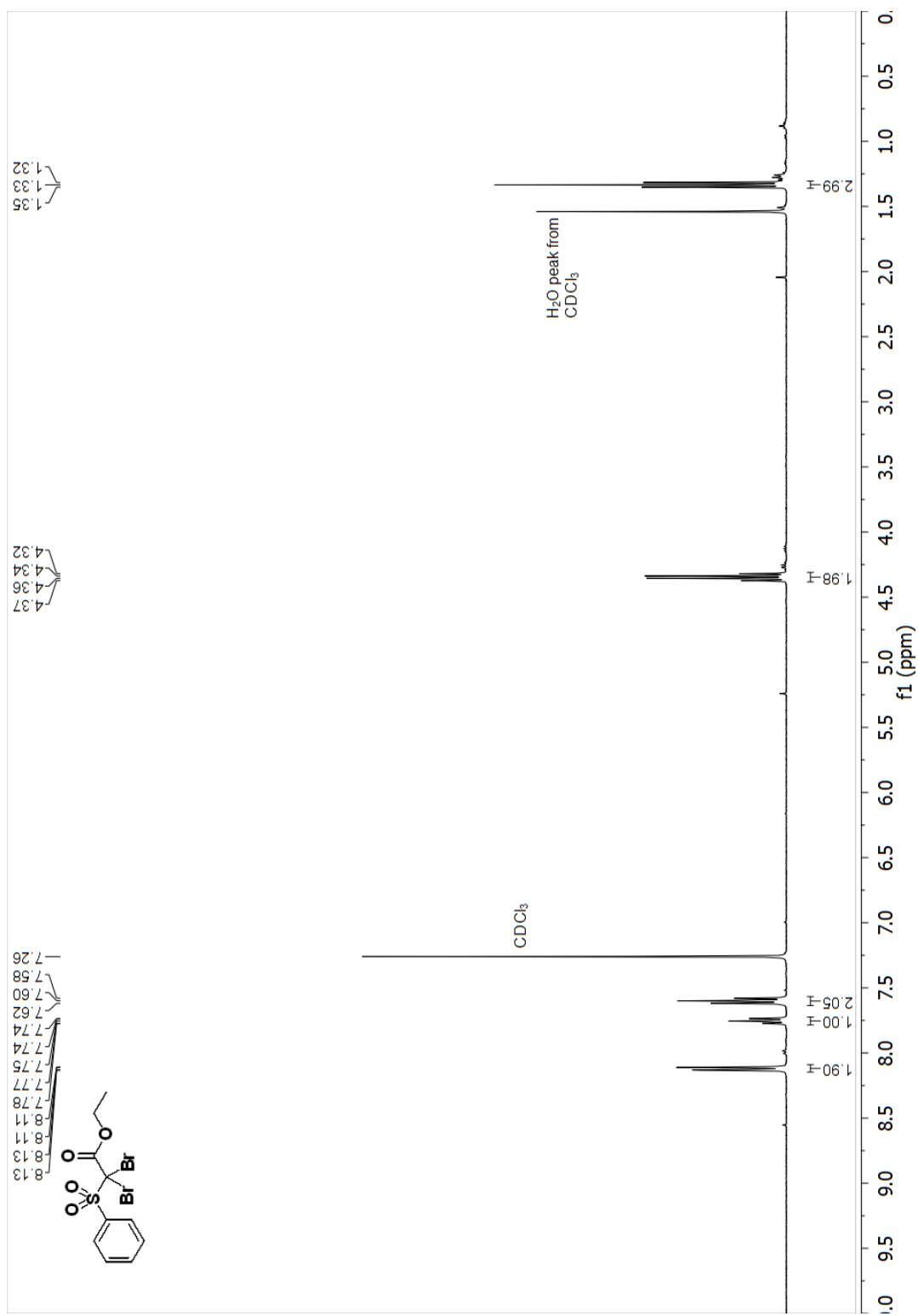
^{19}F NMR (376 MHz, CDCl_3) spectrum of 1b Ethyl 2,2-dibromo-2-((2,6-difluorophenyl)sulfonyl)acetate



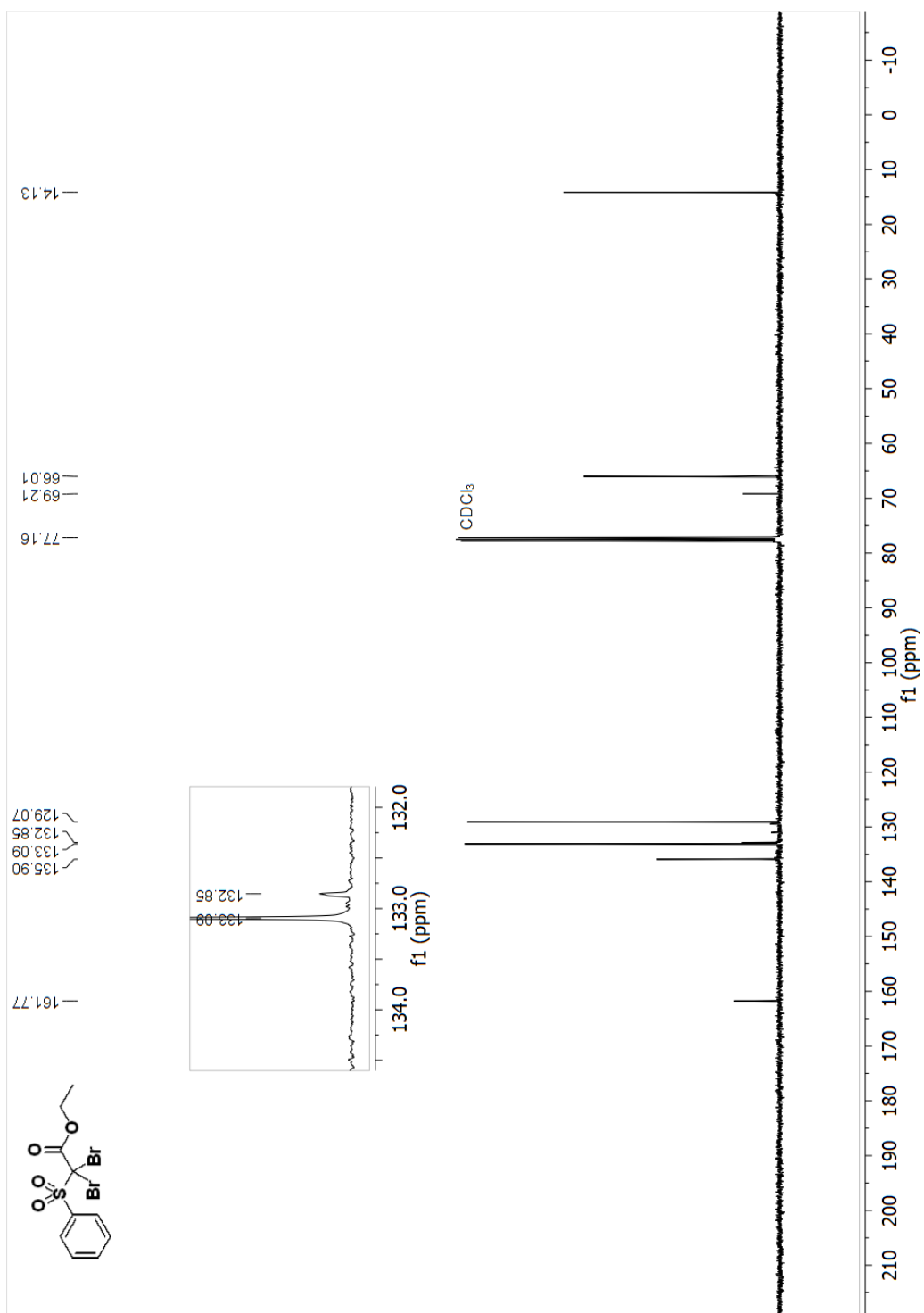
^{13}C NMR (101 MHz, CDCl_3) spectrum of 1b Ethyl 2,2-dibromo-2-((2,6-difluorophenyl)sulfonyl)acetate



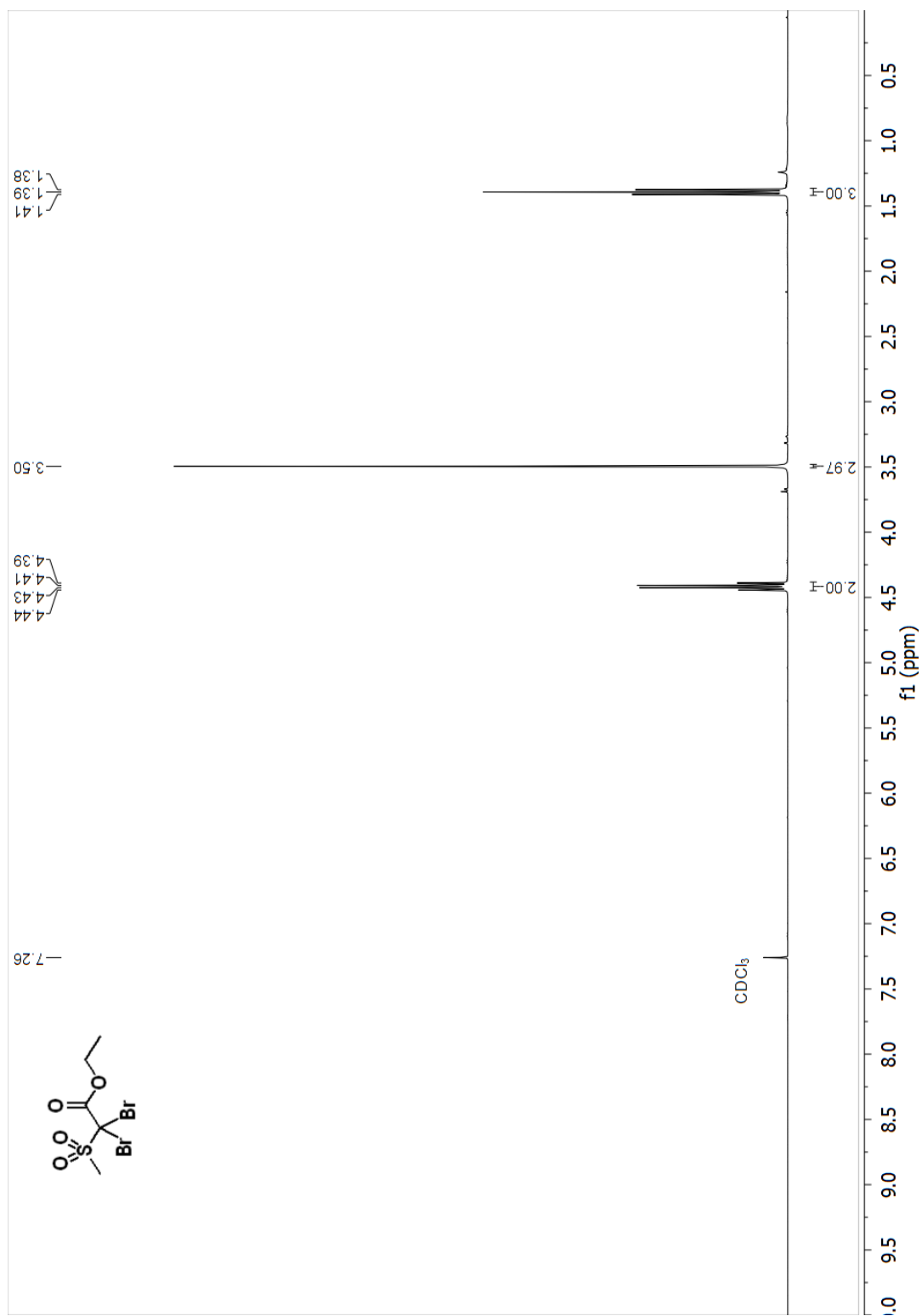
^1H NMR (400 MHz, CDCl_3) spectrum of 2b Ethyl 2,2-dibromo-2-(phenylsulfonyl)acetate



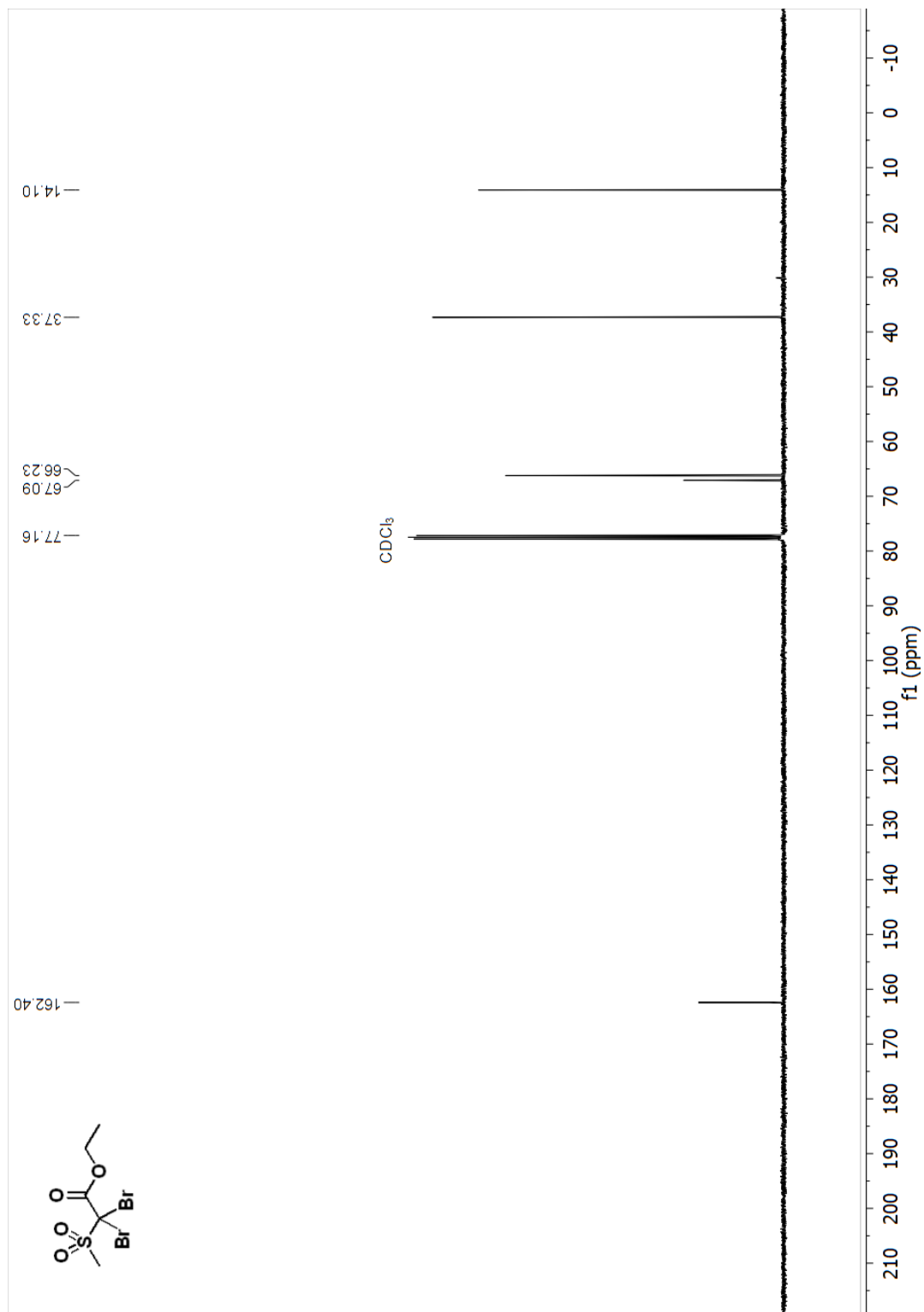
¹³C NMR (101 MHz, CDCl₃) spectrum of 2b Ethyl 2,2-dibromo-2-(phenylsulfonyl)acetate



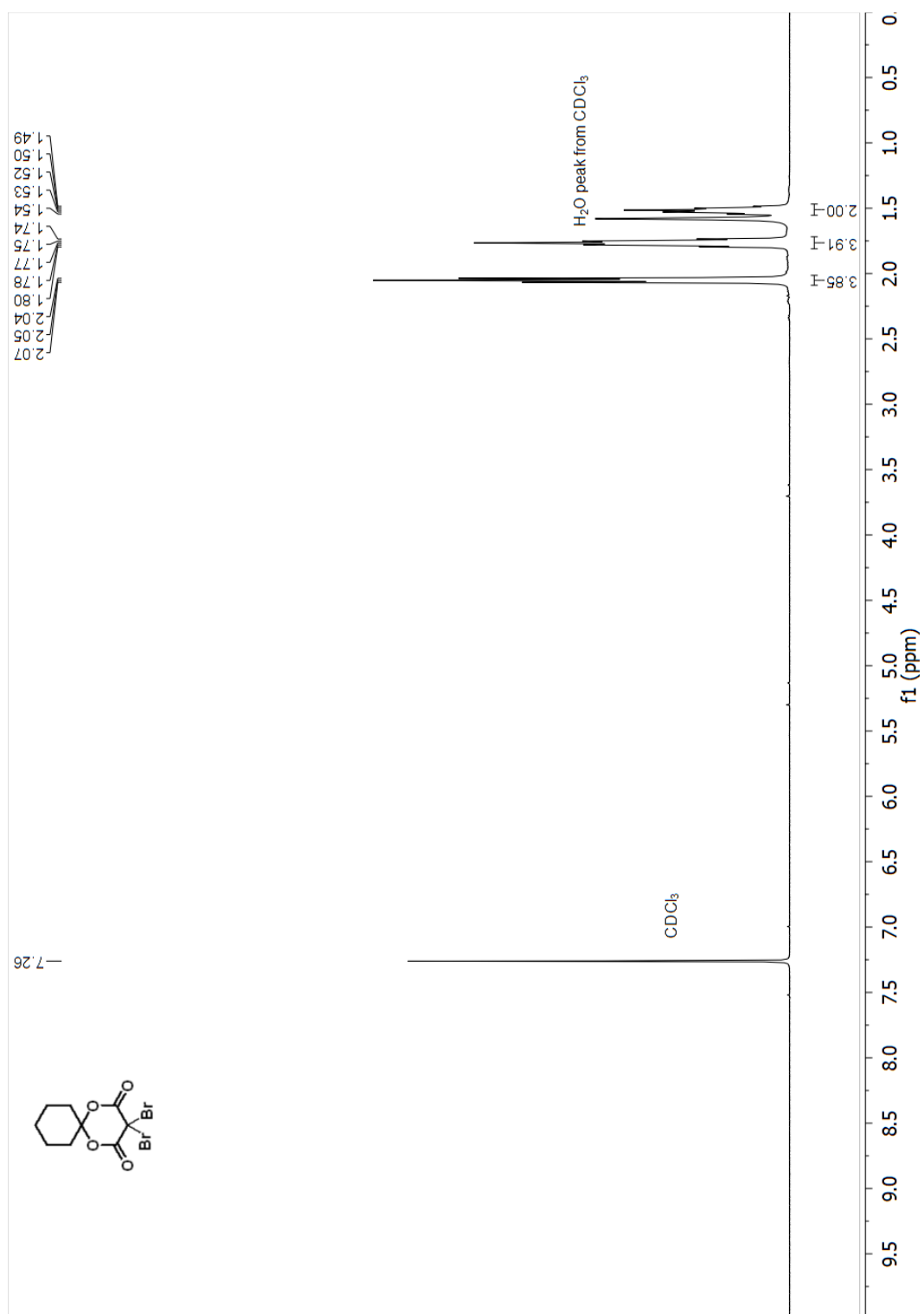
^1H NMR (400 MHz, CDCl_3) spectrum of 3b Ethyl 2,2-dibromo-2-(methylsulfonyl)acetate



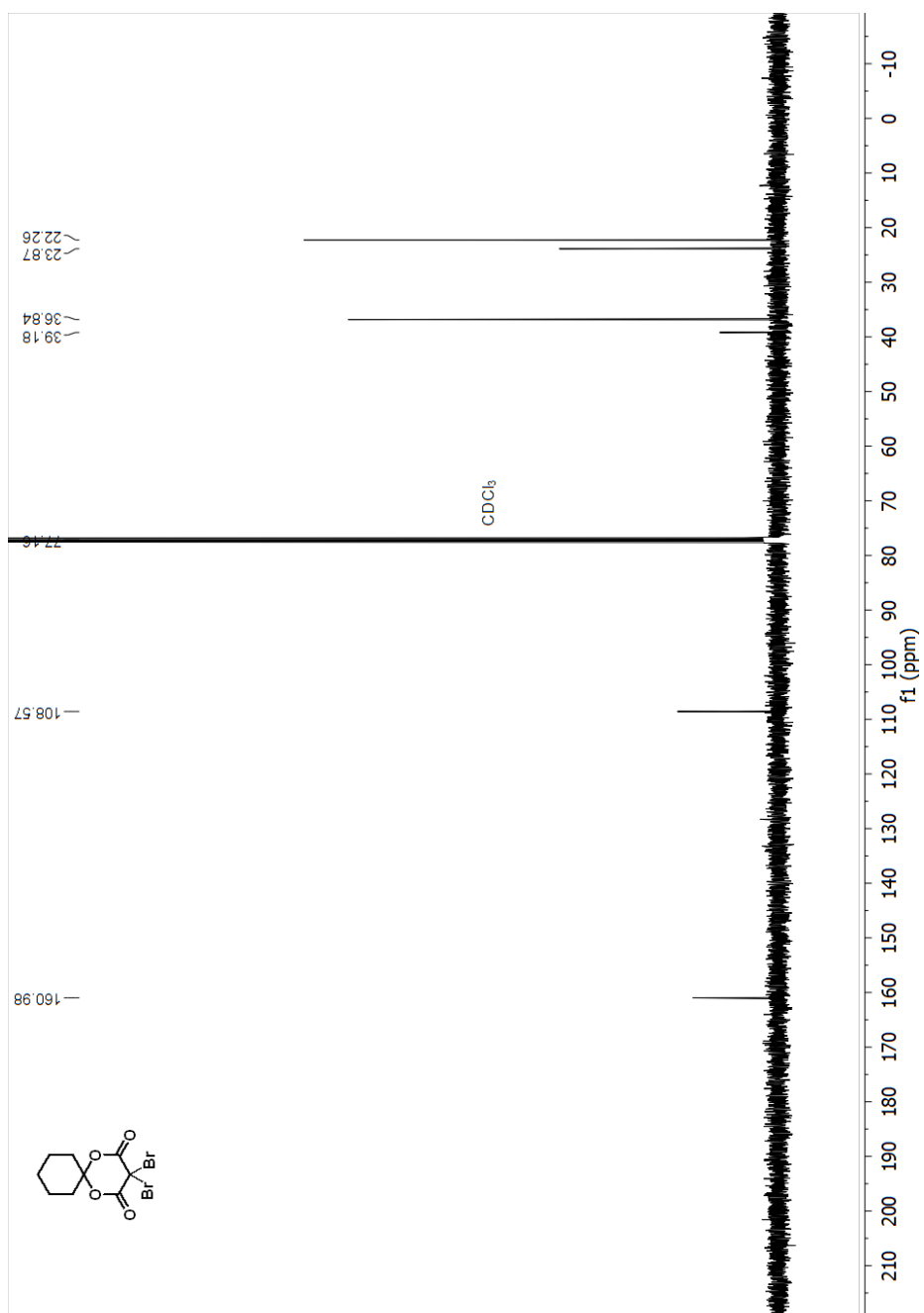
¹³C NMR (101 MHz, CDCl₃) spectrum of 3b Ethyl 2,2-dibromo-2-(methylsulfonyl)acetate



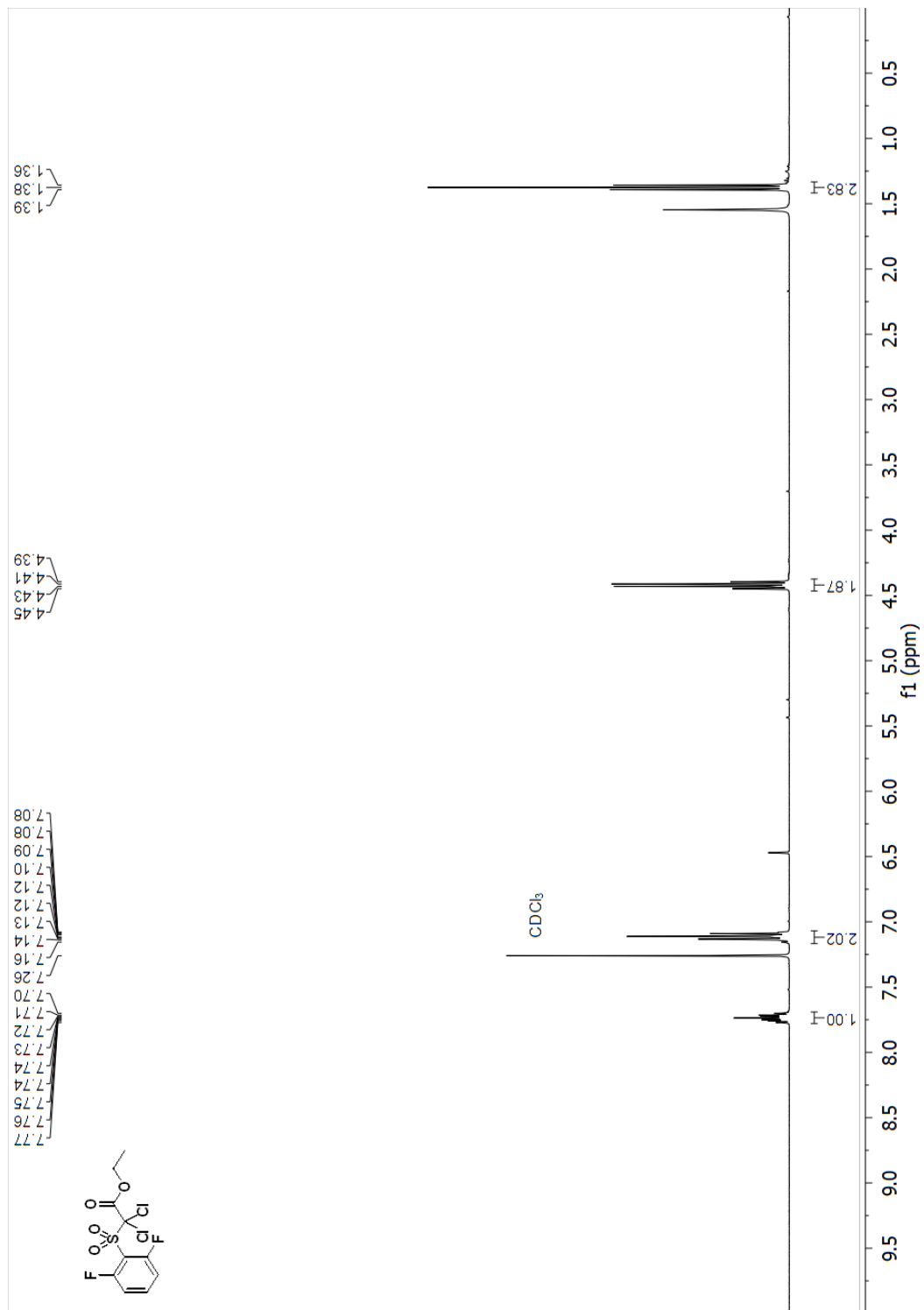
^1H NMR (400 MHz, CDCl_3) spectrum of 6b 3,3-Dibromo-1,5-dioxaspiro[5.5]undecane-2,4-dione



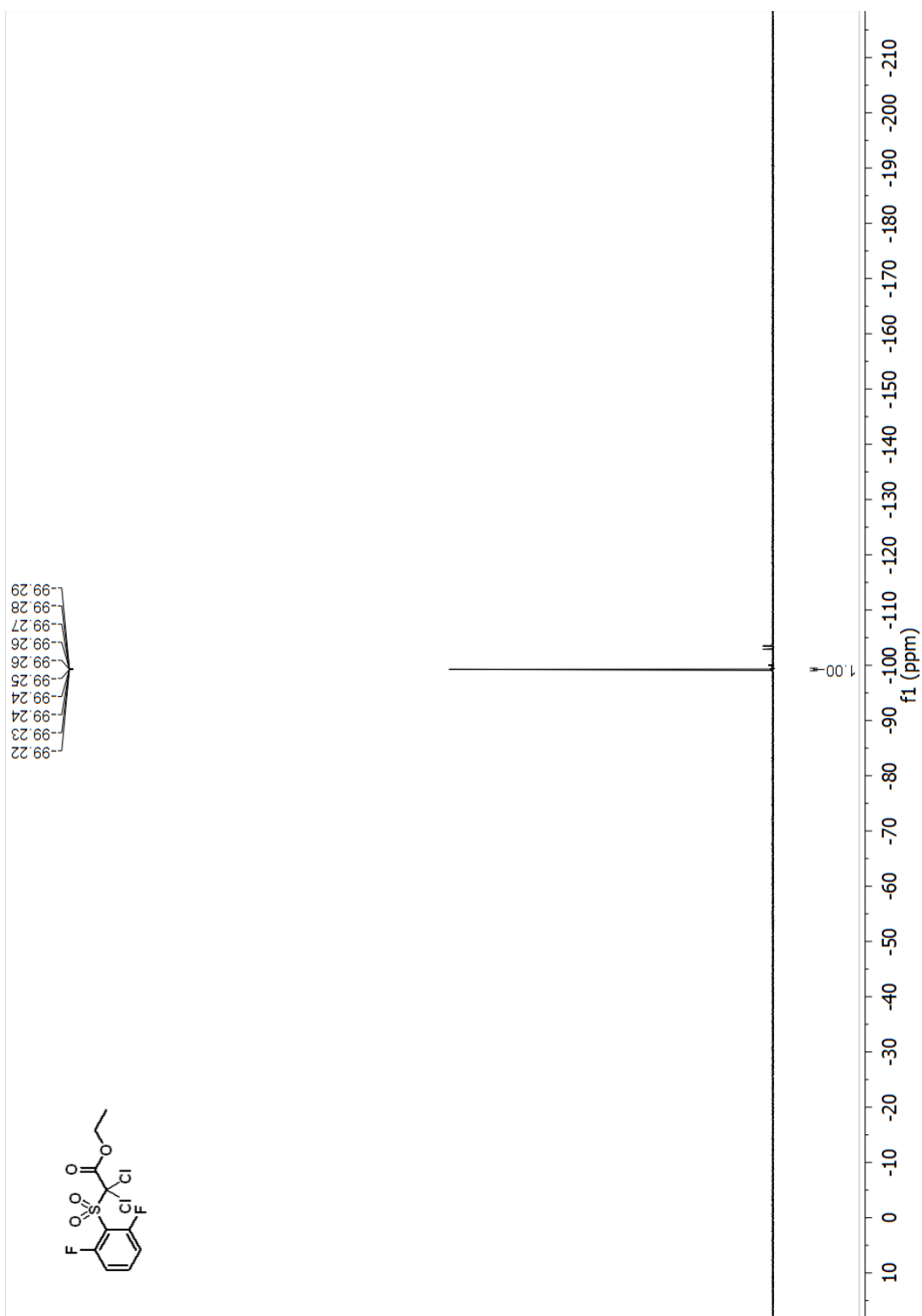
^{13}C NMR (101 MHz, CDCl_3) spectrum of 6b 3,3-Dibromo-1,5-dioxaspiro[5.5]undecane-2,4-dione



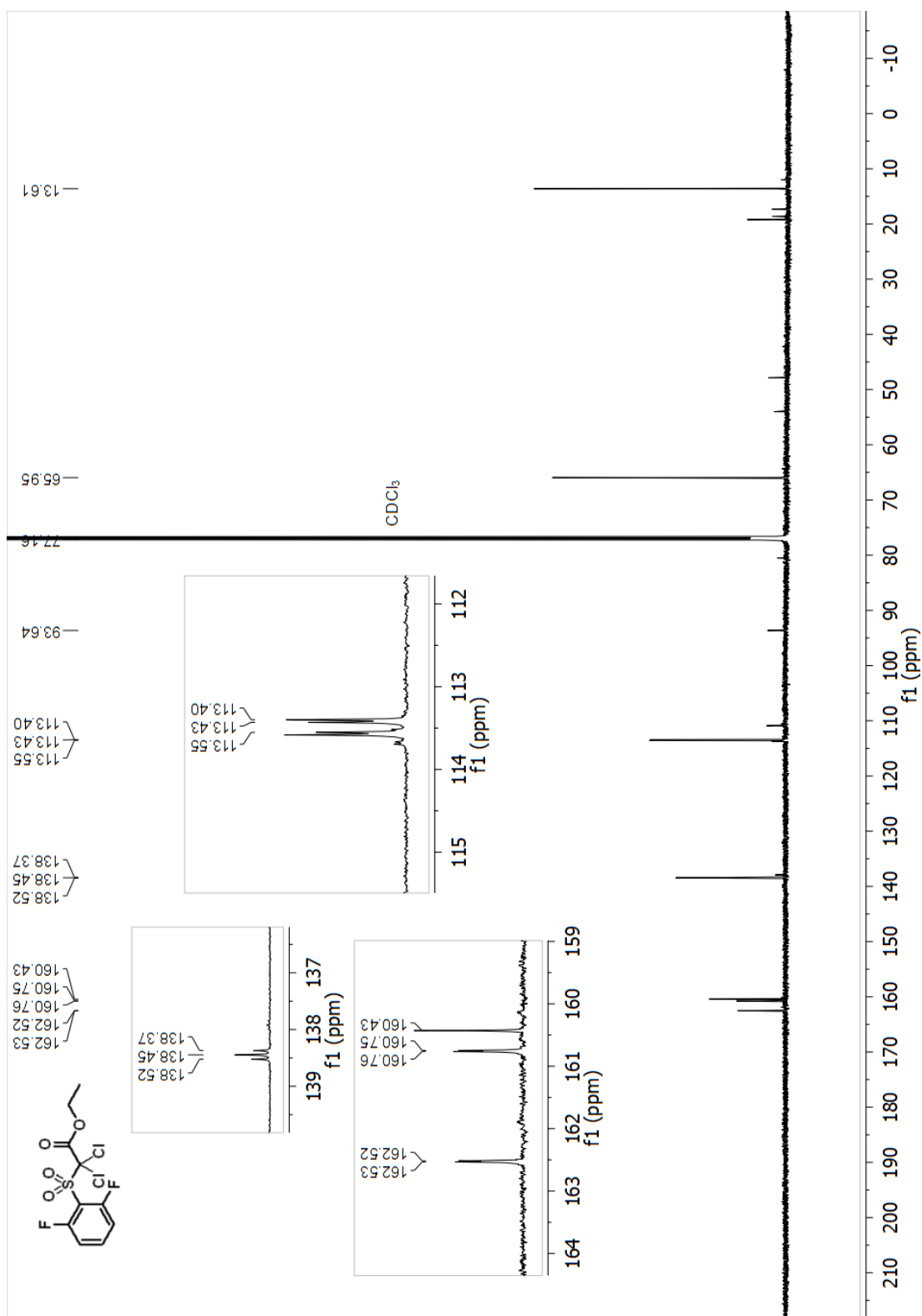
¹H NMR (400 MHz, CDCl₃) spectrum of 14b Ethyl 2,2-dichloro-2-((2,6-difluorophenyl)sulfonyl)acetate



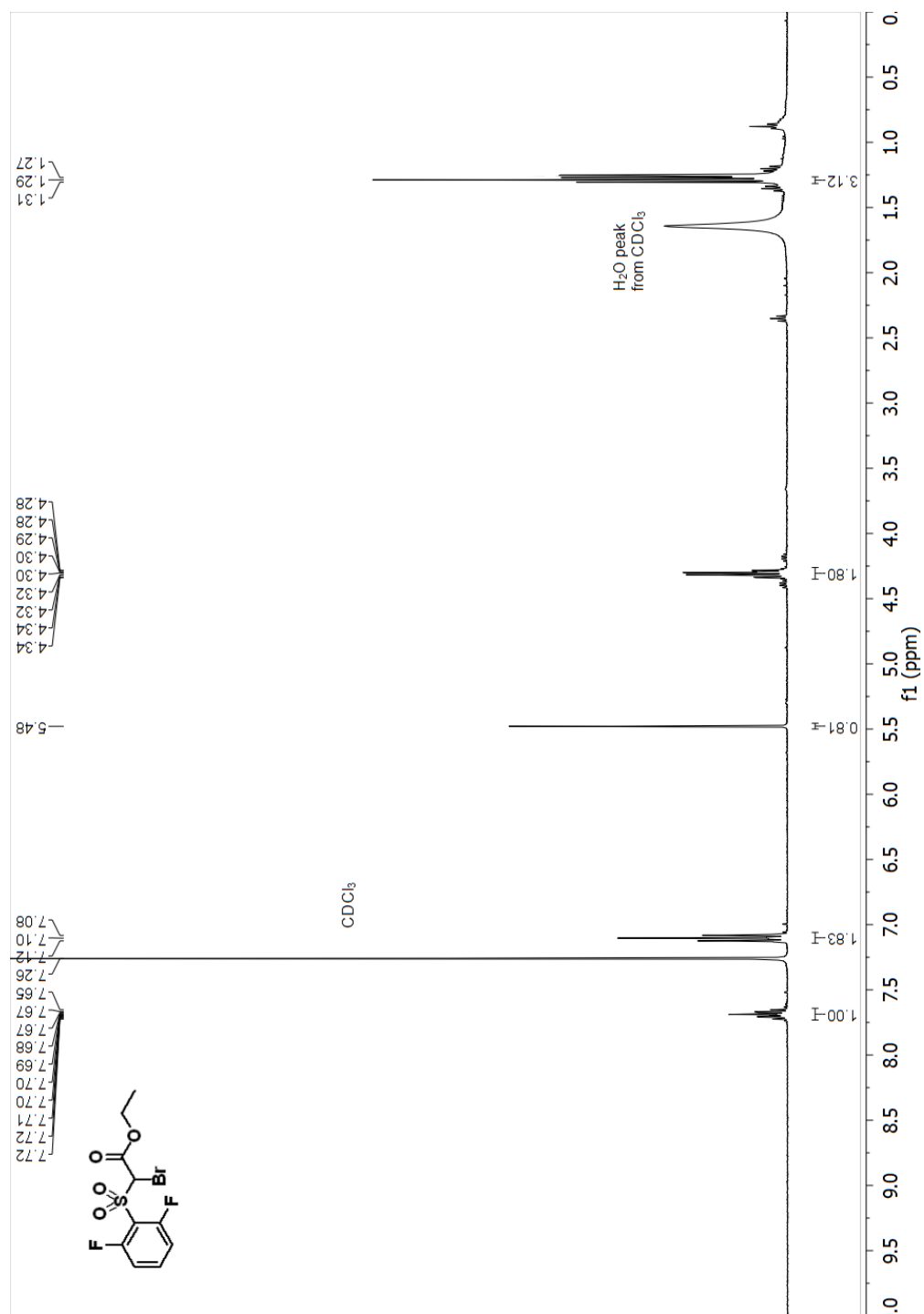
^{19}F NMR (376 MHz, CDCl_3) spectrum of 14b Ethyl 2,2-dichloro-2-((2,6-difluorophenyl)sulfonyl)acetate



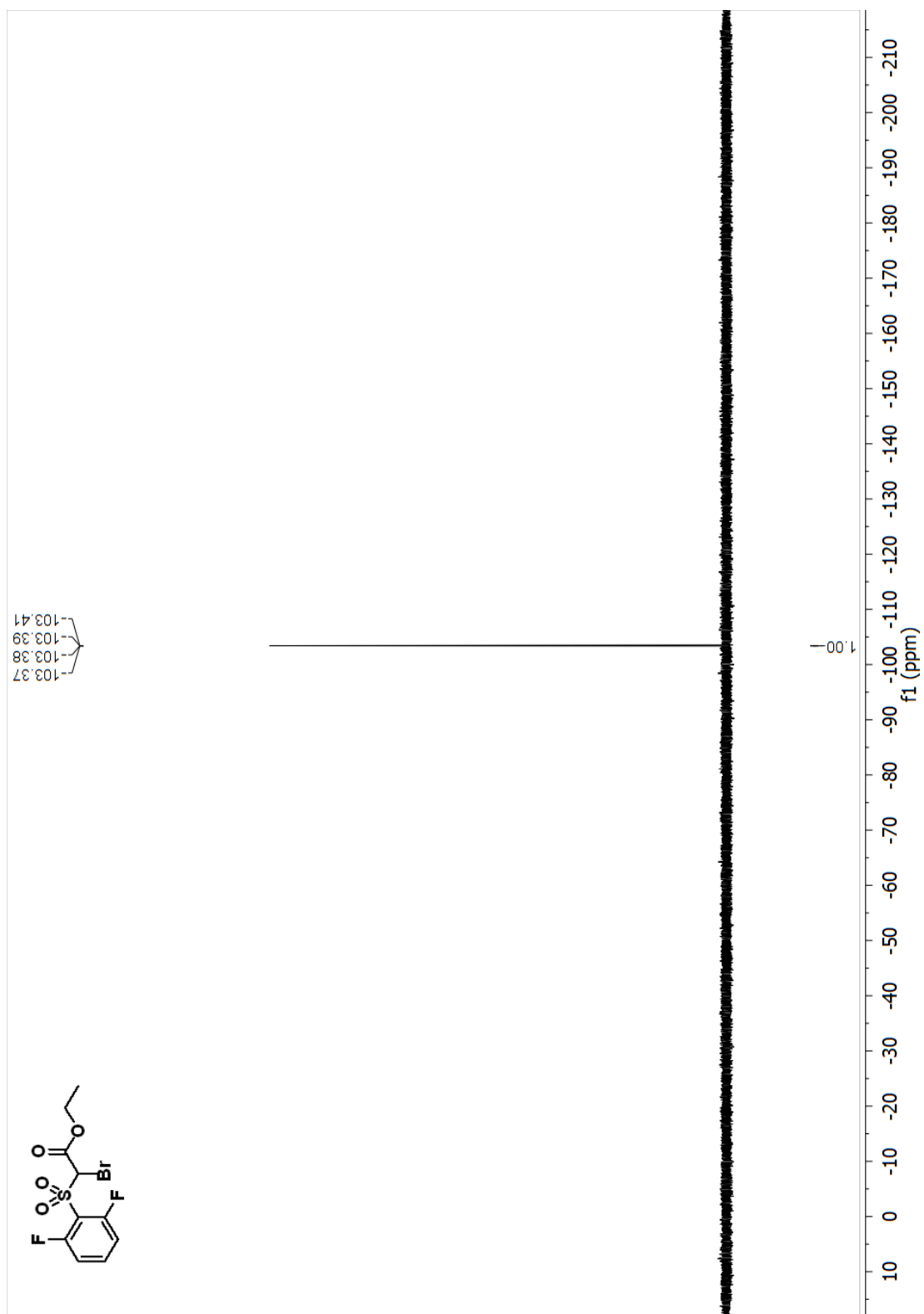
^{13}C NMR (151 MHz, CDCl_3) spectrum of 14b Ethyl 2,2-dichloro-2-((2,6-difluorophenyl)sulfonyl)acetate



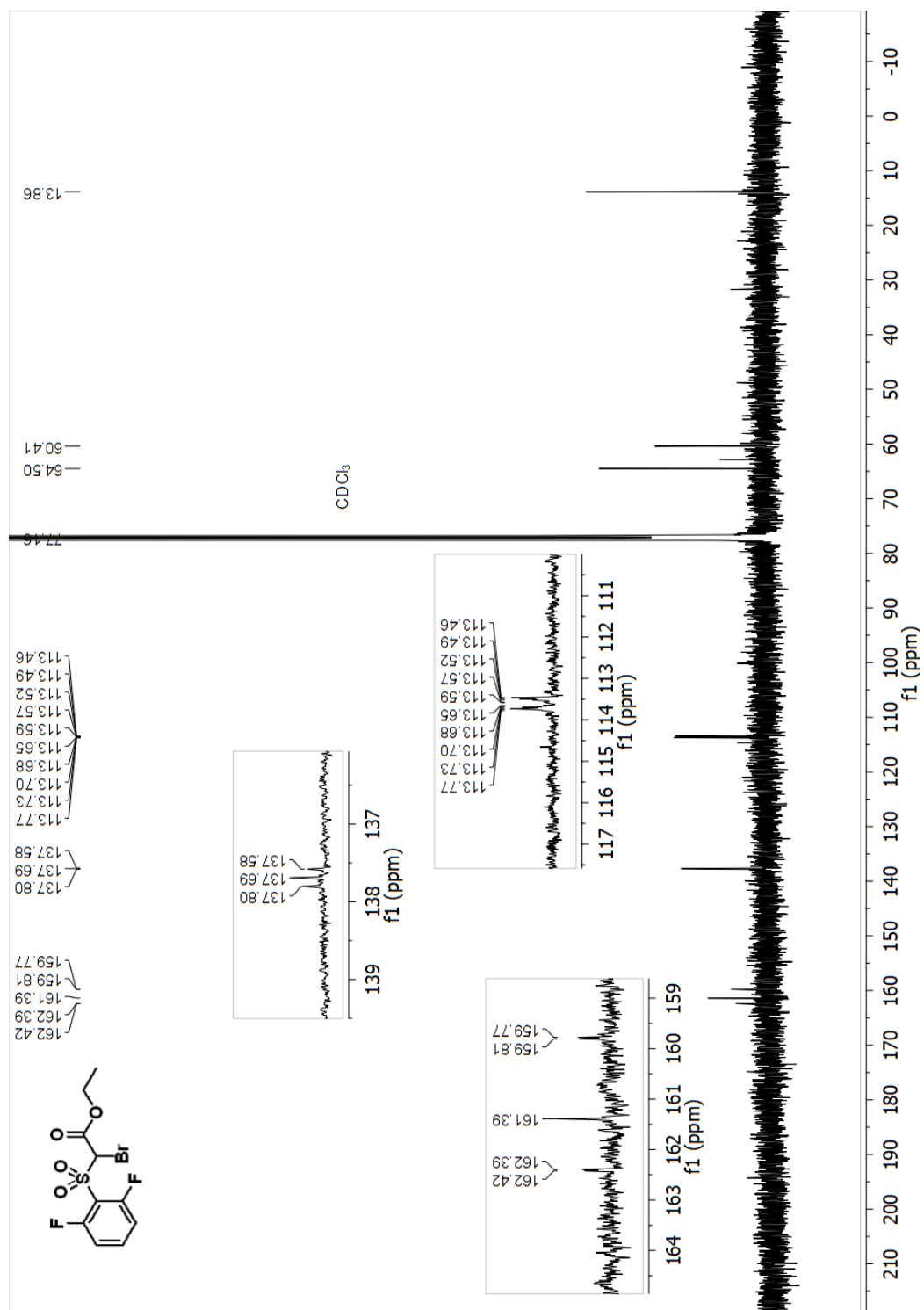
^1H NMR (400 MHz, CDCl_3) spectrum of 1c ethyl 2-bromo-2-((2,6-difluorophenyl)sulfonyl)acetate



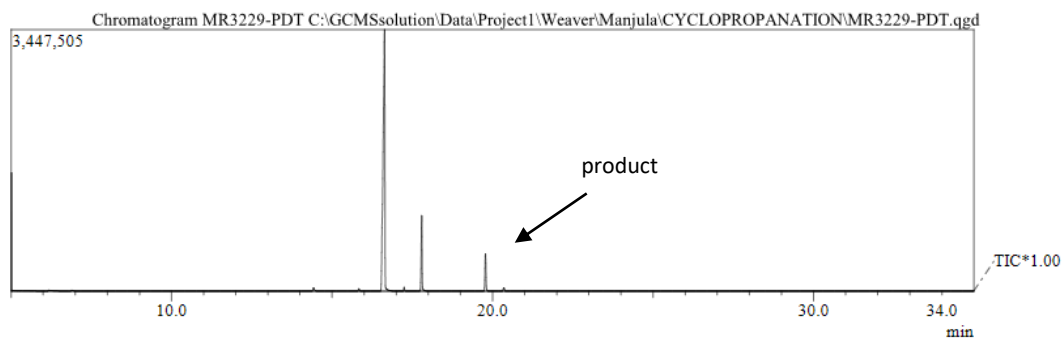
^{19}F NMR (376 MHz, CDCl_3) spectrum of 1c ethyl 2-bromo-2-((2,6-difluorophenyl)sulfonyl)acetate



^{13}C NMR (101 MHz, CDCl_3) spectrum of 1c ethyl 2-bromo-2-((2,6-difluorophenyl)sulfonyl)acetate

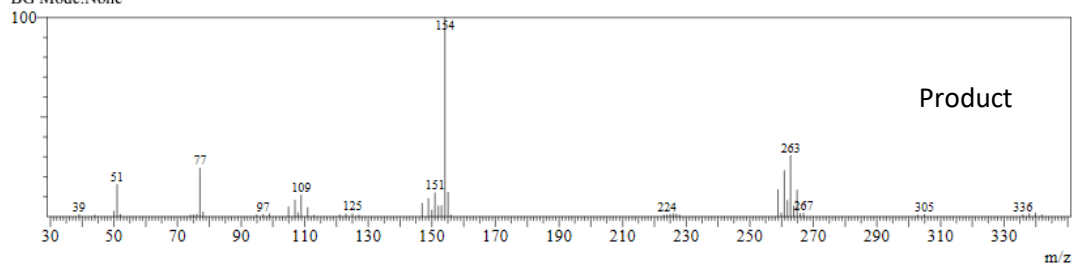


GC and MS of 1c ethyl 2-bromo-2-((2,6-difluorophenyl)sulfonyl)acetate

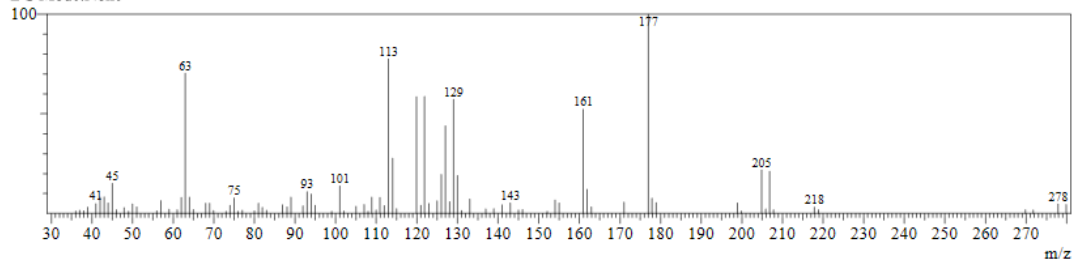


Spectrum

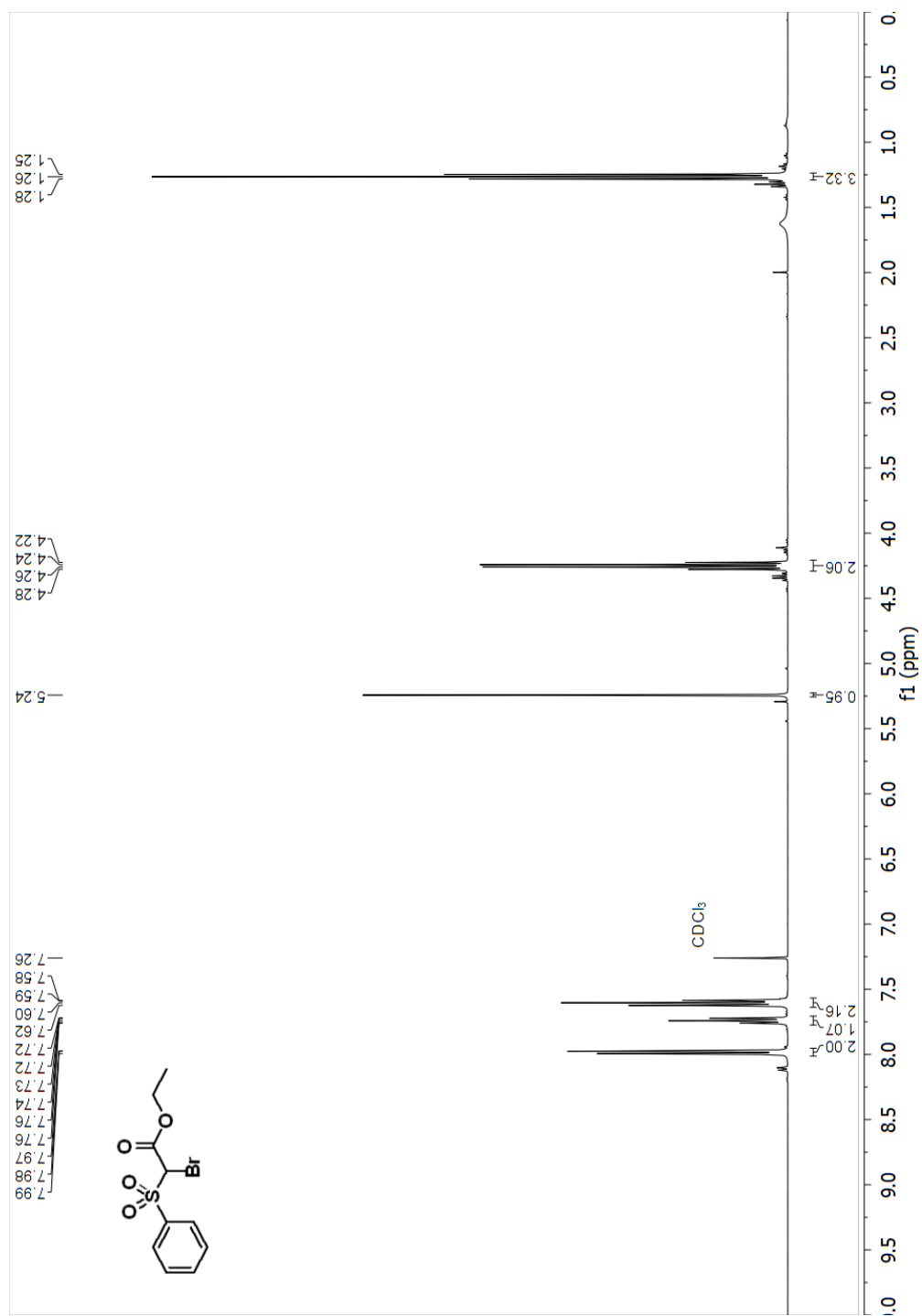
Line#:1 R.Time:19.8(Scan#:1775)
MassPeaks:53
RawMode:Single 19.8(1775) BasePeak:154(138135)
BG Mode:None



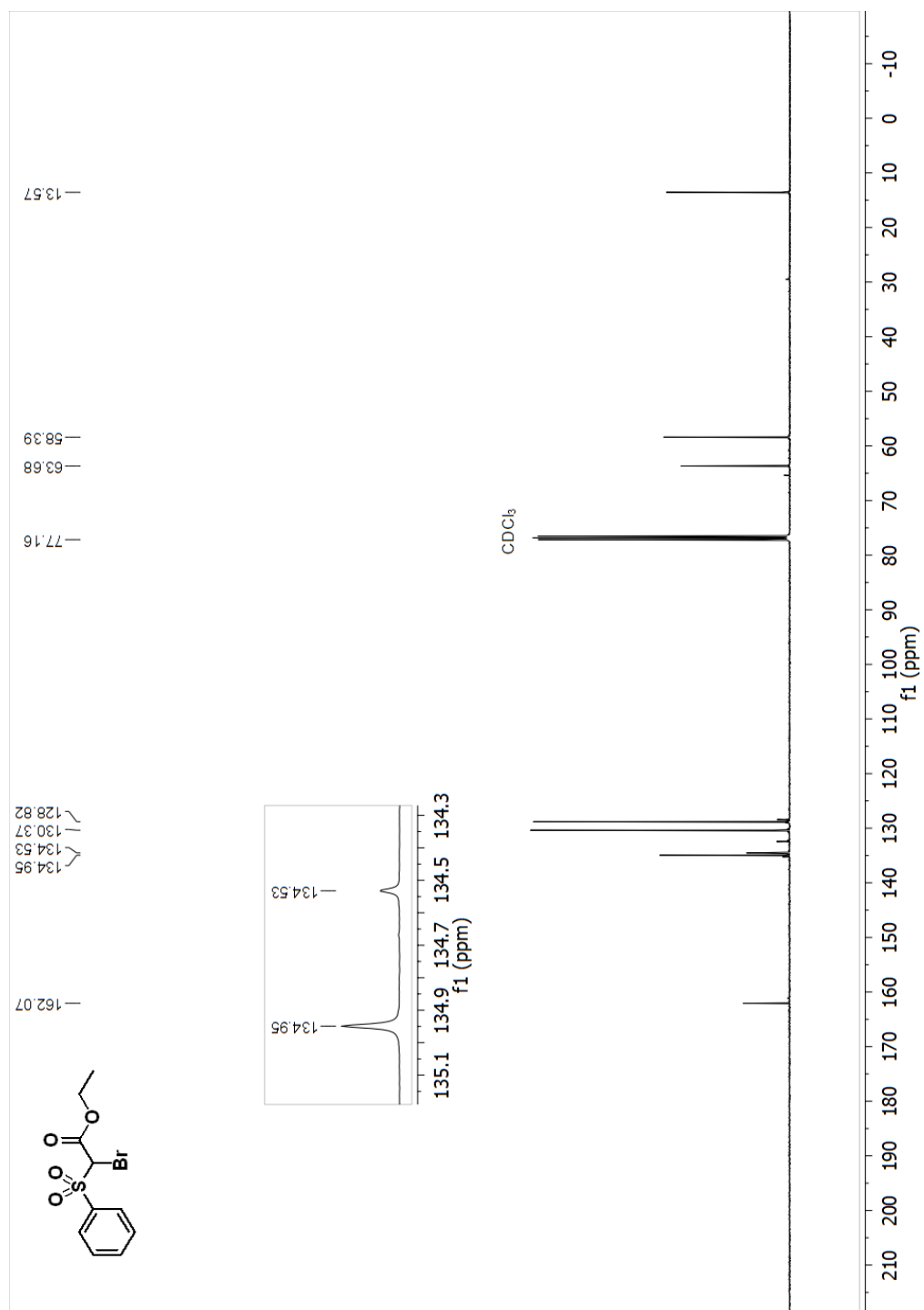
Line#:2 R.Time:17.8(Scan#:1536)
MassPeaks:94
RawMode:Single 17.8(1536) BasePeak:177(102340)
BG Mode:None



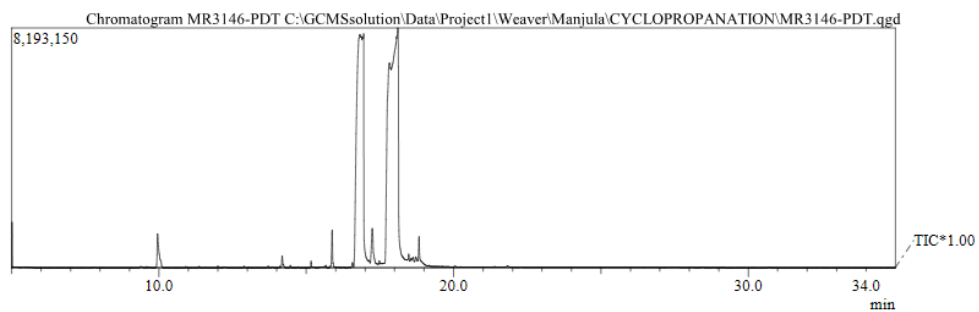
^1H NMR (400 MHz, CDCl_3) spectrum of 2c ethyl 2-bromo-2-(phenylsulfonyl)acetate



^{13}C NMR (101 MHz, CDCl_3) spectrum of 2c ethyl 2-bromo-2-(phenylsulfonyl)acetate



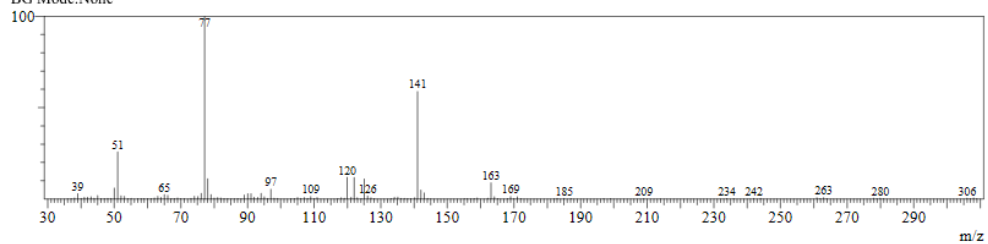
GC and MS of 2c ethyl 2-bromo-2-(phenylsulfonyl)acetate



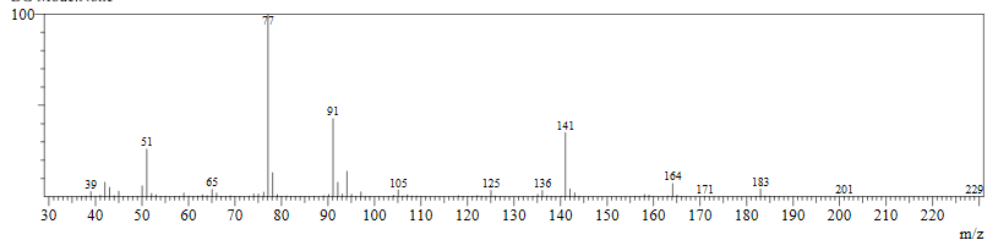
Spectrum

Line#:1 R.Time:17.9(Scan#:1552)
MassPeaks:134
RawMode:Single 17.9(1552) BasePeak:77(2102633)
BG Mode:None

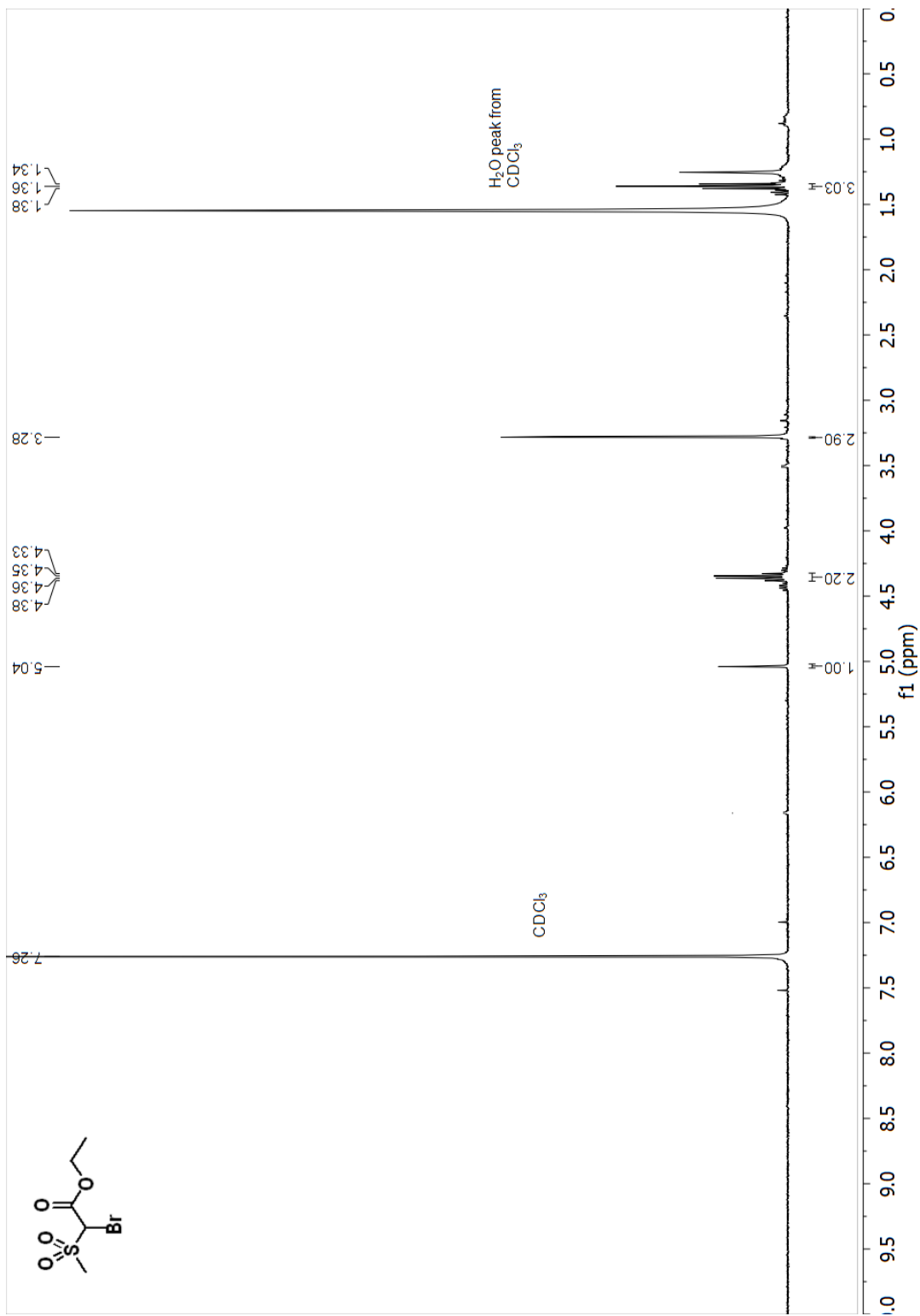
Product



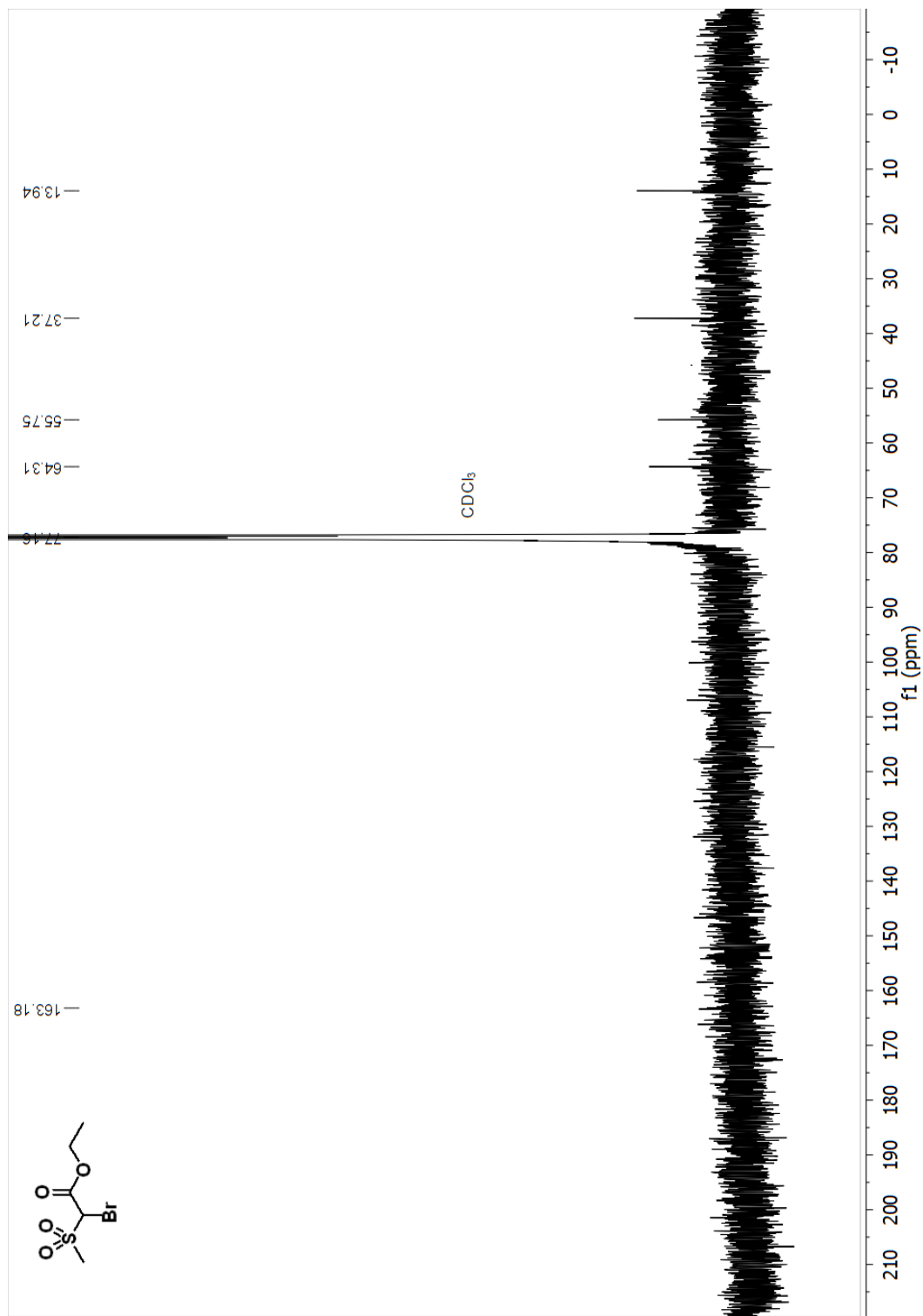
Line#:2 R.Time:16.8(Scan#:1419)
MassPeaks:107
RawMode:Single 16.8(1419) BasePeak:77(2358321)
BG Mode:None



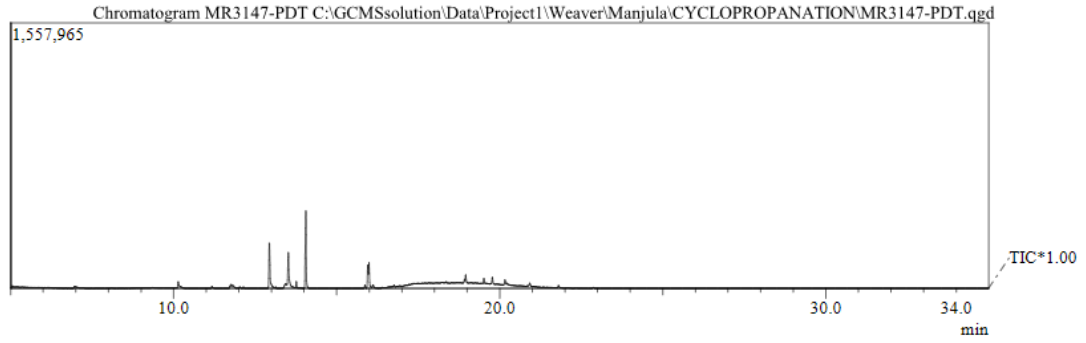
^1H NMR (400 MHz, CDCl_3) spectrum of 3c ethyl 2-bromo-2-(methylsulfonyl)acetate



^{13}C NMR (101 MHz, CDCl_3) spectrum of 3c ethyl 2-bromo-2-(methylsulfonyl)acetate

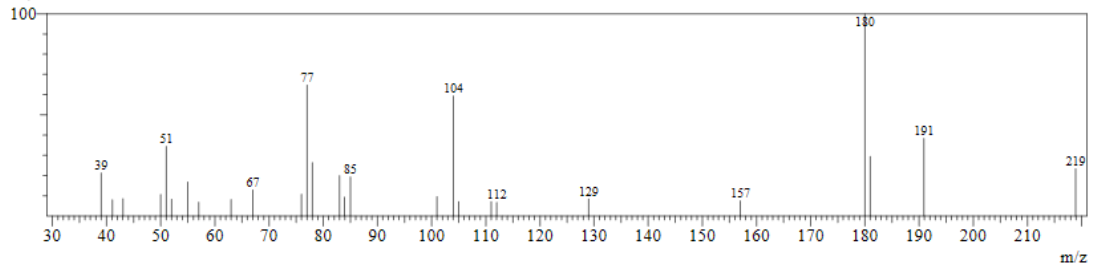


GC and MS of 3c ethyl 2-bromo-2-(methylsulfonyl)acetate

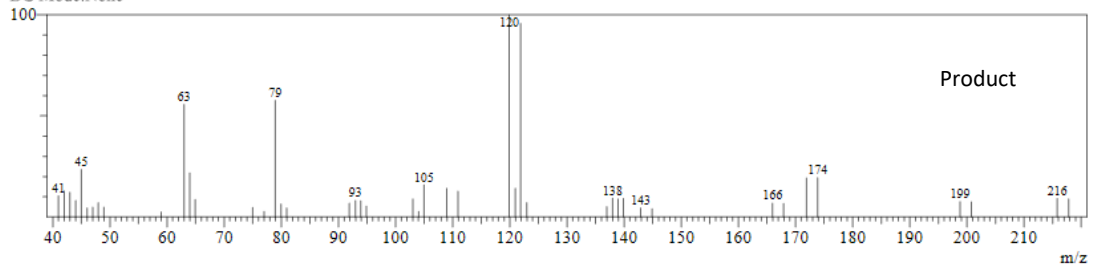


Spectrum

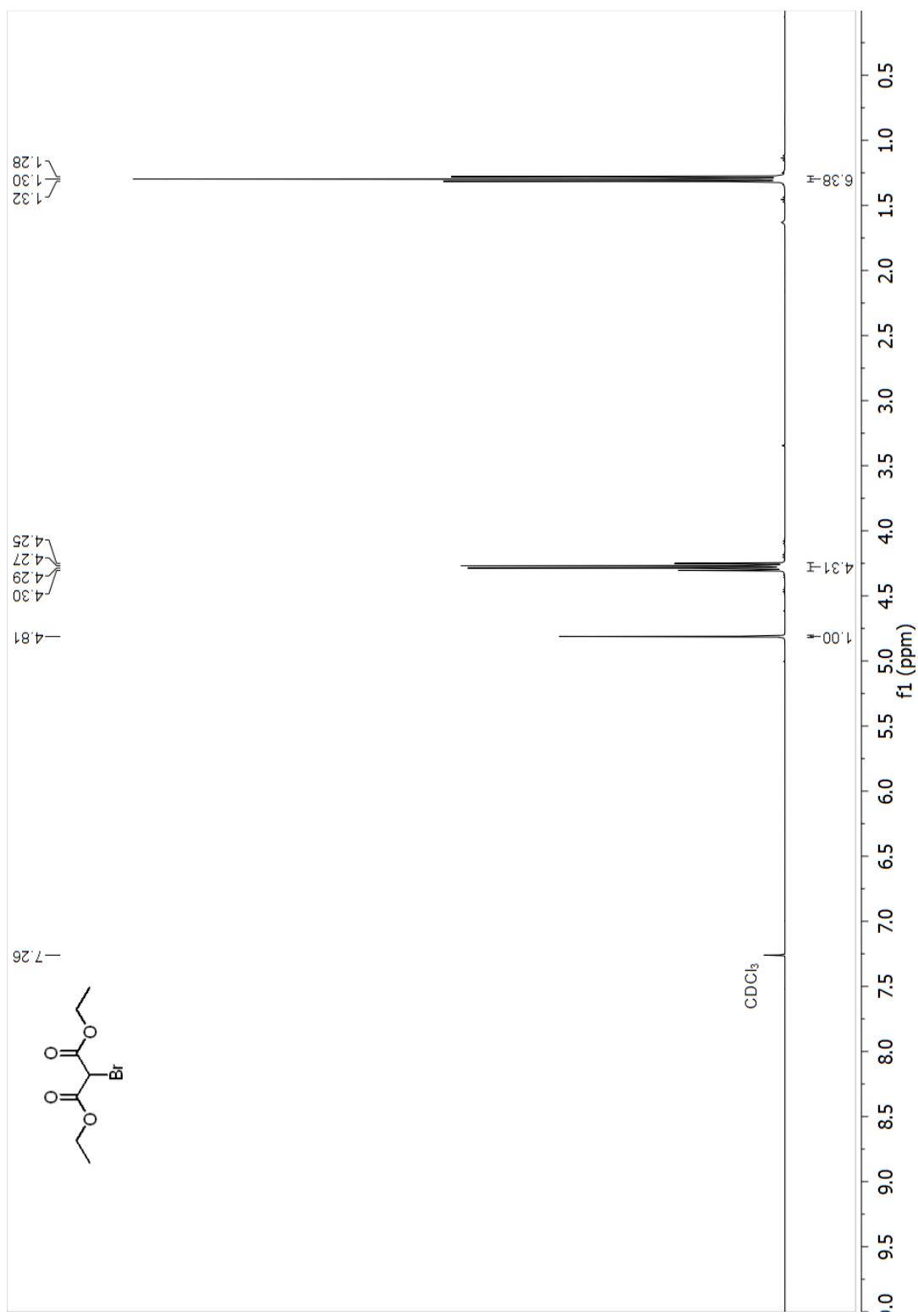
Line#:1 R.Time:16.0(Scan#:1318)
MassPeaks:27
RawMode:Single 16.0(1318) BasePeak:180(14954)
BG Mode:None



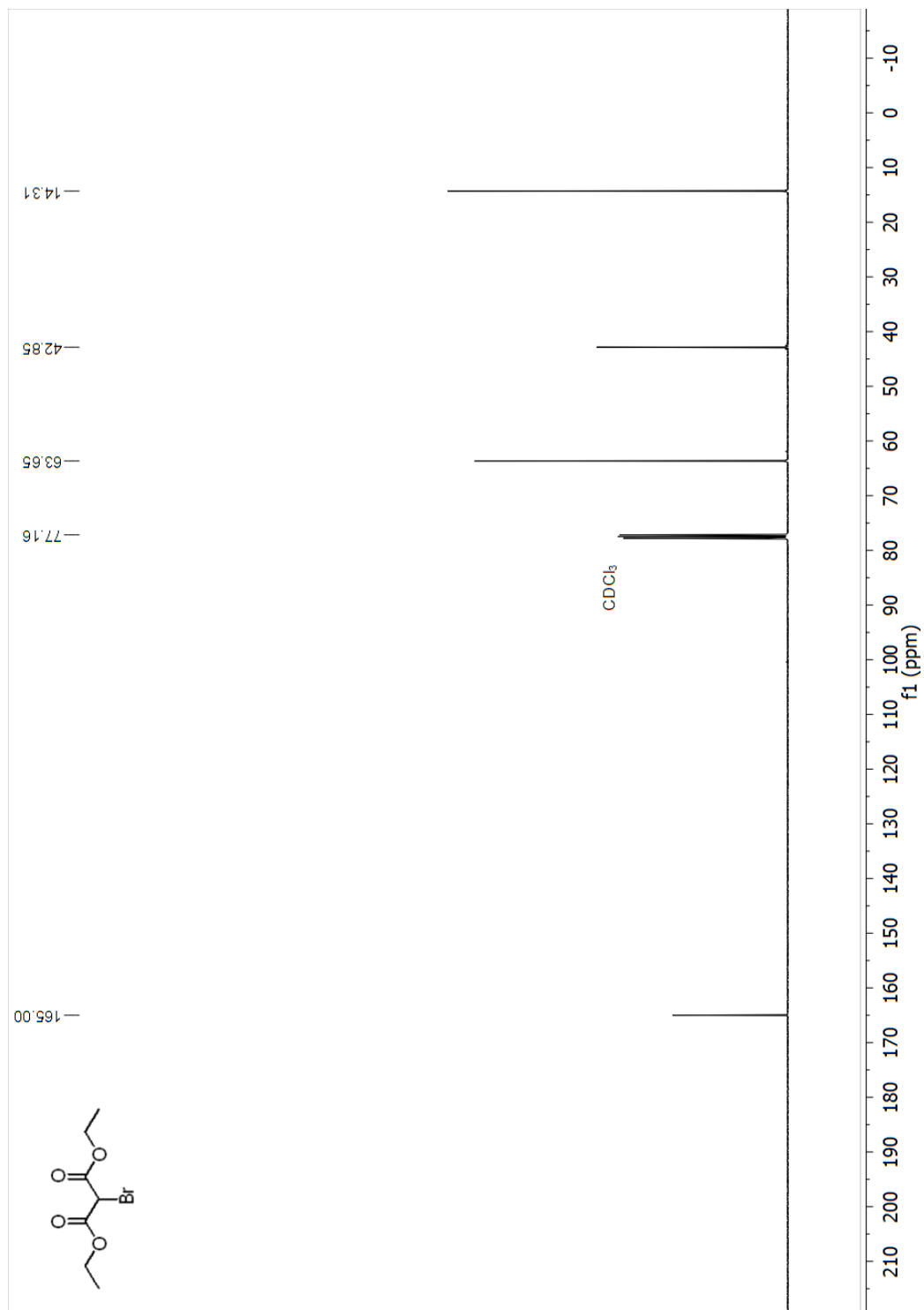
Line#:2 R.Time:14.1(Scan#:1088)
MassPeaks:45
RawMode:Single 14.1(1088) BasePeak:120(46498)
BG Mode:None



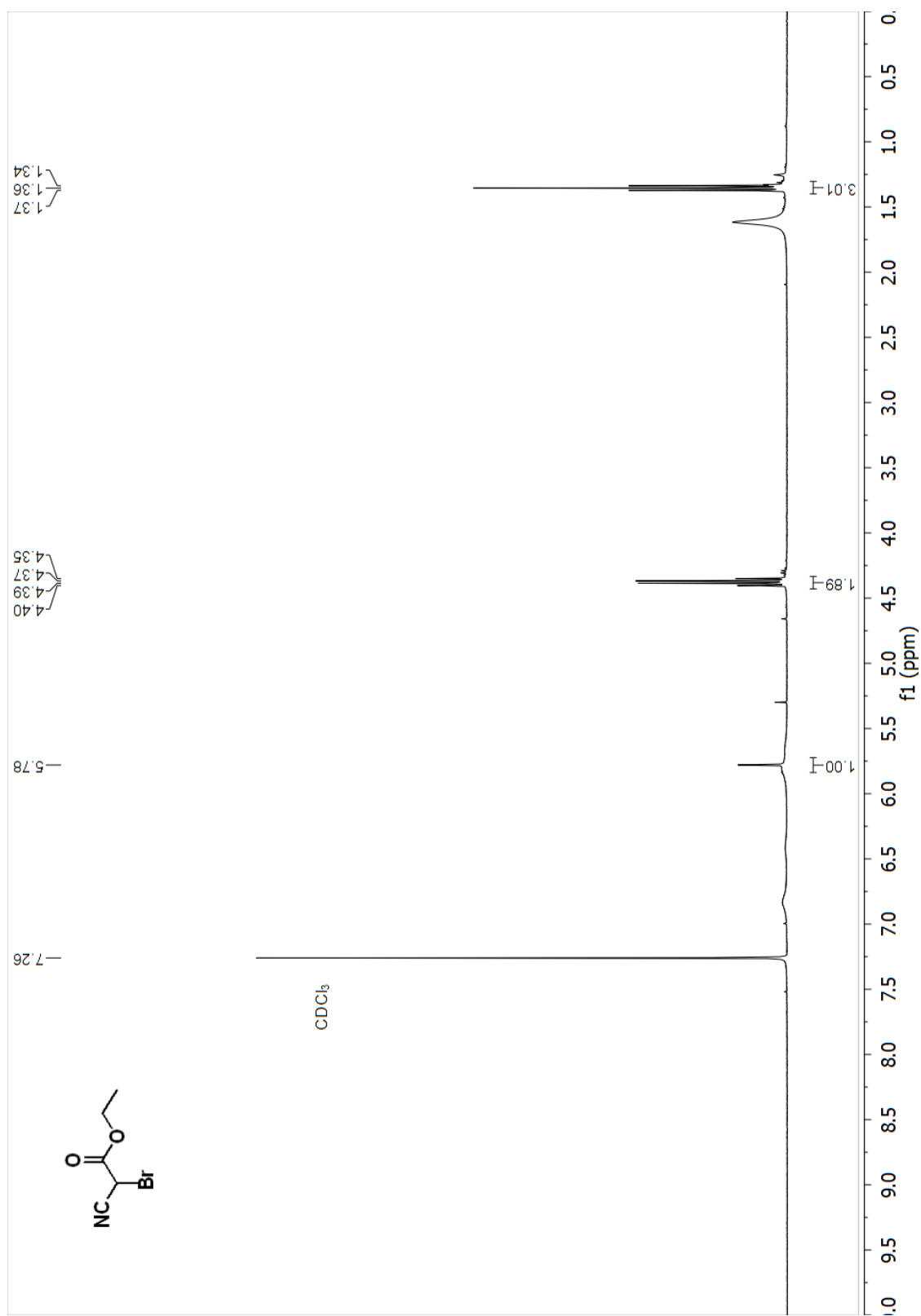
^1H NMR (400 MHz, CDCl_3) spectrum of 4c diethyl 2-bromomalonate



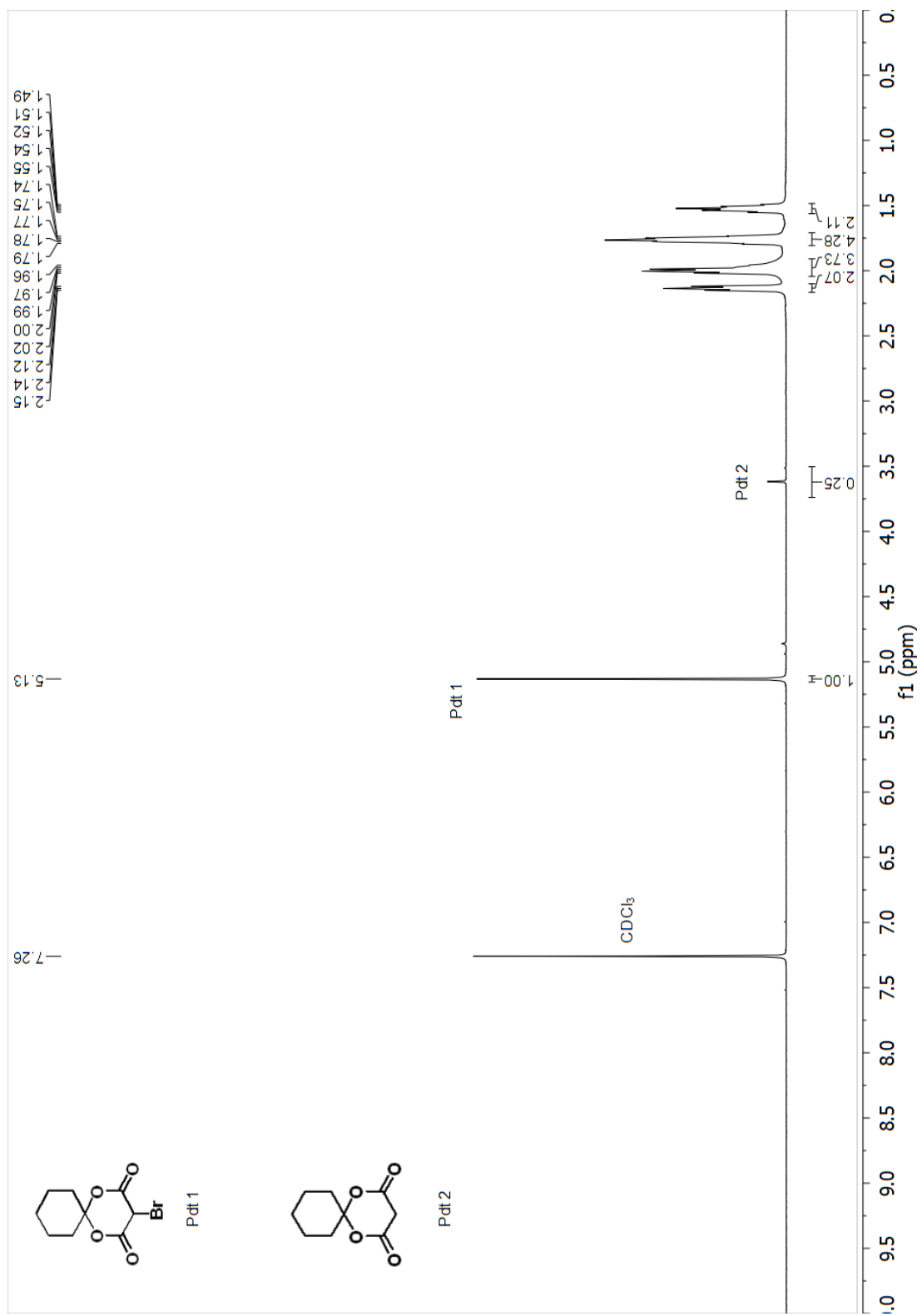
^{13}C NMR (101 MHz, CDCl_3) spectrum of 4c diethyl 2-bromomalonate



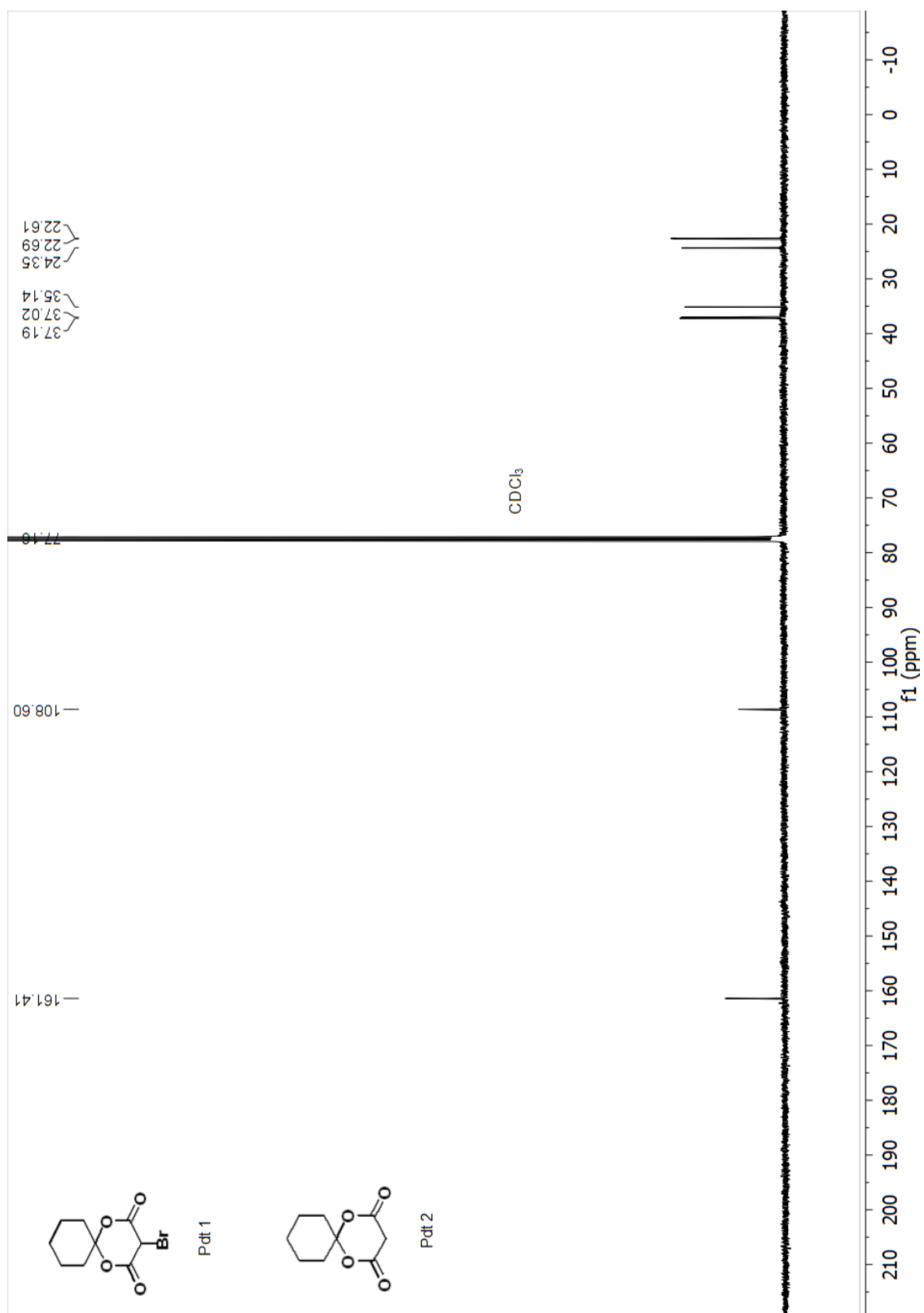
^1H NMR (400 MHz, CDCl_3) spectrum of 5c ethyl 2-bromo-2-cyanoacetate



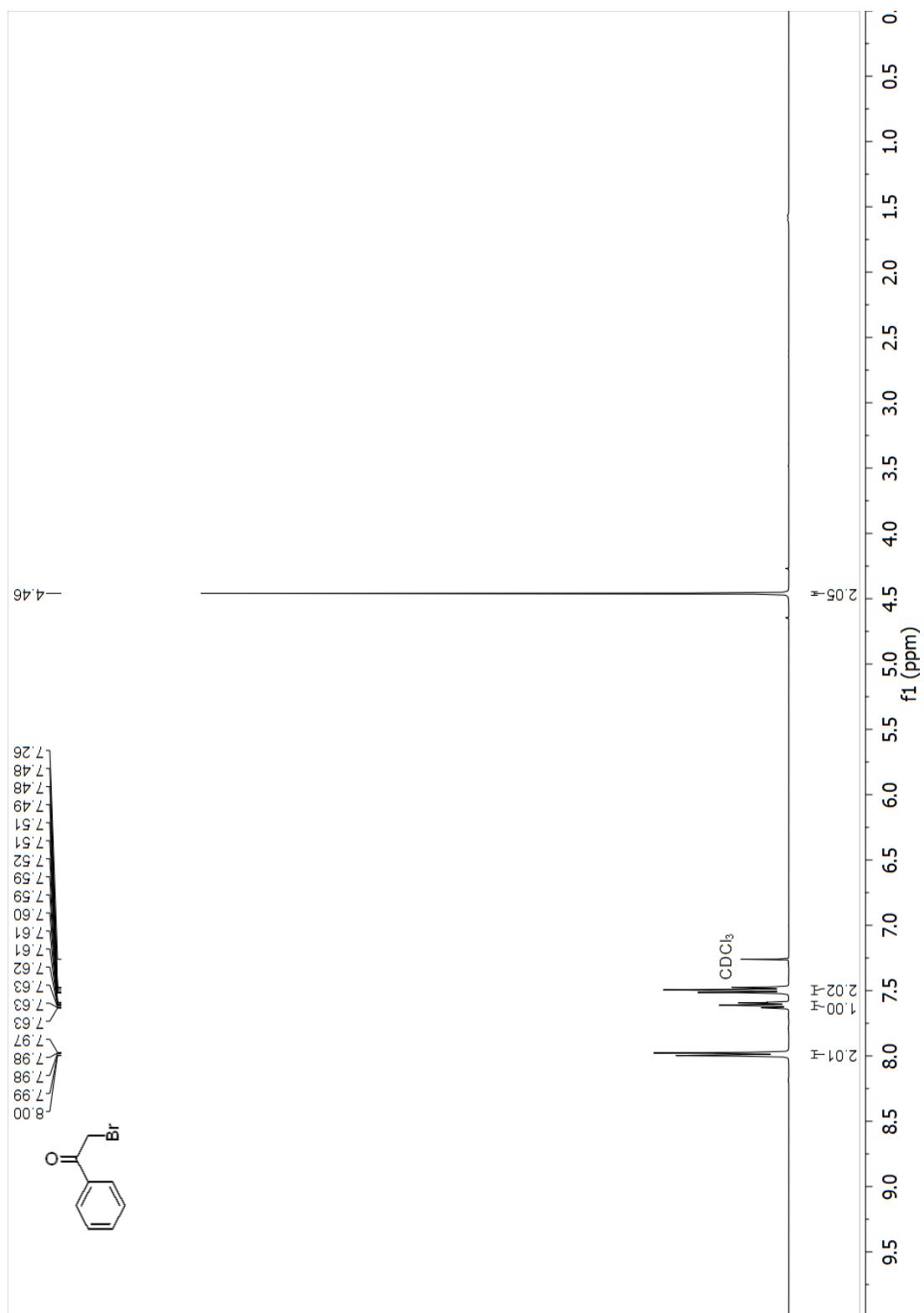
¹H NMR (400 MHz, CDCl₃) spectrum of 6c 3-bromo-1,5-dioxaspiro[5.5]undecane-2,4-dione



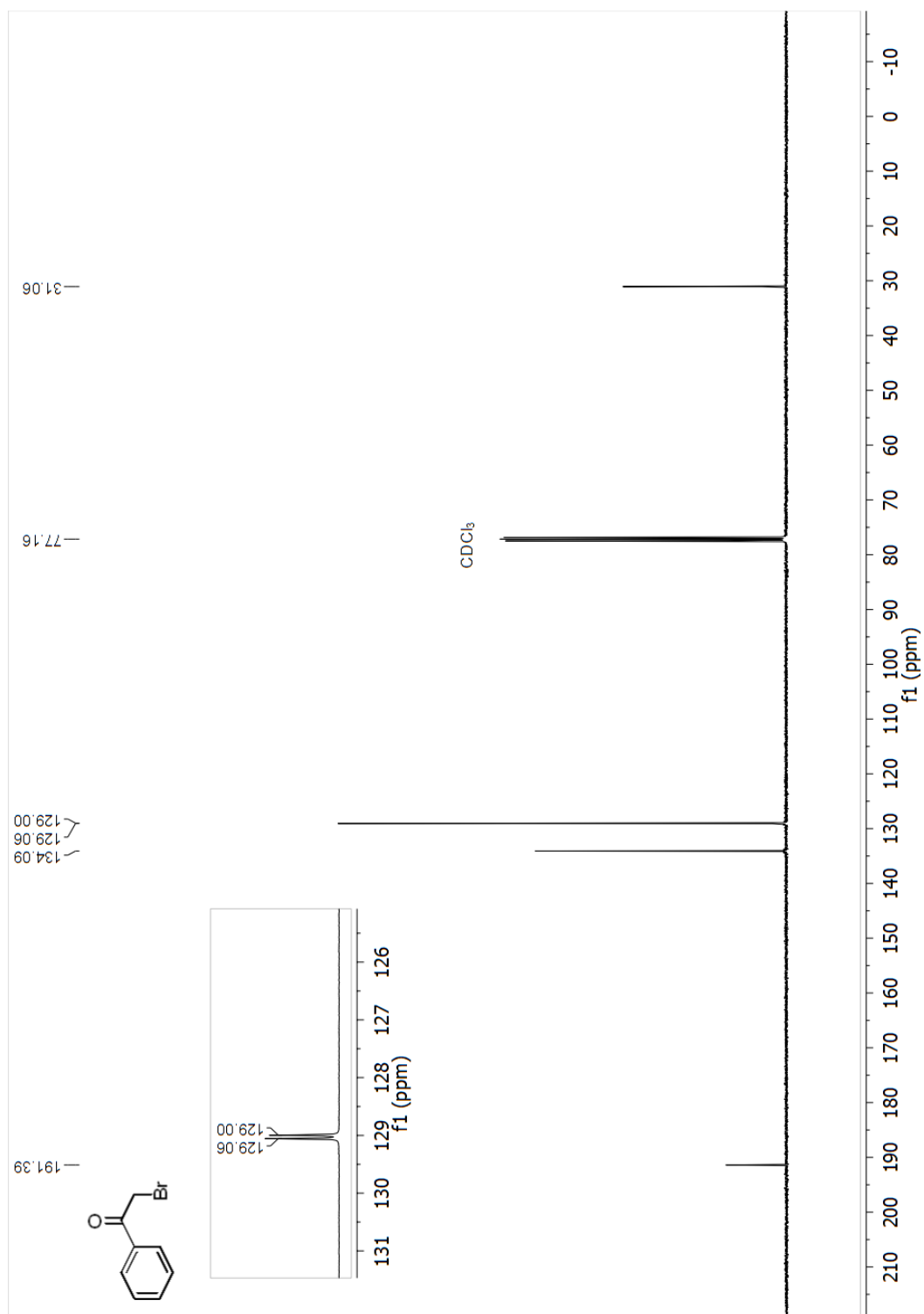
^{13}C NMR (101 MHz, CDCl_3) spectrum of 6c 3-bromo-1,5-dioxaspiro[5.5]undecane-2,4-dione



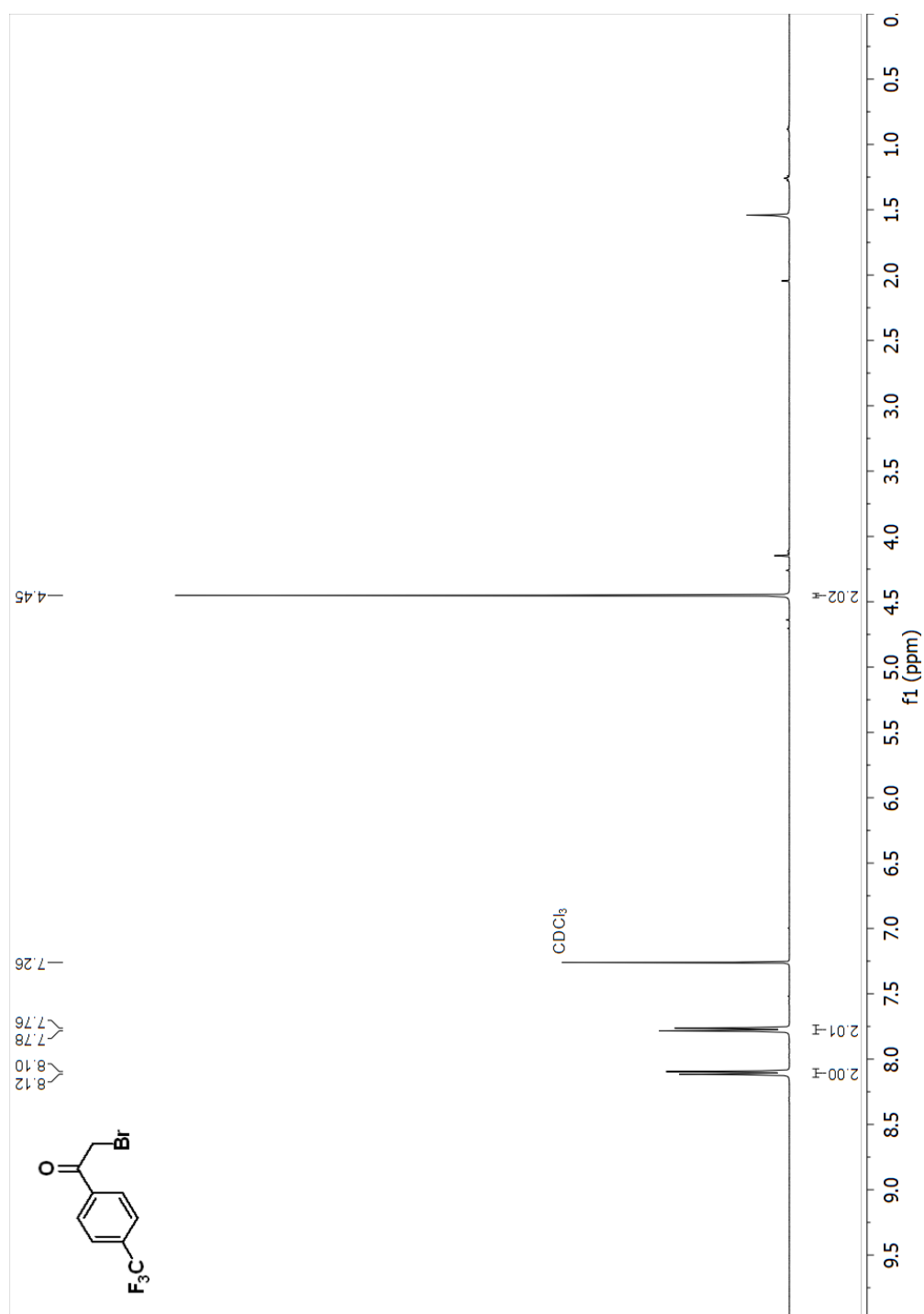
^1H NMR (400 MHz, CDCl_3) spectrum of 7c 2-Bromo-1-phenylethan-1-one



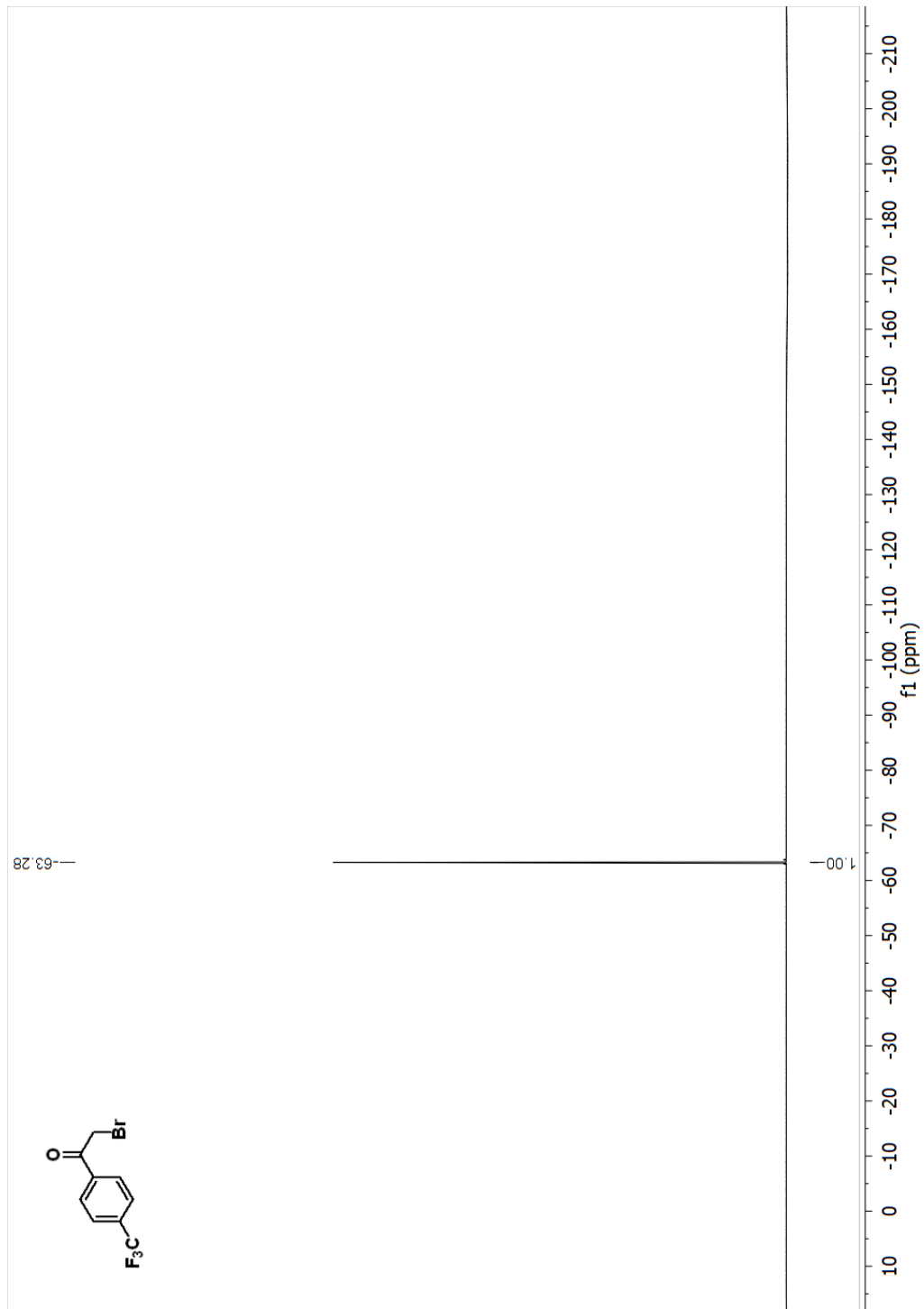
^{13}C NMR (101 MHz, CDCl_3) spectrum of 7c 2-Bromo-1-phenylethan-1-one



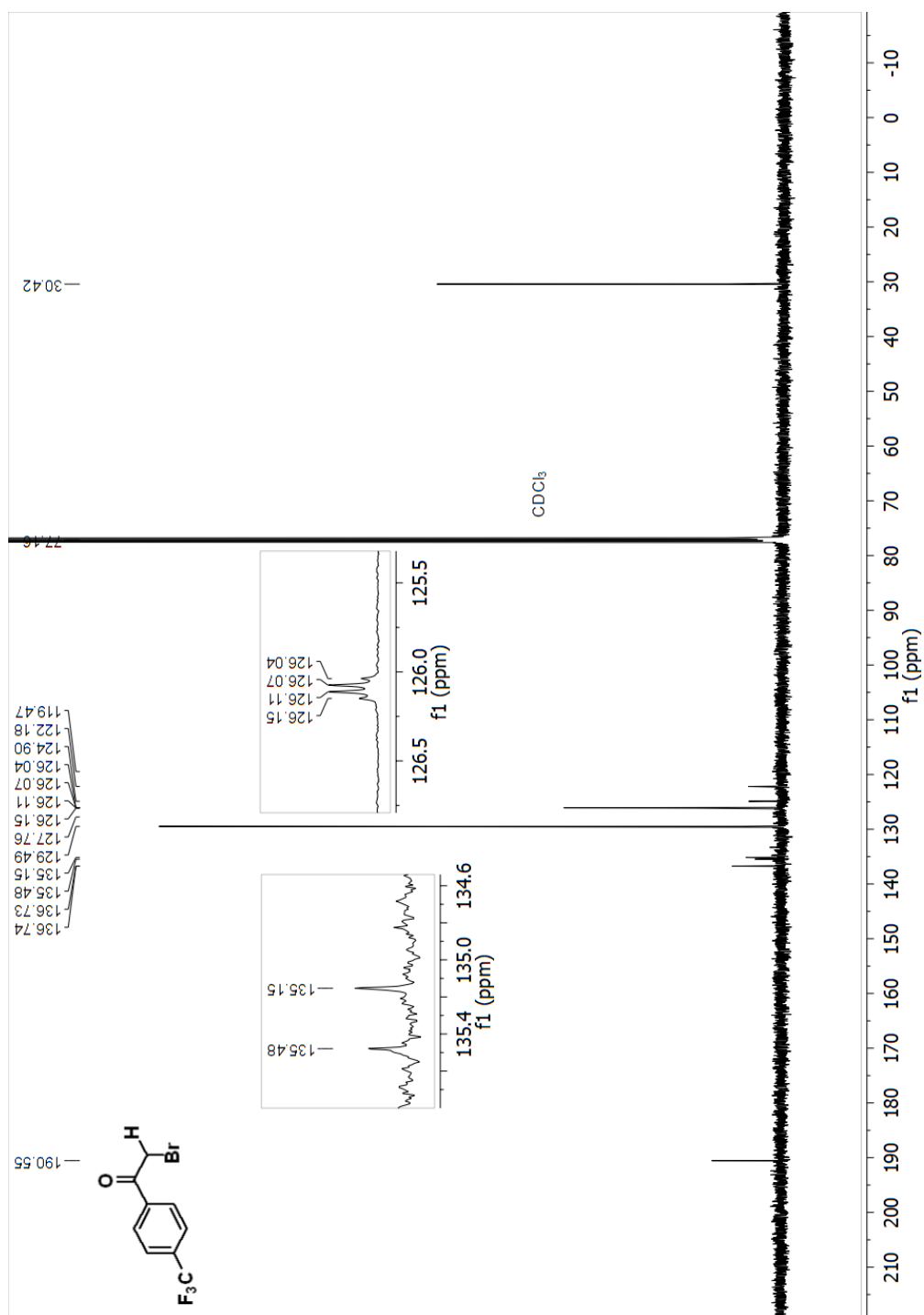
^1H NMR (400 MHz, CDCl_3) spectrum of 8c 2-bromo-1-(4-(trifluoromethyl)phenyl)ethan-1-one



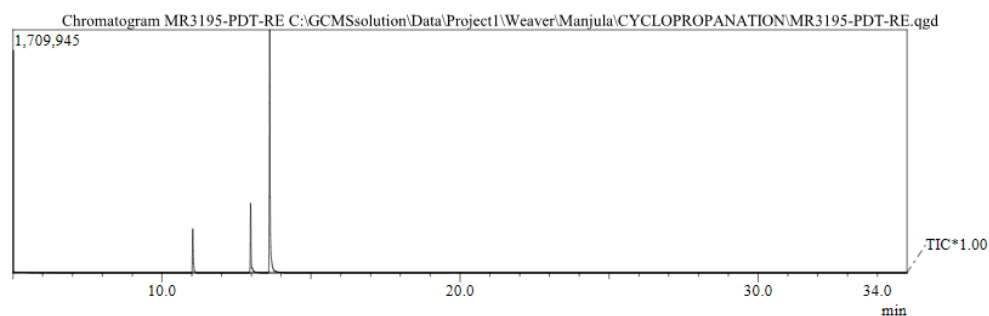
^{19}F NMR (376 MHz, CDCl_3) spectrum of 8c 2-bromo-1-(4-(trifluoromethyl)phenyl)ethan-1-one



^{13}C NMR (101 MHz, CDCl_3) spectrum of 8c 2-bromo-1-(4-(trifluoromethyl)phenyl)ethan-1-one

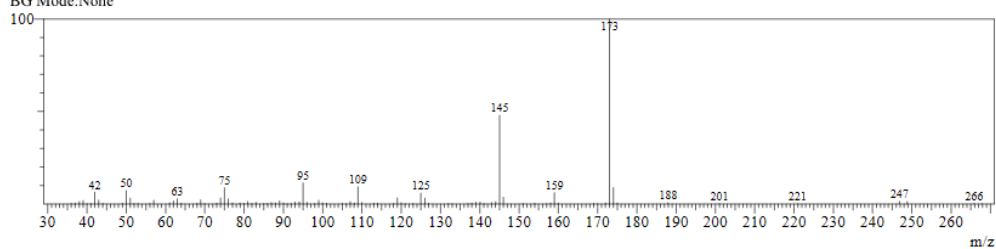


GC and MS of 8c 2-bromo-1-(4-(trifluoromethyl)phenyl)ethan-1-one

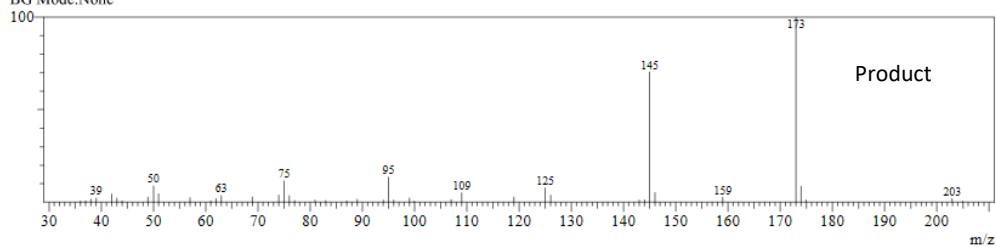


Spectrum

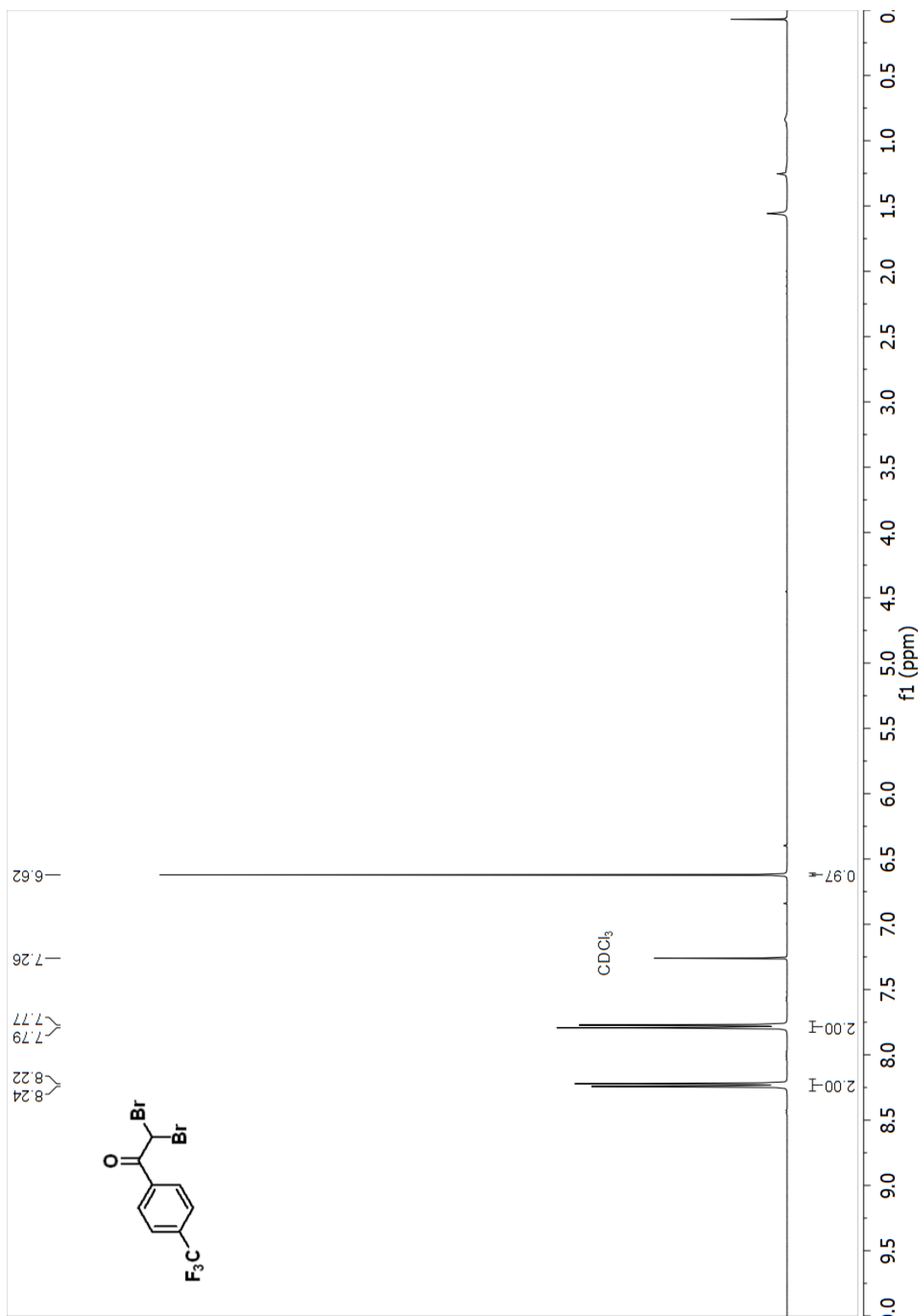
Line#:1 R.Time:13.6(Scan#:1035)
MassPeaks:95
RawMode:Single 13.6(1035) BasePeak:173(601558)
BG Mode:None



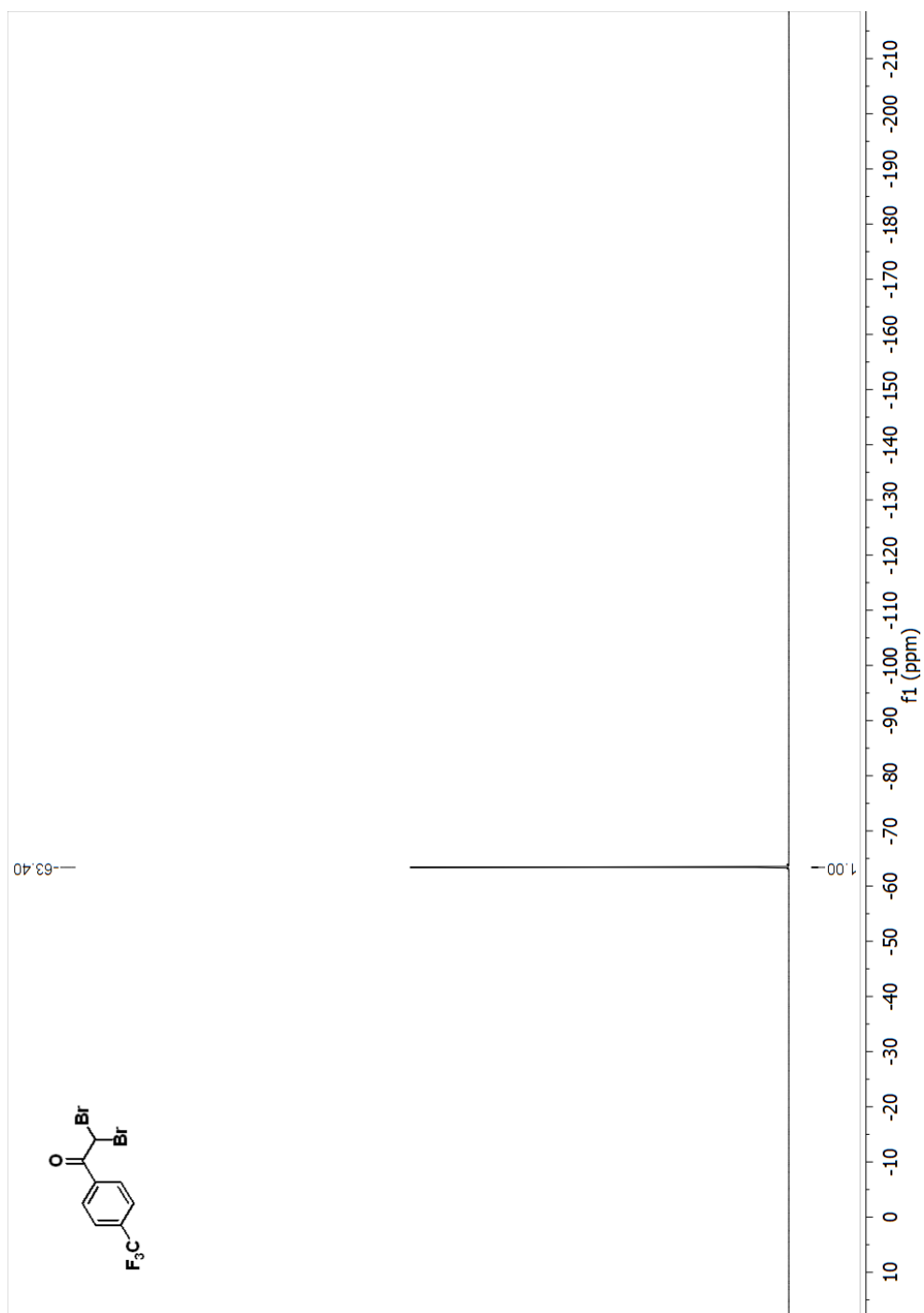
Line#:2 R.Time:13.0(Scan#:958)
MassPeaks:43
RawMode:Single 13.0(958) BasePeak:173(151463)
BG Mode:None



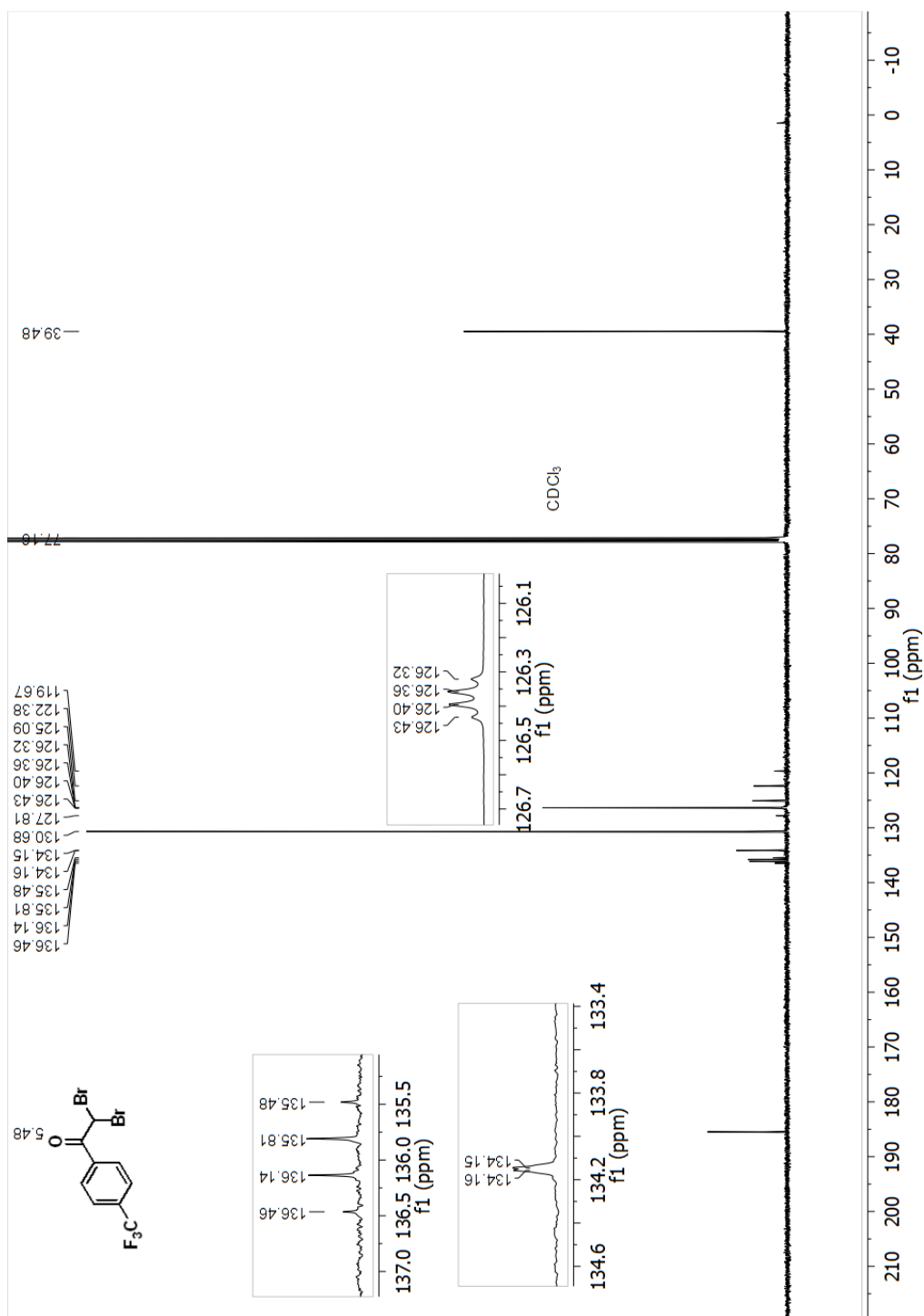
^1H NMR (400 MHz, CDCl_3) spectrum of 9c 2,2-dibromo-1-(4-(trifluoromethyl)phenyl)ethan-1-one



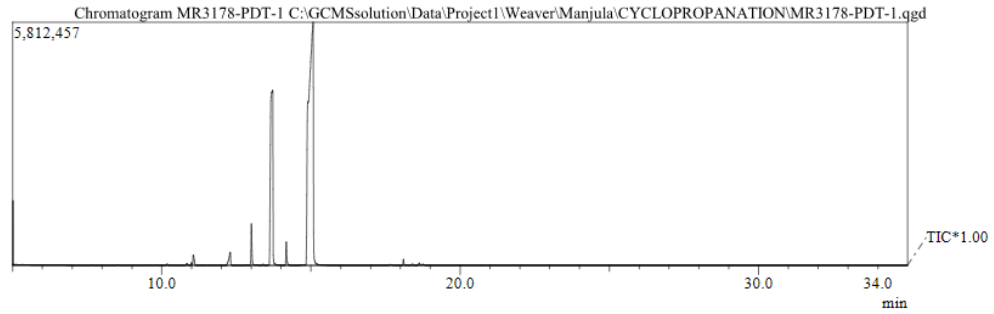
^{19}F NMR (376 MHz, CDCl_3) spectrum of 9c 2,2-dibromo-1-(4-(trifluoromethyl)phenyl)ethan-1-one



^{13}C NMR (101 MHz, CDCl_3) spectrum of 9c 2,2-dibromo-1-(4-(trifluoromethyl)phenyl)ethan-1-one

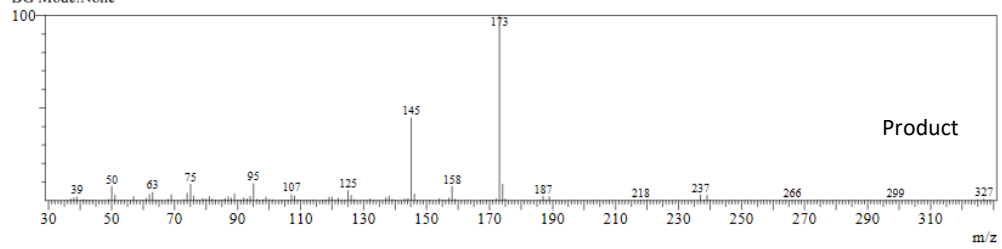


GC and MS of 9c 2,2-dibromo-1-(4-(trifluoromethyl)phenyl)ethan-1-one

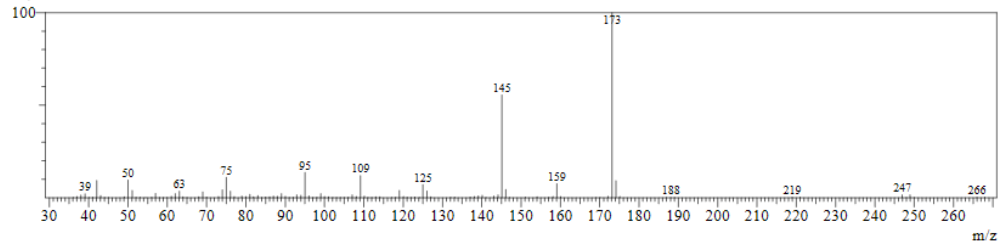


Spectrum

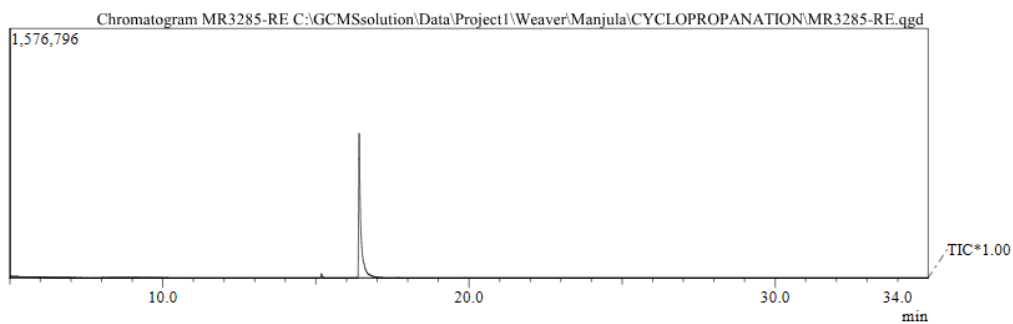
Line#:1 R.Time:14.9(Scan#:1194)
MassPeaks:123
RawMode:Single 14.9(1194) BasePeak:173(1408385)
BG Mode:None



Line#:2 R.Time:13.7(Scan#:1044)
MassPeaks:116
RawMode:Single 13.7(1044) BasePeak:173(1278081)
BG Mode:None

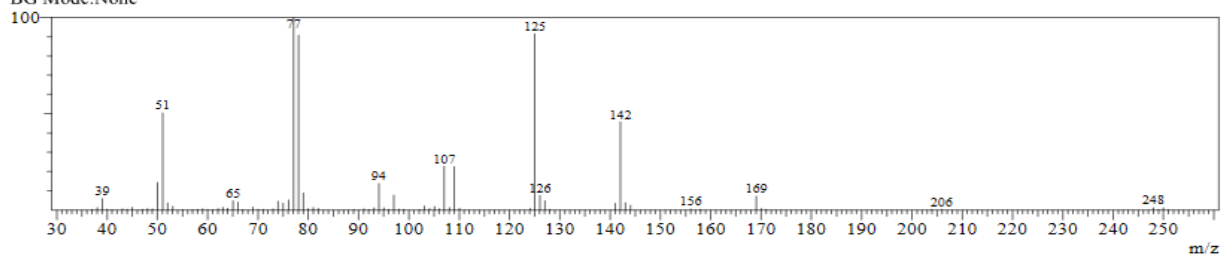


GC and MS of 10c ((1-Bromoethyl)sulfonyl)benzene

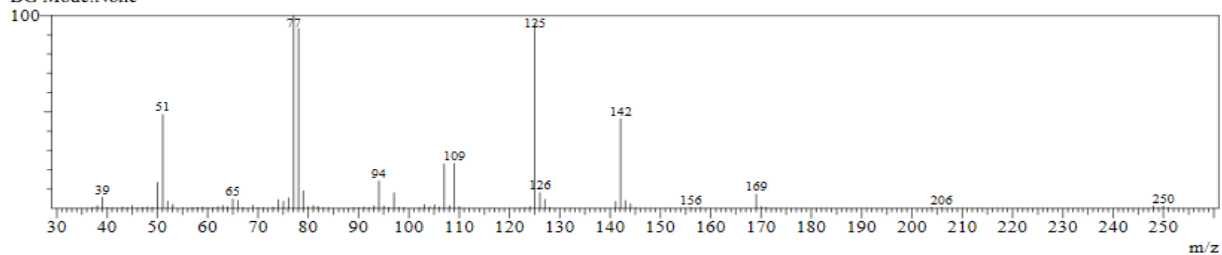


Spectrum

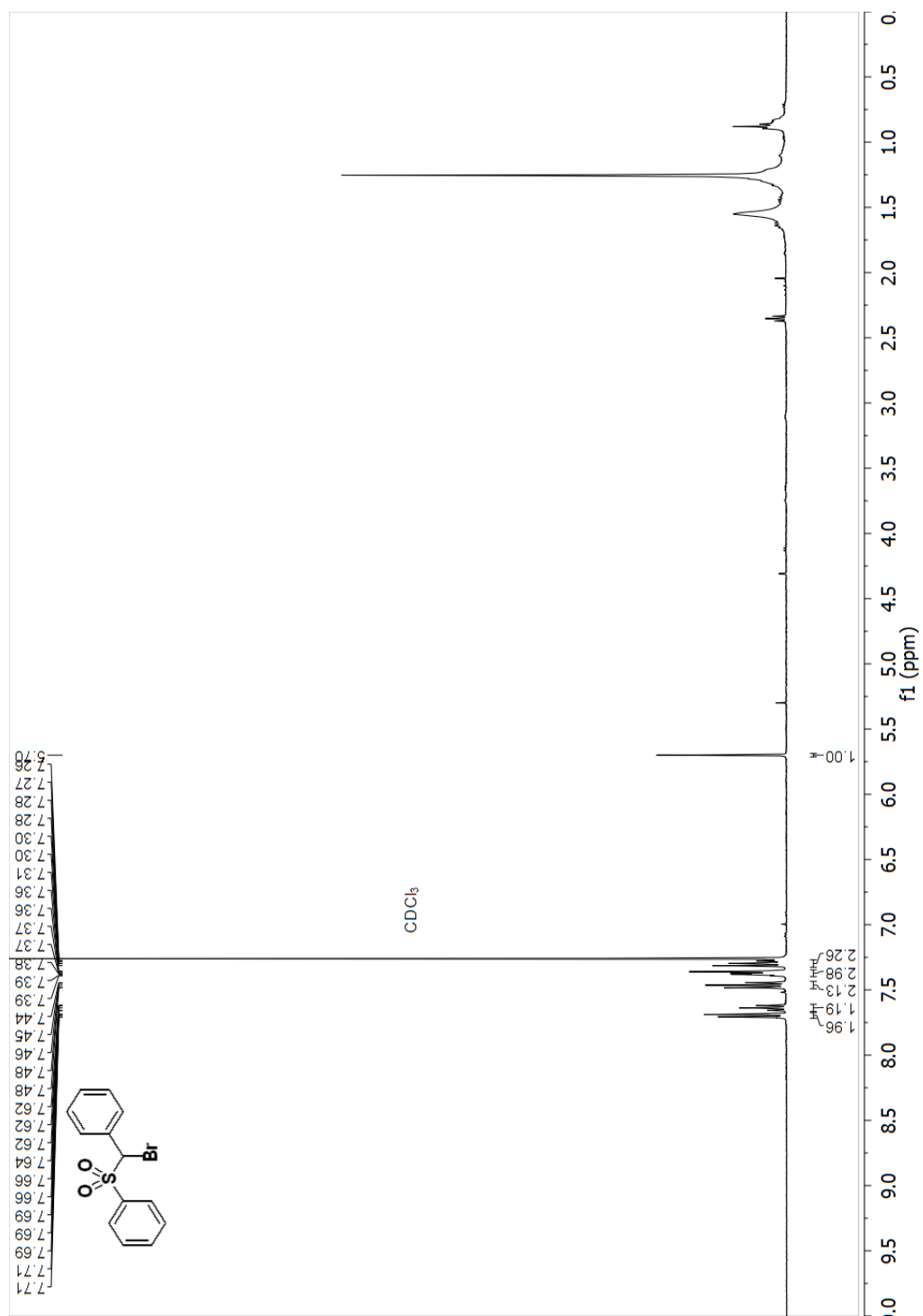
Line#:1 R.Time:16.1(Scan#:1330)
MassPeaks:79
RawMode:Single 16.1(1330) BasePeak:77(530170)
BG Mode:None



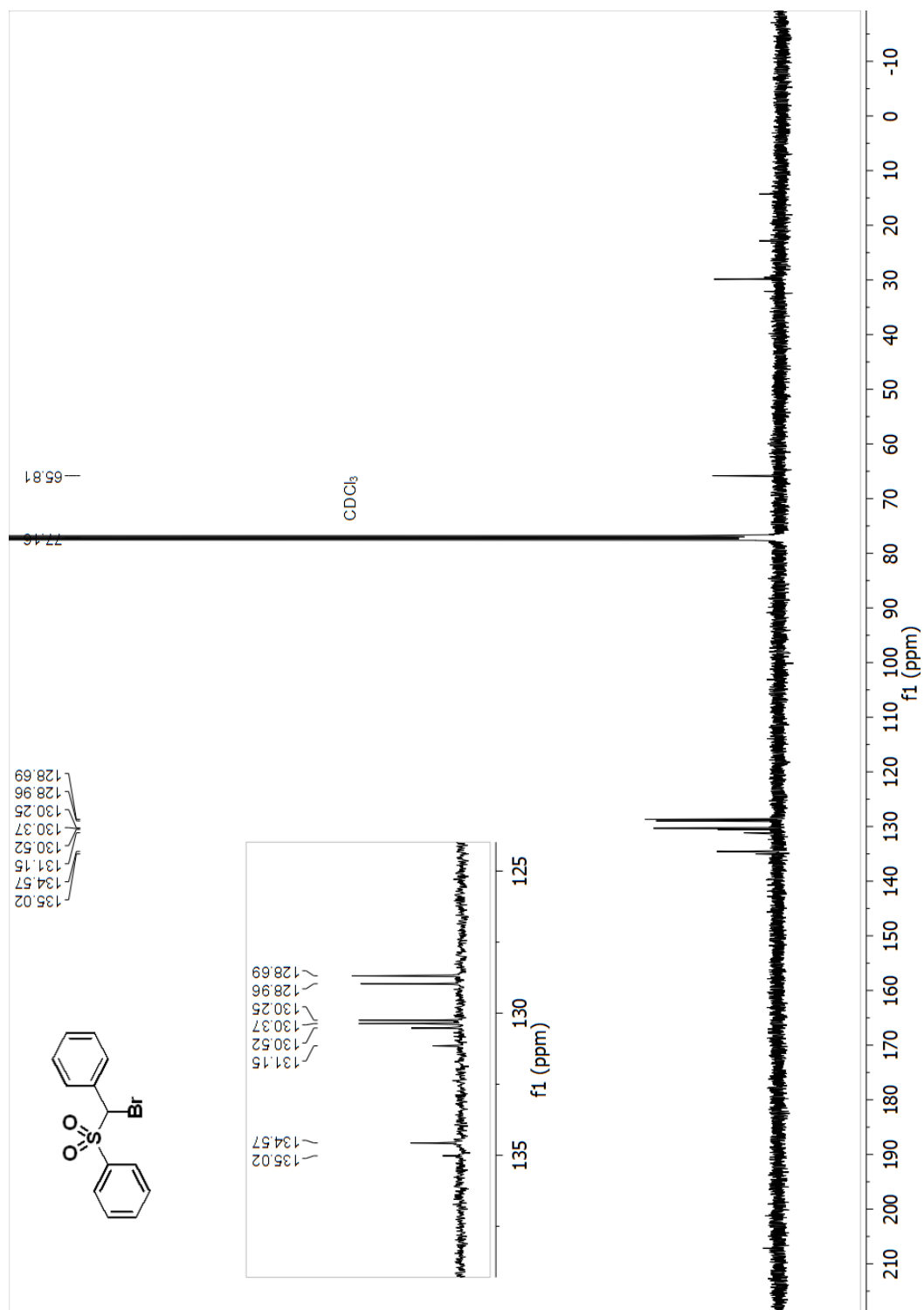
Line#:2 R.Time:16.1(Scan#:1333)
MassPeaks:85
RawMode:Single 16.1(1333) BasePeak:77(744030)
BG Mode:None



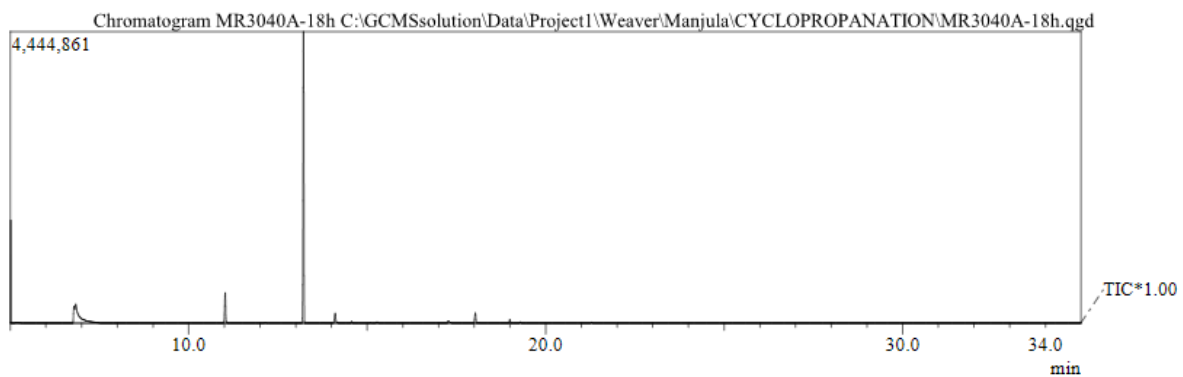
^1H NMR (400 MHz, CDCl_3) spectrum of 11c ((Bromo(phenyl)methyl)sulfonyl)benzene



^{13}C NMR (101 MHz, CDCl_3) spectrum of 11c ((Bromo(phenyl)methyl)sulfonyl)benzene



GC and MS of 12c 6-Bromo-2,2-dimethylcyclohexan-1-one



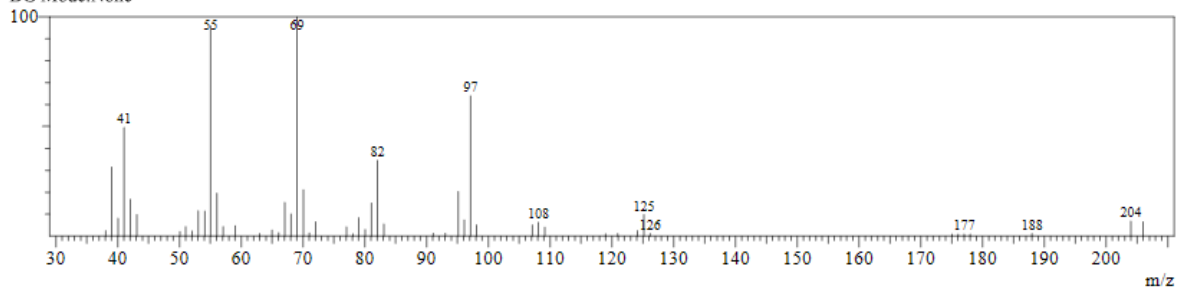
Spectrum

Line#:1 R.Time:13.2(Scan#:989)

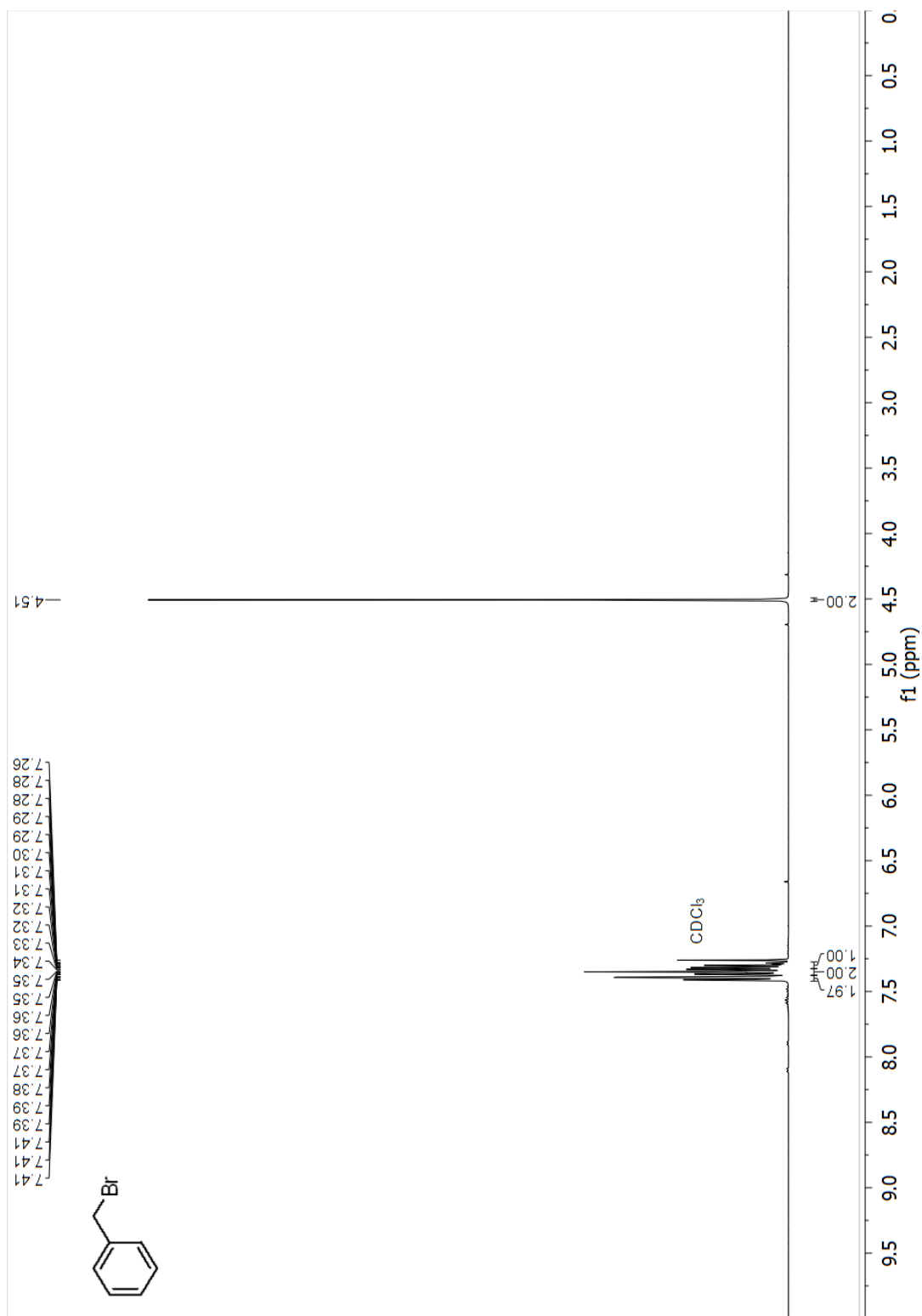
MassPeaks:52

RawMode:Single 13.2(989) BasePeak:69(120745)

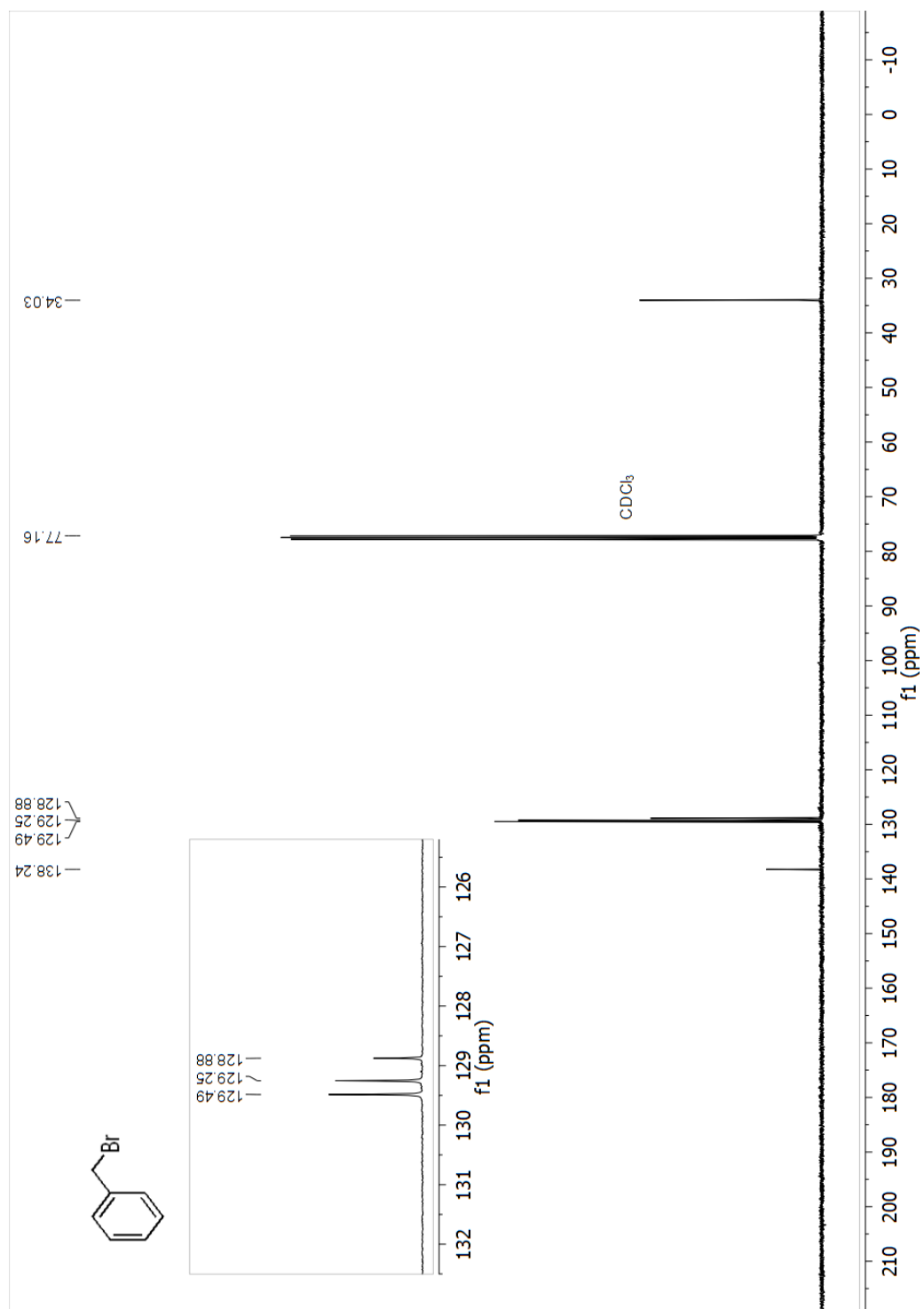
BG Mode:None



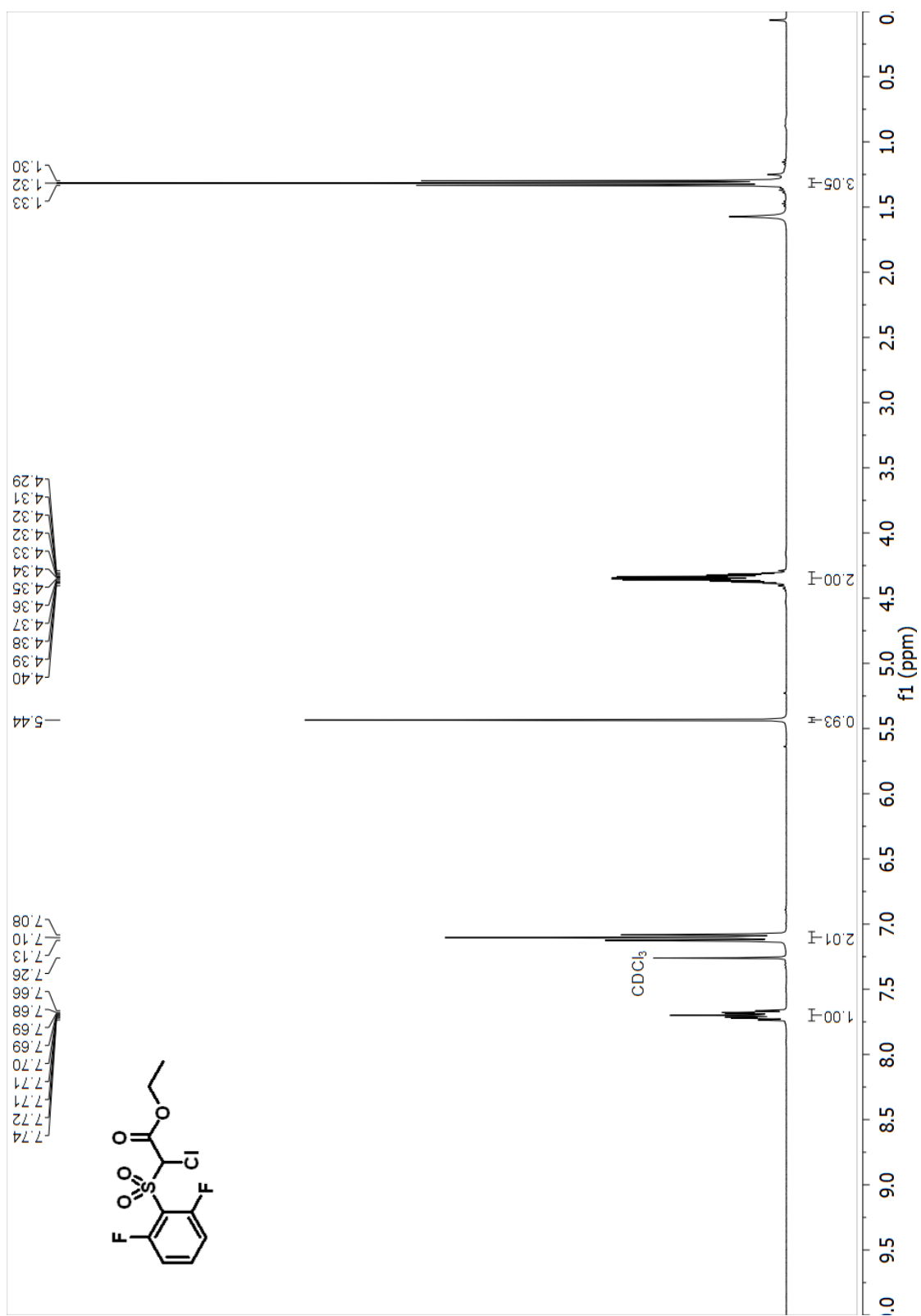
^1H NMR (400 MHz, CDCl_3) spectrum of 13c (Bromomethyl)benzene



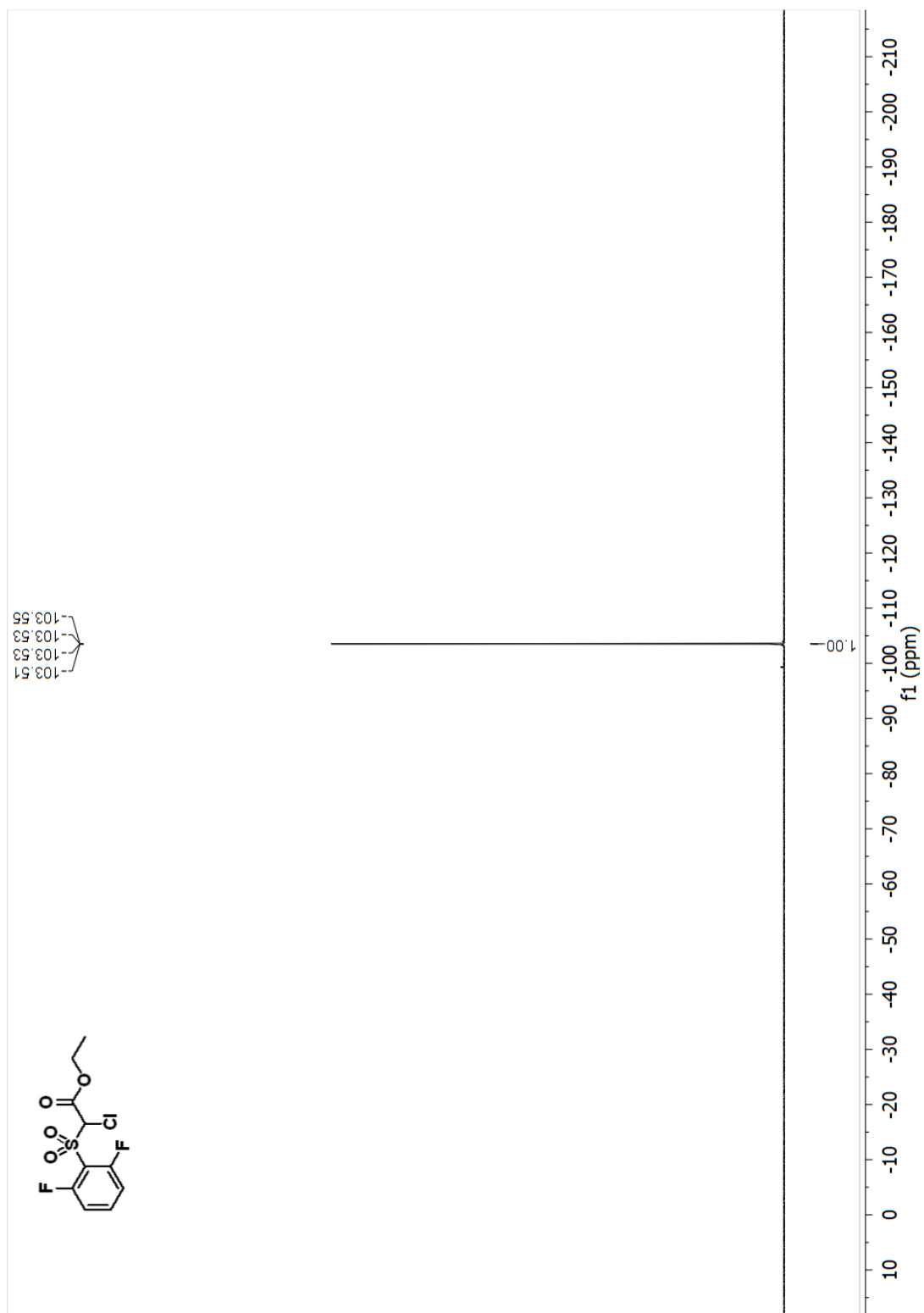
^{13}C NMR (101 MHz, CDCl_3) spectrum of 13c (Bromomethyl)benzene



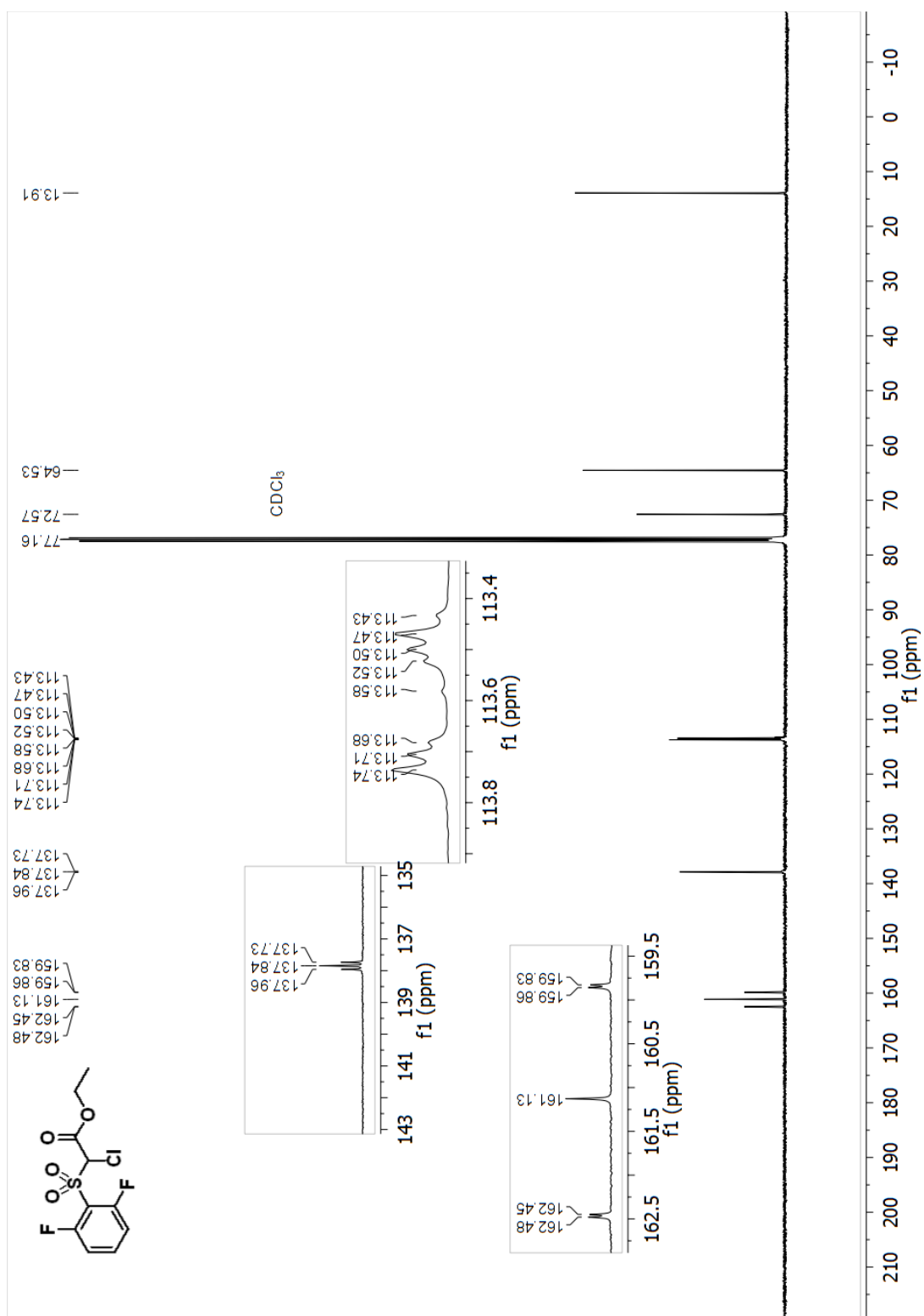
¹H NMR (400 MHz, CDCl₃) spectrum of 14c ethyl 2-chloro-2-((2,6-difluorophenyl)sulfonyl)acetate



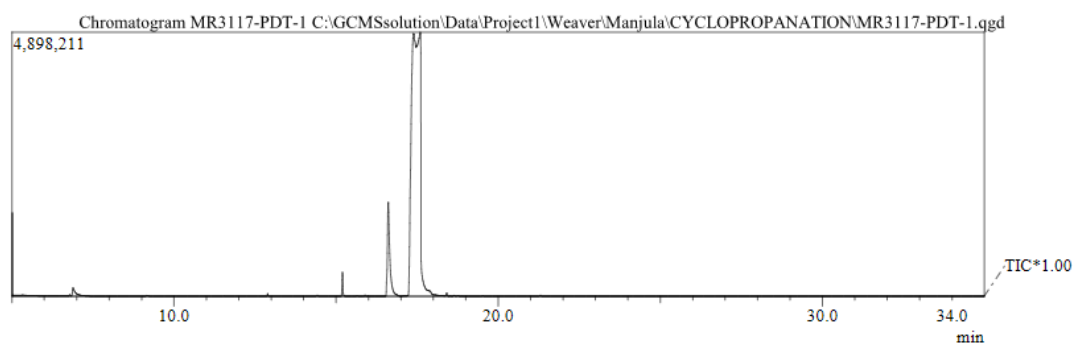
^{19}F NMR (376 MHz, CDCl_3) spectrum of 14c ethyl 2-chloro-2-((2,6-difluorophenyl)sulfonyl)acetate



¹³C NMR (101 MHz, CDCl₃) spectrum of 14c ethyl 2-chloro-2-((2,6-difluorophenyl)sulfonyl)acetate

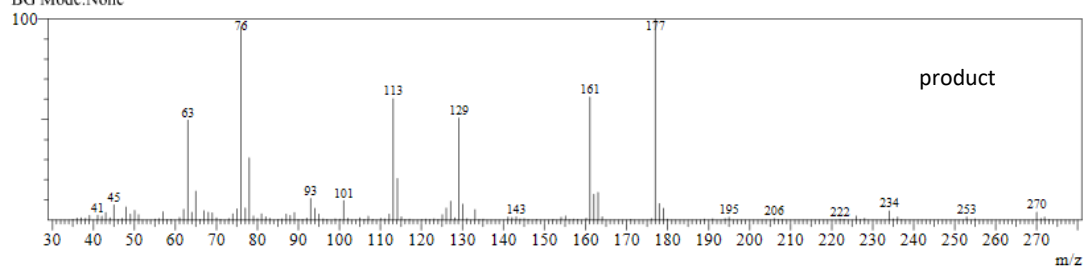


GC and MS of 14c ethyl 2-chloro-2-((2,6-difluorophenyl)sulfonyl)acetate

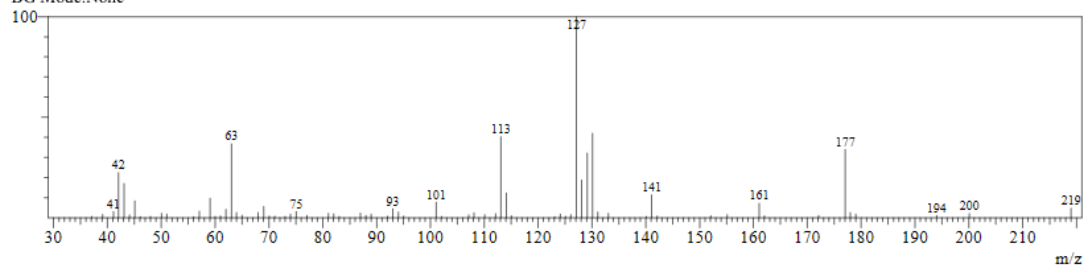


Spectrum

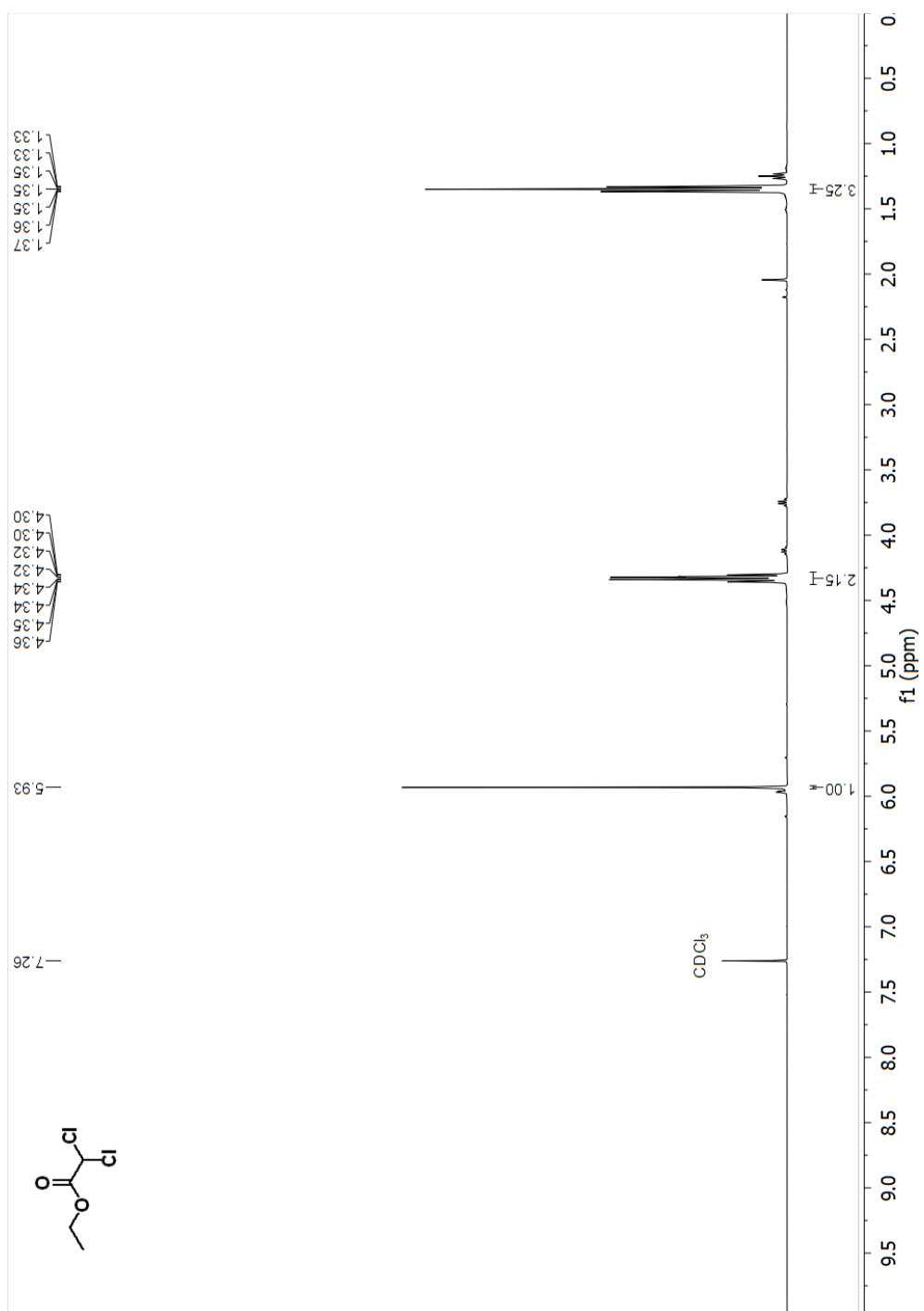
Line#:1 R.Time:17.5(Scan#:1498)
MassPeaks:133
RawMode:Single 17.5(1498) BasePeak:177(626318)
BG Mode:None



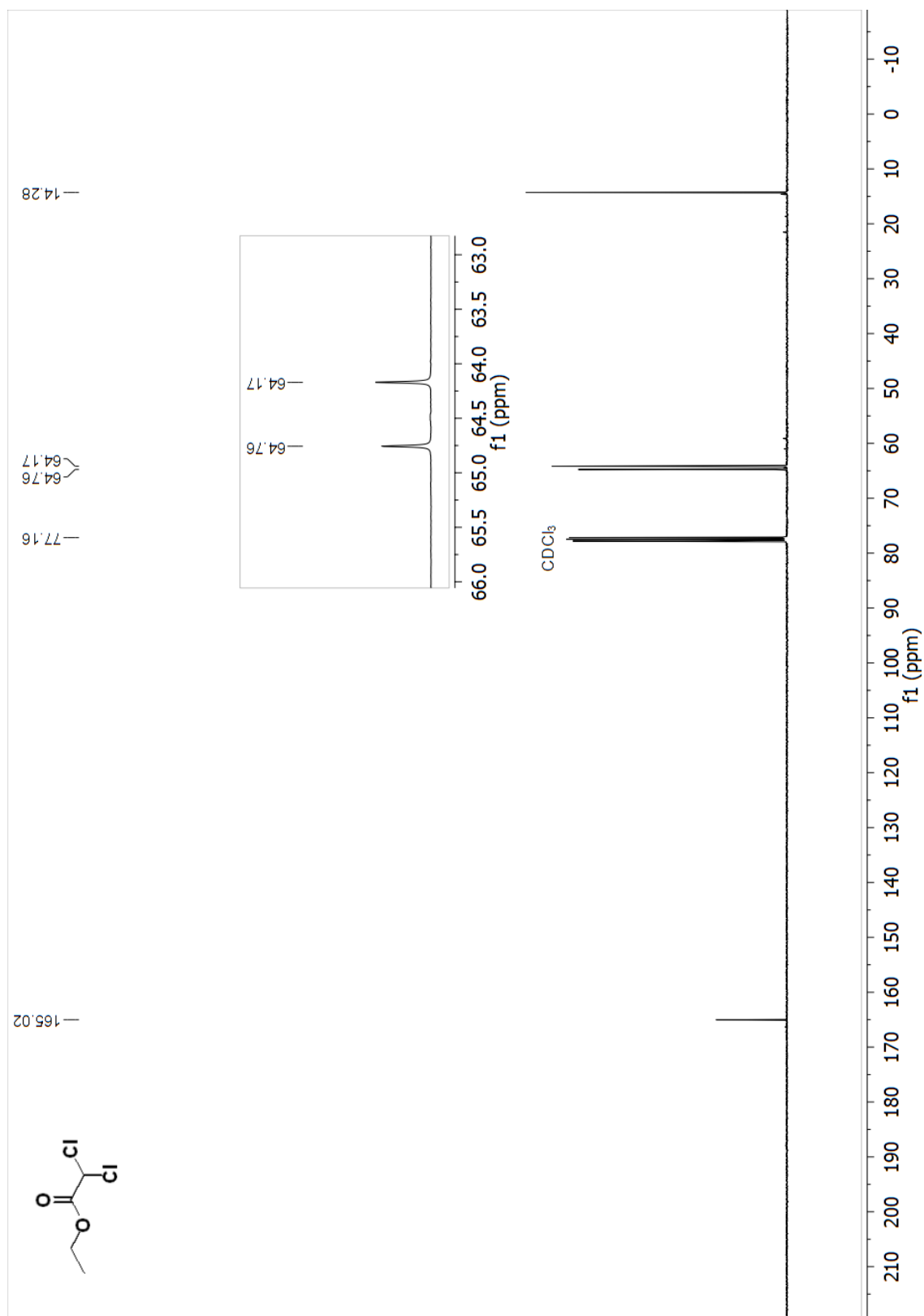
Line#:2 R.Time:16.6(Scan#:1398)
MassPeaks:71
RawMode:Single 16.6(1398) BasePeak:127(193636)
BG Mode:None



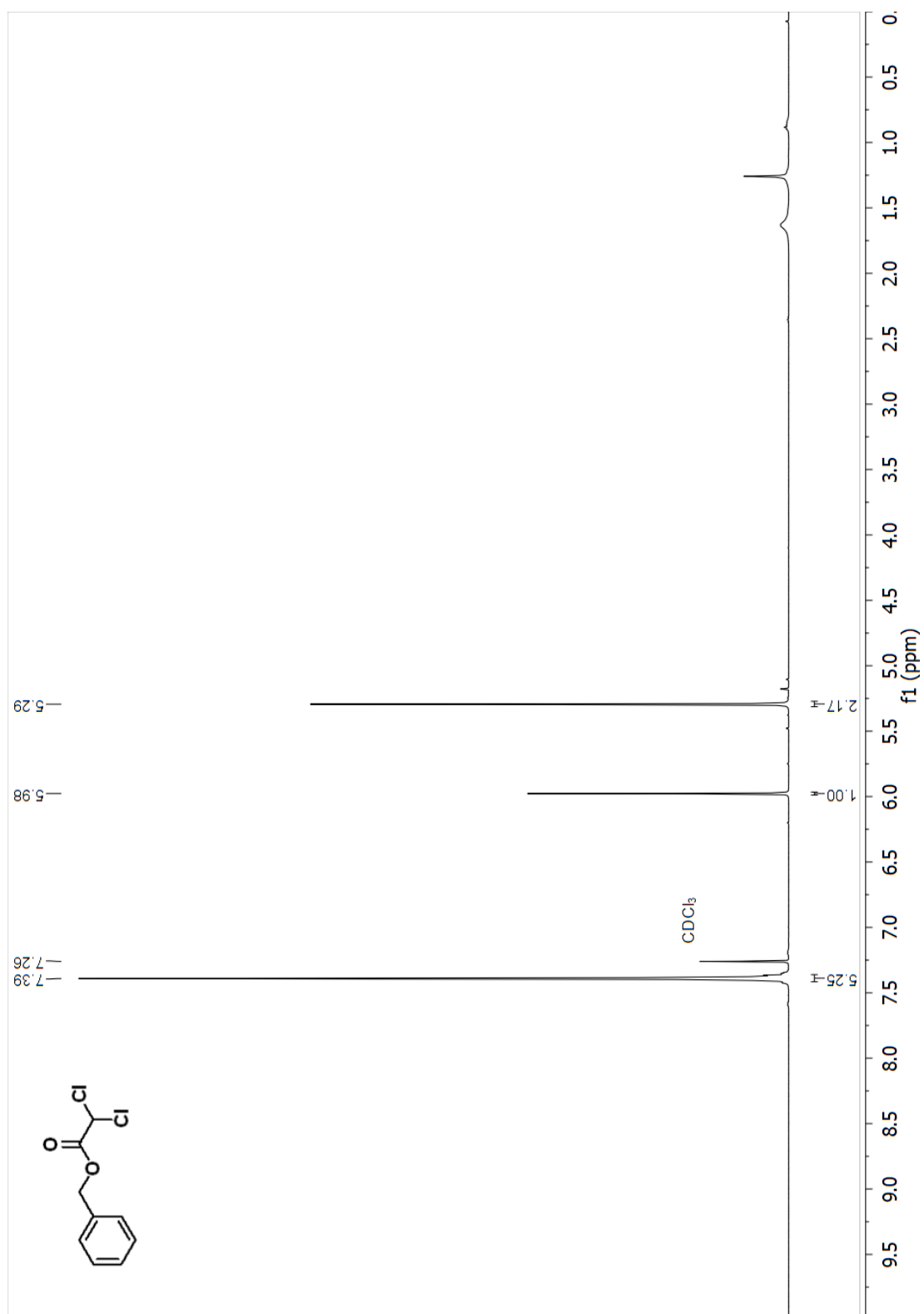
^1H NMR (400 MHz, CDCl_3) spectrum of 15c ethyl 2,2-dichloroacetate



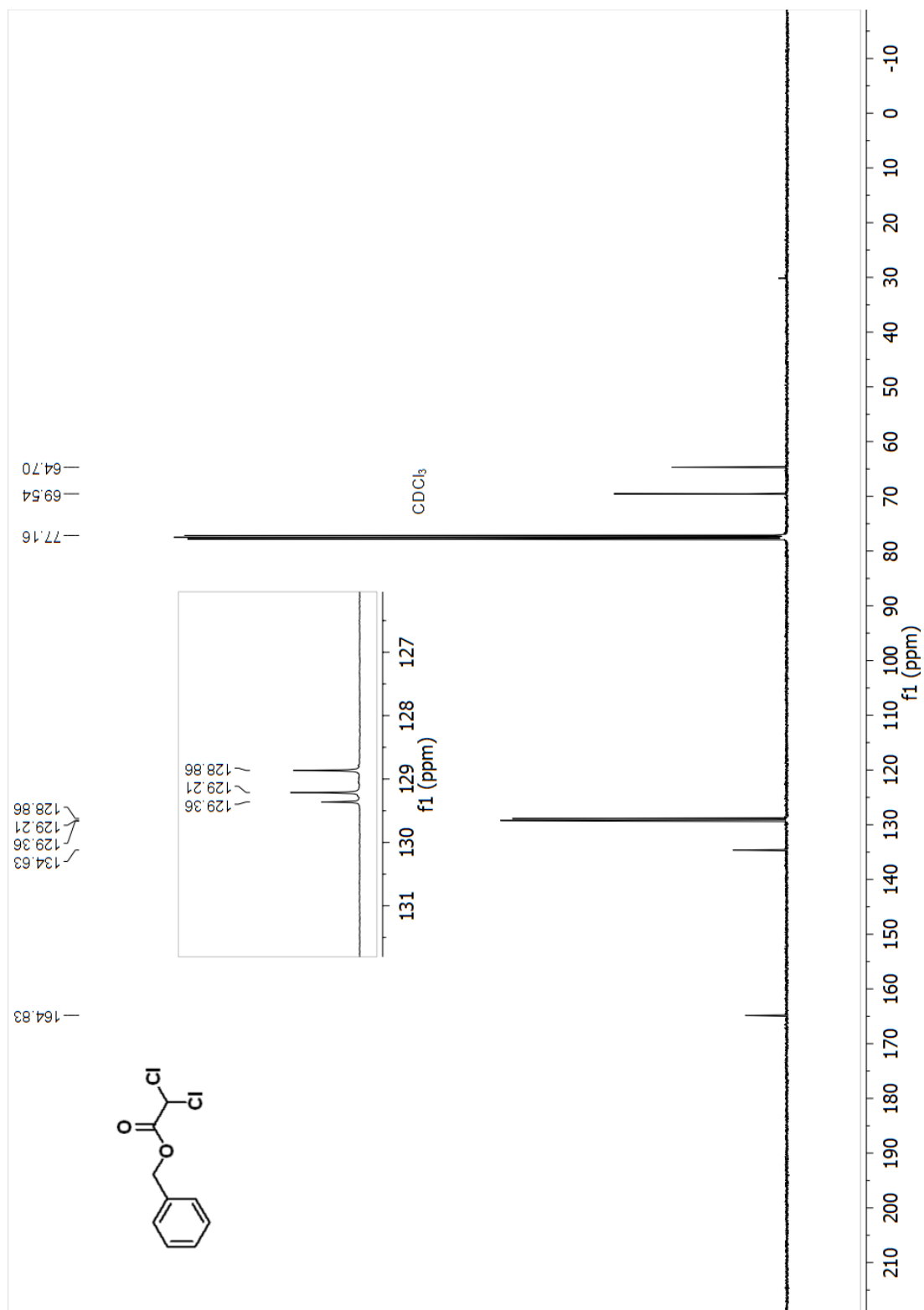
^{13}C NMR (101 MHz, CDCl_3) spectrum of 15c ethyl 2,2-dichloroacetate



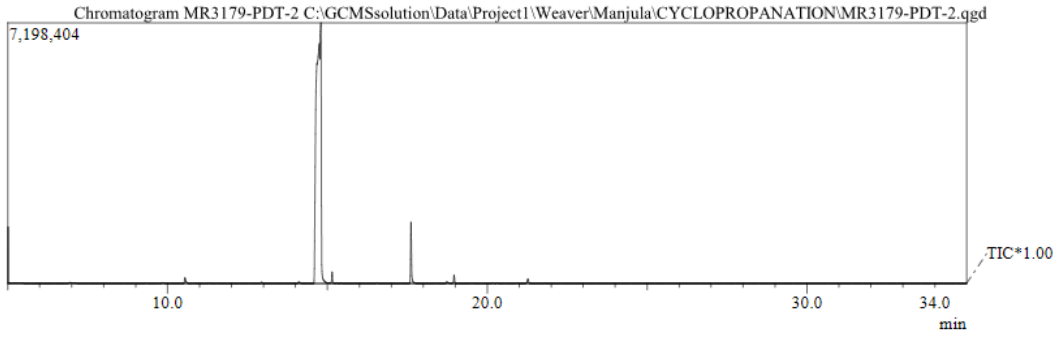
^1H NMR (400 MHz, CDCl_3) spectrum of 16c benzyl 2,2-dichloroacetate



^{13}C NMR (101 MHz, CDCl_3) spectrum of 16c benzyl 2,2-dichloroacetate



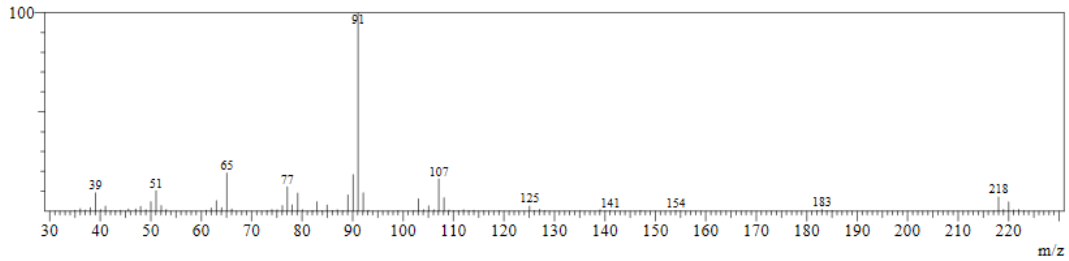
GC and MS of 16c benzyl 2,2-dichloroacetate



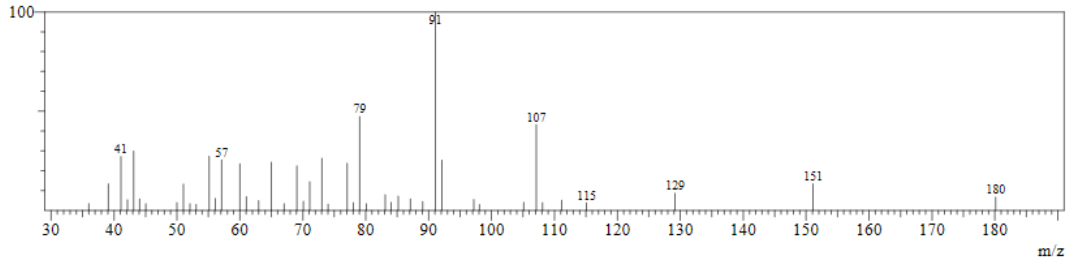
Spectrum

Line#:1 R.Time:14.7(Scan#:1163)
MassPeaks:82
RawMode:Single 14.7(1163) BasePeak:91(2023471)
BG Mode:None

product



Line#:2 R.Time:17.6(Scan#:1518)
MassPeaks:45
RawMode:Single 17.6(1518) BasePeak:91(33849)
BG Mode:None



3.5 References

- 1.(a) Gál, B.; Bucher, C.; Burns, N. Z., Chiral Alkyl Halides: Underexplored Motifs in Medicine. *Mar drugs* **2016**, *14*, 206; (b) Chung, W.-j.; Vanderwal, C. D., Stereoselective Halogenation in Natural Product Synthesis. *Angew. Chem. Int. Ed. Engl.* **2016**, *55*, 4396; (c) Gribble, G. W., *Naturally Occurring Organohalogen Compounds - A Comprehensive Update*. Springer Vienna: 2009; (d) Gribble, G. W., The diversity of naturally produced organohalogens. *Chemosphere* **2003**, *52*, 289; (e) Gerebtzoff, G.; Li-Blatter, X.; Fischer, H.; Frenzel, A.; Seelig, A., Halogenation of drugs enhances membrane binding and permeation. *Chembiochem : a European journal of chemical biology* **2004**, *5*, 676; (f) Gentry, C. L.; Egleton, R. D.; Gillespie, T.; Abbruscato, T. J.; Bechowski, H. B.; Hruby, V. J.; Davis, T. P., The effect of halogenation on blood–brain barrier permeability of a novel peptide drug☆. *Peptides* **1999**, *20*, 1229.
- 2.(a) Kambe, N.; Iwasaki, T.; Terao, J., Pd-catalyzed cross-coupling reactions of alkyl halides. *Chem. Soc. Rev* **2011**, *40*, 4937; (b) Saito, B.; Fu, G. C., Alkyl–Alkyl Suzuki Cross-Couplings of Unactivated Secondary Alkyl Halides at Room Temperature. *J. Am. Chem. Soc.* **2007**, *129*, 9602; (c) Terao, J.; Kambe, N., Cross-Coupling Reaction of Alkyl Halides with Grignard Reagents Catalyzed by Ni, Pd, or Cu Complexes with π -Carbon Ligand(s). *Acc. Chem. Res.* **2008**, *41*, 1545; (d) McMurry, J., *Organic Chemistry*. Brooks/Cole Cengage Learning: 2011.
- 3.(a) Brochu, M. P.; Brown, S. P.; MacMillan, D. W. C., Direct and Enantioselective Organocatalytic α -Chlorination of Aldehydes. *J. Am. Chem. Soc.* **2004**, *126*, 4108; (b) Halland, N.; Braunton, A.; Bachmann, S.; Marigo, M.; Jørgensen, K. A., Direct Organocatalytic Asymmetric α -Chlorination of Aldehydes. *J. Am. Chem. Soc.* **2004**, *126*, 4790; (c) Bertelsen, S.; Halland, N.; Bachmann, S.; Marigo, M.; Braunton, A.; Jørgensen, K. A., Organocatalytic asymmetric α -bromination of aldehydes and ketones. *Chem. Commun.* **2005**, 4821; (d) Ueda, M.; Kano, T.; Maruoka, K., Organocatalyzed direct asymmetric α -halogenation of carbonyl compounds. *Org. Biomol. Chem.* **2009**, *7*, 2005.

4.(a) Saikia, I.; Borah, A. J.; Phukan, P., Use of Bromine and Bromo-Organic Compounds in Organic Synthesis. *Chem. Rev.* **2016**, *116*, 6837; (b) Podgoršek, A.; Zupan, M.; Iskra, J., Oxidative Halogenation with “Green” Oxidants: Oxygen and Hydrogen Peroxide. *Angew. Chem. Int. Ed. Engl.* **2009**, *48*, 8424; (c) Kolvari, E.; Koukabi, N.; Khoramabadi-zad, A.; Shiri, A.; Ali Zolfigol, M., Alternative Methodologies for Halogenation of Organic Compounds. *Curr. Org. Synth.* **2013**, *10*, 837; (d) Sabuzi, F.; Pomarico, G.; Floris, B.; Valentini, F.; Galloni, P.; Conte, V., Sustainable bromination of organic compounds: A critical review. *Coord. Chem. Rev.* **2019**, *385*, 100; (e) Nishina, Y.; Ohtani, B.; Kikushima, K., Bromination of hydrocarbons with CBr₄, initiated by light-emitting diode irradiation. *Beilstein J. Org. Chem.* **2013**, *9*, 1663; (f) Cantillo, D.; Kappe, C. O., Halogenation of organic compounds using continuous flow and microreactor technology. *React. Chem. Eng.* **2017**, *2*, 7; (g) Smith, A. M. R.; Hii, K. K., Transition Metal Catalyzed Enantioselective α -Heterofunctionalization of Carbonyl Compounds. *Chem. Rev.* **2011**, *111*, 1637; (h) Suryakiran, N.; Prabhakar, P.; Srikanth Reddy, T.; Chinni Mahesh, K.; Rajesh, K.; Venkateswarlu, Y., Chemoselective mono halogenation of β -keto-sulfones using potassium halide and hydrogen peroxide; synthesis of halomethyl sulfones and dihalomethyl sulfones. *Tetrahedron Lett.* **2007**, *48*, 877; (i) Poteat, C. M.; Lindsay, V. N. G., Controlled α -mono- and α,α -di-halogenation of alkyl sulfones using reagent–solvent halogen bonding. *Chem. Commun.* **2019**, *55*, 2912; (j) Erian, A. W.; Sherif, S. M.; Gaber, H. M., The Chemistry of α -Haloketones and Their Utility in Heterocyclic Synthesis. *Molecules* **2003**, *8*, 793; (k) Mohan, R. B.; Reddy, N. C. G., Regioselective α -Bromination of Alkyl Ketones Using N-Bromosuccinimide in the Presence of Montmorillonite K-10 Clay: A Simple and Efficient Method. *Synth. Commun.* **2013**, *43*, 2603; (l) Pravst, I.; Zupan, M.; Stavber, S., Halogenation of ketones with N-halosuccinimides under solvent-free reaction conditions. *Tetrahedron* **2008**, *64*, 5191; (m) Jagatheesan, R.; Joseph Santhana Raj, K.; Lawrence, S.; Christopher, C., Electroselective α -bromination of acetophenone using in situ bromonium ions from ammonium bromide. *RSC Adv* **2016**, *6*, 35602.

5.(a) Senaweera, S. M.; Singh, A.; Weaver, J. D., Photocatalytic Hydrodefluorination: Facile Access to Partially Fluorinated Aromatics. *J. Am. Chem. Soc.* **2014**, *136*, 3002; (b) Khaled, M. B.; El Mokadem,

R. K.; Weaver, J. D., Hydrogen Bond Directed Photocatalytic Hydrodefluorination: Overcoming Electronic Control. *J. Am. Chem. Soc.* **2017**, *139*, 13092; (c) Singh, A.; Fennell, C. J.; Weaver, J. D., Photocatalyst size controls electron and energy transfer: selectable E/Z isomer synthesis via C–F alkenylation. *Chem. Sci.* **2016**, *7*, 6796; (d) Senaweera, S.; Weaver, J. D., Dual C–F, C–H Functionalization via Photocatalysis: Access to Multifluorinated Biaryls. *J. Am. Chem. Soc.* **2016**, *138*, 2520; (e) Singh, A.; Kubik, J. J.; Weaver, J. D., Photocatalytic C–F alkylation; facile access to multifluorinated arenes. *Chem. Sci.* **2015**, *6*, 7206; (f) Priya, S.; Weaver, J. D., Prenyl Praxis: A Method for Direct Photocatalytic Defluoroprenylation. *J. Am. Chem. Soc.* **2018**, *140*, 16020.

6. Bailey, W. F.; Patricia, J. J., The mechanism of the lithium - halogen Interchange reaction : a review of the literature. *J Organomet Chem* **1988**, *352*, 1.

7. Yoon, N. M., Selective reduction of organic compounds with aluminum and boron hydrides. In *Pure and Applied Chemistry*, 1996; Vol. 68, p 843.

8.(a) Neumann, W. P., Tri-n-butyltin Hydride as Reagent in Organic Synthesis. *Synthesis* **1987**, *1987*, 665; (b) Curran, D. P., The Design and Application of Free Radical Chain Reactions in Organic Synthesis. Part 1. *Synthesis* **1988**, *1988*, 417; (c) Curran, D. P., The Design and Application of Free Radical Chain Reactions in Organic Synthesis. Part 2. *Synthesis* **1988**, *1988*, 489; (d) O'Mahony, G., Triethylborane (Et₃B). *Synlett* **2004**, *2004*, 572.

9. Alonso, F.; Beletskaya, I. P.; Yus, M., Metal-Mediated Reductive Hydrodehalogenation of Organic Halides. *Chem. Rev.* **2002**, *102*, 4009.

10. Khattab, M. A.; Elgamal, M. A.; El-Batouti, M., Evaluation of thermal hazard of azobisisobutyronitrile using accelerating rate calorimetry. *Fire Mater.* **1996**, *20*, 253.

11. Baguley, P. A.; Walton, J. C., Flight from the Tyranny of Tin: The Quest for Practical Radical Sources Free from Metal Encumbrances. *Angew. Chem. Int. Ed.* **1998**, *37*, 3072.

12. Devery, J. J.; Nguyen, J. D.; Dai, C.; Stephenson, C. R. J., Light-Mediated Reductive Debromination of Unactivated Alkyl and Aryl Bromides. *ACS Catal* **2016**, *6*, 5962.

13. Maji, T.; Karmakar, A.; Reiser, O., Visible-Light Photoredox Catalysis: Dehalogenation of Vicinal Dibromo-, α -Halo-, and α,α -Dibromocarbonyl Compounds. *J. Org. Chem.* **2011**, *76*, 736.
- 14.(a) Moteki, S. A.; Usui, A.; Selvakumar, S.; Zhang, T.; Maruoka, K., Metal-Free C-H Bond Activation of Branched Aldehydes with a Hypervalent Iodine(III) Catalyst under Visible-Light Photolysis: Successful Trapping with Electron-Deficient Olefins. *Angew. Chem. Int. Ed. Engl.* **2014**, *53*, 11060; (b) Tan, H.; Li, H.; Ji, W.; Wang, L., Sunlight-Driven Decarboxylative Alkynylation of α -Keto Acids with Bromoacetylenes by Hypervalent Iodine Reagent Catalysis: A Facile Approach to Ynones. *Angew. Chem. Int. Ed. Engl.* **2015**, *54*, 8374; (c) Li, L.; Mu, X.; Liu, W.; Wang, Y.; Mi, Z.; Li, C.-J., Simple and Clean Photoinduced Aromatic Trifluoromethylation Reaction. *J. Am. Chem. Soc.* **2016**, *138*, 5809; (d) Xie, X.; Li, P.; Shi, Q.; Wang, L., Visible-light-induced tandem cyclization of 2-alkynylanilines with disulfides: a convenient method for accessing benzothiophenes under transition-metal-free and photocatalyst-free conditions. *Org. Biomol. Chem.* **2017**, *15*, 7678.
15. Lima, C. G. S.; de M. Lima, T.; Duarte, M.; Jurberg, I. D.; Paixão, M. W., Organic Synthesis Enabled by Light-Irradiation of EDA Complexes: Theoretical Background and Synthetic Applications. *ACS Catal* **2016**, *6*, 1389.
16. Zhao, G.-J.; Han, K.-L., Hydrogen Bonding in the Electronic Excited State. *Acc. Chem. Res.* **2012**, *45*, 404.
- 17.(a) Foster, R., Electron donor-acceptor complexes. *J. Phys. Chem.* **1980**, *84*, 2135; (b) Rosokha, S. V.; Kochi, J. K., Fresh Look at Electron-Transfer Mechanisms via the Donor/Acceptor Bindings in the Critical Encounter Complex. *Acc. Chem. Res.* **2008**, *41*, 641.
18. Postigo, A., Electron Donor-Acceptor Complexes in Perfluoroalkylation Reactions. *Eur. J. Org. Chem.* **2018**, *2018*, 6391.
- 19.(a) Rosokha, S. V.; Kochi, J. K., Fresh Look at Electron-Transfer Mechanisms via the Donor/Acceptor Bindings in the Critical Encounter Complex. *Acc. Chem. Res.* **2008**, *41*, 641; (b) Hilinski, E. F.; Masnovi, J. M.; Amatore, C.; Kochi, J. K.; Rentzepis, P. M., Charge-transfer excitation of electron donor-acceptor complexes. Direct observation of ion pairs by time-resolved (picosecond)

spectroscopy. *J. Am. Chem. Soc.* **1983**, *105*, 6167; (c) Hubig, S. M.; Bockman, T. M.; Kochi, J. K., Optimized Electron Transfer in Charge-Transfer Ion Pairs. Pronounced Inner-Sphere Behavior of Olefin Donors. *J. Am. Chem. Soc.* **1996**, *118*, 3842; (d) Mulliken, R. S., Molecular compounds and their spectra. III. The interaction of electron donors and acceptors. *J. Phys. Chem.* **1952**, *56*, 801.

20. Fox, M. A.; Younathan, J.; Fryxell, G. E., Photoinitiation of the SRN1 reaction by excitation of charge-transfer complexes. *J. Org. Chem.* **1983**, *48*, 3109.

21. Sankararaman, S.; Haney, W. A.; Kochi, J. K., Aromatic nitration with ion radical pairs [ArH.cntdot.+NO2.cntdot.] as reactive intermediates. Time-resolved studies of charge-transfer activation of dialkoxybenzenes. *J. Am. Chem. Soc.* **1987**, *109*, 5235.

22. Tobisu, M.; Furukawa, T.; Chatani, N., Visible Light-mediated Direct Arylation of Arenes and Heteroarenes Using Diaryliodonium Salts in the Presence and Absence of a Photocatalyst. *Chem. Lett.* **2013**, *42*, 1203.

23. Davies, J.; Booth, S. G.; Essafi, S.; Dryfe, R. A. W.; Leonori, D., Visible-Light-Mediated Generation of Nitrogen-Centered Radicals: Metal-Free Hydroimination and Iminohydroxylation Cyclization Reactions. *Angew. Chem. Int. Ed. Engl.* **2015**, *54*, 14017.

24. Arceo, E.; Jurberg, I. D.; Álvarez-Fernández, A.; Melchiorre, P., Photochemical activity of a key donor–acceptor complex can drive stereoselective catalytic α -alkylation of aldehydes. *Nat Chem* **2013**, *5*, 750.

25. Franz, J. F.; Kraus, W. B.; Zeitler, K., No photocatalyst required – versatile, visible light mediated transformations with polyhalomethanes. *Chem. Commun.* **2015**, *51*, 8280.

26. (a) Pandey, G., Photoinduced electron transfer (PET) in organic synthesis. In *Photoinduced Electron Transfer V*, Mattay, J., Ed. Springer Berlin Heidelberg: Berlin, Heidelberg, 1993; pp 175; (b) Mattay, J., Charge Transfer and Radical Ions in Photochemistry. *Angew. Chem. Int. Ed. Engl.* **1987**, *26*, 825; (c) Kavarnos, G. J.; Turro, N. J., Photosensitization by reversible electron transfer: theories, experimental evidence, and examples. *Chem. Rev.* **1986**, *86*, 401.

27. Wypych, J.-C.; Nguyen, T. M.; Bénéchie, M.; Marazano, C., Reaction of Aldimine Anions with Vinamidinium Chloride: Three-Component Access to 3-Alkylpyridines and 3-Alkylpyridinium Salts and Access to 2-Alkyl Glutaconaldehyde Derivatives. *J. Org. Chem.* **2008**, *73*, 1169.

28.(a) Raghunadh, A.; Meruva, S. B.; Kumar, N. A.; Kumar, G. S.; Rao, L. V.; Syam Kumar, U. K., An Efficient and Practical Synthesis of Aryl and Hetaryl α -Keto Esters. *Synthesis* **2012**, *44*, 283; (b) Lenihan, B. D.; Shechter, H., Chemistry of Conversions of [o-[1-Halo-1-(p-tolylsulfonyl)alkyl]benzyl]trimethylsilanes to o-Quinodimethanes and Benzocyclobutenes. *J. Org. Chem.* **1998**, *63*, 2086; (c) Zhang, G.-B.; Wang, F.-X.; Du, J.-Y.; Qu, H.; Ma, X.-Y.; Wei, M.-X.; Wang, C.-T.; Li, Q.; Fan, C.-A., Toward the Total Synthesis of Palhinine A: Expedient Assembly of Multifunctionalized Isotwistane Ring System with Contiguous Quaternary Stereocenters. *Org. Lett.* **2012**, *14*, 3696; (d) 5,5-Dibromo-2,2-dimethyl-1,3-dioxane-4,6-dione. In *Encyclopedia of Reagents for Organic Synthesis*.

29. A UV-Vis study is included in the SI.

30.(a) Here, EDA complex is likely halogen bonding interaction between haloalkane and amine; (b) Blackstock, S. C.; Lorand, J. P.; Kochi, J. K., Charge-transfer interactions of amines with tetrahalomethanes. X-ray crystal structures of the donor-acceptor complexes of quinuclidine and diazabicyclo [2.2.2]octane with carbon tetrabromide. *J. Org. Chem.* **1987**, *52*, 1451; (c) Cavallo, G.; Metrangolo, P.; Milani, R.; Pilati, T.; Priimagi, A.; Resnati, G.; Terraneo, G., The Halogen Bond. *Chem. Rev.* **2016**, *116*, 2478; (d) Sun, C.; Chang, W.; Ma, W.; Chen, C.; Zhao, J., Photoreductive Debromination of Decabromodiphenyl Ethers in the Presence of Carboxylates under Visible Light Irradiation. *Environ. Sci. Technol.* **2013**, *47*, 2370.

31.(a) Semenov, S. N.; Belding, L.; Cafferty, B. J.; Mousavi, M. P. S.; Finogenova, A. M.; Cruz, R. S.; Skorb, E. V.; Whitesides, G. M., Autocatalytic Cycles in a Copper-Catalyzed Azide-Alkyne Cycloaddition Reaction. *J. Am. Chem. Soc.* **2018**, *140*, 10221; (b) Ferrer Flegeau, E.; Bruneau, C.; Dixneuf, P. H.; Jutand, A., Autocatalysis for C-H Bond Activation by Ruthenium(II) Complexes in

Catalytic Arylation of Functional Arenes. *J. Am. Chem. Soc.* **2011**, *133*, 10161; (c) Bissette, A. J.; Fletcher, S. P., Mechanisms of Autocatalysis. *Angew. Chem. Int. Ed. Engl.* **2013**, *52*, 12800.

32. Böhm, A.; Bach, T., Radical Reactions Induced by Visible Light in Dichloromethane Solutions of Hünig's Base: Synthetic Applications and Mechanistic Observations. *Chem. Eur. J.* **2016**, *22*, 15921.

33.(a) Taft, R. W., *Progress in Physical Organic Chemistry*. Wiley: 2009; (b) Guieu, V.; Izquierdo, A.; Garcia-Alonso, S.; André, C.; Madaule, Y.; Payrastré, C., Fluorescent Streptocyanine Dyes: Synthesis and Photophysical Properties – Synthesis of a New Hemicarboxonium Salt. *Eur. J. Org. Chem.* **2007**, *2007*, 804.

34.(a) Raghavachari, R., *Near-Infrared Applications in Biotechnology*. Taylor & Francis: 2000; (b) Bricks, J. L.; Kachkovskii, A. D.; Slominskii, Y. L.; Gerasov, A. O.; Popov, S. V., Molecular design of near infrared polymethine dyes: A review. *Dyes and Pigments* **2015**, *121*, 238; (c) Ishchenko, A. A., Structure and spectral-luminescent properties of polymethine dyes. *Russ. Chem. Rev.* **1991**, *60*, 865.

35.(a) Shindy, H. A., Fundamentals in the chemistry of cyanine dyes: A review. *Dyes Pigm* **2017**, *145*, 505; (b) Panigrahi, M.; Dash, S.; Patel, S.; Mishra, B. K., Syntheses of cyanines: a review. *Tetrahedron* **2012**, *68*, 781; (c) Hunger, K., *Industrial Dyes: Chemistry, Properties, Applications*. Wiley: 2007.

36.(a) Le Guennic, B.; Jacquemin, D., Taking Up the Cyanine Challenge with Quantum Tools. *Acc. Chem. Res.* **2015**, *48*, 530; (b) Lenhard, J. R.; Cameron, A. D., Electrochemistry and electronic spectra of cyanine dye radicals in acetonitrile. *J. Phys. Chem.* **1993**, *97*, 4916; (c) Schreiber, M.; Buß, V.; Fülischer, M. P., The electronic spectra of symmetric cyanine dyes: A CASPT2 study. *Phys. Chem. Chem. Phys.* **2001**, *3*, 3906; (d) Gayton, J. N.; Autry, S.; Fortenberry, R. C.; Hammer, N. I.; Delcamp, J. H., Counter Anion Effect on the Photophysical Properties of Emissive Indolizine-Cyanine Dyes in Solution and Solid State. *Molecules* **2018**, *23*, 3051; (e) Levitz, A.; Marmarchi, F.; Henary, M., Introduction of various substitutions to the methine bridge of heptamethine cyanine dyes Via substituted dianil linkers. *Photochem. Photobiol. Sci.* **2018**, *17*, 1409; (f) Taniguchi, M.; Lindsey, J. S., Database of Absorption and Fluorescence Spectra of >300 Common Compounds for use in PhotochemCAD. *Photochem. Photobiol.* **2018**, *94*, 290.

- 37.(a) Ryzhova, O.; Tarabara, U.; Trusova, V.; Kurutos, A. In *Aggregation of cyanine dyes in lipid environment*, 2015 International Young Scientists Forum on Applied Physics (YSF), 29 Sept.-2 Oct. 2015; 2015; pp 1; (b) Lu, T.; Lin, Z.; Ren, J.; Yao, P.; Wang, X.; Wang, Z.; Zhang, Q., The Non-Specific Binding of Fluorescent-Labeled MiRNAs on Cell Surface by Hydrophobic Interaction. *PLoS One* **2016**, *11*, e0149751.
- 38.Miyamoto, N.; Kuroda, K.; Ogawa, M., Visible Light Induced Electron Transfer and Long-Lived Charge Separated State in Cyanine Dye/Layered Titanate Intercalation Compounds. *J. Phys. Chem. B* **2004**, *108*, 4268.
- 39.(a) Zhao, J.; Chen, C.; Ma, W., Photocatalytic Degradation of Organic Pollutants Under Visible Light Irradiation. *Top Catal* **2005**, *35*, 269; (b) Yang, S.; Tian, H.; Xiao, H.; Shang, X.; Gong, X.; Yao, S.; Chen, K., Photodegradation of cyanine and merocyanine dyes. *Dyes and Pigments* **2001**, *49*, 93; (c) Touthkine, A.; Nguyen, D.-V.; Hahn, K. M., Merocyanine Dyes with Improved Photostability. *Org. Lett.* **2007**, *9*, 2775; (d) Renikuntla, B. R.; Rose, H. C.; Eldo, J.; Waggoner, A. S.; Armitage, B. A., Improved Photostability and Fluorescence Properties through Polyfluorination of a Cyanine Dye. *Org. Lett.* **2004**, *6*, 909; (e) Wang, M.; Holmes-Davis, R.; Rafinski, Z.; Jedrzejewska, B.; Choi, K. Y.; Zwick, M.; Bupp, C.; Izmailov, A.; Paczkowski, J.; Warner, B.; Koshinsky, H., Accelerated Photobleaching of a Cyanine Dye in the Presence of a Ternary Target DNA, PNA Probe, Dye Catalytic Complex: A Molecular Diagnostic. *Anal. Chem.* **2009**, *81*, 2043; (f) Sha, X.-L.; Niu, J.-Y.; Sun, R.; Xu, Y.-J.; Ge, J.-F., Synthesis and optical properties of cyanine dyes with an aromatic azonia skeleton. *Org Chem Front* **2018**, *5*, 555.
- 40.(a) Ivanov, I. V.; Dolotov, S. M.; Kobeleva, O. I.; Valova, T. M.; Barachevsky, V. A.; Traven, V. F., Photoactivation of fluorescence of rhodamine dyes in the presence of haloalkanes. *Russ. Chem. Bull.* **2013**, *62*, 1195; (b) Diethyl Dibromomalonate. In *Encyclopedia of Reagents for Organic Synthesis*.
- 41.Zou, L.-H.; Li, Y.-C.; Li, P.-G.; Zhou, J.; Wu, Z., Solvent-Controlled α -Monobromination, α,α -Dibromination or Imidation of 1,3-Diketones with N-Bromosuccinimide. *Eur. J. Org. Chem.* **2018**, *2018*, 5639.

42. Tajbakhsh, M.; Khazaei, A.; Mahalli, M. S.; Vaghi, R. G., N,N-DIBROMOBENZENESULFONAMIDE: A USEFUL REGENRABLE REAGENT FOR BROMINATION OF VARIOUS CARBANIONIC SUBSTRATES. *Phosphorus, Sulfur, and Silicon and the Related Elements* **2004**, *179*, 1159.
43. Wu, P.; Xu, S.; Xu, H.; Hu, H.; Zhang, W., One-pot syntheses of α,α -dibromoacetophenones from aromatic alkenes with 1,3-dibromo-5,5-dimethylhydantoin. *Tetrahedron Lett.* **2017**, *58*, 618.
44. Wu, C.; Xin, X.; Fu, Z.-M.; Xie, L.-Y.; Liu, K.-J.; Wang, Z.; Li, W.; Yuan, Z.-H.; He, W.-M., Water-controlled selective preparation of α -mono or α,α' -dihalo ketones via catalytic cascade reaction of unactivated alkynes with 1,3-dihalo-5,5-dimethylhydantoin. *Green Chem.* **2017**, *19*, 1983.
45. Jayaraman, A.; Cho, E.; Kim, J.; Lee, S., Decarboxylative Tribromination for the Selective Synthesis of Tribromomethyl Ketone and Tribromovinyl Derivatives. *Adv. Synth. Catal.* **2018**, *360*, 3978.
46. Corey, E. J.; Topie, T. H.; Wozniak, W. A., Stereochemistry of α -halo ketones. VI. The stereochemistry of α -brominated α -methyl-, α,α -dimethyl-, and α,α' -dibenzylcyclohexanones. *J. Am. Chem. Soc.* **1955**, *77*, 5415.
47. Smela, M. P.; Hoye, T. R., A Traceless Tether Strategy for Achieving Formal Intermolecular Hexadehydro-Diels–Alder Reactions. *Org. Lett.* **2018**, *20*, 5502.
48. Tang, H.; Radosz, M.; Shen, Y., Synthesis and self-assembly of thymine- and adenine-containing homopolymers and diblock copolymers. *J. Polym. Sci., Part A: Polym. Chem.* **2006**, *44*, 5995.
49. Taichi, S.; Wataru, K.; Teruaki, M., Efficient Method for the Preparation of Carboxylic Acid Alkyl Esters or Alkyl Phenyl Ethers by a New-Type of Oxidation–Reduction Condensation Using 2,6-Dimethyl-1,4-benzoquinone and Alkoxydiphenylphosphines. *Bulletin of the Chemical Society of Japan* **2003**, *76*, 1645.
50. (a) Nunes, C. M.; Steffens, D.; Monteiro, A. L., Synthesis of Tri- and Tetrasubstituted Olefins by Palladium Cross-Coupling Reaction. *Synlett* **2007**, *2007*, 0103; (b) Hirose, T.; Miyazaki, Y.; Watabe, M.; Akimoto, S.; Tachikawa, T.; Kodama, K.; Yasutake, M., Trialkylsilylethynyl-substituted

triphenylenes and hexabenzocoronenes: highly soluble liquid crystalline materials and their hole transport abilities. *Tetrahedron* **2015**, *71*, 4714.

51.(a) Delon, L.; Laurent, P.; Blancou, H., New synthesis of polyfluoroalkyl racemic α -amino acids. *J. Fluor. Chem.* **2005**, *126*, 1487; (b) Terent'ev, A. B.; Vasil'eva, T. T.; Mysova, N. E.; Chakhovskaya, O. V., Reactions of Diethyl Dibromomalonate and Ethyl 2,2-Dichloroacetoacetate with Water and Carbonyl Compounds (Aldehydes and Ketones) in the Presence of Pentacarbonyliron. *Russ. J. Org. Chem.* **2004**, *40*, 924.

52.(a) Alinezhad, H.; Tajbakhsh, M.; Tehrani, S. S., **2011**, *32*; (b) Yamada, Y.; Yasuda, H., A Convenient Synthesis of Dialkyl (E)-2,3-Dicyanobutendioates. *Synthesis* **1990**, *1990*, 768.

53.Xing, Y.; Zhang, M.; Ciccarelli, S.; Lee, J.; Catano, B., AuIII-Catalyzed Formation of α -Halomethyl Ketones from Terminal Alkynes. *Eur. J. Org. Chem.* **2017**, *2017*, 781.

54.Frimer, A. A.; Gilinsky-Sharon, P.; Aljadeff, G.; Gottlieb, H. E.; Hameiri-Buch, J.; Marks, V.; Philosof, R.; Rosental, Z., Superoxide anion radical (O₂^{•-})-mediated base-catalyzed autoxidation of enones. *J. Org. Chem.* **1989**, *54*, 4853.

55.Lee, C.-H.; Lee, S.-M.; Min, B.-H.; Kim, D.-S.; Jun, C.-H., Ferric(III) Chloride Catalyzed Halogenation Reaction of Alcohols and Carboxylic Acids Using α,α -Dichlorodiphenylmethane. *Org. Lett.* **2018**, *20*, 2468.

56.(a) Tsurugi, H.; Hayakawa, A.; Kando, S.; Sugino, Y.; Mashima, K., Mixed-ligand complexes of paddlewheel dinuclear molybdenum as hydrodehalogenation catalysts for polyhaloalkanes. *Chem Sci* **2015**, *6*, 3434; (b) Gallucci, R. R.; Going, R., Chlorination of aliphatic ketones in methanol. *J. Org. Chem.* **1981**, *46*, 2532.

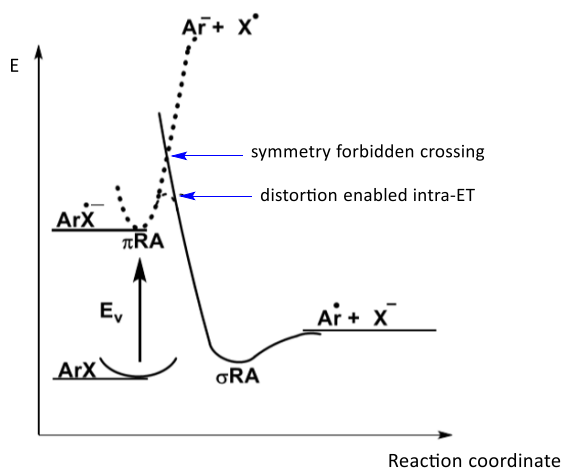
CHAPTER IV

COUPLING PHOTOCATALYSIS AND SUBSTITUTION CHEMISTRY; ENGAGING NON- REDOX ACTIVE HALIDES

4.1 Introduction

The use of visible light in conjunction with visible light absorbing catalysts to drive reactions has the potential to be energy efficient, green, and can reveal new mechanistic possibilities that enable synthesis.¹ Often, central to these methods is the controlled generation of radicals which are the critical reactive intermediates² whose formation is enabled and governed by absorption of a photon by the photocatalyst. Alternatively, the photocatalyst may first undergo oxidation or reduction by another reagent before interacting with the substrate. Some substrates that can be reductively activated by SET include aryl halides³ and pseudo-halides.⁴ Reaction is possible due to the relatively low-lying unoccupied pi-star orbitals of the aromatic system into which an electron is transferred. En route to radical formation, an intramolecular electron transfer (ET) to the C–X sigma* orbital takes place, allowing the critical mesolytic fragmentation which yields the halide ion and carbon centered radical (scheme 4.1).⁵ The rate of this intramolecular ET is dependent on a number of factors, including the energy of the pi*-orbitals, and electronic overlap with the fragmenting groups, among other factors.^{5b, 6-7} Practically speaking, useful rates of radical anion fragmentation are observed for ipso substituted halides, and alpha halo species, but drops with greater structural separation, and represents a real mechanistic limitation of radical anion fragmentation mechanism.

Scheme 4.1 Radical anion fragmentation⁶

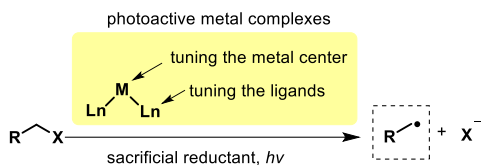


This sensitivity to structure is particularly revealing in the case of benzylic halides in which the rate of fragmentation becomes highly dependent on the structure and functional groups attached to the aromatic component which result in significant variation in the reduction potential and the nature of the orbitals involved.^{7b, 7c} In general, the substantial variation in reduction potential (scheme 4.2d) of the substrates prevents the development of broadly applicable methodology.

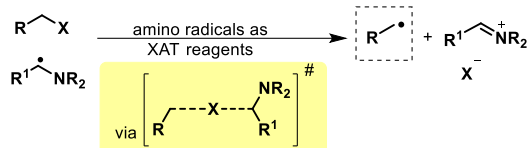
Recently, several diverse strategies have been explored to engage such aliphatic halides that would otherwise be hard to directly engage photocatalytically. Evolution of the photocatalyst structure aimed at pushing the reduction limits has been pursued by several groups⁸ (scheme 4.2a). As such, low-valent group 6 (Cr, Mo, W) isocyanide complexes have demonstrated very appealing photophysical and redox attributes,⁸ and some early success in photoredox transformations of difficult substrates.^{8b, 8c} Remarkably, Gray & Rachford have introduced the homoleptic arylisocyanide tungsten complex $W(CNIph)_6$ as one of the most powerful photoreductant that has been generated with visible light. The estimated reduction potential for the $[W(CNIph)_6]^+/*W$ couple is -2.8 V (vs $Cp_2Fe^{+/0}$). Further, Teets and co-workers have reported a new class of heteroleptic bis-cyclometalated iridium photosensitizers with the general formula $Ir(ppy)_2(NacNac)$, which have excited-state reduction potentials more potent than *fac*- $Ir(ppy)_3$, by ~ 300 – 500 mV.^{8d}

Scheme 4.2. Emerging strategies for radical formation

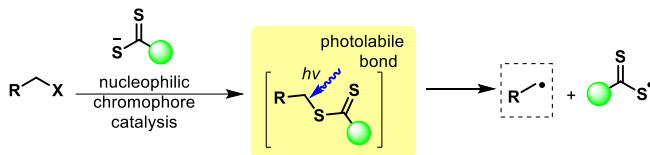
a) Expanding the reduction potential limits by photocatalyst design



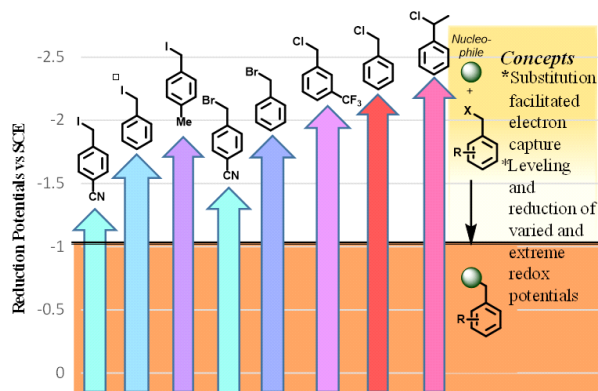
b) Use of alpha amino radicals as halogen atom transfer reagent



c) Nucleophilic chromophore bond weakening



d) Nucleophilic enabled electron capture



Alternatively, Leonori has recently proposed the use of alpha amino radicals to facilitate halogen transfer (scheme 4.2b).⁹ The alkyl and aryl halides are converted to carbon radicals by halogen-atom transfer (XAT) using α -aminoalkyl radicals. Generated alkyl radicals can be utilized to construct new carbon-carbon bonds under mild conditions with high chemoselectivity. More relevant to this work, Melchiorre has identified a clever system that capitalizes on the electrophilicity of alkyl halides to be displaced by a nucleophilic chromophore, dithioacid anion (scheme 4.2c).¹⁰ Upon displacement of the alkyl halide with a nucleophilic chromophore, the alkyl substrate which was optically transparent becomes photoactive, and after absorption of a photon, undergoes homolysis of the inherently weak C-

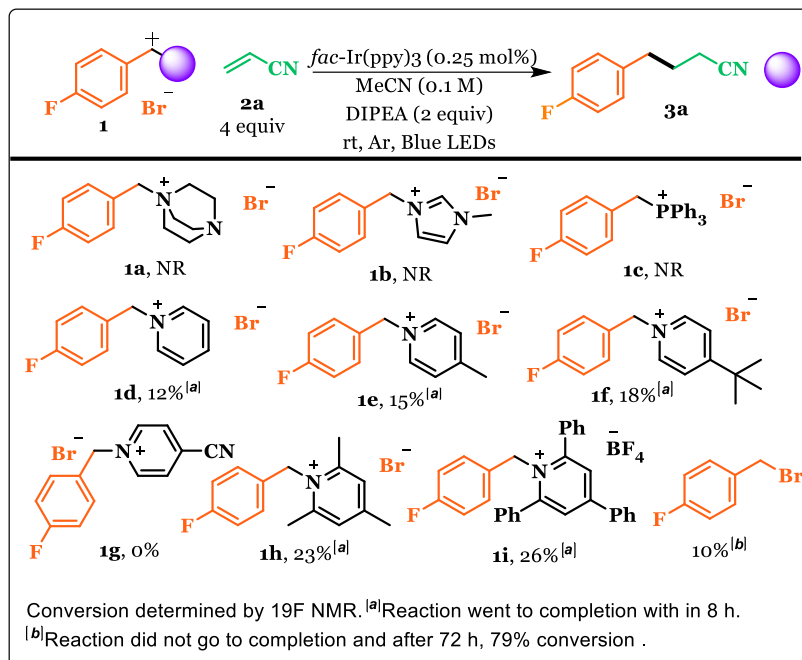
S bond. In the catalytic cycle, dithioacid anion is regenerated by formal reduction of the sulfur radical. This method allows the generation of alkyl radicals under mild conditions which takes place with high functional group tolerance leading to the development of new C–C and C–X bond forming reactions. One potential liability of this conceptually elegant approach is the inherent coupling of the nucleophilic and the chromophoric functions of the catalyst, which may limit both the scope of reactions and the range of mechanistically diverse reactions that would be possible if these two aspects of the catalysts operated independently.

Thus, we set about to develop a conceptually related idea (scheme 4.2d)¹¹ that capitalized on the electrophilicity of alkyl halides but one that decoupled the photon absorbing aspects of the catalyst from its nucleophilic aspects. Our objective was to identify a nucleophile that, upon addition to the alkyl halide, would serve as the electron capturing component where the halide failed, which could then be reduced by an appropriate photocatalyst. Importantly, this would have the effect of leveling substrate reduction potentials, which are often highly dependent on the exact structure of the alkyl halide. Thus, we began our studies by exploring a Giese type reaction¹² using a range of benzyl bromide derived salts and conditions that have been used for reductive coupling in our lab.¹³

4.2 Generating radicals from non-redox active halides

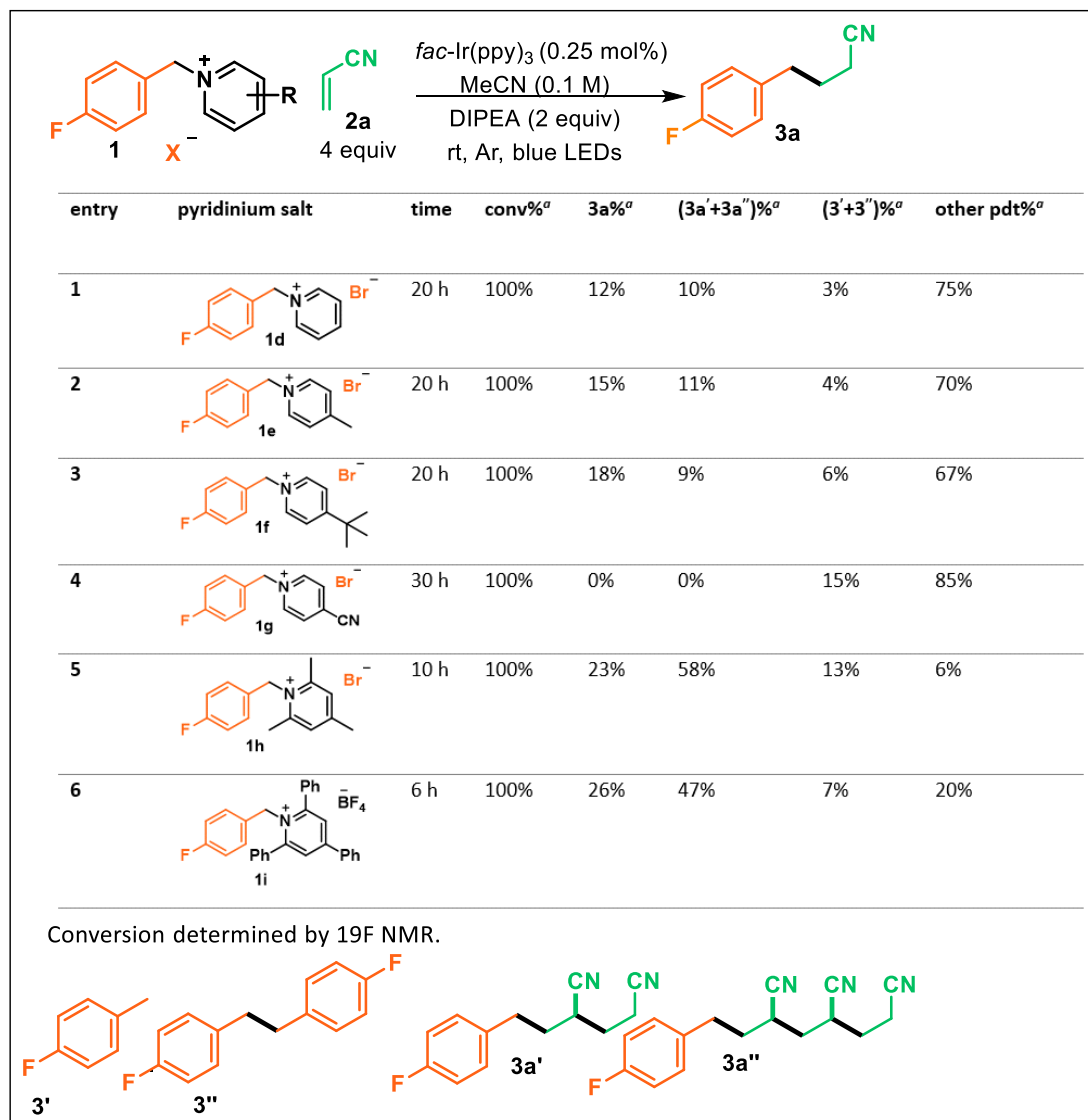
We found that quaternary ammonium, imidazolium, and phosphonium salts showed no reactivity under these conditions (scheme 4.3). Calculation of the molecular orbitals using semi-empirical Hückel calculations demonstrate that the LUMO orbital lies primarily on the fluorobenzene fragment rather than on the added nucleophilic component and explains a lack of reactivity. In contrast, pyridinium 1d, which displays LUMO density on the pyridinium motif, provided the product, albeit in low yield (12%).

Scheme 4.3 Search for redox active salts



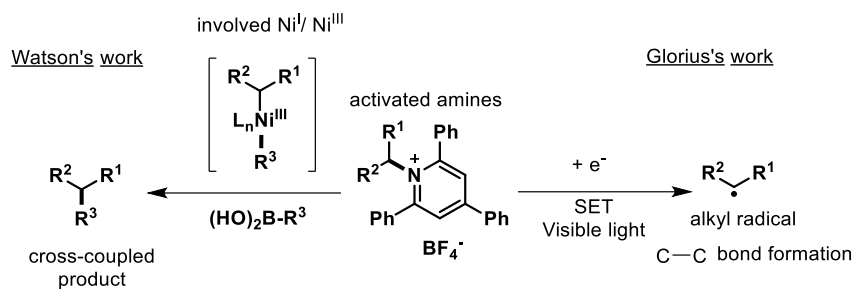
Inspection of the corresponding reaction mixtures by GCMS suggested the formation of fluorobenzylated pyridine byproducts were a major contributor to the mass balance. Thus, we speculated that fluorobenzyl radical was forming under reaction conditions and either attacking the pyridinium salt (1d) or the resulting pyridine in a Minisci-type reaction.¹⁴ Indeed, when the 4-position was blocked (1e and 1f) we observed a slight improvement to the yield, albeit meager. 1g resulted in the formation of a colored EDA complex that was consumed, but did not result in product formation. We next explored both collidinium (1h) and Katritzky¹⁵ (1i) salts, whose susceptible positions were blocked. In both cases, the Minisci-product could not be detected, and yields nearly doubled. All the pyridinium salts' conversion details are given below (scheme 4.4). A direct comparison with the corresponding benzyl bromide revealed the enhanced reactivity of the pyridinium derived salts, suggesting electron capture could be enhanced by substitution.

Scheme 4.4 Redox activity of pyridinium salts



Katritzky salts are formed by condensation of the corresponding primary amine with the commercially available pyrylium salt. In 2017, their application as redoxactive species to construct new C–C bonds was reported. Of particular relevance, Watson¹⁶ reported the first example of a cross-coupling reaction using Katritzky salts through a C–N bond activation of amines with unactivated alkyl groups (scheme 4.5 left). Encouraged by Watson's work, Glorius¹⁷ proposed the generation of similar alkyl radicals via a single-electron-reduction of Katritzky salts using photocatalysis (scheme 4.5 right).

Scheme 4.5 First reports on reduction of Katritzky salts with unactivated alkyl groups



Encouraged by the positive results of our initial exploration and that of Glorius^{17b, 17c} and Lautens^{17b} whose efforts to use of Katritzky salts in deaminative couplings of primary amines via photoredox and other related work^{16, 18} provided strong precedent, and we set out to optimize the reaction conditions (table 4.1). While both the trimethyl- (1h) and triphenyl-pyridinium (1i) salts resulted in the higher yields compared to less substituted versions, a closer inspection of the ¹⁹F NMR spectra of the reaction mixtures revealed that the tri-methyl pyridinium (1h, collidinium) produced far fewer side products (scheme 4.4). Given that tri-phenyl pyridinium (1i) is derived from the corresponding expensive oxopyrylium salt (\$2,376/mol) rather than inexpensive collidine (\$29/mol), we elected to continue optimization using the collidinium salt, 1h. With reductive conditions, that included catalytic Ir(ppy)₃, DIPEA, and blue light, we observed complete conversion within 6 h, but the desired product was minor (23%, entry 1). While minor amounts of radical termination products were identified (3' and 3''), we were encouraged to see that the majority of the mass balance appeared to derived from an intermediate that had formed the desired C-C bond and could, if nudged in the right mechanistic direction, lead to product. More specifically, it appeared that rather than terminating to give the desired product, it underwent one or two propagation steps to give products 3a' and 3a''. Dilution of the reaction mixture (entry 2) somewhat diminished these propagation products and gave a corresponding higher yield, but slowed the reaction. Together these experiments suggested that controlling the rate of termination would be vital to achieving product selectivity. We postulated that identification of the appropriate catalyst could facilitate reduction of the intermediate radical.¹⁹ Indeed, a photocatalyst screen showed

that while iridium catalyst Ir[dF(CF₃)ppy]₂(dtbbpy)PF₆ gave more sluggish conversion (entry 3), the critical ratio of desired to undesired products had improved by an order of magnitude. Furthermore, increasing or decreasing the photocatalyst loading increased (entry 5) or decreased the product ratio (entry 6). Attempts to use NBU₃ (entry 8) instead of DIPEA (entry 3) led to slightly faster conversion but gave substantial amounts of a compound derived from the amine and nitrile.²⁰ A similar adduct was observed using DIPEA, but by comparison it was substantially diminished. Speculating that the off cycle use of the amine was resulting in reaction retardation at higher conversions, we investigated the use of more amine (entry 3 vs 9 and 10). Indeed, moving from 2 equivalents to 4 equivalents increased the conversion from 50% to 100% and the reaction time decreased from 46 h to 16 h. Importantly, as the desired reaction was able to take place throughout the entirety of the reaction, the product distribution shifted in favor of the desired product. With evidence suggesting the involvement of photocatalyst in the termination step, we investigated the effect of water on the reaction (entry 11 and 12). Indeed, the inclusion of 10 equivalents of H₂O further enhanced the product distribution to 29.3:1 and accelerated the reaction (12 h), resulting in an 88% yield. Finally, individual control studies evidenced the critical aspect of each reaction component (entry 13).

Table 4.1 Optimization table

entry	modification	time	conv% ^a	3a% ^a	3a/3a'+3a''
1	none	6 h	100%	23%	0.37
2	MeCN (0.05 M)	10 h	100%	38%	1.36
3	Ir[dF(CF ₃)ppy] ₂ (dtbbpy)PF ₆	46 h	50%	38%	3.5
4	[Ru(bpy) ₃]PF ₆	44 h	1%	0%	0
5	Entry 3 (0.5 mol% photocatalyst)	48 h	70%	52%	5.2
6	Entry 3 (0.05 mol% photocatalyst)	48 h	85%	19%	0.3
7	Entry 3 MeCN (0.05 M)	72 h	39%	33%	5.2
8	Entry 3, NBU ₃ instead of DIPEA	48 h	65%	34%	3.4
9	Entry 3, DIPEA 3 equiv	47 h	79%	66%	6.6
10	Entry 3, DIPEA 4 equiv	16 h	100%	77%	9.63
11	Entry 10, H ₂ O 5 equiv	12 h	100%	85%	21.25
12	Entry 10, H ₂ O 10 equiv	12 h	100%	88%	29.3
13	No amine, no photocatalyst, no light	24 h	0	0	0

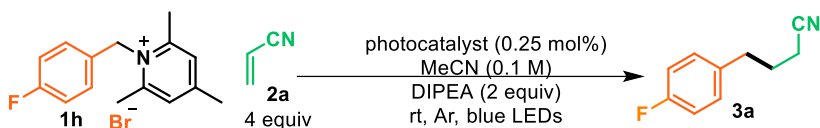
Conversion determined by ¹⁹F NMR.

Radical termination

Radical propagation

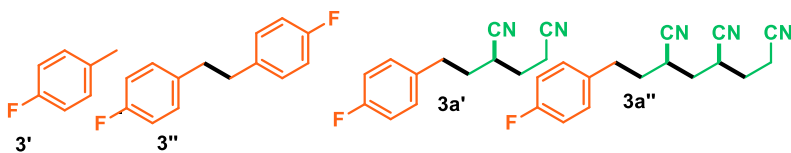
These data were summarized after a broad study that involved variations in several parameters.

Table 4.2 Photocatalyst screening



entry	photocatalyst	time	conv% ^a	3a% ^a	(3a'+3a'')% ^a	(3'+3'')% ^a	3a/(3a'+3a'')
1	<i>fac</i> -Ir(ppy) ₃	6 h	100%	21%	57%	22%	0.4
2	<i>fac</i> -Ir(4'-tb-ppy) ₃	10 h	100%	19%	68%	13%	0.3
3	<i>fac</i> -Ir(4'-F-ppy) ₃	48 h	100%	26%	51%	23%	0.5
4	<i>fac</i> -Ir(4'-CF ₃ -ppy) ₃	72 h	79%	18%	48%	13%	0.4
5	<i>fac</i> -Ir(4'-me-ppy) ₃	48 h	100%	24%	52%	24%	0.5
6	<i>fac</i> -Ir(2',4'-dF-ppy) ₃	44 h	100%	26%	57%	17%	0.5
7	[Ir(3,4'-dm-ppy) ₂ (4,4'-dtb-bpy)]PF ₆	48 h	100%	25%	60%	15%	0.4
8	[Ir(2',4'-dF-5-CF ₃ -ppy) ₂ (4,4'-dtb-bpy)]PF ₆	46 h	50%	38%	11%	1%	3.5
9	[Ir(4,4'-dtb-ppy) ₂ (3,4'-dtb-bpy)]PF ₆	72 h	100%	19%	37%	44%	0.5
10	[Ru(bpz) ₃](PF ₆) ₂	44 h	100%	16%	81%	3%	0.2
11	[Ru(4,4'-me-bpy) ₃](PF ₆) ₂	24 h	100%	10%	90%	0%	0.1
12	[Ru(4,4'-dtb-bpy) ₃](PF ₆) ₂	24 h	100%	14%	86%	0%	0.2
13	[Ru(bpy) ₃]PF ₆	24 h	0%	0%	0%	0%	0
14	Eosin Y	48 h	100%	17%	66%	17%	0.3
15	No photocatalyst	24 h	0%	0%	0%	0%	0

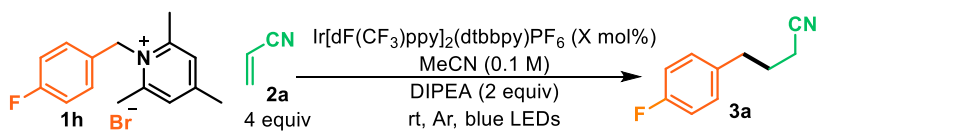
Conversion determined by ¹⁹F NMR.



As indicated by the control experiment (table 4.2, entry 15), the presence of the photocatalyst was required to carry out the reaction. The reactions were monitored quite closely by ¹⁹F NMR to watch how long each reaction takes to reach completion or to give the highest conversion. We began the screening with *fac*-Ir(ppy)₃ (entry 1) and it formed a poor amount of desired product. However, we noticed that the majority of the mass balance appeared from propagation products (3a' and 3a'') that had formed the desired C–C bond. A minor amounts of radical termination products were observed (3' and 3''). More reducing catalyst *fac*-Ir(4'-tb-ppy)₃ (entry 2) formed more propagation products (3a' and

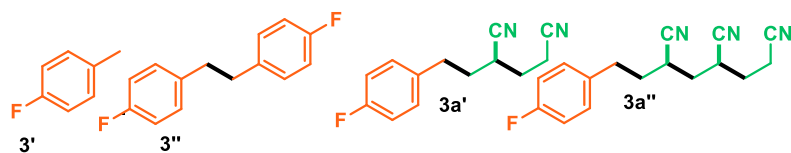
3a'') when compared to *fac*-Ir(ppy)₃. With less reducing Ir catalysts (entries 3, 4, 5 & 6), the reaction was slow and resulted similar product distribution as *fac*-Ir(ppy)₃. Next, the reaction was carried out with more oxidizing heteroleptic Ir catalysts (entries 7, 8 & 9). More specifically, catalyst [Ir(2',4'-dF-5-CF₃-ppy)₂(4,4'-dtb-bpy)]PF₆ (entry 8) formed desired product (38%) rather propagation products (3a' and 3a'') and termination products (3' and 3'') were just 1%. Though, the reaction did not go to completion, we were encouraged to use [Ir(2',4'-dF-5-CF₃-ppy)₂(4,4'-dtb-bpy)]PF₆ for further optimization. The reaction set up with Ru catalysts (entries 10, 11 & 12) resulted more propagation product and [Ru(bpy)₃](PF₆)₂ (entry 13) did not show any reactivity.

Table 4.3 Photocatalyst loading - Ir[dF(CF₃)ppy]₂(dtbbpy)PF₆ (X mol%)



entry	Ir[dF(CF ₃)ppy] ₂ (dtbbpy)PF ₆ (X mol%)	time	conv% ^a	3a% ^a	(3a'+3a'')% ^a	(3'+3'')% ^a	3a/(3a'+3a'')
1	2.5 mol%	48 h	71%	52%	16%	3%	3.3
2	0.5 mol%	48 h	57%	43%	13%	1%	3.3
3	0.25 mol%	48 h	50%	38%	11%	1%	3.5
4	0.05 mol%	48 h	85%	19%	65%	2%	0.3
5	0.025 mol%	48 h	87%	17%	66%	4%	0.3

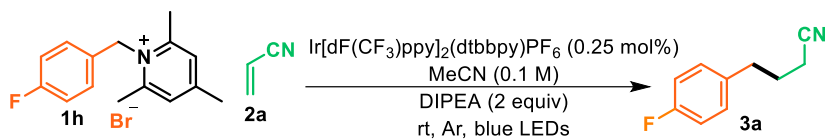
Conversion determined by ¹⁹F NMR.



The catalyst loading experiments revealed that higher concentration of the catalyst (table 4.3, entry 1) produced more desired product (52%). However, the starting material was not fully consumed. With a decrease in concentration of the catalyst, the amount of desired product significantly decreased with a concomitant increase in the amount of propagation product formed. These results suggest that desired product is formed as a result of the photocatalyst, while the formation of the oligomers was less

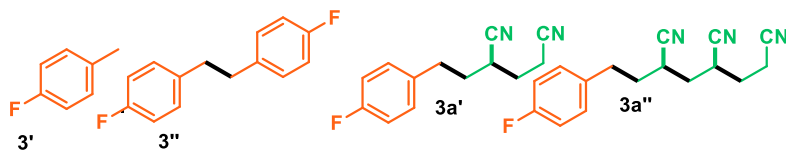
dependent on the photocatalyst. This would be consistent with a reaction that underwent a photocatalyzed termination step, but the by-product could propagate without the photocatalyst.

Table 4.4 Acrylonitrile loading



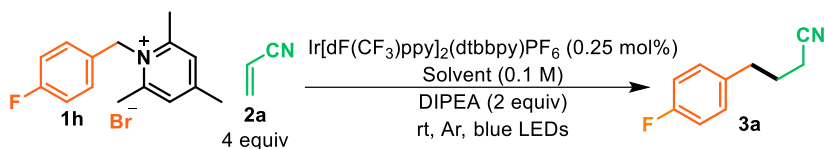
entry	acrylonitrile equivalent	time	conv% ^a	3a% ^a	(3a'+3a'')% ^a	(3'+3'')% ^a	3a/(3a'+3a'')
1	1	48 h	45%	26%	3%	16%	8.7
2	2	48 h	45%	30%	7%	8%	4.3
3	3	48 h	46%	35%	8%	3%	4.4
4	4	48 h	50%	38%	11%	1%	3.5
5	5	48 h	60%	42%	17%	1%	2.5

Conversion determined by ¹⁹F NMR.



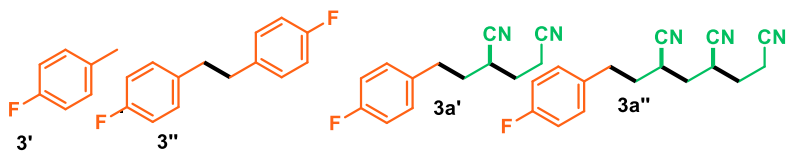
Acrylonitrile loading experiments demonstrated that the amount of desired product formation slightly increased with higher equivalent of acrylonitrile (table 4.4). The starting material was not fully consumed in the presence of 5 equivalent of acrylonitrile.

Table 4.5 Optimization of solvent



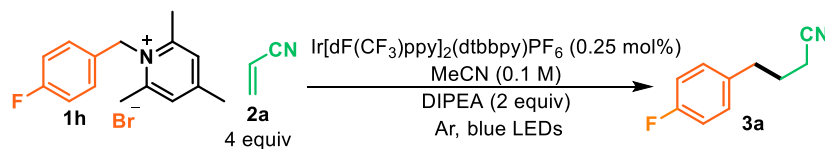
entry	solvent	time	conv% ^a	3a% ^a	(3a'+3a'')% ^a	(3'+3'')% ^a	3a/(3a'+3a'')
1	DMSO	48 h	37%	7%	30%	0%	0.2
2	DMF	48 h	64%	18%	46%	0%	0.4
3	DMA	48 h	89%	25%	60%	4%	0.4
4	MeCN	48 h	50%	38%	11%	1%	3.5
5	DCM	48 h	79%	36%	39%	4%	0.9
6	MeOH	24 h	100%	15%	30%	55%	0.5

Conversion determined by ¹⁹F NMR.



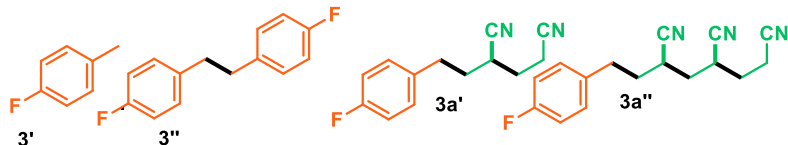
Pyridinium salt 1h is completely soluble in all the above solvents (table 4.5). The reaction carried out in DMSO, DMF, DMA, DCM, and MeOH formed more propagation products (3a' and 3a'').

Table 4.6 Optimization of temperature



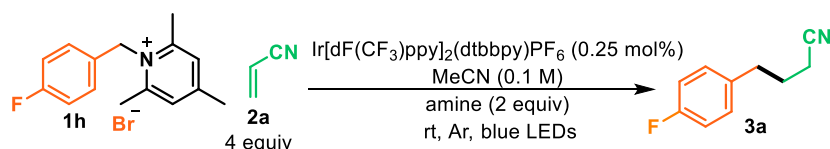
entry	temperature	time	conv% ^a	3a% ^a	(3a'+3a'')% ^a	(3'+3'')% ^a	3a/(3a'+3a'')
1	0 °C	72 h	44%	25%	15%	4%	1.7
2	26 °C	48 h	50%	38%	11%	1%	3.5
3	45 °C	48 h	72%	29%	38%	5%	0.8

Conversion determined by ¹⁹F NMR.



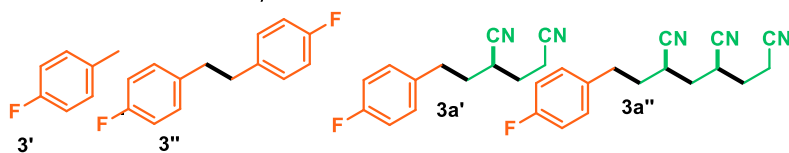
The reaction was slow at 0 °C and formed only 25% of desired product (table 4.6, entry 1). At higher temperature (45 °C), it formed more propagation product and only 29% of desired product.

Table 4.7 Optimization of amine



entry	amine	time	conv% ^a	3a% ^a	(3a'+3a'')% ^a	(3'+3'')% ^a	3a/(3a'+3a'')
1	DIPEA	49 h	50%	38%	11%	1%	3.5
2	Et ₃ N	49 h	21%	19%	2%	0%	9.5
3	Bu ₃ N	49 h	65%	34%	12%	19%	2.8
4	N,N-dimethyl-tert-butylamine	49 h	94%	18%	4%	72%	4.5
5	2,2,6,6-tetramethylpiperidine	42 h	33%	7%	26%	0%	0.3
6	Ethyl 2,2,6,6-tetramethyl-1-piperidineacetate	77 h	95%	5%	90%	0%	0.1
7	2,2,6,6-tetramethyl-1-(phenylmethyl)piperidine	77 h	100%	6%	94%	0%	0.1
8	Morpholine	42 h	15%	3%	12%	0%	0.3
9	N-ethylmorpholine	77 h	100%	23%	44%	33%	0.5
10	No amine	24 h	0%	0%	0%	0%	0

Conversion determined by ¹⁹F NMR.



The presence of the amine was required to carry out the reaction (table 4.7, entry 10). Among all the amines DIPEA formed the highest amount of desired product with better product distribution (entry 1). In the presence of NBu₃, the reaction formed substantial amounts of an undesired compound derived from the addition of the amine to the nitrile, based on GCMS. Presumably this is product arises via the C–H functionalization of the amine, but no attempt to further characterize the adduct was made. Indeed, an analogous adduct was observed using DIPEA, but by comparison, the amount was substantially

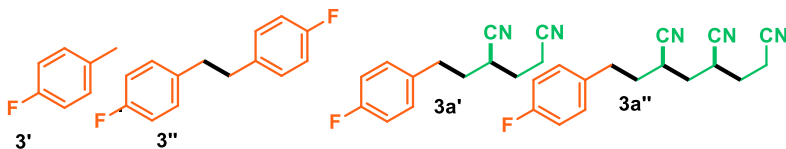
diminished. In the optimization, it was observed that secondary amine reacted with acrylonitrile and formed an *aza-Michael* product rather than the desired product.

Table 4.8 Optimization of DIPEA equivalent



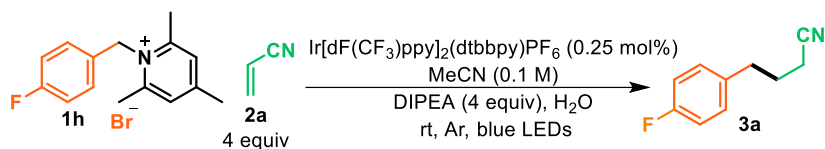
entry	DIPEA equiv	time	conv% ^a	3a% ^a	(3a'+3a'')% ^a	(3'+3'')% ^a	3a/(3a'+3a'')
1	0.8	47 h	19%	10%	9%	0%	1.1
2	1	47 h	20%	14%	6%	0%	2.3
3	2	47 h	50%	38%	11%	1%	3.5
4	3	47 h	79%	66%	10%	3%	6.6
5	4	16 h	100%	77%	8%	15%	9.6

Conversion determined by ¹⁹F NMR.



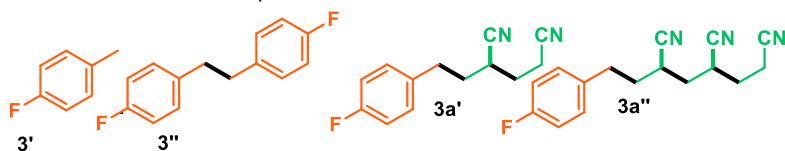
Next, the use of more amine in the reaction was investigated. Indeed, moving from 2 equivalents to 4 equivalents increased the conversion from 50% to 100% and the reaction time decreased from 46 h to 16 h (table 4.8, entry 3, 5). The reaction formed 77% of desired product in the presence of 4 equivalents of DIPEA.

Table 4.9 Effect of water



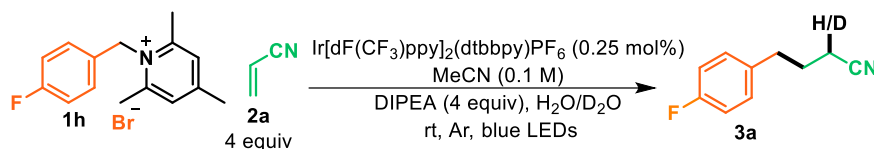
entry	modification	time	conv% ^a	3a% ^a	(3a'+3a'')% ^a	(3'+3'')% ^a	3a/(3a'+3a'')
1	none	16 h	100%	77%	8%	15%	9.6
2	5 equiv H ₂ O	12 h	100%	85%	4%	11%	21.3
3	10 equiv H ₂ O	12 h	100%	88%	3%	9%	29.3
4	15 equiv H ₂ O	15 h	100%	89%	1%	10%	89

Conversion determined by ¹⁹F NMR.



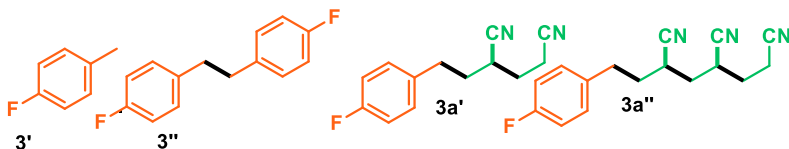
The inclusion of water improved the reaction rate and the product distribution significantly (table 4.9). However, adding 15 equivalents of H₂O caused the reaction slow compared to in the presence of 10 or 5 equivalents of H₂O. The inclusion of 10 equivalents of water resulted 88% desired product within 12 h.

Table 4.10 Deuterium incorporation



entry	modification	time	conv% ^a	3a-H/D% ^a	(3a'+3a'')% ^a	(3'+3'')% ^a	3a/(3a'+3a'')
1	no H ₂ O	16 h	100%	77%	8%	15%	9.6
2	10 equiv H ₂ O	12 h	100%	88%	3%	9%	29.3
3	10 equiv H ₂ O, d-MeCN	12 h	100%	83%	5%	12%	16.6
4	10 equiv D ₂ O	20 h	100%	89%	3%	8%	29.7
5	10 equiv D ₂ O, d-MeCN	20 h	100%	88%	3%	8%	29.3

Conversion determined by ¹⁹F NMR.

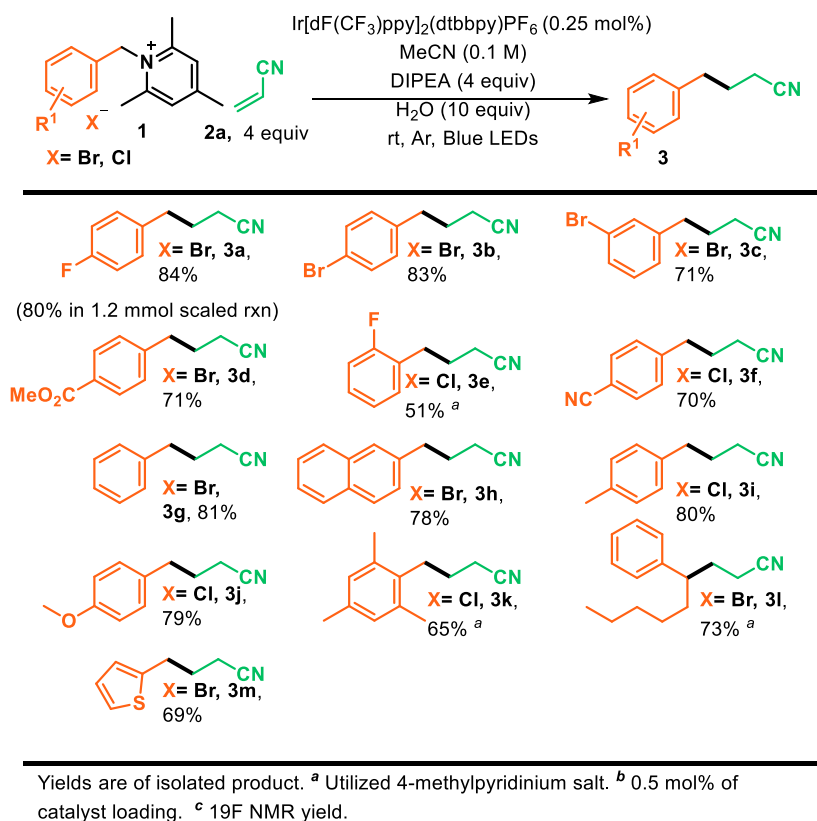


While the inclusion of 10 equivalents of H₂O (table 4.10, entry 2) resulted 88% yield within 12 h, the addition of 10 equivalents of heavy water (entry 4) slowed the reaction (20 h), but resulted in a similar product distribution as the reaction with H₂O. This demonstrates a substantial solvent isotope effect and partially affirmed the protic nature of the termination step. This will be discussed in detail in the reaction mechanism part.

Having identified optimal conditions (entry 12 in table 4.1), we examined the scope of collidinium salts with acrylonitrile (scheme 4.6). Thus, a range of collidinium salts were prepared. To our delight, the reaction worked well for benzylic collidinium salts with electron withdrawing - (3a, 3d, and 3f) neutral-groups (3b, 3c, and 3g) and electron-donating (3i and 3j)- which would have been a challenging feat for the corresponding halides. In addition, this strategy could be extended to sterically demanding, ortho flanked, benzylic substrates (3e and 3k) by use of the 4-methyl pyridine derived salts. Apparently, the bulk of benzyl component, which made nucleophilic substitution more challenging, also served to

protect these salts from undergoing Minisci-type benzylation which we had observed earlier with less sterically demanding benzyl pyridinium salts. Furthermore, 4-methyl pyridinium salt of a secondary benzylic substrate (3l) also gave a good yield, highlighting the ability to rapidly alter the carbon framework of the substrates. The mild reaction conditions are compatible with a wide range of functional groups such as a nitrile (3f), ester (3d), ethers (3j) and bromides (3b and 3c). Importantly, all of these substrates were engaged photocatalytically using the same conditions—a feat that would have been challenging using the corresponding halides given their range of reduction potentials. The collidinium salts offer some protection to otherwise sensitive heterocycles such as thiophene²¹ (3m) and naphthalene²² (3h), which might be expected to undergo radical addition upon themselves. We expect the broad functional group tolerance to facilitate further synthetic elaboration.

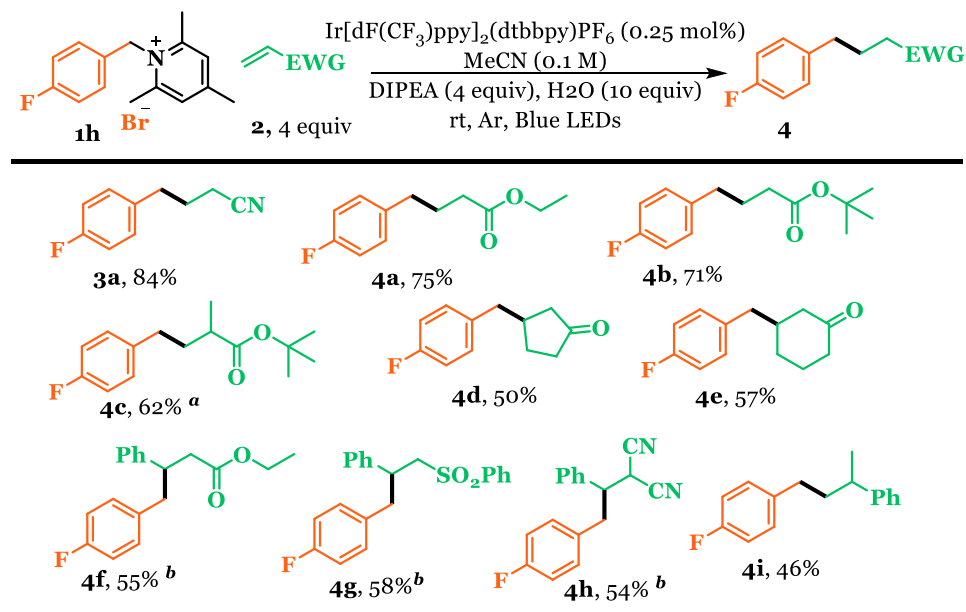
Scheme 4.6 Scope of pyridinium salts



The use of the bench stable, crystalline collidinium salts also facilitate workup of the reaction. Simple extraction followed by acidic washes removes any excess DIPEA, collidine by-product, and any unreacted collidinium salts- though it was not typical to find any unconsumed starting material. This is in stark contrast to the Katritzky salt that produces triphenyl pyridine which must be removed chromatographically. Likewise, if the benzyl halide were used, any excess would also be expected to need to be removed from the organic extracts.

Next, we examined the scope of the alkene receptor partner (scheme 4.7). A range of electron- deficient alkenes worked well in the reaction. While the ester substituent of acrylates exhibited minimal influence (4a and 4b), alpha substitution (methacrylate 4c) was slightly more prone to propagation. Similarly, beta substitution (cinnamate, 4f) gave the product in modest yield.

Scheme 4.7 Scope of acceptors



Yields are of isolated product. ^a 0.5 mol% of catalyst loading. ^b ¹⁹F NMR yield.

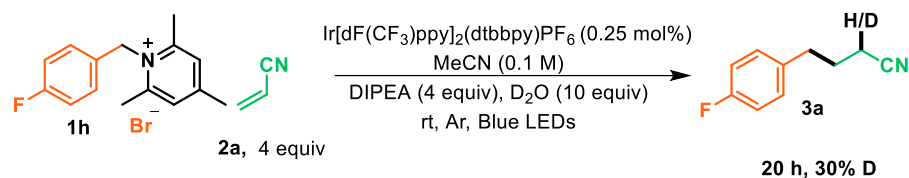
Cyclic enones proved competent (4d, and 4e) giving the benzylated products in good yield after isolation. Furthermore, with no further optimization unsaturated sulfones (4g), alkylidene malononitriles (4h) also proved reasonably competent. Interestingly, the use of styrene was also

possible, though it resulted in the formation of higher order oligomers which led to a more challenging isolation (4i). The broad substrate scope, i.e. both electronically activated and unactivated alkenes, suggests different reaction mechanisms may be operative across the scope.

Turning to the mechanism, a Stern-Volmer analysis was performed using the photocatalyst Ir[dF(CF₃)ppy]₂(dtbbpy)PF₆, collidinium salt 1h, and DIPEA (scheme 4.9C). Rather than observing quenching by the collidinium salt, we observed enhanced fluorescence of the salt. This is likely due to the anion metathesis that inevitably occurs upon addition which Yoon has shown can affect fluorescence of these types of photocatalysts.²³ However, DIPEA did quench the photocatalyst, suggesting a reductive quenching pathway is operative.

Our working understanding of the reaction (scheme 4.9A) begins with the irradiation of the photocatalyst Ir(III) to give an excited state catalyst Ir(III)* which is a strong oxidant (Ir*(III)/Ir(II) = 1.21 V vs SCE in CH₃CN).²⁴ This results in electron transfer from the tertiary amine to give Ir(II) and DIPEA-radical cation (DIPEA ~0.50 V).²⁵ Next, the reducing Ir(II) (Ir(II/III) = -1.37 V vs SCE)²⁴ is expected to undergo SET to the collidinium salt 1g, (E_{1/2} = estimated -1.27 V vs SCE in DMF)²⁶ giving the collidinium radical, I, and completing cycle A. Subsequently, radical I undergoes unimolecular fragmentation²⁷ to give collidine and benzylic radical, II. Addition of II to acrylonitrile generates radical intermediate III. HAT from the amine radical cation yields product (path a). However, several observations called this simple explanation into question, namely, the effect of photocatalyst loading on the product distribution (Table 4.1, entries 1, 5 and 6), and enhanced rate and selectivity upon addition of water (entry 12). We set up an experiment to observe a solvent kinetic isotope effect by replacing 10 equivalents of H₂O with D₂O (scheme 4.8). Indeed, we observed a solvent kinetic isotope effect.

Scheme 4.8 Deuterium incorporation experiment

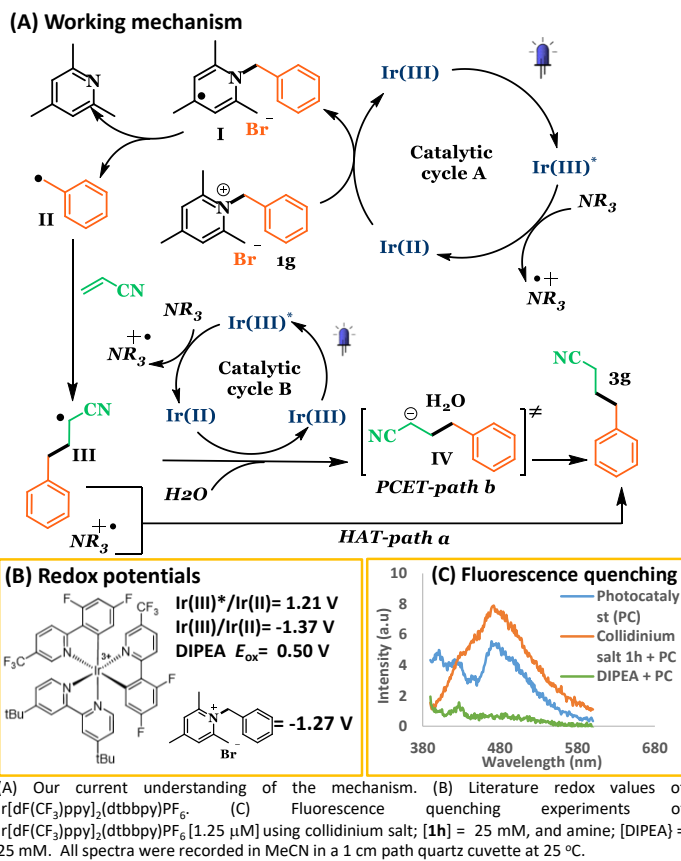


entry	time	k_H/k_D
1	1 h	No detectable deuterium incorporation
2	2 h	2.03
3	4 h	1.97
4	8 h	1.87

At 2 hours into the reaction, we found a solvent kinetic isotope effect of $k_H/k_D = 2.0$ (based on ^1H NMR conversions). Furthermore, a deuterium incorporation experiment revealed that use of D_2O resulted in only partial incorporation of the deuterium (30%) in the alpha position of the nitrile product. Given the O–H bond strength of water (118.8 kcal/mol)²⁸ and the $\text{C}_{\text{alpha}}\text{--H}$ bond strength of the product (89.0 kcal/mol),²⁹ HAT from water is improbable. However, protium incorporation (70%) in the presence of D_2O , suggests that HAT (path a) is indeed occurring—the likely donor being the DIPEA radical cation.^{1c}

³⁰ The observed rate enhancement of the desired reaction upon inclusion of water may be due to a proton-coupled electron transfer (path B) that facilitates a reduction of the radical to carbanion IV (estimated reduction potential ~ -0.9 – -1.1).³¹ Given that the photocatalyst concentration is expected to influence the lifetime of III, which may also undergo oligimerization, it is expected to impact product distribution— which we observe.

Scheme 4.8 Working mechanism



The addition of KI to the reaction of **1h** and acrylonitrile, was shown to significantly retard the rate of the reaction and decrease the yield, which is likely due to redox-active nature of iodide ($\text{I}^-/\text{I}_2 = 0.4 \text{ V}$ vs SCE in H_2O)³² Consequently, an anion metathesis may be needed if iodides are used in the preparation of the collidinium salt.

4.3 Summary

We have demonstrated that the use of collidinium salts are a viable strategy that can enable photoredox catalysis to engage previously sluggish, and unreactive alkyl halides in a mild and efficient manner. Practically speaking, we have shown that the collidinium salts are easy to make, handle, photochemically- and bench-stable, crystalline salts, which are redox active alternatives to alkyl

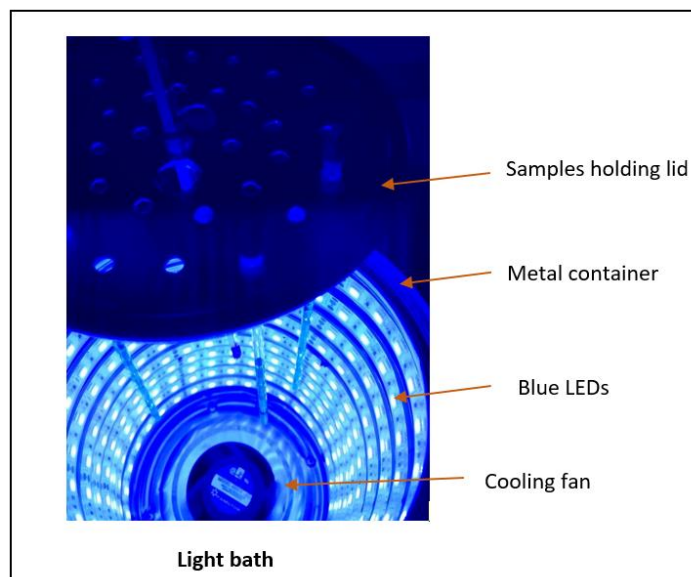
halides. Furthermore, all reaction components are water soluble which facilitates product isolation, and potentially allows their use in biological settings.

4.4 Experimental section

All reagents were obtained from commercial suppliers (Aldrich, VWR, TCI Chemicals, and Oakwood Chemicals) and used without further purification unless otherwise noted. Acetonitrile (CH₃CN) was dried for 48 h over activated 3 Å molecular sieves. Distilled diisopropylethylamine was stored over KOH pellets under an argon atmosphere in an amber bottle.

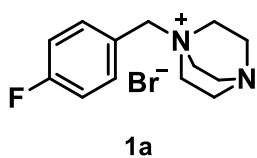
Reactions were monitored by a combination of thin layer chromatography (TLC), (obtained from sorbent technologies Silica XHL TLC Plates, w/UV254, glass backed, 250 µm, 20 x 20 cm) and were visualized with ultraviolet light, potassium permanganate stain, GC-MS (QP 2010S, Shimadzu equipped with auto sampler), ¹⁹F NMR and ¹H NMR (*vide infra*). Isolations were carried out using Teledyne Isco Combiflash Rf 200i flash chromatograph with Redisep Rf normal phase silica (4 g, 12 g, 24 g, 40 g) with product detection at 254 and 288 nm and by ELSD (evaporative light scattering detection). NMR spectra were obtained on a 400 MHz Bruker Avance III spectrometer and Neo 600 MHz. ¹H, ¹⁹F and ¹³C NMR chemical shifts are reported in ppm relative to the residual protio solvent peak (¹H, ¹³C). Mass spectra (HRMS) analysis was performed on LTQ-OrbitrapXL by Thermo Scientific ltd using a Heatedelectrospray ionization (H-ESI) source.

Reactions were set up in a light bath which consists of high intensity Blue LEDs (λ_{max} emission ~ 450 nm) as described below. Blue LEDs (200 LEDs) were wrapped around the inner walls of cylindrical metal container. The lid which was placed on the top of bath made with holes such that reaction tubes were held firmly in the bath. Temperature of the bath was maintained at 26 °C using a cooling fan at the bottom of the metal container.

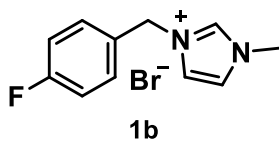


Synthesis of substrates

Synthesis of salts:

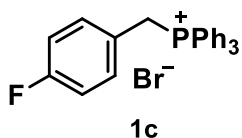


1,4-Diazabicyclo[2.2.2]octane (297 mg, 2.65 mmol, 1equiv) was dissolved in diethyl ether (10 mL). 1-(bromomethyl)-4-fluorobenzene (501 mg, 2.65 mmol, 1 equiv) was added. After stirring the solution for 6 h at room temperature a white precipitate was formed. The precipitate was filtered off and washed thoroughly with hexane and diethyl ether and dried under reduced pressure to afford 1-(4-fluorobenzyl)-1,4-diazabicyclo[2.2.2]octan-1-ium bromide (**1a**) in 90% yield after isolation (718 mg, 2.4 mmol) as a white solid.



1-Methylimidazole (297 mg, 2.65 mmol, 1.1 equiv) was dissolved in acetonitrile (10 mL) and 1-(bromomethyl)-4-fluorobenzene (501 mg, 2.65 mmol, 1equiv) was added. After refluxing the solution for 12 h, the solvent was removed under reduced pressure and the resulting oil was washed thoroughly with hexane and

diethyl ether and dried under reduced pressure to afford 3-(4-fluorobenzyl)-1-methyl-1H-imidazol-3-ium bromide (**1b**) in 80% yield after isolation (575 mg, 2.1 mmol) as a colorless oil. NMR chemical shifts match with the literature values.³²

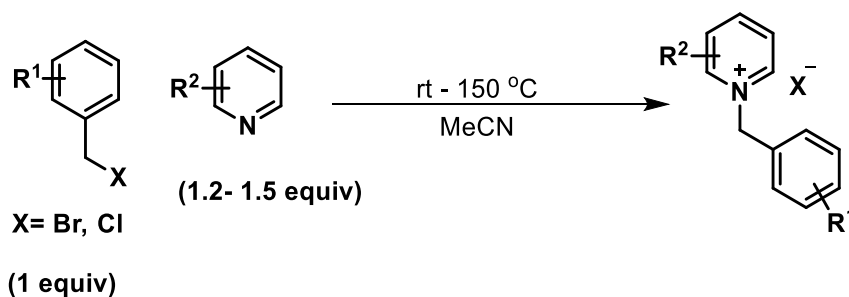


Triphenylphosphine (765 mg, 2.92 mmol, 1.1 equiv) was dissolved in acetonitrile (10 mL) and 1-(bromomethyl)-4-fluorobenzene (501 mg, 2.65 mmol, 1 equiv) was added. After refluxing the solution for 12 h, the solvent was removed under reduced pressure and the resulting oil was washed thoroughly with hexane and diethyl ether and dried under reduced pressure to afford (4-fluorobenzyl)triphenylphosphonium bromide (**1c**) in 75% yield after isolation (896 mg, 2.0 mmol) as a colorless oil. NMR chemical shifts match with the literature values.³³

Synthesis of pyridinium salts:

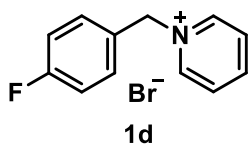
Pyridinium salts were prepared according to general procedure A

General Procedure A

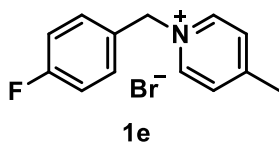


Anhydrous pyridine (1.2- 1.5 equiv) was added to a solution of benzyl bromide or chloride (1 equiv) in dry acetonitrile (~0.5M). Some pyridinium salt syntheses were carried out at room temperature, or under reflux condition (85 °C). The rest of the pyridinium salt syntheses were carried out in microwave reactor or in an oil bath at elevated temperatures using a pressure vial. The progress of the reaction was

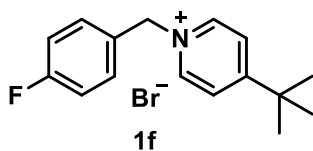
monitored by TLC. After consumption of the starting material, the reaction mixture was allowed to cool to room temperature. Diethyl ether was then added to the reaction mixture and precipitated pyridinium salt was collected by filtration and washed thoroughly with hexane and diethyl ether and dried under reduced pressure.



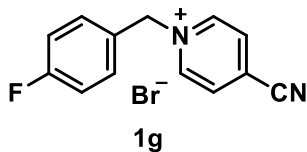
The general procedure **A** was followed using 1-(bromomethyl)-4-fluorobenzene (1.00 g, 5.3 mmol, 1 equiv), pyridine (502 mg, 6.4 mmol, 1.2 equiv) and 10 mL of MeCN and refluxed for 7 h to afford 1-(4-fluorobenzyl)pyridin-1-ium bromide (**1d**) in 95% yield after isolation (1.35 g, 5.0 mmol) as a solid. NMR chemical shifts match with the literature values ³⁴



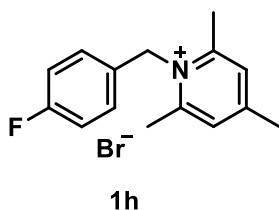
The general procedure **A** was followed using 1-(bromomethyl)-4-fluorobenzene (1.00 g, 5.3 mmol, 1equiv), 4-methylpyridine (595 mg, 6.4 mmol, 1.2 equiv) and 10 mL of MeCN and refluxed for 7 h to afford 1-(4-fluorobenzyl)-4-methylpyridin-1-ium bromide in (**1e**) 96% yield after isolation (1.44 g, 5.1 mmol) as a solid.



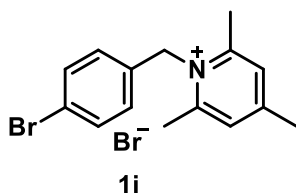
The general procedure **A** was followed using 1-(bromomethyl)-4-fluorobenzene (1.00 g, 5.3 mmol, 1equiv), 4-(tert-butyl)pyridine (864 mg, 6.4 mmol, 1.2 equiv) and 10 mL of MeCN and refluxed for 5 h to afford 4-(tert-butyl)-1-(4-fluorobenzyl)pyridin-1-ium bromide (**1f**) in 96% yield after isolation (1.65 g, 5.1 mmol) as a solid.



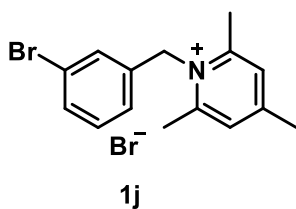
The general procedure **A** was followed using 1-(bromomethyl)-4-fluorobenzene (1.00 g, 5.3 mmol, 1 equiv), isonicotinonitrile (661 mg, 6.4 mmol, 1.2 equiv) and 10 mL of MeCN and refluxed for 5 h to afford 4-(tert-butyl)-1-(4-fluorobenzyl)pyridin-1-ium bromide (**1g**) in 90% yield after isolation (1.4 g, 4.8 mmol) as a solid.



The general procedure **A** was followed using 1-(bromomethyl)-4-fluorobenzene (1.00 g, 5.3 mmol, 1equiv), 2,4,6-trimethylpyridine (968 mg, 8.0 mmol, 1.5 equiv) and 10 mL of MeCN in pressure vial heated to 120 °C in an oil bath for 18 h to afford 1-(4-fluorobenzyl)-2,4,6-trimethylpyridin-1-ium bromide (**1h**) in 88% yield after isolation (1.45 g, 4.7 mmol) as a solid.

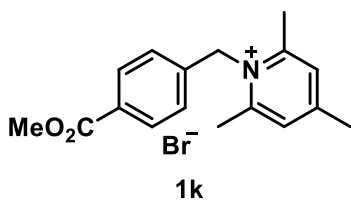


The general procedure **A** was followed using 1-bromo-4-(bromomethyl)benzene (750 mg, 3.0 mmol, 1 equiv), 2,4,6-trimethylpyridine (546 mg, 4.5 mmol, 1.5 equiv) and 5 mL of MeCN in pressure vial heated to 120 °C in an oil bath for 18 h to afford 1-(4-bromobenzyl)-2,4,6-trimethylpyridin-1-ium bromide (**1i**) in 86% yield after isolation (957 mg, 2.6 mmol) as a solid.

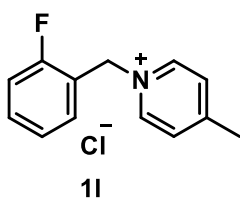


The general procedure **A** was followed using 1-bromo-3-(bromomethyl)benzene (750 mg, 3.0 mmol, 1 equiv), 2,4,6-trimethylpyridine (546 mg, 4.5 mmol, 1.5 equiv) and 5 mL of MeCN in pressure vial heated to 150 °C in a microwave reactor 1.5 h to afford 1-(3-

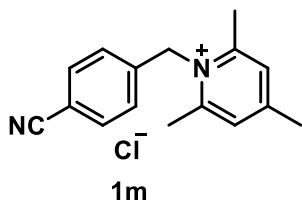
bromobenzyl)-2,4,6-trimethylpyridin-1-ium bromide (**1j**) in 88% yield after isolation (665 mg, 1.8 mmol) as a solid.



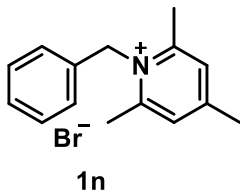
The general procedure **A** was followed using methyl 4-(bromomethyl)benzoate (687 mg, 3.0 mmol, 1 equiv), 2,4,6-trimethylpyridine (546 mg, 4.5 mmol, 1.5 equiv) and 5 mL of MeCN in a pressure vial heated to 150 °C in a microwave reactor for 1.5 h to afford 1-(4-(methoxycarbonyl)benzyl)-2,4,6-trimethylpyridin-1-ium bromide (**1k**) in 70% yield after isolation (735 mg, 2.1 mmol) as a solid.



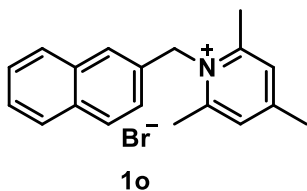
The general procedure **A** was followed using 1-(chloromethyl)-2-fluorobenzene (434 mg, 3.0 mmol, 1equiv), 4-methylpyridine (419 mg, 4.5 mmol, 1.5 equiv) and 5 mL of MeCN in a flask and refluxed for 10 h to afford 1-(2-fluorobenzyl)-4-methylpyridin-1-ium chloride (**1l**) in 80% yield after isolation (571 mg, 2.4 mmol) as a solid.



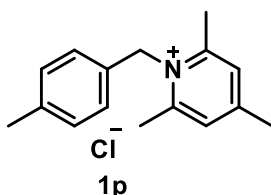
The general procedure **A** was followed using 4-(bromomethyl)benzotrile (582 mg, 3.0 mmol, 1equiv), 2,4,6-trimethylpyridine (546 mg, 4.5 mmol, 1.5 equiv) and 5 mL of MeCN in a pressure vial heated to 120 °C in an oil bath for 24 h to afford 1-(4-cyanobenzyl)-2,4,6-trimethylpyridin-1-ium chloride (**1m**) in 45% yield after isolation (369 mg, 1.35 mmol) as a solid.



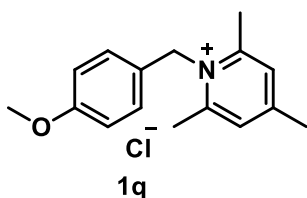
The general procedure **A** was followed using (bromomethyl)benzene (513 mg, 3.0 mmol, 1equiv), 2,4,6-trimethylpyridine (546 mg, 4.5 mmol, 1.5 equiv) and 5 mL of MeCN in pressure vial heated to 150 °C in a microwave reactor for 2 h to afford 1-benzyl-2,4,6-trimethylpyridin-1-ium bromide (**1n**) in 83% yield after isolation (727 mg, 2.5 mmol) as a solid.



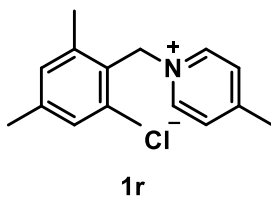
The general procedure **A** was followed using 2-(bromomethyl)naphthalene (663 mg, 3.0 mmol, 1equiv), 2,4,6-trimethylpyridine (546 mg, 4.5 mmol, 1.5 equiv) and 5 mL of MeCN in pressure vial heated to 150 °C in a microwave reactor for 1.5 h to afford 2,4,6-trimethyl-1-(naphthalen-2-ylmethyl)pyridin-1-ium bromide (**1o**) in 60% yield after isolation (616 mg, 1.8 mmol) as a solid.



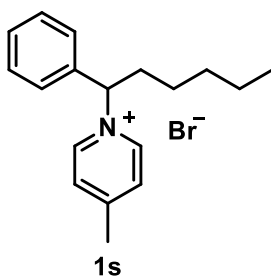
The general procedure **A** was followed using 1-(chloromethyl)-4-methylbenzene (422 mg, 3.0 mmol, 1equiv), 2,4,6-trimethylpyridine (546 mg, 4.5 mmol, 1.5 equiv) and 5 mL of MeCN in pressure vial heated to 120 °C oil bath for 24 h to afford 2,4,6-trimethyl-1-(4-methylbenzyl)pyridin-1-ium chloride (**1p**) in 50% yield after isolation (393 mg, 1.5 mmol) as a solid.



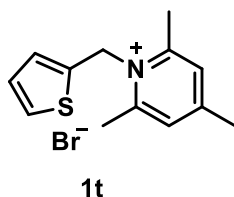
The general procedure **A** was followed using 1-(chloromethyl)-4-methoxybenzene (468 mg, 3.0 mmol, 1 equiv), 2,4,6-trimethylpyridine (546 mg, 4.5 mmol, 1.5 equiv) and 5 mL of MeCN in pressure vial heated to 120 °C in an oil bath for 24 h to afford 1-(4-methoxybenzyl)-2,4,6-trimethylpyridin-1-ium chloride (**1q**) in 60% yield after isolation (500 mg, 1.8 mmol) as a solid.



The general procedure **A** was followed using 2-(chloromethyl)-1,3,5-trimethylbenzene (506 mg, 3.0 mmol, 1equiv), 4-methylpyridine (419 mg, 4.5 mmol, 1.5 equiv) and 5 mL of MeCN and refluxed for 10 h to afford 4-methyl-1-(2,4,6-trimethylbenzyl)pyridin-1-ium chloride (**1r**) in 80% yield after isolation (629 mg, 2.4 mmol) as a solid.

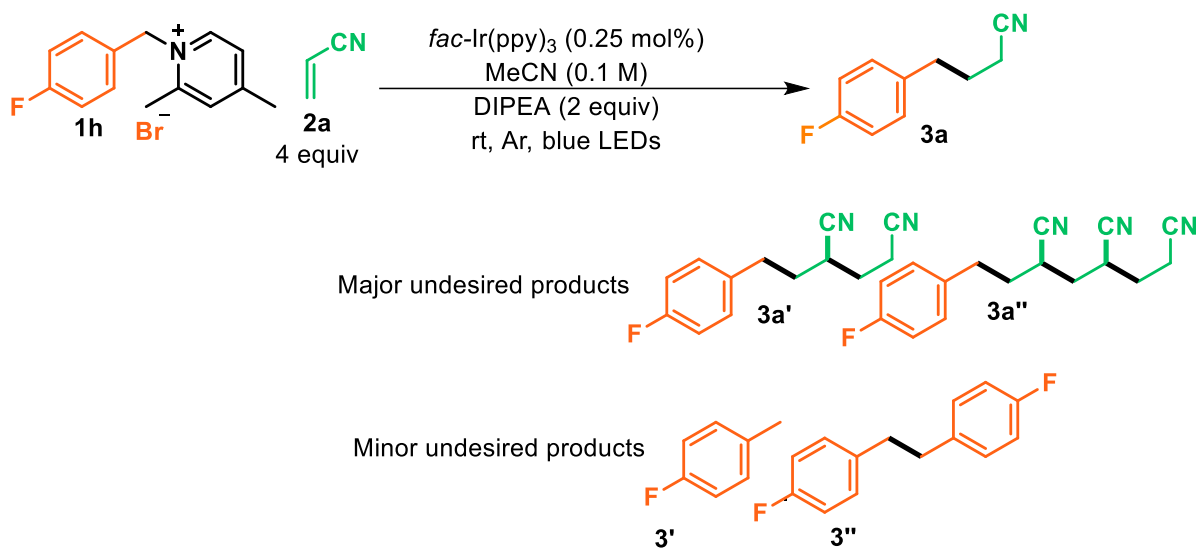


The general procedure **A** was followed using (1-bromohexyl)benzene (723 mg, 3.0 mmol, 1equiv), 4-methylpyridine (419 mg, 4.5 mmol, 1.5 equiv) and 5 mL of MeCN in a flask at room temperature for 24 h to afford 4-methyl-1-(1-phenylhexyl)pyridin-1-ium bromide (**1s**) in 70% yield after isolation (701 mg, 2.1 mmol) as a solid.



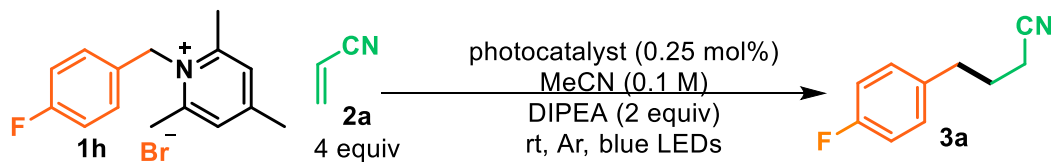
The general procedure **A** was followed using 2-(bromomethyl)thiophene (991 mg, 5.6 mmol, 1equiv), 2,4,6-trimethylpyridine (1.02 g, 8.4 mmol, 1.5 equiv) and 5 mL of MeCN in a flask and refluxed for 10 h to afford 2,4,6-trimethyl-1-(thiophen-2-ylmethyl)pyridin-1-ium bromide (**1t**) in 72% yield after isolation (1.2 g, 4.0 mmol) as a solid.

Optimization of photocatalytic reaction



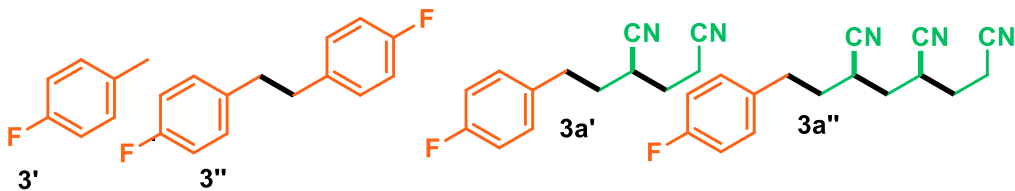
In addition to desired product (**3a**), it formed several undesired products in the reaction. Therefore, a more extensive study that included variations of several parameters and careful optimization was carried out to improve the yield of desired product.

Photocatalyst identity

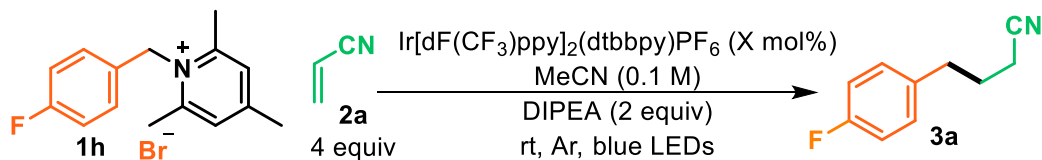


entry	photocatalyst	time	conv% ^a	3a% ^a	(3a'+3a'')% ^a	(3'+3'')% ^a	3a/(3a'+3a'')
1	<i>fac</i> -Ir(ppy) ₃	6 h	100%	21%	57%	22%	0.4
2	<i>fac</i> -Ir(4'-tb-ppy) ₃	10 h	100%	19%	68%	13%	0.3
3	<i>fac</i> -Ir(4'-F-ppy) ₃	48 h	100%	26%	51%	23%	0.5
4	<i>fac</i> -Ir(4'-CF ₃ -ppy) ₃	72 h	79%	18%	48%	13%	0.4
5	<i>fac</i> -Ir(4'-me-ppy) ₃	48 h	100%	24%	52%	24%	0.5
6	<i>fac</i> -Ir(2',4'-dF-ppy) ₃	44 h	100%	26%	57%	17%	0.5
7	[Ir(3,4'-dm-ppy) ₂ (4,4'-dtb-bpy)]PF ₆	48 h	100%	25%	60%	15%	0.4
8	[Ir(2',4'-dF-5-CF ₃ -ppy) ₂ (4,4'-dtb-bpy)]PF ₆	46 h	50%	38%	11%	1%	3.5
9	[Ir(4,4'-dtb-ppy) ₂ (3,4'-dtb-bpy)]PF ₆	72 h	100%	19%	37%	44%	0.5
10	[Ru(bpz) ₃](PF ₆) ₂	44 h	100%	16%	81%	3%	0.2
11	[Ru(4,4'-me-bpy) ₃](PF ₆) ₂	24 h	100%	10%	90%	0%	0.1
12	[Ru(4,4'-dtb-bpy) ₃](PF ₆) ₂	24 h	100%	14%	86%	0%	0.2
13	[Ru(bpy) ₃]PF ₆	24 h	0%	0%	0%	0%	0
14	Eosin Y	48 h	100%	17%	66%	17%	0.3
15	No photocatalyst	24 h	0%	0%	0%	0%	0

Conversion determined by ¹⁹F NMR.

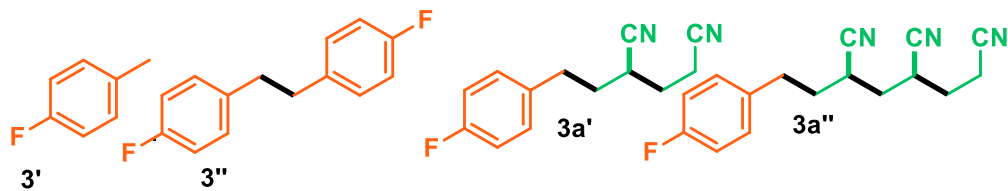


Photocatalyst loading- Ir[dF(CF₃)ppy]₂(dtbbpy)PF₆ (X mol%)

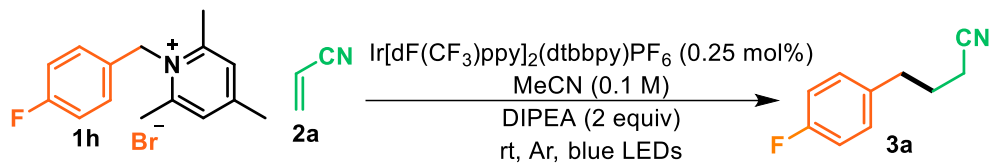


entry	Ir[dF(CF ₃)ppy] ₂ (dtbbpy)PF ₆ (X mol%)	time	conv% ^a	3a% ^a	(3a'+3a'')% ^a	(3'+3'')% ^a	3a/(3a'+3a'')
1	2.5 mol%	48 h	71%	52%	16%	3%	3.3
2	0.5 mol%	48 h	57%	43%	13%	1%	3.3
3	0.25 mol%	48 h	50%	38%	11%	1%	3.5
4	0.05 mol%	48 h	85%	19%	65%	2%	0.3
5	0.025 mol%	48 h	87%	17%	66%	4%	0.3

Conversion determined by ¹⁹F NMR.

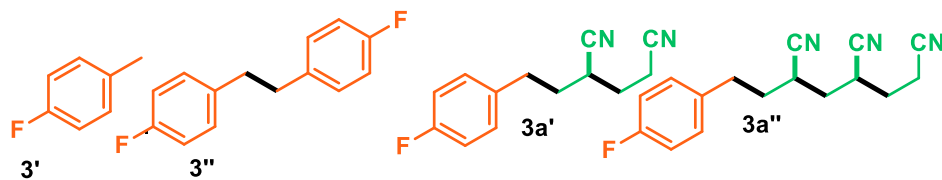


Acrylonitrile loading

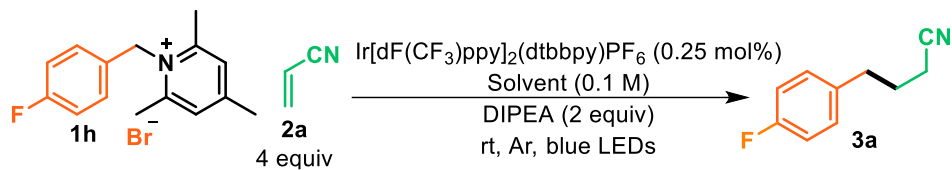


entry	acrylonitrile equivalent	time	conv% ^a	3a% ^a	(3a'+3a'')% ^a	(3'+3'')% ^a	3a/(3a'+3a'')
1	1	48 h	45%	26%	3%	16%	8.7
2	2	48 h	45%	30%	7%	8%	4.3
3	3	48 h	46%	35%	8%	3%	4.4
4	4	48 h	50%	38%	11%	1%	3.5
5	5	48 h	60%	42%	17%	1%	2.5

Conversion determined by ¹⁹F NMR.

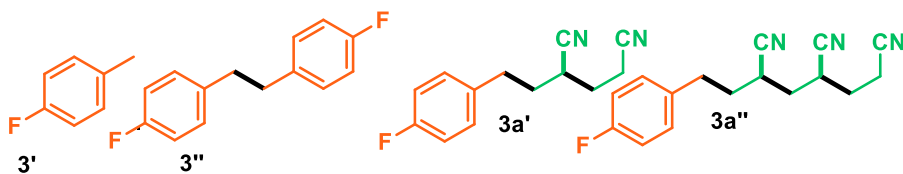


Optimization of solvent



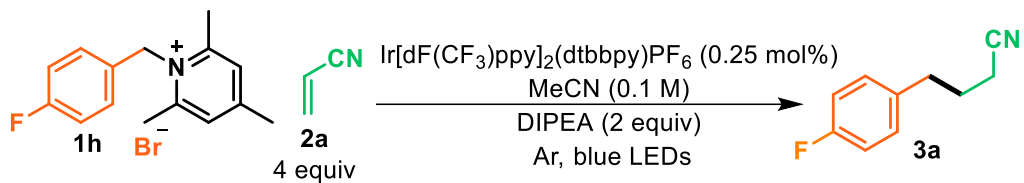
entry	solvent	time	conv% ^a	3a% ^a	(3a'+3a'')% ^a	(3'+3'')% ^a	3a/(3a'+3a'')
1	DMSO	48 h	37%	7%	30%	0%	0.2
2	DMF	48 h	64%	18%	46%	0%	0.4
3	DMA	48 h	89%	25%	60%	4%	0.4
4	MeCN	48 h	50%	38%	11%	1%	3.5
5	DCM	48 h	79%	36%	39%	4%	0.9
6	MeOH	24 h	100%	15%	30%	55%	0.5

Conversion determined by ¹⁹F NMR.



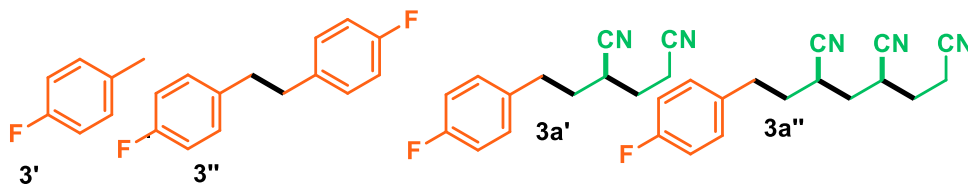
Pyridinium salt **1h** is completely soluble in all the above solvents.

Optimization of temperature

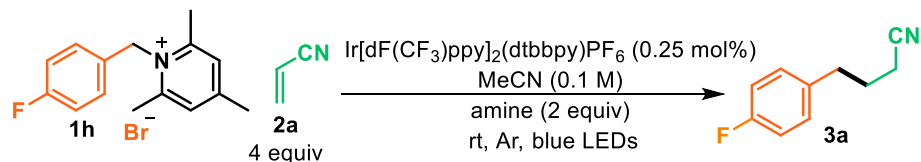


entry	temperature	time	conv% ^a	3a% ^a	(3a'+3a'')% ^a	(3'+3'')% ^a	3a/(3a'+3a'')
1	0 °C	72 h	44%	25%	15%	4%	1.7
2	26 °C	48 h	50%	38%	11%	1%	3.5
3	45 °C	48 h	72%	29%	38%	5%	0.8

Conversion determined by ¹⁹F NMR.

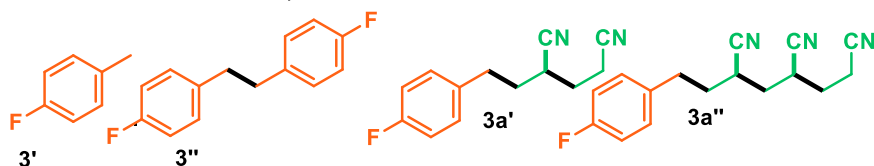


Optimization of amine



entry	amine	time	convl% ^a	3a% ^a	(3a'+3a'')% ^a	(3'+3'')% ^a	3a/(3a'+3a'')
1	DIPEA	49 h	50%	38%	11%	1%	3.5
2	Et ₃ N	49 h	21%	19%	2%	0%	9.5
3	Bu ₃ N	49 h	65%	34%	12%	19%	2.8
4	N,N-dimethyl-tert-butylamine	49 h	94%	18%	4%	72%	4.5
5	2,2,6,6-tetramethylpiperidine	42 h	33%	7%	26%	0%	0.3
6	Ethyl 2,2,6,6-tetramethyl-1-piperidineacetate	77 h	95%	5%	90%	0%	0.1
7	2,2,6,6-tetramethyl-1-(phenylmethyl)piperidine	77 h	100%	6%	94%	0%	0.1
8	Morpholine	42 h	15%	3%	12%	0%	0.3
9	N-ethylmorpholine	77 h	100%	23%	44%	33%	0.5
10	No amine	24 h	0%	0%	0%	0%	0

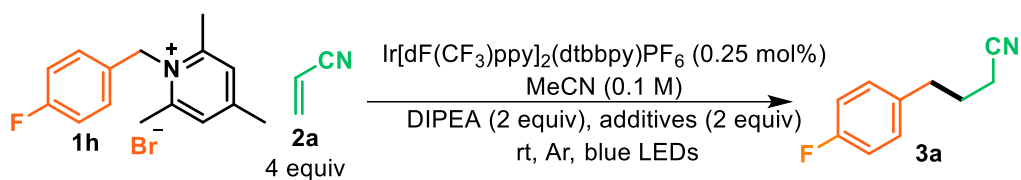
Conversion determined by ¹⁹F NMR.



In the optimization it was observed that secondary amine reacts with acrylonitrile and formed an *aza-Michael* product rather than the desired product.

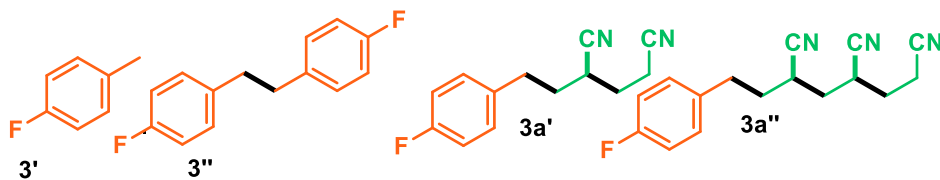
In the presence of NBu₃, the reaction formed substantial amounts of an undesired compound derived from the addition of the amine to the nitrile, based on GCMS. Presumably this is product arises via the C–H functionalization of the amine, but no attempt to further characterize the adduct was made. Indeed, an analogous adduct was observed using DIPEA, but by comparison, the amount was substantially diminished.

Effect of additives

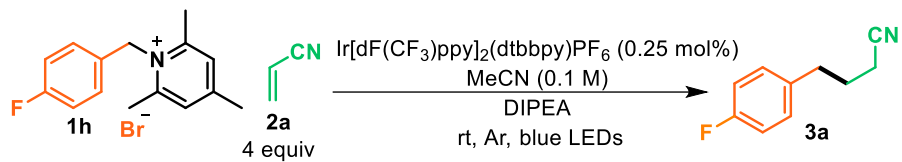


entry	additives	time	conv% ^a	3a% ^a	(3a'+3a'')% ^a	(3'+3'')% ^a	3a/(3a'+3a'')
1	none	46 h	50%	38%	11%	1%	3.5
2	HCOOH	46 h	79%	31%	15%	33%	2.1
3	Hantzsch ester	46 h	100%	85%	9%	6%	9.4
4	KHCO ₃	49 h	69%	62%	7%	0%	8.9

Conversion determined by ¹⁹F NMR.

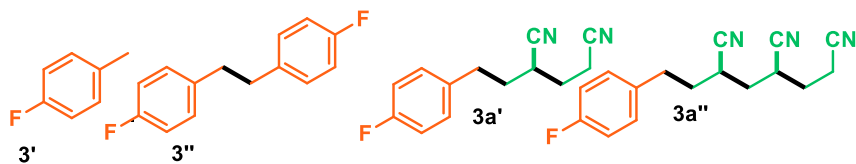


Optimization of DIPEA equivalent

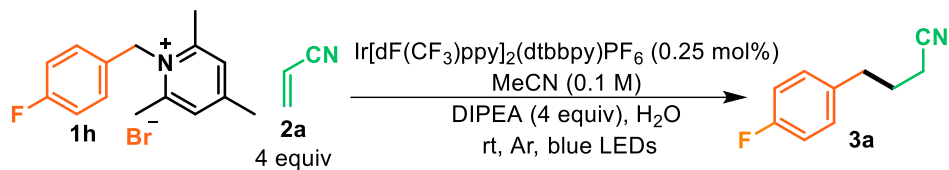


entry	DIPEA equiv	time	conv% ^a	3a% ^a	(3a'+3a'')% ^a	(3'+3'')% ^a	3a/(3a'+3a'')
1	0.8	47 h	19%	10%	9%	0%	1.1
2	1	47 h	20%	14%	6%	0%	2.3
3	2	47 h	50%	38%	11%	1%	3.5
4	3	47 h	79%	66%	10%	3%	6.6
5	4	16 h	100%	77%	8%	15%	9.6

Conversion determined by ¹⁹F NMR.

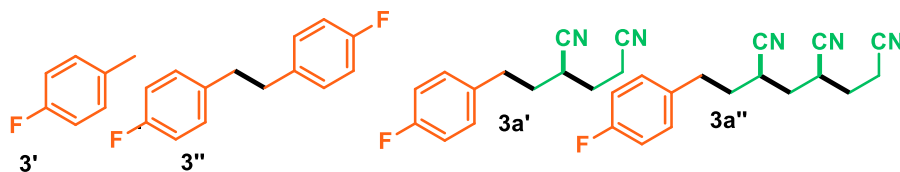


Effect of water

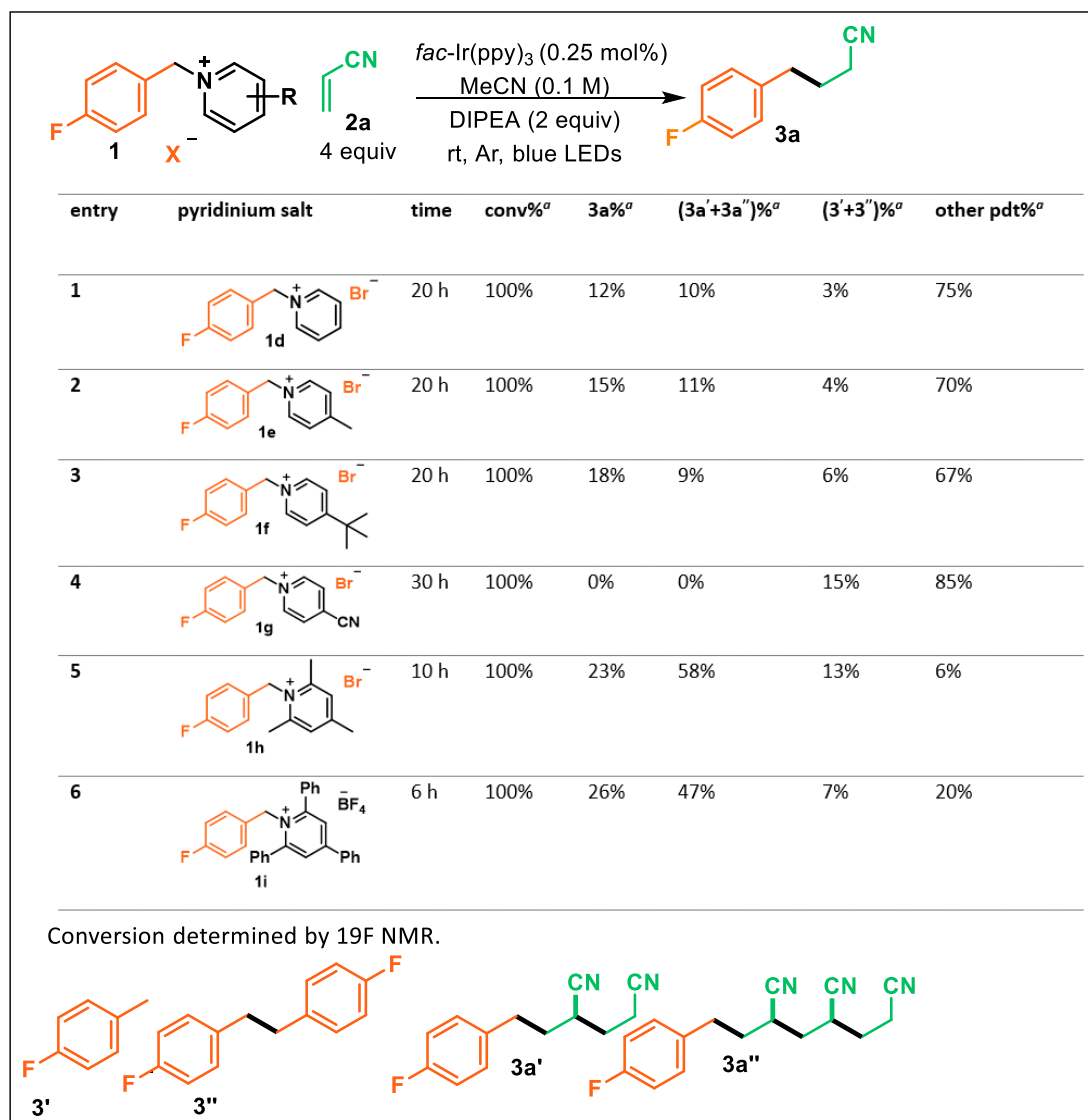


entry	modification	time	conv% ^a	3a% ^a	(3a'+3a'')% ^a	(3'+3'')% ^a	3a/(3a'+3a'')
1	none	16 h	100%	77%	8%	15%	9.6
2	5 equiv H ₂ O	12 h	100%	85%	4%	11%	21.3
3	10 equiv H ₂ O	12 h	100%	88%	3%	9%	29.3
4	15 equiv H ₂ O	15 h	100%	89%	1%	10%	89

Conversion determined by ¹⁹F NMR.

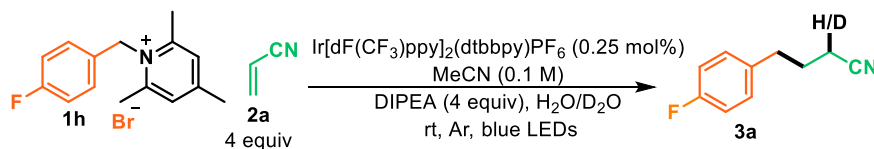


Search for redox active pyridinium salt



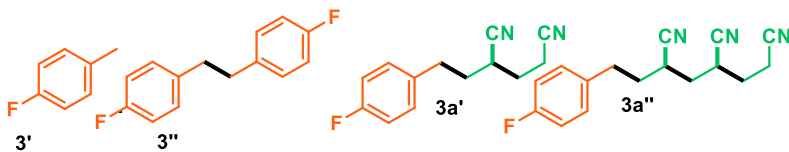
Mechanistic experiments

Deuterium incorporation experiments



entry	modification	time	conv% ^a	3a-H/D% ^a	(3a'+3a'')% ^a	(3'+3'')% ^a	3a/(3a'+3a'')
1	no H ₂ O	16 h	100%	77%	8%	15%	9.6
2	10 equiv H ₂ O	12 h	100%	88%	3%	9%	29.3
3	10 equiv H ₂ O, d-MeCN	12 h	100%	83%	5%	12%	16.6
4	10 equiv D ₂ O	20 h	100%	89%	3%	8%	29.7
5	10 equiv D ₂ O, d-MeCN	20 h	100%	88%	3%	8%	29.3

Conversion determined by ¹⁹F NMR.

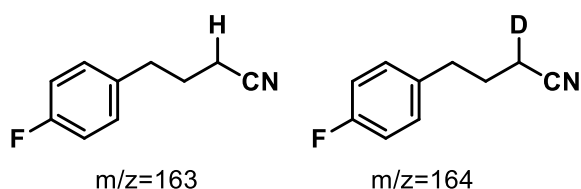


entry	modification	3a-D % ^a
1	10 equiv H ₂ O	9%
2	10 equiv H ₂ O, d-MeCN	11%
3	10 equiv D ₂ O	39%
4	10 equiv D ₂ O, d-MeCN	41%

^a GCMS conversions

Determination of deuterium incorporation:

The reaction was set up according to the general procedure. The reaction was monitored by ^{19}F NMR. After the complete consumption of starting material (**1h**), the volatiles (MeCN, acrylonitrile and some DIPEA) were removed via rotovap and the residue was dissolved in ethyl acetate (6 mL) and washed with 1M aqueous HCl solution (3 x 2 mL) and brine solution (2 mL). The organic layer was dried over anhydrous MgSO_4 and concentrated in vacuo. From the concentrated crudes of entry 1,2,3, and 4 reactions, GCMS samples were prepared with the same concentration and subjected to GCMS (SIM Mode).

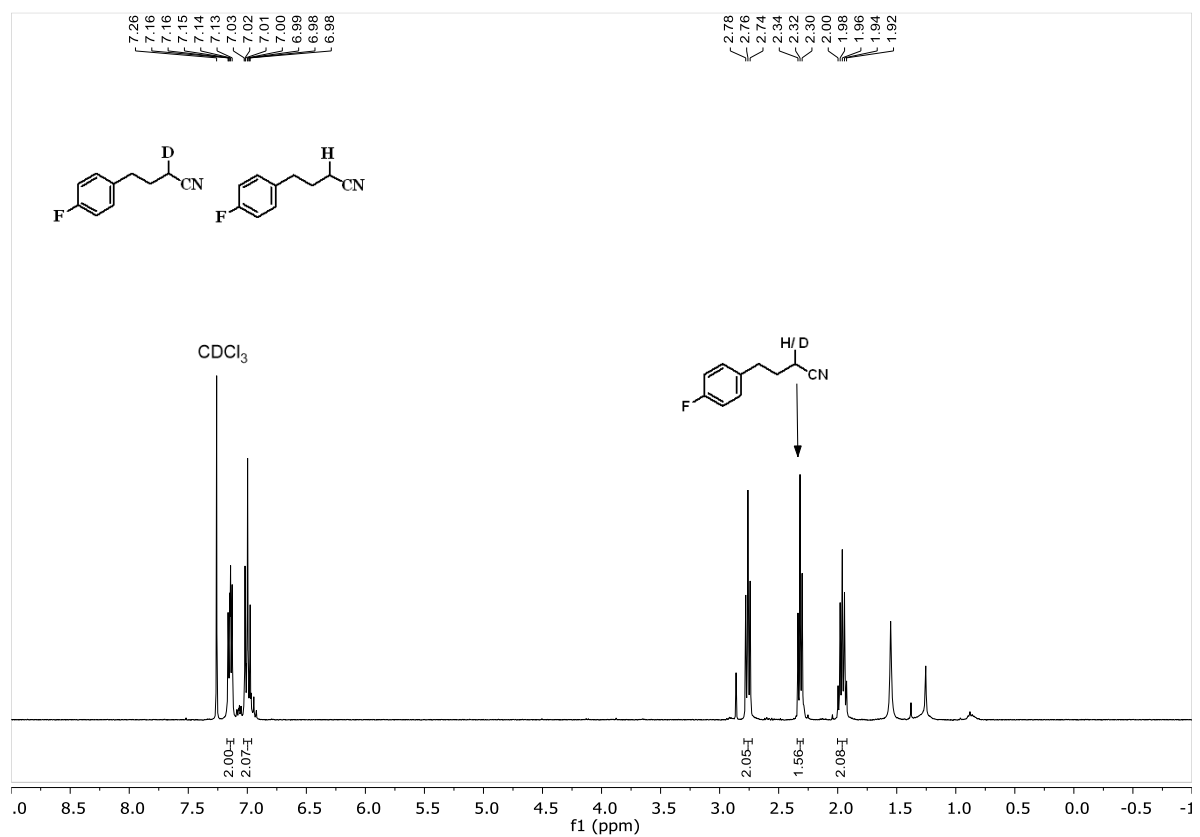


Total Ion Count (TIC) was measured for 163 (M^+) and 164 ($\text{M}+1$) separately. Deuterium incorporated product % was calculated using following formula.

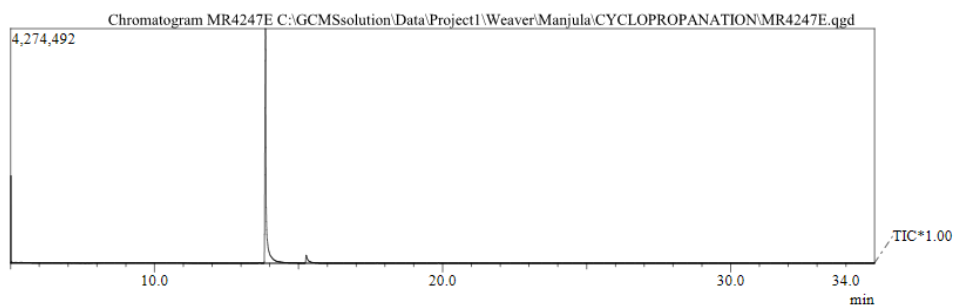
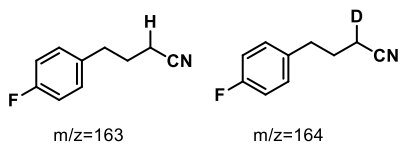
$$\mathbf{3a-D} \% = \text{TIC of (M+1)} / [\text{TIC of (M+1)} + \text{TIC of (M+)}]$$

Deuterium incorporation experiments revealed that D_2O resulted in partial incorporation of the deuterium (30%) at the alpha position to the nitrile product.

¹H NMR of the crude mixture of **3a-H/D** has shown below. The difference in the integration of the highlighted signal (2.32 ppm) is due to the presence of **3a-D**.

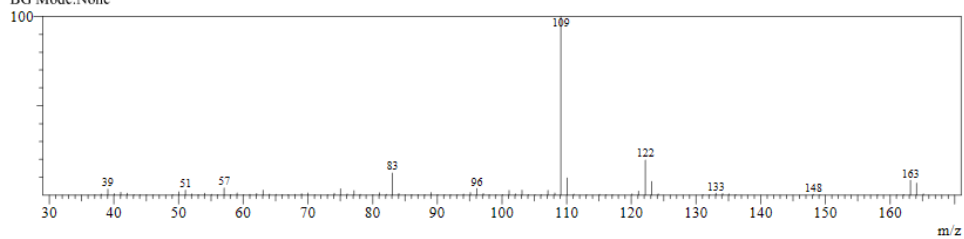


GC and MS of deuterium incorporated product mixture:

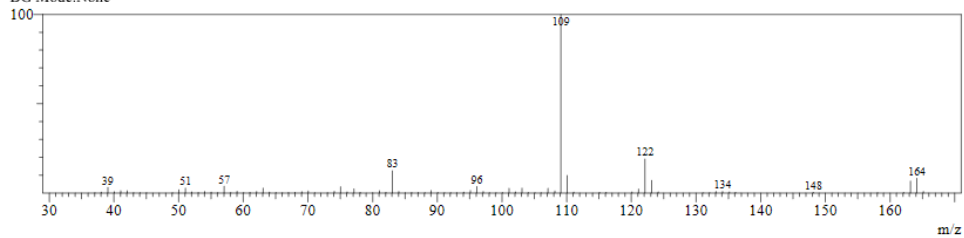


Spectrum

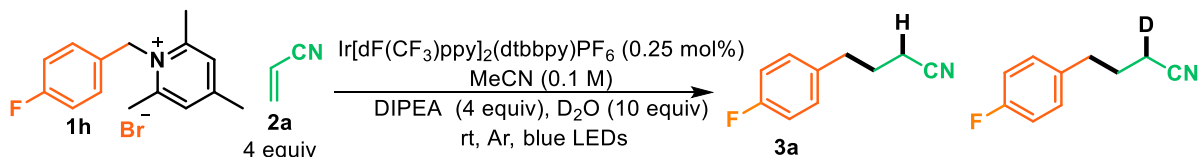
Line#:1 R.Time:13.8(Scan#:1062)
MassPeaks:94
RawMode:Single 13.8(1062) BasePeak:109(1577671)
BG Mode:None



Line#:2 R.Time:13.8(Scan#:1061)
MassPeaks:89
RawMode:Single 13.8(1061) BasePeak:109(1219246)
BG Mode:None



Kinetic isotope effect



entry	time	k_H/k_D
1	1 h	Deuterium incorporation did not observed
2	2 h	2.03
3	4 h	1.97
4	8 h	1.87

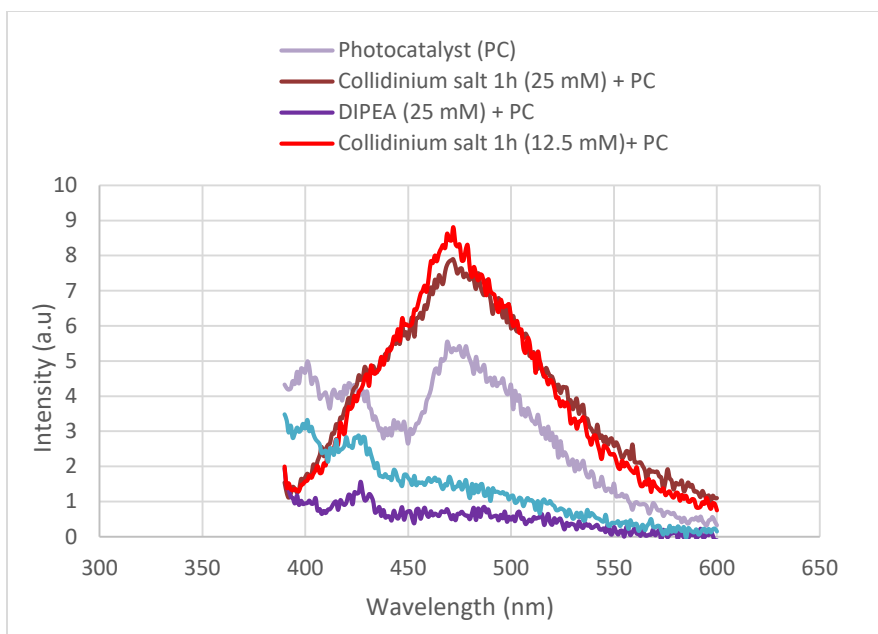
k_H/k_D was calculated based on ¹H NMR conversions.

All the reagents (DIPEA, MeCN) were dried. Then, they were used in the reaction. A 18×150 mm borosilicate tube fitted with a rubber septum was charged with a solution of [Ir(2',4'-dF-5-CF₃-ppy)₂(4,4'-dtbbpy)]PF₆ (0.25 mM, 2.4 mL in MeCN), 1-(4-fluorobenzyl)-2,4,6-trimethylpyridin-1-ium bromide (**1h**) (74.4 mg, 0.24 mmol), DIPEA (0.96 mmol, 124.0 mg 172.6 μL, 4 equiv), DI water (2.4 mmol, 43.2 mg, 43.2 μL, 10 equiv), and acrylonitrile (0.96 mmol, 51 mg, 62.8 μL, 4 equiv). Then the reaction mixture was degassed via Ar bubbling for 15 min and then left under positive Ar pressure by removing the exit needle. The tube was placed in a light bath (description above) which was maintained at 26 °C and the reaction was stirred. Reaction mixture (0.6 ml) was pulled out from the reaction tube for 1 h, 2 h, 4 h and 8 h time points. Each time point reaction mixture was monitored by ¹⁹F NMR. Then a careful work up was carried out. The volatiles (MeCN, acrylonitrile and some DIPEA) were removed via rotovap and the residue was dissolved in ethyl acetate (3 mL) and washed with 1M aqueous

HCl solution (2 x 2 mL) and brine solution (2 mL). The organic layer was dried over anhydrous MgSO₄. The crude product was concentrated *in vacuo* and ¹H NMR was taken with internal standard (1,2,3-Trimethoxybenzene) to calculate deuterium incorporation. Then, k_H/k_D was calculated for each time point.

Quenching study on 1-(4-fluorobenzyl)-2,4,6-trimethylpyridin-1-ium bromide (**1h**) and DIPEA with catalyst [Ir(2',4'-dF-5-CF₃-ppy)₂(4,4'-dtbbpy)]PF₆

2.5 μM solutions of catalyst [Ir(2',4'-dF-5-CF₃-ppy)₂(4,4'-dtbbpy)]PF₆ was prepared in acetonitrile. 50 mM stock solutions of 1-(4-fluorobenzyl)-2,4,6-trimethylpyridin-1-ium bromide (**1h**) and DIPEA were prepared in acetonitrile. 50 mM stock solutions of 1-(4-fluorobenzyl)-2,4,6-trimethylpyridin-1-ium bromide (2 mL) was taken in a vial. 1 mL of this solution was transferred to the second vial and diluted with 1 mL of acetonitrile. 1 mL of this diluted solution was transferred to the third vial and this way a series of dilution was performed. Same dilution was carried out with DIPEA. After that 2.5 μM of catalyst (1 mL) solution was added to all the vials. The solution was mixed properly and the mixture was degassed via Ar bubbling for 5 min and then left under positive Ar pressure by removing the exit needle and fluorescence was measured. Catalyst was excited at 380 nm. The emission was observed at 468 nm for the catalyst.

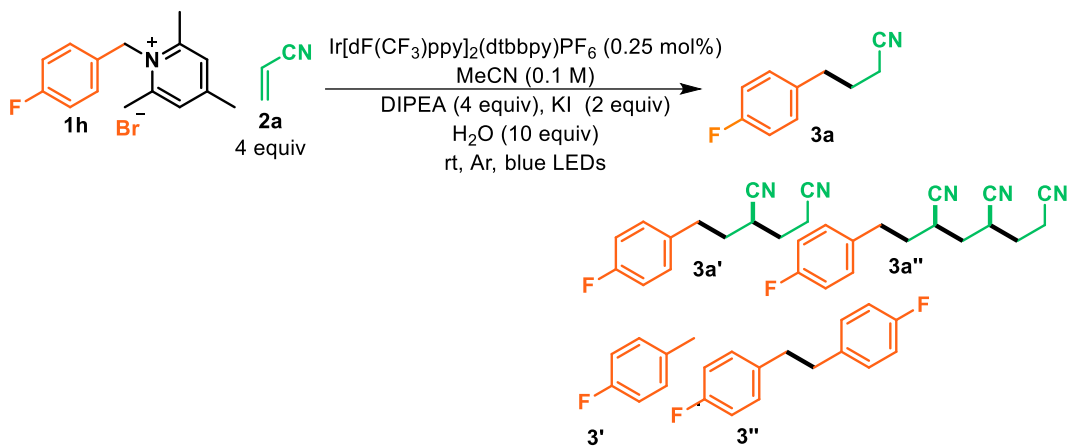


Fluorescence quenching experimental spectra recorded in MeCN in a 1 cm path quartz cuvettes at 25 °C

Rather than observing quenching by the collidinium salt, we observed enhanced fluorescence of the salt. This is likely due to the anion metathesis that inevitably occurs upon addition which Yoon²² has shown can affect fluorescence of these types of photocatalysts. However, DIPEA did quench the photocatalyst, suggesting a reductive quenching pathway is operative.

Effect of KI salt

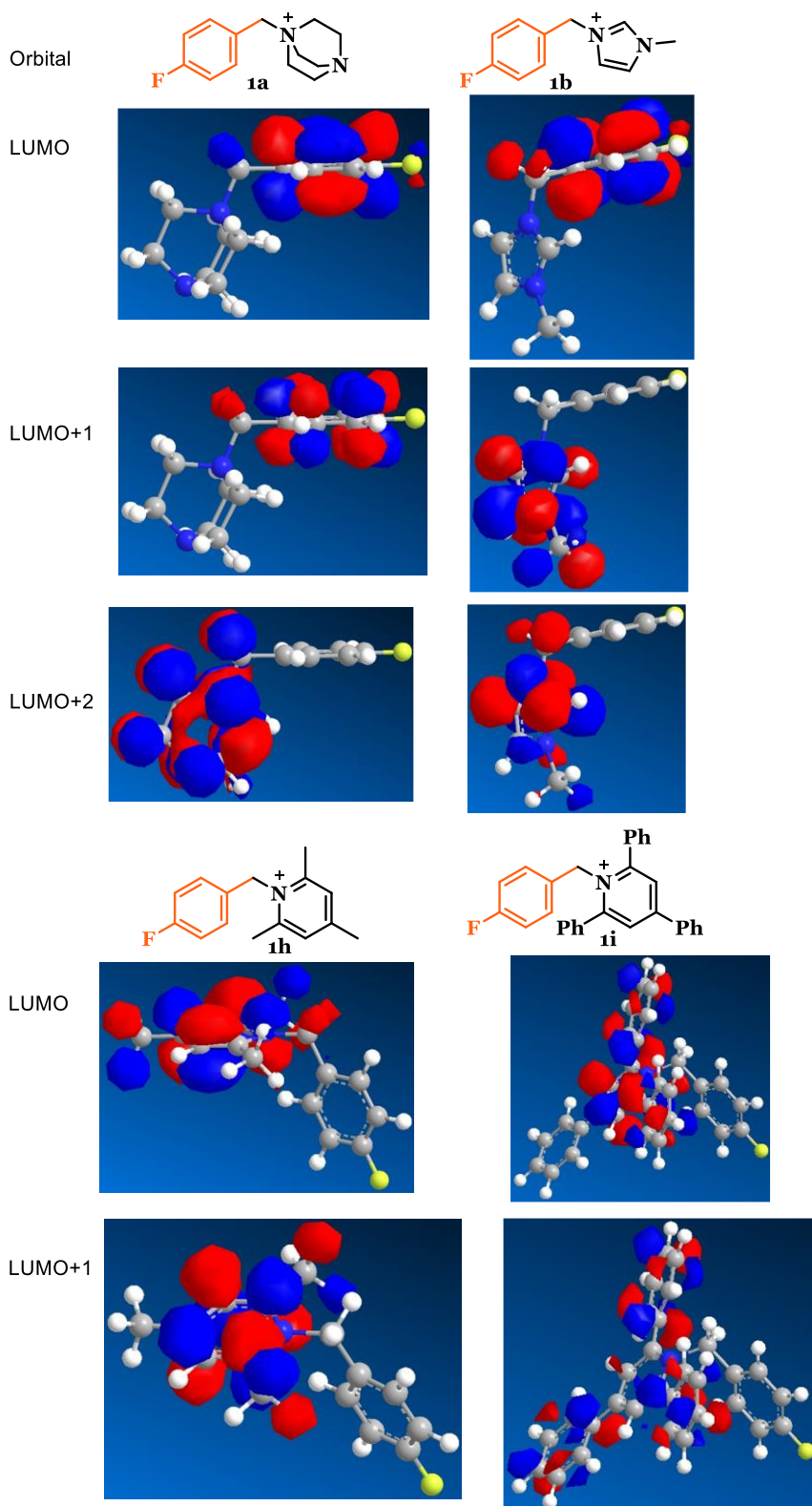
The addition of KI to the reaction of **1h** and acrylonitrile, was shown to significantly retard the rate of the reaction and decrease the yield.



entry	modification	time	conv% ^a	3a % ^a	(3a' + 3a'')% ^a	(3' + 3'')% ^a
1	KI	26 h	80%	60%	19%	1%
2	Control (no KI)	12 h	100%	88%	3%	9%

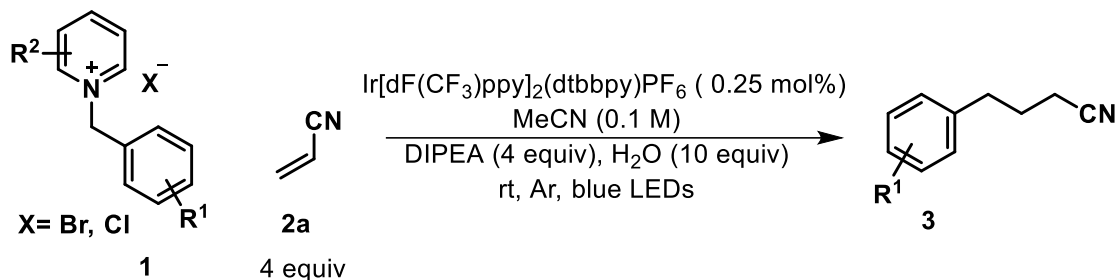
^a ¹⁹F NMR conversions

Calculation of the molecular orbitals using semi-empirical Hückel calculations



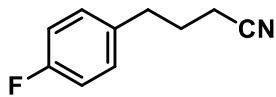
Photocatalytic reactions:

General procedure B



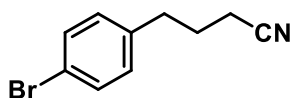
A NMR tube fitted with a rubber septum was charged with a solution of [Ir(2',4'-dF-5-CF₃-ppy)₂(4,4'-dtbbpy)]PF₆ (0.25 mM, 1.2 mL in MeCN), benzylpyridinium bromide/ chloride (0.12 mmol, 1 equiv), DIPEA (0.48 mmol, 62.0 mg 83.6 μ L, 4 equiv), DI water (1.2 mmol, 21.6 mg, 21.6 μ L, 10 equiv) and acrylonitrile (0.48 mmol, 25.5 mg, 31.4 μ L, 4 equiv). Then the reaction mixture was degassed via Ar bubbling for 10 min and then left under positive Ar pressure by removing the exit needle. The tube was placed in a light bath (description above) which was maintained at 26 °C. The reaction was monitored by ¹H or ¹⁹F NMR. After the complete consumption of benzylpyridinium bromide/ chloride, the volatiles (MeCN, acrylonitrile and some DIPEA) were removed via rotovap and the residue was dissolved in ethyl acetate (6 mL) and washed with 1M aqueous HCl solution (3 x 2 mL) and brine solution (2 mL). The organic layer was dried over anhydrous MgSO₄. The crude product was concentrated in vacuo and purified via normal phase chromatography.

4-(4-fluorophenyl)butanenitrile (**3a**)



The general procedure **B** was followed using 1-(4-fluorobenzyl)-2,4,6-trimethylpyridin-1-ium bromide (**1h**) (37.2 mg, 0.12 mmol), DIPEA (0.48 mmol, 62.0 mg 83.6 μ L, 4 equiv), DI water (1.2 mmol, 21.6 mg, 21.6 μ L, 10 equiv), acrylonitrile (0.48 mmol, 25.5 mg, 31.4 μ L, 4 equiv) and 1.2 mL of stock solution of $[\text{Ir}(2',4'\text{-dF-5-CF}_3\text{-ppy})_2(4,4'\text{-dtbbpy})]\text{PF}_6$ in MeCN. After the completion of the reaction 12 h, the crude was purified via automated flash chromatography using EtOAc in hexanes (0% to 100%) with product eluting at 3.5% on a 4 g silica column to afford **3a** in 84% yield (16 mg, 0.10 mmol) as an oil. NMR chemical shifts match with the literature values.³⁵ ^1H NMR (400 MHz, CDCl_3) δ 7.14 (dd, $J = 8.4, 5.5$ Hz, 2H), 6.99 (t, $J = 8.7$ Hz, 2H), 2.76 (t, $J = 7.5$ Hz, 2H), 2.32 (t, $J = 7.0$ Hz, 2H), 1.96 (p, $J = 7.2$ Hz, 2H). ^{19}F NMR (376 MHz, CDCl_3) δ -116.5 – -116.6 (m). ^{13}C NMR (101 MHz, CDCl_3) δ 161.4 (d, $J = 244.5$ Hz), 135.1 (d, $J = 3.2$ Hz), 129.6 (d, $J = 7.9$ Hz), 119.1, 115.2 (d, $J = 21.2$ Hz), 33.3, 26.8, 16.1. GC/MS (m/z , relative intensity) 163 (M^+ , 15), 122 (25), 109 (100).

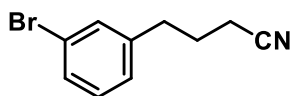
4-(4-bromophenyl)butanenitrile (**3b**)



The general procedure **B** was followed using 1-(4-bromobenzyl)-2,4,6-trimethylpyridin-1-ium bromide (**1i**) (44.5 mg, 0.12 mmol), DIPEA (0.48 mmol, 62.0 mg 83.6 μ L, 4 equiv), DI water (1.2 mmol, 21.6 mg, 21.6 μ L, 10 equiv), acrylonitrile (0.48 mmol, 25.5 mg, 31.4 μ L, 4 equiv) and 1.2 mL of stock solution of $[\text{Ir}(2',4'\text{-dF-5-CF}_3\text{-ppy})_2(4,4'\text{-dtbbpy})]\text{PF}_6$ in MeCN. After the completion of the reaction 12 h, the crude was purified via automated flash chromatography using EtOAc in hexanes (0% to 100%) with product eluting at 2.8% on a 4 g silica column to afford **3b** in 83% yield (22 mg, 0.10 mmol) as an oil. NMR chemical shifts match with the literature values.¹⁷ ^1H NMR (400 MHz, CDCl_3) δ 7.43 (app.d, $J = 8.4$ Hz, 2H), 7.07 (app.d, $J = 8.4$ Hz, 2H), 2.74 (t, $J = 7.5$ Hz, 2H), 2.32 (t, $J = 7.0$ Hz, 2H), 1.96 (p, $J = 7.1$ Hz, 2H). ^{13}C NMR (101

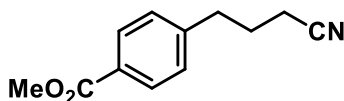
MHz, CDCl₃) δ 139.1, 132.2, 130.6, 120.8, 119.7, 34.2, 27.1, 16.8. GC/MS (m/z, relative intensity) 225 (M+ 2, 30), 223 (M⁺, 30), 182 (30), 169 (100).

4-(3-bromophenyl)butanenitrile (**3c**)



The general procedure **B** was followed using 1-(3-bromobenzyl)-2,4,6-trimethylpyridin-1-ium bromide (**1j**) (44.5 mg, 0.12 mmol), DIPEA (0.48 mmol, 62.0 mg 83.6 μ L, 4 equiv), DI water (1.2 mmol, 21.6 mg, 21.6 μ L, 10 equiv), acrylonitrile (0.48 mmol, 25.5 mg, 31.4 μ L, 4 equiv) and 1.2 mL of stock solution of [Ir(2',4'-dF-5-CF₃-ppy)₂(4,4'-dtbbpy)]PF₆ in MeCN. After the completion of the reaction 14 h, the crude was purified via automated flash chromatography using EtOAc in hexanes (0% to 100%) with product eluting at 3% on a 4 g silica column to afford **3c** in 71% yield (19 mg, 0.09 mmol) as an oil. ¹H NMR (400 MHz, CDCl₃) δ 7.39 – 7.30 (m, 2H), 7.18 (t, *J* = 7.7 Hz, 1H), 7.12 (d, *J* = 7.7 Hz, 1H), 2.75 (t, *J* = 7.5 Hz, 2H), 2.33 (t, *J* = 7.1 Hz, 2H), 1.97 (p, *J* = 7.1 Hz, 2H). ¹³C NMR (101 MHz, CDCl₃) δ 142.1, 131.6, 130.4, 129.8, 127.3, 122.8, 119.3, 34.1, 26.8, 16.5. GC/MS (m/z, relative intensity) 223 (M⁺, 50), 225 (M⁺ + 2, 50), 183 (30), 169 (100). HRMS (ESI) calcd. for [C₁₀H₁₁BrN]⁺ [M+H]⁺ m/z, 224.0075 found 224.0078.

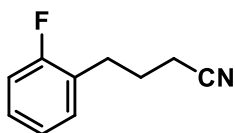
methyl 4-(3-cyanopropyl)benzoate (**3d**)



The general procedure **B** was followed using 1-(4-(methoxycarbonyl)benzyl)-2,4,6-trimethylpyridin-1-ium bromide (**1k**) (42.0 mg, 0.12 mmol), DIPEA (0.48 mmol, 62.0 mg 83.6 μ L, 4 equiv), DI water (1.2 mmol, 21.6 mg, 21.6 μ L, 10 equiv), acrylonitrile (0.48 mmol, 25.5 mg, 31.4 μ L, 4 equiv) and 1.2 mL of stock solution of [Ir(2',4'-dF-5-CF₃-ppy)₂(4,4'-dtbbpy)]PF₆ in MeCN. After the completion of the reaction 13 h, the crude was purified via automated flash chromatography using EtOAc in hexanes (0% to 100%) with

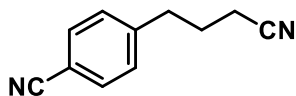
product eluting at 10% on a 4 g silica column to afford **3d** in 71% yield (17 mg, 0.09 mmol) as an oil. NMR chemical shifts match with the literature values.¹⁷ ¹H NMR (400 MHz, CDCl₃) δ 7.99 (d, *J* = 8.2 Hz, 2H), 7.26 (d, *J* = 8.2 Hz, 2H), 3.91 (s, 3H), 2.84 (t, *J* = 7.5 Hz, 2H), 2.34 (t, *J* = 7.0 Hz, 2H), 2.01 (p, *J* = 7.1 Hz, 2H). ¹³C NMR (101 MHz, CDCl₃) δ 167.0, 145.2, 130.2, 128.7, 128.6, 119.3, 52.2, 34.5, 26.7, 16.6. GC/MS (m/z, relative intensity) 203 (M⁺, 20), 172 (100), 149 (30).

4-(2-fluorophenyl)butanenitrile (**3e**)



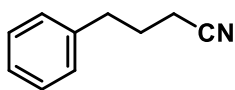
The general procedure **B** was followed using 1-(2-fluorobenzyl)-4-methylpyridin-1-ium chloride (**11**) (28.5 mg, 0.12 mmol), DIPEA (0.48 mmol, 62.0 mg 83.6 μL, 4 equiv), DI water (1.2 mmol, 21.6 mg, 21.6 μL, 10 equiv), acrylonitrile (0.48 mmol, 25.5 mg, 31.4 μL, 4 equiv) and 1.2 mL of stock solution of [Ir(2',4'-dF-5-CF₃-ppy)₂(4,4'-dtbbpy)]PF₆ in MeCN. After the completion of the reaction 15 h, the crude was purified via automated flash chromatography using EtOAc in hexanes (0% to 100%) with product eluting at 3% on a 4 g silica column to afford **3e** in 51% yield (10 mg, 0.06 mmol) as an oil. ¹H NMR (400 MHz, CDCl₃) δ 7.25 – 7.16 (m, 2H), 7.09 (td, *J* = 7.5, 1.1 Hz, 1H), 7.04 (t, *J* = 7.3 Hz, 1H), 2.81 (t, *J* = 7.4 Hz, 2H), 2.35 (t, *J* = 7.2 Hz, 2H), 1.99 (p, *J* = 7.2 Hz, 2H). ¹⁹F NMR (376 MHz, CDCl₃) δ -118.5 – -118.6 (m). ¹³C NMR (101 MHz, CDCl₃) δ 161.0 (d, *J* = 245.2 Hz), 130.6 (d, *J* = 4.8 Hz), 128.2 (d, *J* = 8.1 Hz), 126.4 (d, *J* = 15.8 Hz), 124.1 (d, *J* = 3.6 Hz), 119.2, 115.3 (d, *J* = 22.0 Hz), 27.9, 25.5, 16.4. GC/MS (m/z, relative intensity) 163 (M⁺, 15), 123 (20), 109 (100). HRMS (ESI) calcd. for [C₁₀H₁₁FN]⁺ [M+H]⁺ m/z, 164.0876 found 164.0875.

4-(3-cyanopropyl)benzonitrile (**3f**)



The general procedure **B** was followed using 1-(4-cyanobenzyl)-2,4,6-trimethylpyridin-1-ium bromide (**1m**) (38.1 mg, 0.12 mmol), DIPEA (0.48 mmol, 62.0 mg 83.6 μ L, 4 equiv), DI water (1.2 mmol, 21.6 mg, 21.6 μ L, 10 equiv), acrylonitrile (0.48 mmol, 25.5 mg, 31.4 μ L, 4 equiv) and 1.2 mL of stock solution of $[\text{Ir}(2',4'\text{-dF-5-CF}_3\text{-ppy})_2(4,4'\text{-dtbbpy})]\text{PF}_6$ in MeCN. After the completion of the reaction 13 h, the crude was purified via automated flash chromatography using EtOAc in hexanes (0% to 100%) with product eluting at 9.5% on a 4 g silica column to afford **3f** in 70% yield (14 mg, 0.08 mmol) as an oil with minor contamination of DIPEA-acrylonitrile oligomer. Crude ^1H NMR yield of the reaction is 64% with respect to an internal standard (1,2,3-Trimethoxybenzene). NMR chemical shifts match with the literature values.¹⁷ ^1H NMR (400 MHz, CDCl_3) δ 7.62 (d, J = 8.2 Hz, 2H), 7.31 (d, J = 8.2 Hz, 2H), 2.86 (t, J = 7.6 Hz, 2H), 2.36 (t, J = 7.0 Hz, 2H), 2.00 (p, J = 7.1 Hz, 2H). ^{13}C NMR (101 MHz, CDCl_3) δ 145.4, 132.7, 129.4, 119.1, 118.9, 110.8, 34.6, 26.5, 16.7. GC/MS (m/z , relative intensity) 170 (M^+ , 15), 130 (70), 116 (100).

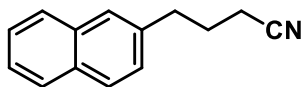
4-phenylbutanenitrile (**3g**)



The general procedure **B** was followed using 1-benzyl-2,4,6-trimethylpyridin-1-ium bromide (**1n**) (35.1 mg, 0.12 mmol), DIPEA (0.48 mmol, 62.0 mg 83.6 μ L, 4 equiv), DI water (1.2 mmol, 21.6 mg, 21.6 μ L, 10 equiv), acrylonitrile (0.48 mmol, 25.5 mg, 31.4 μ L, 4 equiv) and 1.2 mL of stock solution of $[\text{Ir}(2',4'\text{-dF-5-CF}_3\text{-ppy})_2(4,4'\text{-dtbbpy})]\text{PF}_6$ in MeCN. After the completion of the reaction 13 h, the crude was purified via automated flash chromatography using EtOAc in hexanes (0% to 100%) with product eluting at 3% on a 4 g silica column to afford **3g** in 81% yield (14 mg, 0.10 mmol) as an oil. NMR chemical shifts match with the literature values.¹⁷ ^1H NMR (400 MHz, CDCl_3) δ 7.32 (t, J = 7.5 Hz, 2H), 7.24 (t, J = 7.4 Hz, 1H), 7.19 (d, J = 7.3 Hz, 2H), 2.79 (t, J = 7.4 Hz, 2H), 2.32 (t, J = 7.1 Hz, 2H), 1.99 (p, J = 7.2 Hz, 2H). ^{13}C NMR (101 MHz, CDCl_3) δ 140.1,

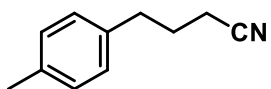
129.1, 128.9, 126.9, 119.9, 34.8, 27.4, 16.8. GC/MS (m/z, relative intensity) 145 (M⁺, 15), 104 (15), 91 (100).

4-(naphthalen-2-yl)butanenitrile (**3h**)



The general procedure **B** was followed using 2,4,6-trimethyl-1-(naphthalen-2-ylmethyl)pyridin-1-ium bromide (**1o**) (41.1 mg, 0.12 mmol), DIPEA (0.48 mmol, 62.0 mg 83.6 μ L, 4 equiv), DI water (1.2 mmol, 21.6 mg, 21.6 μ L, 10 equiv), acrylonitrile (0.48 mmol, 25.5 mg, 31.4 μ L, 4 equiv) and 1.2 mL of stock solution of [Ir(2',4'-dF-5-CF₃-ppy)₂(4,4'-dtbbpy)]PF₆ in MeCN. After the completion of the reaction 14 h, the crude was purified via automated flash chromatography using EtOAc in hexanes (0% to 100%) with product eluting at 2.5% on a 4 g silica column to afford **3h** in 78% yield (18 mg, 0.09 mmol) as a solid. NMR chemical shifts match with the literature values.¹⁷ ¹H NMR (400 MHz, CDCl₃) δ 7.86 – 7.78 (m, 3H), 7.65 (s, 1H), 7.48 (dddd, *J* = 7.3, 5.8, 1.5 Hz, 2H), 7.32 (dd, *J* = 8.4, 1.7 Hz, 1H), 2.95 (t, *J* = 7.4 Hz, 2H), 2.34 (t, *J* = 7.1 Hz, 2H), 2.07 (p, *J* = 7.1 Hz, 2H). ¹³C NMR (101 MHz, CDCl₃) δ 137.5, 133.9, 132.6, 128.8, 128.1, 127.9, 127.3, 127.2, 126.6, 126.0, 119.9, 34.9, 27.2, 16.8. GC/MS (m/z, relative intensity) 145 (M⁺, 15), 104 (15), 91 (100).

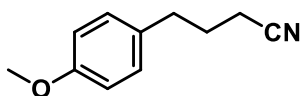
4-(p-tolyl)butanenitrile (**3i**)



The general procedure **B** was followed using 2,4,6-trimethyl-1-(4-methylbenzyl)pyridin-1-ium chloride (**1p**) (31.4 mg, 0.12 mmol), DIPEA (0.48 mmol, 62.0 mg 83.6 μ L, 4 equiv), DI water (1.2 mmol, 21.6 mg, 21.6 μ L, 10 equiv), acrylonitrile (0.48 mmol, 25.5 mg, 31.4 μ L, 4 equiv) and 1.2 mL of stock solution of [Ir(2',4'-dF-5-CF₃-ppy)₂(4,4'-dtbbpy)]PF₆ in MeCN. After the completion of the reaction 15 h, the crude was purified via automated

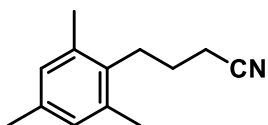
flash chromatography using EtOAc in hexanes (0% to 100%) with product eluting at 3% on a 4 g silica column to afford **3i** in 80% yield (15 mg, 0.10 mmol) as an oil. NMR chemical shifts match with the literature values.³⁵ ¹H NMR (400 MHz, CDCl₃) δ 7.13 (d, *J* = 8.0 Hz, 2H), 7.08 (d, *J* = 8.1 Hz, 2H), 2.74 (t, *J* = 7.4 Hz, 2H), 2.33 (s, 3H), 2.30 (t, *J* = 7.1 Hz, 2H), 1.96 (p, *J* = 7.2 Hz, 2H). ¹³C NMR (101 MHz, CDCl₃) δ 136.4, 135.9, 129.1, 128.1, 119.4, 33.8, 26.8, 20.8, 16.2. GC/MS (*m/z*, relative intensity) 159 (M⁺, 25), 118 (20), 105 (100).

4-(4-methoxyphenyl)butanenitrile (**3j**)



The general procedure **B** was followed using 1-(4-methoxybenzyl)-2,4,6-trimethylpyridin-1-ium chloride (**1q**) (33.3 mg, 0.12 mmol), DIPEA (0.48 mmol, 62.0 mg 83.6 μL, 4 equiv), DI water (1.2 mmol, 21.6 mg, 21.6 μL, 10 equiv), acrylonitrile (0.48 mmol, 25.5 mg, 31.4 μL, 4 equiv) and 1.2 mL of stock solution of [Ir(2',4'-dF-5-CF₃-ppy)₂(4,4'-dtbbpy)]PF₆ in MeCN. After the completion of the reaction 15 h, the crude was purified via automated flash chromatography using EtOAc in hexanes (0% to 100%) with product eluting at 3% on a 4 g silica column to afford **3j** in 79% yield (17 mg, 0.10 mmol) as an oil. NMR chemical shifts match with the literature values.³⁵ ¹H NMR (400 MHz, CDCl₃) δ 7.10 (d, *J* = 8.6 Hz, 2H), 6.85 (d, *J* = 8.6 Hz, 2H), 3.79 (s, 3H), 2.72 (t, *J* = 7.4 Hz, 2H), 2.30 (t, *J* = 7.1 Hz, 2H), 1.95 (p, *J* = 7.2 Hz, 2H). ¹³C NMR (101 MHz, CDCl₃) δ 158.4, 131.8, 129.5, 119.7, 114.2, 55.4, 33.6, 27.3, 16.4. GC/MS (*m/z*, relative intensity) 175 (M⁺, 15), 121 (100), 91 (10).

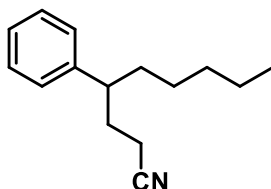
4-mesitylbutanenitrile (**3k**)



The general procedure **B** was followed using 4-methyl-1-(2,4,6-trimethylbenzyl)pyridin-1-ium chloride (**1r**) (31.4 mg, 0.12 mmol), DIPEA

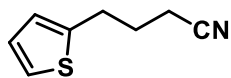
(0.48 mmol, 62.0 mg 83.6 μ L, 4 equiv), DI water (1.2 mmol, 21.6 mg, 21.6 μ L, 10 equiv), acrylonitrile (0.48 mmol, 25.5 mg, 31.4 μ L, 4 equiv) and 1.2 mL of stock solution of [Ir(2',4'-dF-5-CF₃-ppy)₂(4,4'-dtbbpy)]PF₆ in MeCN. After the completion of the reaction 15 h, the crude was purified via automated flash chromatography using EtOAc in hexanes (0% to 100%) with product eluting at 3% on a 4 g silica column to afford **3k** in 65% yield (15 mg, 0.08 mmol) as an oil. NMR chemical shifts match with the literature values.¹⁷ ¹H NMR (400 MHz, CDCl₃) δ 6.86 (s, 2H), 2.80 – 2.70 (m, 2H), 2.44 (t, *J* = 7.0 Hz, 2H), 2.31 (s, 6H), 2.26 (s, 3H), 1.87 – 1.76 (m, 2H). ¹³C NMR (101 MHz, CDCl₃) δ 136.1, 135.8, 133.9, 129.2, 119.7, 28.5, 25.1, 20.9, 19.8, 17.6. GC/MS (*m/z*, relative intensity) 187 (M⁺, 18), 133 (100), 105 (5).

4-phenylnonanenitrile (**3l**)



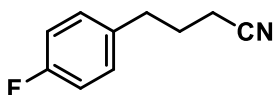
The general procedure **B** was followed using 4-methyl-1-(1-phenylhexyl)pyridin-1-ium bromide (**1s**) (40.1 mg, 0.12 mmol), DIPEA (0.48 mmol, 62.0 mg 83.6 μ L, 4 equiv), DI water (1.2 mmol, 21.6 mg, 21.6 μ L, 10 equiv), acrylonitrile (0.48 mmol, 25.5 mg, 31.4 μ L, 4 equiv) and 1.2 mL of stock solution of [Ir(2',4'-dF-5-CF₃-ppy)₂(4,4'-dtbbpy)]PF₆ in MeCN. After the completion of the reaction 15 h, the crude was purified via automated flash chromatography using EtOAc in hexanes (0% to 100%) with product eluting at 3.1% on a 4 g silica column to afford **3l** in 73% yield (19 mg, 0.09 mmol) as an oil. ¹H NMR (400 MHz, CDCl₃) δ 7.32 (t, *J* = 7.4 Hz, 2H), 7.23 (td, *J* = 7.3, 6.4, 3.2 Hz, 1H), 7.15 (d, *J* = 7.4 Hz, 2H), 2.65 (tq, *J* = 8.7, 4.1 Hz, 1H), 2.17 (pd, *J* = 9.8, 8.7, 4.8 Hz, 1H), 2.10 – 1.96 (m, 2H), 1.83 (ddt, *J* = 15.8, 10.5, 5.7 Hz, 1H), 1.61 (dt, *J* = 8.4, 4.9 Hz, 2H), 1.27 – 1.16 (m, 6H), 0.83 (t, *J* = 6.7 Hz, 3H). ¹³C NMR (101 MHz, CDCl₃) δ 143.6, 129.2, 128.0, 127.2, 120.2, 45.4, 36.9, 32.7, 32.2, 27.5, 22.9, 15.9, 14.5. GC/MS (*m/z*, relative intensity) 215 (M⁺, 10), 161 (15), 144 (50). HRMS (ESI) calcd. for [C₁₅H₂₂N]⁺ [M+H]⁺ *m/z*, 216.1752 found 216.1754.

4-(thiophen-2-yl)butanenitrile (**3m**)



The general procedure **B** was followed using 2,4,6-trimethyl-1-(thiophen-2-ylmethyl)pyridin-1-ium bromide (**1t**) (36 mg, 0.12 mmol), DIPEA (0.48 mmol, 62.0 mg 83.6 μ L, 4 equiv), DI water (1.2 mmol, 21.6 mg, 21.6 μ L, 10 equiv), acrylonitrile (0.48 mmol, 25.5 mg, 31.4 μ L, 4 equiv) and 1.2 mL of stock solution of $[\text{Ir}(2',4'\text{-dF-5-CF}_3\text{-ppy})_2(4,4'\text{-dtbbpy})]\text{PF}_6$ in MeCN. After the completion of the reaction 14 h, the crude was purified via automated flash chromatography using EtOAc in hexanes (0% to 100%) with product eluting at 3% on a 4 g silica column to afford **3m** in 69% yield (17 mg, 0.08 mmol) as an oil. NMR chemical shifts match with the literature values.³⁵ ^1H NMR (400 MHz, CDCl_3) δ 7.17 (d, $J = 5.1$ Hz, 1H), 6.94 (dd, $J = 5.0, 3.5$ Hz, 1H), 6.84 (d, $J = 3.3$ Hz, 1H), 3.01 (t, $J = 7.2$ Hz, 2H), 2.37 (t, $J = 7.1$ Hz, 2H), 2.03 (p, $J = 7.1$ Hz, 2H). ^{13}C NMR (101 MHz, CDCl_3) δ 142.2, 127.2, 125.4, 124.0, 119.4, 28.6, 27.4, 16.4. GC/MS (m/z, relative intensity) 151 (M^+ , 20), 110 (10), 97 (100).

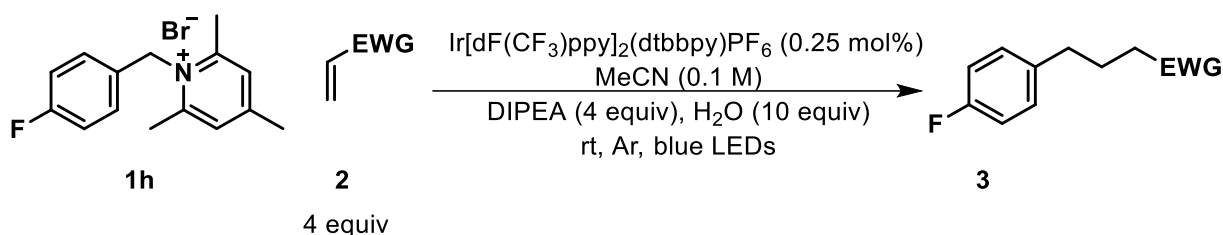
Photocatalytic reaction in large scale



A 18 \times 150 mm borosilicate tube fitted with a rubber septum was charged with a solution of $[\text{Ir}(2',4'\text{-dF-5-CF}_3\text{-ppy})_2(4,4'\text{-dtbbpy})]\text{PF}_6$ (0.25 mM, 12 mL in MeCN), 1-(4-fluorobenzyl)-2,4,6-trimethylpyridin-1-ium bromide (**1h**) (372 mg, 1.2 mmol), DIPEA (4.8 mmol, 620 mg 0.84 mL, 4 equiv), DI water (12 mmol, 216 mg, 0.22 mL, 10 equiv), acrylonitrile (4.8 mmol, 255 mg, 0.31 mL, 4 equiv). Then the reaction mixture was degassed via Ar bubbling for 30 min and then left under positive Ar pressure by removing the exit needle. The tube was placed in a light bath (description above) which was maintained at 26 $^\circ\text{C}$. The reaction was monitored by ^{19}F NMR. After the complete consumption of starting material (**1h**), crude reaction showed 84% of **3a** product according to ^{19}F NMR and the volatiles (MeCN, acrylonitrile and some

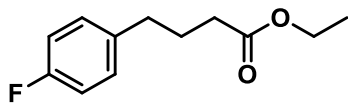
DIPEA) were removed via rotovap and the residue was dissolved in ethyl acetate (40 mL) and washed with 1M aqueous HCl solution (3 x 20 mL) and brine solution (20 mL). The organic layer was dried over anhydrous MgSO₄. The crude product was concentrated *in vacuo* and purified via normal phase chromatography using EtOAc in hexanes (0% to 100%) with product eluting at 4% on a 24 g silica column to afford **3a** in 80% (156.5 mg, 0.96 mmol) as an oil.

General procedure C



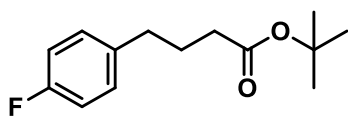
A NMR tube fitted with a rubber septum was charged with [Ir(2',4'-dF-5-CF₃-ppy)₂(4,4'-dtbbpy)]PF₆ (2-(2,4-difluorophenyl)-5-trifluoromethylpyridine 4,4'-di-tert-butyl-2,2'-bipyridine) (0.25 mM, 1.2 mL in MeCN), 1-(4-fluorobenzyl)-2,4,6-trimethylpyridin-1-ium bromide (**1h**) (37.2 mg, 0.12 mmol, 1 equiv), DIPEA (0.48 mmol, 62.0 mg 83.6 μL, 4 equiv), DI water (1.2 mmol, 21.6 mg, 21.6 μL, 10 equiv) and Michael acceptor (0.48 mmol, 25.5 mg, 31.4 μL, 4 equiv). Then the reaction mixture was degassed via Ar bubbling for 10 min and then left under positive Ar pressure by removing the exit needle. The tube was placed in a light bath (description above) which was maintained at 26 °C. The reaction was monitored by ¹⁹F NMR. After the complete consumption of benzylpyridinium bromide, MeCN was removed via rotovap and the residue was dissolved in ethyl acetate (6 mL) and washed with 1M aqueous HCl solution (3 x 2 mL) and brine solution (2 mL). The organic layer was dried over anhydrous MgSO₄. The crude product was concentrated *in vacuo* and purified via normal phase chromatography.

ethyl 4-(4-fluorophenyl)butanoate (**4b**)



The general procedure **C** was followed using 1-(4-fluorobenzyl)-2,4,6-trimethylpyridin-1-ium bromide (**1h**) (37.2 mg, 0.12 mmol), DIPEA (0.48 mmol, 62.0 mg 83.6 μ L, 4 equiv), DI water (1.2 mmol, 21.6 mg, 21.6 μ L, 10 equiv), ethyl acrylate (0.48 mmol, 48.0 mg, 52.0 μ L, 4 equiv) and 1.2 mL of stock solution of [Ir(2',4'-dF-5-CF₃-ppy)₂(4,4'-dtbbpy)]PF₆ in MeCN. After the completion of the reaction 15 h, the crude was purified via automated flash chromatography using EtOAc in hexanes (0% to 100%) with product eluting at 2.8% on a 4 g silica column to afford **4b** in 75% yield (20.0 mg, 0.09 mmol) as an oil. NMR chemical shifts match with the literature values.³⁶ ¹H NMR (400 MHz, CDCl₃) δ 7.13 (dd, J = 8.5, 5.5 Hz, 2H), 7.01 – 6.91 (m, 2H), 4.12 (q, J = 7.1 Hz, 2H), 2.62 (t, J = 7.6 Hz, 2H), 2.30 (t, J = 7.4 Hz, 2H), 1.93 (p, J = 7.5 Hz, 2H), 1.25 (t, J = 7.1 Hz, 3H). ¹⁹F NMR (376 MHz, CDCl₃) δ -117.5 – -117.6 (m). ¹³C NMR (101 MHz, CDCl₃) δ 173.9, 161.8 (d, J = 243.5 Hz), 137.5 (d, J = 3.2 Hz), 130.3 (d, J = 7.8 Hz), 115.6 (d, J = 21.1 Hz), 60.8, 34.8, 34.0, 27.1, 14.7. GC/MS (m/z , relative intensity) 210 (M⁺, 20), 165 (40), 109 (100).

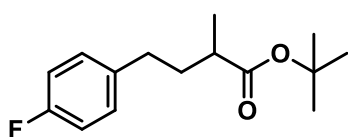
tert-butyl 4-(4-fluorophenyl)butanoate (**4c**)



The general procedure **C** was followed using 1-(4-fluorobenzyl)-2,4,6-trimethylpyridin-1-ium bromide (**1h**) (37.2 mg, 0.12 mmol), DIPEA (0.48 mmol, 62.0 mg 83.6 μ L, 4 equiv), DI water (1.2 mmol, 21.6 mg, 21.6 μ L, 10 equiv), *tert*-butyl acrylate (0.48 mmol, 62.0 mg, 70.0 μ L, 4 equiv) and 1.2 mL of stock solution of [Ir(2',4'-dF-5-CF₃-ppy)₂(4,4'-dtbbpy)]PF₆ in MeCN. After the completion of the reaction 15 h, the crude was purified via automated flash chromatography using EtOAc in hexanes (0% to 100%) with product eluting at 2.5% on a 4 g silica column to afford **4c** in 71% yield (20.3 mg, 0.09 mmol) as an oil. ¹H NMR (400 MHz, CDCl₃) δ 7.13 (dd, J = 8.5, 5.5 Hz, 2H), 7.00 – 6.91 (m, 2H), 2.61 (t, J = 7.5 Hz, 2H), 2.22 (t, J = 7.4 Hz, 2H), 1.88 (p, J = 7.5 Hz, 2H), 1.45 (s, 9H). ¹⁹F NMR (376 MHz, CDCl₃) δ -117.6 – -117.8 (m). ¹³C

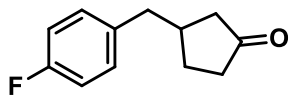
NMR (101 MHz, CDCl₃) δ 173.2, 161.8 (d, $J = 243.4$ Hz), 137.7 (d, $J = 3.2$ Hz), 130.3 (d, $J = 7.8$ Hz), 115.5 (d, $J = 21.0$ Hz), 80.6, 35.2, 34.8, 28.6, 27.3. GC/MS (m/z, relative intensity) 182 (20), 122 (40), 109 (40). The *tert-butyl* group was thermally removed upon injection in the GCMS. HRMS (ESI) calcd. for [C₁₄H₂₀FO₂]⁺ [M+H]⁺ m/z, 239.1447 found 239.1450.

tert-butyl 4-(4-fluorophenyl)-2-methylbutanoate (**4d**)



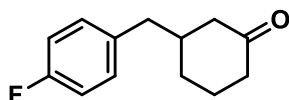
The general procedure **C** was followed using 1-(4-fluorobenzyl)-2,4,6-trimethylpyridin-1-ium bromide (**1h**) (37.2 mg, 0.12 mmol), DIPEA (0.48 mmol, 62.0 mg 83.6 μ L, 4 equiv), DI water (1.2 mmol, 21.6 mg, 21.6 μ L, 10 equiv), *tert*-butyl methacrylate (0.48 mmol, 68.0 mg, 80.0 μ L, 4 equiv) and 1.2 mL of stock solution of 0.5 mM [Ir(2',4'-dF-5-CF₃-ppy)₂(4,4'-dtbbpy)]PF₆ (double the normal concentration) in MeCN. After the completion of the reaction 15 h, the crude was purified via Prep TLC using EtOAc: hexanes (1:9) to afford **4d** in 62% yield (18.8 mg, 0.07 mmol) as an oil. ¹H NMR (400 MHz, CDCl₃) δ 7.12 (ddd, $J = 8.4, 5.3, 2.5$ Hz, 2H), 7.00 – 6.92 (m, 2H), 2.65 – 2.51 (m, 1H), 2.40 – 2.27 (m, 1H), 1.92 (dddd, $J = 13.6, 9.3, 8.2, 6.5$ Hz, 1H), 1.63 (dddd, $J = 13.4, 9.4, 6.9, 6.0$ Hz, 1H), 1.46 (s, 9H), 1.14 (d, $J = 7.0$ Hz, 3H). ¹⁹F NMR (376 MHz, CDCl₃) δ -117.7 – -117.9 (m). ¹³C NMR (101 MHz, CDCl₃) δ 176.0, 161.4 (d, $J = 243.3$ Hz), 137.7 (d, $J = 3.2$ Hz), 129.9 (d, $J = 7.8$ Hz), 115.2 (d, $J = 21.1$ Hz), 80.2, 40.1, 35.9, 32.9, 28.3, 17.4. GC/MS (m/z, relative intensity) 196 (20), 179 (15), 109 (80). The *tert-butyl* group was thermally removed upon injection in the GCMS. HRMS (ESI) calcd. for [C₁₅H₂₂FO₂]⁺ [M+H]⁺ m/z, 253.1604 found 253.1607.

3-(4-fluorobenzyl)cyclopentan-1-one (**4e**)



The general procedure **C** was followed using 1-(4-fluorobenzyl)-2,4,6-trimethylpyridin-1-ium bromide (**1h**) (37.2 mg, 0.12 mmol), DIPEA (0.36 mmol, 46.4 mg 62.8 μ L, 3 equiv), DI water (1.2 mmol, 21.6 mg, 21.6 μ L, 10 equiv), cyclopent-2-en-1-one (0.48 mmol, 40.0 mg, 40.0 μ L, 4 equiv) and 1.2 mL of stock solution of [Ir(2',4'-dF-5-CF₃-ppy)₂(4,4'-dtbbpy)]PF₆ in MeCN. After the completion of the reaction 17 h, the crude was purified via automated flash chromatography using EtOAc in hexanes (0% to 100%) with product eluting at 20% on a 4 g silica column to afford **4e** in 50% yield (11.5 mg, 0.06 mmol) as an oil. ¹H NMR (400 MHz, CDCl₃) δ 7.12 (dd, *J* = 8.5, 5.5 Hz, 2H), 7.02 – 6.95 (m, 2H), 2.78 – 2.64 (m, 2H), 2.49 – 2.38 (m, 1H), 2.38 – 2.25 (m, 2H), 2.20 – 2.14 (m, 1H), 2.14 – 2.05 (m, 1H), 1.89 (ddd, *J* = 18.1, 9.9, 1.4 Hz, 1H), 1.68 – 1.52 (m, 1H). ¹⁹F NMR (376 MHz, CDCl₃) δ -117.0 – -117.1 (m). ¹³C NMR (101 MHz, CDCl₃) δ 218.7, 161.3 (d, *J* = 244.1 Hz), 135.5 (d, *J* = 3.3 Hz), 129.9 (d, *J* = 7.8 Hz), 115.1 (d, *J* = 21.1 Hz), 44.7, 40.5, 38.8, 38.1, 28.8. GC/MS (*m/z*, relative intensity) 192 (M⁺, 20), 135 (5), 109 (100). HRMS (ESI) calcd. for [C₁₂H₁₄FO]⁺ [M+H]⁺ *m/z*, 193.1029 found 193.1031.

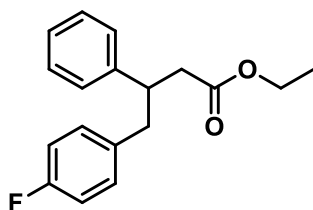
3-(4-fluorobenzyl)cyclohexan-1-one (**4f**)



The general procedure **C** was followed using 1-(4-fluorobenzyl)-2,4,6-trimethylpyridin-1-ium bromide (**1h**) (37.2 mg, 0.12 mmol), DIPEA (0.36 mmol, 46.4 mg 62.8 μ L, 3 equiv), DI water (1.2 mmol, 21.6 mg, 21.6 μ L, 10 equiv), cyclohex-2-en-1-one (0.48 mmol, 46.0 mg, 48.0 μ L, 4 equiv) and 1.2 mL of stock solution of [Ir(2',4'-dF-5-CF₃-ppy)₂(4,4'-dtbbpy)]PF₆ in MeCN. After the completion of the reaction 17 h, the crude was purified via automated flash chromatography using EtOAc in hexanes (0% to 100%) with product eluting at 10% on a 4 g silica column to afford **4f** in 57% yield (14.1 mg, 0.07 mmol) as an oil. ¹H NMR (400 MHz, CDCl₃) δ 7.08 (dd, *J* = 8.7, 3.1 Hz, 1H), 7.01 – 6.92 (m, 1H), 2.67 – 2.51 (m, 1H), 2.40 – 2.32 (m, 2H),

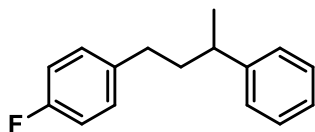
2.26 (td, $J = 13.9, 13.2, 6.2$ Hz, 1H), 2.09 – 1.97 (m, 3H), 1.90 – 1.81 (m, 1H), 1.69 – 1.59 (m, 1H), 1.36 (qd, $J = 13.7, 3.6$ Hz, 1H). ^{19}F NMR (376 MHz, CDCl_3) δ -117.1 (tt, $J = 8.7, 5.4$ Hz). ^{19}F NMR (376 MHz, CDCl_3) δ -117.0 – -117.1 (m). ^{13}C NMR (101 MHz, CDCl_3) δ 211.3, 161.3 (d, $J = 244.0$ Hz), 134.8 (d, $J = 3.2$ Hz), 130.2 (d, $J = 7.8$ Hz), 115.0 (d, $J = 21.2$ Hz), 47.5, 41.9, 41.2, 40.8 (d, $J = 0.9$ Hz), 30.6, 24.9. GC/MS (m/z , relative intensity) 206 (M^+ , 15), 148 (90), 109 (70). HRMS (ESI) calcd. for $[\text{C}_{13}\text{H}_{16}\text{FO}]^+ [\text{M}+\text{H}]^+ m/z$, 207.1185 found 207.1187.

ethyl 4-(4-fluorophenyl)-3-phenylbutanoate (**4g**)



The general procedure **C** was followed using 1-(4-fluorobenzyl)-2,4,6-trimethylpyridin-1-ium bromide (**1h**) (37.2 mg, 0.12 mmol), DIPEA (0.36 mmol, 46.4 mg 62.8 μL , 3 equiv), DI water (1.2 mmol, 21.6 mg, 21.6 μL , 10 equiv), ethyl cinnamate (0.48 mmol, 84.5 mg, 80.0 μL , 4 equiv) and 1.2 mL of stock solution of $[\text{Ir}(2',4'\text{-dF-5-CF}_3\text{-ppy})_2(4,4'\text{-dtbbpy})]\text{PF}_6$ in MeCN. After the completion of the reaction 19 h, the crude was purified via automated flash chromatography using EtOAc in hexanes (0% to 100%) with product eluting at 5% on a 4 g silica column to afford **3s** as a mixture with hydrogenated ethyl cinnamate (SM) as an oil. ^{19}F NMR yield of the reaction is 55% with respect to an internal standard (fluorobenzene). ^1H NMR (400 MHz, CDCl_3) of the mixture δ 7.32 – 7.23 (m, 5H), 7.10 (dd, $J = 8.4, 5.5$ Hz, 2H), 6.94 (t, $J = 8.7$ Hz, 2H), 3.94 (q, $J = 7.1$ Hz, 2H), 3.01 – 2.85 (m, 3H), 2.82 – 2.71 (m, 2H), 1.00 (t, $J = 7.1$ Hz, 3H). ^{19}F NMR (376 MHz, CDCl_3) of the mixture δ -117.1 – -117.3 (m). ^{13}C NMR (101 MHz, CDCl_3) of the mixture δ 174.8, 173.1, 161.7 (d, $J = 244.2$ Hz), 140.7, 139.1, 134.9 (d, $J = 3.2$ Hz), 130.4 (d, $J = 7.9$ Hz), 129.0, 128.6, 128.5, 128.4, 126.6, 126.4, 115.3 (d, $J = 21.2$ Hz), 60.6, 60.4, 49.9, 38.5, 37.5, 36.1, 31.1, 14.4, 14.2. GC/MS (m/z , relative intensity) 178 (M^+ , 20), 133 (10), 104 (100). HRMS (ESI) calcd. for $[\text{C}_{18}\text{H}_{20}\text{FO}_2]^+ [\text{M}+\text{H}]^+ m/z$, 287.1447 found 287.1450.

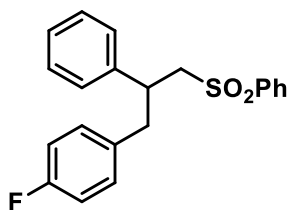
1-fluoro-4-(3-phenylbutyl)benzene (**4i**)



The general procedure **C** was followed using 1-(4-fluorobenzyl)-2,4,6-trimethylpyridin-1-ium bromide (37.2 mg, 0.12 mmol), DIPEA (0.36 mmol, 46.4 mg 62.8 μ L, 3 equiv), DI water (1.2 mmol, 21.6 mg, 21.6 μ L, 10 equiv), prop-1-en-2-ylbenzene (0.48 mmol, 46.8 mg, 37.0 μ L, 4 equiv) and 1.2 mL of stock solution of [Ir(2',4'-dF-5-CF₃-ppy)₂(4,4'-dtbbpy)]PF₆ in MeCN. After the completion of the reaction 19 h, the crude was purified via a Prep TLC using hexanes (100%) to afford **4i** in 46% yield (12.6 mg, 0.06 mmol) as an oil. ¹H NMR (400 MHz, CDCl₃) δ 7.25 – 7.15 (m, 3H), 7.06 (d, *J* = 7.1 Hz, 1H), 7.00 (ddd, *J* = 9.1, 5.6, 3.9 Hz, 2H), 6.92 (td, *J* = 8.7, 1.3 Hz, 3H), 2.41 – 2.24 (m, 3H), 2.14 – 2.02 (m, 1H), 1.94 – 1.77 (m, 1H), 1.37 (d, *J* = 29.0 Hz, 3H). ¹⁹F NMR (376 MHz, CDCl₃) δ -118.0 – -118.1 (m). ¹³C NMR (101 MHz, CDCl₃) δ 161.6 (d, *J* = 243.1 Hz), 143.7, 139.4, 130.0 (d, *J* = 7.7 Hz), 129.9, 127.3 (d, *J* = 15.7 Hz), 126.2, 115.5 (d, *J* = 21.9 Hz), 48.5, 38.1, 30.2, 22.0. GC/MS (m/z, relative intensity) 227 (10), 149 (5), 109 (100).

Following acceptors were also tried in the reaction. However, they did not work well.

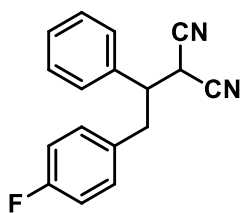
1-fluoro-4-(2-phenyl-3-(phenylsulfonyl)propyl)benzene (**4h**)



The general procedure **C** was followed using 1-(4-fluorobenzyl)-2,4,6-trimethylpyridin-1-ium bromide (**1h**) (37.2 mg, 0.12 mmol), DIPEA (0.36 mmol, 46.4 mg 62.8 μ L, 3 equiv), DI water (1.2 mmol, 21.6 mg, 21.6 μ L, 10 equiv), (E)-(2-(phenylsulfonyl)vinyl)benzene (0.48 mmol, 107.6 mg, 4 equiv) and 1.2 mL of stock solution of [Ir(2',4'-dF-5-CF₃-ppy)₂(4,4'-dtbbpy)]PF₆ in MeCN. After the completion of the reaction 20 h, the crude was purified via automated flash chromatography using EtOAc in hexanes (0% to 100%) with product eluting at 5% on a 4 g silica column to afford in 63% yield (27 mg) as an oil with a mixture of hydrogenated (E)-(2-(phenylsulfonyl)vinyl)benzene impurities. ¹H NMR (400 MHz, CD₂Cl₂) δ 7.94 – 7.90 (m, 1H), 7.68 (d, *J* = 7.7 Hz, 2H), 7.63 – 7.54

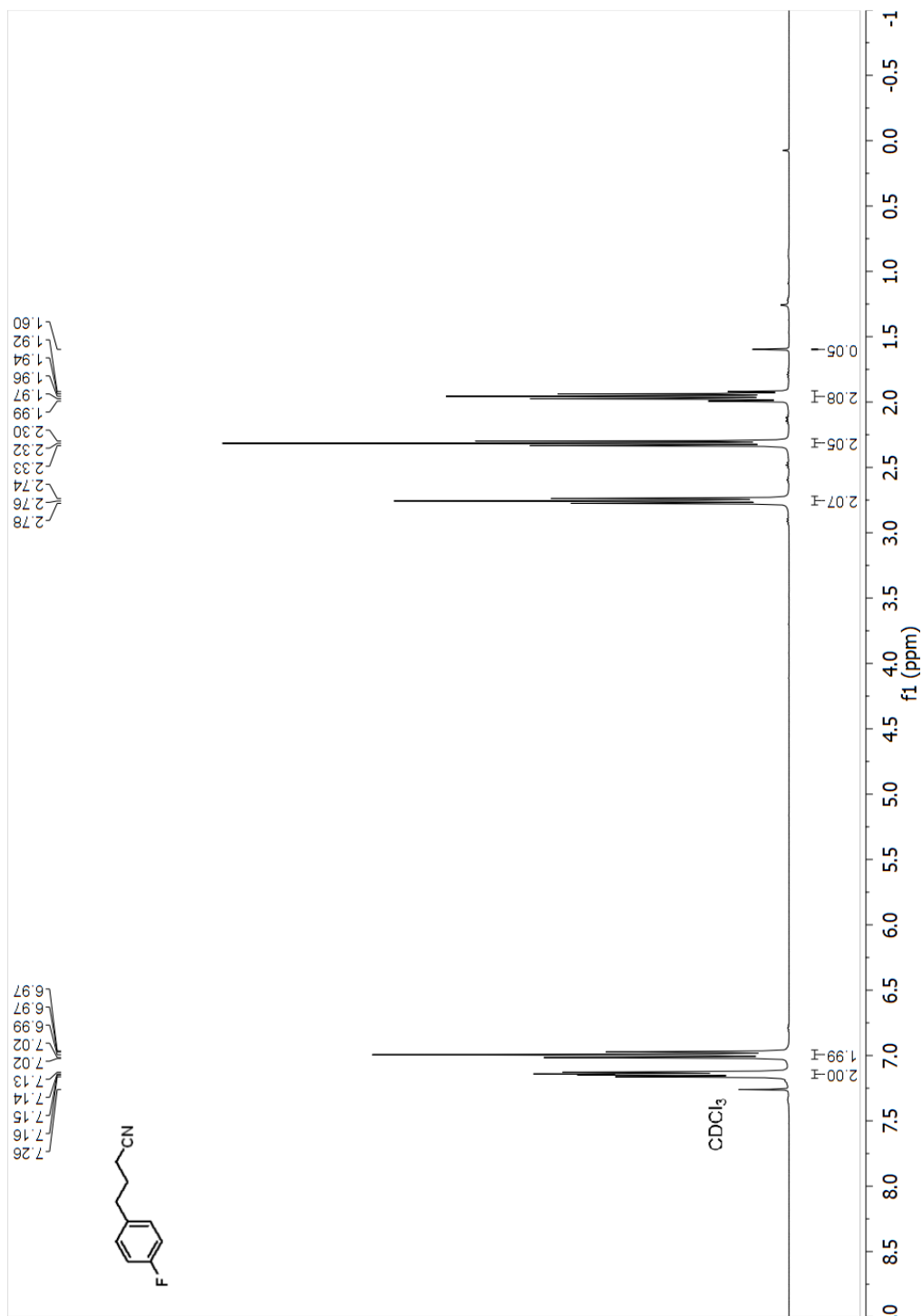
(m, 2H), 7.43 (t, $J = 7.8$ Hz, 1H), 7.29 – 7.24 (m, 2H), 7.13 (t, $J = 5.6$ Hz, 3H), 6.95 – 6.92 (m, 1H), 6.90 – 6.85 (m, 2H), 3.48 (dd, $J = 12.0, 6.5$ Hz, 1H), 3.44 – 3.32 (m, 2H), 3.07 (dd, $J = 13.8, 6.2$ Hz, 1H), 3.04 – 2.97 (m, 1H). ^{19}F NMR (376 MHz, CD_2Cl_2) δ -117.4 (tt, $J = 8.8, 5.8$ Hz). ^{13}C NMR (101 MHz, CD_2Cl_2) δ 162.1 (d, $J = 245.2$ Hz), 134.1 (d, $J = 36.2$ Hz), 131.2 (d, $J = 7.8$ Hz), 129.9, 129.7, 129.3, 129.0, 128.8, 128.6, 128.3, 128.2, 115.5 (d, $J = 21.3$ Hz), 61.1, 57.9, 43.2, 42.6, 30.3, 29.3. GC/MS (m/z, relative intensity) 245(1), 212 (20), 109 (100). HRMS (ESI) calcd. for $[\text{C}_{21}\text{H}_{20}\text{FO}_2\text{S}]^+$ $[\text{M}+\text{H}]^+$ m/z, 355.1168 found 355.1921.

2-(2-(4-fluorophenyl)-1-phenylethyl)malononitrile

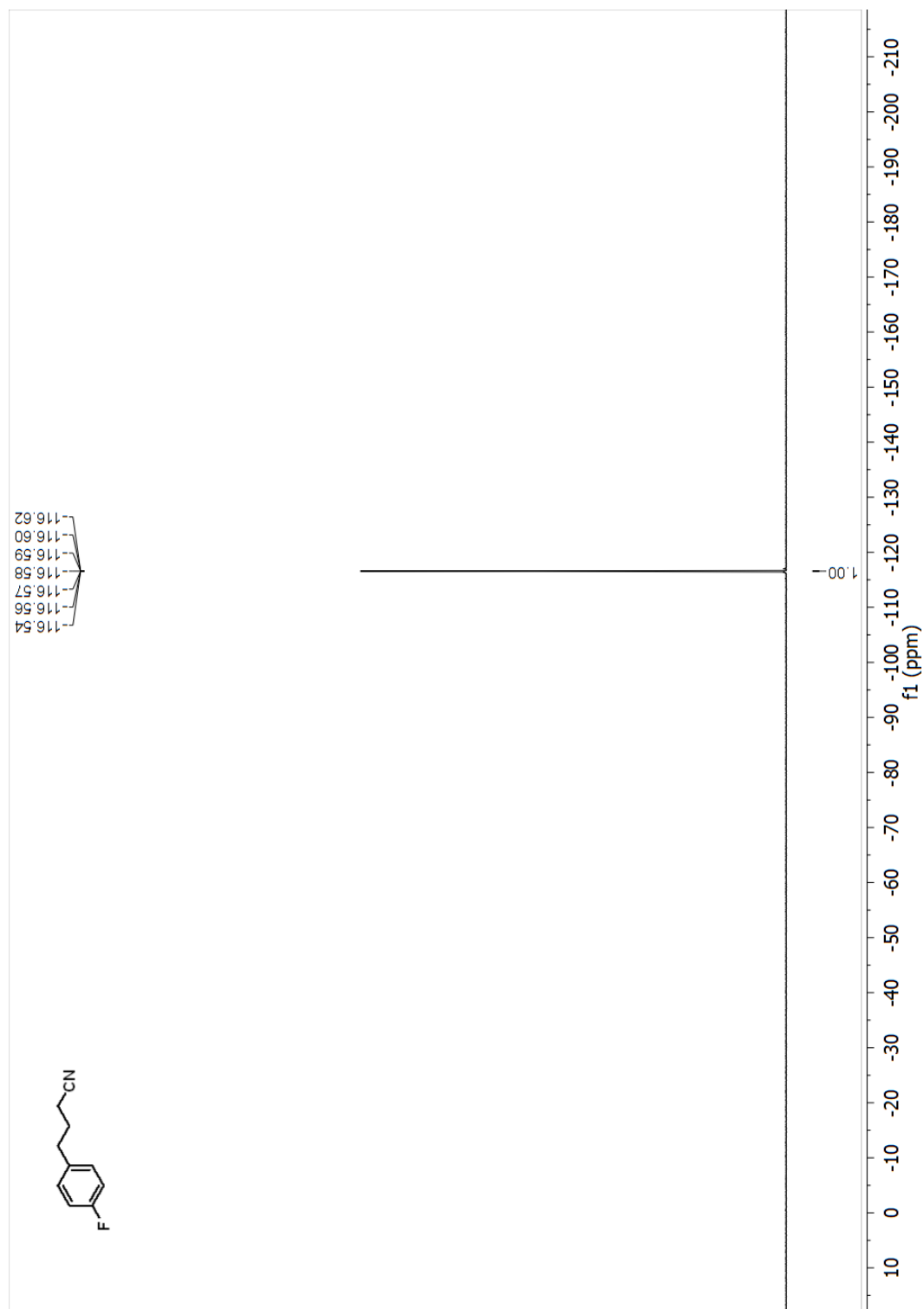


The general procedure **C** was followed using 1-(4-fluorobenzyl)-2,4,6-trimethylpyridin-1-ium bromide (**1h**) (37.2 mg, 0.12 mmol), DIPEA (0.36 mmol, 46.4 mg 62.8 μL , 3 equiv), DI water (1.2 mmol, 21.6 mg, 21.6 μL , 10 equiv), 2-benzylidenemalononitrile (0.48 mmol, 74.0 mg, 4 equiv) and 1.2 mL of stock solution of $[\text{Ir}(2',4'\text{-dF-5-CF}_3\text{-ppy})_2(4,4'\text{-dtbbpy})]\text{PF}_6$ in MeCN. After the completion of the reaction 20 h, the crude was purified via automated flash chromatography using EtOAc in hexanes (0% to 100%) with product eluting at 3% on a 4 g silica column to afford with other product (22 mg) as an oil. ^{19}F NMR chemical shifts match with the literature values.³⁷ ^{19}F NMR yield of the reaction is 4%. ^1H NMR (400 MHz, CD_2Cl_2) δ 7.39 – 7.30 (m, 9H), 7.09 (t, $J = 8.7$ Hz, 2H), 7.01 – 6.95 (m, 2H), 6.90 – 6.82 (m, 2H), 3.56 (d, $J = 11.0$ Hz, 1H), 3.37 (q, $J = 12.8, 12.2$ Hz, 2H), 3.07 (d, $J = 13.9$ Hz, 1H), 2.83 (d, $J = 13.9$ Hz, 1H). ^{19}F NMR (376 MHz, CD_2Cl_2) δ -113.8 – -114.0 (m). ^{13}C NMR (101 MHz, CD_2Cl_2) δ 163.6 (d, $J = 247.4$ Hz), 135.4, 133.7, 132.6 (d, $J = 8.3$ Hz), 131.1 (d, $J = 7.9$ Hz), 129.7, 129.6, 128.1, 127.9, 116.4, 116.2, 116.0, 115.7 (d, $J = 21.3$ Hz), 114.9, 46.0, 42.1, 38.3, 30.3. GC/MS (m/z, relative intensity) 263 (M-1, 1), 199 (8), 109 (100).

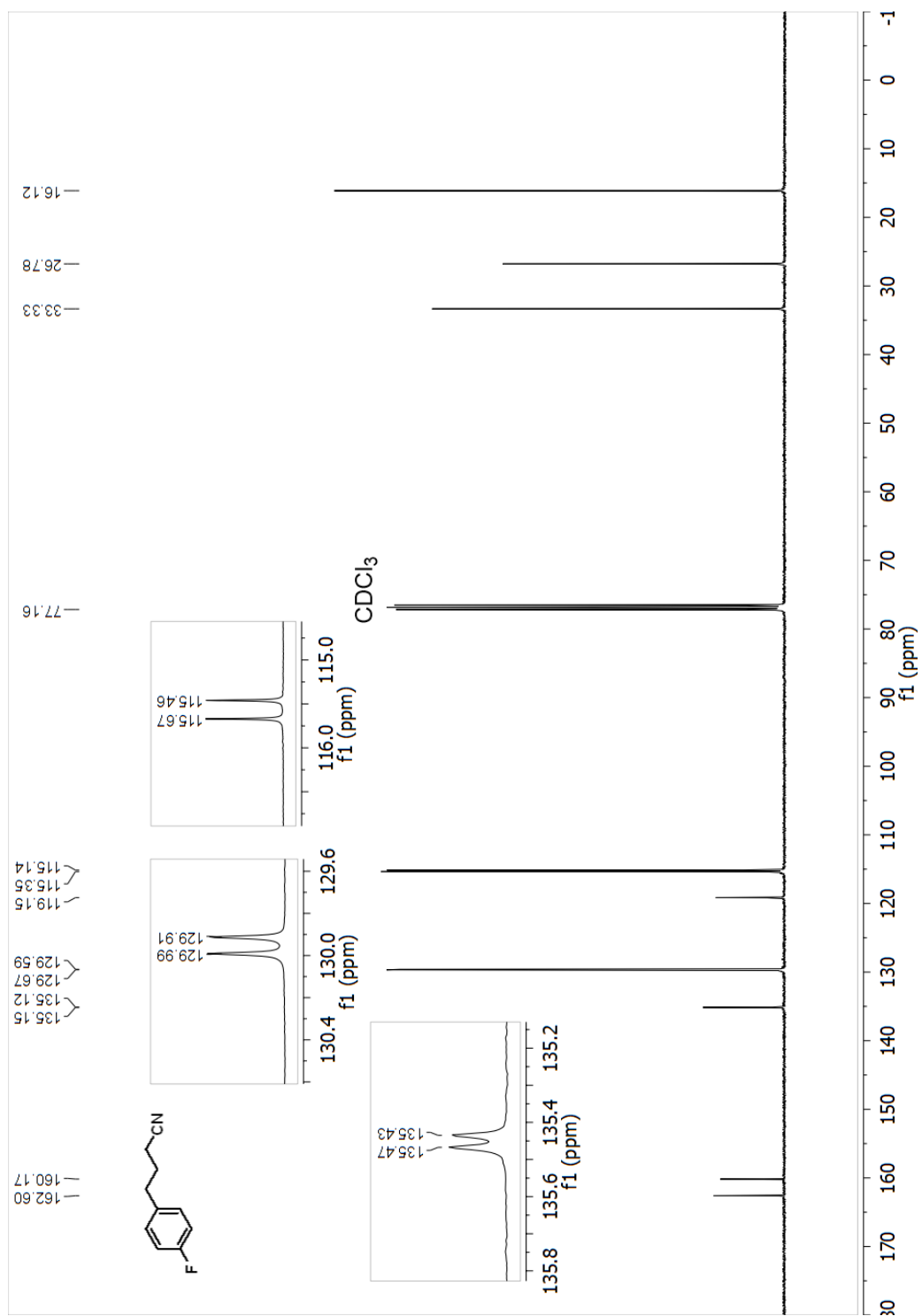
¹H NMR (400 MHz, Chloroform-d) spectrum of 3a 4-(4-fluorophenyl)butanenitrile



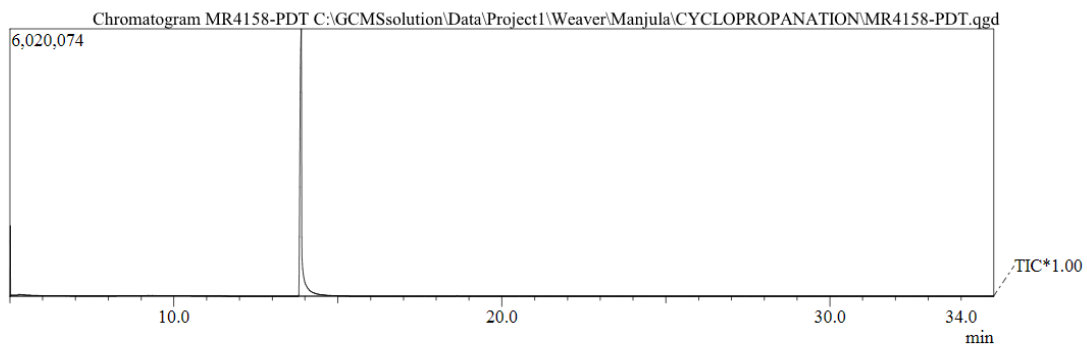
^{19}F NMR (376 MHz, Chloroform-d) spectrum of 3a 4-(4-fluorophenyl)butanenitrile



¹³C NMR (101 MHz, Chloroform-d) spectrum of 3a 4-(4-fluorophenyl)butanenitrile

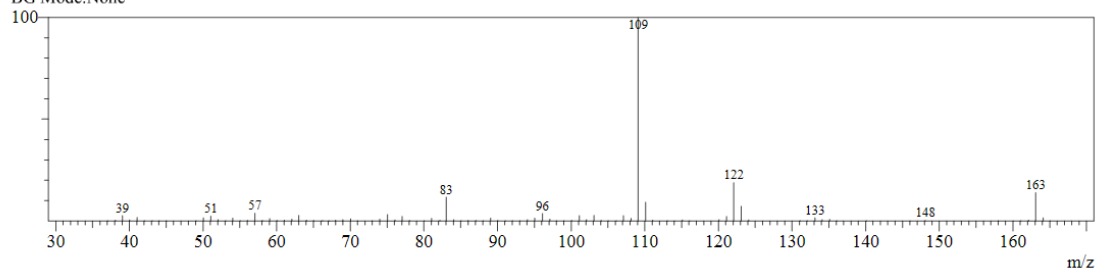


GC and MS of 3a 4-(4-fluorophenyl)butanenitrile

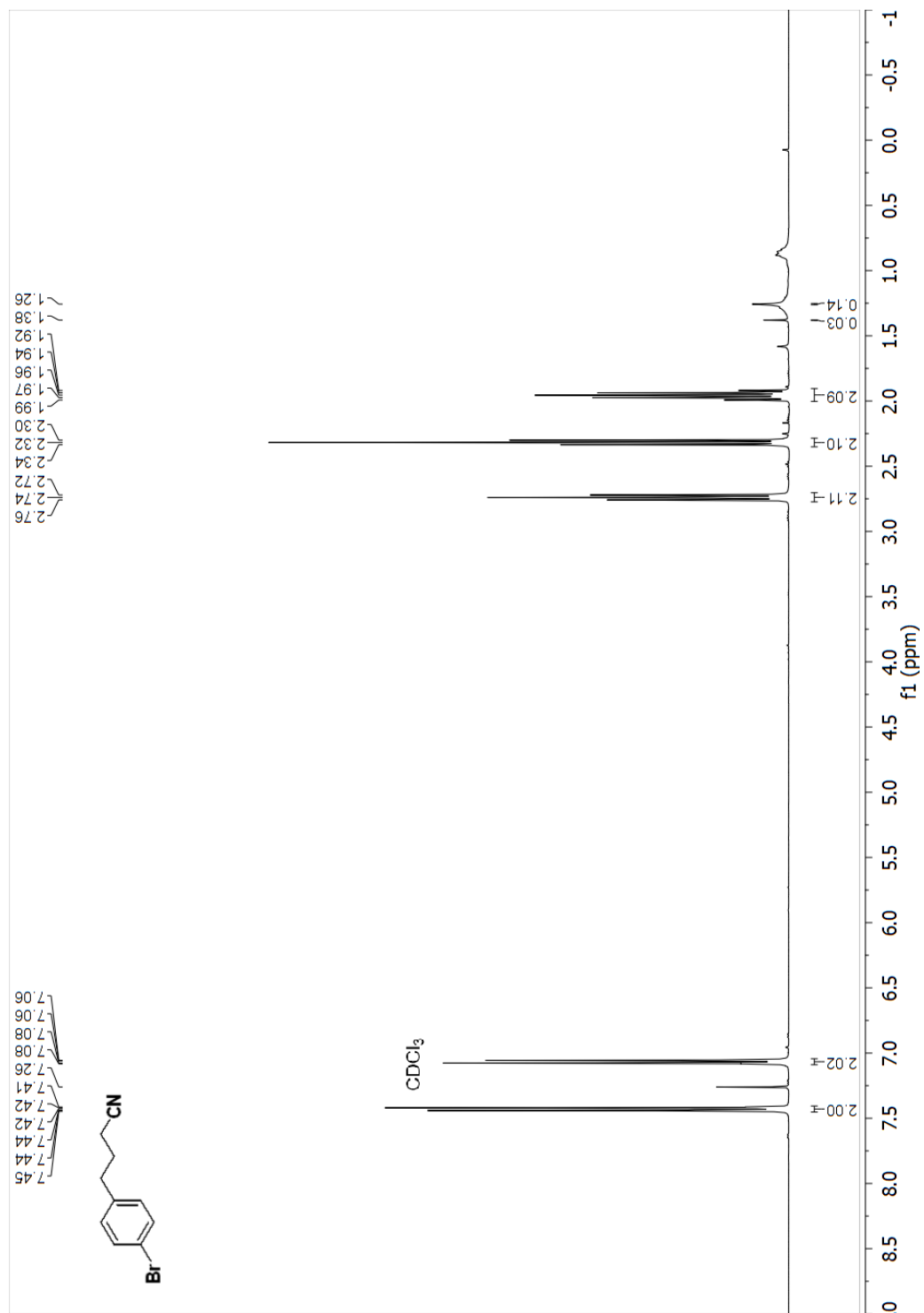


Spectrum

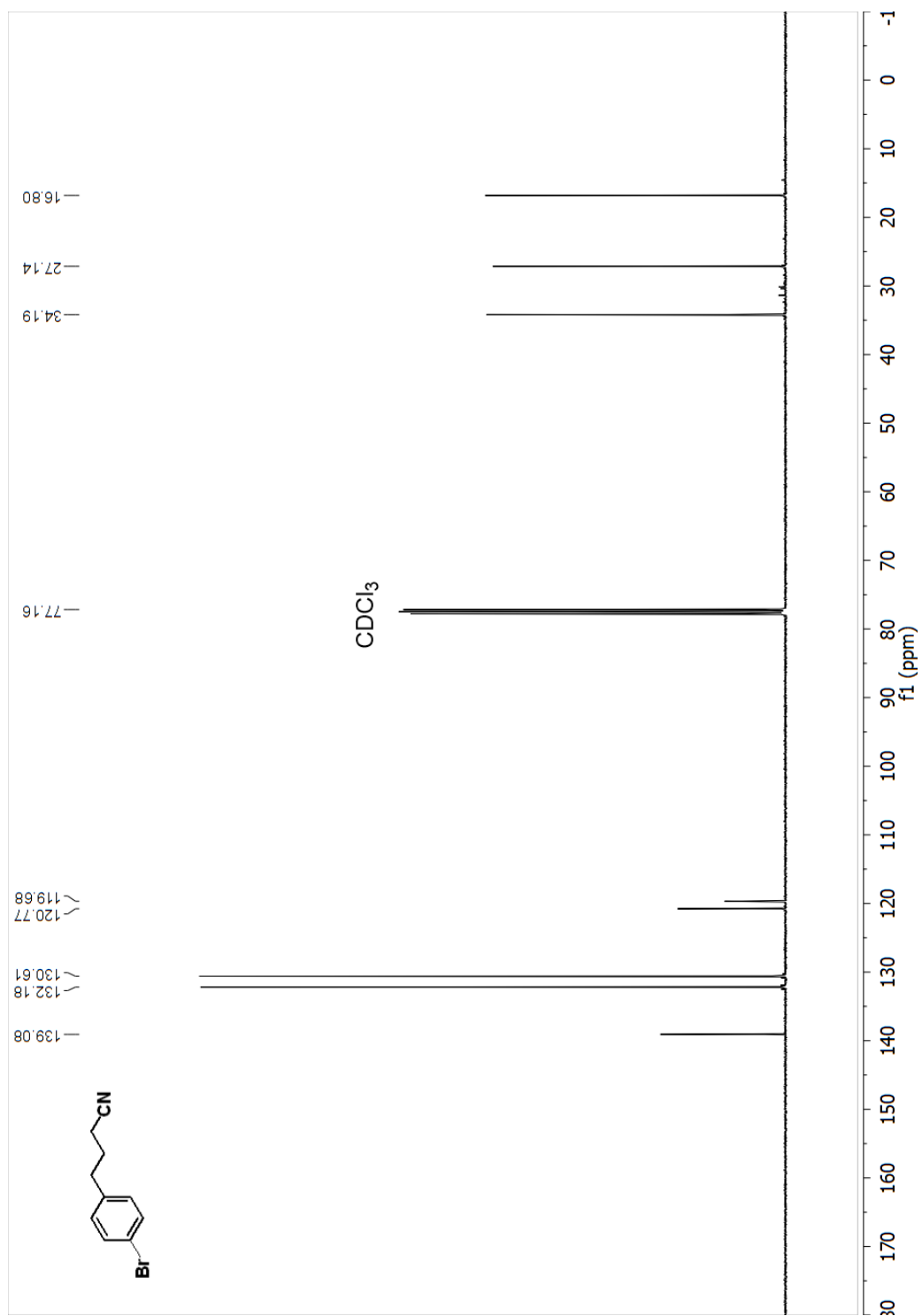
Line#:1 R.Time:13.9(Scan#:1063)
MassPeaks:95
RawMode:Single 13.9(1063) BasePeak:109(1961732)
BG Mode:None



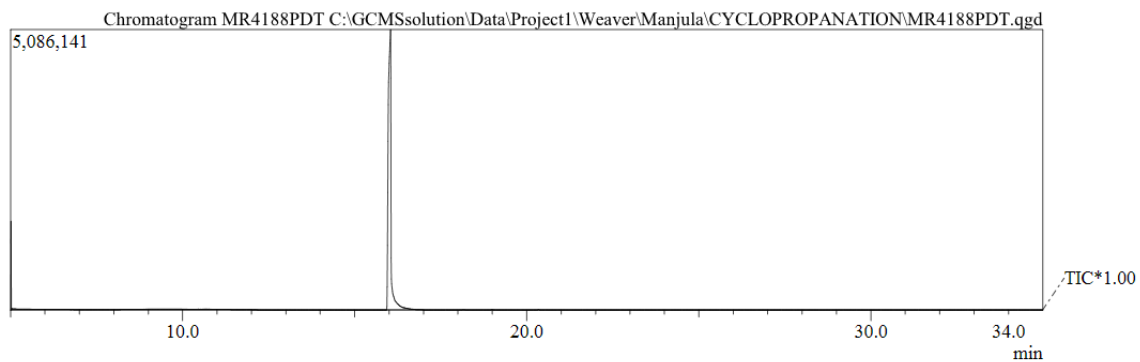
¹H NMR (400 MHz, Chloroform-d) spectrum of 3b 4-(4-bromophenyl)butanenitrile



^{13}C NMR (101 MHz, Chloroform-d) spectrum of 3b 4-(4-bromophenyl)butanenitrile

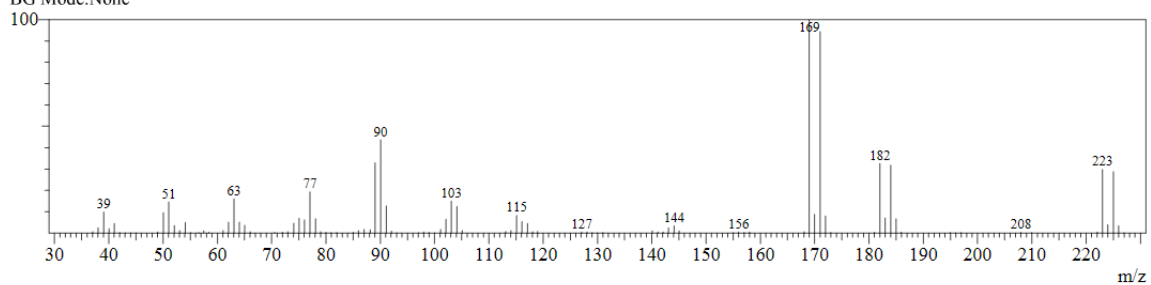


GC and MS of 3b 4-(4-bromophenyl)butanenitrile

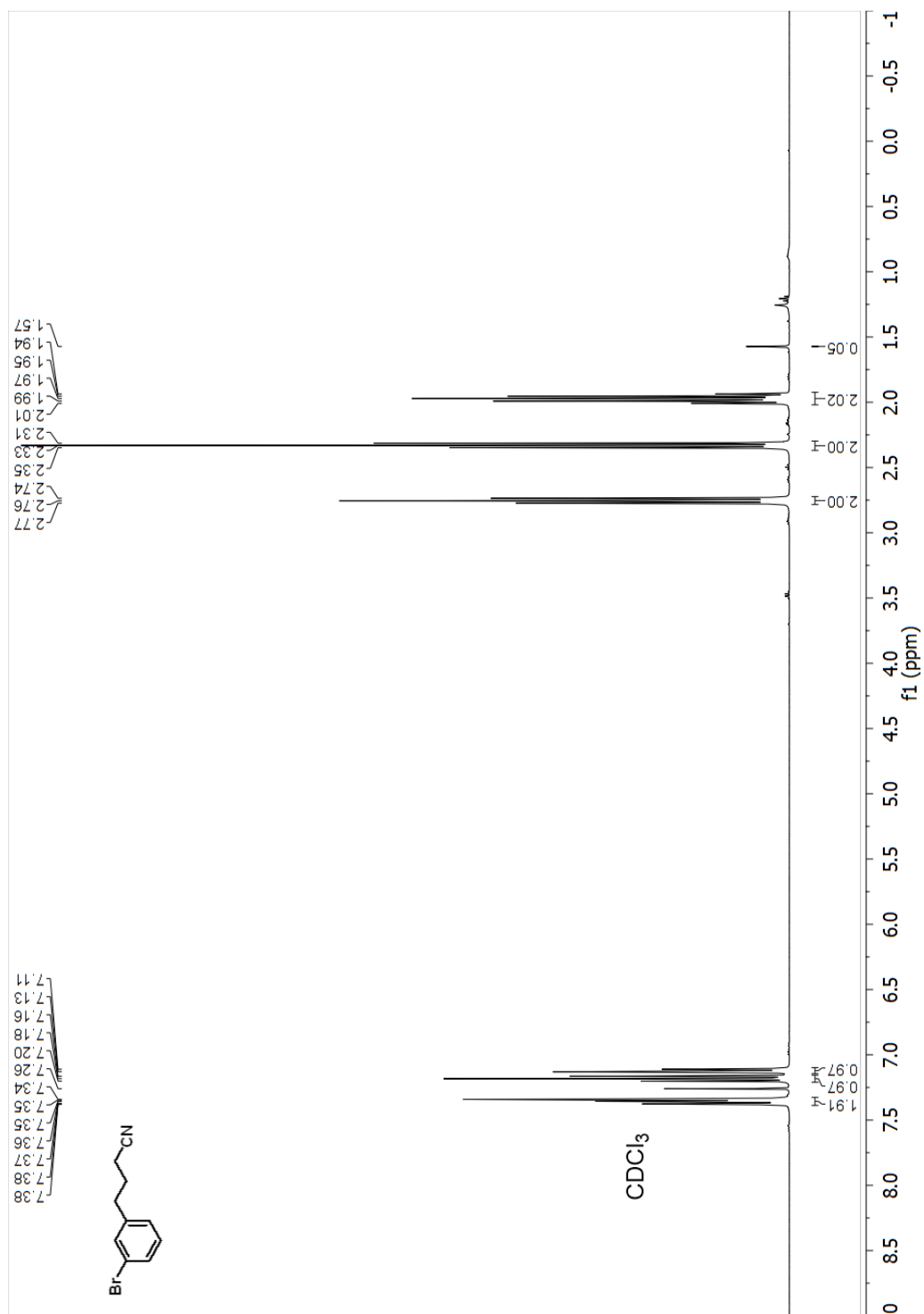


Spectrum

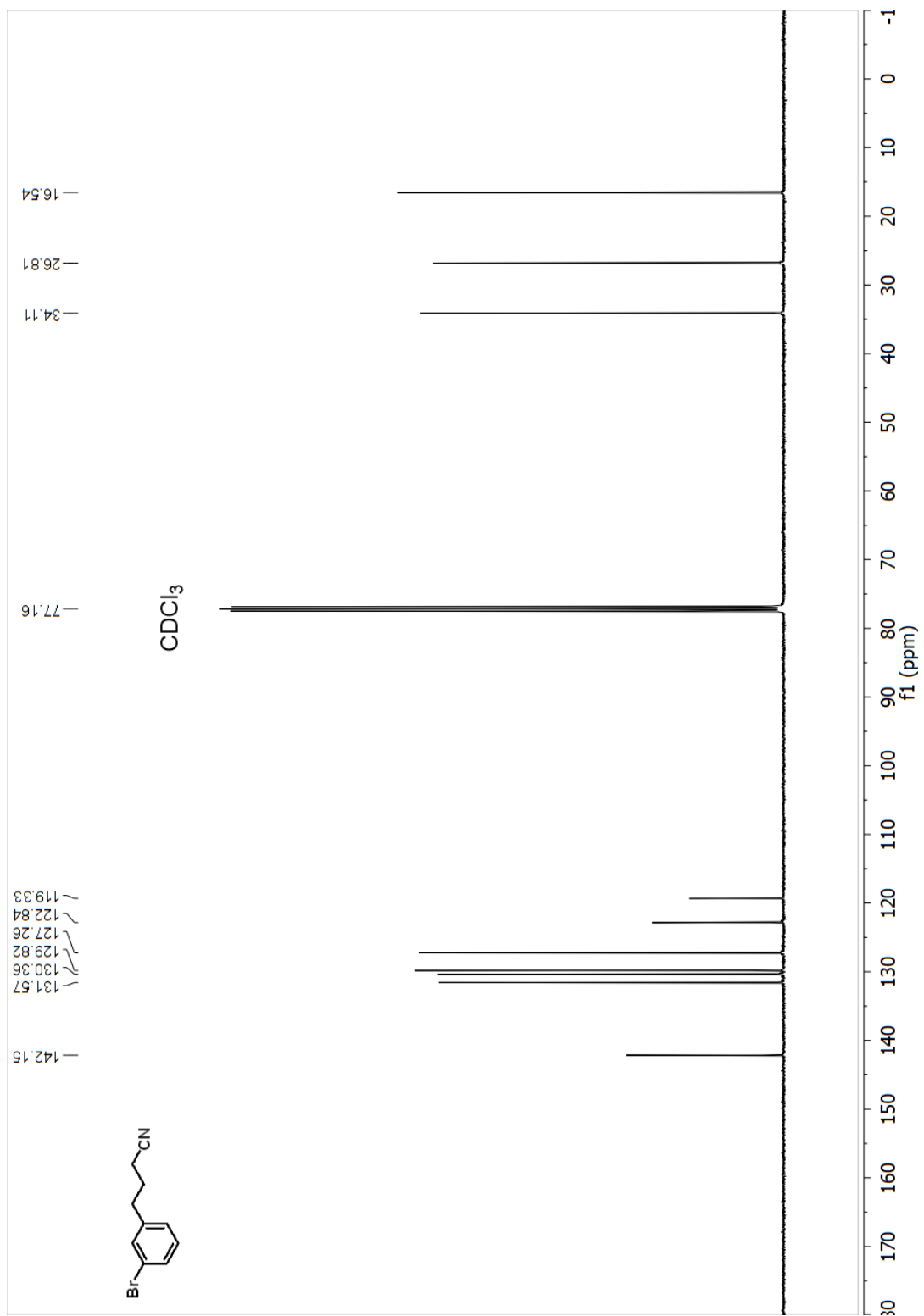
Line#:1 R.Time:16.0(Scan#:1322)
MassPeaks:100
RawMode:Single 16.0(1322) BasePeak:169(694862)
BG Mode:None



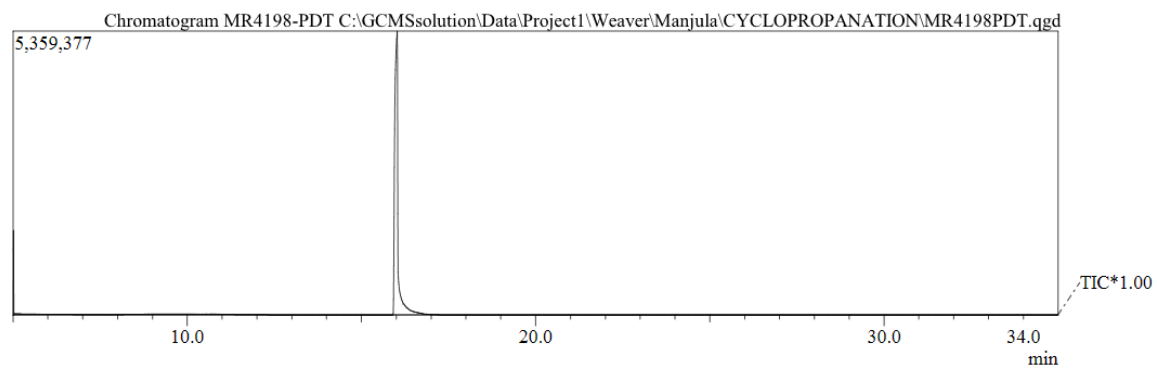
¹H NMR (400 MHz, Chloroform-d) spectrum of 3c 4-(3-bromophenyl)butanenitrile



¹³C NMR (101 MHz, Chloroform-d) spectrum of 3c 4-(3-bromophenyl)butanenitrile

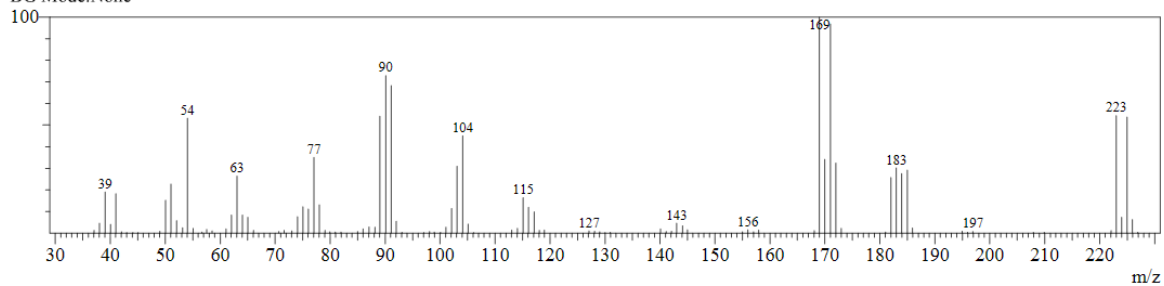


GC and MS of 3c 4-(3-bromophenyl)butanenitrile

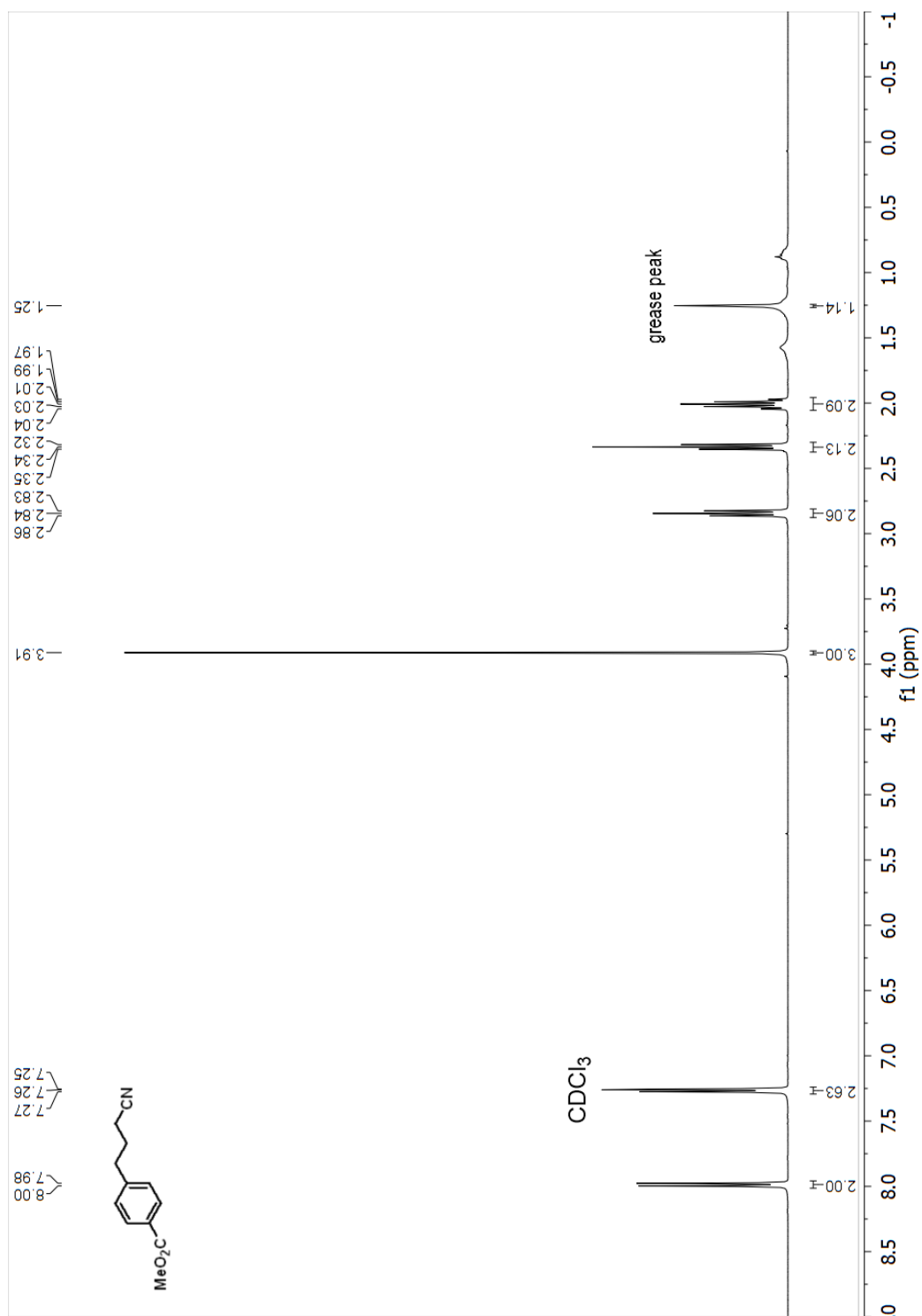


Spectrum

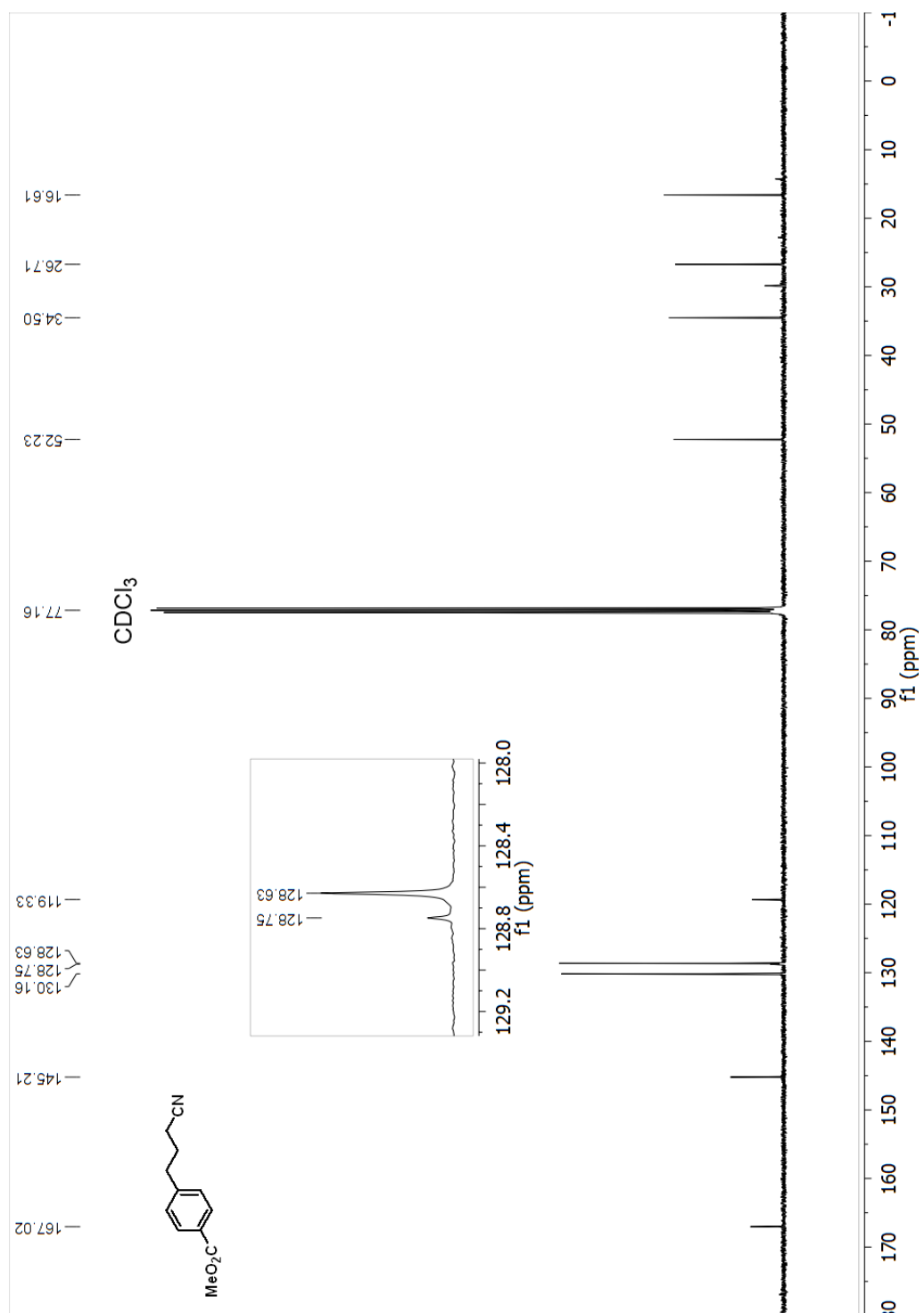
Line#:1 R.Time:16.0(Scan#:1321)
MassPeaks:101
RawMode:Single 16.0(1321) BasePeak:169(433370)
BG Mode:None



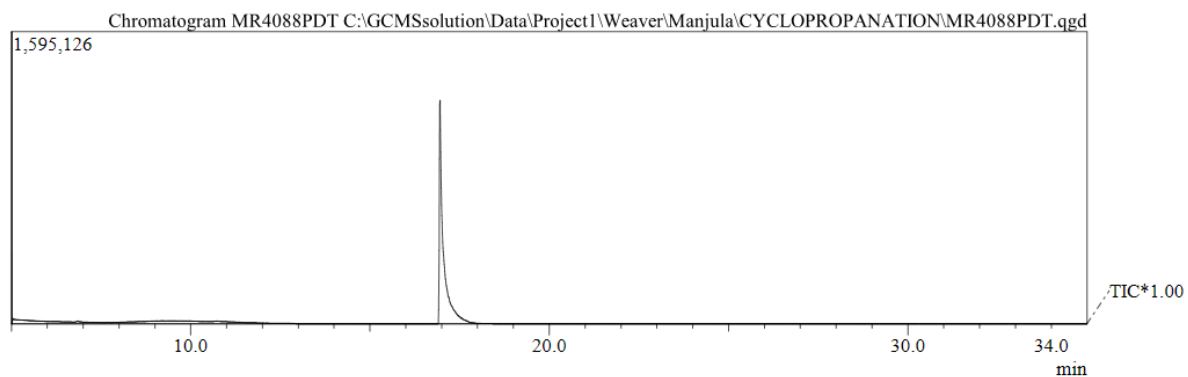
¹H NMR (400 MHz, Chloroform-d) spectrum of 3d methyl 4-(3-cyanopropyl)benzoate



^{13}C NMR (101 MHz, Chloroform-d) spectrum of 3d methyl 4-(3-cyanopropyl)benzoate

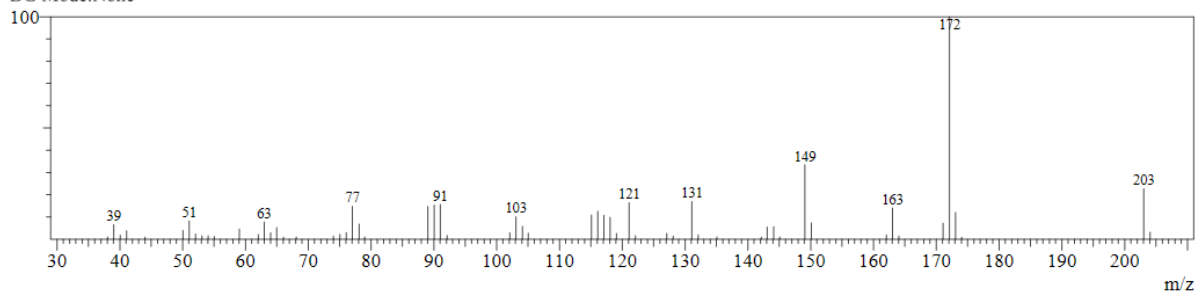


GC and MS of 3d methyl 4-(3-cyanopropyl)benzoate

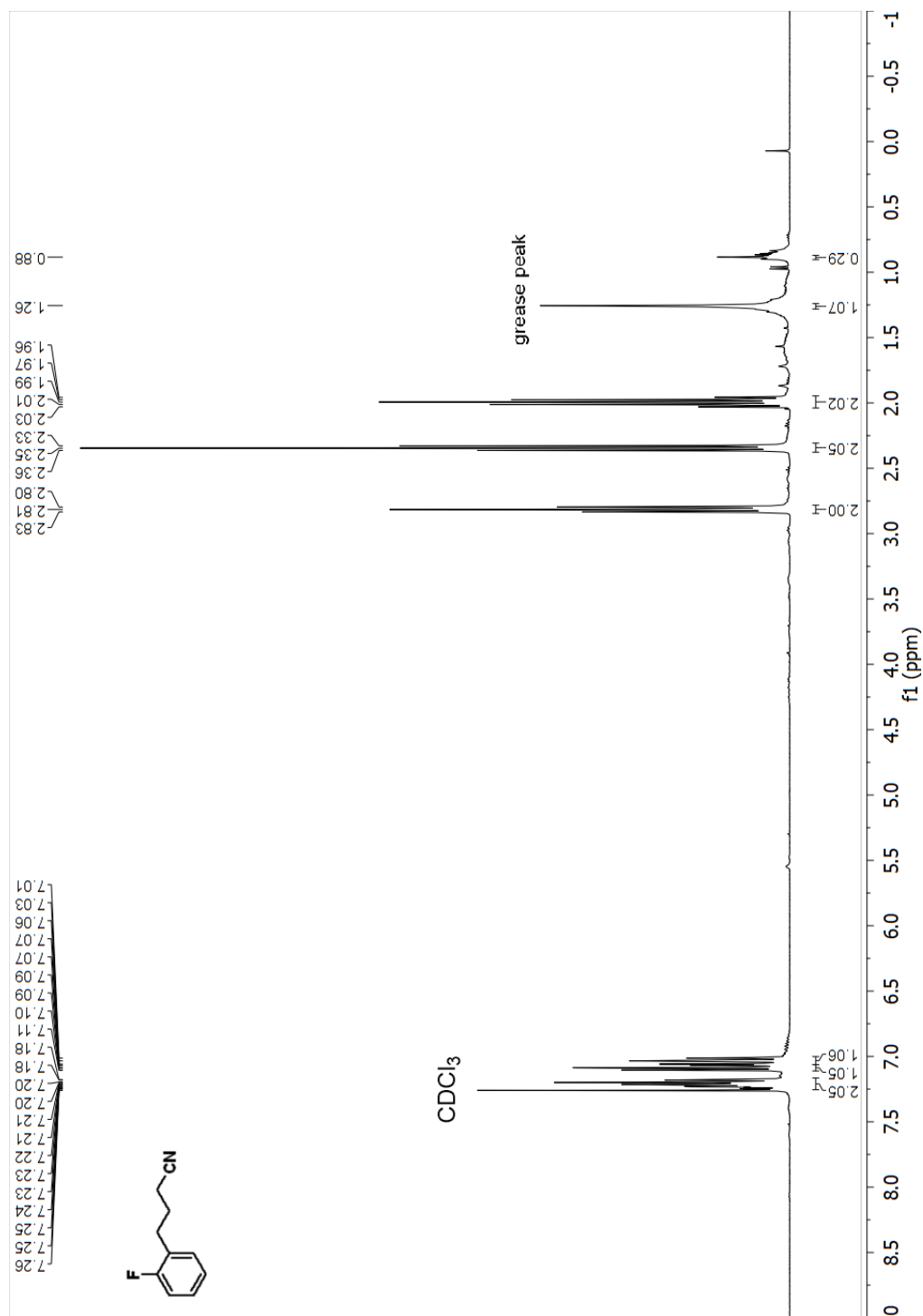


Spectrum

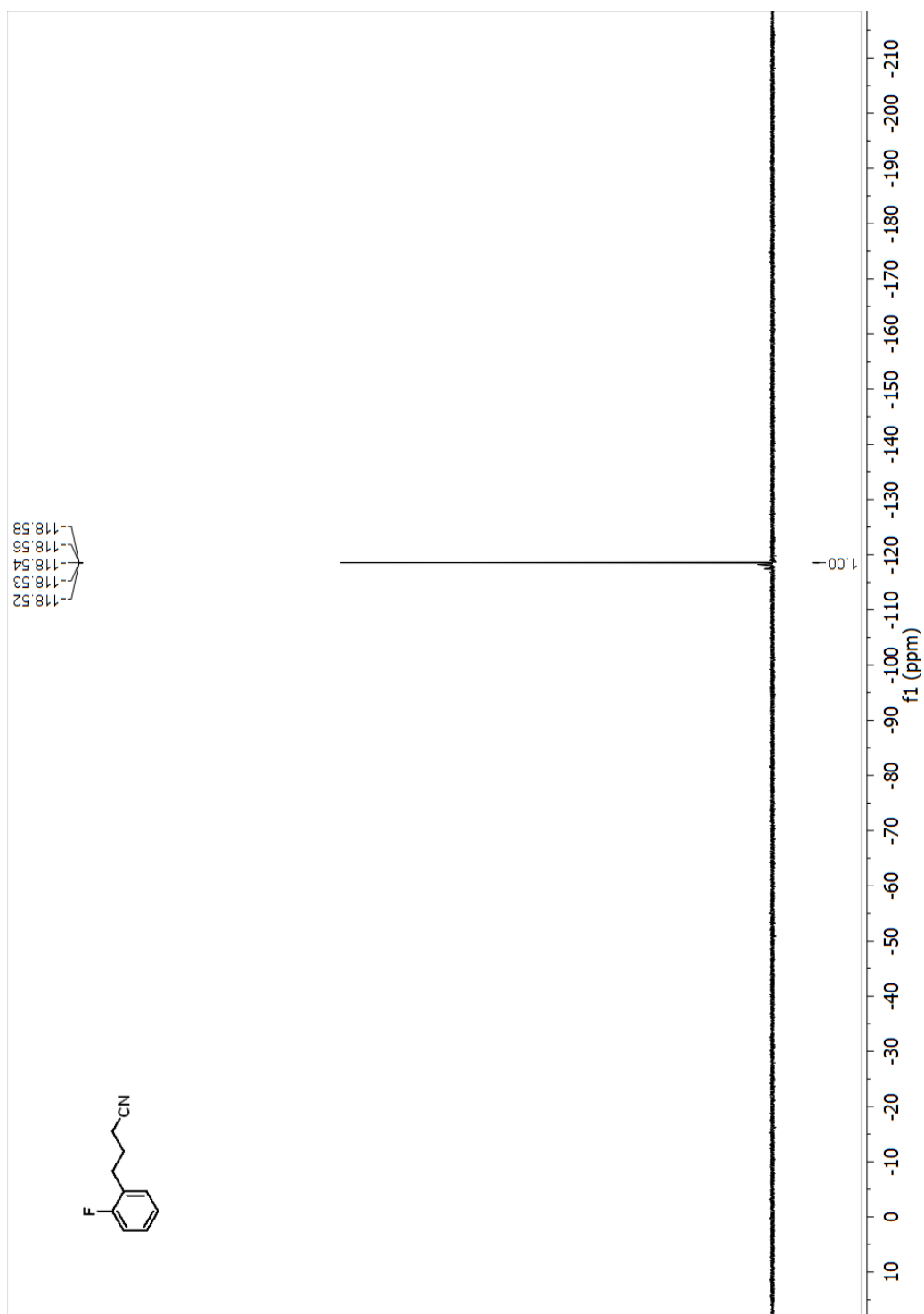
Line#:1 R.Time:17.0(Scan#:1442)
MassPeaks:59
RawMode:Single 17.0(1442) BasePeak:172(119839)
BG Mode:None



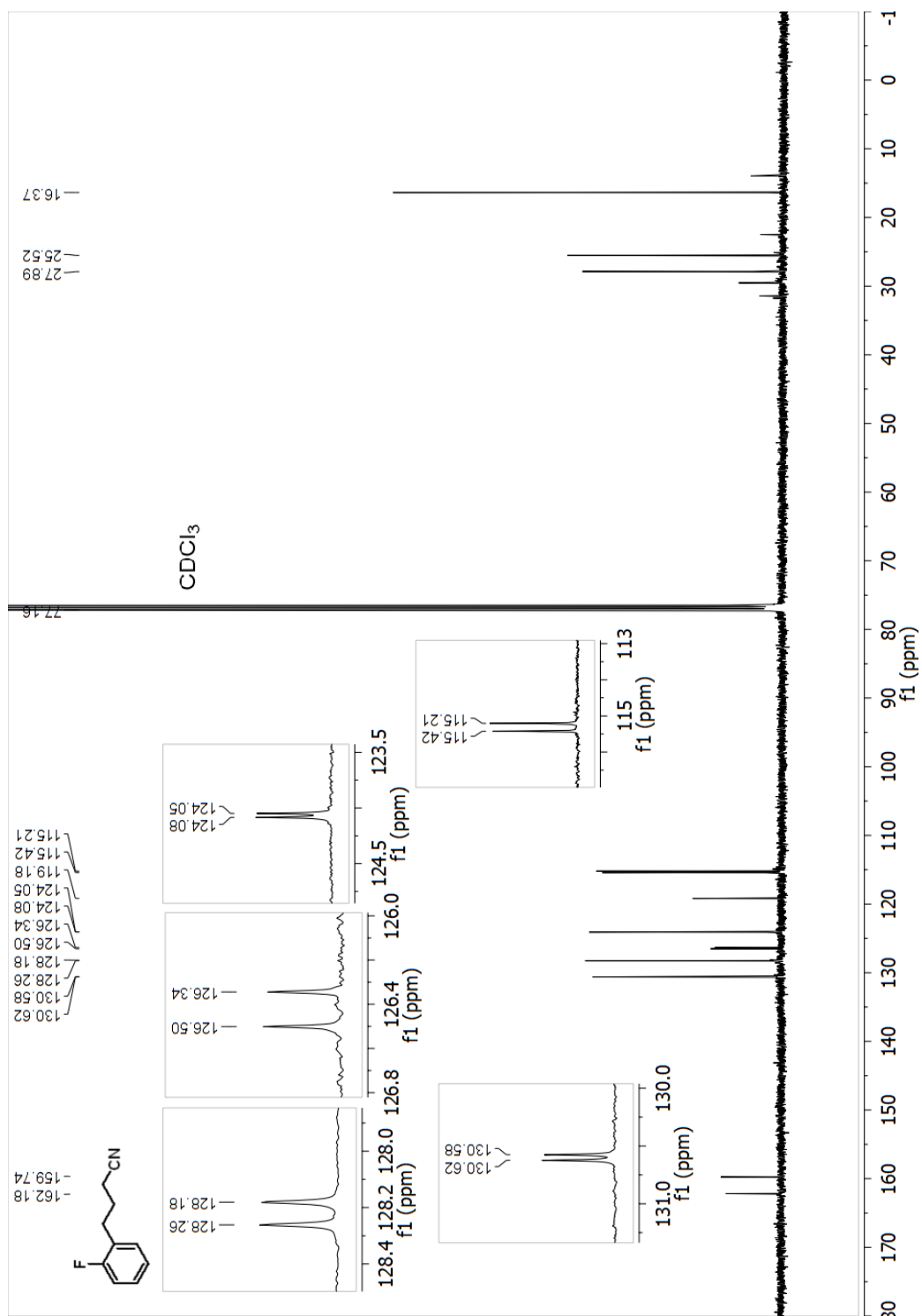
^1H NMR (400 MHz, Chloroform-d) spectrum of 3e 4-(2-fluorophenyl)butanenitrile



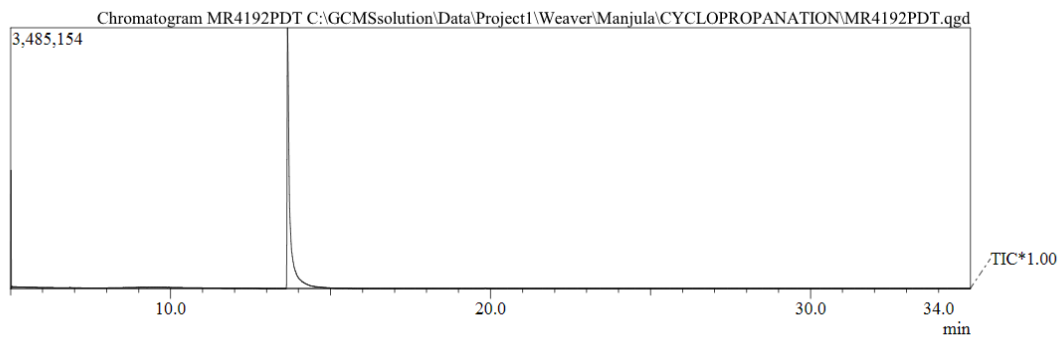
^{19}F NMR (376 MHz, Chloroform-d) spectrum of 3e 4-(2-fluorophenyl)butanenitrile



¹³C NMR (101 MHz, Chloroform-d) spectrum of 3e 4-(2-fluorophenyl)butanenitrile

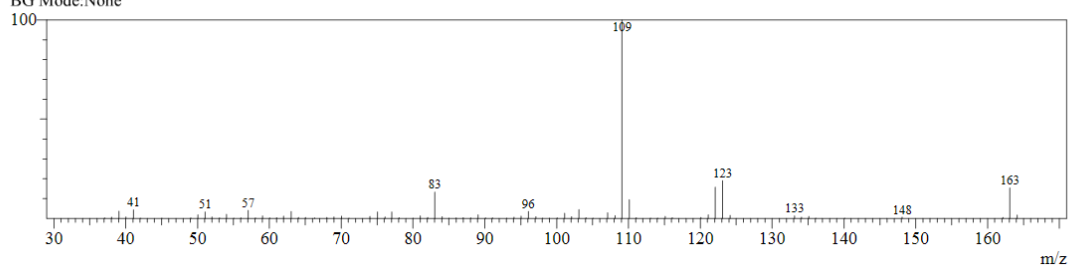


GC and MS of 3e 4-(2-fluorophenyl)butanenitrile

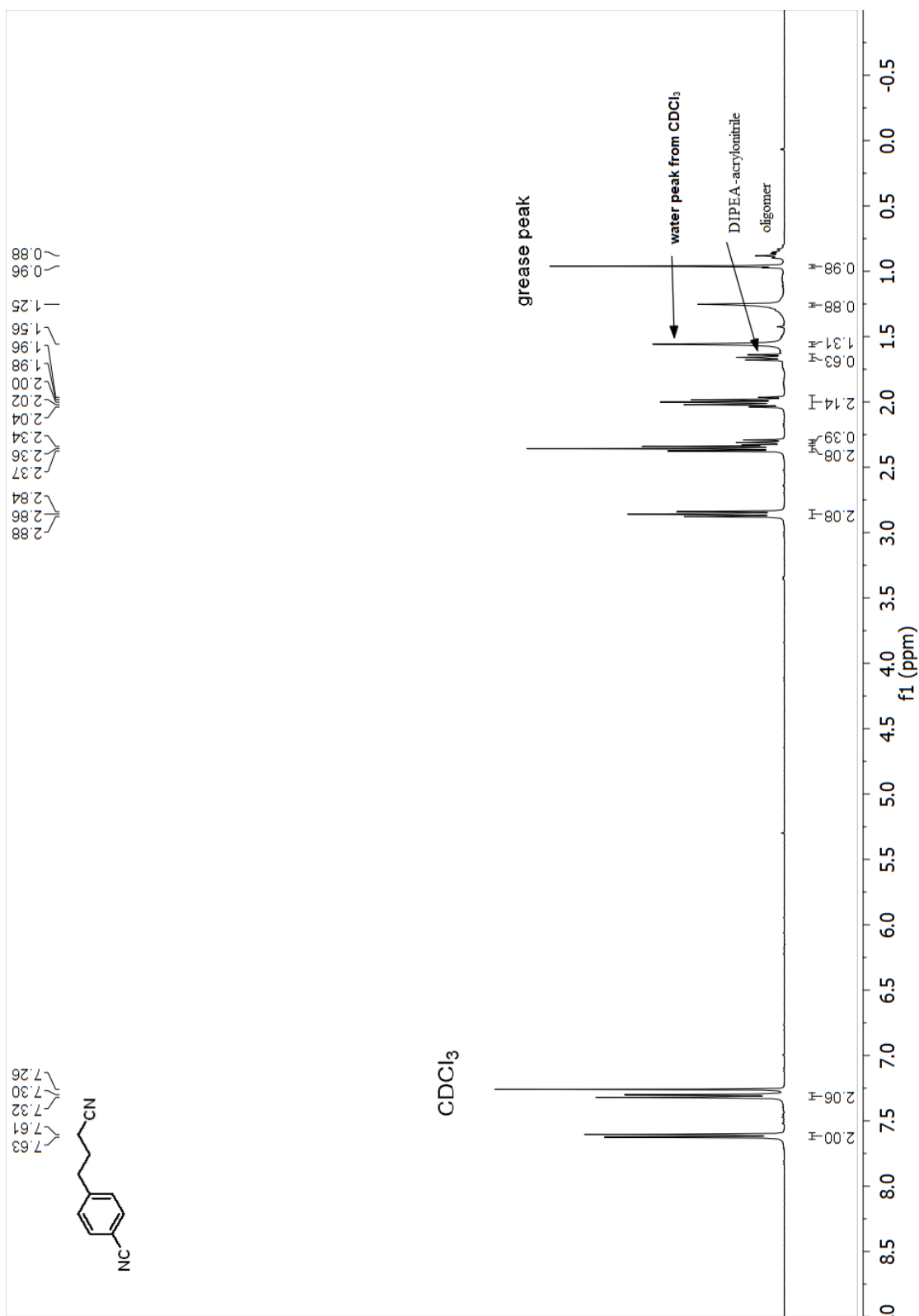


Spectrum

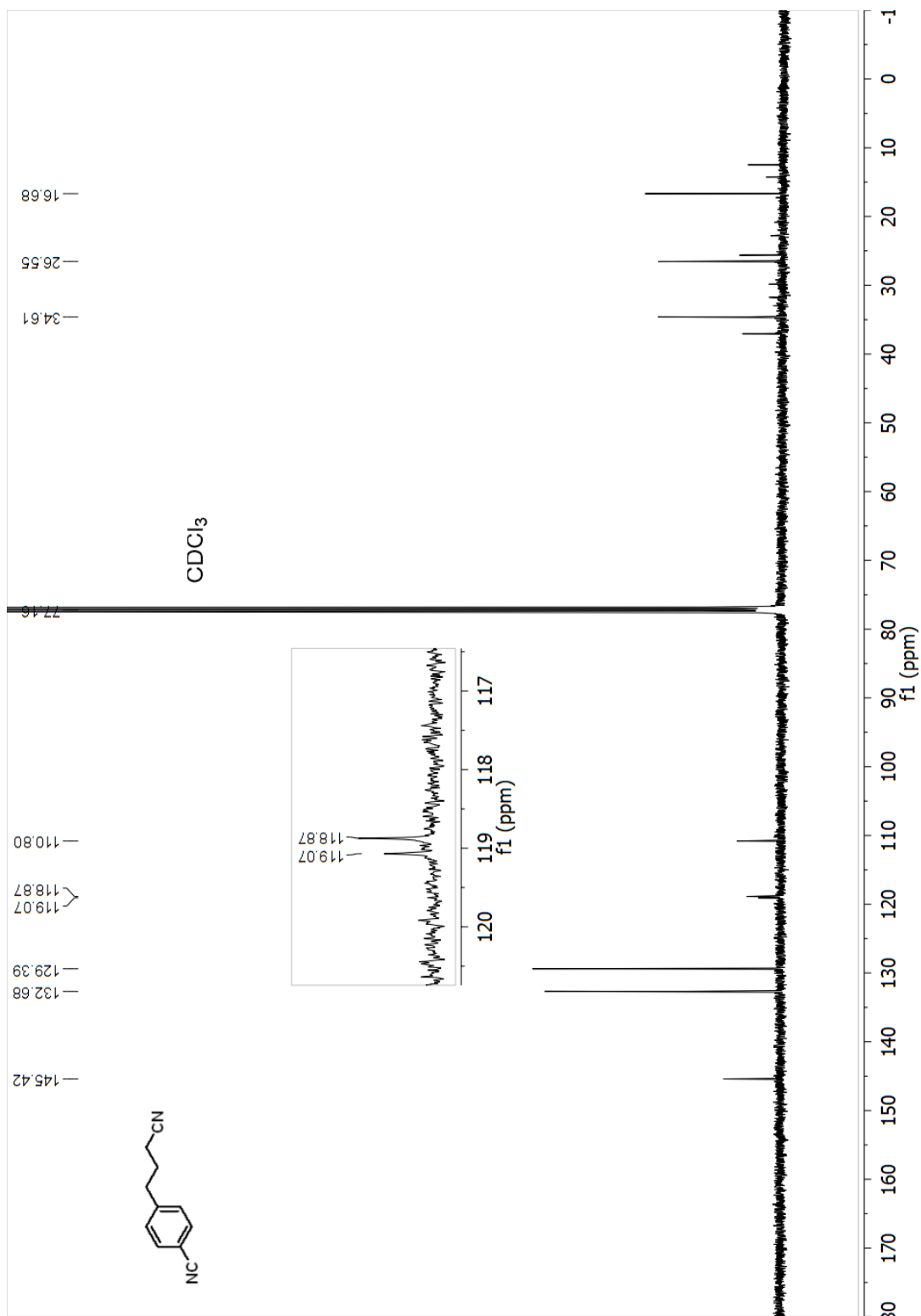
Line#:1 R. Time:13.7(Scan#:1044)
MassPeaks:82
RawMode:Single 13.7(1044) BasePeak:109(728703)
BG Mode:None



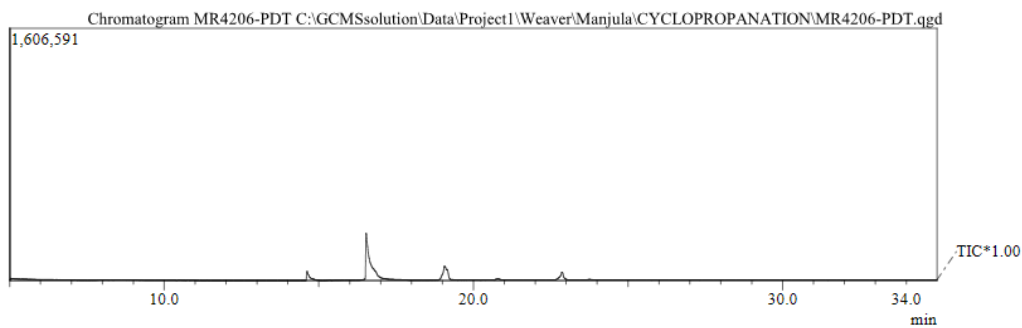
¹H NMR (400 MHz, Chloroform-d) spectrum of 3f 4-(3-cyanopropyl)benzonitrile



¹³C NMR (101 MHz, Chloroform-d) spectrum of 3-(4-(3-cyanopropyl)phenyl)benzonitrile

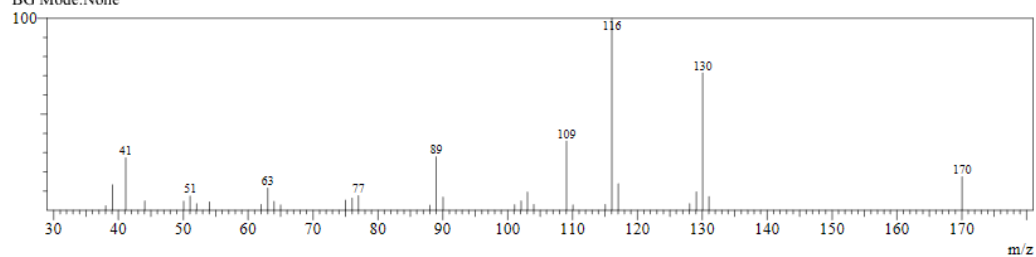


GC and MS of 3f 4-(3-cyanopropyl)benzonitrile

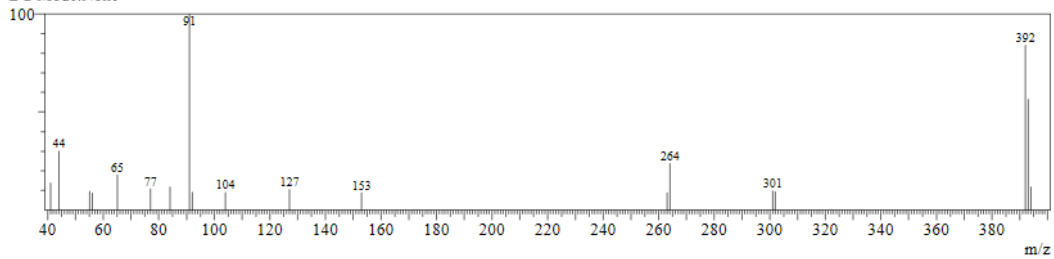


Spectrum

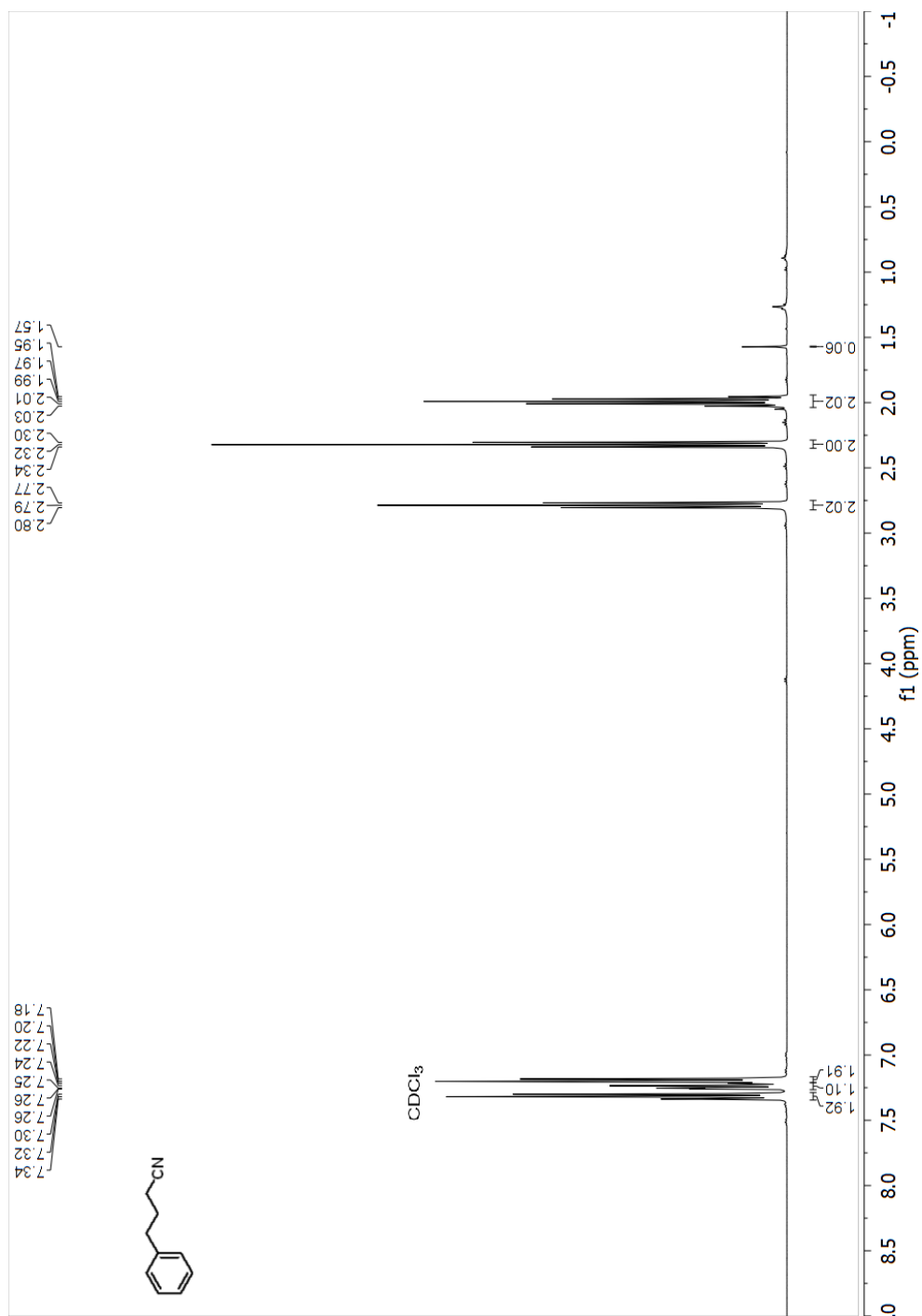
Line#:1 R.Time:16.6(Scan#:1392)
MassPeaks:32
RawMode:Single 16.6(1392) BasePeak:116(42034)
BG Mode:None



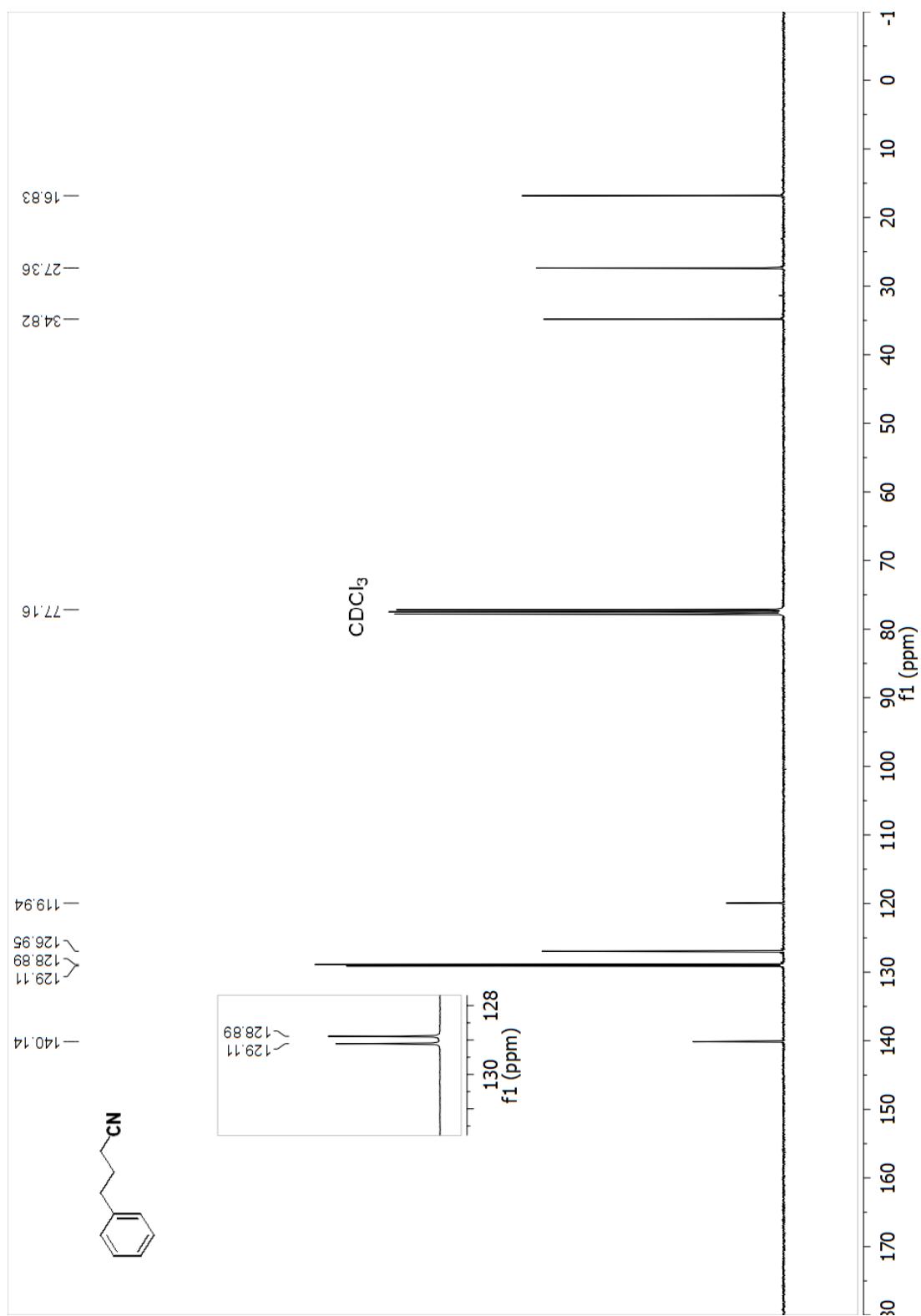
Line#:3 R.Time:22.9(Scan#:2143)
MassPeaks:19
RawMode:Single 22.9(2143) BasePeak:91(11866)
BG Mode:None



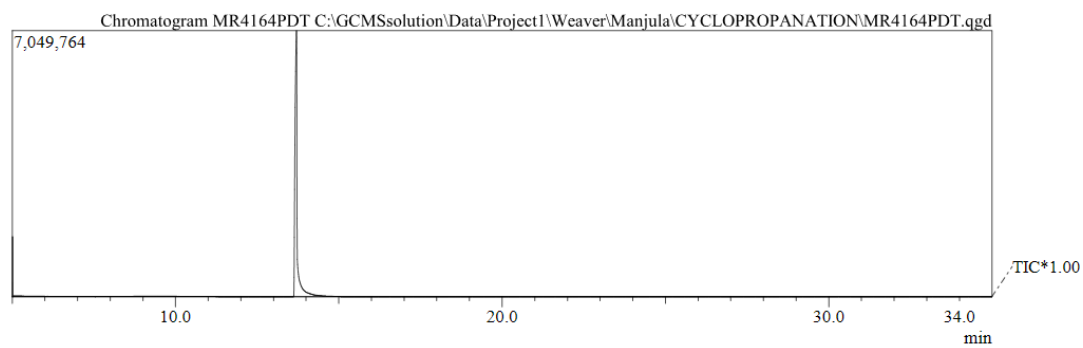
¹H NMR (400 MHz, Chloroform-d) spectrum of 3g 4-phenylbutanenitrile



¹³C NMR (101 MHz, Chloroform-d) spectrum of 3g 4-phenylbutanenitrile



GC and MS of 3g 4-phenylbutanenitrile



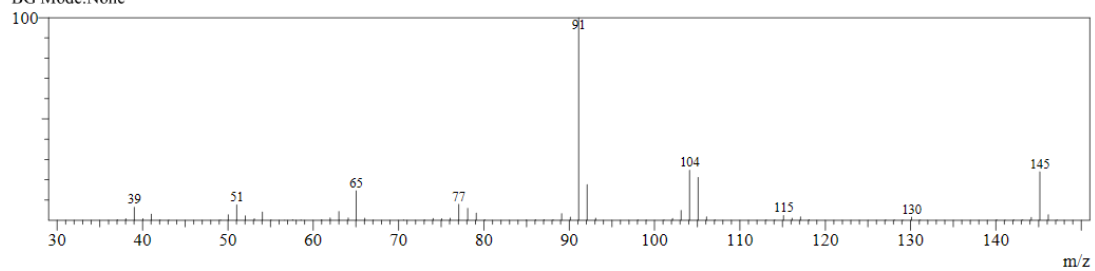
Spectrum

Line#:1 R.Time:13.7(Scan#:1044)

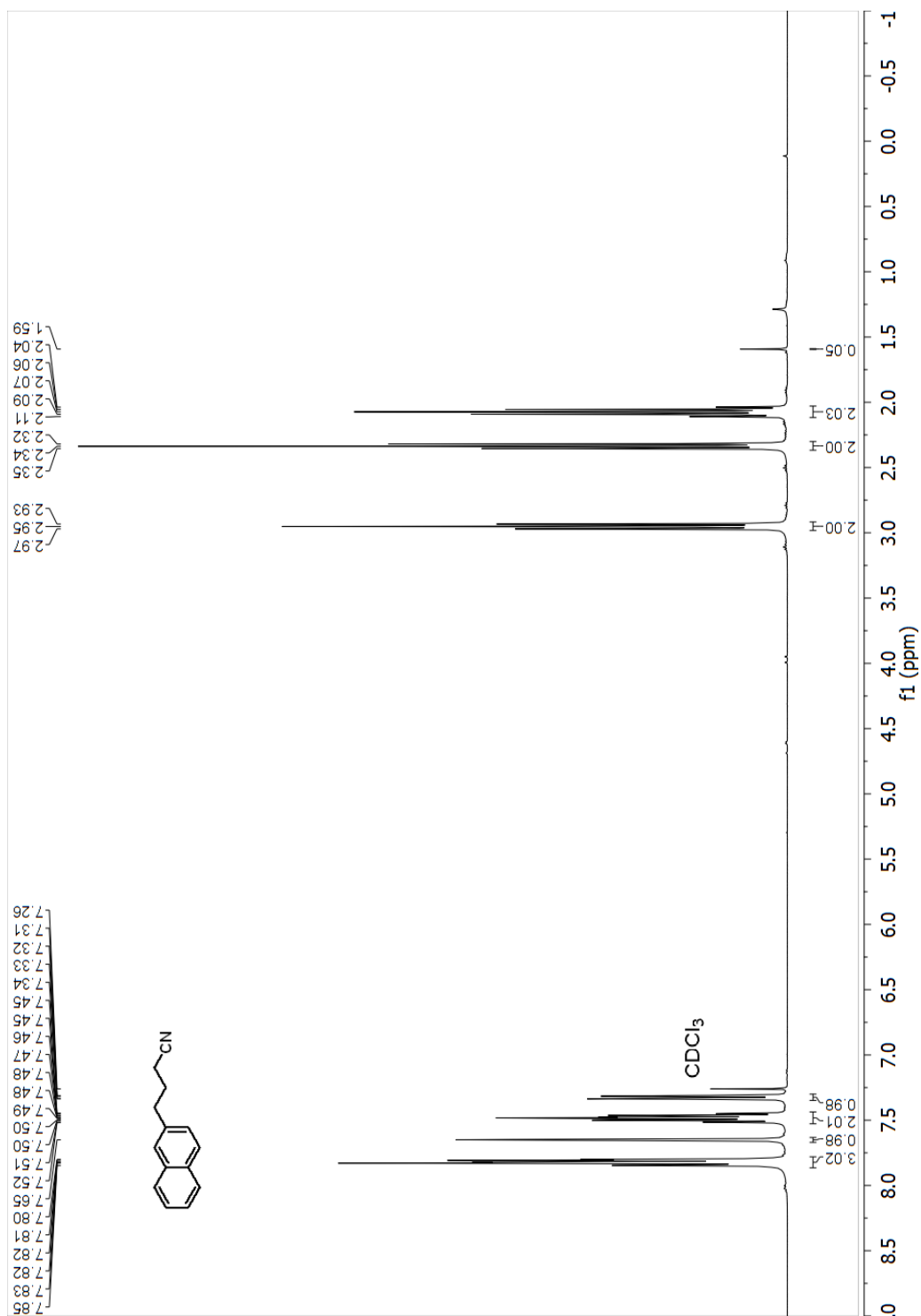
MassPeaks:70

RawMode:Single 13.7(1044) BasePeak:91(2347796)

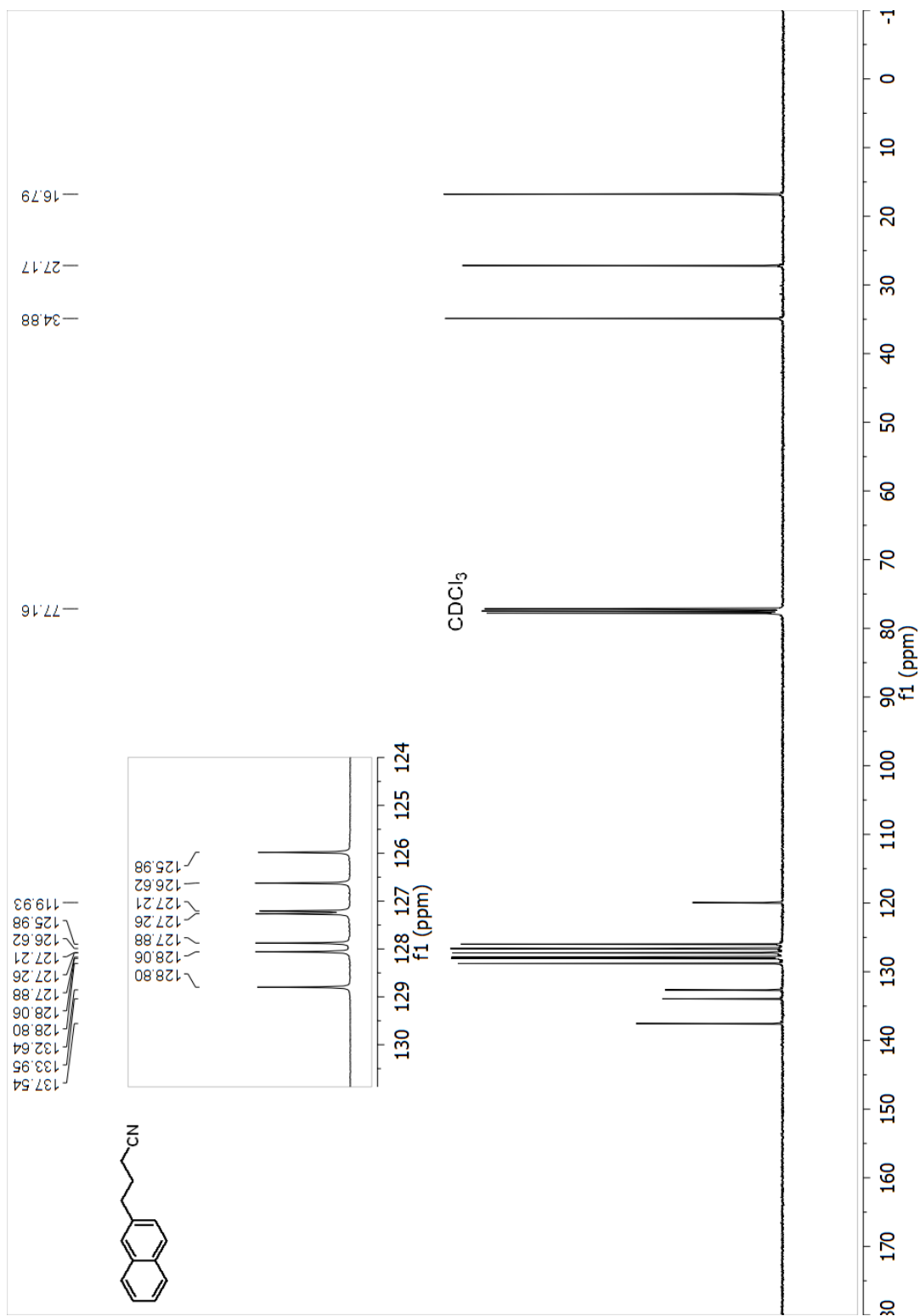
BG Mode:None



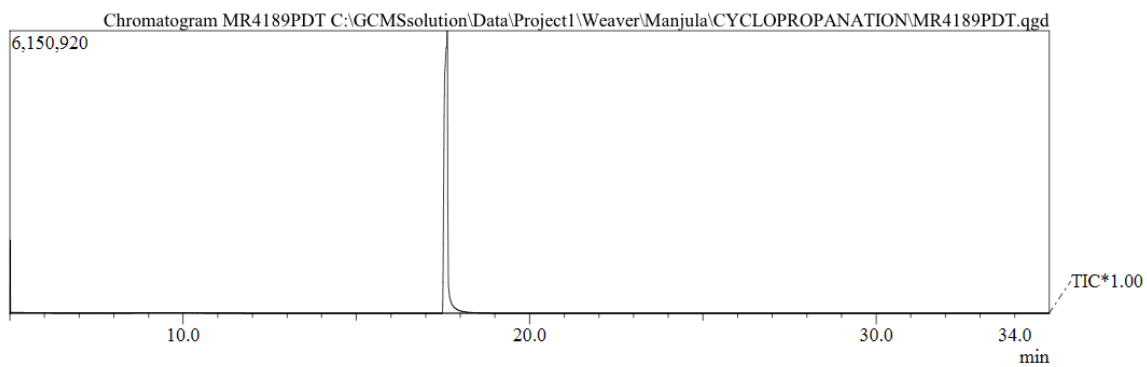
¹H NMR (400 MHz, Chloroform-d) spectrum of 3h 4-(naphthalen-2-yl)butanenitrile



¹³C NMR (101 MHz, Chloroform-d) spectrum of 3h 4-(naphthalen-2-yl)butanenitrile

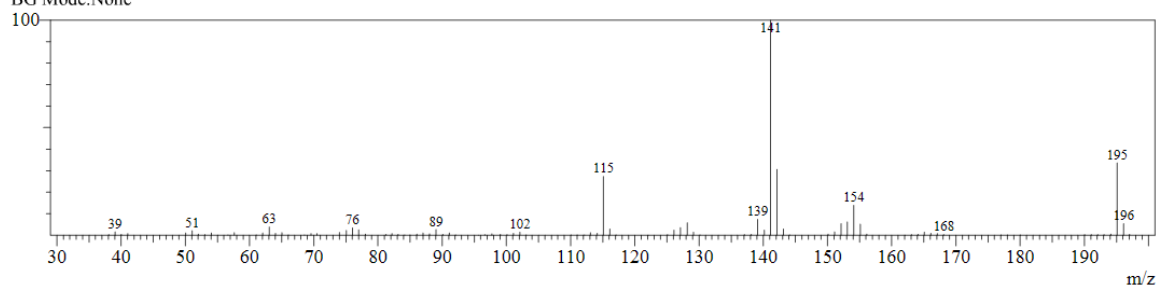


GC and MS of 3h 4-(naphthalen-2-yl)butanenitrile

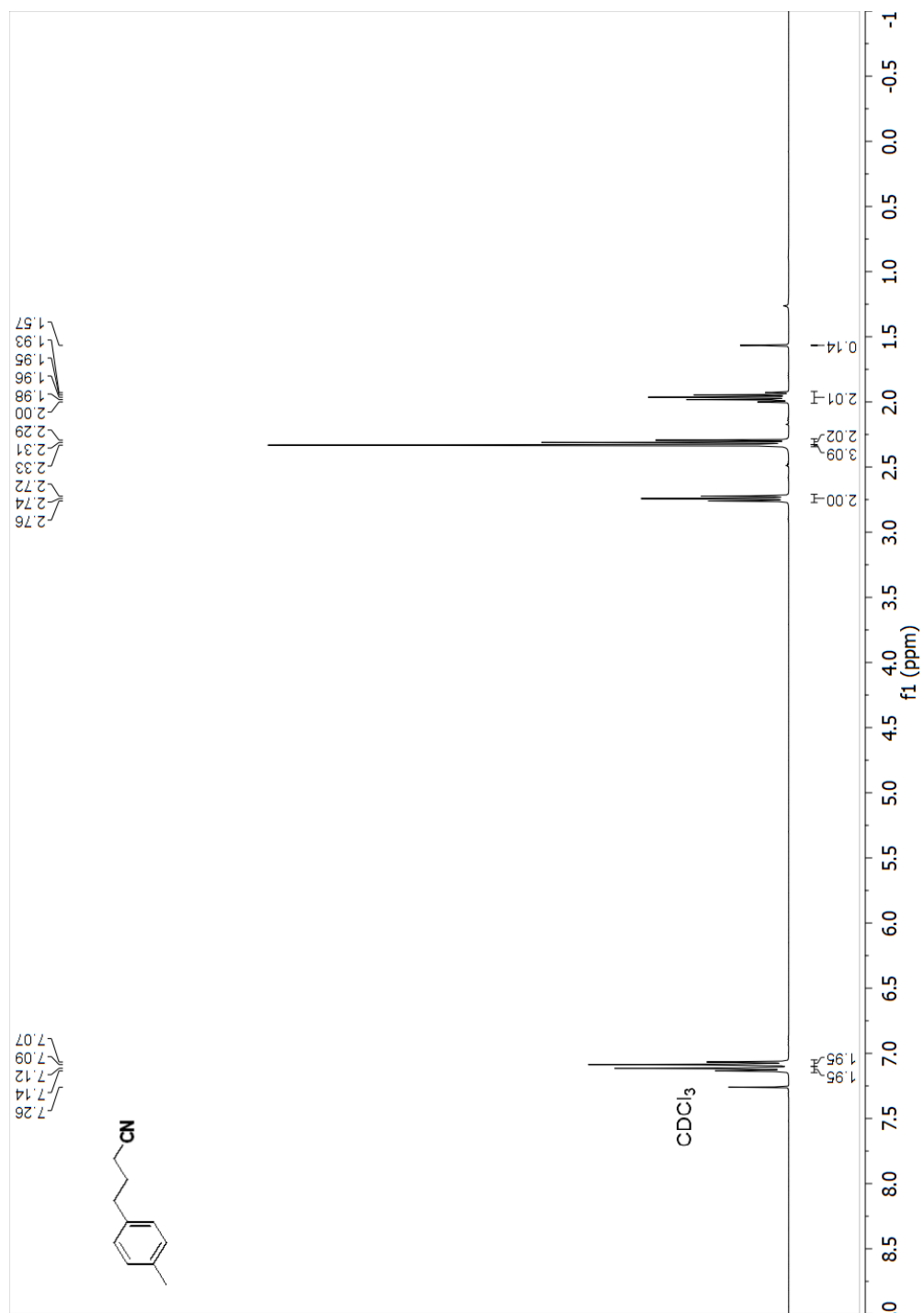


Spectrum

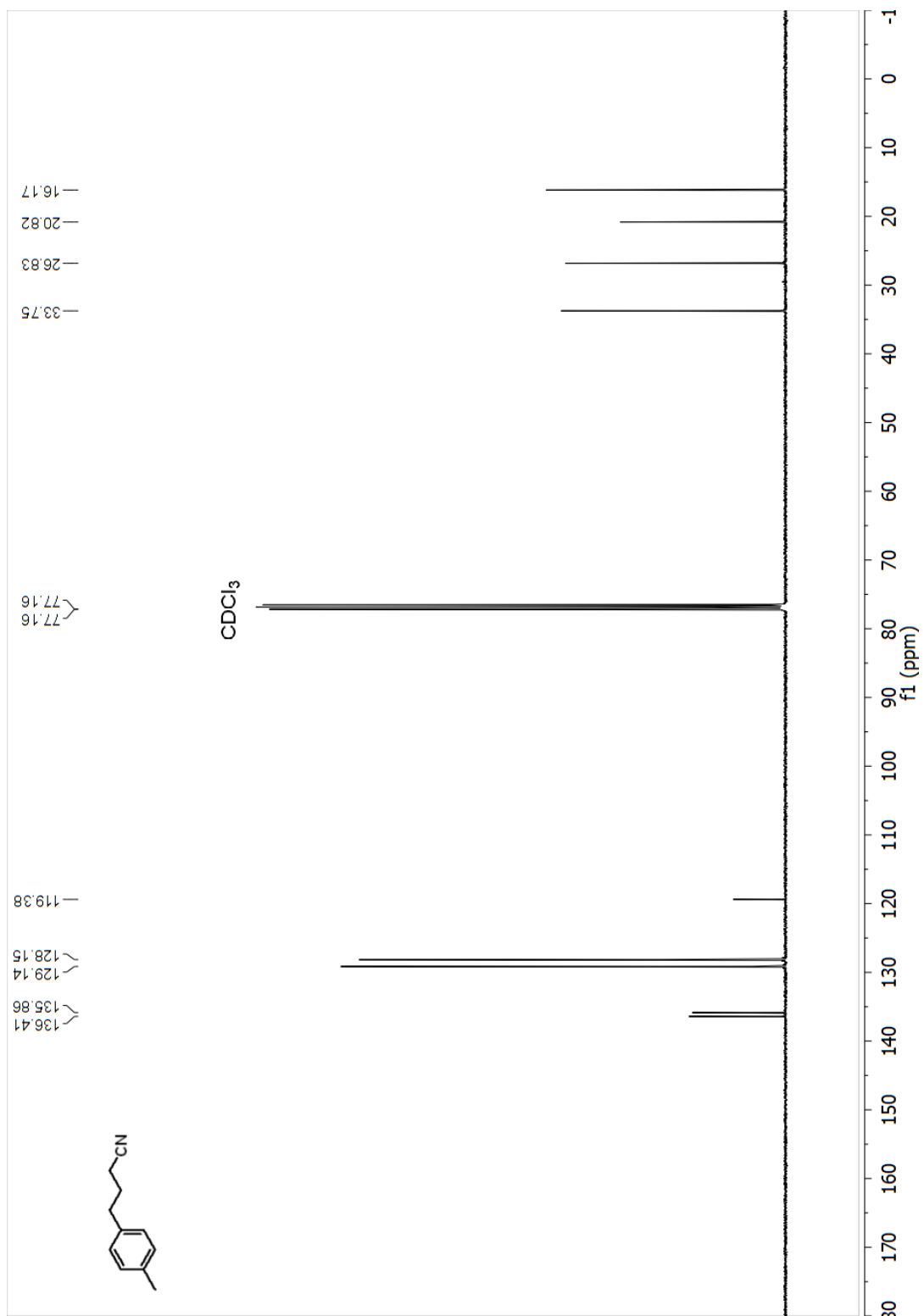
Line#:1 R.Time:17.6(Scan#:1510)
MassPeaks:94
RawMode:Single 17.6(1510) BasePeak:141(1790775)
BG Mode:None



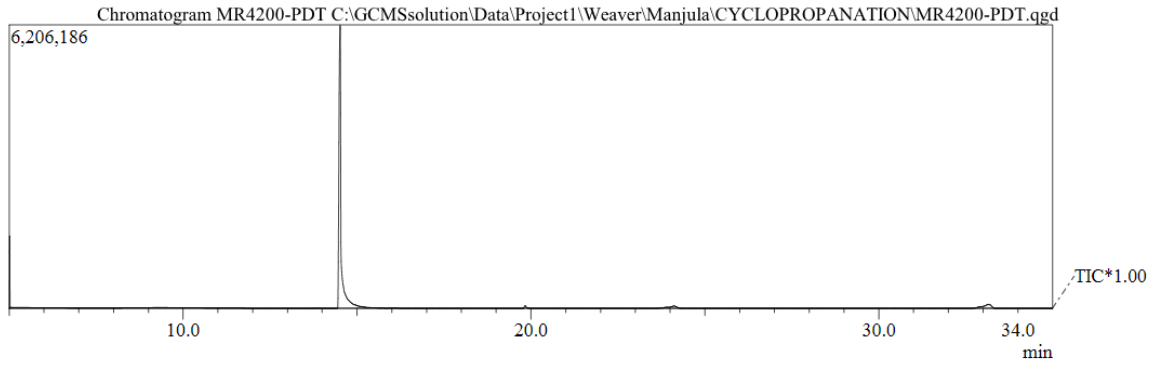
^1H NMR (400 MHz, Chloroform-d) spectrum of 3i 4-(p-tolyl)butanenitrile



¹³C NMR (101 MHz, Chloroform-d) spectrum of 3i 4-(p-tolyl)butanenitrile

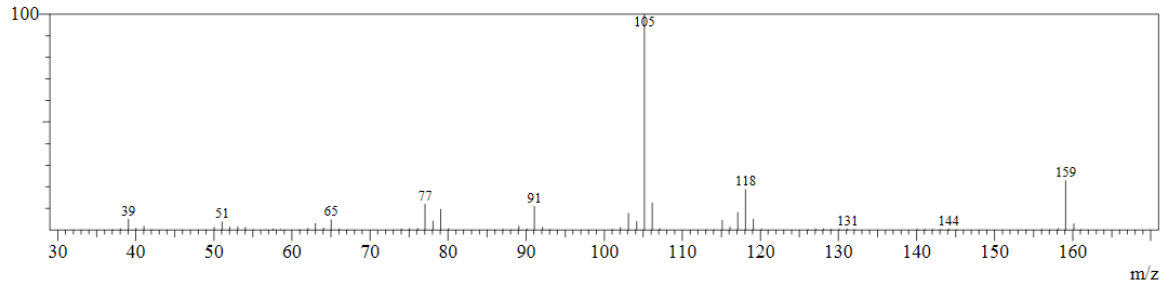


GC and MS of 3i 4-(p-tolyl)butanenitrile

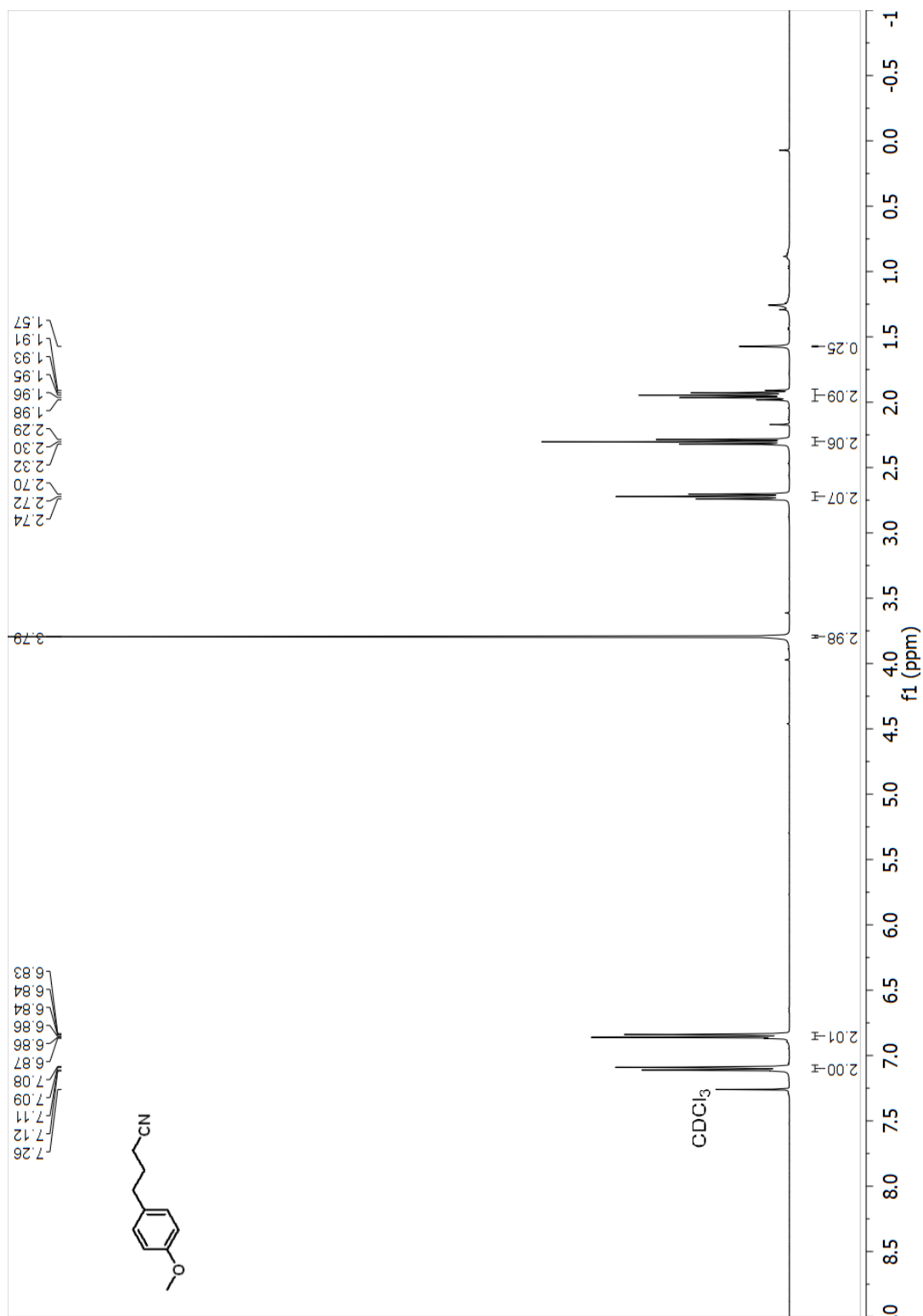


Spectrum

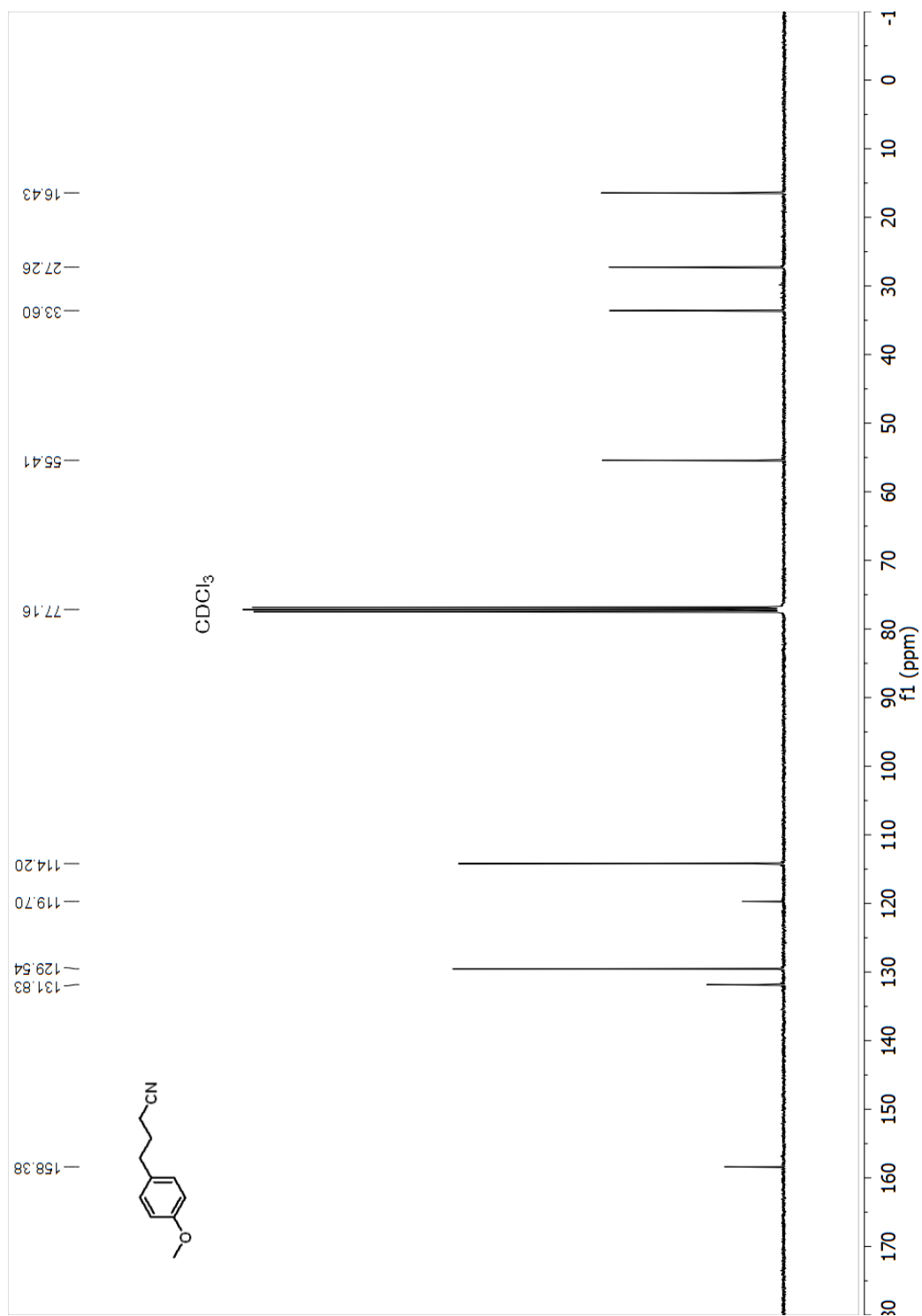
Line#:1 R.Time:14.5(Scan#:1141)
MassPeaks:75
RawMode:Single 14.5(1141) BasePeak:105(2189032)
BG Mode:None



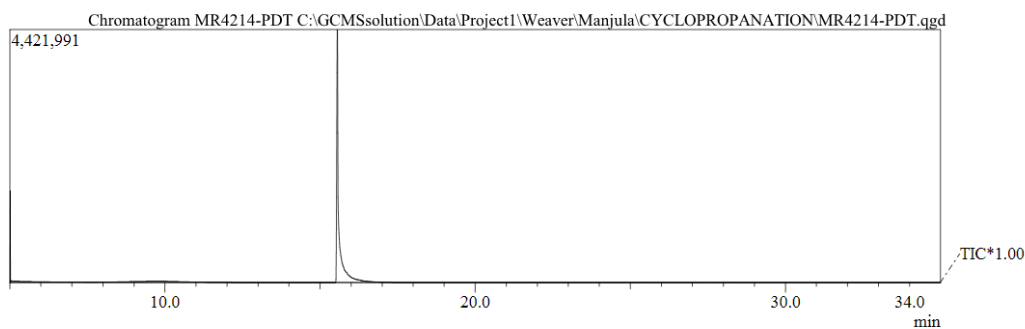
^1H NMR (400 MHz, Chloroform-d) spectrum of 3j 4-(4-methoxyphenyl)butanenitrile



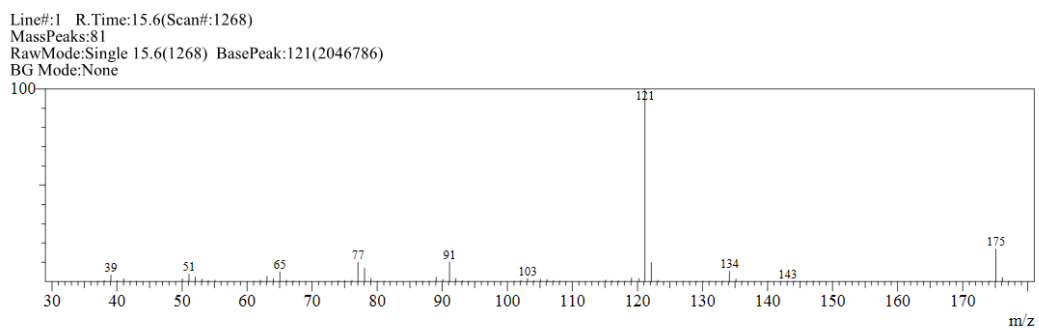
^{13}C NMR (101 MHz, Chloroform-d) spectrum of 3j 4-(4-methoxyphenyl)butanenitrile



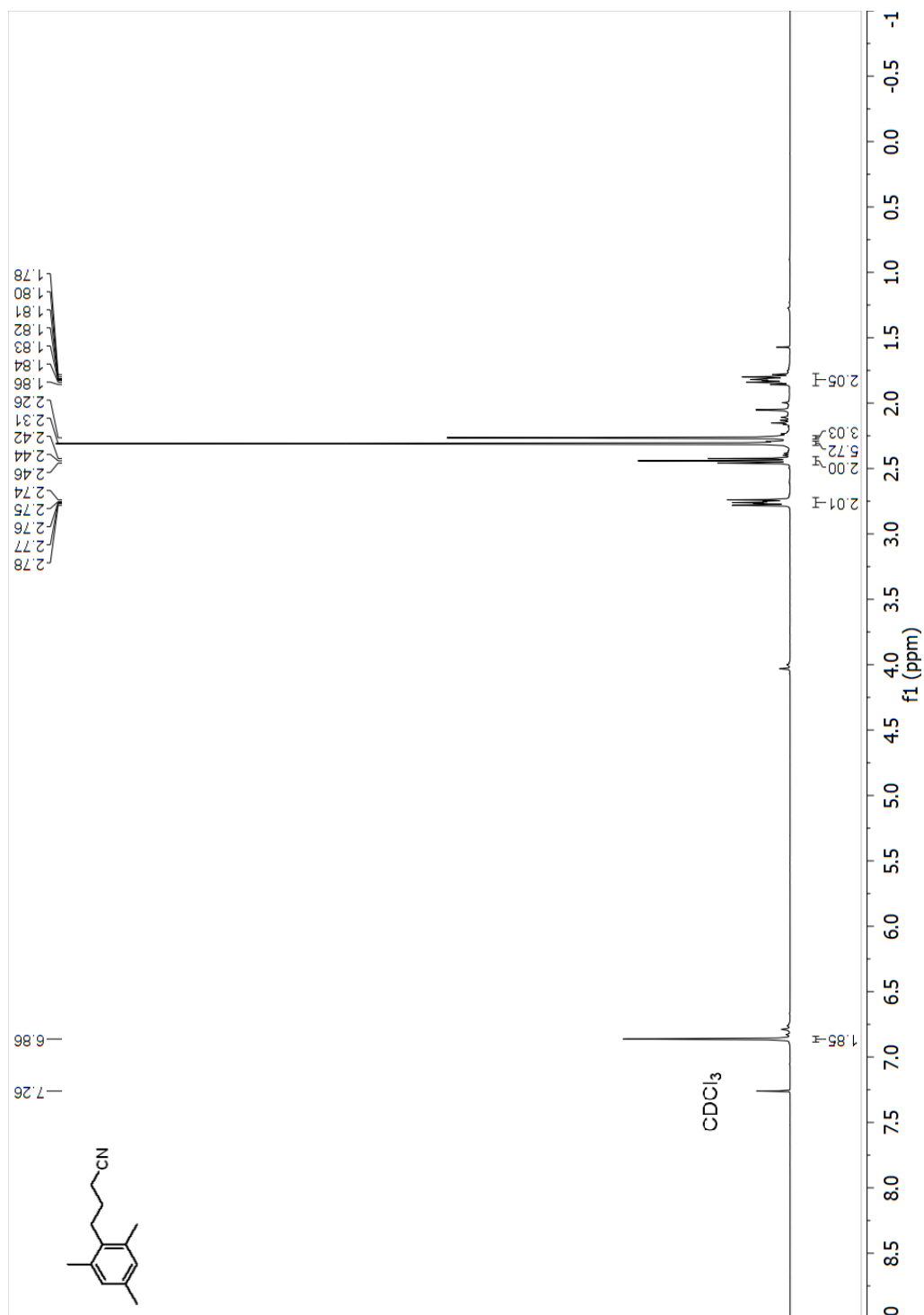
GC and MS of 3j 4-(4-methoxyphenyl)butanenitrile



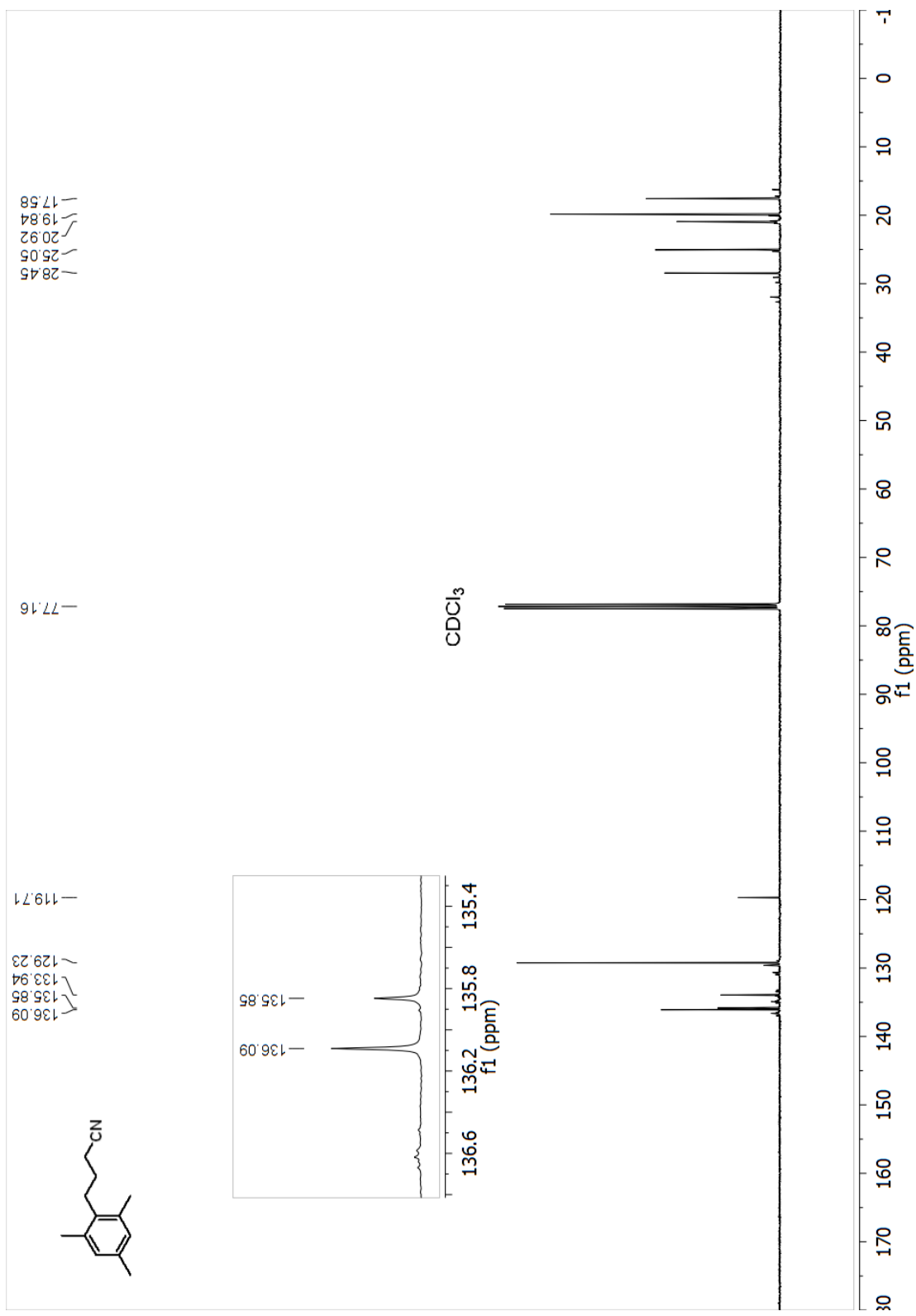
Spectrum



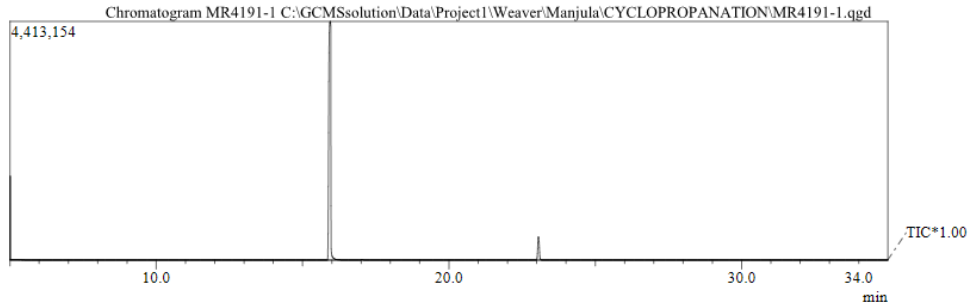
^1H NMR (400 MHz, Chloroform-d) spectrum of 3k 4-mesitylbutanenitrile



¹³C NMR (101 MHz, Chloroform-d) spectrum of 3k 4-mesitylbutanenitrile

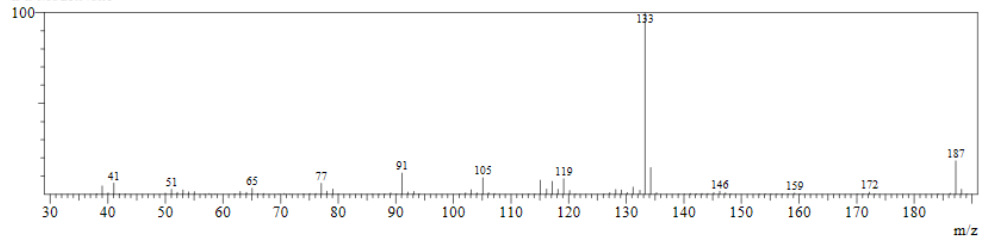


GC and MS of 3k 4-mesitylbutanenitrile

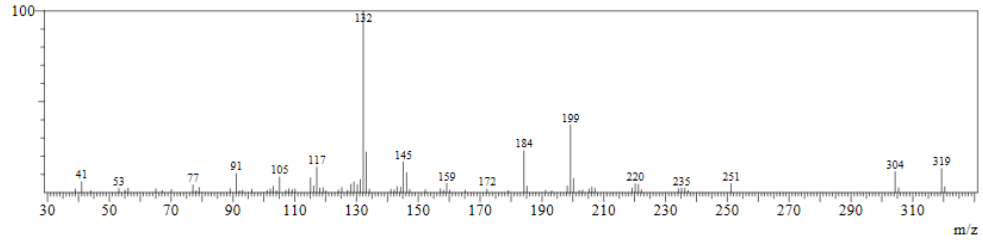


Spectrum

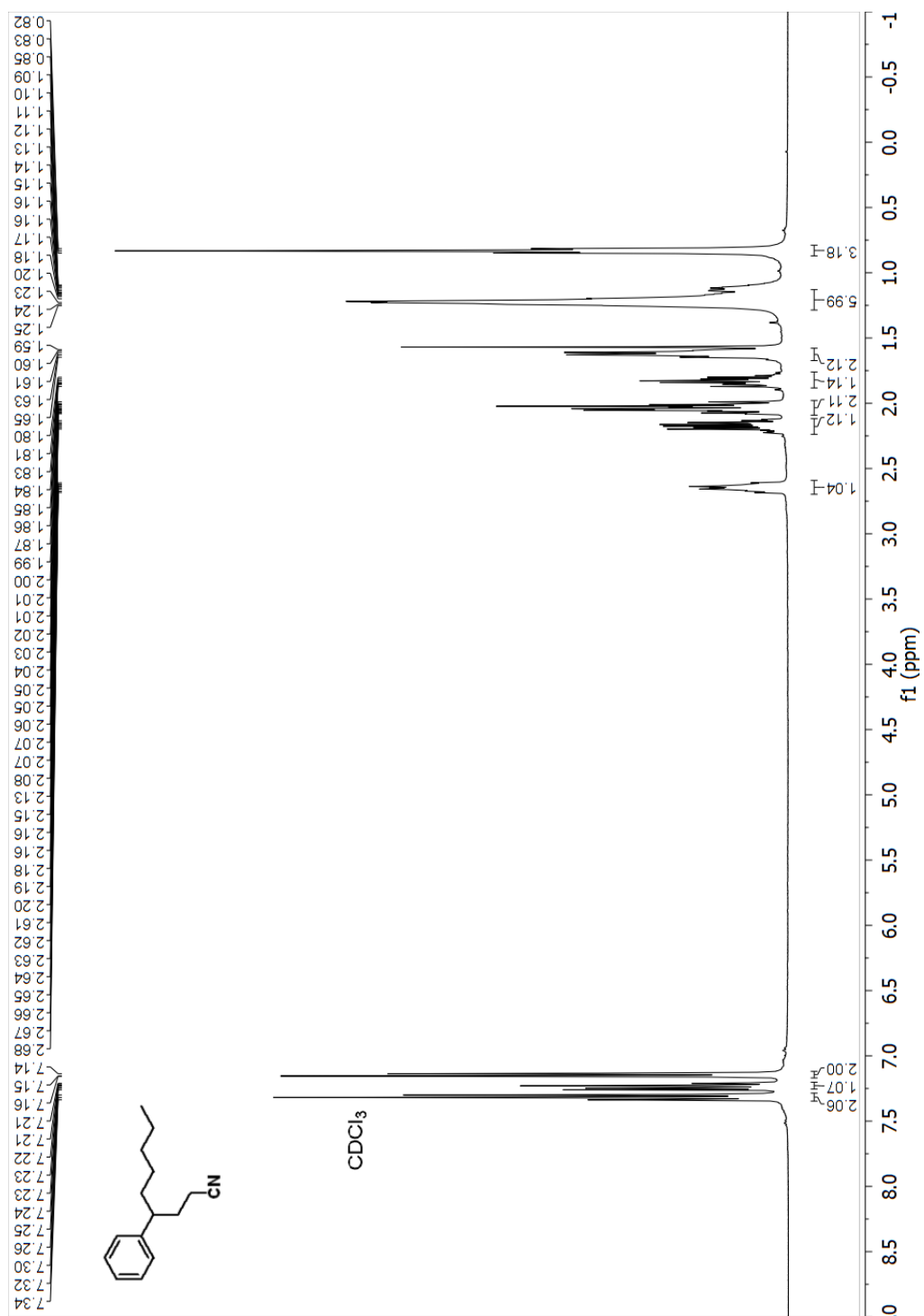
Line#:1 R.Time:15.9(Scan#:1313)
MassPeaks:93
RawMode:Single 15.9(1313) BasePeak:133(1665697)
BG Mode:None



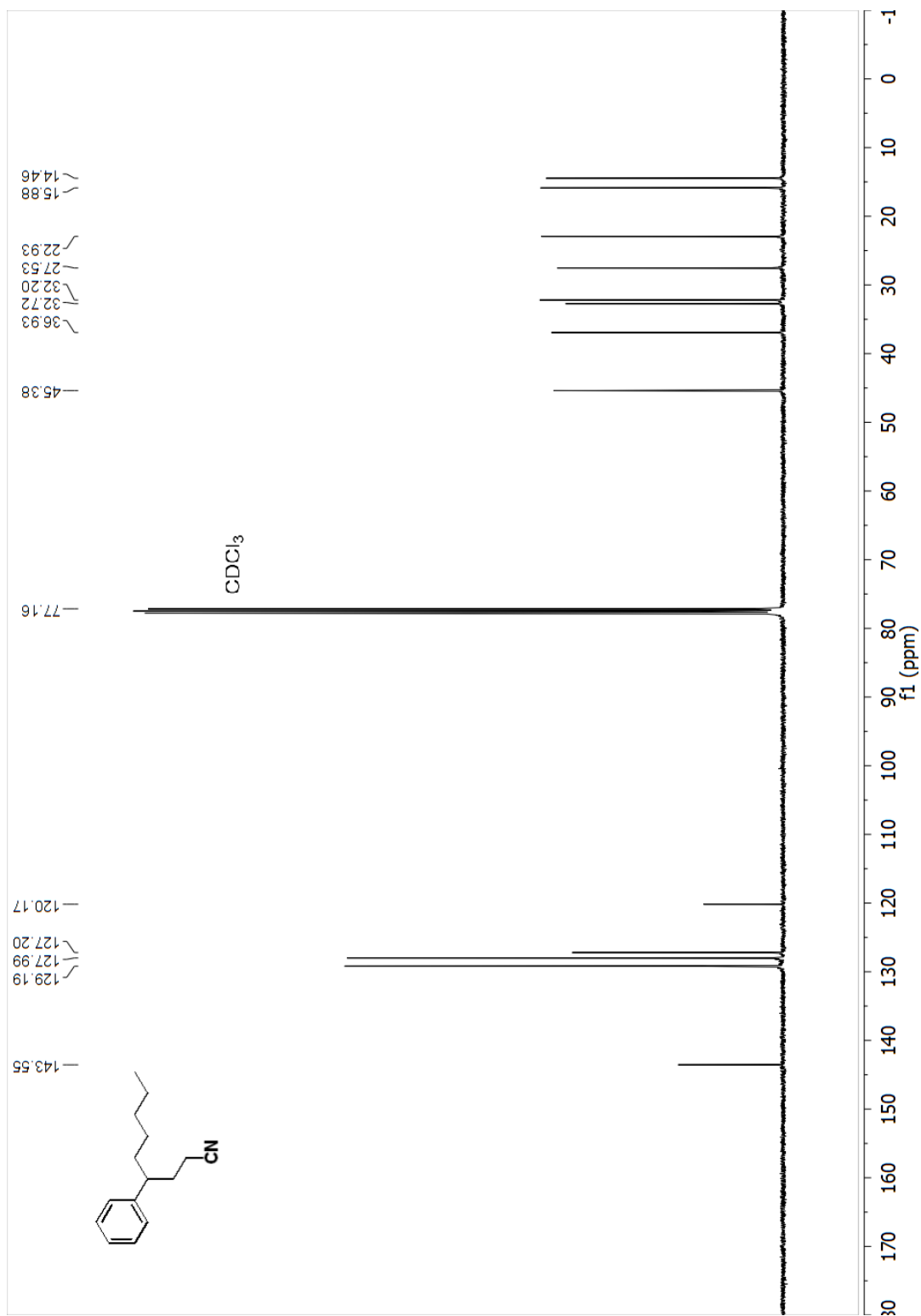
Line#:2 R.Time:23.1(Scan#:2168)
MassPeaks:82
RawMode:Single 23.1(2168) BasePeak:132(95927)
BG Mode:None



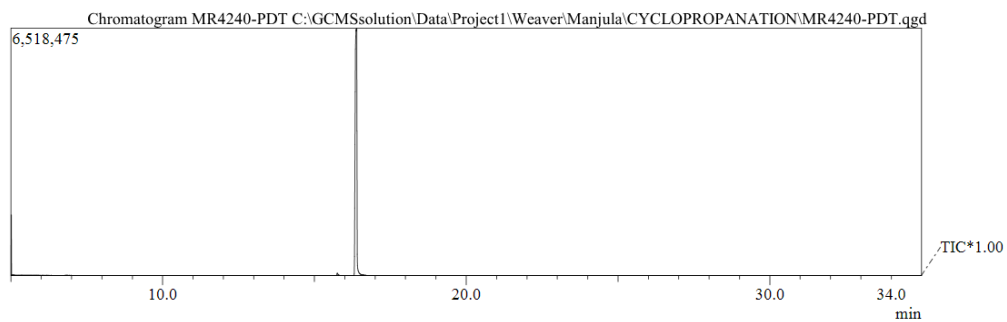
¹H NMR (400 MHz, Chloroform-d) spectrum of 3-(4-phenylnonanenitrile)



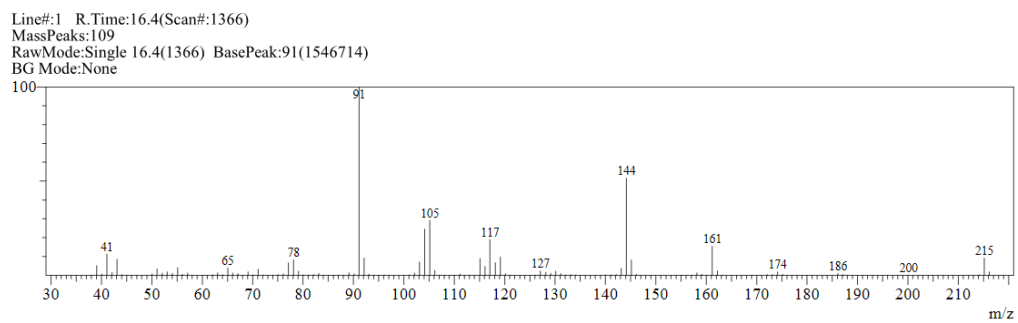
¹³C NMR (101 MHz, Chloroform-d) spectrum of 3-(4-phenyl)nonanenitrile



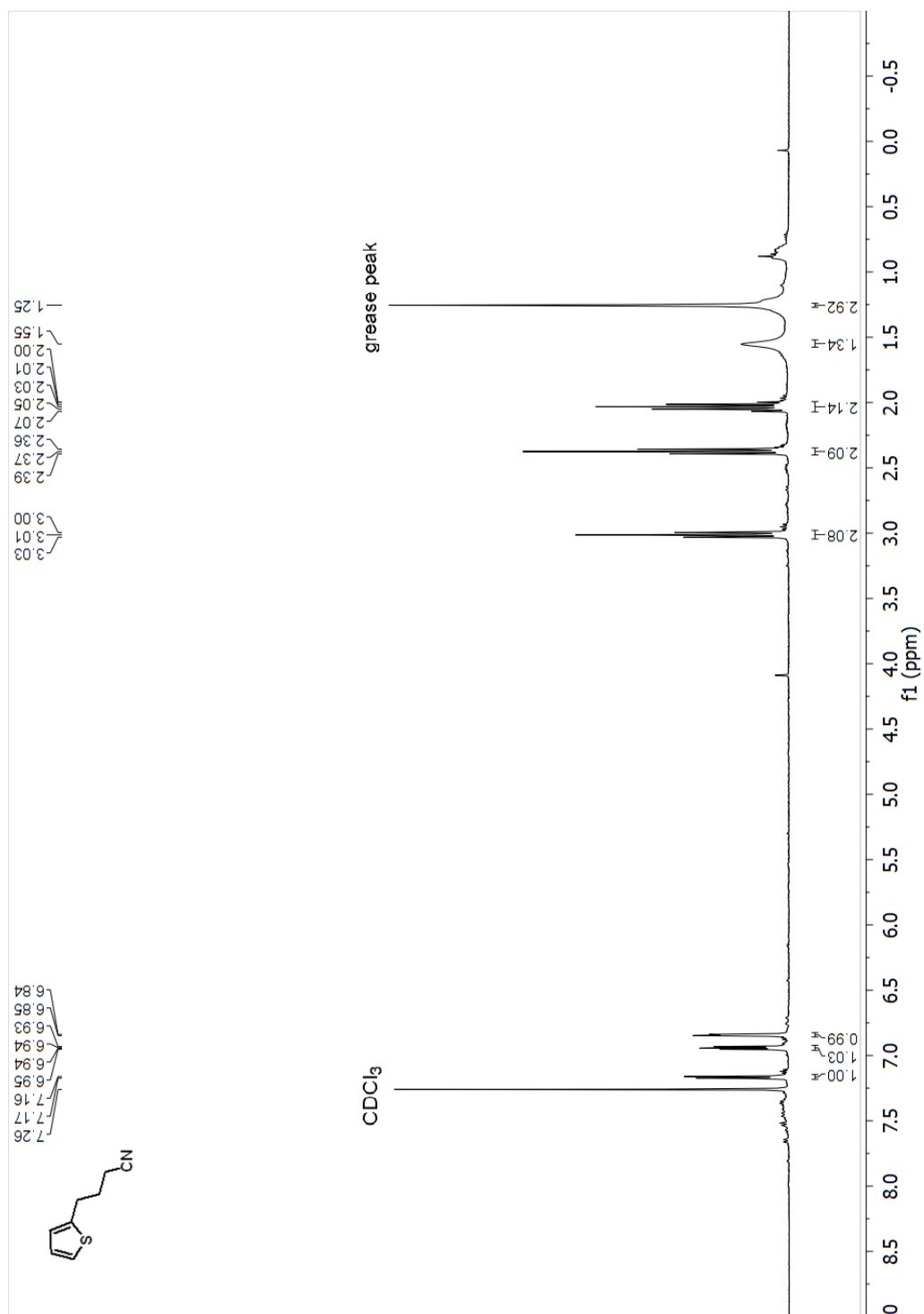
GC and MS of 31 4-phenylnonanenitrile



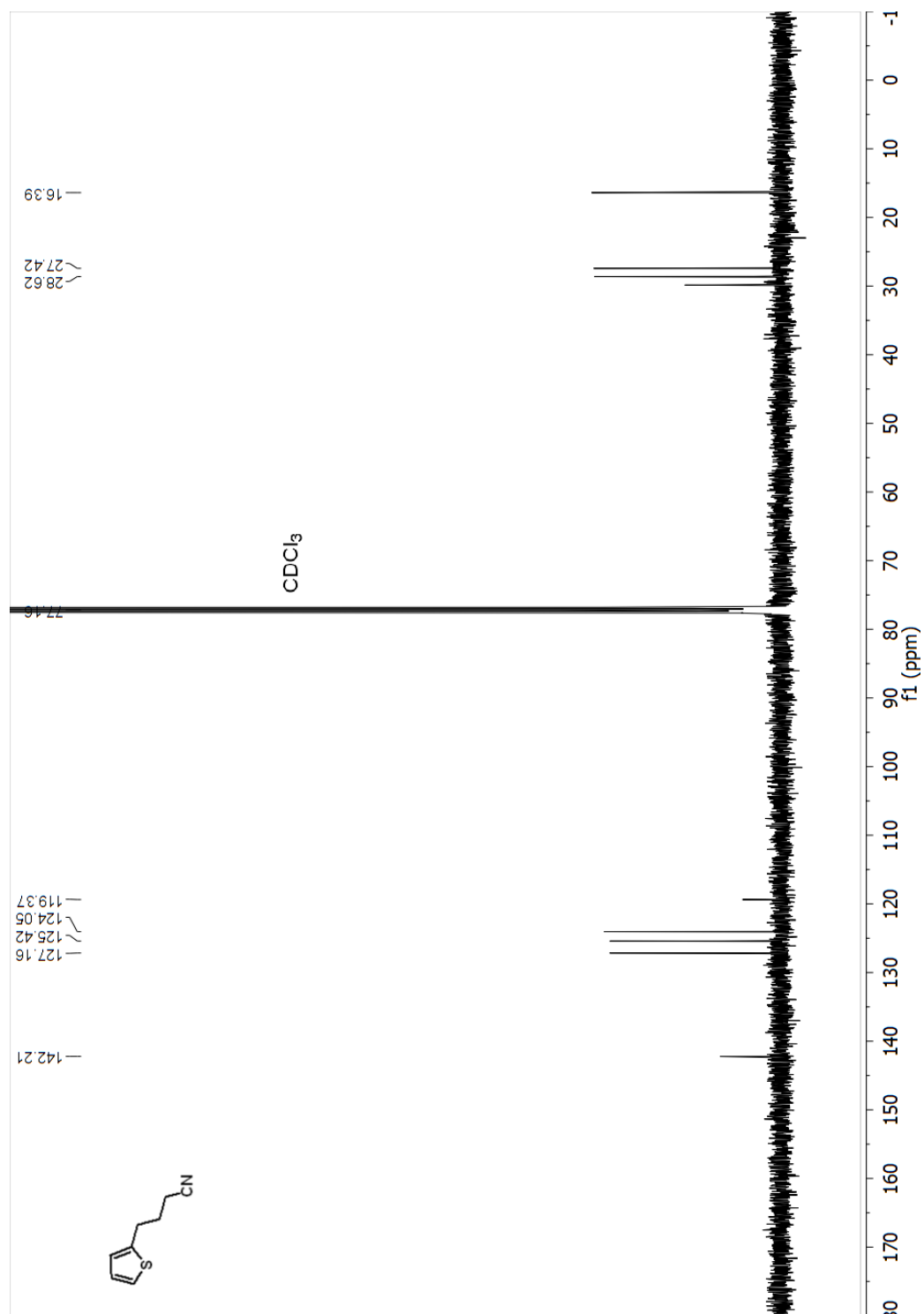
Spectrum



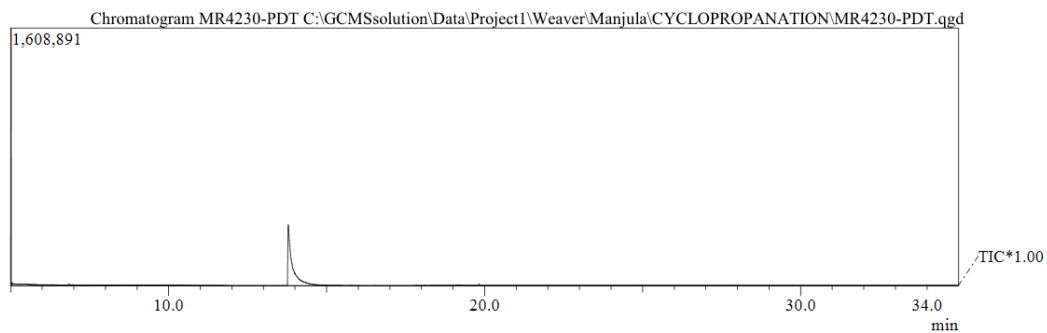
^1H NMR (400 MHz, Chloroform-d) spectrum of 3m 4-(thiophen-2-yl)butanenitrile



^{13}C NMR (101 MHz, Chloroform-d) spectrum of 3m 4-(thiophen-2-yl)butanenitrile

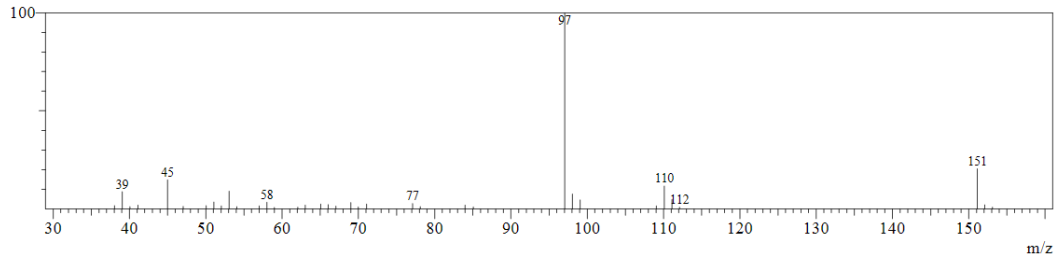


GC and MS of 3m 4-(thiophen-2-yl)butanenitrile

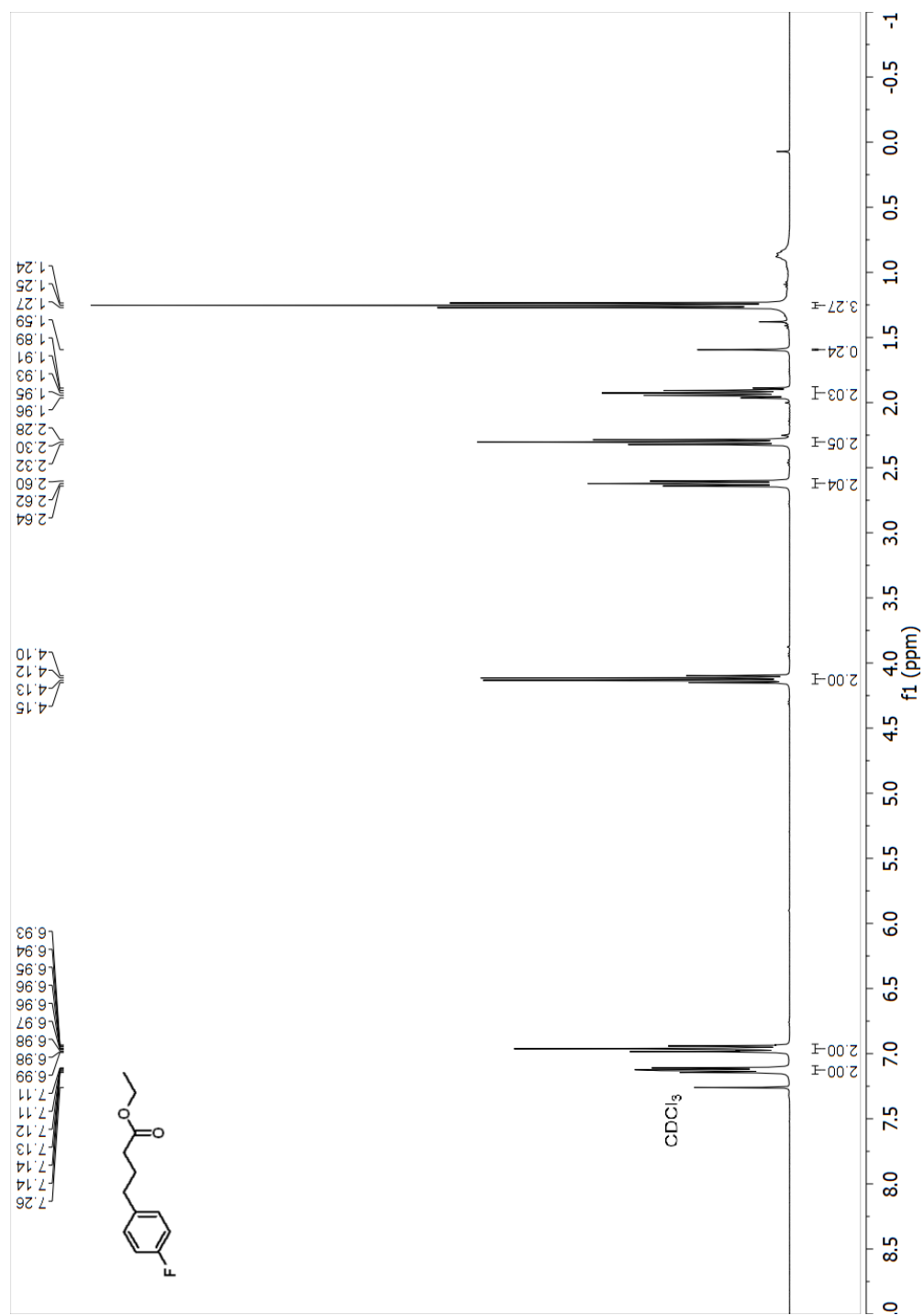


Spectrum

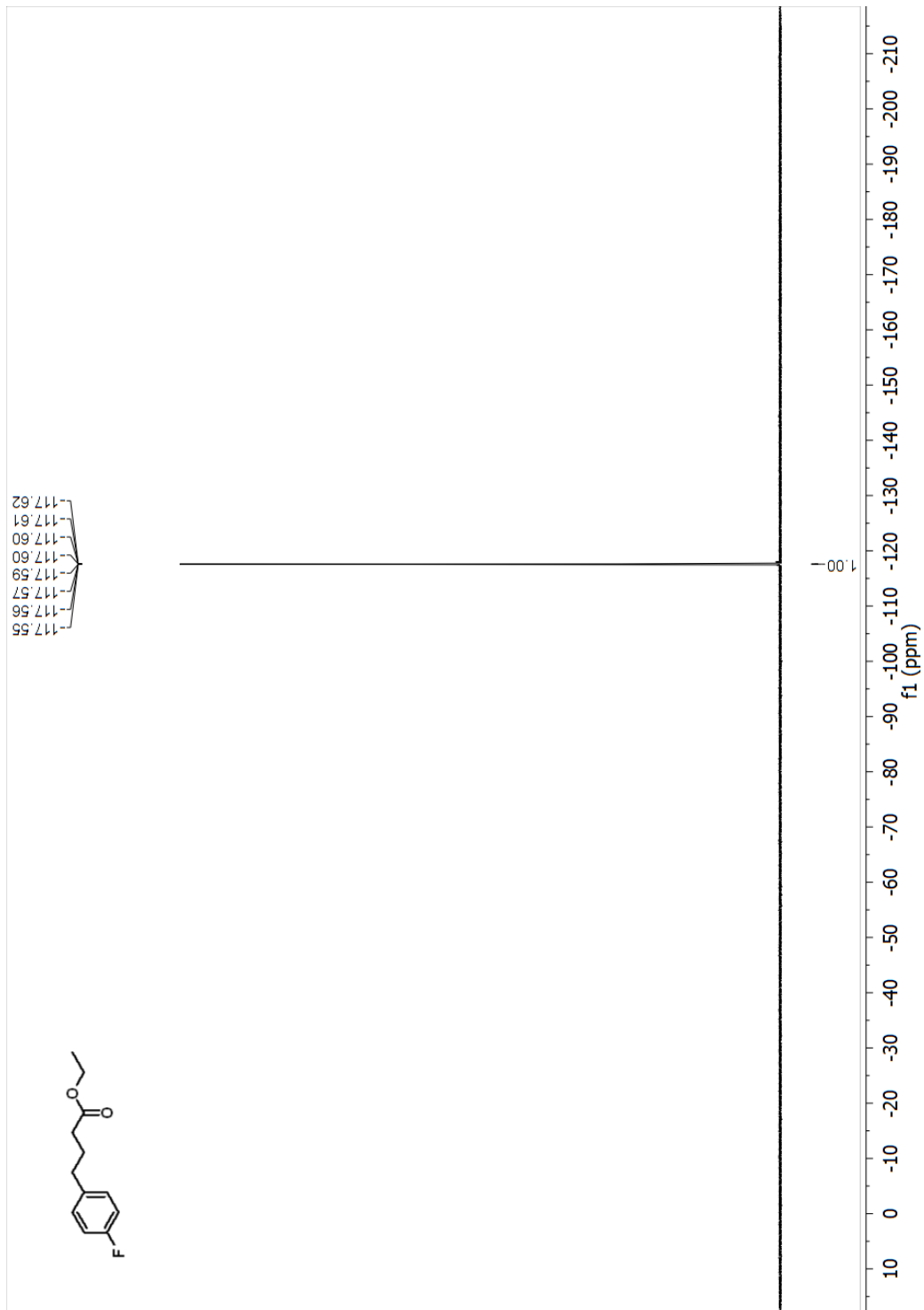
Line#:1 R.Time:13.8(Scan#:1059)
MassPeaks:36
RawMode:Single 13.8(1059) BasePeak:97(123729)
BG Mode:None



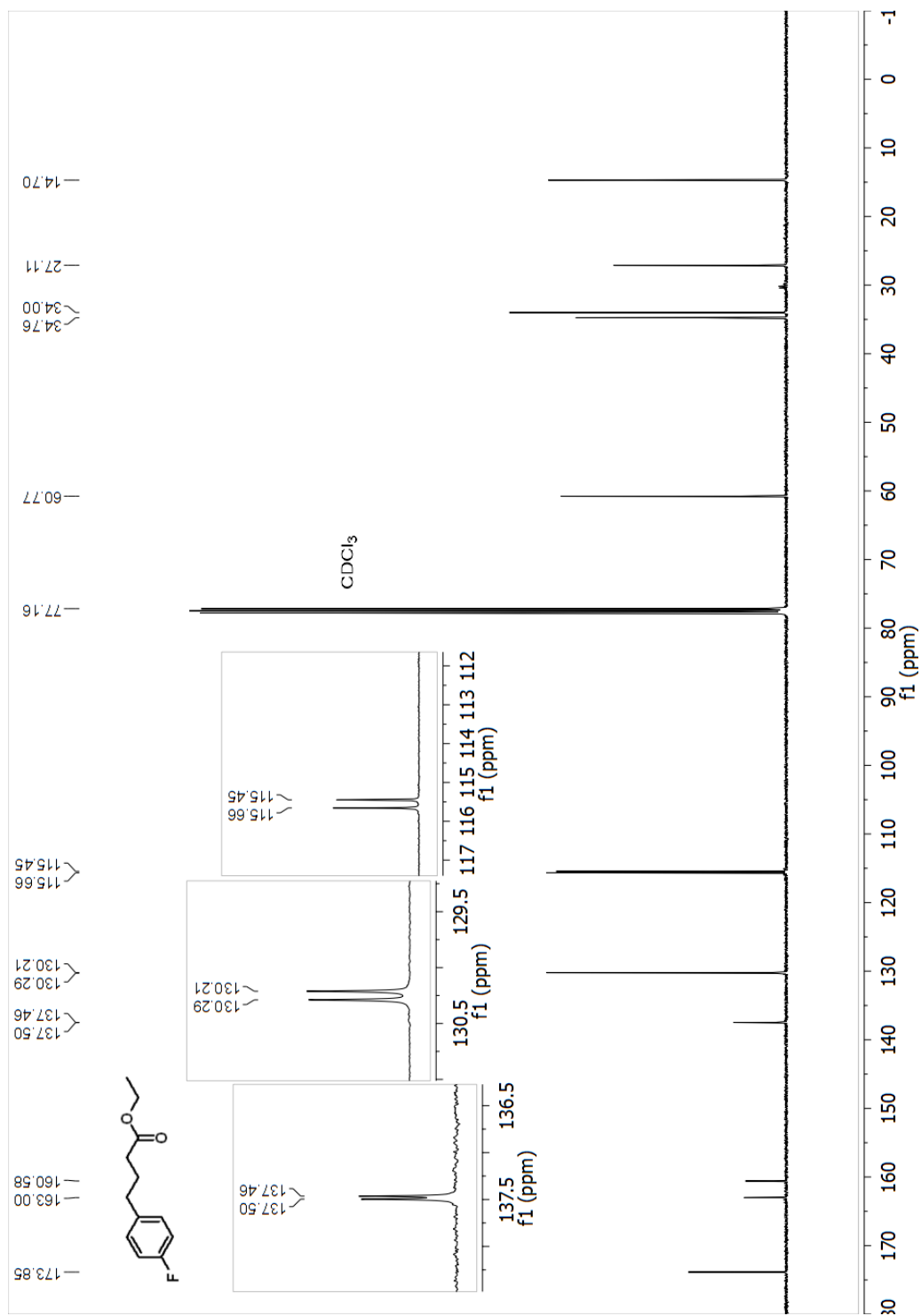
¹H NMR (400 MHz, Chloroform-d) spectrum of 4b ethyl 4-(4-fluorophenyl)butanoate



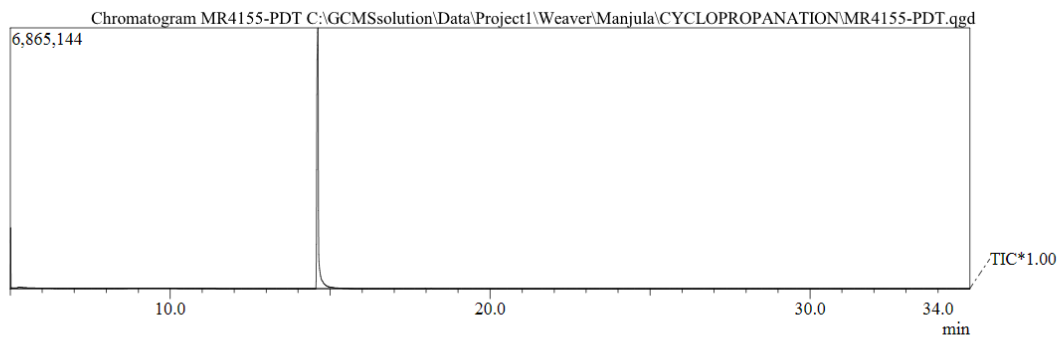
^{19}F NMR (376 MHz, Chloroform-d) spectrum of 4b ethyl 4-(4-fluorophenyl)butanoate



¹³C NMR (101 MHz, Chloroform-d) spectrum of 4b ethyl 4-(4-fluorophenyl)butanoate

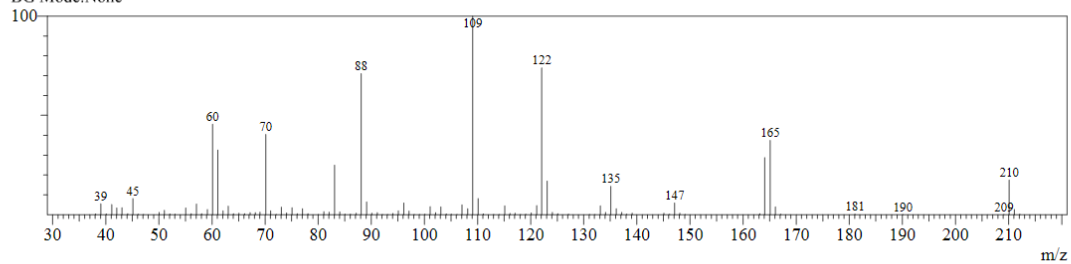


GC and MS of 4b ethyl 4-(4-fluorophenyl)butanoate

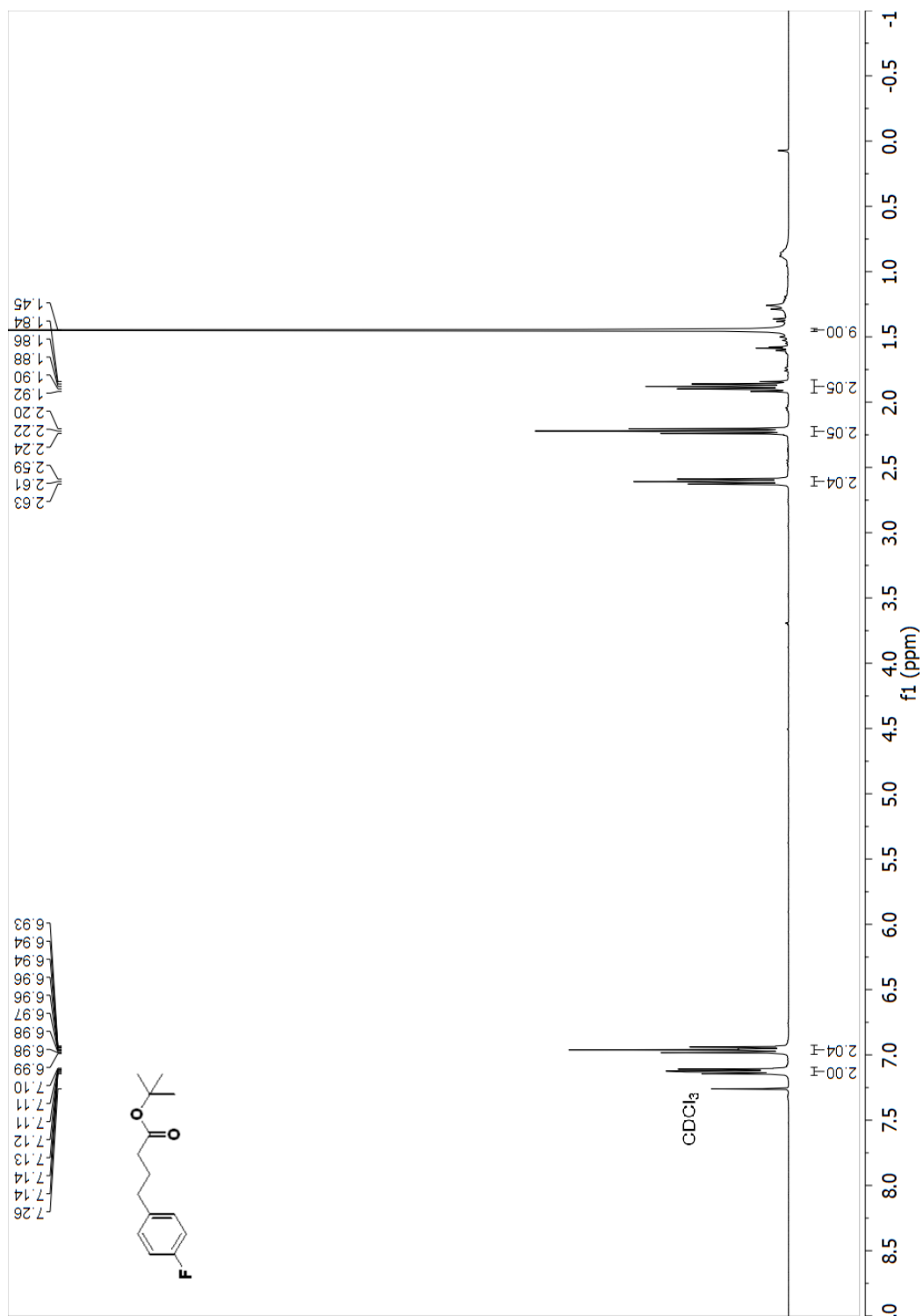


Spectrum

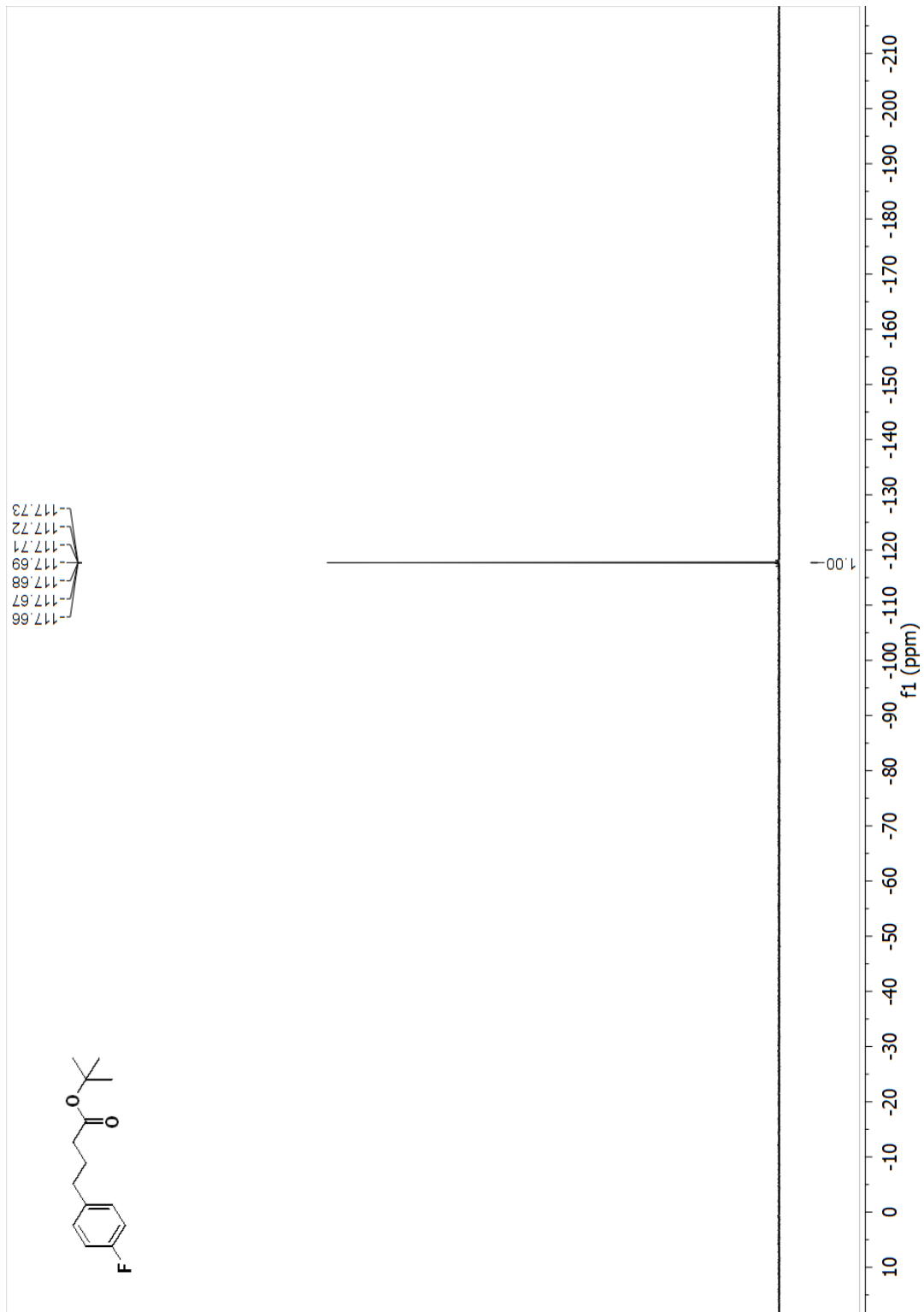
Line#:1 R. Time:14.6(Scan#:1154)
MassPeaks:109
RawMode:Single 14.6(1154) BasePeak:109(1011330)
BG Mode:None



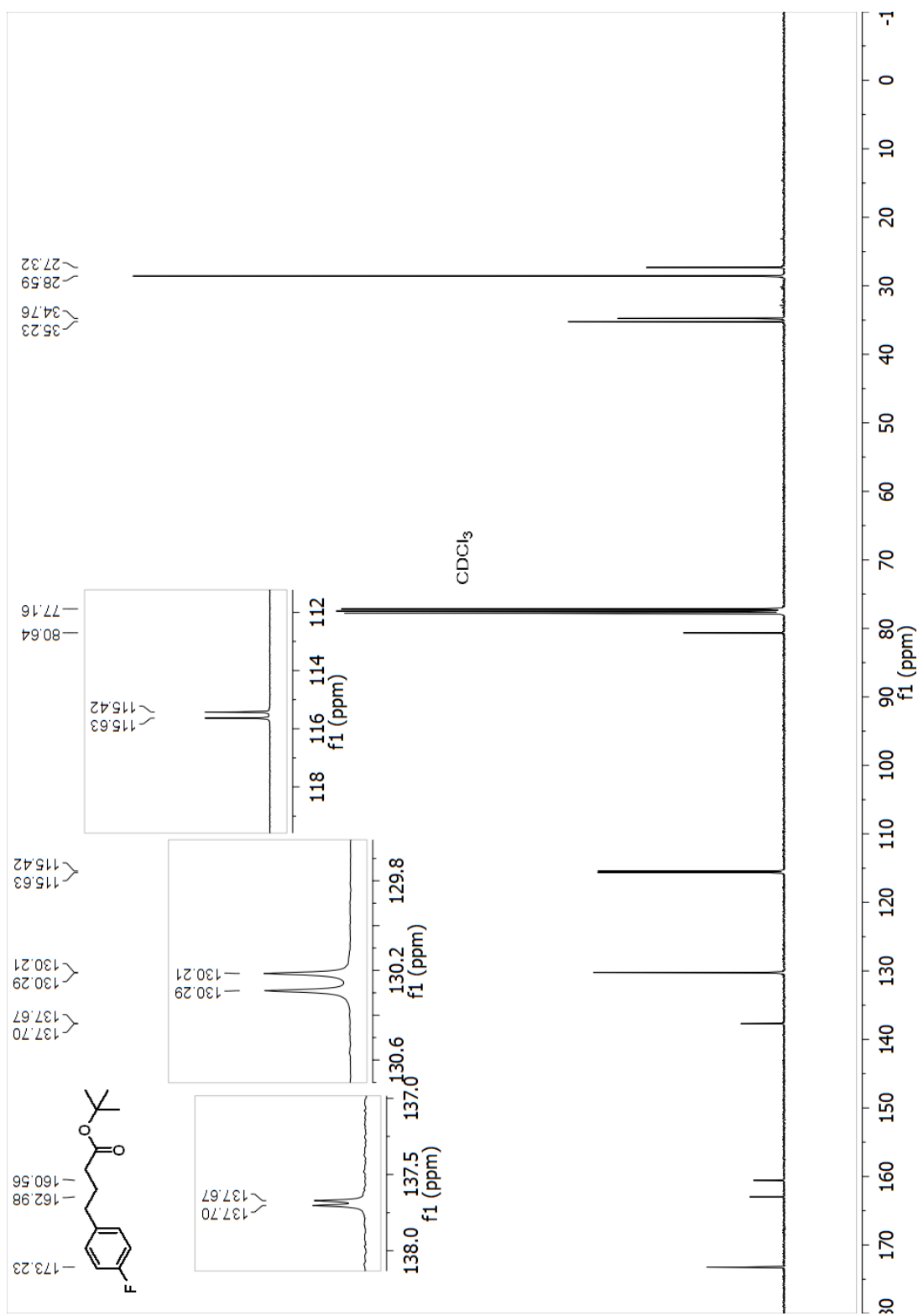
¹H NMR (400 MHz, Chloroform-d) spectrum of 4c tert-butyl 4-(4-fluorophenyl)butanoate



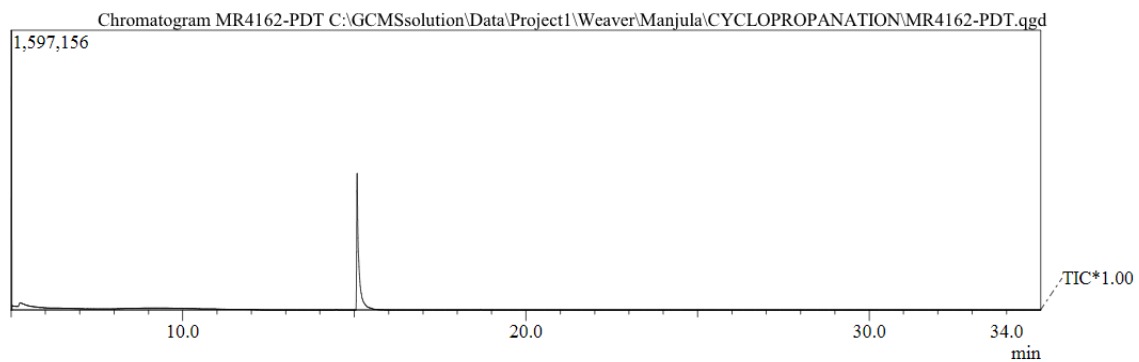
¹⁹F NMR (376 MHz, Chloroform-d) spectrum of 4c tert-butyl 4-(4-fluorophenyl)butanoate



^{13}C NMR (101 MHz, Chloroform-d) spectrum of 4c tert-butyl 4-(4-fluorophenyl)butanoate

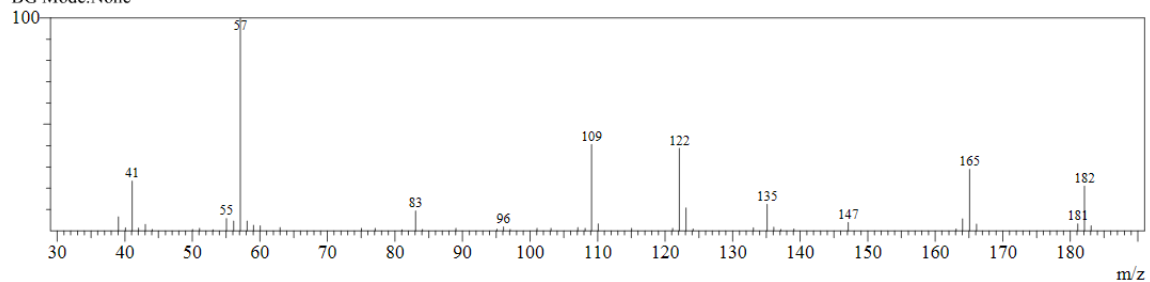


GC and MS of 4c tert-butyl 4-(4-fluorophenyl)butanoate

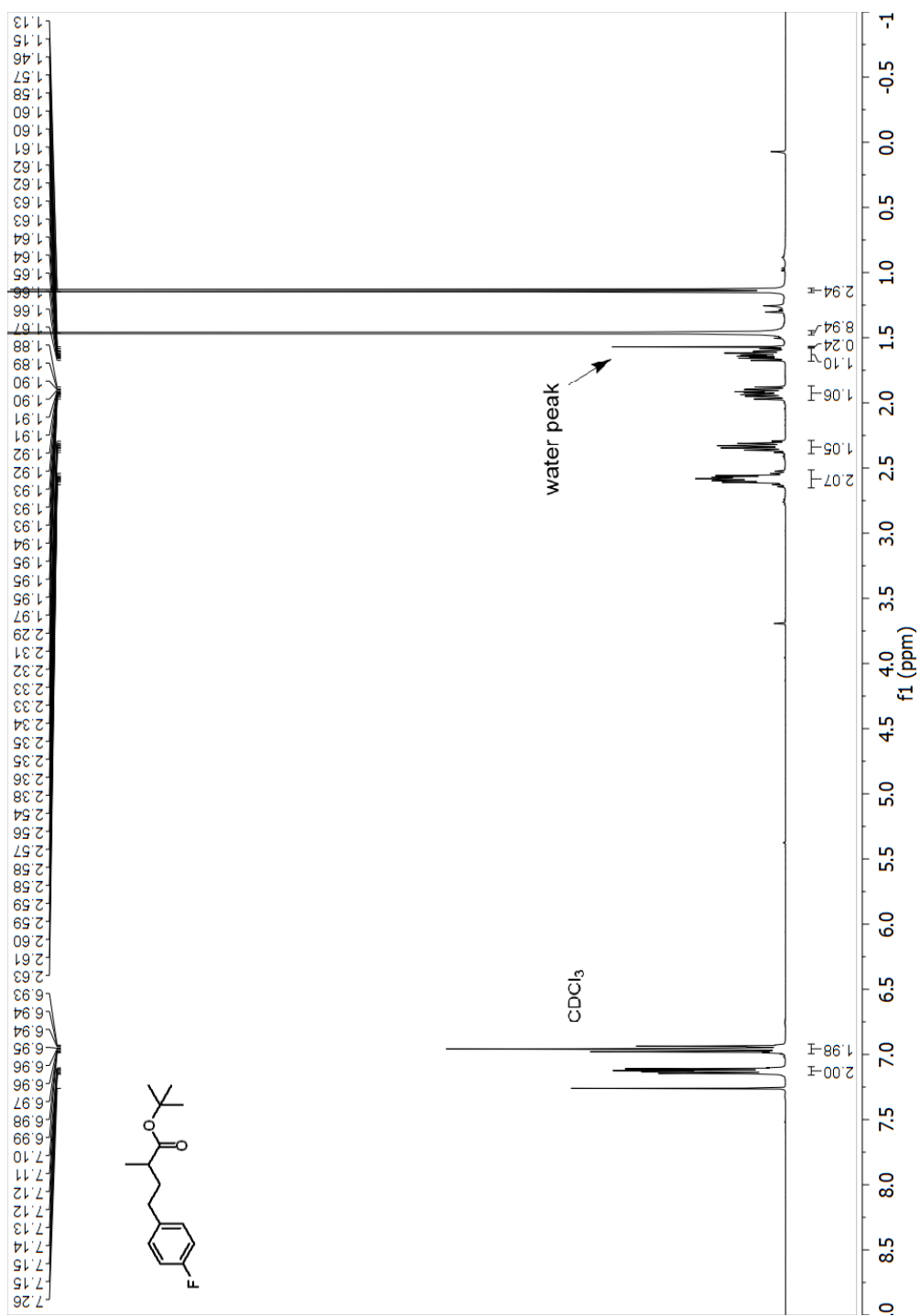


Spectrum

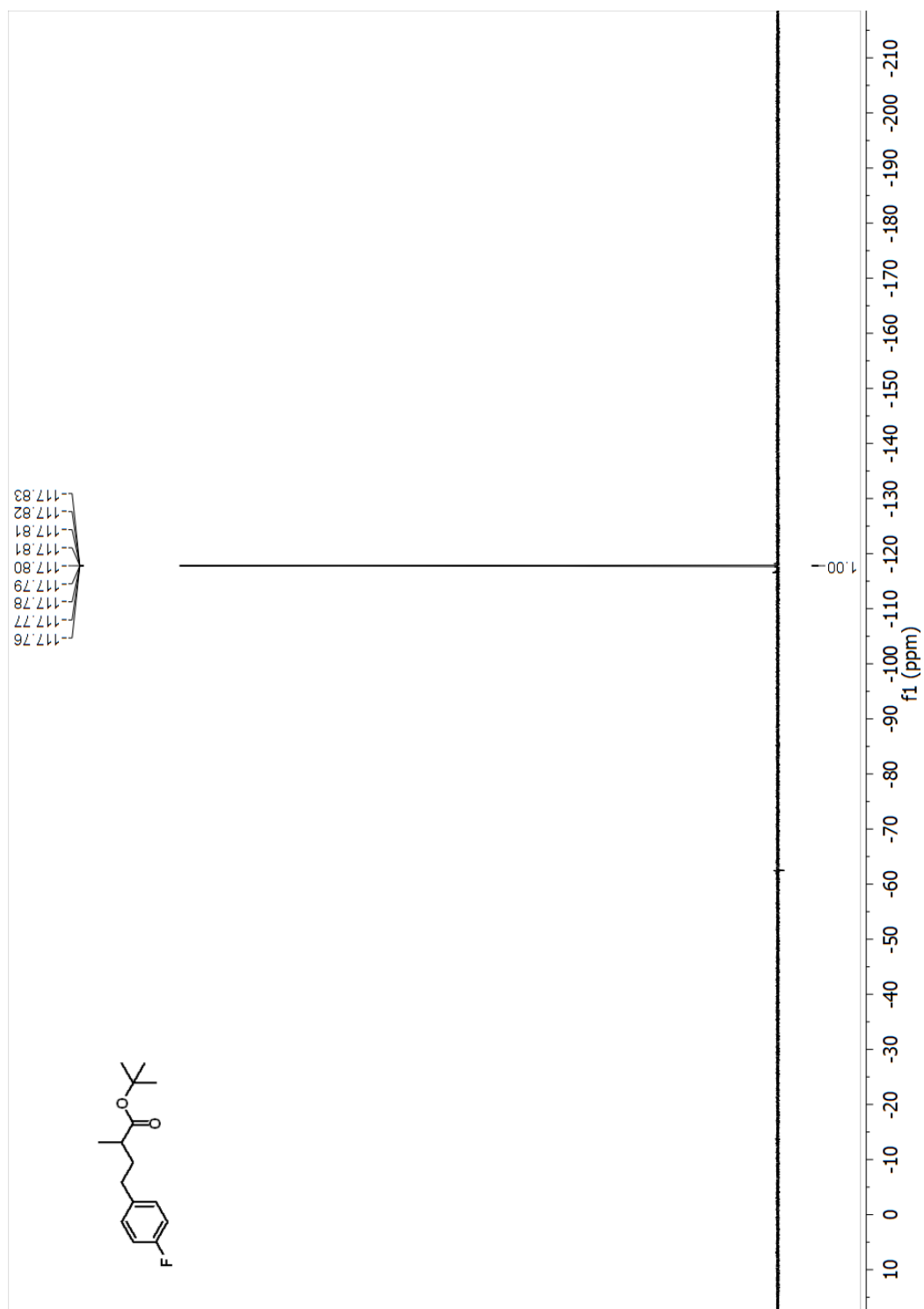
Line#:1 R.Time:15.1(Scan#:1211)
MassPeaks:49
RawMode:Single 15.1(1211) BasePeak:57(213820)
BG Mode:None



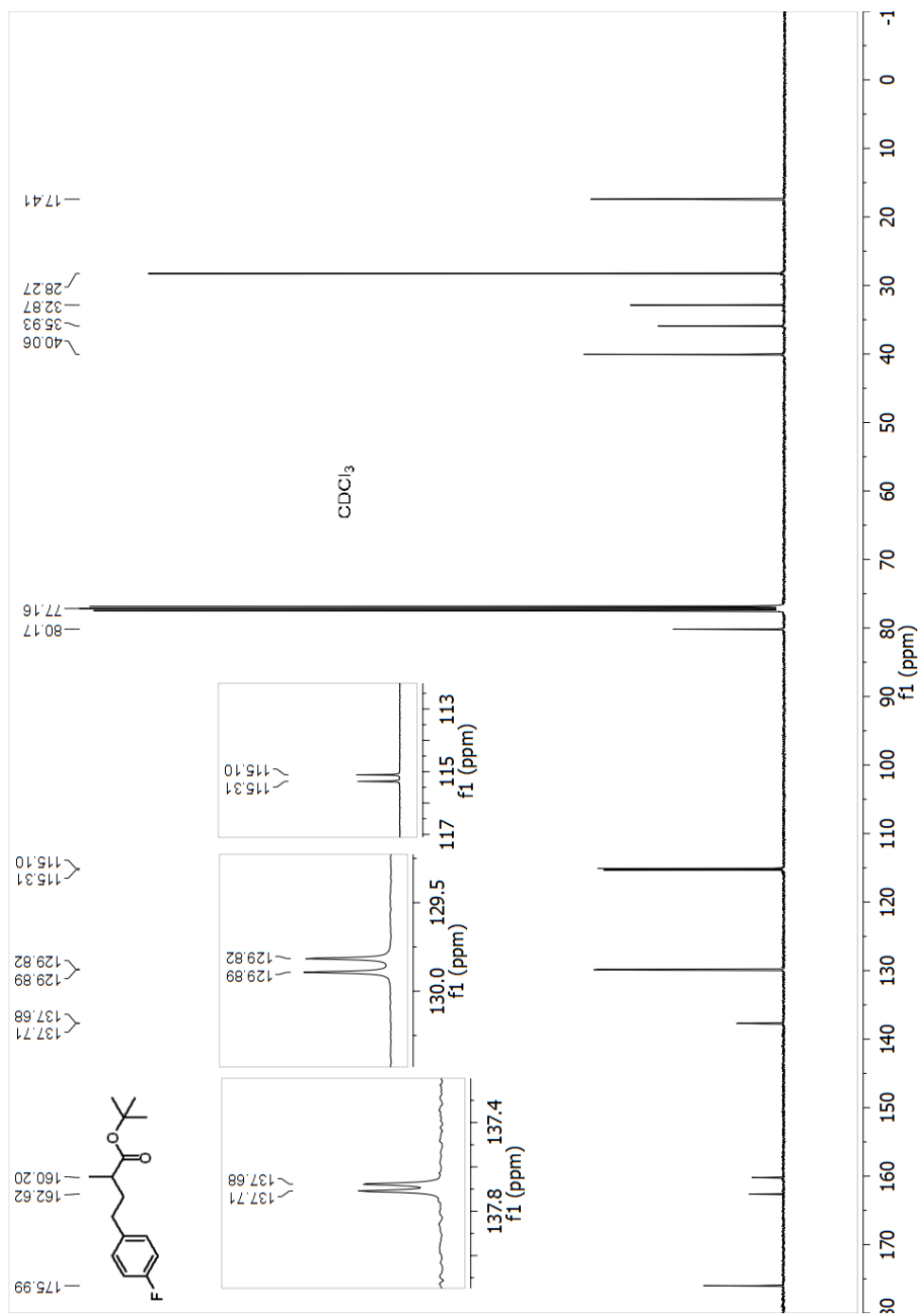
¹H NMR (400 MHz, Chloroform-d) spectrum of 4d tert-butyl 4-(4-fluorophenyl)-2-methylbutanoate



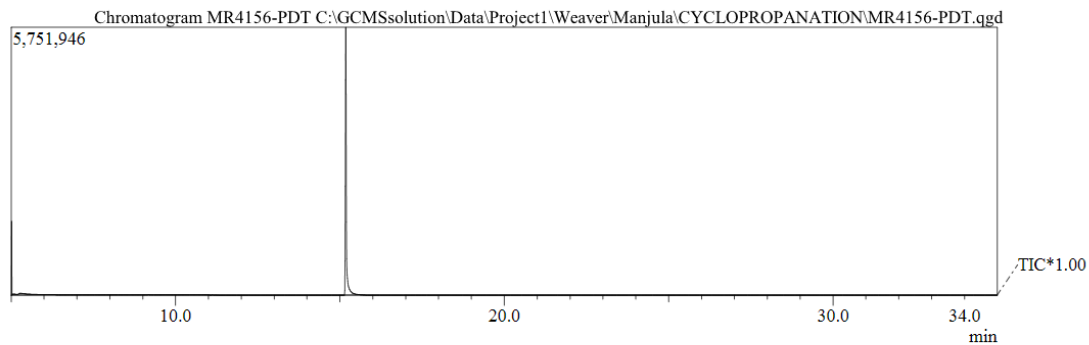
^{19}F NMR (376 MHz, Chloroform-d) spectrum of 4d tert-butyl 4-(4-fluorophenyl)-2-methylbutanoate



¹³C NMR (101 MHz, Chloroform-d) spectrum of 4d tert-butyl 4-(4-fluorophenyl)-2-methylbutanoate

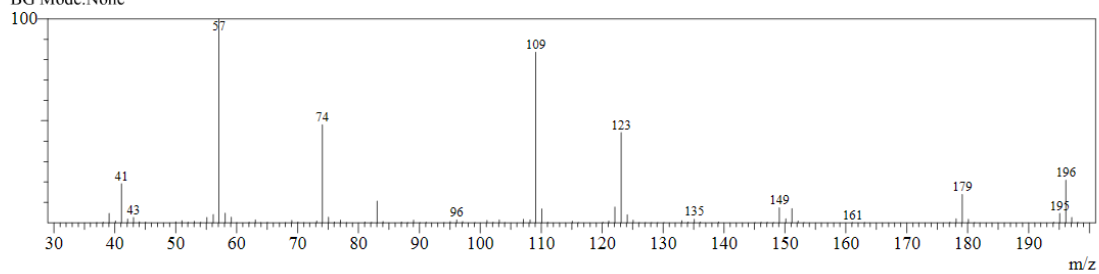


GC and MS of 4d tert-butyl 4-(4-fluorophenyl)-2-methylbutanoate

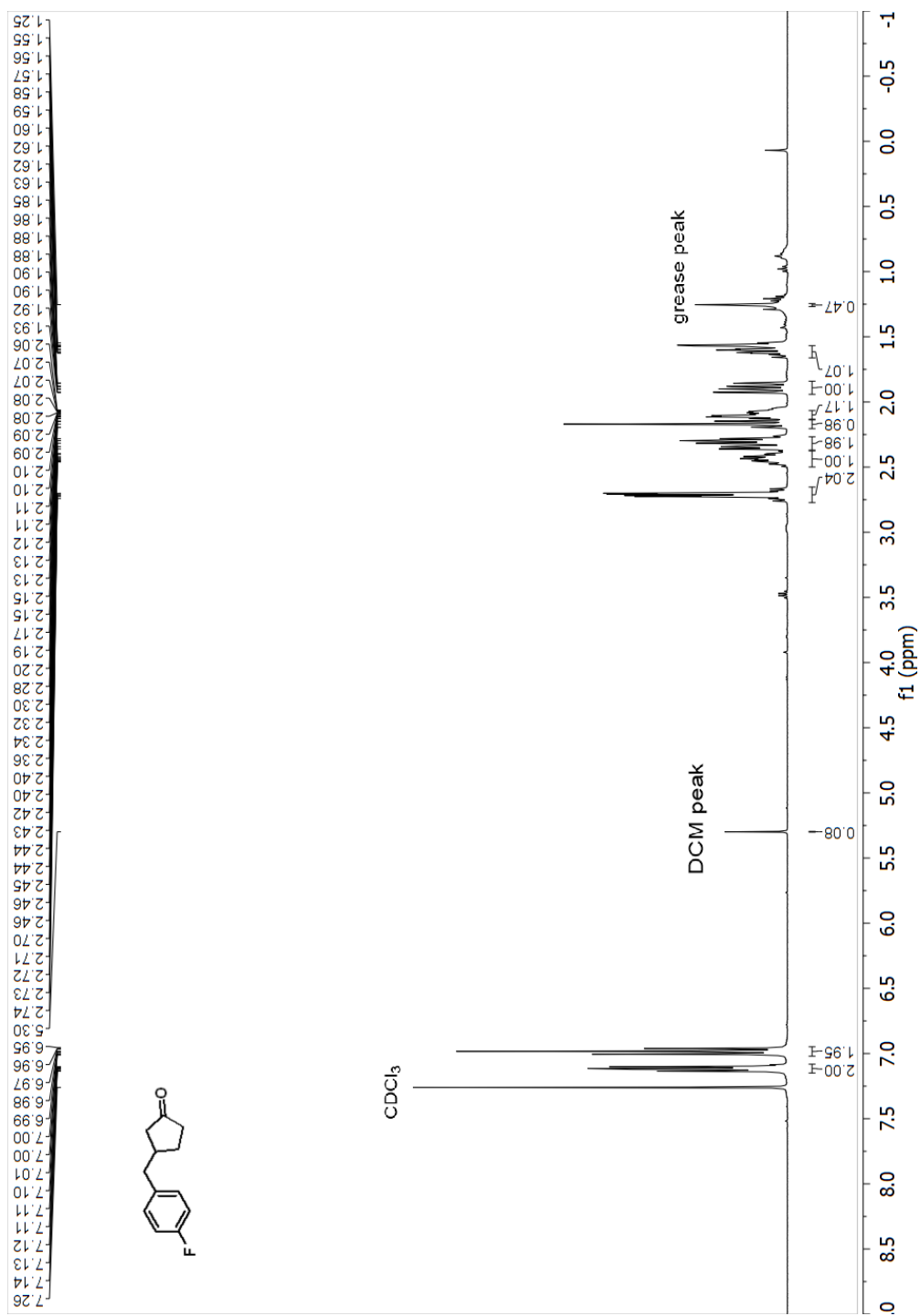


Spectrum

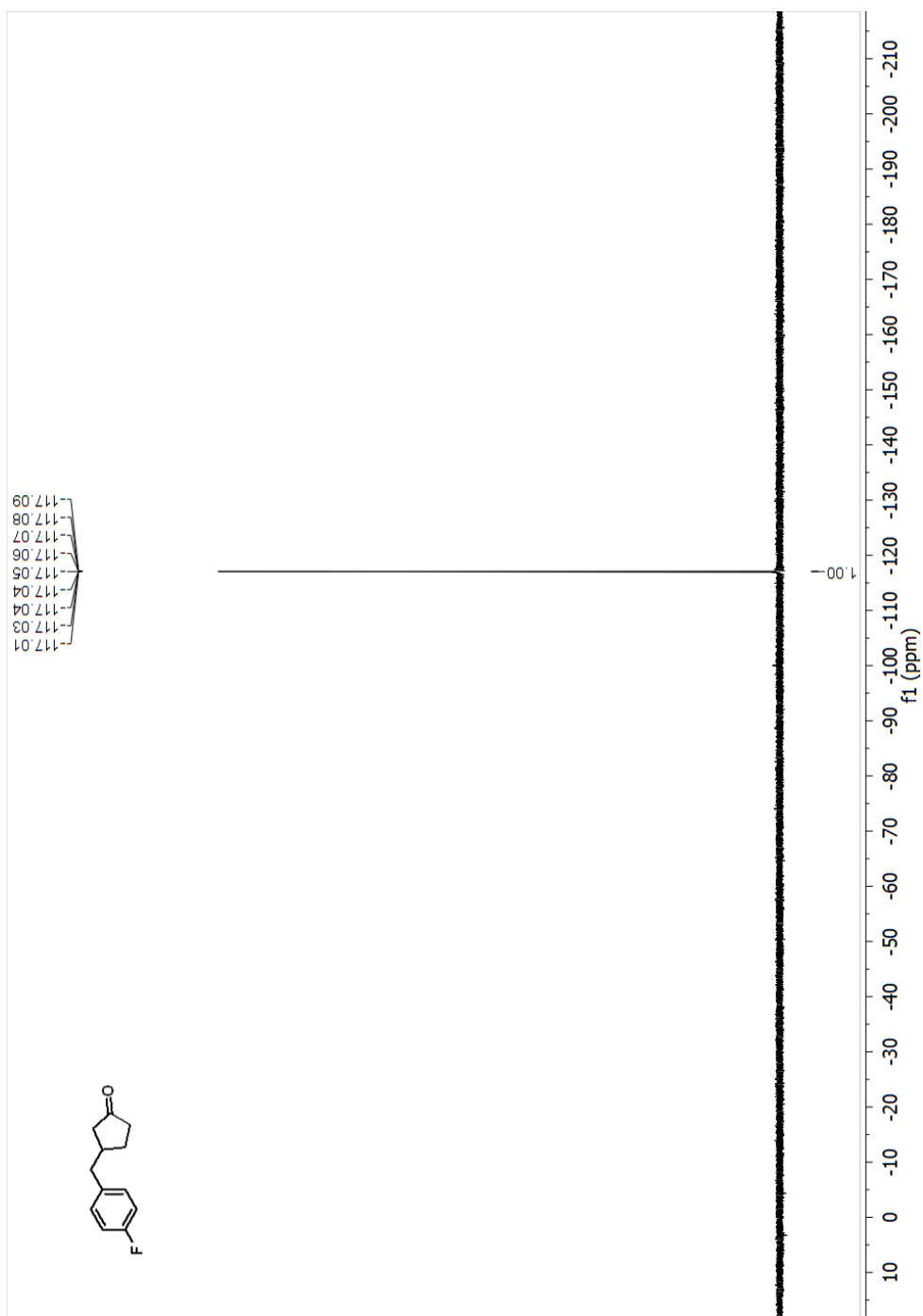
Line#:1 R.Time:15.2(Scan#:1222)
MassPeaks:96
RawMode:Single 15.2(1222) BasePeak:57(1283529)
BG Mode:None



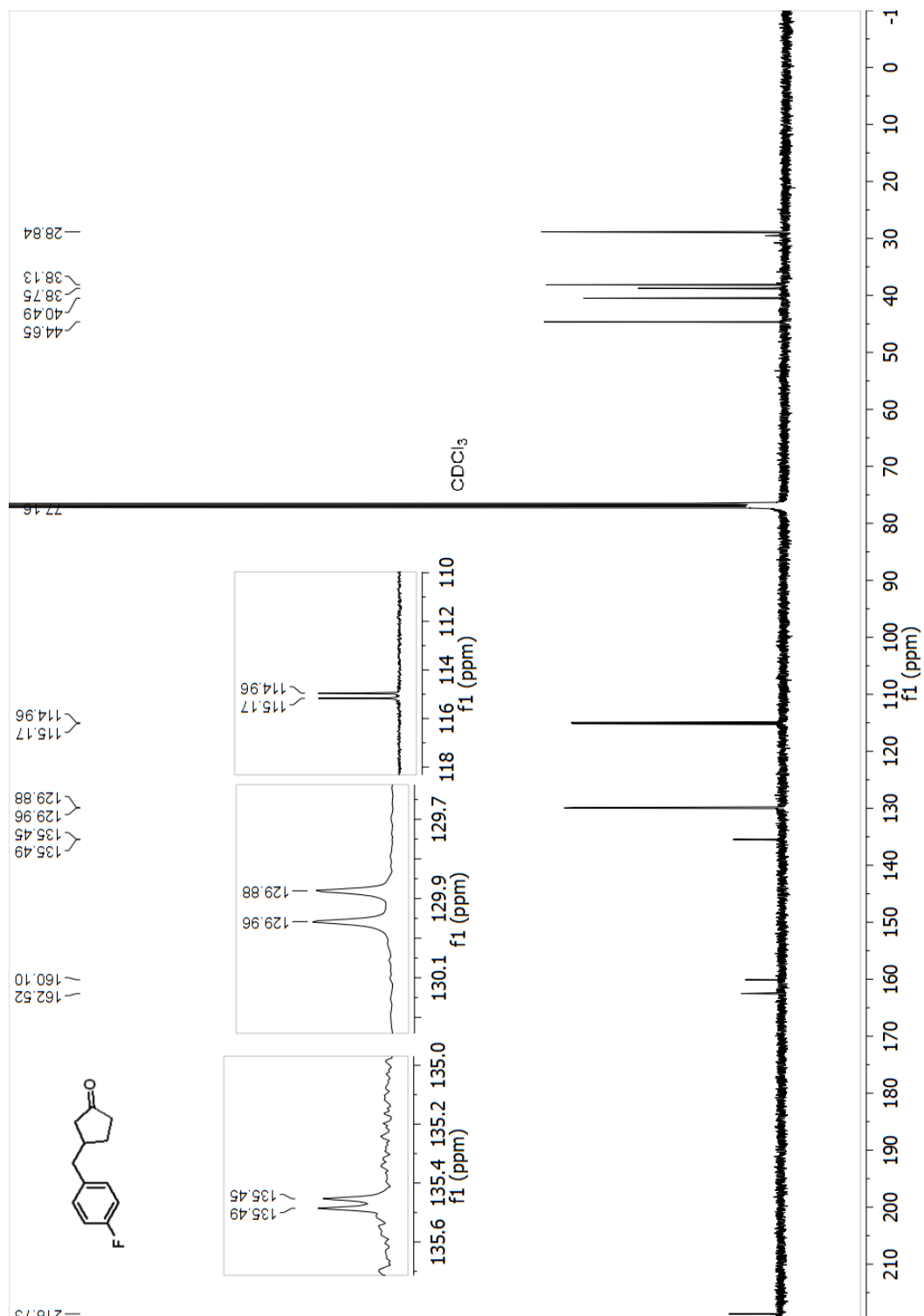
¹H NMR (400 MHz, Chloroform-d) spectrum of 4e 3-(4-fluorobenzyl)cyclopentan-1-one



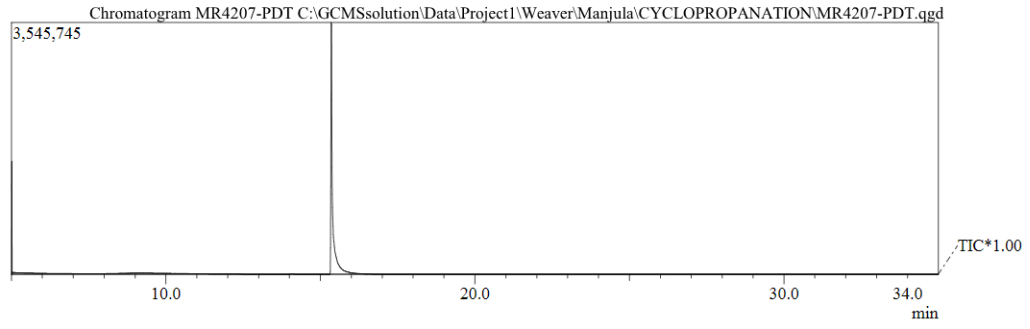
^{19}F NMR (376 MHz, Chloroform-d) spectrum of 4e 3-(4-fluorobenzyl)cyclopentan-1-one



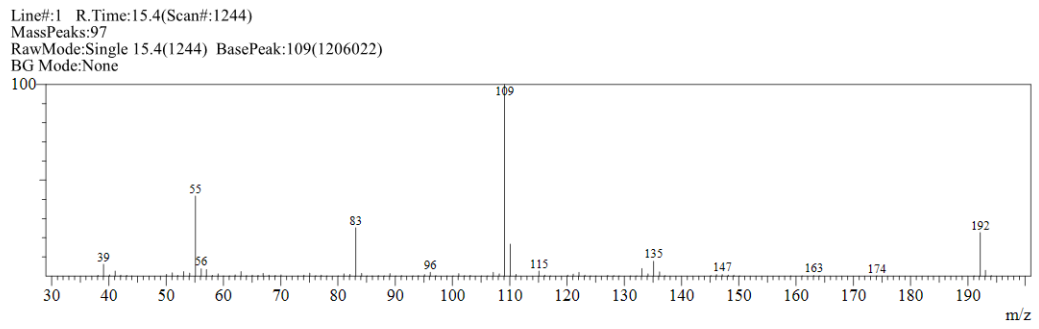
¹³C NMR (101 MHz, Chloroform-d) spectrum of 4e 3-(4-fluorobenzyl)cyclopentan-1-one



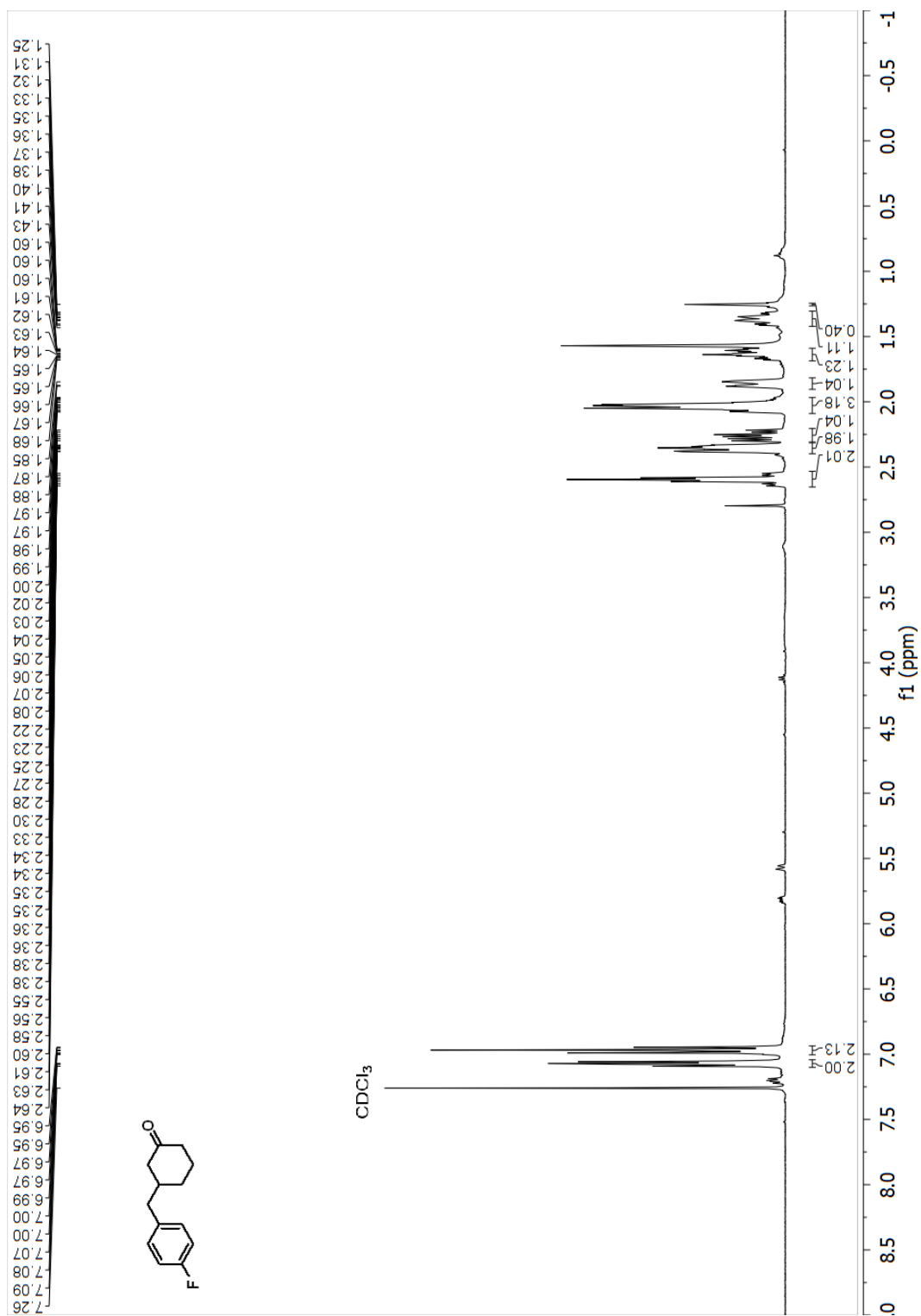
GC and MS of 4e 3-(4-fluorobenzyl)cyclopentan-1-one



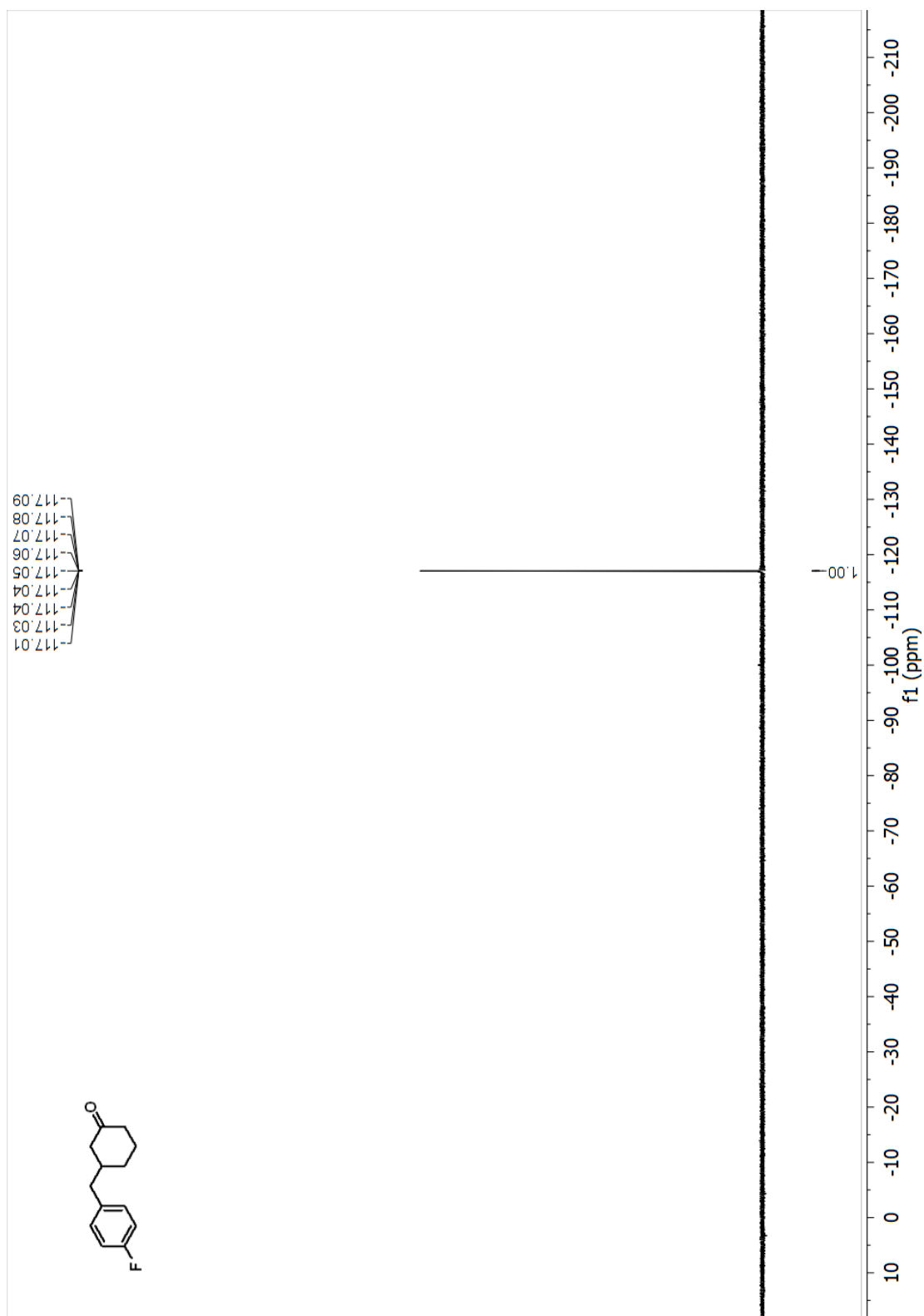
Spectrum



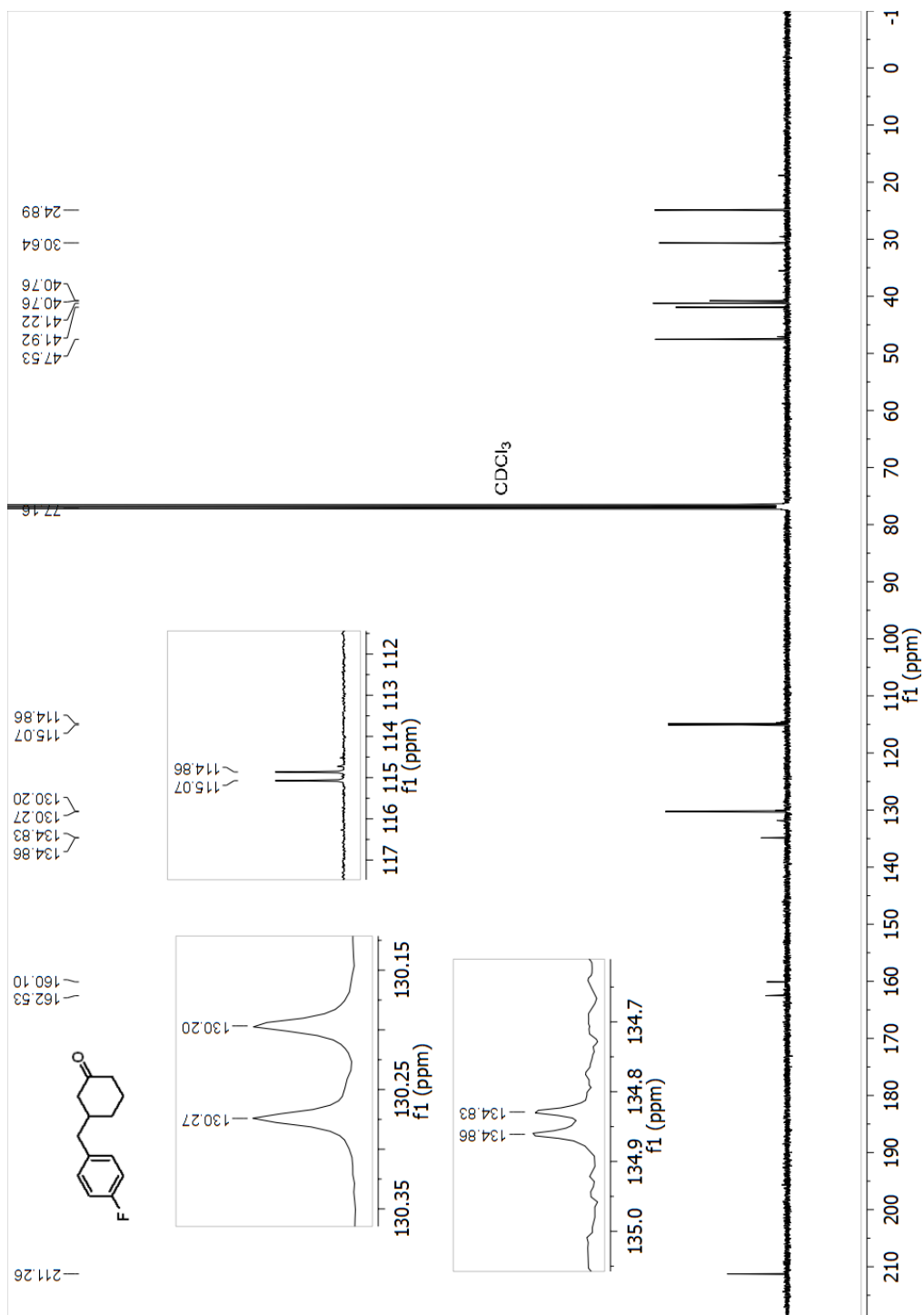
¹H NMR (400 MHz, Chloroform-d) spectrum of 4f 3-(4-fluorobenzyl)cyclohexan-1-one



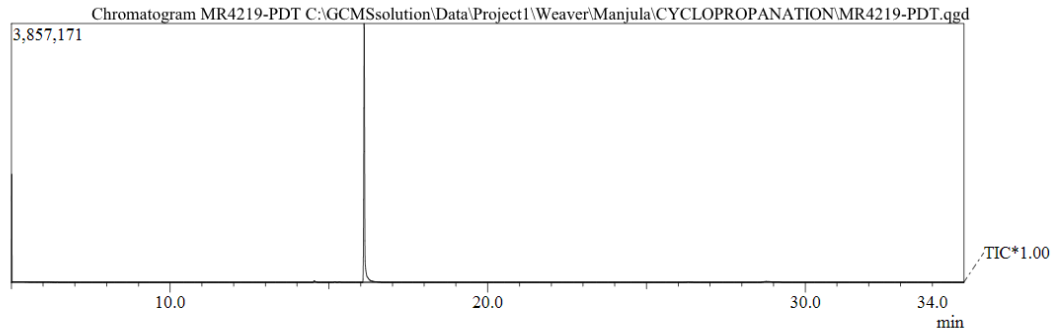
^{19}F NMR (376 MHz, Chloroform-d) spectrum of 4-(3-(4-fluorobenzyl)cyclohexan-1-one)



¹³C NMR (101 MHz, Chloroform-d) spectrum of 4f 3-(4-fluorobenzyl)cyclohexan-1-one

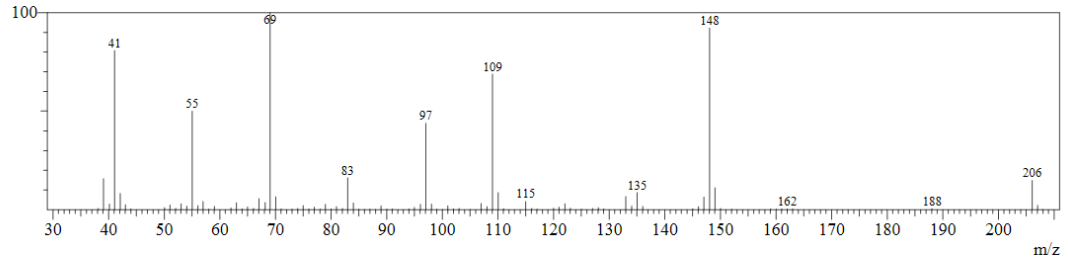


GC and MS of 4f 3-(4-fluorobenzyl)cyclohexan-1-one

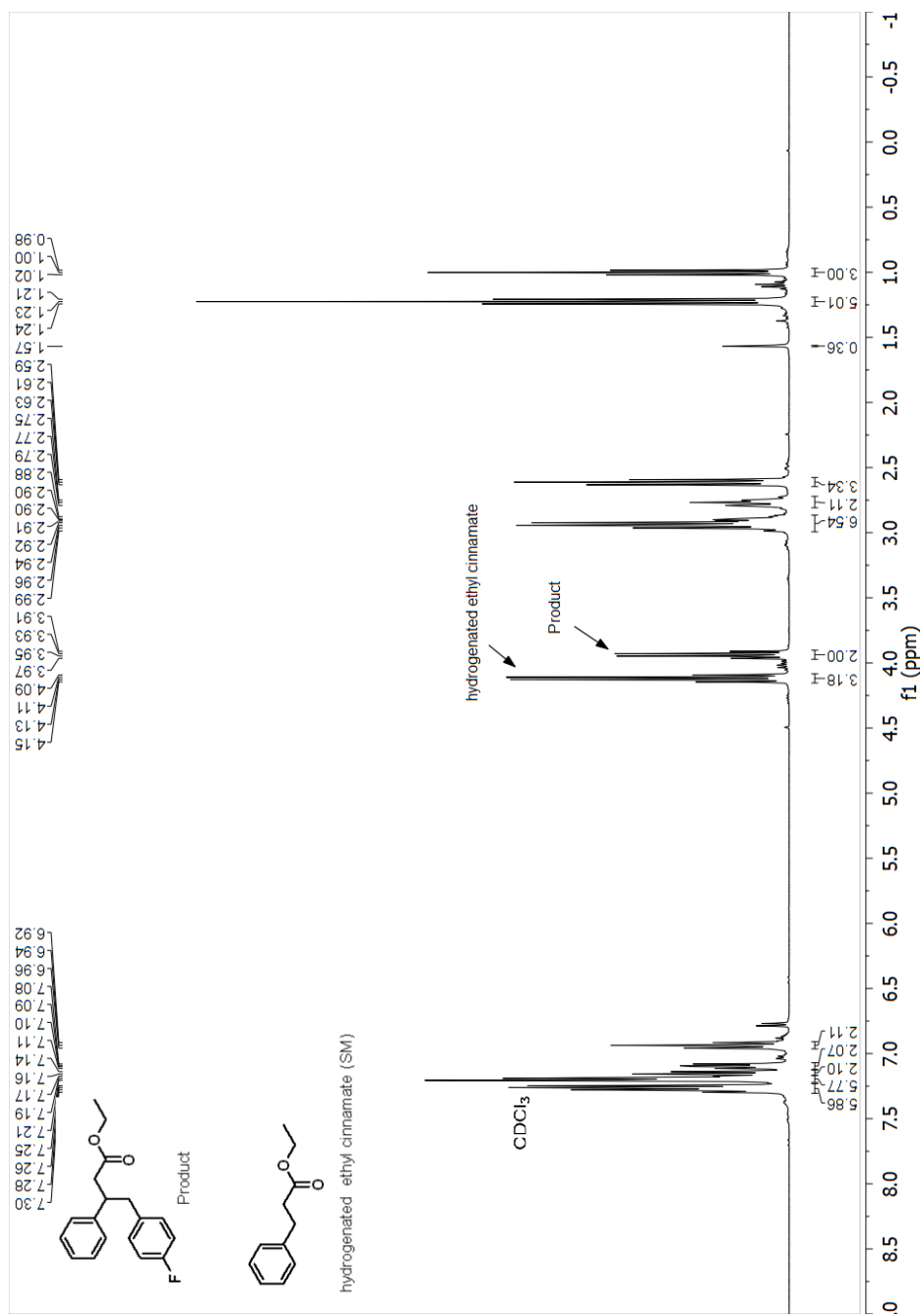


Spectrum

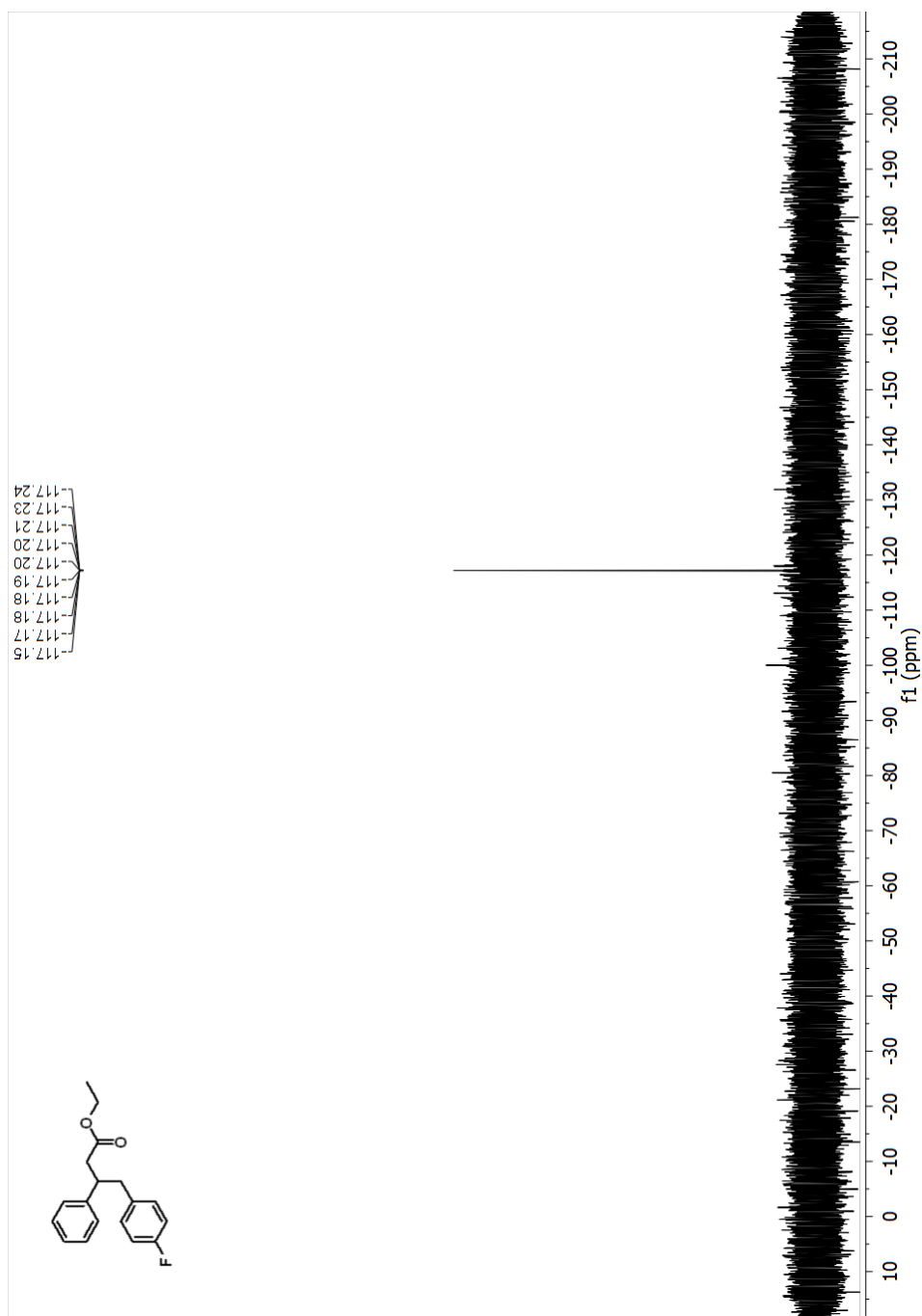
Line#:1 R.Time:16.1(Scan#:1334)
MassPeaks:93
RawMode:Single 16.1(1334) BasePeak:69(604454)
BG Mode:None



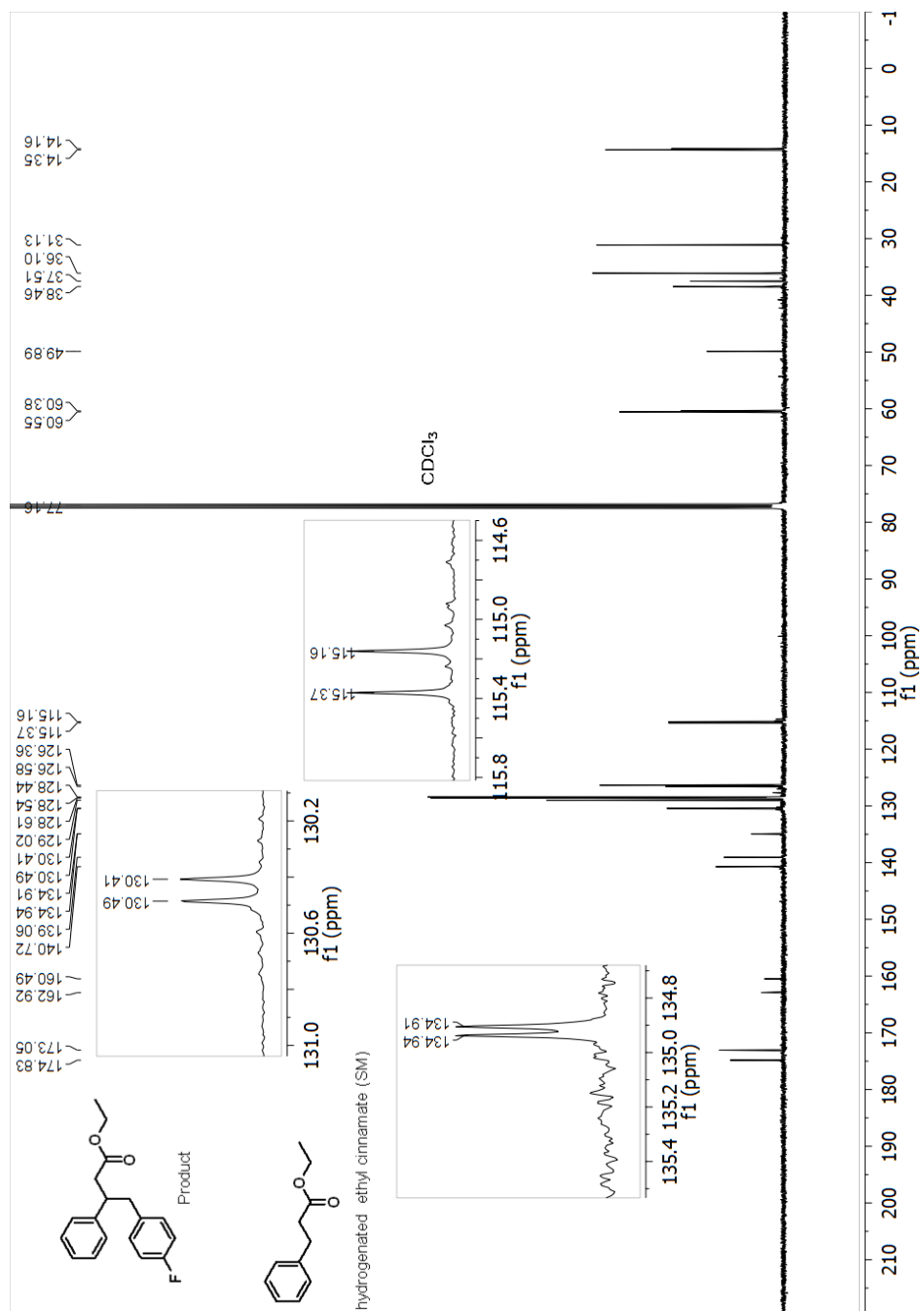
¹H NMR (400 MHz, Chloroform-d) spectrum of 4g ethyl 4-(4-fluorophenyl)-3-phenylbutanoate



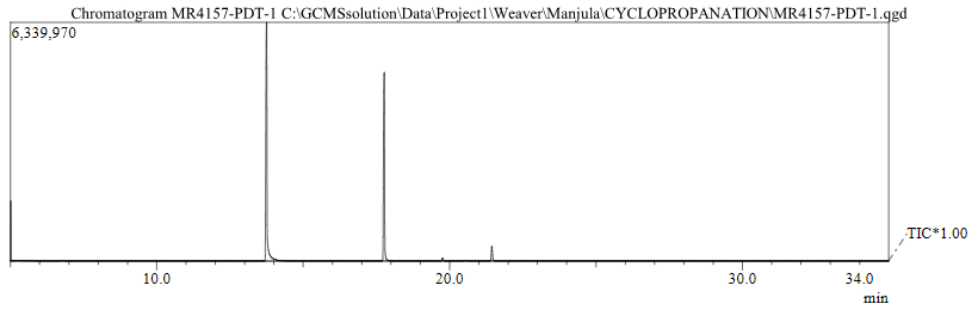
¹⁹F NMR (376 MHz, Chloroform-d) spectrum of 4g ethyl 4-(4-fluorophenyl)-3-phenylbutanoate



^{13}C NMR (101 MHz, Chloroform-d) spectrum of 4g ethyl 4-(4-fluorophenyl)-3-phenylbutanoate

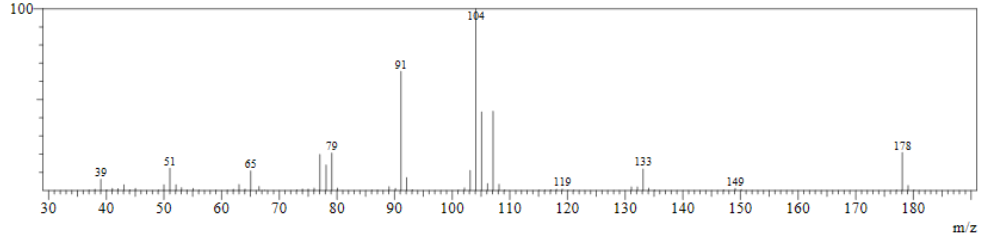


GC and MS of 4g ethyl 4-(4-fluorophenyl)-3-phenylbutanoate

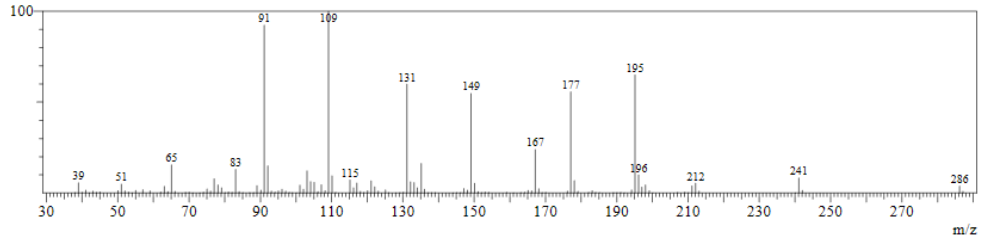


Spectrum

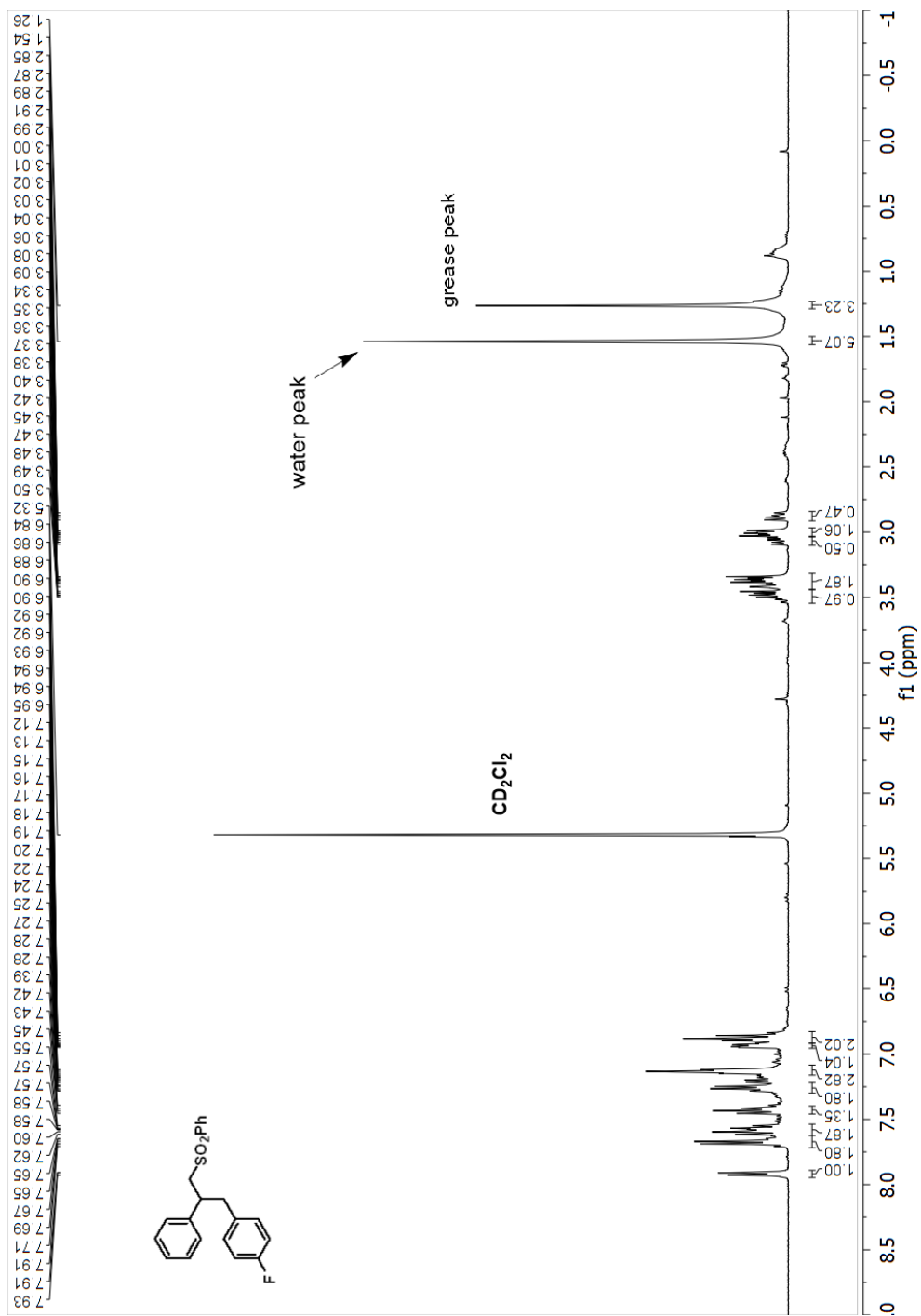
Line#:1 R.Time:13.7(Scan#:1050)
MassPeaks:68
RawMode:Single 13.7(1050) BasePeak:104(1417900)
BG Mode:None



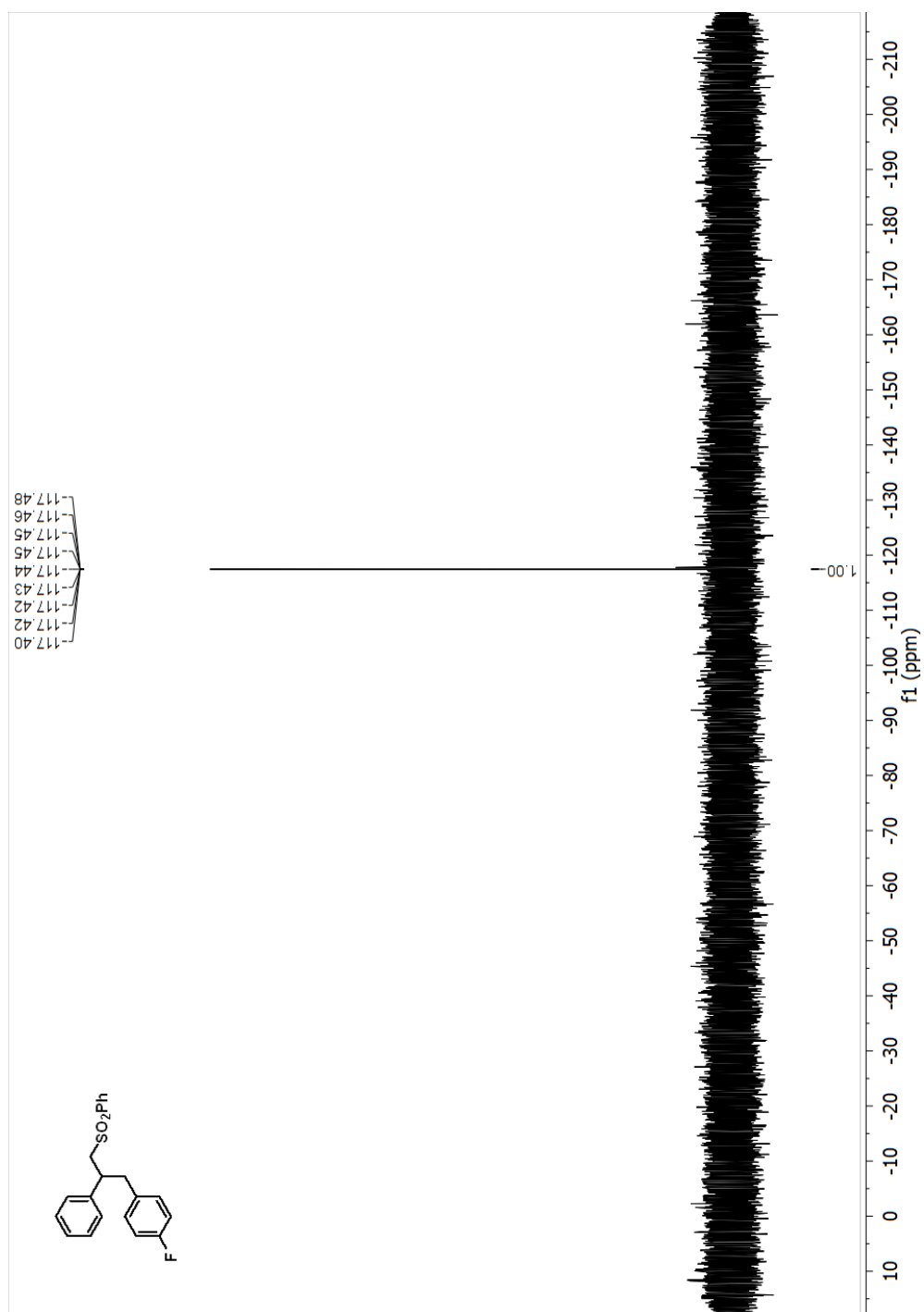
Line#:2 R.Time:17.8(Scan#:1532)
MassPeaks:136
RawMode:Single 17.8(1532) BasePeak:109(658986)
BG Mode:None



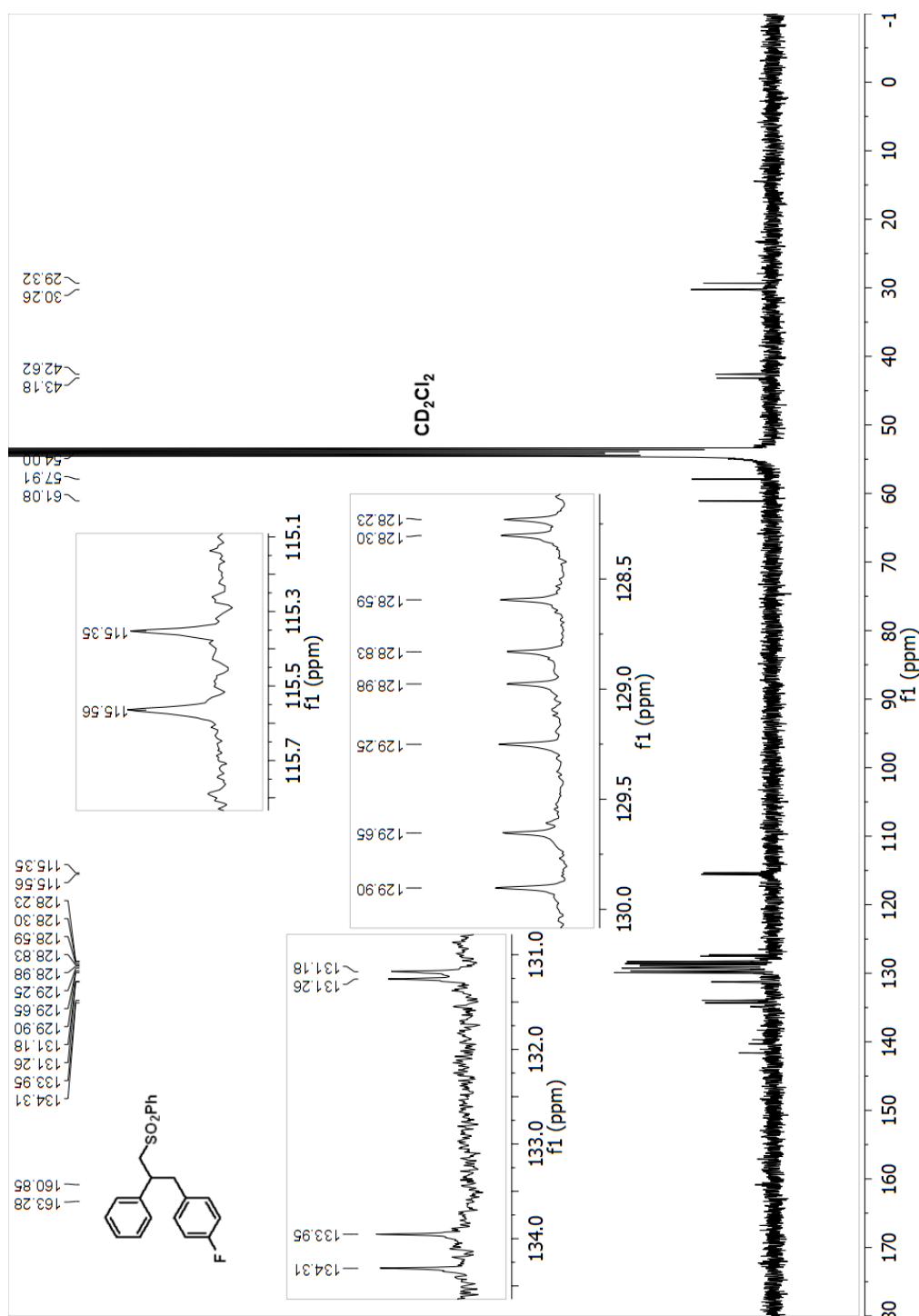
^1H NMR (400 MHz, Methylene chloride- d_2) spectrum of 4h 1-fluoro-4-(2-phenyl-3-(phenylsulfonyl)propyl)benzene



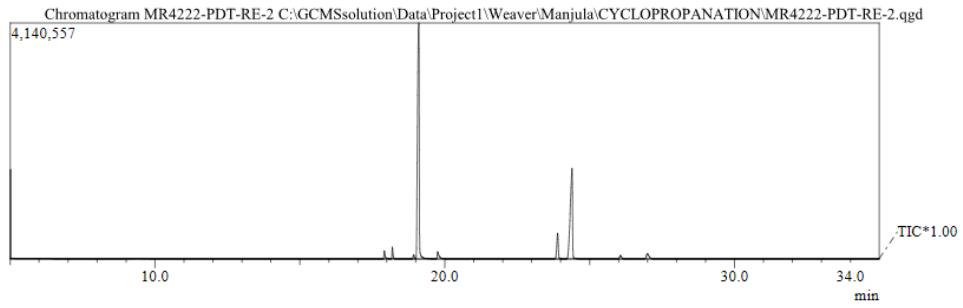
^{19}F NMR (376 MHz, Methylene chloride- d_2) spectrum of 4-fluoro-4-(2-phenyl-3-(phenylsulfonyl)propyl)benzene



¹³C NMR (101 MHz, Methylene chloride-d₂) spectrum of 4-fluoro-4-(2-phenyl-3-(phenylsulfonyl)propyl)benzene

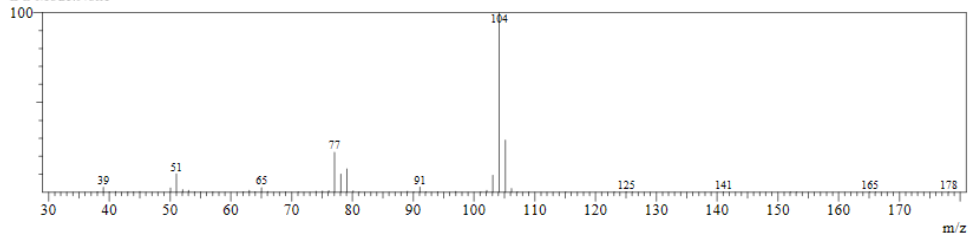


GC and MS of 4h 1-fluoro-4-(2-phenyl-3-(phenylsulfonyl)propyl)benzene

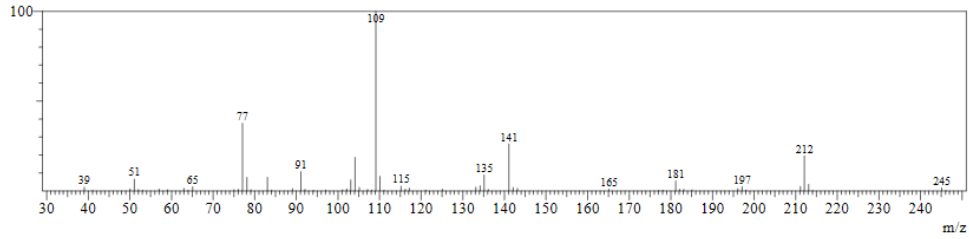


Spectrum

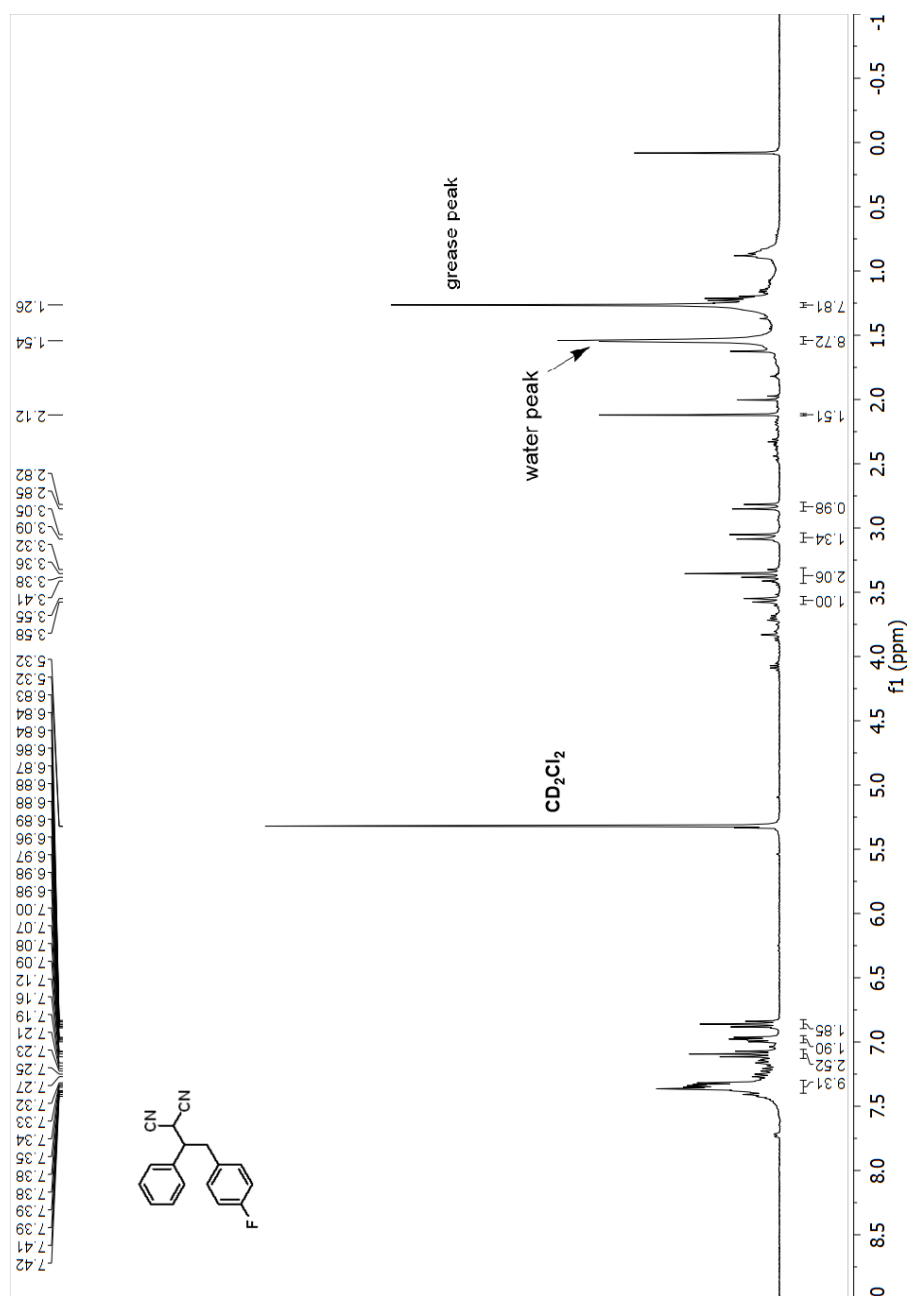
Line#:1 R.Time:19.1(Scan#:1690)
MassPeaks:53
RawMode:Single 19.1(1690) BasePeak:104(1488381)
BG Mode:None



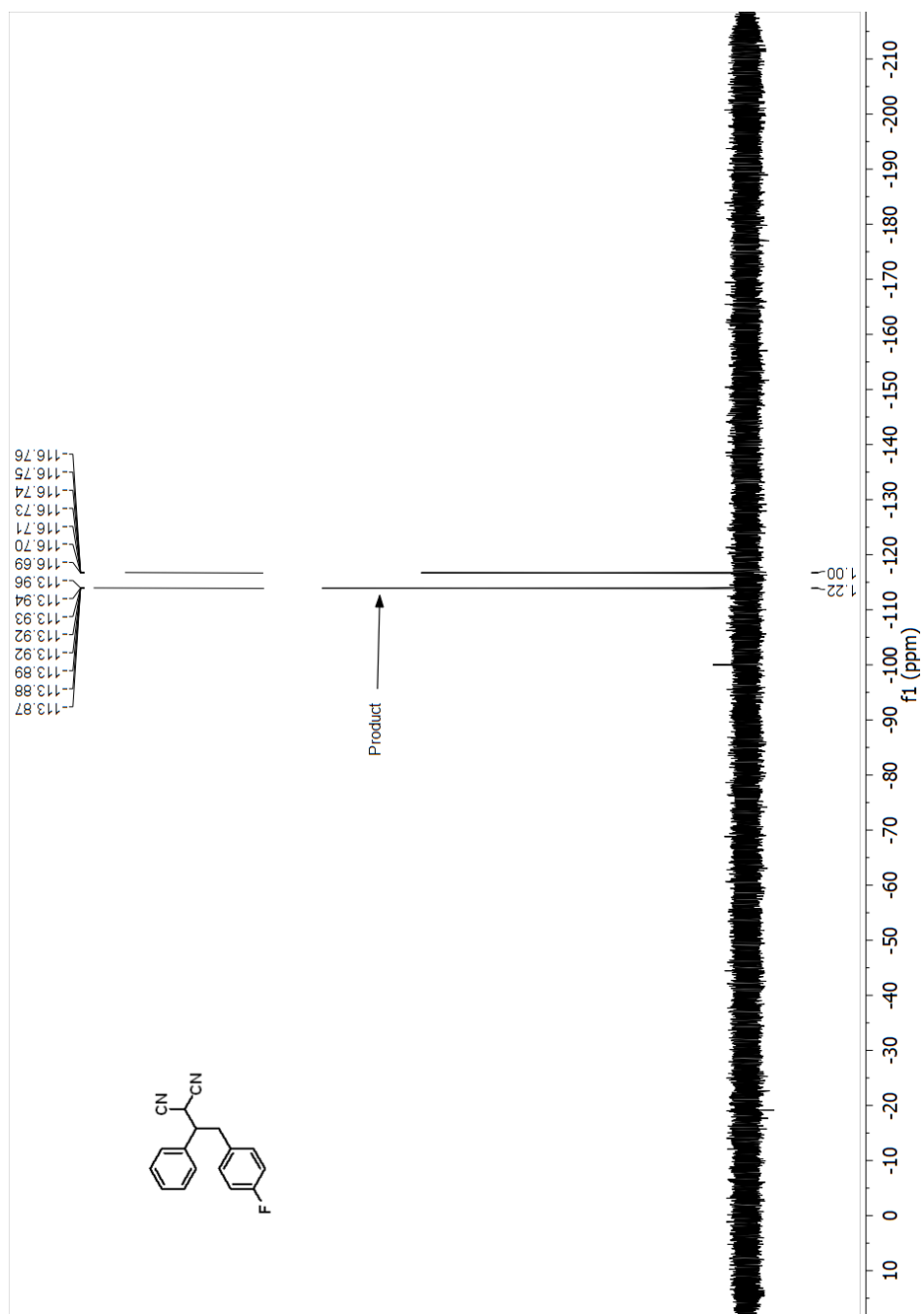
Line#:2 R.Time:24.3(Scan#:2322)
MassPeaks:61
RawMode:Single 24.3(2322) BasePeak:109(324782)
BG Mode:None



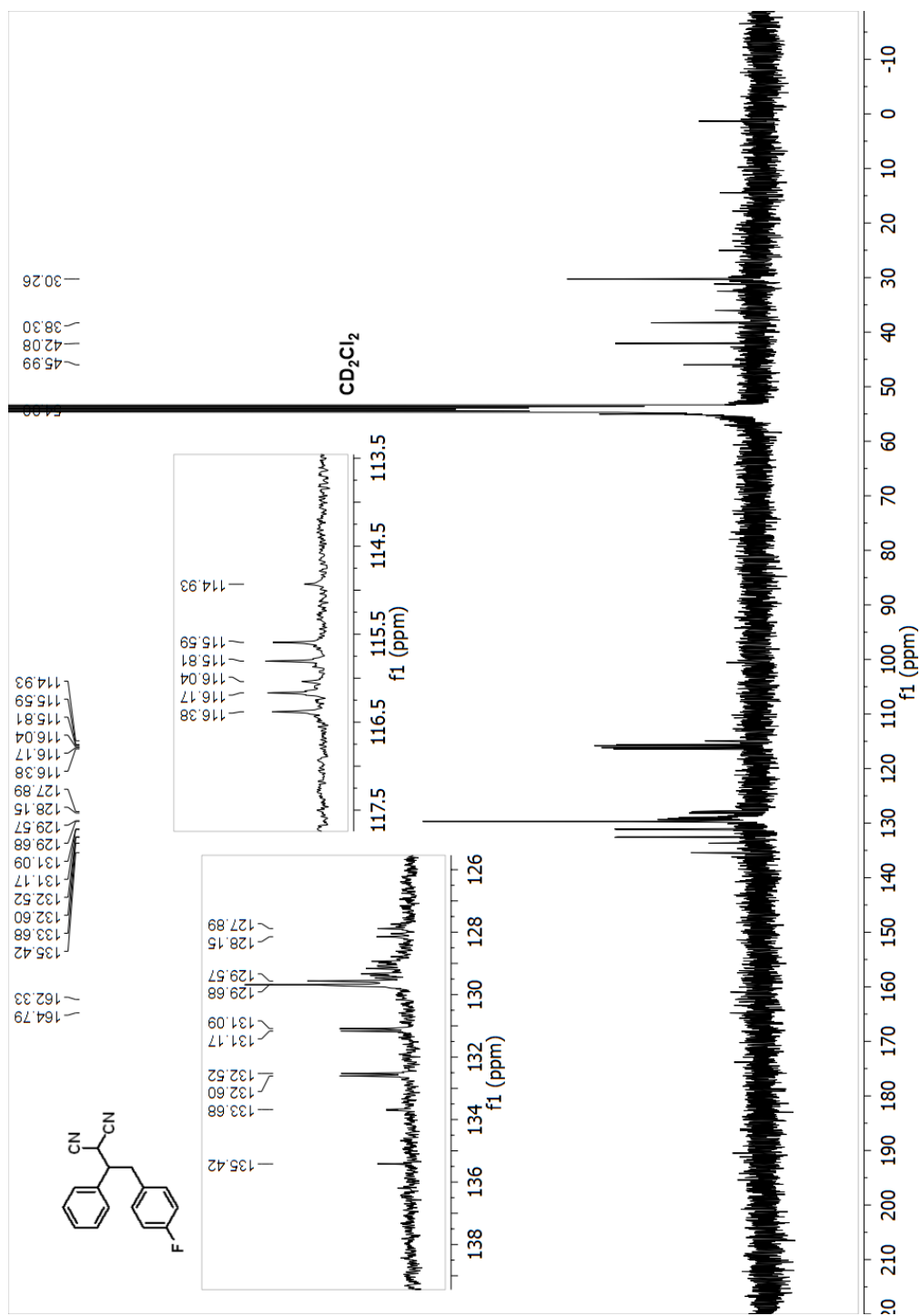
^1H NMR (400 MHz, Methylene chloride- d_2) spectrum of 2-(2-(4-fluorophenyl)-1-phenylethyl)malononitrile



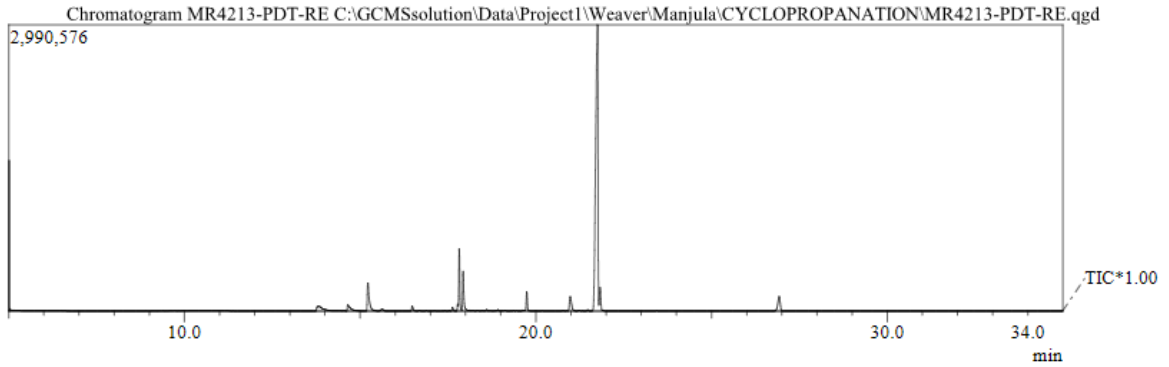
^{19}F NMR (376 MHz, Methylene chloride- d_2) spectrum of 2-(2-(4-fluorophenyl)-1-phenylethyl)malononitrile



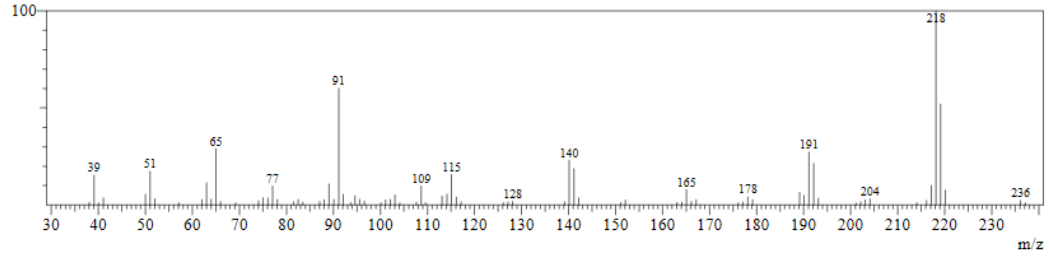
^{13}C NMR (101 MHz, Methylene chloride- d_2) spectrum of 2-(2-(4-fluorophenyl)-1-phenylethyl)malononitrile



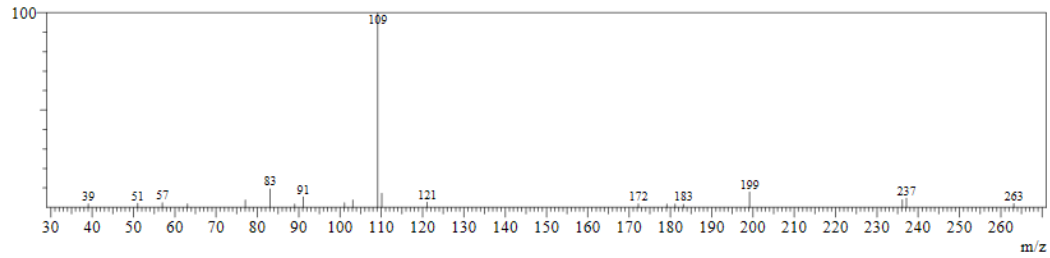
GC and MS of 2-(2-(4-fluorophenyl)-1-phenylethyl)malononitrile



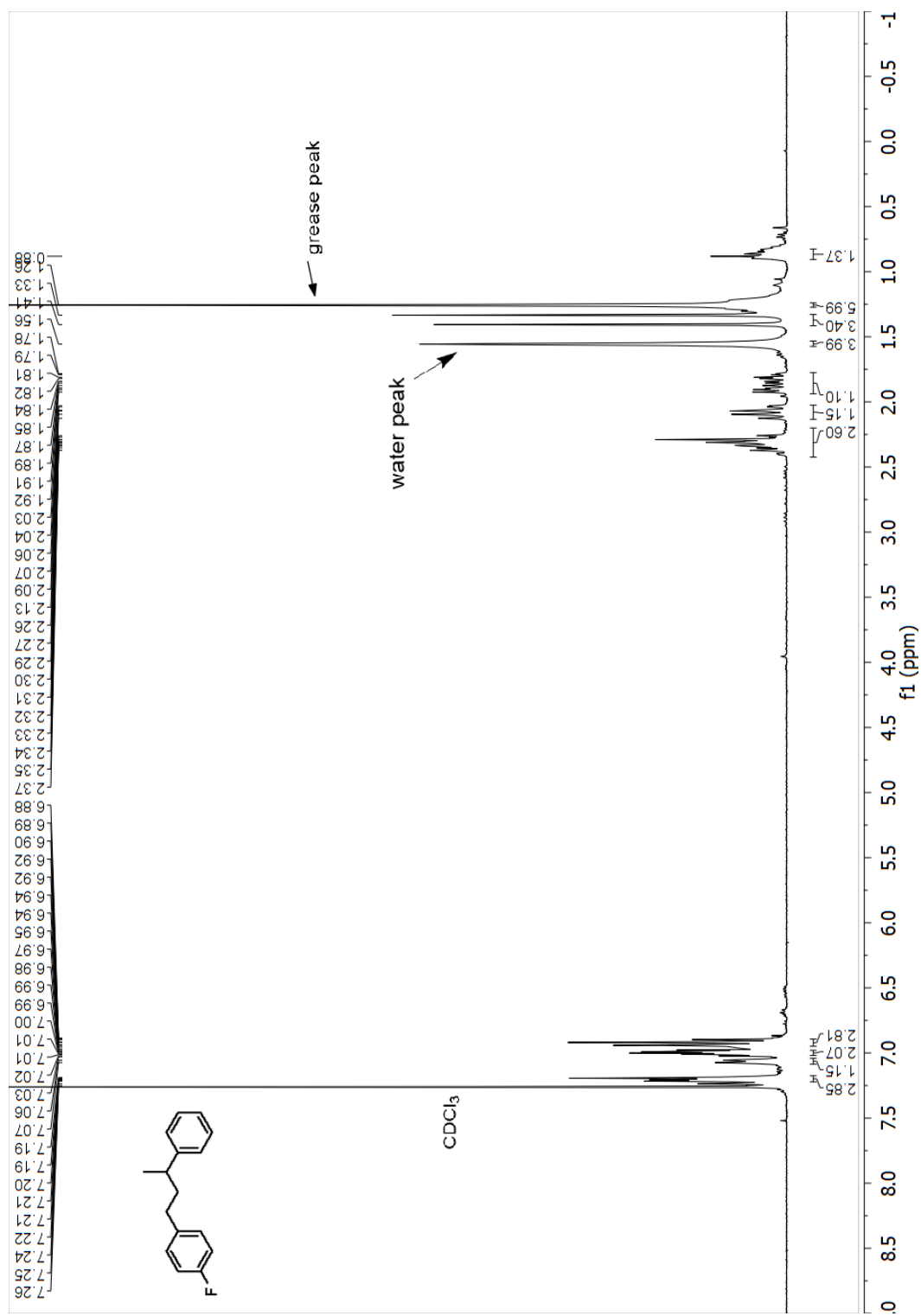
Line#:2 R.Time:17.8(Scan#:1539)
MassPeaks:80
RawMode:Single 17.8(1539) BasePeak:218(107409)
BG Mode:None



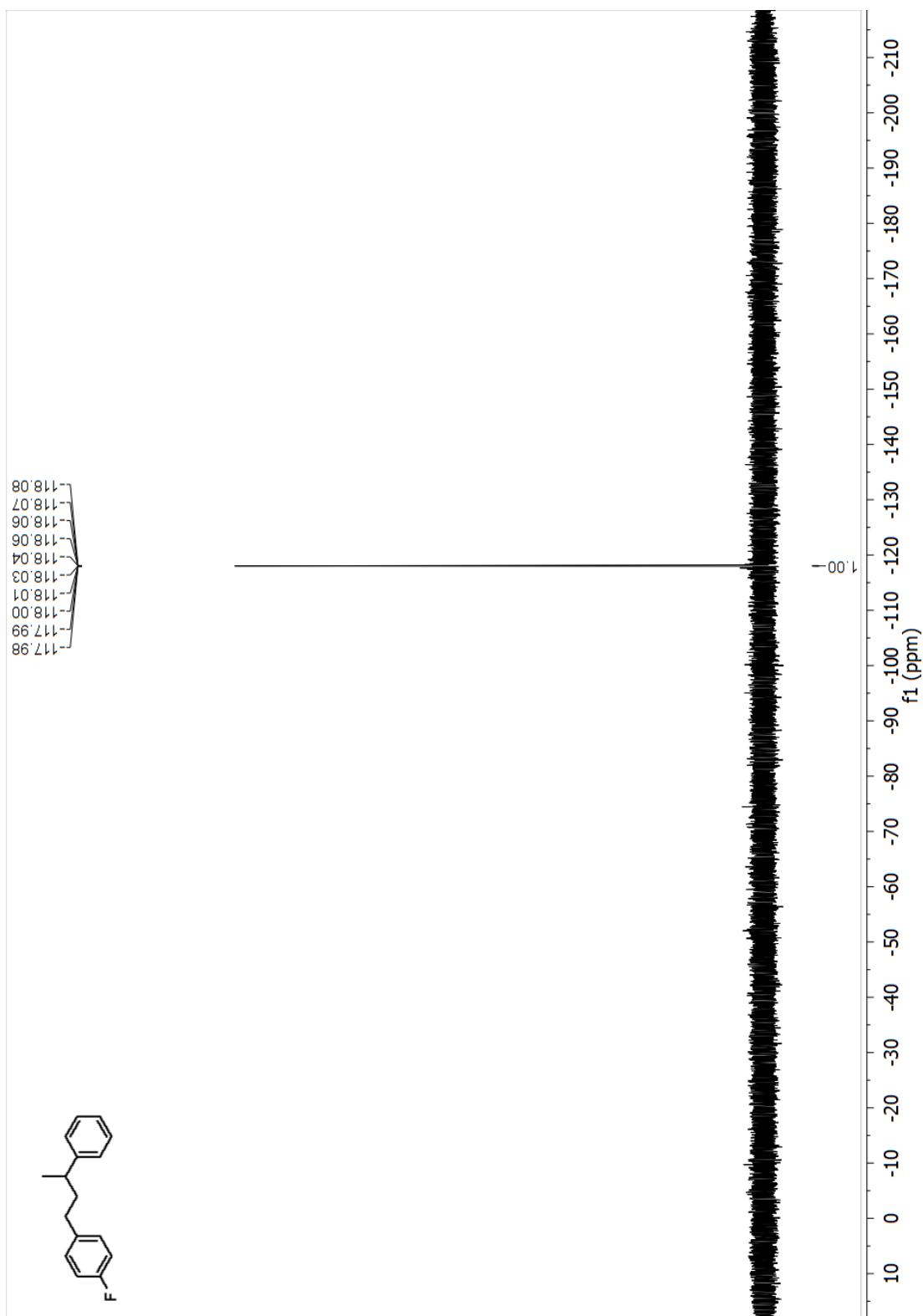
Line#:6 R.Time:21.8(Scan#:2015)
MassPeaks:21
RawMode:Single 21.8(2015) BasePeak:109(64999)
BG Mode:None



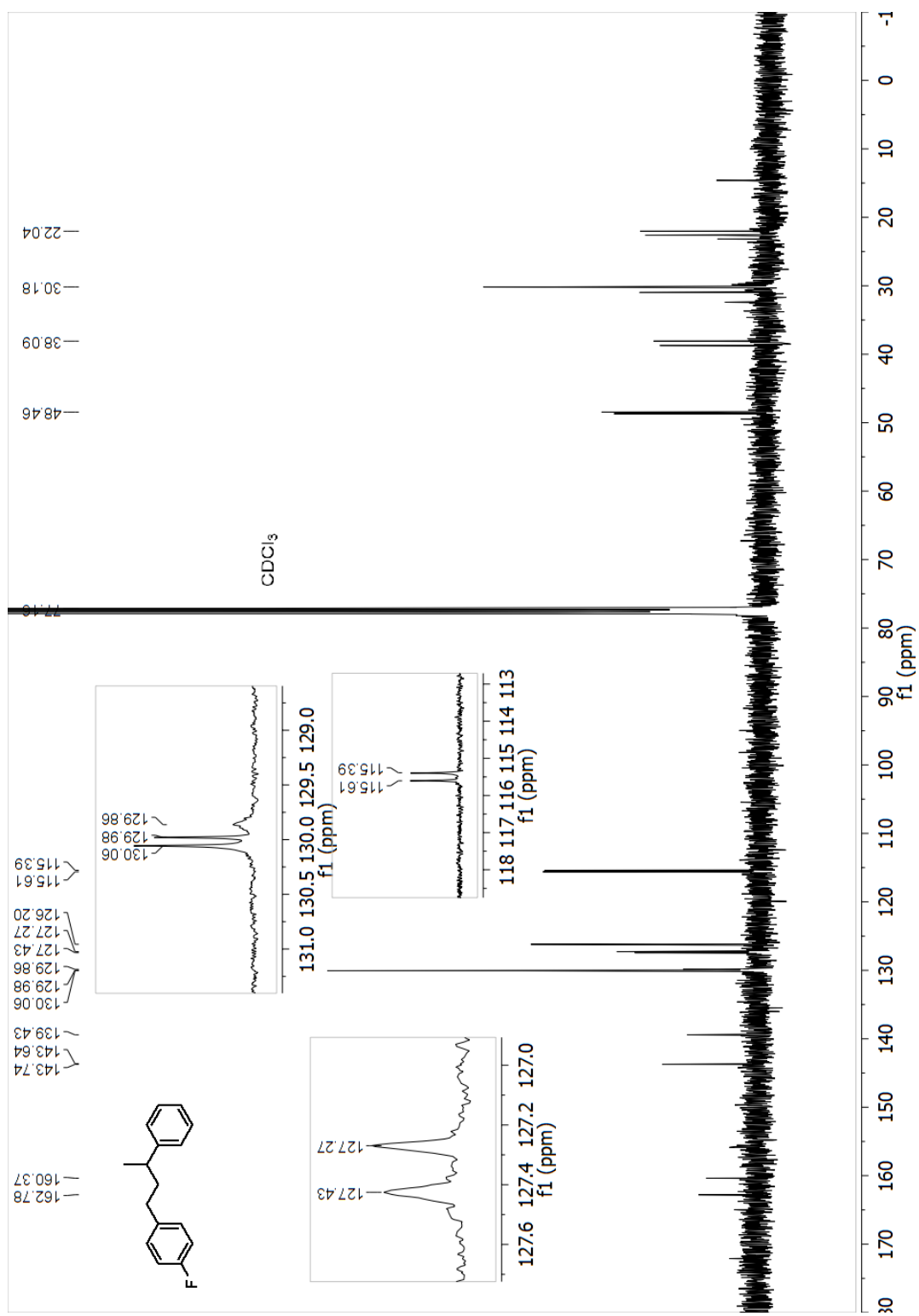
¹H NMR (400 MHz, Chloroform-d) spectrum of 4-(1-fluoro-4-(3-phenylbutyl)benzene



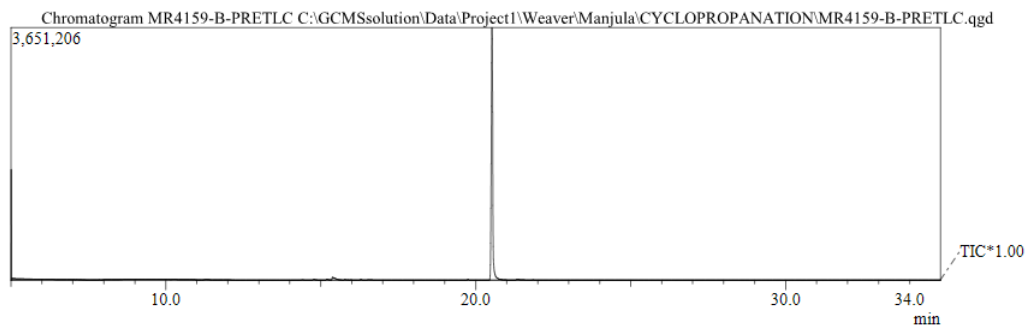
^{19}F NMR (376 MHz, Chloroform-d) spectrum of 4i 1-fluoro-4-(3-phenylbutyl)benzene



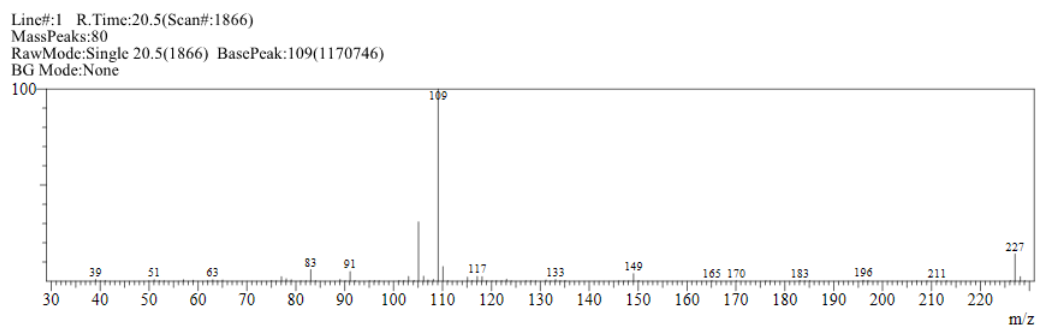
^{13}C NMR (101 MHz, Chloroform-d) spectrum of 4-(1-fluoro-4-(3-phenylbutyl)benzene



GC and MS of 4i 1-fluoro-4-(3-phenylbutyl)benzene



Spectrum



4.5 References

- 1.(a) Prier, C. K.; Rankic, D. A.; MacMillan, D. W. C., Visible Light Photoredox Catalysis with Transition Metal Complexes: Applications in Organic Synthesis. *Chem. Rev.* **2013**, *113*, 5322; (b) Romero, N. A.; Nicewicz, D. A., Organic Photoredox Catalysis. *Chem. Rev.* **2016**, *116*, 10075; (c) Beatty, J. W.; Stephenson, C. R. J., Amine Functionalization via Oxidative Photoredox Catalysis: Methodology Development and Complex Molecule Synthesis. *Acc. Chem. Res.* **2015**, *48*, 1474; (d) Marzo, L.; Pagire, S. K.; Reiser, O.; König, B., Visible-Light Photocatalysis: Does It Make a Difference in Organic Synthesis? *Angew. Chem. Int. Ed.* **2018**, *57*, 10034.
- 2.(a) Ischay, M. A.; Anzovino, M. E.; Du, J.; Yoon, T. P., Efficient Visible Light Photocatalysis of [2+2] Enone Cycloadditions. *J. Am. Chem. Soc.* **2008**, *130*, 12886; (b) Nicewicz, D. A.; MacMillan, D. W. C., Merging Photoredox Catalysis with Organocatalysis: The Direct Asymmetric Alkylation of Aldehydes. *Science* **2008**, *322*, 77; (c) Nguyen, J. D.; D'Amato, E. M.; Narayanam, J. M. R.; Stephenson, C. R. J., Engaging unactivated alkyl, alkenyl and aryl iodides in visible-light-mediated free radical reactions. *Nat Chem* **2012**, *4*, 854; (d) Tucker, J. W.; Nguyen, J. D.; Narayanam, J. M. R.; Krabbe, S. W.; Stephenson, C. R. J., Tin-free radical cyclization reactions initiated by visible light photoredox catalysis. *Chem. Commun.* **2010**, *46*, 4985; (e) Guindon, Y.; Jung, G.; Guerin, B.; Ogilvie, W. W., Hydrogen and allylation transfer reactions in acyclic free radicals. *Synlett* **1998**, 213; (f) Cheng, Y.; Yang, J.; Qu, Y.; Li, P., Aerobic Visible-Light Photoredox Radical C–H Functionalization: Catalytic Synthesis of 2-Substituted Benzothiazoles. *Org. Lett.* **2012**, *14*, 98; (g) Barton, D. H. R.; Csiba, M. A.; Jaszberenyi, J. C., Ru(bpy)₃²⁺-mediated addition of Se-phenyl p-tolueneselenosulfonate to electron rich olefins. *Tetrahedron Lett.* **1994**, *35*, 2869; (h) Nguyen, J. D.; Tucker, J. W.; Konieczynska, M. D.; Stephenson, C. R. J., Intermolecular Atom Transfer Radical Addition to Olefins Mediated by Oxidative Quenching of Photoredox Catalysts. *J. Am. Chem. Soc.* **2011**, *133*, 4160; (i) Wallentin, C.-J.; Nguyen, J. D.; Finkbeiner, P.; Stephenson, C. R. J., Visible Light-Mediated Atom

Transfer Radical Addition via Oxidative and Reductive Quenching of Photocatalysts. *J. Am. Chem. Soc.* **2012**, *134*, 8875.

3. Qiu, G.; Li, Y.; Wu, J., Recent developments for the photoinduced Ar–X bond dissociation reaction. *Org. Chem. Front.* **2016**, *3*, 1011.

4.(a) Galli, C., Radical reactions of arenediazonium ions: An easy entry into the chemistry of the aryl radical. *Chem. Rev.* **1988**, *88*, 765; (b) Allongue, P.; Delamar, M.; Desbat, B.; Fagebaume, O.; Hitmi, R.; Pinson, J.; Savéant, J.-M., Covalent Modification of Carbon Surfaces by Aryl Radicals Generated from the Electrochemical Reduction of Diazonium Salts. *J. Am. Chem. Soc.* **1997**, *119*, 201; (c) Milanesi, S.; Fagnoni, M.; Albini, A., (Sensitized) Photolysis of Diazonium Salts as a Mild General Method for the Generation of Aryl Cations. Chemoselectivity of the Singlet and Triplet 4-Substituted Phenyl Cations. *J. Org. Chem.* **2005**, *70*, 603; (d) Hari, D. P.; Schroll, P.; König, B., Metal-Free, Visible-Light-Mediated Direct C–H Arylation of Heteroarenes with Aryl Diazonium Salts. *J. Am. Chem. Soc.* **2012**, *134*, 2958; (e) Kundu, D.; Ahammed, S.; Ranu, B. C., Visible Light Photocatalyzed Direct Conversion of Aryl-/Heteroarylamines to Selenides at Room Temperature. *Org. Lett.* **2014**, *16*, 1814.

5.(a) Pause, L.; Robert, M.; Savéant, J.-M., Can Single-Electron Transfer Break an Aromatic Carbon–Heteroatom Bond in One Step? A Novel Example of Transition between Stepwise and Concerted Mechanisms in the Reduction of Aromatic Iodides. *J. Am. Chem. Soc.* **1999**, *121*, 7158; (b) Costentin, C.; Robert, M.; Savéant, J.-M., Fragmentation of Aryl Halide π Anion Radicals. Bending of the Cleaving Bond and Activation vs Driving Force Relationships. *J. Am. Chem. Soc.* **2004**, *126*, 16051; (c) Devery, J. J.; Nguyen, J. D.; Dai, C.; Stephenson, C. R. J., Light-Mediated Reductive Debromination of Unactivated Alkyl and Aryl Bromides. *ACS Catal.* **2016**, *6*, 5962.

6. Arora, A.; Weaver, J. D., Visible Light Photocatalysis for the Generation and Use of Reactive Azolyl and Polyfluoroaryl Intermediates. *Acc. Chem. Res.* **2016**, *49*, 2273.

7.(a) Konovalov, V. V.; Laev, S. S.; Beregovaya, I. V.; Shchegoleva, L. N.; Shteingarts, V. D.; Tsvetkov, Y. D.; Bilkis, I., Fragmentation of Radical Anions of Polyfluorinated Benzoates. *J. Phys.*

Chem. A **2000**, *104*, 352; (b) Neta, P.; Behar, D., Intramolecular electron transfer in the anion radicals of nitrobenzyl halides. *J. Am. Chem. Soc.* **1980**, *102*, 4798; (c) Neta, P.; Behar, D., Intramolecular electron transfer and dehalogenation of anion radicals. 3. Halobenzonitriles and cyanobenzyl halides. *J. Am. Chem. Soc.* **1981**, *103*, 103; (d) Behar, D.; Neta, P., Intramolecular electron transfer and dehalogenation of anion radicals. 4. Haloacetophenones and related compounds. *J. Am. Chem. Soc.* **1981**, *103*, 2280; (e) Andrieux, C. P.; Blocman, C.; Dumas-Bouchiat, J. M.; M'Halla, F.; Saveant, J. M., Determination of the lifetimes of unstable ion radicals by homogeneous redox catalysis of electrochemical reactions. Application to the reduction of aromatic halides. *J. Am. Chem. Soc.* **1980**, *102*, 3806; (f) Andrieux, C. P.; Saveant, J. M.; Zann, D., Relationship between reduction potentials and anion radical cleavage rates in aromatic molecules. *Nouv. J. Chim.* **1984**, *8*, 107.

8.(a) Sattler, W.; Ener, M. E.; Blakemore, J. D.; Rachford, A. A.; LaBeaume, P. J.; Thackeray, J. W.; Cameron, J. F.; Winkler, J. R.; Gray, H. B., Generation of Powerful Tungsten Reductants by Visible Light Excitation. *J. Am. Chem. Soc.* **2013**, *135*, 10614; (b) Büldt, L. A.; Guo, X.; Prescimone, A.; Wenger, O. S., A Molybdenum(0) Isocyanide Analogue of Ru(2,2'-Bipyridine)₃²⁺: A Strong Reductant for Photoredox Catalysis. *Angew. Chem. Int. Ed.* **2016**, *55*, 11247; (c) Herr, P.; Glaser, F.; Büldt, L. A.; Larsen, C. B.; Wenger, O. S., Long-Lived, Strongly Emissive, and Highly Reducing Excited States in Mo(0) Complexes with Chelating Isocyanides. *J. Am. Chem. Soc.* **2019**, *141*, 14394; (d) Shon, J.-H.; Teets, T. S., Potent Bis-Cyclometalated Iridium Photoreductants with β -Diketiminato Ancillary Ligands. *Inorg. Chem.* **2017**, *56*, 15295.

9. Constantin, T.; Zanini, M.; Regni, A.; Sheikh, N. S.; Juliá, F.; Leonori, D., Aminoalkyl radicals as halogen-atom transfer agents for activation of alkyl and aryl halides. *Science* **2020**, *367*, 1021.

10.(a) Schweitzer-Chaput, B.; Horwitz, M. A.; de Pedro Beato, E.; Melchiorre, P., Photochemical generation of radicals from alkyl electrophiles using a nucleophilic organic catalyst. *Nat. Chem.* **2019**, *11*, 129; (b) Mazzearella, D.; Magagnano, G.; Schweitzer-Chaput, B.; Melchiorre, P., Photochemical Organocatalytic Borylation of Alkyl Chlorides, Bromides, and Sulfonates. *ACS Catal.* **2019**, *9*, 5876;

(c) Cuadros, S.; Horwitz, M. A.; Schweitzer-Chaput, B.; Melchiorre, P., A visible-light mediated three-component radical process using dithiocarbamate anion catalysis. *Chem. Sci.* **2019**, *10*, 5484.

11.(a) Isse, A. A.; Falciola, L.; Mussini, P. R.; Gennaro, A., Relevance of electron transfer mechanism in electrocatalysis: the reduction of organic halides at silver electrodes. *Chem. Commun.* **2006**, 344; (b) Koch, D. A., Carbanion and Radical Intermediacy in the Electrochemical Reduction of Benzyl Halides in Acetonitrile. *J. Electrochem. Soc.* **1987**, *134*, 3062; (c) Andrieux, C. P.; Le Gorande, A.; Saveant, J. M., Electron transfer and bond breaking. Examples of passage from a sequential to a concerted mechanism in the electrochemical reductive cleavage of arylmethyl halides. *J. Am. Chem. Soc.* **1992**, *114*, 6892; (d) Tanner, D. D.; Plambeck, J. A.; Reed, D. W.; Mojelsky, T. W., Polar radicals. 15. Interpretation of substituent effects on the mechanism of electrolytic reduction of the carbon-halogen bond in series of substituted benzyl halides. *J. Org. Chem.* **1980**, *45*, 5177.

12.(a) Giese, B.; González-Gómez, J. A.; Witzel, T., The Scope of Radical CC-Coupling by the “Tin Method”. *Angew. Chem. Int. Ed. Engl.* **1984**, *23*, 69; (b) Giese, B., Formation of CC Bonds by Addition of Free Radicals to Alkenes. *Angew. Chem. Int. Ed. Engl.* **1983**, *22*, 753; (c) Zhang, W., Intramolecular free radical conjugate additions. *Tetrahedron* **2001**, *57*, 7237; (d) Srikanth, G. S. C.; Castle, S. L., Advances in radical conjugate additions. *Tetrahedron* **2005**, *61*, 10377.

13.(a) Arora, A.; Teegardin, K. A.; Weaver, J. D., Reductive Alkylation of 2-Bromoazoles via Photoinduced Electron Transfer: A Versatile Strategy to Csp²-Csp³ Coupled Products. *Org. Lett.* **2015**, *17*, 3722; (b) Arora, A.; Weaver, J. D., Photocatalytic Generation of 2-Azoly radicals: Intermediates for the Azolylation of Arenes and Heteroarenes via C-H Functionalization. *Org. Lett.* **2016**, *18*, 3996; (c) Senaweera, S.; Weaver, J. D., Dual C-F, C-H Functionalization via Photocatalysis: Access to Multifluorinated Biaryls. *J. Am. Chem. Soc.* **2016**, *138*, 2520; (d) Priya, S.; Weaver, J. D., 3rd, Prenyl Praxis: A Method for Direct Photocatalytic Defluoroprenylation. *J. Am. Chem. Soc.* **2018**, *140*, 16020.

14.(a) Minisci, F., Recent Developments of Free-Radical Substitutions of Heteroaromatic Bases. *Heterocycles* **1989**, *28*, 489; (b) Minisci, F.; Vismara, E.; Fontana, F., Homolytic alkylation of

protonated heteroaromatic bases by alkyl iodides, hydrogen peroxide, and dimethyl sulfoxide. *J. Org. Chem.* **1989**, *54*, 5224.

15. Eweiss, N. F.; Katritzky, A. R.; Nie, P.-L.; Ramsden, C. A., The Conversion of Amines into Iodides. *Synthesis* **1977**, *1977*, 634.

16. Liao, J.; Basch, C. H.; Hoerrner, M. E.; Talley, M. R.; Boscoe, B. P.; Tucker, J. W.; Garnsey, M. R.; Watson, M. P., Deaminative Reductive Cross-Electrophile Couplings of Alkylpyridinium Salts and Aryl Bromides. *Org. Lett.* **2019**, *21*, 2941.

17.(a) Klauck, F. J. R.; James, M. J.; Glorius, F., Deaminative Strategy for the Visible-Light-Mediated Generation of Alkyl Radicals. **2017**, *56*, 12336; (b) Klauck, F. J. R.; Yoon, H.; James, M. J.; Lautens, M.; Glorius, F., Visible-Light-Mediated Deaminative Three-Component Dicarbofunctionalization of Styrenes with Benzylic Radicals. *ACS Catalysis* **2019**, *9*, 236; (c) Klauck, F. J. R.; James, M. J.; Glorius, F., Deaminative Strategy for the Visible-Light-Mediated Generation of Alkyl Radicals. *Angew. Chem. Int. Ed.* **2017**, *56*, 12336.

18. Suga, T.; Shimazu, S.; Ukaji, Y., Low-Valent Titanium-Mediated Radical Conjugate Addition Using Benzyl Alcohols as Benzyl Radical Sources. *Org. Lett.* **2018**, *20*, 5389.

19.(a) Maji, T.; Karmakar, A.; Reiser, O., Visible-Light Photoredox Catalysis: Dehalogenation of Vicinal Dibromo-, α -Halo-, and α,α -Dibromocarbonyl Compounds. *J. Org. Chem.* **2011**, *76*, 736; (b) Pac, C.; Ihama, M.; Yasuda, M.; Miyauchi, Y.; Sakurai, H., Tris(2,2'-bipyridine)ruthenium(2+)-mediated photoreduction of olefins with 1-benzyl-1,4-dihydronicotinamide: a mechanistic probe for electron-transfer reactions of NAD(P)H-model compounds. *J. Am. Chem. Soc.* **1981**, *103*, 6495.

20. Hu, J.; Wang, J.; Nguyen, T. H.; Zheng, N., The chemistry of amine radical cations produced by visible light photoredox catalysis. *Beilstein J. Org. Chem.* **2013**, *9*, 1977.

21. Crich, D.; Patel, M., Facile Dearomatizing Radical Arylation of Furan and Thiophene. *Org. Lett.* **2005**, *7*, 3625.

22. Castro, S.; Fernández, J. J.; Vicente, R.; Fañanás, F. J.; Rodríguez, F., Base- and metal-free C–H direct arylations of naphthalene and other unbiased arenes with diaryliodonium salts. *Chem. Commun.* **2012**, *48*, 9089.
23. Farney, E. P.; Chapman, S. J.; Swords, W. B.; Torelli, M. D.; Hamers, R. J.; Yoon, T. P., Discovery and Elucidation of Counteranion Dependence in Photoredox Catalysis. *J. Am. Chem. Soc.* **2019**, *141*, 6385.
24. Lowry, M. S.; Goldsmith, J. I.; Slinker, J. D.; Rohl, R.; Pascal, R. A.; Malliaras, G. G.; Bernhard, S., Single-Layer Electroluminescent Devices and Photoinduced Hydrogen Production from an Ionic Iridium(III) Complex. *Chem. Mater.* **2005**, *17*, 5712.
25. (a) McTiernan, C. D.; Morin, M.; McCallum, T.; Scaiano, J. C.; Barriault, L., Polynuclear gold(i) complexes in photoredox catalysis: understanding their reactivity through characterization and kinetic analysis. *Catal. Sci. Technol.* **2016**, *6*, 201; (b) Cherevatskaya, M.; Neumann, M.; Fuldner, S.; Harlander, C.; Kümmel, S.; Dankesreiter, S.; Pfitzner, A.; Zeitler, K.; König, B., Visible-Light-Promoted Stereoselective Alkylation by Combining Heterogeneous Photocatalysis with Organocatalysis. *Angew. Chem. Int. Ed.* **2012**, *51*, 4062.
26. Grimshaw, J., *Electrochemical Reactions and Mechanisms in Organic Chemistry*. Elsevier Science: 2000.
27. Maslak, P.; Narvaez, J. N., Mesolytic Cleavage of C–C Bonds. Comparison with Homolytic and Heterolytic Processes in the Same Substrate. *Angew. Chem. Int. Ed. Engl.* **1990**, *29*, 283.
28. Blanksby, S. J.; Ellison, G. B., Bond Dissociation Energies of Organic Molecules. *Acc. Chem. Res.* **2003**, *36*, 255.
29. Gribov, L. A.; Novakov, I. A.; Pavlyuchko, A. I.; Korolkov, V. V.; Orlinson, B. S., Spectroscopic Calculation of CH Bond Dissociation Energies for Aliphatic Nitriles. *J. Struct. Chem.* **2004**, *45*, 771.
30. Wayner, D. D. M.; Dannenberg, J. J.; Griller, D., Oxidation potentials of α -aminoalkyl radicals: bond dissociation energies for related radical cations. *Chem. Phys. Lett.* **1986**, *131*, 189.

- 31.(a) Schmittl, M.; Lal, M.; Lal, R.; Röck, M.; Langels, A.; Rappoport, Z.; Basheer, A.; Schlirf, J.; Deiseroth, H.-J.; Flörke, U.; Gescheidt, G., A comprehensive picture of the one-electron oxidation chemistry of enols, enolates and α -carbonyl radicals: oxidation potentials and characterization of radical intermediates. *Tetrahedron* **2009**, *65*, 10842; (b) Abbas, S. Y.; Zhao, P.; Overman, L. E., 1,6-Addition of Tertiary Carbon Radicals Generated From Alcohols or Carboxylic Acids by Visible-Light Photoredox Catalysis. *Org. Lett.* **2018**, *20*, 868.
- 32.Iniesta, J.; Cooper, H. J.; Marshall, A. G.; Heptinstall, J.; Walton, D. J.; Peterson, I. R., Specific electrochemical iodination of horse heart myoglobin at tyrosine 103 as determined by Fourier transform ion cyclotron resonance mass spectrometry. *Archives of Biochemistry and Biophysics* **2008**, *474*, 1.
- 33.Dou, J.; Liu, Z.; Mahmood, K.; Zhao, Y., Synthesis of poly(ethylene terephthalate) in benzyl imidazolium ionic liquids. *Polym Int* **2012**, *61*, 1470.
- 34.Nomura, S.; Endo-Umeda, K.; Aoyama, A.; Makishima, M.; Hashimoto, Y.; Ishikawa, M., Styrylphenylphthalimides as Novel Transrepression-Selective Liver X Receptor (LXR) Modulators. *ACS Med. Chem. Lett.* **2015**, *6*, 902.
- 35.Kerner, C.; Lang, J.; Gaffga, M.; Menges, F. S.; Sun, Y.; Niedner-Schatteburg, G.; Thiel, W. R., Mechanistic Studies on Ruthenium(II)-Catalyzed Base-Free Transfer Hydrogenation Triggered by Roll-Over Cyclometalation. *ChemPlusChem* **2017**, *82*, 212.
- 36.Kumar, Y.; Jaiswal, Y.; Kumar, A., Visible-Light-Mediated Remote γ -C(sp³)-H Functionalization of Alkylimidates: Synthesis of 4-Iodo-3,4-dihydropyrrole Derivatives. *Org. Lett.* **2018**, *20*, 4964.
- 37.Everson, D. A.; Jones, B. A.; Weix, D. J., Replacing Conventional Carbon Nucleophiles with Electrophiles: Nickel-Catalyzed Reductive Alkylation of Aryl Bromides and Chlorides. *J. Am. Chem. Soc.* **2012**, *134*, 6146.
- 38.Uchikura, T.; Moriyama, K.; Toda, M.; Mouri, T.; Ibáñez, I.; Akiyama, T., Benzothiazolines as radical transfer reagents: hydroalkylation and hydroacylation of alkenes by radical generation under photoirradiation conditions. *Chem. Commun.* **2019**, *55*, 11171.

APPENDICES

Intersystem crossing (ISC)

Metal Ligand Charge Transfer (MLCT)

Single Electron Transfer (SET)

Ultraviolet (UV)

Lowest unoccupied molecular orbital (LUMO)

Hydrogen atom transfer (HAT)

Electron Donor-Acceptor (EDA)

Trimethylamine (TEA, Et₃N)

Tributylamine (Bu₃N)

Di-isopropylethylamine (DIPEA)

Dichloromethane (DCM)

Acetonitrile (MeCN)

Methanol (MeOH)

N, N-Dimethylformamide (DMF)

Dimethyl sulfoxide (DMSO)

Dimethylacetamide (DMA)

Tetrahydrofuran (THF)

Thin layer chromatography (TLC)

1,8-Diazabicyclo[5.4.0]undec-7-ene (DBU)

1,4-Diazabicyclo[2.2.2]octane (DABCO)

Phenyl (Ph)

Benzyl (Bn)

Methyl (Me)

Starting material (SM)

Pdt (product)

PC (photocatalyst)

rt (room temperature)

EWG (electron withdrawing group)

VITA

Rathnayake Mudiyansele Manjula Damayanthi Rathnayake

Candidate for the Degree of

Doctor of Philosophy

Thesis: THE DEVELOPMENT OF REAGENTS AND REACTIONS TO BE USED IN
VISIBLE LIGHT PHOTOCATALYSIS

Major Field: Chemistry

Biographical:

Education:

Completed the requirements for the Doctor of Philosophy in Organic Chemistry
at Oklahoma State University, Stillwater, Oklahoma in July, 2020.

Completed the requirements for the Bachelor of Science in Chemistry at
University of Kelaniya, Sri Lanka, 2013.

Professional Memberships:

Phi Kappa Phi

American Chemical Society